MDOT RC-1412
CSD-2002-02

MDOT

Research

CAUSES & CURES FOR PRESTRESSED CONCRETE I-BEAM END DETERIORATION

AUGUST 2002

WAYNE STATE UNIVERSITY

MichiganTech

Center for Structural Durability
A Michigan DOT Center of Excellence

TESTING AND RESEARCH SECTION
CONSTRUCTION AND TECHNOLOGY DIVISION
RESEARCH REPORT NO. RC-1412

This report presents the results of research conducted by the authors and does not necessarily reflect the views of the Michigan Department of Transportation. This report does not constitute a standard or specification.

Technical Report Documentation Page

1. Report No. Research Report RC-1412	2. Government Accession No.	3. MDOT Project Manager Roger D. Till
4. Title and Subtitle Causes and Cures for Prestressed Concrete I-Beam End Deterioration		5. Report Date August 2002
7. Author(s) Dr. Theresa M. (Tess) Ahlborn, Mr. James M. Kasper (MTU) Dr. Haluk Aktan, Mr. Yilmaz Koyuncu, Mr. Jason Rutyna (WSU)		6. Performing Organization Code MTU and WSU
9. Performing Organization Name and Address Center for Structural Durability – a joint research effort between Michigan Technological University, CEE Department 1400 Townsend Drive, Houghton, MI 49931 and Wayne State University, CEE Department 5050Anthony Wayne Dr., Detroit, MI 48202		8. Performing Org Report No. CSD-2002-02
12. Sponsoring Agency Name and Address Michigan Department of Transportation Construction and Technology Division P.O. Box 30049 Lansing, MI 48909		10. Work Unit No. (TRAIS) 11. Contract Number: WSU # 01-0364 11(a). Authorization Number: MTU # 01-MTU-8-1
15. Supplementary Notes		13. Type of Report & Period Covered Final Report, 5/01-6/02 14. Sponsoring Agency Code

16. Abstract

Prestressed concrete (PC) for highway bridges was first introduced in Michigan in the 1950s. In 2002, Michigan had over 1900 prestressed box beam and 700 prestressed I-beam structures. A recent study focusing on the condition of Michigan's PC bridges revealed that while most were in fair or better than fair condition, older bridges are showing signs of deterioration, particularly in the ends of I-beam structures. End deterioration needs to be addressed through various inspection and repair techniques for these structures. The specific goals of this research were to a) *develop an inspection procedure* for prestressed concrete I-beam bridges that will clearly distinguish distress severity and disclose potential problems, b) *identify preventive maintenance* strategies to extend the service life of prestressed concrete I-beam ends, and c) *evaluate repair techniques* for I-beam ends to avoid performing complete beam replacement.

The information presented here begins with field survey inspection data and results of a multi-state survey to determine nationwide practices for inspection and repair of prestressed concrete I-beam ends. Analytical studies incorporated extensive field inspection data and showed beam-end deterioration to significantly influence the load path through the member to the bearing. An experimental investigation of shrinkage/cracking and adhesion of vertically patched shallow and deep repairs was conducted. Three repair materials were used in patches and specimens were thermally cycled. All repair materials showed cracking larger than 6 mils and no material met the minimum bond performance criteria of 400 psi. A master listing of suggested preventative maintenance and repair techniques is provided.

17. Key Words bridges, prestressed concrete, precast girders, inspection, repair, finite element, cracking	18. Distribution Statement No restrictions. This document is available to the public through the Michigan Department of Transportation.		
19. Security Classification (report) Unclassified	20. Security Classification (Page) Unclassified	21. No. of Pages 390	22. Price

August 22, 2002

CAUSES & CURES FOR PRESTRESSED CONCRETE I-BEAM END DETERIORATION

Submitted to the

RESEARCH ADVISORY PANEL

MDOT

WAYNE STATE UNIVERSITY

Wayne State University
Civil & Environmental Eng. Dept.
5050 Anthony Wayne Dr.
Detroit, Michigan 48202
fax: 313/577-3881

Dr. Haluk Aktan, P.E.
Professor
313/577-3825
haluk.aktan@wayne.edu

Mr. Yilmaz Koyuncu
Graduate Research Assistant
313/577-3785
ykoyuncu@eng.wayne.edu

Mr. Jason M. Rutyna
Undergraduate Research Assistant
313/577-3785
jrutyna@eng.wayne.edu

MichiganTech

Michigan Technological University
Civil & Environmental Eng. Dept.
1400 Townsend Dr.
Houghton, Michigan 49931
fax: 906/487-1620

Dr. Tess Ahlborn, P.E.
Assistant Professor
906/487-2625
tess@mtu.edu

Mr. James M. Kasper, P.E.
Graduate Research Assistant
906/487-1952
jmkasper@mtu.edu

Executive Summary

The research study focus was the evaluation and abatement of girder end deterioration in prestressed concrete I-beam bridges. Details of the research conducted, including the quarterly report, notes of research meetings and detailed field inspection data can be found at http://webpages.eng.wayne.edu/durabilitycenter. The initial work task was the documentation of observed girder end condition by inspecting twenty prestressed concrete I-beam bridges constructed in Michigan between 1961 and 1998. The following table documents the list of inspected bridges and summary of girder end condition. Also, in the following table "corr" and "del" are abbreviations for corrosion and delamination, respectively.

Condition Summary

Bridge ID	County	Region	Year Built	No. of Spans	No. of Girders	Total No. of Beam-ends Inspected	% Beam-ends w/ No Cracks & No Corr	% Beam-ends w/ cracks	% Beam-ends w/ cracks & corr	% Beam-ends w/ del	% Beam-ends w/ spall	Sum (%)
29011 S03	Gratiot	Bay	1961	3	27	54	0	0	28	39	33	100
06111 S04	Arenac	Bay	1968	3	18	35	0	4	21	34	40	100
06111 S05	Arenac	Bay	1968	3	15	30	0	17	16	17	51	100
06111 S06	Arenac	Bay	1968	3	15	30	0	2	17	13	67	100
06111 S11	Arenac	Bay	1968	6	54	62	0	15	19	31	35	100
25042 S12-8	Genesee	Bay	1969	4	16	28	0	26	26	17	31	100
25042 S12-3	Genesee	Bay	1969	4	22	44	0	7	33	30	30	100
25042 S12-4	Genesee	Bay	1969	4	22	43	0	3	33	27	37	100
25042 S12-7	Genesee	Bay	1969	4	16	32	0	19	5	10	66	100
25132 S34	Genesee	Bay	1971	4	24	48	4	4	18	14	61	100
41025 S07	Kent	Grand	1961	4	24	47	0	0	9	11	80	100
41027 S06	Kent	Grand	1963	3	36	71	0	0	7	12	81	100
41029 S16-3	Kent	Grand	1964	3	24	46	0	0	13	16	72	100
41029 S16-4	Kent	Grand	1964	3	24	48	0	21	21	35	23	100
41029 S23	Kent	Grand	1972	3	24	48	0	58	6	10	25	100
67016 S09	Oceola	North	1984	1	6	11	0	18	18	55	9	100
67016 S10	Oceola	North	1984	1	7	14	0	64	14	7	14	100
53034 S05	Mason	North	1986	4	24	27	0	19	52	22	7	100
83033 S06	Wexford	North	1997	1	8	16	0	94	6	0	0	100
83033 S05	Wexford	North	1998	2	8	16	13	81	6	0	0	100
Total					414	750	0	17	18	20	44	100

Upon documenting the prestressed concrete I-beam end condition in Michigan a survey of State Departments of Transportation was conducted to document the observations in other states. A survey return-rate of 40 percent was achieved with 20 states responding. Responding states were located across the country. Two of Michigan's five neighboring states responded to the survey. One survey respondent indicated that the state did not have a prestressed concrete I-beam end deterioration problem and did not include a completed survey. Over 70 percent of the respondents indicated that they use some unique internal software for management of their state's bridge structural / safety data. All respondents indicated they do not gather specific inspection data on prestressed concrete beam end conditions. It was unclear from the survey responses if any states are using existing documentation (reports, etc.) to aid in the preventive maintenance of prestressed concrete I-beams.

While most states have not repaired prestressed I-beams for end deterioration, roughly 50 percent of the respondents indicated that their state DOT specifications would be used in the rehabilitation of prestressed concrete I-beam ends. The only responding state to indicate that I-beam end repair has been attempted was Michigan.

An inspection procedure is proposed specifically for early identification of prestressed concrete I-beam ends prone to deterioration. The inspection technique is based on data collected visually (at an arms length). In reviewing the observations and data obtained during the inspections, there are three inspection items of importance that are related to I-beam end deterioration. These items are presence of beam end cracking, bearing condition and beam end restraints, and drainage and expansion joint condition.

Categories of condition of deteriorated prestressed concrete beam-ends have been developed to define a distress level and an associated preventative maintenance or repair technique. Condition states for a prestressed concrete I-beam also describe the progression of distress at the beam-end with time. The information shown in the table below has been assembled to assist an inspection crew with accurately assessing the condition of a beam-end.

Condition States of Prestressed Concrete I-Beam Ends

Rating	Condition State
1	No cracks observed, no staining
2	Efflorescence, water-stains, and/or corrosion
3	Hairline Cracks. They can be horizontal, vertical, and/or diagonal
4	Map Cracks
5	Hairline Cracks with efflorescence, water-stains, and/or corrosion with a horizontal crack propagating from the sole plate
6	Cracked and Deformed Neoprene Pad, probably non-functional
7	Moderate Cracks
8	Moderate Cracks with efflorescence, water-stains, and/or corrosion
9	Major Cracks with efflorescence, water-stains, and/or corrosion
10	Delamination with Moderate and/or Major Cracks
11	Spall, Delamination, Corrosion, and Cracks
12	Spall, Exposed Reinforcement, and Corrosion

The study identified four major families of preventive maintenance approaches that can be applied to beam-ends. These techniques were: structure modification, surface insulating

methods, electrical control methods, and environment modifying methods. The study developed three analysis tools for successfully executing a beam-end repair project. The tools are: testing procedures and distress severity criteria for PC I-beam end deterioration, cause-evidence relationships for beam end distress and an example performance matrix for preventive maintenance techniques.

The finite element modeling of a PC I-girder is performed to evaluate the causes of observed beam-end distress. The discrete beam analysis identified the effects of prestressing loads, and design changes with respect to tendon geometry and arrangement. Three types of prestressed concrete I-beams were modeled from existing bridges to determine the cause for initial bursting cracks at the end zones. The first model is a beam with straight tendons, the second beam is a Wisconsin type with and without bond breakers, and the third beam is with draped tendons. The stress formation at the end zones and cracking potential are studied. The table below describes the calculated shear and uniaxial stress in the girder ends. In all cases cracking is anticipated by high shear and tension stresses upon release of tendons.

Stresses in Prestressed I-Beam Ends Under Prestressing Loads

Girder Type Tendons		Maximum Shear Stress (ksi)	Axial Stress (ksi)	
			Compression	Tension
Straight (Uniform) Tendon		0.8	3.0	0.4
Draped Tendon		1.5	3.2	$>f_{ct}$
Bond-breakers	With Bond-breakers	3.0	5.4	$>f_{ct}$ (424 psi)
	Without Bond-breakers	4.0	$>>f_c'$ (5,000 psi)	$>f_{ct}$ (424 psi)

The structural interactions between the bridge members and the load-transfer mechanism to the beam-ends is analyzed on a full bridge model. The analytical modeling is performed on the bridge with ID 06111-S04. The three-span bridge has exterior spans of 31 feet 3 inches in length and a mid-span of 49 feet in length. The bridge deck has a uniform width of 43 feet 2 inches with two lanes. The minimum deck thickness is 8 inches. Two types of AASHTO prestressed I-girder types, Type III and Type I, are used. Type III girders are located in the mid-span and as fascia girders in the exterior spans. Type I girders are located in the exterior spans as interior girders. The girders are designed as simply supported. The structural behavior of a bridge under several service-loading stages is analyzed. The impact of the diaphragms on beam-ends is investigated by describing diaphragms with different geometry and cross sections and having different material properties. The following table summarizes the shear and moments near beam-ends with various diaphragm types under various load conditions. It is seen that change in the stresses at the beam-ends are insignificant with the use of different diaphragms.

Full Bridge Analysis Results near the Beam-ends

Without Diaphragms			With Diaphragms						Steel Bracing						Loading			
Dead Load			Dead Load			Live Load			Dead Load			Live Load						
V (k)	M (in-k)	T (in-k)	V (k)	M (in-k)	T (in-k)	V (k)	M (in-k)	T (in-k)	V (k)	M (in-k)	T (in-k)	V (k)	M (in-k)	T (in-k)				
10	82	1	12	105	0	28	230	8	11	92	1	17	142	10	ID	A	Exterior	First Span Beams
8	193	3	8	242	7	8	518	18	8	206	3	9	282	26	OD			
8	193	3	8	211	11	9	301	27	8	206	3	9	275	23	OD	P		
10	82	1	11	91	1	15	126	6	11	92	1	16	136	9	ID			
12	106	0	11	95	0	21	181	9	12	102	0	30	253	10	ID	A	Interior	
10	243	1	11	221	0	31	440	24	10	238	1	30	625	26	OD			
10	243	1	10	237	0	19	397	5	10	238	1	20	413	5	OD	P		
12	106	0	12	103	1	22	182	0	12	102	0	21	172	1	ID			
16	137	2	18	150	1	NA	NA	NA	18	149	0	NA	NA	NA	ID	P	Exterior	Middle Span Beams
14	326	6	15	352	4	NA	NA	NA	15	347	1	NA	NA	NA	OD			
19	164	1	19	158	0	NA	NA	NA	19	158	0	NA	NA	NA	ID	P	Interior	
17	383	4	16	370	0	NA	NA	NA	16	372	0	NA	NA	NA	OD			

A: Abutment end
ID: Inside of Diaphragm (Span Side)
OD: Outside of Diaphragm (Beam-end Side)
M: Moment
NA: Not Available
P: Pier-cap end
T: Torsion
V: Shear Force

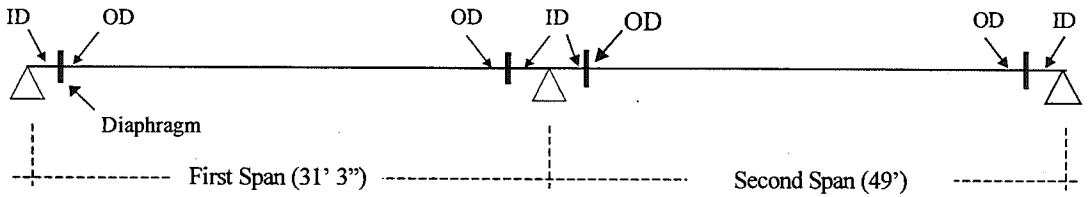

Forms of distress at the beam-ends include concrete spalling, delamination, cracking, and corrosion of reinforcement. The loss of concrete permits accelerated deterioration of reinforcing and prestressing steels, allows detensioning of prestressing steel, and increases the stress demand (bearing, shear, flexural) on the remaining section. Properly functioning repairs can restore cover to reinforcing and prestressing steels and re-establish the original intended cross section of the concrete. The two of the most important properties of concrete repair are crack resistance and substrate adhesion (bond). Crack resistance is needed to prohibit ingress of contaminants that can adversely affect the performance of the repair. Adhesion is required to assist the parent member in carrying loads as well as protecting the parent member (or repair) steel reinforcement from corrosion. A performance evaluation of vertical repair material was conducted and focused on evaluating crack development and repair bond tensile strength at the conclusion of a thermal cycling period. The performance measure for maximum repair cracking width for this study was 6-mils. Visual observations of the repair condition at the conclusion of the post-curing period revealed cracking within the repair material itself and at the repair-substrate joints (i.e. top and bottom repair joints). Not considering the cracking at these joints, some observations made were:

- All brands of repair material showed cracking greater than 6-mils in width.
- Those specimens with fine-width (2-mil) pattern cracking generally did not exhibit cracks within the repair greater than 6-mils in width.
- Those specimens repaired with materials produced with a liquid polymer exhibited more cracking than the material mixed with potable water.
- Repair depth (1-inch or 3-inch) did not have an impact on frequency of cracked specimens relative to the total number of specimens tested. About 1/3 of each repair depth group exhibited cracking greater than 6-mils.
- Post-curing environment showed 43% of specimens exceeded the 6-mil performance measure, whereas 28% of ambient cured specimens exceeded the measure.

For bond tensile strength, two sets of performance measures were observed. First, repairs cannot delaminate from the substrate and second, a bond tensile strength of 400-psi was required. Over 1/3 of the repair specimens did not meet the delamination performance criteria and none of the specimens were able to develop a bond tensile strength of greater than 400-psi.

The focus for the next phase of work should be related to safety assessment. In order to understand the relation between girder-end condition states and their load performance, the proposed approach is to development an analytical model for various bridge types calibrated by the full scale testing of decommissioned girders. The experimental component is further divided into laboratory experiments for condition characterization of in-service girders and field-testing of full-scale girders. Evaluation of actual beam structural capacity is needed to truly understand the damage due to deterioration. Full scale testing results of individual beams in flexure and shear can give insight into the actual strength reduction and can be compared with analytical models. Corresponding models can then be used for future bridge analysis of deteriorated structures to more accurately determine the capacity of the structure. In addition, repaired beams can also be tested for effectiveness in restoring strength.

Acknowledgements

The Michigan Department of Transportation and the Departments of Civil and Environmental Engineering at Wayne State University and Michigan Technological University provided funds for this study. This support is gratefully acknowledged.

The authors would like to acknowledge the support and efforts of Mr. Roger Till for initiating this research and for providing direction as the Project Manager. The authors would also like to acknowledge the continuing assistance of the Research Advisory Panel (RAP) in contributing to the advancement of this study: Steve Beck, David Calabrese, Christopher Idusuyi, Raja Jildeh, Steve Kahl, Ali Mahdavi, Tony Olson, Neil Pullman, and Tom Tellier. Their guidance and supervision of the project and valuable input regarding these research efforts are appreciated.

We would also like to thank the following individuals who helped with bridge inspection: Recep Birgul and Kraig and Kristofer Warnemuende. Anna Ovanesova is also acknowledged for her work on this project. In addition, the physical work and data entry for the experimental study portion of this project is greatly appreciated. Individuals contributing to that effort include Joel Prusi, Jeff Diephuis, Archie Kollmorgen, Rob Fritz, Jim Vivian, and Karl Peterson.

We sincerely extend our appreciation to the manufacturers and their representatives that provided repair materials for this study. Scott Perry of Chemrex, Inc. provided the ThoRoc HB2 and MBT Emaco R350-CI repair materials. Wesley Pringle of Sika USA was able to provide the Sika Top 126 Plus repair mortar.

TABLE OF CONTENTS

List of Figures

List of Tables

List of Photographs

1.0 Introduction

1.1 Overview

Deterioration of in-service civil engineering infrastructure in the United States has become an issue in recent years (ASCE, 2002). Due in part to its versatility, availability, and economy, portland cement concrete has been selected as the building material of choice for roads, bridges, and dams, among other infrastructure elements. When properly designed and placed, portland cement concrete is also a very durable material (Mindess and Young, 1981). However, portland cement concrete can deteriorate during its service life if proper design and placement practices are not followed or if the service conditions are different from those anticipated. An example of insufficient durability is evidenced in the ends of some in-service prestressed concrete I-beams in Michigan bridges.

The basic concept of prestressed concrete dates back to the late eighteen hundreds, nearly as old as reinforced concrete. However, it was the material properties that prevented the application of prestressed concrete to structures like bridges. It was first Eugene Freyssinet of France who in 1928 first began the use of high strength steel wire for prestressed concrete, and he is known as the originator of practical prestressed concrete (Nawy, 2000). After Freyssinet's original work, prestressed concrete was increasingly utilized in both Europe and North America, and the first prestressed bridge was the Walnut Lane Bridge in Philadelphia, which was finished in 1951.

This bridge type quickly became popular because the beams could be built economically in plants, and their span lengths could compete with that of steel beams. Michigan's first prestressed concrete bridge was built in 1951 (Moore et al, 1970). In 1996, Michigan had 1,696 prestressed box beam and 696 prestressed I-beam structures that were owned and operated by the state (Needham and Juntunen, 1997).

Work performed by others has concluded that in midwestern states, such as Michigan, corrosion is more pronounced in older bridges near the beam-ends (Whiting et al, 1999). This is likely due to the beam-ends being located below poorly maintained deck joints and thus exposed to deicing salts draining from the deck surface. Photo 1-1 shows an example of the end deterioration problem that some of Michigan's prestressed concrete I-beam bridges face.

Corrosion induced deterioration of prestressed concrete bridges are more critical than similar deterioration in a conventionally reinforced portland cement concrete element for several reasons. One reason is that even minor corrosion of prestressing strands may affect the load carrying capacity of beams to a greater degree than in conventional reinforced concrete. Also, because of the relatively small diameter and large number of prestressing strands compared to the fewer number of larger bars that are used in conventionally reinforced concrete, a greater

surface area is available for corrosion. Lastly, the increase in reinforcement density and surface area within a prestressed concrete section can lead to increased corrosion activity when compared to a conventionally reinforced member.

Photo 1-1. End deterioration of prestressed concrete I-beam ends

Recent practice in Michigan is to use a continuous-for-live-load (CLL) superstructure design where the diaphragms are cast integral with the deck over the piers. As shown in Figure 1-1, this design eliminates the joints over the piers and eliminates the direct exposure of the prestressing strands at the beam-ends to chlorides. While the current Michigan detail is similar, positive moment reinforcement is not used.

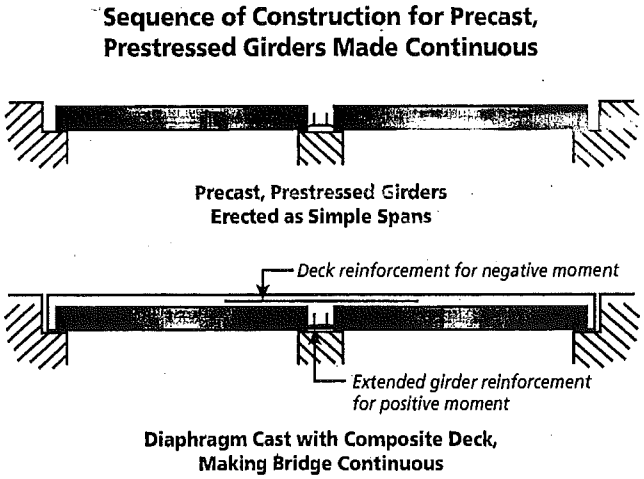

Figure 1-1. Example of Constructing Decks Continuous for Live Load (Rabbat and Aswad, 2002)

If this practice is effective, the corrosion problem will be constrained and corrective actions may be limited to prestressed concrete bridges constructed prior to CLL structures. For the remaining limited group of bridges with joints, there is a potential for corrosion of prestressed strands and mild steel reinforcement. There will be a need for inspection techniques that can identify problems in advance so that corrective action can be taken.

For existing deteriorated prestressed concrete bridges, however, there is a need for effective repair procedures. The Michigan Department of Transportation (MDOT) and the Federal Highway Administration (FHWA) developed one such repair procedure for prestressed concrete I-beams (Needham, 1999). The repair procedure was experimentally verified on one salvaged prestressed I-beam. The procedure was then applied to three in-service structures with some modifications, and it was economically beneficial compared to a total superstructure replacement (Needham, 2000). The effectiveness of this and other similar procedures, however, should be further verified using analytical tools and some experimental demonstrations.

Therefore, for bridges that may be at risk for end deterioration, there is a serious need for:

- **Evaluating** and **assessing** the deterioration level of these prestressed concrete bridges,
- **preventing** further deterioration from occurring, and
- **repairing** prestressed concrete bridges with corroding strands.

Research activity in the field of concrete repair has been on going for over 30 years, however at a relatively low volume, compared to other areas of concrete research. Through the completion of a state-of-the art literature review, multi-state survey, analytical modeling and experimental studies, this study examined the potential deterioration mechanisms that can affect a prestressed concrete beam-end, and what components of concrete durability are required to resist the deterioration. Although several deterioration mechanisms exist, one mechanism dominates all others in terms of frequency: corrosion-induced deterioration by deicer penetration.

1.2 Objectives

This research project, "Causes and Cures for Prestressed Concrete I-Beam End Deterioration," was sponsored by the Michigan Department of Transportation (MDOT) and performed by the Center for Structural Durability, a collaborative effort between Michigan Technological University and Wayne State University, the Research Team. Work has focused exclusively on prestressed concrete I-beams with end deterioration.

There were two main objectives for the research program:

- Development of an inspection procedure for existing prestressed concrete I-beams with potential end deterioration problems, and
- Evaluation of repair techniques for existing deteriorated prestressed concrete I-beam ends.

To satisfy these objectives, the project was organized in two phases with thirteen tasks. Sections 1.3 and 1.4 list the tasks with respect to their appropriate phase as they were presented in the original proposal. Also, any changes to the original tasks are discussed. Each task corresponds to one chapter of this report.

1.3 Phase I

Phase I contained Tasks 1-8 as listed below.

Task 1. State-of-the-Art Literature Review (Chapter 2)

The objective of the literature review was to identify, review, and synthesize information related to prestressed concrete I-beam end deterioration. It has been an ongoing study throughout the project, and the result is a comprehensive chapter describing many different aspects of prestressed concrete I-beams ranging from history of design to inspection, preventive maintenance and repair methods.

Task 2. Field Investigation (Chapter 3)

The objective of the field investigation was to conduct an extensive examination of 20 prestressed concrete I-beam bridges to observe the distress at the beam-ends. Bridges ranged from 2 to 40 years old and were previously FHWA condition rated between 4 (poor) and 8 (very good). The result is a complete documentation of the research team's process of selection of field specimens, field inspection and observations, and data organization.

Task 3. Identify Bridges Prone to Deterioration (Chapter 4)

The objective of this analysis was to identify bridges that are at risk of distress. Information gathered from the field investigation was used to describe why I-beams are in the current state of distress. This chapter thoroughly describes the methodology and results of the analysis.

Task 4. Conduct a Survey of State Highway Officials (Chapter 5)

The objectives of the survey include determining practices that are used for inspecting and repairing prestressed concrete I-beam ends, and identifying reports relating to the evaluation or repair of prestressed concrete I-beam ends. This task was completed in Phase I, and the result is a discussion of the returned surveys.

Task 5. Survey of PC I-beam End Inspection Techniques (Chapter 6)

A significant review of inspection techniques was provided in the literature review. This review, in conjunction with the field inspection of Chapter 3, has resulted in the proposed condition states and corresponding tabulated photos to aid inspectors in identifying the condition of a beam-end.

Task 6. Preventive Maintenance Techniques for Beam-End Deterioration (Chapter 7)

While families of preventative maintenance approaches were identified in the literature review, this chapter focuses on three analysis tools: tests applicable in classifying the severity of end distress, cause/evidence relationships for beam-end deterioration, and a performance matrix to aid in the selection of effective approaches.

Task 7. Project Website (Chapter 8)

The objective of the website was to create a centralized location of information pertaining to the projects that the Center for Structural Durability have completed or currently working on. This task was continually updated through both phases, and the result is a project homepage for the research project "Causes & Cures for Prestressed Concrete I-beam End Deterioration" that provides pertinent information.

Task 8. Interim Report

The Interim Report was submitted on October 25, 2001. It included all information that was completed within Tasks 1-7.

1.4 Phase II

Phase II contained Tasks 9-13 as listed below.

Task 9. Repair Techniques for Beam-End Deterioration (Chapter 9)

The initial task definition was to determine feasible repair/strengthening techniques including their benefit/cost analysis. Initial items within this task included identifying a performance matrix and identifying methods to assign repair techniques to different levels of distress based on literature review (Task 1), inspection and survey observations (Tasks 2-6), analytical study (Task 10) and laboratory testing results (Task 11). This matrix was discussed in Chapter 7, and benefit/cost analysis became beyond the scope/timeline of this project (see Chapter 14). Included in this chapter are basic suggestions for beam end repair, including comments/suggested changes for MDOT related documents.

Task 10. Analytical Modeling (Chapter 10)

The original purpose of this task was to develop an analytical model of a "prestressed concrete I-beam bridge" to be used for evaluating repair techniques. The task evolved to the evaluation of shear stresses during production, load paths near the girder-end under dead and live loads, and diaphragm effects in a bridge load response. Two models were developed (a discrete I-beam model and a full bridge model) using one of the inspected bridge as a reference for design and material characteristics. Models help to identify the cause of end cracking and can be used to potentially propose new reinforcement details or changes to precasting practices.

Task 11. Experimental Study of Repair Materials (Chapter 11)

The initial task definition was to conduct lab testing / implementation of the selected repair techniques based on Phase I outcome including 1) conduct specimen preparation 2) identify surface preparation technique and 3) state visible repair techniques for damage treatment. The outcome of this task was the experimental study of three repair materials used for partial patching of vertical and overhead repairs, and an evaluation of both shrinkage/cracking potential and bond tensile strength for all three materials.

Task 12. Data Analysis

This task has been incorporated into each respective chapter. For example, the analysis of field inspection data was included in Tasks 2 and 3, or Chapters 3 and 4, respectively. Results of the analytical study are included in Task 10 (Chapter 10), and laboratory data analysis is included in Task 11 (Chapter 11).

Task 13. Final Report

This document constitutes the final report. In addition to the above chapters, the following three chapters are included:

Chapter 12 – includes a discussion on a bridge management approach to managing the preventative maintenance and repair of prestressed concrete beam end distress.

Chapter 13 – provides a summary of the significant conclusions of this work.

Chapter 14 – as with any quality research project, many questions can be answered but some remain unanswered. This chapter includes a list of future studies for consideration.

2.0 State-of-the-Art Literature Review (Task 1)

2.1 Objectives and Approach

A state-of-the-art literature review was conducted for this project. The objective of the literature review was to identify, review, and synthesize information related to prestressed concrete I-beam end deterioration. Concentration areas for the review were established for the project, and included:

- Concrete durability and deterioration mechanisms
- Inspection, preventive maintenance, and repair tools for prestressed concrete bridges
- Past and current MDOT practices with prestressed concrete design and repairs

To effectively convey the results of the literature review, other topics related to prestressed concrete were reviewed and have been included in this report.

The resources of the Michigan Tech and Wayne State University libraries were used for this project. In addition to the collections of reference material housed at these facilities, a significant number of references were identified through electronic index searches including National Technical Information Service, Transportation Research Information Service, Engineering Village, and World Cat. An extensive review of information available on the Internet was also conducted. The resources of professional and government organizations were explored through web searches and telephone interviews. These organizations included:

- American Concrete Institute (ACI),
- ASTM International (ASTM),
- Federal Highway Administration (FHWA),
- American Association of State Highway and Transportation Officials (AASHTO),
- National Cooperative Highway Research Program (NCHRP),
- Transportation Research Board (TRB), and
- Michigan Department of Transportation (MDOT).

2.2 Overview of Prestressed Concrete

Prestressed concrete, a product of the twentieth century, announced a significant new direction in structural engineering. The idea of prestressing opened up new possibilities for form. Freyssinet outlined the "conditions for the practical use of prestressing" and had established the need for high strength steel, tensioning it to a high initial stress, and high strength concrete to reduce the loss of initial prestress to a minimum (Billington, 1976).

The first design guide for prestressed concrete was in the form of a recommended practice, rather than a building code. In the United States, the "ACI-ASCE Joint Committee Recommendations for the Design of Prestressed Members" published in 1958, included the state of art knowledge, which had developed with the limited use of prestressed concrete by the mid-1950's.

The Prestressed Concrete Institute, founded in 1954, published the first U.S. Building Code for prestressed concrete in 1961. At that time, the American Concrete Institute (ACI) Building Code Requirements for Reinforced Concrete (ACI, 1956) contained no reference to prestressed concrete, but the inclusion of new material on this subject was being considered for the next revision.

In 1963, the ACI Building Code Requirements for Reinforced Concrete (ACI, 1963) included a chapter covering prestressed concrete, much of which was carried forward into the 1971 revision of the ACI Building Code Requirements for Reinforced Concrete (ACI, 1971). Since 1971, annual revisions have been made. A similar evolution occurred with the AASHTO "Standard Specification for Highway Bridges" (AASHTO, 1996). The provisions for prestressed concrete in the current AASHTO Standard Specification for Highway Bridges are very similar to those of the ACI Code. Some differences are the allowable stress values and load factors that have been traditionally more conservative for bridges than buildings (Lin and Burns, 1981).

Representatives of the Federal Highway Administration (FHWA, formerly the Bureau of Public Roads), AASHTO, and the Prestressed Concrete Institute (PCI) developed a series of standard AASHTO-PCI sections for bridge beams to reduce the cost of design. Standard beam Types I through IV were developed in the late 1950's, and Types V and VI in the early 1960's. Additional modifications were made in the 1980's to further optimize sections (Rabbat and Russell, 1982). The current AASHTO shapes include these modifications (Rabbat and Russell, 1982).

2.3 Durability and Deterioration

There has been great concern about durability, especially in materials for structures that are subjected to harsh environments. Durability is the ability of concrete to resist weathering action, chemical attack, abrasion and other service conditions (ACI, 1990). Considerable emphasis is still given to high quality concrete as the first line of defense against corrosion. The heightened awareness of the importance of durability is evidenced by the ACI Building Code Requirements

for Reinforced Concrete (ACI, 1989) that featured a new chapter devoted to the issue of durability.

The ACI 318-89 Code mandated the latest Post Tensioning Institute (PTI) standards for improved corrosion protection of unbonded tendons. Unbonded tendons used in corrosive environments must be completely encapsulated and be further protected with high quality greases. With an extra layer of protection provided by sheathing, post-tensioned structures are more corrosion resistant than pre-tensioned construction (Whiting et al, 1998). Because beam end deterioration has been observed, it suggests that prestressed concrete I-beams lack durability. This statement is only partially true, as prestressed concrete I-beams are subjected to diverse set of environmental and loading conditions.

Environmental conditions are not the only constituent behind the potential deterioration of a member. Concrete, prestressing steel type, and the environment affect whether or not a reinforcing steel will be susceptible to corrosion (Whiting et al, 1993). Concrete needs to have a water/cement ratio less than 0.45 and be free of chloride admixtures. Segregation of the concrete may occur at the bottom of cast members and the resulting concrete may lack acceptable durability (Emmons, 1994). In another example, concrete cover over top of slab reinforcement needs to be greater than 2-inches, per AASHTO, when exposed to deicers (AASHTO, 1996). AASHTO specifies that additional cover beyond the minimum 1.5-inches should be provided for prestressed beams when the contact of deicing agents is unavoidable.

Prestressing steel needs to be from cold-drawn wires; quenched and tempered wires are hard and brittle (Whiting et al, 1993). Whiting et al note that quenched and tempered wires are not approved for use in the United States.

What types of environmental conditions must prestressed concrete I-beams resist? In Michigan, the most common conditions that require concrete durability are thermal cycles, freeze-thaw cycles, exposure to acidic gasses (carbon dioxide), and exposure to deicing solutions. Other states may experience similar conditions (Enright and Frangopol, 2000). However, different aggressive conditions will not be discussed (alkali-silica reaction, delayed ettringite formation, etc.) in detail for this report. It is suggested that concrete deterioration can be categorized as dismemberment, dissolution, or erosion (Emmons, 1994). Forms of concrete distress can vary widely but are mainly dismemberment related for prestressed concrete I-beam end deterioration. This can include cracking, spalling, delaminations, and minor surface damage (Xanthakos, 1996).

2.3.1 Thermal Distortion

Nearly all Michigan bridges are situated in a location that allows fascia beams to be exposed to un-even (diurnal) solar heating. Like all materials, concrete expands when heated and shrinks when cooled. Having a temperature differential on an element such as a prestressed concrete I-beam would cause expansion on the outward-facing side and induce weak-axis bending stresses. Fixity of the top flange may cause an out-of-plumb condition for the beam web and induce additional stress into the member. A partially fixed beam end, such as one created by a frozen bearing may impose additional stress at the beam end. When stress build-up is relieved, tension cracks, shear cracks, or buckling may result (Emmons, 1994).

The coefficient of thermal expansion of the concrete and freedom from restraint affect the amount of thermal distortion related distress. To date, no information is available that suggests thermal distortion causes prestressed concrete I-beam end distress.

2.3.2 Freeze-thaw Deterioration

Without entrained air, the cement matrix surrounding the aggregate particles may fail when it becomes critically saturated and frozen (ACI, 1992). Freeze-thaw deterioration is a function of porosity, moisture saturation, number of freeze-thaw cycles, air entrainment, member surface, and aggregate quality (Emmons, 1994). An important fact to consider regarding freeze-thaw damage is that concrete that is dry or contains only a small amount of moisture is essentially not affected by even a large number of cycles of freezing and thawing (Kosmatka and Panarese, 1988). Evidence of freeze-thaw deterioration is usually in the form of small surface disintegration (Emmons, 1994). Freeze thaw damage is resisted by proper structure design to minimize exposure, low water-cement ratio (*w/c*), appropriate air entrainment, quality materials, adequate curing, and special attention to construction practices (ACI, 1992).

Observations by other researchers indicate that freeze-thaw damage is not presently occurring in Michigan's prestressed concrete I-beam ends (Ahlborn et al, 2001). Past practices have apparently adequately resisted this form of deterioration.

2.3.3 Corrosion-induced Deterioration

Corrosion of reinforcing steel is the single most destructive deterioration mechanism for reinforced concrete bridges in the United States (Weyers et al, 1993). An improved understanding of the influence of corrosion damage upon structural performance would assist owners and operators of structures to plan strategic, cost-effective remedial treatment (Cairns and Millard, 1999). Based on the observations of on-going research, damage to prestressed concrete I-beam ends is largely attributed to corrosion-related damage (Ahlborn et al, 2001). Corrosion can be generally defined as the deterioration of a substance or its properties because of a reaction with its environment (NACE, 1970). Numerous references were reviewed to gain an understanding of how steel reinforcement corrodes in concrete.

2.3.3.1 *Background*

In 1960, NCHRP Report No. 90 stated that corrosion of prestressing in concrete was not and would not be a problem if certain precautions were considered (Moore et al, 1970). These precautions include cover thickness in conformance with AASHTO specifications and protection of prestressing steel during shipment and storage. Issues being addressed by this project clearly indicate that some past practices (e.g. design, construction, and maintenance) have been insufficient and ineffective. Corrosion of metals in concrete has been studied for many years, both in the field and in the laboratory. Whiting et al collaborated and discussed several programs that intended to simulate corrosion of stressed reinforcement in the laboratory by immersion in a solution (Whiting et al, 1993). Researchers have also performed laboratory testing of prestressing steel in concrete to more closely simulate in-situ conditions (Moore et al, 1970). The Moore study also looked at two bridges, 2 and 11 years old. For these relatively young bridges, it was shown that the cement paste around the wires in the prestressing strands was providing corrosion protection.

Corrosion of steel reinforcement in concrete is commonly known to be an electrochemical process, rather than chemical or physical (NACE, 1970). One of two environments must exist for corrosion to occur, either aqueous or in air (Heldt, 2001). For electrochemical corrosion to occur, a cathode and an anode are required along with an electrical conductor and an aqueous medium (ACI, 1996). Any metal surface on which corrosion is taking place is a composite of anodes and cathodes electrically connected through the body of the material itself. Concrete provides the aqueous environment, containing water with dissolved oxygen (ACI, 1996). Figure 2-1 shows the basic corrosion cell than can occur in a section of prestressed concrete (Emmons, 1994).

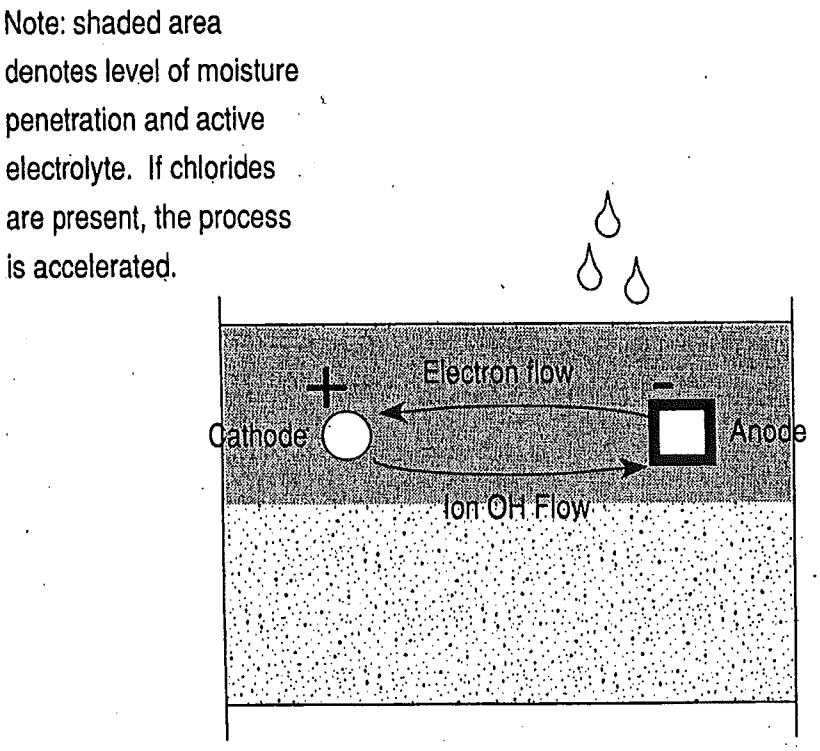

Figure 2-1. Basic Corrosion Cell Between Two Metals in Concrete (Emmons, 1994)

The presence of oxygen is essential for corrosion to occur. Oxygen is introduced into concrete most quickly through several wetting and drying processes. It has been shown that steel within concrete in a continuously wet environment has a slow rate of corrosion, even if the environment is seawater. For oxygen to be consumed in the cathodic half-cell reaction, it must be in an aqueous state. ACI 222R-96 shows that corrosion rate, discussed in later sections of this report, is paralleled with the oxygen concentration (ACI, 1996).

The inherently high pH of concrete is able to sustain a passive hydrated oxide film on the steel reinforcement. The film is actually a corrosion product that acts as a barrier to the anodic dissolution reaction (Jones, 1992). The composition of this thin and invisible film has been difficult to determine, however it is believed to be composed of chemical compounds of oxygen. The presence of the film is able to resist current flow at low voltages (driving forces). Current will flow at higher voltages on steel that has an adhered passive film due to the electrolysis of water (ACI, 1996).

Two types of corrosion are generally recognized in prestressed concrete: stress corrosion and pitting corrosion (Whiting et al, 1993; Leonhardt, 1964). Pitting corrosion is a localized form of galvanic corrosion (Novokshchenov, 1989). Pitting corrosion is most prevalent in reinforced concrete and prestressed concrete structures. Concrete carbonation and chloride ion penetration are the two primary causes of pitting corrosion. The presence of sufficient chloride ion with water, oxygen, and a corrodible metal leads to pitting corrosion. Carbonation reduces the alkalinity in the concrete and may lead to hydrogen embrittlement type of stress corrosion (Whiting et al, 1993). Stress corrosion cracking of chloride-laden concrete is unlikely to occur (Moore et al, 1970). Research by Legat et al showed that corrosion is mainly due to high concentration of chlorides and in a few cases the carbonization of concrete (Legat et al, 1996).

Different types of cements and pozzolans affect the pH of concrete. For example, blended cements may reduce alkalinity but increase electrical resistivity and decrease permeability. Aggregates have been shown to have little effect on corrosion of steel in concrete. However, exceptions are noted for porous aggregates or those aggregates previously exposed to seawater (ACI, 1996).

Dry, unsaturated concrete is more electrically resistive than wet concrete (ACI, 1996). Even in the presence of moisture, oxygen, and chloride ions (discussed in later sections of this report), corrosion damage can be prevented with highly resistive concrete (ACI, 1996). High quality concrete (low *w/c*, low permeability, certain admixtures) will also limit the ingress of moisture, oxygen, and chlorides. Concrete cover and degree of carbonation also affect the rate of corrosion (Tilly, 1987; ACI, 1996).

Epoxy coated strands showed excellent corrosion resistance performance in the laboratory in a study conducted by Perenchio et al (Perenchio et al, 1988; Whiting et al, 1993).

An electrochemical corrosion reaction can be separated into two component reactions called half-cell reactions. In the corrosion of steel reinforcement, iron is oxidized into ferrous ions at the anode, which in turn forms into ferrous oxide through several reactions (ACI, 1996). A second half-cell forms at the cathode, involving oxygen, water, and a free electron from the anodic reaction, generating a hydroxyl ion (ACI, 1996). Ferrous oxide precipitates on the surface of the reinforcing steel at the anode and occupies a volume several times greater than of the atomic / ionic iron consumed in the reaction (Kosmatka et al, 2001).

The anodic half-cell reaction has a standard redox potential (SRP, also known as standard electrode potential) of E=-0.440 mV. The SRP of the cathodic reaction is E=+0.401. SRP's are considered to be reversible potentials, in reference to a hydrogen half-cell having zero potential (ACI, 1996).

The SRP differs from corrosion potential (also known as rest potential or open circuit potential). The corrosion potential is related to the temperature, composition of the aqueous medium, and polarizations of the half-cells (ACI, 1996). It is the difference in magnitude of the two half-cell reactions (or SRPs) that determines the driving force of an electrochemical corrosion reaction.

Corrosion rate in concrete is typically influenced by environmental and other factors and controlled by one of two mechanisms. These mechanisms are the rate of oxygen diffusion through concrete and electrical resistance within the concrete (ACI, 1996). Both factors will affect the electrochemical corrosion reactions that produce or consume electrons (Jones, 1992). The rate of electron flow (current) is therefore a measure of the reaction rate. From manipulation

of Faraday's Law, it can be shown that corrosion current density is proportional to the mass loss per unit time (Jones, 1992).

As previously mentioned, every half-cell reaction is reversible. The current density and potential at which a half cell reaction occurs in known as the exchange current density and half cell electrode potential, respectively (Jones, 1992). For an anodic (oxidation) half cell electrochemical reaction to occur, there must be a positive shift in the current density and potential from the equilibrium state. A cathodic (reduction) reaction will occur when a negative potential and positive current density is applied to the equilibrium state.

Deviation of half-cell electrode potential from the equilibrium state is known as polarization. Two kinds of polarization can occur simultaneously and are known as activation and concentration polarization (Jones, 1992). Concentration polarization occurs when the level of ions from the cathodic reaction are depleted more aggressively at the surface of the corroding metal, thus governing the rate of the reaction. Activation polarization occurs when one step in the electrochemical corrosion reaction controls the rate or charge flow.

2.3.3.2 *Carbonation-induced corrosion deterioration*

Carbonation of concrete is a reaction between acidic gases in the atmosphere or dissolved in water and the products of cement hydration (Emmons, 1994; ACI, 1992). This reaction produces carbonates ($CaCO_3$) and is accompanied by shrinkage. Concrete carbonation is a function of humidity, concrete permeability, and the concentration of carbon dioxide.

Carbonated concrete has properties that can be considered both beneficial and detrimental to concrete performance. Favorable effects of carbonation can be found in increased strength, hardness, and dimensional stability. Adverse effects of carbonation can be a porous and less wear resistant surface. Probably the most detrimental effect is a reduction in the concrete alkalinity, from a pH of around 13 to a pH of around 10 (ACI, 1992). When the pH of the concrete approaches 10, the passivity of steel is destroyed and more rapid corrosion may occur (Emmons, 1994).

Whiting et al, used petrography to determine the depth of carbonation in several prestressed concrete bridges in the Midwest (Whiting et al, 1993). At the time of the study, the Midwest bridges ranged in age from 31 to 36 years old. The depth of carbonation was generally on the order of 0.1 to 0.4 inches, with the exception of one bridge that had 0.6 to 1.3-inches of carbonated concrete. Cover to prestressing steel was greater than 1.5-inches for the same bridges. It is estimated that an upper limit for carbonation in concrete is 0.04-inches per year (Emmons, 1994).

It is uncertain whether or not Michigan's prestressed concrete I-beam ends are affected by carbonation-induced deterioration. Refer to the cited references for additional information on the mechanisms by which carbonation-induced corrosion damage occurs and is resisted.

2.3.3.3 *Deicer-induced corrosion deterioration*

Chloride ions have a well-documented detrimental role in reinforced concrete. Chloride ions are considered to be the major cause of premature corrosion of steel reinforcement (ACI, 1996). Even sound concrete is not immune from chloride ion penetration (ACI, 1996). Several theories exist as to the exact mechanism by which chloride ions affect corrosion. Two theories consider the chloride ion to be essentially a catalyst in the electrochemical corrosion reaction. Another

theory states that chloride ions disrupt the performance of the passive oxide film on the reinforcement, in turn promoting corrosion (ACI, 1996). Other researchers (Whiting et al, 1993; Needham and Juntunen, 1997) have indicated that concrete alkalinity may be lowered when chloride concentration is increased to a certain level. However, steel corrosion may occur even in highly alkaline concrete if enough chlorides are present with water and oxygen (Emmons, 1994).

The amount of chloride ions in the concrete is typically expressed as a percentage of the weight of cement (ACI, 1992). The concentration of chlorides necessary to initiate corrosion varies greatly depending upon the pH of the concrete (Emmons, 1994). The amount of chloride ion required to accelerate corrosion (threshold) is 0.2 percent weight of cement, as determined by water-soluble testing techniques. Chlorides may be acid-soluble (naturally occurring aggregates) or water-soluble (admixtures) in form (Emmons, 1994). Water-soluble chlorides are of greatest concern to concrete durability since they "readily become free to attack surrounding reinforcing steel" (Emmons, 1994). As such, design Codes and many references suggest limiting the amount of water-soluble chloride ion to 0.06 percent weight of cement (ACI, 1999; ACI, 1996; Emmons, 1994).

A potential advantage of prestressing steel over reinforcing steel may be a higher resistance to chloride ion attack. A study (Rengaswamy and Rajagopalan, 1977) cited by Whiting et al (1993) indicated that 2 to 3 times the amount of chloride ion was required to initiate corrosion in prestressing steel, compared to mild reinforcement. Interestingly, design codes such as ACI 318-99 limit the maximum chloride ion content of concrete mixes more severely in prestressed concrete than in conventionally reinforced concrete (Whiting et al, 1993).

From a study conducted by Needham and Juntunen (1997), it was found that the bridge inspection superstructure rating and chloride ion content did not relate to beam end conditions, such as deterioration and water staining, for the prestressed concrete I-beam bridges studied. Other researchers have drawn opposite conclusions regarding the level of chloride ions and deterioration. Novokshchenov found elevated levels of chloride ion in prestressed concrete I-beams at deck joints where the greatest corrosion-related deterioration took place (Novokshchenov, 1989). In Michigan, Needham and Juntunen found that the chloride ion content was related to average daily traffic (Needham and Juntunen, 1997).

The origin of deicer agents onto prestressed concrete I-beam ends is fairly well understood. Numerous authors have recognized that the majority of prestressed concrete I-beam end distress occurs at transverse bridge deck joints (Tilly, 1987; Novokshchenov, 1989; Whiting et al, 1998; Jadun, 1990; Needham, 1999; Enright and Frangopol, 2000). The actions of traffic and environment degrade joints and lead to beam-end deterioration (Whiting et al, 1998). When the deck joint is not watertight, leakage of deicing solutions onto the beam end is permitted.

Tilly cites few overall problems with prestressed concrete bridges, but notes that the damage caused by leaking transverse deck joints was, even in 1987, a significant problem in the United States (Tilly, 1987).

Work by Novokshchenov in FHWA-RD-88-269 "Salt Penetration and Corrosion in Prestressed Concrete Members", cited by Whiting et al (1993), also showed that deck joints were the cause of corrosion-related deterioration in prestressed concrete I-beam ends (Novokshchenov, 1989). Novokshchenov cited several attributes of a failed joint, including deteriorated sealer, lack of

sealer, and cracking of concrete at the joint. Novokshchenov also cited insufficient concrete cover as causing pre-mature corrosion failure.

Whiting et al evaluated 12 prestressed concrete bridges in various environments to document causes of corrosion and deterioration (Whiting et al, 1993). Whiting et al had similar conclusions to Novokshchenov in that the deicer solution passing through deck joints was the cause of the deterioration. However, another pathway for deicers was from deteriorated drains or gaps in the bridge railings (Whiting et al, 1993).

MDOT sought to determine chloride ion content in a select group of prestressed concrete bridges and perform an inspection of a portion of the prestressed concrete bridges around the state of Michigan (Jadun, 1990; Whtiting et al, 1993). Of the 12 bridges selected, it was reported that any deterioration on the beams was minor. Beam end deterioration was noted in I-beams and box beams in the study, and the distress was attributed to leaking deck joints. The study also showed that vehicular traffic underneath a prestressed concrete bridge increased the chloride ion contents of the beams, I-beams had higher chloride ion contents than box beams, and that box beams were in worse condition (Jadun, 1990; Whiting et al, 1993).

One research program was identified that sought to replicate leaking deck joints in a laboratory setting by periodically wetting I-beam ends with a 15% NaCl solution (Whiting et al, 1998). I-beams tested for the project were AASHTO Type II, cast specifically for the research project. Mix proportions for the laboratory beams included a *w/c* of 0.39 and an air content of 5.0% to 7.5% (Whiting et al, 1998). The beam end wetting approach did not produce distress for the eight months the equipment was operational. Further testing of the beam end specimens was consequently abandoned by Whiting (Whiting et al, 1998).

Enright and Frangopol studied prestressed concrete bridges in the Midwest and Colorado (Enright and Frangopol, 2000). They also concluded that the most common location of prestressed concrete I-beam distress was at the transverse deck joints. Further, this damage was corrosion related and due to chloride ion ingress (Enright and Frangopol, 2000).

2.3.4 Other Forms of Deterioration

Review of literature and conversations with state engineers have identified impact damage, alkali-silica reaction (ASR), and delayed ettringite formation (DEF) as some other forms of distress that may or have been documented for prestressed concrete I-beams. These distresses either do not appear to be common in Michigan (ASR and DEF), or routinely occur at locations beyond the beam end (impact damage).

2.4 Tools for Identifying Prestressed Concrete I-Beam End Deterioration

In the following subsections of this report, distinction is made between "current" and "new" approaches. The rationale for assigning a category to each technique is whether or not the approach is being used by Michigan or other states, as indicated from a multi-state survey (see Chapter 5).

2.4.1 Inspection / Assessment Techniques

From the suggestion of other researchers (Shanafelt and Horn, 1980) and for the purposes of this report, the term *inspection* is used to refer to the physical act of obtaining data on the condition of a structural element. *Assessment* is defined as the process of reviewing or making an interpretation of (inspection) data/conditions, structural analysis, and other decision-making processes. Although Shanafelt and Horn's work dealt with practices related to accidental (vehicular) damage of prestressed concrete bridge beams, this approach could be applied to assessment of beam end deterioration.

Both assessment and inspection practices are discussed in this section. As an example, the Michigan Pontis Bridge Inspection Manual has defined pre-determined assessment criteria for an inspector to follow for assigning a condition state and potential feasible actions (MDOT, 1999). In contrast, the Michigan Structure Inventory and Appraisal Coding Guide, used for National Bridge Inspection Standards (NBIS) inspections, allows for greater latitude in assigning condition ratings to a structural element (MDOT, 1997b). In this case, assessment is left to the judgment of the bridge inspector.

2.4.1.1 *Current Approaches*

Responses from a survey of state bridge engineers, discussed in Chapter 5, have indicated that all responding states use the *FHWA Bridge Inspectors Training Manual 90* (Manual 90) as a reference guide for the inspection and assessment of prestressed concrete I-beam bridges (Hartle et al, 1995). This document is the current standard for inspecting bridges and generally covers bridge mechanics, materials, and inspection practices. Guidelines are established to aid the bridge inspector in defined tasks. Of particular interest to this project are the suggested means and methods to inspect the ends of prestressed concrete I-beams.

The tools for cleaning, inspection, visual aid, measuring, and documentation that many states use for inspecting prestressed concrete I-beams are covered in Manual 90. Included in this list are chipping hammers, mirrors, and optical crack gauges. Conventional non-destructive evaluation equipment (pachometers, ultrasonic thickness gauge, etc.) is not part of the bridge inspector's equipment (Hartle et al, 1995).

Shanafelt and Horn identified similar tools that aid in the inspection of damaged prestressed concrete beams (Shanafelt and Horn, 1980) including a magnifying glass, flashlight, camera, and mirror. In addition to physical tools used by an inspector, good eyesight and a critical mind are essential personal qualities.

Photography, one of the technologies included in Manual 90, has benefited from advances in recent technology. The Tennessee Department of Transportation (TDOT) Bridge Inspection and Repair Office conducted an evaluation of the feasibility of using digital cameras to replace conventional cameras (FHWA, 1991). Digital cameras are greatly enhancing the usefulness of bridge inspections, since state-of-the-art computer programs allow engineers in the office quickly view the conditions of a bridge at the time the last inspection was performed.

Manual 90 provides inspection procedures for prestressed concrete I-beams (Hartle et al, 1995). Included in these procedures are specific instructions to "Examine the areas near the bearings and the cast-in-place end diaphragms for spalling concrete." among other detailed documentation requirements (Hartle et al, 1995).

The following is an except from the Manual's basic concrete inspection section:

When inspecting concrete structures, note all visible cracks, recording their type, width, length, and location. Any rust or efflorescence stains should also be recorded. Concrete scaling can occur on any exposed face of the concrete surface, and its area, location, depth, and general characteristics should be recorded. Inspect concrete surfaces for delamination or hollow zones, which are areas of incipient spalling, using a hammer or a chain drag. Delamination should be carefully documented using sketches showing the location and pertinent dimensions.

Unlike delamination, spalling is readily visible. Spalling should also be documented using sketches, noting the depth of the spalling, the presence of exposed reinforcing steel, and any deterioration or section loss that may be present on the exposed bars.

There are many common defects that occur on concrete bridges: cracking, scaling, delamination, spalling chloride contamination, honeycombs, pop-outs, wear, collision damage, abrasion, overload damage, reinforcing steel corrosion, prestressed concrete deterioration.

Each of these distresses is defined in the Manual. Cracks can be classified as hairline, medium, or wide cracks. On prestressed structures, all cracks are significant. When reporting cracks, the length, width, location, and orientation (horizontal, vertical, or diagonal) should be noted. The presence of rust stains or efflorescence or evidence of differential movement on either side of the crack should be indicated.

The manual has an eight-step inspection procedure for prestressed concrete I-beam bridge structures:

- *Examine the areas near the bearings and the cast-in-place end diaphragms for spalling concrete.*
- *Inspect the fixed diaphragms for diagonal cracking. This is a possible sign of shear failure caused by structure movement.*
- *Investigate the intermediate diaphragms for cracking and spalling concrete.*
- *Check beam flange surfaces for longitudinal cracks. This may indicate a deficiency of prestressing steel.*
- *Inspect the tension and shear zones of the beams for structural cracks. Any crack should be carefully measured with an optical crack gauge and documented.*
- *Examine underneath the beams for alignment and camber of the prestressed beams. Signs of deflection usually indicate loss of prestress.*
- *Investigate the beams for any collision damage. This is a major cause of damage to prestressed I-beams.*
- *Examine thoroughly any repairs that have been made previously. Determine if the repaired areas are functioning properly. Effective repairs and patching are usually limited to protection of exposed tendons and reinforcement.*

In terms of assessment, Manual 90 requires that inspectors rate bridge elements, including prestressed concrete I-beams, as a whole, rather than allowing individual locations of distress to lower an element's rating. However, inspectors are expected to modify the condition rating accordingly if an isolated distress (possibly beam end deterioration) influences the load carrying capacity or serviceability of the element (Hartle et al, 1995). The condition rating for a

superstructure element, such as a prestressed concrete I-beam, is based on a scale of 0 to 9, in Manual 90. Manual 90 does not have a uniform damage severity classification for various concrete distresses. Shanafelt and Horn suggest ranking damage assessment into four categories: minor, moderate, severe, and critical (Shanafelt and Horn, 1980).

One recent study revealed significant variability from state to state on assigned condition ratings and field notes. In 1998 the FHWA's Nondestructive Evaluation Validation Center undertook a study to evaluate visual inspection of bridges (Graybeal et al, 2001). The Center performed a series of inspection trials among 49 state departments of transportation bridge inspectors. The bridges used in this study were located in northern Virginia and central Pennsylvania. "The primary data used to evaluate the routine inspections were the National Bridge Inspection Standards Condition Ratings assigned by the inspectors to the primary bridge components (deck, superstructure, and substructure)." In depth inspections were rated on the inspector's field notes. The study showed a significant variability from state to state on assigned condition ratings and field notes. The Center's recommendations were to revise the condition rating system to increase accuracy and reliability, increase the training of inspectors with respect to methods that identify reoccurring defects, and study the types and sizes of specific defects that will be found in an in-depth inspection.

Other studies have been performed to determine current policies and practices that may affect the accuracy and reliability of visual inspection (Rolander et al, 2001). A survey of state departments of transportation, a local-level department of transportation, and selected bridge inspection contractors showed how inspection management might influence the reliability of inspections (Rolander et al, 2001).

Effects of the deterioration should be understood through engineering assessments (Shanafelt and Horn, 1980). For accidental impact damage of prestressed concrete bridge beams, Shanafelt and Horn do not recommend field assessment of damage, due to the potential for making premature assessments. More innovative repair techniques appear to be generated by having repair assessments be office-based, away from the field process. However, ideas and alternatives for repair are suggested from the field inspector. Shanafelt and Horn concluded that complex engineering calculations were not required to develop in-place repairs, but that a basic level of calculations should be performed to verify restoration of strength and durability. Procedures for performing a capacity analysis of a prestressed concrete beam, considering compromised prestressing strands, have been developed by Xanthakos (1996).

Shanafelt and Horn provide recommendations for assessment of exposed, damaged, and severed strands. Nearly all states allow beams with one to three severed strands to remain in service (Shanafelt and Horn, 1980). Location of a damaged beam within a structure should be given consideration in the assessment stage. For example, fascia beams may not be loaded to the same levels as internal beams and therefore a greater amount of deterioration may be permitted (Shanafelt and Horn, 1985).

2.4.1.2 *New Approaches*

A manual of recommended practice for the inspection, assessment, and repair of deteriorated prestressed concrete bridge beams has been developed within NCRHP Report 280 (Shanafelt and Horn, 1985). These practices can be applied to deteriorated ends of prestressed concrete beams with engineering judgment (Ahlborn et al, 2001).

A rivet gun chipper is a tool that may be used by inspectors to evaluate the quality of concrete around a prestressing strand (Shanafelt and Horn, 1985). Deflection and elastic shortening techniques have been used in the past to estimate tension in exposed prestressing strands.

To evaluate box beams for a New York State DOT project, engineers used techniques consisting of visual examination, counting broken / deteriorated / corroded strands, and measuring remaining concrete section (Hag-Elsafi and Alampalli, 2000).

In addition to a visual inspection, Whiting et al, (1993) used a variety of survey techniques for a research project involving the inspection of prestressed concrete bridges. These techniques included half-cell potential measurements, delamination survey, cover measurements, corrosion rate measurements, petrographic analysis, chloride sampling and analysis, and penetrating sealer effectiveness. Techniques showing results fairly consistent with prestressed concrete I-beam end deterioration included half-cell potential measurements, corrosion rate measurements, and chloride sampling. The deicer-environment bridges reviewed by Whiting et al generally had deterioration consisting of cracked and spalled concrete with exposed corroding strand and stirrups.

Similar techniques were chosen by Arner and Panganiban (1986) and Kennedy (1991) for the investigation of deteriorating bridge decks. These techniques included half-cell potential testing, cover measurements, and chloride ion content testing. Arner and Panganiban suggested that delaminations could affect half-cell potential testing by creating an insulating plane in the concrete.

The result of a study conducted on the condition of prestressed concrete bridge elements located in corrosive environments is presented by Novokshchenov (Novokshchenov, 1989). Five bridges were subjected to a detailed inspection and other bridges in the study received a visual inspection. The bridges selected were in northern areas (subjected to deicing salts) and in southern areas (subjected to marine spray). Descriptions, visual examination results, corrosion amounts, concentration of chlorides, metallurgical analyses, and metallographic examination results are given with pictures and tables for each bridge surveyed. Recommendations about procedures, parameters and threshold values for detection of corrosive environments and assessment of the condition of prestressing steel in bridge components are also included in the Novokshchenov study.

Monterio et al (Monterio et al, 1998) studied a nondestructive method using a multi-electrode electrical resistivity array to determine the position of the reinforcing bars and their corrosion state. This work was performed by measuring the frequency dependence of the complex impedance of the bars along the surface of the concrete structure. By using this method, the background resistivity of the concrete can also be obtained. The method uses the direct relation between the complex impedance and the corrosion rate of the reinforcing bars to provide a rapid evaluation of the corrosion rate. Two advantages of the technique are that the measurements are taken on the surface of the concrete and that the method does not require removal of the concrete to connect the device to the bars. An experiment was conducted to test and determine the efficiency of the method. Four types of bars were used in the research which included a clean bar, a bar covered with gold, a painted bar, and a corroded bar. Apparatus, measurement technique, instrumentation, and the results of the experiment are presented in the paper. Similar research on the same content is conducted by Zhang et al. (Zhang et. al., 2001). As a conclusion

in this study, the Surface Measurement Method is agreed to be an accurate method to investigate different corrosion states of the reinforcement.

New tools are available not only for the inspection of original bridge elements, but also for monitoring the performance of these repairs. Halstead et al (2000) used strain gauges to monitor potential cross sectional growth of strengthened columns due to the corrosion of reinforcing steel (expansive process). In the study, linear polarization probes were also included in the instrumentation package to measure corrosion rate of internal reinforcement.

Broomfield, et al (1999) studied corrosion monitoring using half-cell potential measurement, linear polarization and macro-cell current measurement methods. Linear polarization, concrete resistivity and other probes have been installed in new structures to monitor durability as well as in existing structures to evaluate rehabilitation strategies such as corrosion inhibitor applications and patch repairs. The types of sensors used, data collection techniques, results and interpretation are discussed.

Data obtained from nondestructive evaluation (NDE) of structures can greatly enhance the maintenance and management of infrastructure systems (Nogueira, 1999). Nogueira has proposed a methodology for a systematic application of NDE methods in periodical bridge inspection.

Pascale, et al (1999) described an experimental program aimed to assess the performance of fiber optic sensors (FOS) in civil engineering applications. This technique has been applied to a reinforced concrete bridge beam externally reinforced by fiber reinforced polymer (FRP) sheets. The paper includes the information about FOS, the experimental program, and a discussion for the results.

NDE for corrosion detection of embedded or encased steel reinforcement or bridge cables using time domain reflectometry is developed and demonstrated by Liu, et al (2001). Modeling, procedures, and a case study are presented.

In the paper presented by Titman (1999), wide ranges of applications of infrared thermography are explored, particularly relating to structural investigation situations. Some guidance is given on optimum timing, conditions, and viewing locations for the various situations are also described.

Settipani (1987) has shown that gammagraphy can be used to determine strand location, size, corrosion, and concrete defects. This technique has shown to be effective on elements 27-inches and less in thickness. According to Settipani, gammagraphy has a high initial cost compared to other non-destructive evaluation methods, but it provides more comprehensive data and a permanent inspection record.

Innovative ways to detect concrete delaminations have emerged in recent years. Henderson et al (2000) reported that an instrument named HollowDeck is an alternate approach to acoustic impact surveys. The technology used involves frequency analysis of sound waves to identify areas of concrete delamination.

Ganji et al (2000) and Gucunski et al (2000) have performed similar testing using a portable seismic pavement analyzer (PSPA). With the PSPA, Ganji et al were able to detect delaminations not found by chain dragging on bridge decks. Gucunski et al were able to place delaminations into four severity levels by interpretation of surface waves.

Due to the size of the PSPA and the time it takes to complete a single test (Gucunski et al, 2000), the PSPA appears to show little promise for use in prestressed concrete I-beam end inspection. HollowDeck technology appears to be similarly inappropriate for beam end inspection. However, non-destructive testing equipment like the HollowDeck and PSPA could be used as calibration and training tools for inspectors performing acoustic impact (delamination) surveys.

A useful tool in performing assessments of beam-end deterioration is the understanding of how distresses may have formed. Juntunen prepared an interim report containing a collection of photographs related to cracking of prestressed concrete I-beams (Juntunen, 2000). From review of this report, a summary of crack location, type, and potential cause has been prepared. This information is presented in Table 2-1.

Table 2-1. Prestressed Concrete Crack Type and Probable Cause

Location	Crack Type	Potential Cause (per Juntunen, 2000)							
		Loss of Bond	Pre-stressing Cut	Load Hit	Diaph. Bond	Strand Slip	Over-load	Insuff. Reinf.	Reinf. Corr'n
End of Member	Horizontal		✓		✓				
	Diagonal		✓	✓			✓	✓	
	Frown		✓						
	Vertical								✓
	Map							✓	
Remainder of Span	Longitudinal Flange	✓							
	Diagonal			✓		✓			
	Map							✓	

2.4.2 Preventive Maintenance Techniques

The efforts described in the literature review and current infrastructure management practices recognize that preventive maintenance is essential in extending the service life of many structures. Prestressed concrete I-beam bridges are no exception as evidenced by end deterioration problems. For the purpose of this report, preventive maintenance of prestressed concrete I-beams is distinguished from repair techniques by the fact that preventive maintenance can be applied to bridges where there is an existing sound substrate. If reconstruction of the substrate is or is part of the requirements for a given technique, then the technique shall be considered a repair technique. Repair techniques are discussed in later sections of this chapter.

2.4.2.1 *Current Approaches*

Preventive maintenance suggestions for existing concrete structures can be separated into four categories according to ACI (ACI, 1996). These categories are insulating methods, environment modifying methods, electron control methods, and a combination of two or more methods. Research performed for this project has suggested that perhaps another category exists: structure modification methods. A summary of all of the preventive maintenance or repair approaches discussed in this chapter, separated per category, is included in Appendix J of this report. All are discussed further in this section.

2.4.2.1.1 Surface Insulating Methods

Insulating methods should be considered as a preventive maintenance option when the parent concrete has been properly prepared (Weyers et al, 1993; ACI, 1996). The objectives of the covering should be to prevent contaminant, moisture, and oxygen intrusion into the concrete. This may include removal of chloride-contaminated concrete and arrest of the corrosion process prior to surface application. To not remove chloride-contaminated concrete prior to the application of an insulating method may accelerate corrosion (ACI, 1996).

PCA publication IS001 identifies 17 protective treatments (coatings and sealers) for use on concrete exposed to chlorides (PCA, 2001). Penetrating sealers in this list included certain formulations of:

- Drying Oils,
- Silanes, and
- Siloxanes

Linseed-oil surface sealers may be safely used on a prestressed concrete member (Weyers et al, 1993). Silanes and siloxanes are inexpensive, easy to apply, and allow the passage of water vapor while resisting a head of water. Silanes have shown better penetration into dried concrete than siloxanes and surfaces can easily be retreated for improved penetration (PCA, 2001). These sealers should not, however, be applied to concrete elements with active corrosion or excessive chloride ion contamination (Whiting, 1999), and silanes may not be an optimum solution when prolonged exposure to freezing and deicing chemicals is expected (PCA, 2001).

Researchers and consultants have also suggested the use of silanes and siloxanes in preventive maintenance (Tilly, 1987; Weyers et al, 1993; Emmons, 1994; Whiting et al, 1998). At least 17 different nationwide manufacturers of drying oils, silanes, and siloxanes exist (PCA, 2001). In addition, drying oils, such as boiled linseed oil, are commercially available.

Sealers are judged by many performance characteristics including water repellency, chloride screening, penetration depth, vapor permeability, alkaline resistance, and UV resistance (Weyers et, al, 1993). Coatings are compared with respect to their chloride screening, vapor permeability, and shrinkage properties. The surface of the substrate must be free of contaminants through surface preparation and cleaning methods to successfully apply coatings and sealers (Weyers et al, 1993). Weyers et al suggest patching surface defects with materials that can accommodate the "high internal stresses" generated by surface coatings.

In 1993, Whiting et al examined the performance of penetrating sealers in accordance with Strategic Highway Research Program (SHRP) guidelines (Whiting et al, 1992; Whiting et al, 1993). Two locations on one bridge were tested with some difficulty and variable results (Whiting et al, 1993).

More recent work in preventive maintenance was also identified in FHWA-RD-98-189. The use of 2-part epoxy, siloxane, silane, and multi-component (silane, siloxane, methyl methacrylate) materials for use as an insulator on various bridge elements was investigated (Whiting et al, 1998). These elements included piers, slabs, and I-beams. For the beam specimens, the silane sealer and the multi-component material were applied. Material performance was measured using half-cell potential testing, macrocell current measurement, and visual observation. Results of the testing indicated that after 50 ponding cycles, corrosion activity increased in the silane treated specimen, as indicated by half-cell potential, and macrocell current measurements. The

multi-component material showed better performance, with seasonal fluctuations in current and potential. Whiting et al concluded that neither material showed promise for a long-term solution to corrosion resistance without consistent reapplication. Better new designs may be more effective in preventing beam end damage than performing periodic repairs or replacing members.

The sealing of cracks is recognized as a means to extend the life of prestressed concrete I-beam ends. Since 1984, MDOT has specified that longitudinal cracks greater than 10-mils in width in the beam end be sealed (MDOT, 1984b). Given the availability of several coatings to bridge cracks in concrete, coatings may have preference over crack treatment techniques.

Other countries are also using coatings as a preventive maintenance measure. The Victoria Department of Transportation in Australia conducted a project aimed at extending the durability of coastal bridge structures by application of protective coating systems (Andrews-Phaedonos et. al., 1997). The first stage of the study focused on a literature review of current world standards and codes related to laboratory based coating testing, assessment of coating performance requirements, evaluation of available products for testing, and a review of the most appropriate laboratory based assessment methods. The second stage included development of a reproducible concrete-type substrate, a chloride ingress-screening test, and their application to examples of four generic types of coatings.

A final means of insulating concrete from deterioration is the treatment of cracks. Durable repairs may be achieved by select epoxy injection of cracks (Shanafelt and Horn, 1980). Michigan has adopted the practice of sealing longitudinal cracks in prestressed concrete beams since 1984 (MDOT, 1984b). However, cracks in prestressed concrete formed by normal loading cannot be effectively repaired by epoxy injection (Shanafelt and Horn, 1980).

2.4.2.1.2 Electrical Control Methods

Only cathodic protection (CP) has been proven to stop corrosion of an existing structure (ACI, 1996). Cathodic protection is a method of controlling electron flow (current) in a structure (ACI 222R-96, 1996). In general, CP can be accomplished by either galvanic / sacrificial anode cathodic protection or impressed current cathodic protection systems (ACI, 1996; Xanthakos, 1996). The advantages and disadvantages of each system are briefly summarized in Table 2-2 (ACI, 1996):

Table 2-2. Comparison of Advantages and Disadvantages of Cathodic Protection Systems

Galvanic or Sacrificial Anode	Impressed Current
No external power required	External power required
Fixed, small driving voltage	Voltage variable over a wide range
Limited, small current output	Current output variable over a wide range
Interference of adjacent structure not likely	Interference can result
Overprotection not likely	Overprotection can result
Anodes rapidly consumed	Anodes slowly consumed
Sensitive to moisture and temperature conditions	Not sensitive to moisture and temperature

Possibly the more desirable cathodic protection system is a sacrificial anode system because it does not require external electricity to operate (ACI, 1996; CIAS, 2001). Sacrificial anodes are composed of a consumable metal such as zinc or aluminum and can be installed on the concrete surface or in an internal application (ACI, 1996) without external electrical requirements. Other consumable anodes include magnesium (ACI, 1996) and aluminum-zinc alloys (Funahashi and Daily, 1996). These systems can be applied to most structures and easily provide localized protection (CIAS, 2001). An impressed current system is not appropriate however where global reinforcement protection is desired, or in especially electrically resistant concrete where the driving voltages may be too low to provide sufficient protection (CIAS, 2001).

A unique type of sacrificial anode is a surface applied anode system. The 3M company has developed the 3M-4727 anode, a surface-mounted self-adhering sacrificial anode for cathodic protection of concrete structures (3M, 1998; 3M, 2001). 3M's literature indicates the anodes may be applied in a wide range of service environments in the vertical, horizontal, and overhead positions (3M, 1998). Like all sacrificial anodes, an electrical connection to the reinforcing steel (cathode) is required. Performance of the 3M-4727 anode has been correlated to NACE Standard RP290-00 (3M, 1998). Others have indicated that the criteria for protection of steel embedded in concrete are not clearly defined (ACI, 1996).

Sacrificial anode cathodic protection using the 3M-4727 anode did not show long-term success in recent Illinois trials on prestressed concrete I-beam ends (IDOT, 2001). Poor long-term performance of the Illinois installations was due to the breakdown of the hydro-gel material (IDOT 2001); a layer that aids in keeping the concrete moist for effective cathodic projection. According to the IDOT report, the hydrogel had changed over a "short period of time" from an ion conductor to an insulator (IDOT, 2001). A project is underway in Michigan that is also using this anode on I-beam ends (Needham, 2001); results of the anode performance have not yet been obtained. Other surface applied sacrificial anode systems include a technique involving thermal-sprayed zinc anodes (Bullard et al, 1996). The applicability of thermal-sprayed zinc anodes to Michigan bridges is being investigated in an internal MDOT project.

Surface-applied anodes appear to have a disadvantage over internal anodes in that they prevent future direct observation of the beam-end concrete. Norcure manufactures two types of internal anodes known as the Galvashield XP and Galvashield CC (Beaudette, 2001a). Both anodes are constructed of a zinc core surrounded by a cement matrix (Beaudette, 2001b; Beaudette, 2001c). In general, XP anodes are more appropriate for repair type projects while the CC anode could be used in a preventive maintenance application. Vector Corrosion Technologies has cited one project in Winnipeg, Manitoba, Canada, where the Galvashield CC anode was used to protect service life and prevent the onset of future corrosion problems (Vector, 2001). The Galvashield CC anode is cylindrical, 2-1/2-inches long and 1-5/8-inches in diameter. The anode is to be installed in predrilled holes in the concrete. A wire lead emitting from the anode is provided to permit an electrical connection to the reinforcing steel. Norcure specifies a maximum anode spacing of 28-inches for the CC anode. The Galvashield CC anodes are reported to have a service life of 10 to 20 years under normal conditions (Beaudette, 2001c).

In a study performed by the Concrete Innovations Appraisal Service, Galvashield anodes were found to be effective in conferring protection to reinforcing steel when used as intended (CAIS, 2001). However, the quantity of steel protected and service life of individual Galvashield anodes in a structure is still being studied. According to Daniel Burns of Vector Corrosion Technologies,

the performance of the Norcure anodes is reportedly in accordance with non-published Vector recommendations (Burns, 2001).

Impressed current cathodic protection has been used since 1977 and is an option for preventive maintenance of prestressed concrete I-beams (CIAS, 2001). Impressed current systems force reinforcing steel into a passive cathodic state by applying a direct current from an anode to the reinforcing steel. Sufficient current is used to stop the anodic reaction at the steel and render the steel cathodic (CIAS, 2001). These systems are suitable for global protection, and can be applied via a variety of systems (CIAS, 2001). Impressed current systems do require constant adjustment and monitoring, as well as a permanent power supply (CIAS, 2001). However, the need for on-site electrical power and continual monitoring makes impressed current CP systems very unattractive for use in beam-end applications. In addition, overprotection (oxygen reduction) in impressed current systems may cause debonding at high current densities or hydrogen embrittlement for high yield strength steels (ACI, 1996).

2.4.2.2 *New Approaches*

2.4.2.2.1 Structure Modification Methods

There are several structure modifications that may help to reduce the beam end deterioration. These modifications include modifications to the deck, support member modifications, and primary framing modifications.

Possible deck modifications include repair or replacement of transverse deck joints, installation of a positive drainage waterproof overlay, or installation of a continuous for live load (CLL) deck. No evidence in the literature review was identified that indicated states are using a joint maintenance approach to prolonging prestressed concrete I-beam life. This is not to say that joints are not receiving attention from state transportation departments, but rather suggests that consideration is not being given to addressing the cause of the distress. Effective joint maintenance appears to be a logical approach to ensuring successful performance of prestressed concrete I-beam ends and other researchers have suggested joint maintenance as the first step in combating beam-end distress (Whiting et al, 1998). More effective joint maintenance, in combination with other approaches discussed in this chapter, can be extremely effective in preventing end deterioration. Design of joints should receive careful consideration, as not all are designed to be watertight. Installing joints and other bridge components in a manner that provides for positive drainage is an additional means of redirecting moisture and deicing solutions away from beam-ends (Whiting et al, 1998).

A recent trend in bridge deck construction has been to construct the decks with out joints, or CLL. In other words, the primary support members are designed to be simply supported members, carrying the dead and live loads. Bridge decks also carry superimposed dead and live loads, however the decks are made continuous over the supports (beam-ends). This design concept permits the elimination of transverse deck joints at the beam-ends and therefore reduces the risk of corrosion-induced concrete deterioration. To this end, reconstructing decks CLL is a preventive maintenance method.

Another option that may achieve the same results, as a continuous for live load deck is a waterproof deck overlay (Tortorete, 2001).

A field investigation performed by this and other researchers indicated frequent distress at the bottom beam flange near the sole plate (Ahlborn et al, 2001). This deterioration was commonly associated with corroding sole plates and masonry plates. Replacement of deteriorating bearings prior to concrete spalling is a means of preventing concrete distress.

Partial depth beam repair is a structure modifying approach that can be used as a preventive maintenance measure for beam-ends with potential deterioration. However, this technique is most applicable to repair projects and is therefore discussed in greater detail later in this chapter.

2.4.2.2.2 Surface Insulating Methods

Preventive maintenance solutions for prestressed concrete I-beams not currently being widely used have also been identified. Sealers and coatings are both considered surface treatments for concrete (PCA, 2001). However, penetrating sealers and surface sealers can be differentiated from coatings by their performance objectives. Sealers aim to prevent or decrease the penetration of liquid or gaseous media (e.g. chlorides, moisture, and sulfates) that can enter the pores of the concrete (PCA, 2001; ACI, 1990). Coatings are designed to act as a barrier to provide complete isolation between the concrete and the contaminating substance (PCA, 2001).

Numerous surface sealers are available for the protective treatment of prestressed concrete I-beam ends. Like penetrating sealers, surface sealers intend to limit the amount of moisture, chlorides, or other materials that can enter the pores of the concrete (PCA, 2001). Responses from the multi-state survey for this project (Chapter 5) did not indicate that any state transportation department is using surface sealers. A recent PCA publication identified 17 families of protective treatments (coatings and sealers) for use on concrete exposed to chlorides (PCA, 2001). Surface sealers in this list included certain formulations of:

- Acrylics,
- Methyl Methacrylate (MMA), and
- High Molecular Weight Methacrylate (HMWM)

At least 22 different manufacturers of acrylics and methyl methacrylates are available (PCA, 2001). A complete listing of these manufacturers is included in PCA publication IS001 (PCA, 2001).

Michigan is moving toward using coatings to protect prestressed concrete I-beam ends (Till, 2001b). In the MDOT Bridge Committee Meeting Minutes of June 14, 2001, MDOT indicated the intent to use an elastomeric sealer to protect beam-ends from chloride-induced corrosion deterioration. Based on the results of the multi-state survey (see Chapter 5), no other state departments of transportation are using coatings to protect beam-ends.

Several coatings were also identified in PCA as being suitable for resistance to chlorides (PCA, 2001). Coatings showing the most promise included:

- Bituminous Paints, Mastics, and Enamels,
- Polyesters,
- Urethanes,
- Epoxies,
- Neoprene,
- Coal Tar-Epoxy,
- Chemical Resistant Mortars and Grouts,
- Sheet Rubber Goods,

- Acrylics,
- Methyl Methacrylate (MMA), and
- High Molecular Weight Methacrylate (HMWM)

Several manufacturers produce products in multiple families of coatings. A recent effort by the Florida Wire and Cable Company has been to develop and bring to commercial production an epoxy coated prestressing strand (Breen, 1990). NCHRP Report 313 indicated excellent creep characteristics and found "epoxy coated prestressing strand to be remarkably tough and effective against corrosion in both pretension and post-tensioned applications" (Perenchio et al, 1989). Fiberglass tendons for anti-corrosion have also been introduced (Breen, 1990).

Partial depth beam repair is a surface insulating approach that can be used as a preventive maintenance measure for beam ends with potential deterioration. However, this technique is most applicable to repair projects and is therefore discussed later in this chapter.

2.4.2.2.3 Environment Modifying Methods

Elimination of water, removal of chlorides, removal of oxygen, impregnation of polymers, and elimination of stray electrical currents are means to create a less corrosive concrete environment (ACI, 1996).

Chloride ion extraction (CIE) and re-alkalization of concrete are two methods that are available to change the properties of concrete. This change generally modifies the environment from one conducive to corrosion-induced deterioration (e.g., high levels of chloride ion, low-alkalinity) to a less corrosive environment. CIE is accomplished electrochemically (ACI, 1996) and involves the use of an electrolyte, ion exchange resin, noble anode, and the reinforcing steel. In CIE, a low voltage direct current is impressed upon the reinforcing steel and chloride ions are driven toward the noble anode (Beaudette, 2002a; ACI, 1996). In the process, the chloride ions become trapped in the ion exchange resin (ACI, 1996). ACI notes that CIE is most applicable for structures exposed in aqueous solution (ACI, 1996). More information on chloride ion extraction and re-alkalization of concrete can be found in the Beaudette (2002a, 2002b).

Partial depth beam repair is an environment modifying approach that can be used as a preventive maintenance measure for beam ends with potential deterioration. However, this technique is most applicable to repair projects and is therefore discussed in greater detail later in this chapter.

2.4.2.2.4 Electrical Control Methods

There are several different methods that are appropriate as preventative maintenance in the control of electrons for reinforcement corrosion prevention in concrete structures. These include surface applied corrosion inhibitors; surface applied sacrificial anodes, and internally applied sacrificial anodes. Discussion on sacrificial anodes is included in the current approaches section on preventive maintenance, as state departments of transportation are currently using them.

Corrosion-inhibiting admixtures chemically arrest the corrosion reaction (Kosmatka and Panarese, 1988). Corrosion inhibitors may be added to the portland cement concrete during beam production as an admixture or be applied to hardened concrete as a spray applied surface treatment. This section will consider only surface applied corrosion inhibitors, however, it should be noted that corrosion inhibitors were once incorporated directly into the concrete used for prestressed concrete I-beams in Michigan (MDOT, 1992). Surface applied products are available from at least two manufacturers in the United States. Penetrating inhibitors have been

shown to reduce the corrosion of reinforcing steel in bridge decks. The method has been tested extensively as described in SHRP-S-666 and may involve heating the concrete above the boiling point of water and then soaking the surface with an aqueous calcium nitrite solution (Al-Qadi et al, 1993). The best results have been found when the contaminated surface layer is either removed or scarified prior to application of inhibitors.

Some penetrating inhibitors that have been shown to be effective with overlays are Alox 901 and Cortec VCI-1337 (MCI 2020). Alox 901 may be applied to un-dried surfaces and has the potential to double the service life of an overlay (or repair material). MCI 2020 also boasts increased overlay service life and has shown nearly a 100% reduction in corrosion rates in laboratory specimens (Al-Qadi et al, 1993). MCI 2020 does not perform as well on un-dried specimens (Al-Qadi et al, 1993), and requires the overlay to contain the inhibiting admixture MCI 2000. Alox 901 must not be overlaid with an admixture-modified concrete (Weyers et al, 1993). Both inhibitors are easily applied with a typical commercial garden sprayer but require a light sandblasting or shotblasting to achieve adequate bond strength with the overlay (Al-Qadi et al, 1993).

Partial depth beam repair is an electrical control approach that can be used as a preventive maintenance measure for beam ends with potential deterioration. However, this technique is most applicable to repair projects and is therefore discussed in greater detail later in the following section of this chapter.

2.4.2.2.5 Analytical Tools

Analytical tools are available to predict when a member may be affected by corrosion-induced distress. Enright and Frangopol (2000) present and summarize methods for damage modeling and predicting service life of concrete beams, specifically with respect to corrosion-initiated distress. According to Frangopol and Enright, the location of damage in a member is related to the type of member, its position in the structure, and the damage source. In other words, the source of the damage can be linked to a damage pattern. Their study included a sampling of bridges in the Midwest and Colorado. A conclusion was that the most common form of prestressed concrete I-beam distress for these bridges is at the transverse deck joints. Further, this damage is corrosion related and due to chloride ion ingress. To this end, Enright and Frangopol modeled resistance and steel area loss over time, for both shear and flexural reinforcement. This may be a valuable modeling tool for determining whether or not strengthening or replacement of a superstructure is required.

Others have also used analytical tools to model future performance. Research by Cairns and Millard predicted the residual lifetime of the structure with no remediation (Canis and Millard, 1999). The qualitative and quantitative effects on residual structural capacity concrete and steel section loss, longitudinal cracking and loss of bond between reinforcement and concrete were investigated by this team.

How a structure behaves over time (i.e. from construction to some point in time) is useful in understanding what structural effects have changed from the original design assumptions. Mari and Valdes considered continuous concrete box beam bridges composed of precast reinforced and prestressed concrete beams with a U cross section and a cast-in-place top slab (Mari and Valdez, 2000). A 1:2 scale model of a two-span continuous bridge was tested to study its behavior during the construction process and under permanent loads. Time-dependent concrete properties, support reactions, deflections, and strains in the concrete and steel were measured for

500 days. Time-dependent redistributions of stresses and internal forces throughout the bridge were also measured. The test results were compared with analytical predictions obtained by means of a numerical model developed for the non-linear and time-dependent analysis of segmentally erected reinforced and prestressed concrete structures. Generally good agreement was obtained, showing the adequacy of the model to reproduce the structural effects of complex time-dependent phenomena.

A probabilistic model has been developed that predicts bridge specific deterioration based on random field simulations (Sterritt and Chryssanthopoulos, 1999). For these simulations, reinforced concrete bridges were targeted, with emphasis placed on structural members for whom field data was collected. As a result of the work by Sterritt and Chryssanthopoulos, models were developed for chloride ingress, spatial corrosion initiation, spatial delamination and corrosion propagation. Nogueira has also investigated employing probabilistic deterioration models (Nogueira, 1999).

Zemajtis and Weyers have also proposed a corrosion deterioration model for bridge structures on the general representation of deterioration versus time relationship (Zemajtis and Weyers, 1998). The Zemajtis and Weyers work considers diffusion period, corrosion stage, bar size, spacing, concrete cover, and the deterioration stages in the modeling.

2.4.3 Repair Techniques

Repair techniques are considered by some researchers to be those that restore a bridge component to an acceptable level of service (Weyers et al, 1993). Repair of prestressed concrete I-beams with end deterioration is cost effective compared to beam replacement, as evidenced by a recent MDOT project that found repairs to cost 35 to 69 percent of full-replacement cost (Needham, 2000).

Repair strategies can be developed with several or no levels of redundancy to assure durable repairs (Emmons, 1994). Different repair scenarios can be used, depending on the degree of exposure and damage (Xanthakos, 1996). Monitoring of repairs is recommended to improve damage inspection and assessment techniques (Shanafelt and Horn, 1980). The ability to perform maintenance or replacement of repair systems should also be considered (Xanthakos, 1996).

Assumptions made by the engineer designing the repairs should be studied carefully. Parameters indicated on the original project documents may not be representative of actual conditions. Tilly cites studies in which long term prestressing losses were 36 percent of the applied stress, compared to the 21 percent loss expected by design (Tilly, 1987). An accurate understanding of prestress loss is important because of the need to compute allowable shear and flexural capacities in beams with more advanced levels of deterioration.

2.4.3.1 *Current Approaches*

2.4.3.1.1 Structure Modification Methods

Beam replacement is known to be an option for prestressed concrete I-beam end deterioration that has been exercised by Michigan and neighboring states. Researchers have also cited complete replacement of damaged members as an option (Shanafelt and Horn, 1985). Removed beams are commonly lifted up and out of a bridge, although some states have developed alternate methods of replacement, such as lateral removal. However, in-place repair techniques were

found to be desirable compared to replacement due to faster completion times and less overall inconvenience to users.

Repairs to bridge decks, support members, and framing members all constitute structure modification methods (see Appendix J). In order for repairs to be successful, the cause of the corrosion induced concrete deterioration should be remedied. Often, improperly functioning bridge decks are associated with end deterioration. Techniques such as joint replacement, deck overlays, and new decks can be used to prolong the life of repairs made directly to the beam-ends.

Support member modifications are also options for the repair of prestressed concrete I-beams. One such retrofit is the addition of a haunch to the pier or abutment to establish a new, sound bearing area (Emmons, 1994). Replacement or repair of bearings is another option that may increase the life of repairs made directly to the beam-ends.

Beam replacement is an option that has been pursued by Minnesota, Illinois, and Michigan. Various methods exist for beam removal including selective vertical removal, selective horizontal removal, or total bridge replacement. A less aggressive approach would be to install a supplemental primary framing beam that would carry a portion of the distressed beams load.

Primary framing members may also be repaired through the use of external beam strengthening methods. Concrete encasement, external post-tensioning, and externally bonded reinforcement could be a means of accomplishing external beam strengthening.

Perhaps the repair technique that holds the most promise for distressed I-beams ends is partial depth repair (PDR). In general, PDR's are those that do not extend the full thickness of the member. PDR's can be performed using relatively simple approaches or with more advanced methods. Summaries of these approaches follow.

Traditional removal and replacement of deteriorated concrete has been applied by Michigan and neighboring states for the distressed prestressed concrete I-beam ends (Xanthakos, 1996; Needham, 2000). In general, concrete repairs must provide protection for the substrate, have an acceptable appearance, and have the ability to carry the required loads (Emmons, 1994).

Needham drafted a repair procedure for prestressed concrete I-beams with end distress (Needham, 1999). Needham's work involved two separate repair and testing scenarios, exposing 12-inches of prestressing and shear reinforcement at the beam ends. From review of Figure 5 in Needham's report, the entire beam cross section was removed to the first stirrup (approximately 3-inches). Concrete was removed at the flange tips to a distance of approximately 12-inches from the "original" end of the member. Removal was tapered back from the flange tips, along two roughly diagonal lines, in plan, to the limits of web removal. Concrete was patched with MDOT Grade D polymer (latex) modified concrete.

Using the described removal and patching procedure, Needham found that through full-scale laboratory testing, there was no stress loss in prestressing strands (Needham, 1999). Needham did conclude that because of a high load hit on the beam that was used for his experiment, some loss in prestressing did occur from the hit. Premature shear cracking and the angles at which the shear cracks formed evidenced this. Bond or tensile testing of the completed patch material to the concrete substrate was compromised when using a 15-pound jackhammer for concrete removal. Other removal methods, such as hydro-demolition, were suggested. As a result of

Needham's research, MDOT plans were prepared detailing an end repair method for prestressed concrete I-beams with and without end blocks.

The suggested prestressed concrete I-beam end repair technique was executed in 1999 in Lower Michigan (Needham, 2000). Although numerous problems were encountered in the field repairs, they appeared to be attributed to contractor/engineer miscommunication and not necessarily the design details. Additionally, prestressed concrete I-beams repaired using the technique were found to be economically attractive compared to complete superstructure replacements (35 to 69 percent of replacement cost) and were estimated to have a life of 30 to 40 years.

Whether to repair or replace a member is an early critical decision that an engineer will need to make. General criteria are stated within NCHRP Report No. 226 for whether to replace or repair prestressed concrete beams having damaged concrete (Shanafelt and Horn, 1980). These criteria appear to have been developed from the findings of their multi-survey.

Load relief for the structure must be provided when performing repairs in compression zones to allow surface repairs to carry load (Emmons, 1994). Others have cited this need as well and refer to it as preloading (Shanafelt and Horn, 1980; Keating and Fisher, 1987; Xanthakos, 1996). Depending on the location of the concrete patching along the span and height of an element, pre-loading may be essential to keep repairs from experiencing in-service tensile stresses (Keating and Fisher, 1987; Xanthakos, 1996).

Dimensionally stable repair materials are required to have the repaired concrete carry load after removal of the load relief provisions (Emmons, 1994). Standard procedures exist in Michigan for shoring of superstructure beams (MDOT, 2001a). Shoring may be required to safely make repairs to beams.

Weyers et al suggest two pairs of techniques to identify concrete that is to be removed (Weyers et al, 1993). They are visual observation and hammer sounding (for low-effort removal over defined areas), and coring and half-cell measurement (for high-effort removal over undefined areas). Removal methods must be selective, preserve the substrate, and provide a quality bonding surface. Weyers et al suggest defining limits of removal by a four-category classification that includes surface, concrete cover, matrix, and core concrete removal.

One of the benefits of performing a partial depth repair is that the process permits unsound or poor quality concrete to be replaced. The limits of removal and quality of concrete can be easily seen during removal operations. Once removal has been performed, other protective strategies, such as the application of a corrosion inhibitor or reinforcement coatings, can be applied (Al-Qadi, 1993). Lastly, the removal of contaminated concrete and subsequent replacement with fresh concrete is an effective means of reducing reinforcing steel corrosion (Al-Qadi, 1993).

Different removal techniques and equipment are used depending on the depth location of the concrete to be removed. Each technique has strengths and weaknesses (Weyers et al, 1993). Hydrodemolition is a technique in which high pressure water is used (around 20 to 40-ksi) to remove concrete of any condition. Hydrodemolition is an attractive removal option because it cleans the reinforcing bars as it removes surrounding concrete without causing damage to the remaining concrete or steel (Weyers et al, 1993). Due to the size and configuration of equipment currently available, this technique has been successful in large, horizontal applications such as parking structures and bridge decks (Weyers et al, 1993). However, the research team has yet to learn that hydrodemolition can effectively be used in difficult access, vertical applications. With

hydrodemolition, variability in the depth of concrete removal may be encountered if the quality of the concrete changes in depth or area (Weyers et al, 1993).

Other concrete removal methods include the use of pneumatic and electric breakers and rotary hammers. These processes are flexible, but also the most labor intensive and production rates are slow (Weyers et al, 1993). In addition, concrete and reinforcing steel in the removal area can be damaged in the process (Weyers et al, 1993). In work conducted for this project, electric rotary hammers were found to be a feasible means of removing deteriorated concrete, after it had first been scored with saw cuts. The rough, angular resulting surface profile was similar to that achieved by pneumatic breakers, and favorable for bonding repair materials (Weyers et al, 1993).

As with concrete removal processes, several options exist for preparing the roughened concrete surface. Depending on the requirements of the repair material, surface preparation methods consisting of compressed air blasting, detergent washing, water blasting, grit blasting, sand blasting, scabbling, or mechanical abrasion may be appropriate. One researcher has found that using sandblasting techniques has increased the bond strength of overlays when specific contact inhibitors are used (Al-Qadi, 1993).

Bond of the repair material to the substrate is of concern. A layer of bonding material is often placed at the transition zone (between the repair material and the substrate) to promote adhesion to the substrate. This material may consist of a thin layer of the repair material or a different material compatible with both the substrate the repair material. The Illinois Department of Transportation has used patches that were mechanically anchored to the concrete using pins and welded wire fabric reinforcement (Xanthakos, 1996).

Protection of reinforcement is considered important to the success of a patch. Methods to prepare exposed reinforcement in a repair are generally similar to those used for concrete. In addition, supplemental measures may be taken to retard corrosion of the reinforcement while the repair is in-service. Some of these methods include placing a highly alkaline material (concrete mortar) around the perimeter of the bar, installing a passive or impressed current cathodic protection system, applying a penetrating corrosion inhibitor, or providing electrical insulation protection (epoxy or zinc-based coatings). Penetrating corrosion inhibitors and cathodic protection are discussed elsewhere in this chapter.

In a study by Whiting et al (1998), coatings were applied to reinforcement in prestressed concrete elements prior to repairs being made. Exposed reinforcement in the patches was coated with either a zinc-rich paint or an epoxy. As a result of the study, epoxy coated reinforcement was found not to perform was well as reinforcement coated with zinc-rich paint.

Conditions in the field may warrant that internal strengthening measures be taken. These conditions may consist of internal reinforcement that has been corroded to a point of significant section loss. If necessary, replacement or supplement of this reinforcement could be performed in accordance with applicable design codes during a PDR.

Repair materials that may be feasible for partial depth repairs include, but are not limited to portland cement concrete, portland cement mortar, magnesium phosphate cement and shotcrete (Emmons, 1994; Kosmatka et al, 2001). Specific selection of the binder, aggregate, fillers, and polymer modifiers, further depends on desired performance of the material and the overall material type selected (e.g.: portland cement mortar vs. shotcrete). More information on the

selection and proportioning of repair materials can be found in Emmons (1994) and Kosmatka et al (2001).

The ability for a surface repair to accommodate the imposed stresses is important (Emmons, 1994). Stresses form due to volume changes of the new and existing concrete as well as from service loads being carried by the repair. Nearly a dozen unique forces exist for the engineer to consider when designing surface repairs (Emmons, 1994).

Portland cement concrete and shotcrete repairs have been investigated by SHRP Report S-360. Weyers et al stress that neither of these techniques will be effective for longer than 15 years if the cause of the distress is not addressed. Additionally, all chloride-contaminated concrete should be removed from the areas surrounding repairs in order for the repair to be effective. Weyers et al also identify concrete and shotcrete containing corrosion inhibitors as repair materials having promise for superstructure repair. Procedures employing corrosion inhibitors in the repair material and as a surface applied treatment for the substrate were investigated. Products were manufactured by W.R. Grace and Company and Cortec Corporation in the Weyers et al study (1993).

For their research on the performance of repairs to prestressed concrete bridge components, Whiting et al selected conventional portland cement concrete, latex modified concrete, and silica fume concrete with corrosion inhibitor repair materials (Whiting et al, 1998). Whiting monitored the performance of the repairs during laboratory induced wetting-drying cycles by the use of half-cell potential, chloride ion, and visual measurements. Prestressed concrete slabs, beams, and piles were included in the research. For the beam specimens, half-cell potential measurements within the patch were more negative than –350mv (copper-copper sulfate half-cell), even after four wetting and drying cycles. These results were discounted as being representative of the steel corroding outside of the patch area. Chloride ion measurements were found to both vary widely (even considering a uniform application of deicer) as well as not be representative of active corrosion, upon visual examination. Silica fume portland cement concrete with an inorganic corrosion inhibitor was found to have the best overall performance on the beam specimens, compared to the conventional portland cement concrete patch and latex modified concrete patch. The overall performance rankings generally correlated with the half-cell potential testing, dissection observation, and surface observation trends. Upon dissection of the patches, corrosion of the central strand was commonly observed. Whiting et al postulated that the corrosion of this strand was caused by a lateral migration of chloride from the surrounding contaminated concrete.

The repair material chosen will largely govern placement and formwork options. Some options include form-and-pump, form and cast-in-place, hand application, low-pressure spraying and others (Emmons, 1994).

Options for curing repair materials primarily consist of moist or membrane curing methods. Moist curing methods (wet burlap covered with polyethylene sheeting) are often viewed as being more efficient than membranes (curing compounds), but application in vertical, difficult access areas, such as beam-ends, may be difficult.

External post tensioning is a technique to restore strength and durability (Keating and Fisher, 1987; Shanafelt and Horn, 1980; Xanthakos, 1996). External post-tensioning may be an option to consider for beam-ends that have distress extending a considerable distance from the end of the beam (Keating and Fisher, 1987).

Post-tensioning, metal sleeve splices, and internal splicing are methods recognized for restoring prestressing (Xanthakos, 1996). Post-tensioning and metal sleeve splices may be applicable to prestressed concrete I-beam end deterioration. Internal splicing does not appear practical due to the absence of a second fixed end for the prestressing strand. All three methods are generally considered when remedying serious damage.

External post-tensioning, internal splices, and sleeve splices are recognized to restore strength and durability to prestressed concrete I-beams (Shanafelt and Horn, 1985). Sleeve splices were also noted to be applicable to I-beams that may have experienced environmental damage.

Preston et al (1987) investigated and looked to restore flexural capacity to distressed prestressed concrete box beam bridges in Pennsylvania. As described in Preston et al, the repair techniques of NCHRP Report 280 were considered and implemented. Repair procedures for the box beam bridge included retrofit with epoxy coated reinforcing bars (not cited in NCHRP Report 280) and post-tensioned, epoxy coated tendons. Preston et al suggest investigating remaining capacity in a distressed beam before making repairs, as earlier designs were likely conservative compared to current design requirements. This conclusion may apply to both the box beams used in Preston's project and the prestressed concrete I-beams included in this research.

Lanyi summarized two projects in Alberta, Canada, where distressed prestressed concrete channel beams were rehabilitated (Lanyi, 1994). Damage to these bridges consisted of a high load hit and extensive corrosion of an exterior bottom channel leg. Repair techniques largely consisted of removing concrete, splicing in new prestressing strands, and patching with conventional concrete.

Fiber reinforced polymer (FRP) laminates appears to be gaining acceptance in the bridge repair arena as evidenced by a recent New York State DOT project (Hag-Elsafi and Alampalli, 2000). To design the FRP retrofit, existing condition data was first input into a computer program. The program was used to determine remaining capacity and design the FRP retrofit (Hag-Elsafi and Alampalli, 2000).

2.4.3.1.2 Electrical Control Methods

The United States is generally recognized as a leader in using cathodic protection as a preventive maintenance and repair technique for concrete bridge elements (Tilly, 1987). In the 1980's, impressed-current cathodic protection systems were preferred for large or important structures and often used in bridge deck applications (Arner and Panganiban, 1986; Tilly, 1987; Kennedy, 1991). Cathodic protection has limitations. Excessive or discontinuous protection may result in hydrogen embrittlement or active corrosion (ACI, 1996).

The success of the protection system used in Kennedy's project was based on whether a 100-mV potential shift could be measured between the reinforcement and a reference half-cell. Impressed current systems appear to be useful in applications where the system can be closely monitored. For the purposes of protecting prestressed concrete I-beam ends, it appears that galvanic or sacrificial anode cathodic protection systems are desirable over impressed current systems.

Response from the multi-state survey discussed in Chapter 5 did not indicate impressed-current cathodic protection is being used, however sacrificial anode systems are receiving attention.

One sacrificial anode available for use in repairs is the Galvashield XP, manufactured by Norcure (Beaudette, 2001b). The anode is constructed of a zinc core surrounded by a cement

matrix. The Galvashield XP anode has been used in repairs to prestressed concrete I-beams in Iowa to provide protection against the accelerated corrosion of reinforcing steel. (Beaudette, 2001d).

The Galvashield XP anode is roughly the shape and size of a hockey puck and is to be installed within the original cross-section of the member during patching. Wire leads from the anode are provided to permit an electrical connection to the reinforcing steel (Beaudette, 2001b). Norcure specifies a maximum anode spacing of 30-inches for the XP anode. The Galvashield XP anodes are reported to have a service life of 10 to 20 years under normal conditions.

According to Daniel Burns of Vector Corrosion Technologies, the performance of the Norcure anodes is reportedly in accordance with non-published Vector recommendations (Burns, 2001).

2.4.3.2 *New Approaches*

Protection of concrete elements can be equated to controlling the cause of deterioration according to Emmons. Protection to eliminate future causes of new deterioration must be provided to prohibit return to a deteriorated state (Emmons, 1994). The high frequency of beam end deterioration with failed transverse deck joints suggests the proper joint maintenance is required (Whiting et al, 1998).

Because of the established link between the leaking transverse deck joints and beam end deterioration, some researchers have suggested modifying the deck drainage and possibly reducing the number and location of joints in a structure (Whiting et al, 1998). A deck overlay may be a means to eliminate the joints, however consideration should be given to providing a high quality overlay that will not foster deterioration of the substrate or support beams.

Bearing modifications are a potential solution to bearing region cracking in prestressed concrete I-beams. Supporting documentation for the need to modify bearings to mitigate distress has not been found.

2.5 MDOT Practice

2.5.1 Use and Evolution of Prestressed Concrete in Michigan

According to a survey submitted for NCHRP Report 90, the first prestressed concrete bridge in Michigan was constructed in 1951 (Moore et al, 1970). Little is known about this first bridge, however, a substantial number of documents are available to document progress since.

Review of MDOT Design Division Informational Memoranda (IM) has provided insight to the changes in MDOT practice in the last 20 years (Till, 2001a). Changes summarized by the IM show progress in the MDOT design philosophy. Probably the most significant changes in the design practices as related to the problem of end-deterioration is the use of CLL design (MDOT, 1989). CLL design is the practice of designing a continuous deck to carry the bridge live load over simply supported beams intended to carry the structure dead load and live load. This practice effectively eliminates deck joints over beam-ends, where a joint would otherwise be placed to accommodate the seasonal movements of the superstructure. Several authors have recognized that the majority of prestressed concrete I-beam end distress occurs at bridge deck joints (Tilly, 1987; Whiting et al, 1998; Needham, 1999; Enright and Frangopol, 2000).

Other important MDOT design changes over the past three decades include use of epoxy-coated shear connectors (IM 320-B), re-designing the placement of bond breakers for strand ends (IM 332-B), omitting corrosion inhibitors from the mix design (IM 447-B), using larger diameter strand (IM 484-B), and sealing of certain width cracks (IM 332-B).

To potentially minimize deck and beam deterioration, shear connector "D" bars were specified to be epoxy coated by IM 320-B (MDOT, 1984a). "D" bars provide horizontal shear resistance between the beam and the deck slab. Since 1984, this is the only epoxy-coated reinforcement used in Michigan prestressed concrete I-beams.

Repair or maintenance of the bridge deck could have a positive, adverse, or no effect on prestressed concrete I-beams. For deck repairs, the use of high-early strength concrete was recommended by MDOT in 1991 (IM 402-B). The required cement content (846 pounds per cubic yard) is the only mix design requirement contained in IM 402-B. High *w/c* concrete could be prone to shrinkage not experienced by lower *w/c* mixes (Kosmatka and Panarese, 1994). Cracks created by the volume change may be of sufficient width to permit intrusion of chloride-laden solutions through the deck and to the beam (Whiting et al, 1998).

Calcium nitrate was used in the casting of prestressed concrete I-beams until 1992 (MDOT, 1992). It is not known when the use of calcium nitrate was initiated. When properly used, calcium nitrate is a corrosion inhibitor effective in reinforcing and stabilizing the passive oxide film on the steel reinforcement (Kosmatka and Panarese, 1994). According to IM 447-B, the use of calcium nitrate was discontinued because there was limited documentation of severe corrosion to prestressed concrete I-beams. MDOT has now recognized that these problems do exist, but only in the end regions near transverse deck joints (Jadun, 1990; Needham, 1999).

Designers recognized the benefits of larger diameter strand with the release of IM 484 (MDOT, 1997a). Permissible prestressing strand diameter changed with this IM from 0.5-inch to 0.6-inch. This change is significant from a design and end deterioration standpoint because material

loss or degradation has a greater effect on a 0.5-inch diameter strand compared to a 0.6-inch diameter strand.

Sealing longitudinal cracks greater than 10-mils in width was recommended by IM 332-B to prevent strand corrosion (MDOT, 1984b). Sealing cracks is a positive step in preventing member deterioration, however cracks as small as 4-mils have been reported to be sufficient to permit localized corrosion of reinforcement (Moore et al, 1970).

Table 2-3 summarizes the design evolution of prestressed concrete I-beams in Michigan.

2.5.2 Current Design

Several MDOT documents are available for the use in the design of new prestressed concrete I-beam bridges. The Bridge Design Manual is intended to be a single source reference for MDOT design engineers and consultants assigned the responsibility of producing bridge plans (MDOT, 2001a). Much of the information in the MDOT Bridge Design Manual originated from Bridge Squad Leaders' Notes.

The types of documents available to the bridge designer to assist in producing plans include maintenance reports, scoping reports, and other inspection data (MDOT, 2001a). The level of detail included in these reports and data is of interest to the project herein. The level of detail potentially indicates how accurate or reliable the data is. Work by other researchers has identified that the greatest amount of distress occurs in an otherwise concealed region behind the diaphragm (Ahlborn et al, 2001). Whether or not field inspectors are getting behind the diaphragms to observe the entire beam end is of interest. From a review of the Scoping Checklist in Appendix 2.02.19 A.3 of the Bridge Design Manual, observations related to beam end repairs are to be performed (MDOT, 2001a).

While past MDOT research projects have example plans for restoration or repair projects (Needham, 2000), the Bridge Design Manual does not. This lack of a sample set of restoration or repair drawings may lead to inconsistencies or omissions between different projects, thereby increasing project costs.

The MDOT Bridge Design Guides serve as an aid for consistently designing and detailing bridges (MDOT, 2001b). In this sense, they serve a similar function to the example plan sheets of the Bridge Design Manual. Of particular interest to this project are the current details that are included in Chapter Six – Superstructure. Section 6.60 contains several current standard design details for prestressed concrete I-beams. In particular, design sheet 6.60.13 contains prestressed concrete I-beam connection details being used at piers and abutments.

Table 2-3. Summary of Changes in MDOT Practice

Changes Occurred in	Bridge Elements	Materials or Section Properties	Years					
			1958	1959	1964	1975	1989	1997
Materials	Beam	f's (psi)	250,000	250,000	250,000	270,000	270,000	270,000
		f'c (psi)	5,000	5,000	5,000	5,000	5,000	5,000
	Deck	f'c (psi)	3,000	3,000	3,000	3,500	3,500	3,500
Design	Beam	Beam Types	AASHTO I-IV	AASHTO I-IV	AASHTO I-IV	AASHTO I-IV WI 70-inch Beam*	AASHTO I-IV	AASHTO I-IV MI 1800 Beam
		E deck / E beam	0.77	0.77	0.77	0.83	0.80	0.80
		Cover on Top (in)	3.00	3.00	3.00	3.00	3.00	3.00
		Cover on Bottom (in)	2.00	2.00	2.00	2.00	2.00	2.00
		Beam Spacing (ft)	5 to 7	4 to 7	5 to 9	6 to 10	Info n/a	6 to 11
		Span Length (ft)	30 to 80	60 to 100	30 to 90	20 to 100	Info n/a	90-150 (MI1800)
		Grade of P. Steel	250	250	250	270	270	270
		Nom. diam of P. Steel (in)	7/16"	7/16"	1/2"	1/2"	1/2"	3/5"
		Draped Strands	No	Yes	Yes	Info n/a	Info n/a	Yes
		Coated reinforcement	No	No	No	No	Epoxied D-Bars	Epoxied D-Bars
		Bond Breaker Used	No	No	No	No	Yes	Yes
	Deck	Thickness (in)	8" constant	8" constant	7" to 9" varies with beam spacing	8" to 9 1/2" varies with beam spacing	Info n/a	Info n/a
		Sections	Precast	Precast	Precast	Precast	Precast	Precast
		Span	Simple	Simple	Simple	Simple	Simple	Simple
		Strands	Pretensioned	Pretensioned	Pretensioned	Pretensioned	Pretensioned	Pretensioned
		Coating	Uncoated	Uncoated	Uncoated	Uncoated	Uncoated	Uncoated
		Calcium Nitrate Added	No	No	No	No	Yes	No
Manufacturing & Construction	Deck	Sections	Cast in Place	Cast in Place	Cast in Place	Cast in Place	Cast in Place	Cast in Place
		Support Conditions	Simple	Simple	Simple	Simple	Continuous for LL	Continuous for LL

*The use of the WI-70 beam began in 1977.

Table 2-3 was compiled with information from the following sources:

Documents

1. General Instructions for Designing Precast Prestressed Concrete I-Beams (6-1957)
2. Prestressed Concrete Beams. AASHO Standard Sections (3-6-1958, Rev. 3-27-1958)
3. Prestressed Concrete Beams. AASHO PCI Standard I Sections with Draped Strands (6.60a, Issued 11-1-1959)
4. Prestressed Concrete I-Beams. AASHO-PCI Standard I Sections (6.60.03, September 1963)
5. Prestressed Concrete I-Beams. AASHO-PCI Standard I Sections (6.60.01, July 1964)
6. Historical Information from Squad Leader Notes, p. BB3a (6-5-1963)
7. Historical Information from Squad Leader Notes, p. BB1 (6-12-1974)
8. Prestressed Concrete I-Beams (6.60.01, April, 1975)
9. MDOT Design Division Informational Memorandum 285B (June 8, 1981)
10. MDOT Design Division Informational Memorandum 318-B (January 4, 1984)
11. MDOT Design Division Informational Memorandum 320-B (February 2, 1984)
12. MDOT Design Division Informational Memorandum 321-B and 268-R (February 2, 1984)
13. MDOT Design Division Informational Memorandum 332-B (July 3, 1984)
14. MDOT Design Division Informational Memorandum 336-B (May 5, 1986)
15. MDOT Design Division Informational Memorandum 348-B (April 8, 1985)
16. MDOT Design Division Informational Memorandum 361-B (December 3, 1985)
17. MDOT Design Division Informational Memorandum 366-B (May 5, 1986)
18. MDOT Design Division Informational Memorandum 368-B and 311-R (June 24, 1986)
19. MDOT Design Division Informational Memorandum 378-B (March 17, 1987)
20. MDOT Design Division Informational Memorandum 385-B, Revised IM 378-B (September 30, 1987)
21. MDOT Design Division Informational Memorandum 402-B (July 1, 1991)
22. MDOT Design Division Informational Memorandum 411-B (August 29, 1989)
23. MDOT Design Division Informational Memorandum 446-B (July 15, 1992)
24. MDOT Design Division Informational Memorandum 447-B (August 3, 1992)
25. MDOT Design Division Informational Memorandum 447-B (August 3, 1992)
26. MDOT Design Division Informational Memorandum 458-B (June 8, 1995)
27. MDOT Design Division Informational Memorandum 484-B (December 5, 1997)

Plans and Drawings

28. Stirrup from Superior Product Company (02-10-1976)
29. Prestressed Concrete I-Beam Details. PC-1B. (7-25-1979)
30. Prestressed Concrete I-Beam Details. PC-1F. (5-16-1985)
31. 70" Prestressed Concrete I-Beam Details. PC-2E. (5-16-1985)
32. Bearing Details for Prestressed Concrete I-Beams (4-10-1990)
33. Bearing at Abutments with Prestressed I-Beams (4-10-1979, 8-9-1971, 11-2-1970, 5-21-1962)

2.5.3 Bridge Management

The thousands of bridges in Michigan require a concerted effort to be maintained in a level safe for the traveling public. Successful efforts are realized in an effective bridge management program. The foundation of a bridge management program is the field inspection. Though it is possible for a field inspection to be performed for any number of reasons, bridge inspections are typically performed as part of a Pontis or NBIS inspection program.

The Pontis inspection is performed to provide estimated future cost information for the maintenance of bridges. Pontis inspections commonly document construction quantities on a bridge, so that repair and replacement estimates can be developed. On the other hand, NBIS inspections are meant to assess the structure and the overall safety of the structure. The NBIS generally apply to all bridges on public roads with a span greater than 20-feet (CFR Title 23, 1999). The NBIS require an inspection organization to be established by each state. Also required of the states is the preparation and maintenance of their bridge inventory. According to the NBIS, a maximum bridge inspection frequency of two years is required. A random review of bridge inspection reports from Michigan has shown conformance with the inspection frequency requirements established by the NBIS.

Inspection procedures to be used to satisfy NBIS requirements are presented in the Manual for Condition Evaluation of Bridges (AASHTO, 2000) and the Interim Revisions to the Manual (AASHTO, 2001). The Manual for Condition Evaluation of Bridges also includes sections for determining the load rating of a bridge. Suggestions for distress conditions to observe in prestressed concrete beams, bridge drainage structures, and bearings are included in the Manual for Condition Evaluation of Bridges. The bearing region condition of prestressed concrete beams is to be checked per the Manual for Condition Evaluation of Bridges. Various types of material tests for the bridge inspector to consider are also included in the Manual. Tests for concrete include strength, sonic, ultrasonic, magnetic, electrical, nuclear, thermography, radar, and radiography based techniques (AASHTO, 2000).

3.0 Field Investigation (Task 2)

3.1 Introduction

The focus of Task 2 was to conduct an extensive field investigation of twenty PC I-beam bridges to observe the distress at the beam-ends. This chapter is divided into seven sections. First, a field visit to a precast concrete plant is described. Next, the process of how the field specimens were selected is documented. Then the inspection preparation and protocol are clearly defined. The research team's field experiences are summaries. A thorough review of each bridge's inspection data is given. Lastly, the organization of the inspection data is explained. This chapter provides a comprehensive outlook on the current sate of distress in PC I-beam ends in Michigan.

3.2 Precast Plant

On June 19, 2001, the research team visited Premarc, a prestressed concrete plant. Premarc is located on Chicago Drive SW of Grand Rapids in Michigan. The Premarc Corporation, is a closely held, family owned Michigan manufacturing concern, founded in 1925. Since then, Premarc has supplied the construction industry with concrete products such as prestressed concrete I-beams for highways and bridges. The manager of the plant showed the research team the products made at Premarc and led them through the process of manufacturing prestressed concrete.

3.2.1 Concrete Plant

The plant has its own facility for concrete mixture design and manufacturing. Commercial software is utilized for the design of concrete mixture. The computerized equipment is used to produce a desired strength from the concrete.

3.2.2 Prestressing Systems and Anchorages

The plant has several open air pretensioning beds. Buckets are used to transport concrete approximately 500-feet from the plant to the beds. Beams are cast in permanent type beds, where forms are fixed in place. A precast stressing bed of a long reinforced concrete slab is cast on the ground with vertical anchor bulkheads at its ends. Prestressing steel is pretensioned

against independent anchorages prior to the placement of concrete around it. Prestressing can be accomplished by prestressing individual strands, or all the strands at one jacking operation.

One of the components of a prestressing operation is the jacking system applied, i.e., the manner in which the prestressing force is transferred to the steel tendons. Such a force is applied through the use of hydraulic jacks of different capacity; depending on whether individual tendons are being prestressed or all the tendons are being stressed simultaneously.

3.2.3 Quality Control

Precast concrete is cast into complex shapes. Plant-cast precast concrete components are not fabricated under optimum conditions of forming. For example, the process of the pretensioning and concrete placement is taking place in the open space. Thus the requirement to maintain the certain temperature is not satisfied. This may be one of the reasons why most of the prestressed concrete I-beams in stock have hairline cracks along the flange.

3.3 Selection of Field Specimens

The objective of this project is to inspect a full spectrum of bridges at different ages and conditions. Beam types were not taken into consideration, however access issues were a primary concern. For this reason, only "highway-over-highway" bridges were selected. Other access parameters such as "bridge clearance" and the presence of a shoulder or sidewalk on the "featured intersection" were reviewed on the site plan.

A total of 20 prestressed concrete I-beam bridges were selected in order to document the detailed beam end conditions and general conditions of the deck and substructure. In order to initiate the field investigation; Grand Region (23 bridges), North Region (26 bridges) and Bay Region (17 bridges) have been selected for the prestressed concrete I-beam bridge pool.

The information collected was reviewed and organized in a tabular form. The tables contain information on bridge ID, year built, geometry, characteristics and ratings/conditions, etc. (see Appendix A for Grand, Appendix B for North and Appendix C for Bay). The primary parameters for selecting the bridges to be inspected were the year built and the deck and stringer ratings/conditions. The bridges subjected to high load hits were automatically eliminated.

In Table 3-1, Table 3-2, and Table 3-3 the shaded bridges indicate that particular bridge was studied for the finite element modeling analysis in Chapter 10.

3.3.1 Grand Region

The research team selected a group of 5 bridges satisfying the criteria (see Table 3-1) out of a pool of 23 prestressed concrete I-beam bridges that are highway-over-highway (see Appendix A).

The selection was made based on the bridge rating during the most recent inspection (6-9 for deck, 6-9 for stringer, 6-8 for abutment, and 5-7 for pier) and year built (1961, 1963, 1964, 1969 and 1972). The list was reviewed with respect to inspection feasibility (traffic control and access issues).

Table 3-1. Bridges Identified for Inspection in Grand Region

NBI No.	County	Year Built	Facility Carried	Feature Intersected
41025 S07	Kent	1961	KNAPP ST	I-96
41027 S06	Kent	1963	US-131 NB	6TH AVE
41029 S16-3	Kent	1964	I-196, M-21 EB	LANE AVE
41029 S16-4	Kent	1964	I-196, M-21 WB	LANE AVE
41029 S23	Kent	1972	I-196 WB	36TH ST

3.3.2 North Region

There is a concentration of new prestressed concrete I-beam bridges in the North Region. Our goal was to inspect these bridges in order to document their condition at an early age. Out of a set of 26 prestressed concrete I-beam bridges located (see Appendix B) in this region, five bridges were selected for inspection (see Table 3-2). The most recent ratings of these bridges were 7-8 for deck, 8 for stringer, 7-8 for abutment, and 7-8 for pier. A bridge engineer verified the easy accessibility of all these bridges, including two located on a portion of US-131 that was not yet open to traffic.

Table 3-2. Bridges Identified for Inspection in North Region

NBI No.	County	Year Built	Facility Carried	Feature Intersected
67016 S09	Oceola	1984	US-131 N B	US-10
67016 S10	Oceola	1984	US-131 S B	US-10
53034 S05	Mason	1986	CHAUVEZ RD	US-31
83033 S06	Wexford	1997	NO. 36 ROAD	US-131
83033 S03	Wexford	1998	WHALEY RD	US-131 RELOC.

3.3.3 Bay Region

Based on the latest bridge rating (4-8 for deck, 4-7 for stringer, 6-7 for abutment, and 4-7 for pier) and year built (1961, 1967, 1968, and 1969, 1971) 10 bridges (see Table 3-3) out of 17 were selected by the research team for inspection (see Appendix C).

Table 3-3. Bridges Identified for Inspection in Bay Region

NBI No.	County	Year Built	Facility Carried	Feature Intersected
06111 S04	Arenac	1968	I-75 NB	M-61
06111 S05	Arenac	1968	LINCOLN RD	I-75 SB
06111 S06	Arenac	1968	LINCOLN RD	I-75 NB
06111 S11	Arenac	1968	M-33	I-75
25042 S12-8	Genesee	1967	I-69 RAMP F	I-75
25042 S12-3	Genesee	1969	I-69 EB	I-75
25042 S12-4	Genesee	1969	I-69 WB	I-75
25042 S12-7	Genesee	1969	I-69 RAMP E	I-75
25132 S34	Genesee	1971	I-475 SB	CLIO RD
29011 S03	Gratiot	1971	US-27 NB	US-27BR (POLK RD)

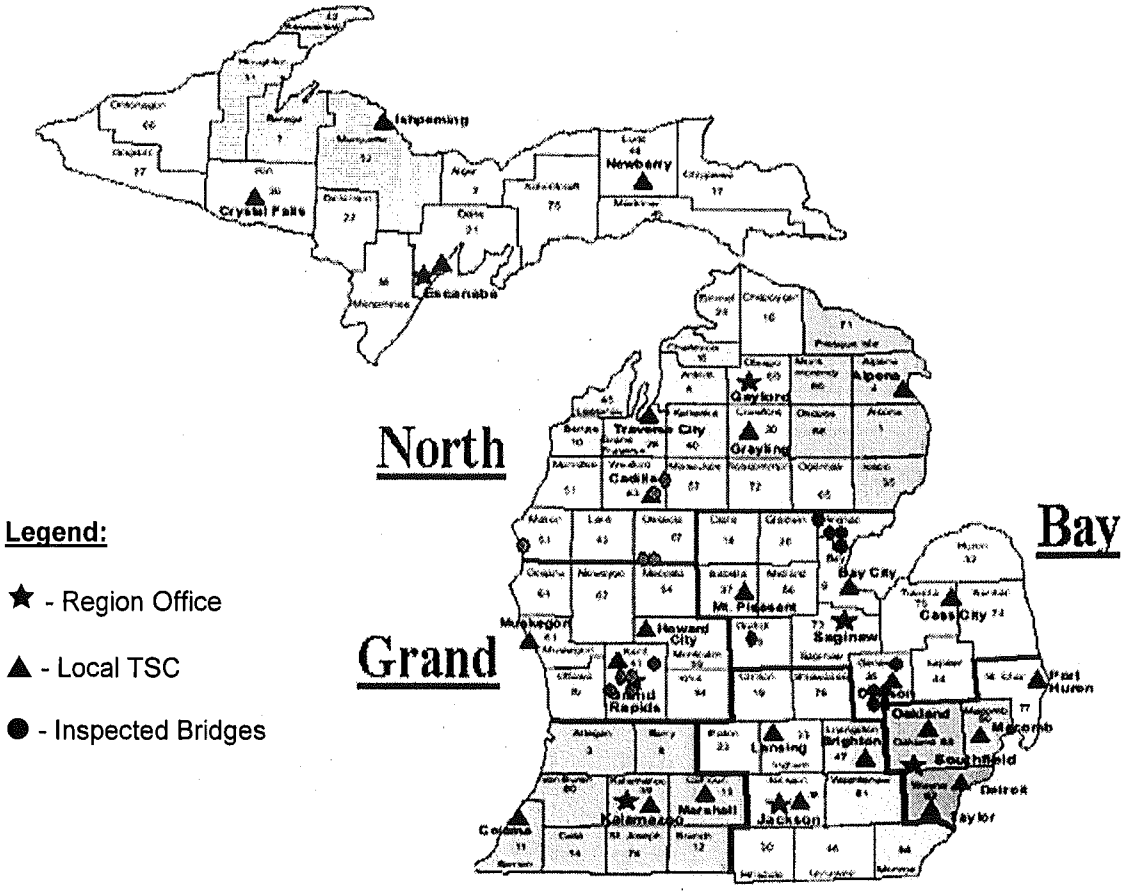

Figure 3-1. Site Location of the 20 Inspected Bridges

Figure 3-1 shows a visual summary of the 20 inspected bridges within their respective region.

3.3.4 Bridge Categories by Design and Loading

The classification of the inspected bridges according to design is based on the data obtained from MDOT, Construction and Technology Division.

Based on the data collected, twenty inspected prestressed concrete I-girder bridges are categorized by their different design characteristics, such as deck type, bearing type, girder type, diaphragm type on piers (end diaphragms) and intermediate diaphragms, diaphragm type on abutments/backwalls, as well as traffic load under and on the bridge. The information below is based on the data summarized in Table I-1 (Appendix I). Also, this information is sorted in order to provide better understanding of bridges distribution according to deck bearing types (see Table 3-4), girder diaphragm (see Table 3-5), and loading on and under bridges (see Table 3-6).

Bridge design categories are subdivided by (1) deck, (2) bearing pads on abutments and piers, (3) girder and (4) diaphragm types, and (5) loading as shown below.

(1) Deck type:

Composite: 41029S23, 41029S163, 41029S164, 41027S060, 41025S070, 67016S090, 67016S100, 53034S050, 83033S050, 25042S124, 25042S123, 25042S128, 25042S127, 06111S11, 25132S34, 29011S03, 06111S04, 06111S05, 06111S06

Continuous: 83033S060

(2) Bearing pad type:

Abutments:

Elastomeric Pad: 41029S23, 67016S090, 67016S100, 53034S05, 83033S060, 83033S050, 25042S124, 25042S123, 25042S128, 25042S127, 06111S11, 25132S34, 29011S03, 06111S04, 06111S05, 06111S06

Neoprene Pad: 41029S163, 41029S164, 41027S06, 41025S07

Piers:

Elastomeric Pad: 41029S23, 53034S05, 83033S050, 25042S124, 25042S123, 25042S128, 25042S127, 06111S11, 25132S34, 06111S04, 06111S05, 06111S06

Neoprene Pad: 41029S163, 41029S164, 41027S06, 41025S07, 29011S03

No: 67016S09, 67016S10, 83033S06

(3) Girder type:

AASHTO I, II, III: 41029S16-3, 41029S16-4, 06111S11, 25132S34

AASHTO I, II: 29011S03

AASHTO I, III: 41029S23, 06111S04

AASHTO II, III: 41027S06, 41025S07, 06111S05, 06111S06

AASHTO III: 25042S12-4, 25042S12-3, 25042S12-8, 25042S12-7

Wisconsin 70": 67016S09, 67016S10, 83033S05

Wisconsin 70", AASHTO I: 53034S05

MI 1800: 83033S06

(4) Diaphragm type:

Abutments/Backwalls:

Type A: 67016S09, 67016S10, 29011S03

Type B: 41025S07, 29011S03

No: 41029S23, 41029S16-3, 41029S16-4, 53034S05, 83033S06, 83033S05, 25042S12-4, 25042S12-3, 25042S12-8, 25042S12-7, 06111S11, 25132S34, 06111S04, 06111S05, 06111S06

End Diaphragms (On Piers):

Type A: 41027S06, 25042S12-4, 25042S12-3, 25042S12-8, 25042S12-7

Type Dm: 83033S05

Multiple (more than one present): 41029S23, 41029S16-3, 41029S16-4, 41025S07, 53034S05, 06111S11, 25132S34, 29011S03, 06111S04, 06111S05, 06111S06

No: 67016S09, 67016S10, 83033S06, 83033S05

Intermediate Diaphragms (At the middle of span):

Type A: 67016S09, 67016S10, 25132S34,

Type Am: 83033S06, 83033S05

Type G: 06111S04

Type I: 25042S12-4, 25042S12-3, 25042S12-8, 25042S12-7

Multiple: 41029S23, 41029S16-3, 41029S16-4, 41027S06, 41025S07, 53034S05, 06111S11, 29011S03, 06111S04, 06111S05, 06111S06

No: 41029S23, 67016S09, 67016S10, 83033S06, 83033S05, 25132S34, 06111S04

(5) Loading:

ADT under:

Less then 1,000: 29011S03

1,000-10,000: 41029S23, 41029S16-3, 41029S16-4, 41027S06, 67016S09, 67016S10, 25132S34, 06111S04, 06111S05, 06111S06

10,000-20,000: 06111S11

20,000-50,000: 41025S07

Over 50,000: 25042S12-4, 25042S12-3, 25042S12-7

N/A: 53034S05, 83033S06, 83033S05, 25042S12-8

ADTT under:

0 or less: 41029S23, 41029S16-3, 41029S16-4, 41027S06

0-1,000: 67016S09, 67016S10, 25132S34, 29011S03, 06111S04, 06111S05, 06111S06

1,000-10,000: 41025S07, 25042S12-4, 25042S12-3, 25042S12-7, 06111S11

N/A: 53034S05, 83033S06, 83033S05, 25042S12-8

ADT on:

Less then 1,000: 06111S05, 06111S06

1,000-10,000: 41025S07, 67016S09, 67016S10, 25042S12-7, 06111S11, 25132S34, 29011S03, 06111S04

10,000-20,000: 41029S23

20,000-50,000: 41029S16-3, 41029S16-4, 25042S12-4, 25042S12-3

over 50,000: 41027S06

N/A: 53034S05, 83033S06, 83033S05, 25042S12-8

ADTT on:

0 or less: 06111S05, 06111S06

0-1,000: 41025S07, 67016S09, 67016S10, 25042S12-7, 06111S11, 25132S34, 29011S03, 06111S04

1,000-10,000: 41029S23, 41029S16-3, 41029S16-4, 41027S06, 25042S12-4, 25042S12-3,

N/A: 53034S05, 83033S06, 83033S05, 25042S12-8

Table 3-4. Bridge Distribution According to Deck and Bearing Pad Type

	Deck Type		Bearing Pad Type					
			On Abutments			On Piers		
	Composite	Continuous	Elastomeric	Neoprene	None	Elastomeric	Neoprene	None
No. of Bridges	19	1	16	4	0	12	5	3

Table 3-5. Bridge Distribution According to Girder and Diaphragm Type

	Girder Type								Diaphragm Type[i]												
									Abutments/ BackWalls			End Diaphragms (On Piers)				Intermediate Diaphragm					
	I, II, III	I, II	I, III	II, III	III	Wisconsin 70",	Wisconsin 70", AASHTO I	MI 1800	Type A	Type B	Not present[ii]	Type A	Type Dm	Multiple[iii]	Not present	Type A	Type Am	Type G	Type I	Multiple	Not present
No. of Bridges	4	1	2	4	4	3	1	1	3	2	16	5	1	11	4	3	2	1	4	11	7

[i] Diaphragm type – see Appendix I, Table I-2, [ii] Not present – No diaphragm is present at the bridge
[iii] Multiple –Two or more different diaphragm types are presented in the bridge
Note: Total number of bridges appearing in the Table 3-5 may be more than twenty. This occurs when bridges fall into two different design categories.

Table 3-6. Bridge Distribution According to Loading On and Under Bridge

	Loading																			
	ADT u[i]						ADTT u[ii]				ADT on[iii]						ADTT on[iv]			
	<1,000	1,000-10,000	10,000-20,000	20,000-50,000	> 50,000	N/A	< 0	0-1,000	1,000-10,000	N/A	< 1,000	1,000-10,000	10,000-20,000	20,000-50,000	> 50,000	N/A	< 0	0-1,000	1,000-10,000	N/A
No. of Bridges	1	10	1	1	3	4	4	7	5	4	2	8	1	4	1	4	2	8	6	4

[i] Average Daily Traffic Under Bridge, [ii] Average Daily Truck Traffic Under Bridge
[iii] Average Daily Traffic On Bridge, [iv] Average Daily Truck Traffic On Bridge

3.4 Inspection Preparation and Training

Prior to the actual fieldwork, the preparation for inspection consisted of planning the inspection, a review of field documentation and inspection procedures, and understanding safety and traffic control issues. A list of the tools used during the inspection is given in Appendix D. Also, the shoulder closure plan and traffic control equipment is given in Appendix E and F respectively.

3.4.1 Planning the Inspection

The principal inspection goal was to document the condition of the prestressed I-beam ends, diaphragms, and general structure of the bridges. The documentation included mapping the beam-end conditions on a template, notes on diaphragm conditions and bearings, and brief notes on the deck, barriers, abutments and piers conditions. Notes also included the structural system such as beam-end restraints, deck system and expansion joints. Also, it was important to note the condition of drainage systems, joints, embankments, and utility lines.

3.4.2 Inspection Schedule

At this stage contacts with the regional MDOT offices were made to help correlate the trips scheduled for bridge inspection. The final schedule for the inspection was established as shown in Table 3-7 and Table 3-8.

Table 3-7. Bridge Inspection Schedule

Region	No. of Inspection Days	Inspection Dates	No. of Bridges	Total No. of Beams Inspected
Grand	4	07/12/01-07/15/01	5	132
North	3	07/18/01-07/20/01	5	53
Bay	3	07/23/01-07/25/01	5	130
	3	08/27/01-08/29/01	5	99

Table 3-8. Prestressed Concrete I-beam Bridges Inspected

Region	NBI No.	County	Year Built	No. of Spans	No. of Beams per Span	Beam Type	Total No. of Beams per Bridge	Inspection Date
Grand	41141029000S230	Kent	1972	3	8	I, III	24	July 12,01
	41141029000S163	Kent	1964	3	8	I, II, III	24	July13,01
	41141029000S164	Kent	1964	3	8	I, II, III	24	July 13,01
	41141027000S060	Kent	1963	3	12	II, III	36	July 14,01
	41141025000S070	Kent	1961	4	6	II, III	24	July 15, 01
North	67167016000S090	Oceola	1984	1	6	Wisc.70	6	July 18, 01
	67167016000S100	Oceola	1984	1	7	Wisc.70	7	July 18, 01
	53153034000S050	Mason	1986	4	6	Wisc.70	24	July 19, 01
	83183033000S060	Wexford	1997	1	8	MI 1800	8	July 20, 01
	83183033000S050	Wexford	1998	2	4	Wisc.70	8	July 20, 01
Bay	25125042000S128	Genesee	1967	4	5/2, 3/2	III	16	July23-24,01
	25125042000S123	Genesee	1969	4	7/2, 4/2	III	22	July23-24,01
	25125042000S124	Genesee	1969	4	7/2, 4/2	III	22	July23-24,01
	25125042000S127	Genesee	1969	4	5/2, 3/2	III	16	July23-24,01
	06106111000S110	Arenac	1968	6	9	I, II, III	54	July 25, 01
	25125132000S340	Genesee	1971	4	6	I, II, III	24	Aug. 27, 01
	29129011000S030	Gratiot	1961	3	9	I, II	27	Aug.27-28, 01
	06106111000S040	Arenac	1968	3	6	I, III	18	Aug. 28, 01
	06106111000S050	Arenac	1968	3	5	II, III	15	Aug. 29, 01
	06106111000S060	Arenac	1968	3	5	II, III	15	Aug. 29, 01

3.4.3 Field Documentation and Inspection Procedures

Based on the general plan of the structure, the team prepared templates that contained a beam plan, beam face templates and room for survey notes and annotations. The main goal was to collect detailed information on beam-end and diaphragm conditions. For use in the field, template plans of beams, diaphragm location and orientation, the beam and diaphragm elevations were prepared for each bridge. The templates were to be completed in the field by the individual inspector looking at a specific beam face.

Prior the inspection trips, the team reviewed procedures and documentation according to the Bridge Inspector Training Manual (Hartle et al, 1995). These procedures included the following:

a. Report all visible cracks, recording their width, length, location and orientation (horizontal, vertical, or diagonal). Check beam flange surfaces for longitudinal cracks. Inspect the beam webs for structural cracks.
b. Note any corrosion and efflorescence stains.
c. Record area, location, depth, and general characteristics of concrete scaling.
d. Document concrete surfaces delamination using sketches showing the location and pertinent dimensions.
e. Sketch spalling and the presence of exposed reinforcing steel.
f. Examine the areas near the bearings and the cast-in-place end diaphragms for spalling concrete, bearing condition and sole plate corrosion.
g. Inspect the end diaphragms for cracking and spalling.
h. Document high load hits on beams.
i. Document any repairs that have been made previously.

3.4.4 Safety & Traffic Control Issues

The fundamental safety practices the inspector should be aware of, according to Manual 90 (Hartle et al, 1995), were reviewed in preparation for the inspection. The most relevant practices pertaining to the particular project were discussed with the inspection team prior to each trip.

A traffic control plan was prepared and presented to everyone on the team (see Appendix E: Traffic Control Plan for a Shoulder Closure and Appendix F: Traffic Control Equipment). The traffic control was limited to a shoulder closure on most inspection sites. The four bridges in Genesee County with featured intersection on I-75 required lane closures. Genesee County provided the traffic control for the inspection team.

3.5 Field Inspection Protocol

The site inspections were performed to visually and physically examine each bridge component to document its condition in detail. The structural components that were inspected were beams, diaphragms, deck, joint, drainage system, piers, and abutments. The details of the inspection procedure for each component are described in the following sub-sections.

3.5.1 Beams & Diaphragms

The first purpose of the beam inspection was to document the condition of the beam-end and to identify the cause of distress. The second purpose was to collect data in order to develop an inspection procedure for identifying corrosion prone beam-ends. Using the templates of the beams and the diaphragms (see Figure 4-6. Example of Field Investigation Template Form) the research team documented the elements' details and documented all their findings. The team also took specific field measurements, such as crack widths and delaminated and spalled areas, which detailed the level of deterioration in elements.

During the time of actual field investigation the research team performed the following tasks:

1. Measurement of cracks (location, orientation, length, width, and coordinates), delaminations and spalls on beam-ends and diaphragms using a crack gage and hammers where necessary. Beam elevation sketches have been used as templates to document the information.
2. Noted the location, length, and corrosion level of any exposed rebar or tendons.
3. Noted the presence of rust stains and efflorescence and location.
4. Took photos of selected beams and diaphragms.
5. Checked and recorded type and condition of sole plates and bearings.

3.5.2 Deck, Joints & Drainage System

During the inspection of the deck the conditions of the joints, deck, wearing surface, and drainage systems were documented. The research team performed the following tasks:

1. Documented the estimates of deck deterioration. Noted how many cracks and orientation in each slab and the amount and location of spalling. Indicated asphalt overlay or other repair if any.
2. Recorded locations of expansion and control joints on the deck.
3. Noted if there was any sidewalk and type and condition of barrier.
4. Took photos depicting the deck condition.

Joints were inspected to document any leakage and presence of debris. The joints are particularly critical because they prevent the leakage of runoff and deicing chemicals to the substructure elements below the deck. Inspection of the bridge surface flow drainage system is performed to document the condition of pipes or channels of the drainage system.

3.5.3 Substructure

Concrete substructure components were inspected for cracking, spalling, delamination, and exposed reinforcement. Pier caps were examined for a buildup of moisture and excessive spalling. The research team performed the following tasks:

1. Documented cracks and spalls on piers and abutments and their location.
2. Identified the cause of any deterioration of substructure elements.
3. Took pictures of piers and abutments.

3.6 Review of Inspection Process and Field Experience

3.6.1 Inspection Process

The inspection of each bridge varied with bridge type, equipment and people available. The following steps provide a common basis of the process for each particular bridge.

Coordination. Prior to the inspections coordination meetings took place between all of the research team members. All arrived at the site with a clear understanding of what was to be accomplished and how to do it safely throughout the completion of the inspection.

Inform Authorities. The local MDOT office was informed prior to beginning the inspection.

Inspection Notes. The research team used a set of bridge plans and sketches as templates. The team supervisor reviewed the notes at the end of each day to make sure that the information was complete. The team took pictures of the structure and structural details, recording the roll and picture number. A description, location, and direction of the picture was also recorded. A digital camera was also utilized primarily to document the beam-ends.

General Course of Action. The research team looked over the entire bridge. It was helpful in order to get a feel of what problems may exist and how to use access equipment in specific areas. Once the plan of inspection was formulated, the inspection was started, generally at one end and worked across the bridge.

One inspector climbed around the bridge taking notes on abutment, pier, and deck conditions. Other members inspected the beam-ends, primarily using ladders. In one case, MDOT "reach all" equipment was utilized. In the inspection of the last five bridges a boom lift was used in addition to ladders.

Direct Physical Measurements. The condition survey of bridges included two stages of direct physical measurements:

1. Visual Inspections and Crack Measurement.

Results of the visual investigation were noted on a field investigation form. Cracks were measured and sketched on the template. The number beside each crack indicated the crack width. Photographs were taken to supplement the field notes since it was often difficult to describe the location and extent of deterioration of a bridge member solely with a written explanation.

2. Delamination Testing.

To test for delaminations, the research team used the most basic method of testing using a hammer and sounding for hollow spots. The presence of delaminations indicates that corrosion of the steel has progressed to the point where distress has occurred at the beam end. Prior training of the team provided fairly uniform documentation of this condition.

3.6.2 Field Experience

The research team took more time than estimated, because of the difficulty in accessing various portions of the bridge structure. The inspection at times could be very dangerous due to traffic and the use of tall ladders, thus making it essential to have technically and physically capable people performing the work.

In the field the research team faced the following difficulties:

- The beam was too high to access by conventional ladders.
- Fitting ladders into the narrow gap between piers and crash barriers.
- Safely placing ladders on the inclined embankments.
- The condition of embankments (deteriorated and/or covered by debris) made it difficult to climb or to place ladder safely.

In all these cases the team was trying to collect the desirable information in as safe a manner as possible.

The MDOT regional office helped the inspection of the bridge in Bay Region, Arenac County (Pontis bridge ID is 06106111000S110) by arranging a "Reach-All" and its operators. It would have been impossible to access the superstructure elements by ladders, because the superstructure was too high and the soil underneath the structure was too soft to safely set the ladders. The "Reach-All" allowed the team access from the bridge deck in order to inspect the fascia and beams.

3.7 Inspection Data Review

The following is the overview of findings from the inspection of each bridge presented in the sequence of inspection.

3.7.1 Grand Region

3.7.1.1 *NBI No: 41029 S23*

The bridge was inspected on July 12, 2001. The inspection took 8 hours and 30 minutes between 1:00 p.m. and 9:30 p.m.

General Bridge Information

The bridge is located in Kent County. Constructed in 1972 the bridge carries I-196 WB over 36th Street in Grand Rapids.

Bridge Geometry

The bridge is 116.6-ft long, 49.8-ft wide, and carries 4 lanes of traffic with 0.9-ft wide sidewalks. The bridge orientation is North-South. This is a skewed three span bridge with eight beams per span. The beam lengths are: 59.00-ft at the central span and 28.8-ft at the side spans. Side spans beams are types I and III, and center span beams are type III.

Abutments, Pier, Deck and Joints

The north abutment has several hairline cracks and minor rust and efflorescence stains. Some of the beam sole plates are corroded. South abutment, bearings and sole plates are in a good condition.

Piers have minor cracks and spalls, light rust, efflorescence and water stains.

Deck shoulders are covered with debris. Main span deck is in good condition. Side span decks have cracks and potholes with some rust and efflorescence stains. Expansion joints have leakage. Spalls are noted along construction joints. The construction joint filler is missing at the barriers. Drainage system is clean and operable. The general view of the deck is shown in Photo 3-1.

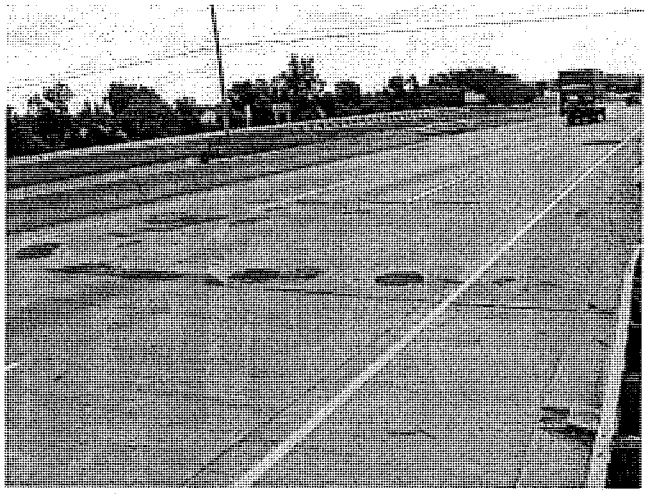

Photo 3-1. Deck Condition of 41029 S23

Stringers, Bearing and Diaphragms

Most beam-ends display cracking and minor spalling, rust and/or efflorescence stains. At some of the beam-ends shear reinforcement is exposed. Examples of the typical beam-end conditions are shown in Photo 3-2 and Photo 3-3:

Photo 3-2. View of beam-end condition with exposed rebars

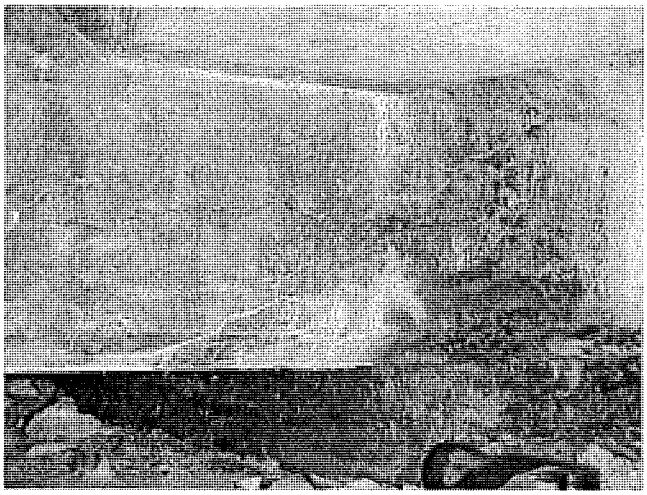

Photo 3-3. Close view of the beam-end condition - note cracking and efflorescence

Most of the sole plates on the piers are rusted. Several diaphragms on both piers are cracked and delaminated. One concrete diaphragm between beams W5 and W6 on pier S1 was partially spalled with exposed shear reinforcement (see Photo 3-4).

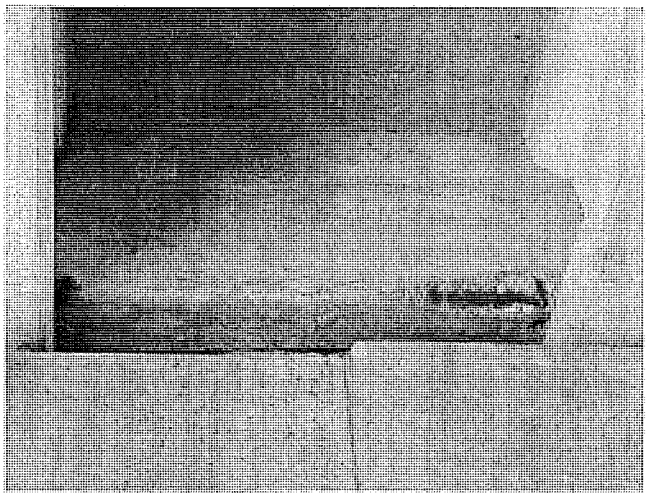

Photo 3-4. Diaphragm condition with exposed rebars

3.7.1.2 *NBI No: 41029 S163*

The bridge was inspected on July 13, 2001. The inspection took 6 hours between 7:00 a.m. and 1:00 p.m.

General Bridge Information

The bridge is located in Kent County. Constructed in 1964, the bridge carries I-196, M-21 EB over Lane Avenue in Grand Rapids.

Bridge Geometry

The bridge is 126-ft long, 45.6-ft wide and carries 2 lanes of traffic with 10.8-ft wide shoulders. The bridge orientation is North-South. This is a non-skewed three span bridge with eight beams per span. The beam lengths are: 63.00-ft at the central span and 31.5-ft at the side spans. Side span beam types are I and III, and center span beam type is II.

Abutments, Pier, Deck and Joints

Both abutments have a few vertical cracks. All piers have random cracks, spalls, delamination, and rust stains. Heavy rust stains and exposed reinforcement are observed on the east fascia of pier S1 and west fascia of pier S3. The severe pier and stringer conditions are shown in Photo 3-5.

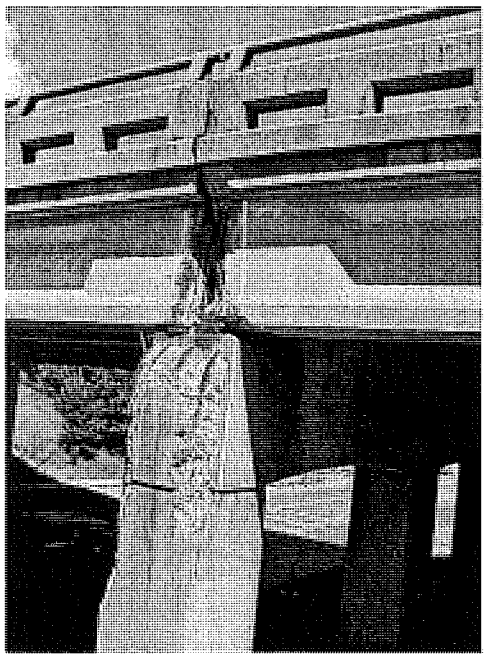

Photo 3-5. Documenting severe deterioration of the pier and beam end

The deck has potholes with bituminous patches. The presence of construction joints packing and seals cannot be detected. Continuous cracking and some openings with patch (bituminous) along joints are noted. Barriers have some cracking, scaling and some rust staining.

Stringers, Bearing and Diaphragms

Most of the beam-ends are partially delaminated and spalled showing exposed shear reinforcement. The example of severe beam-end deterioration is shown on Photo 3-6:

Photo 3-6. Severe deterioration of beam-end

Most of the sole plates are rusted and the neoprene pads appeared to have lost flexibility.

The diaphragms on both piers are cracked, spalled, and delaminated. The concrete diaphragms on pier W1 between beams S4 and S5 and on pier W2 between beams S2 and S3 are heavily spalled with exposed shear reinforcement (see Photo 3-7).

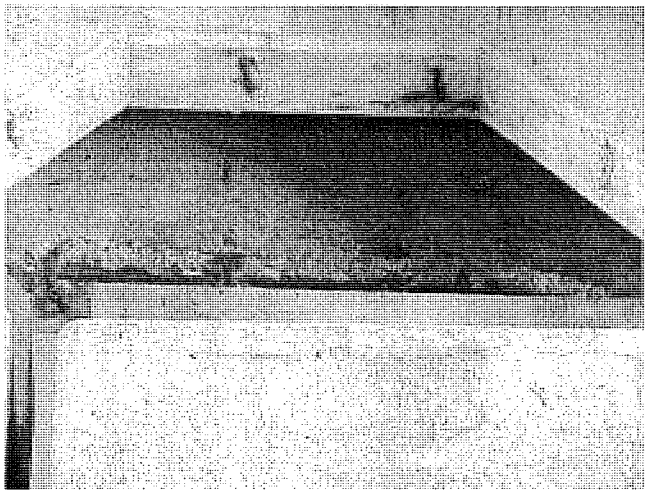

Photo 3-7. Diaphragm condition with some deterioration

3.7.1.3 *NBI No: 41029 S164*

The bridge was inspected on July 13, 2001. The inspection took 6 hours between 2:00 p.m. and 8:00 p.m.

General Bridge Information

The bridge is located in Kent County, constructed in 1964. The bridge carries I-196, M-21 WB over Lane Avenue in Grand Rapids.

Bridge Geometry

The bridge is 126-ft long, 45.6-ft wide and carries 2 lanes of traffic with 10.8-ft wide shoulders. The bridge orientation is West-East. This is a non-skewed three span bridge with eight beams per span. The beam lengths are: 63.00-ft at the central span and 31.5-ft at the side spans. Side spans beam types are I and III, and center span beam type is II.

Abutments, Pier, Deck and Joints

The abutments have a few vertical cracks and minor water and rust stains. Elastometric bearings are deformed. Piers have cracks, spalls, rust, and water stains. Shear reinforcement is exposed, and concrete has spalled at the bottom of the pier cap W1 (see Photo 3-8). Also, notice the difficulty of accessing the beam end behind the diaphragm for visual inspection.

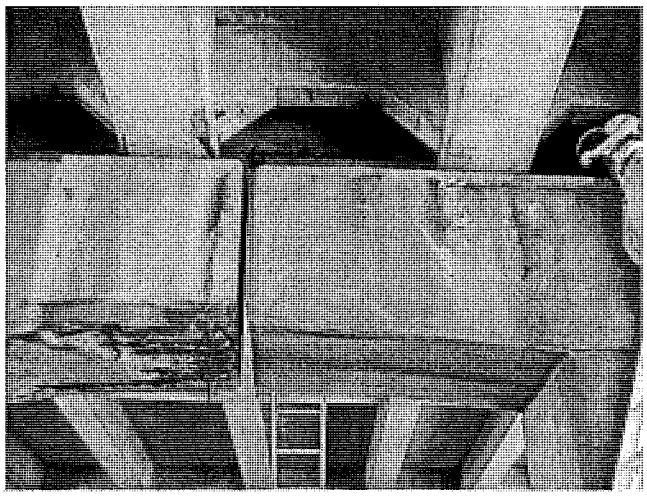

Photo 3-8. Exposed reinforcement and some spalls at piers, beam-end and diaphragms

The deck is overlaid with asphalt (see Photo 3-9)

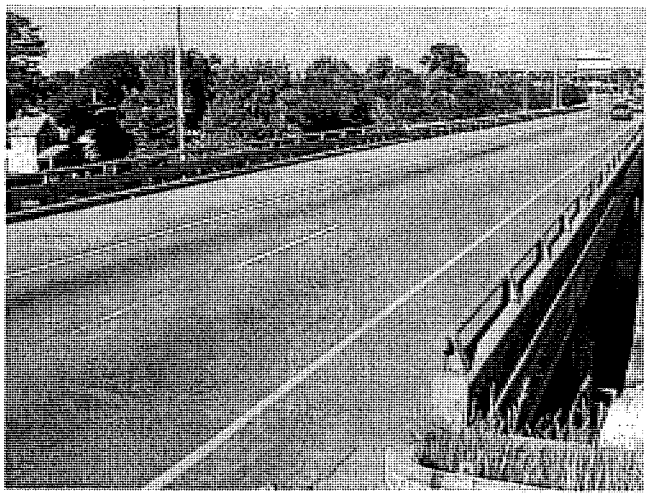

Photo 3-9. General view of the deck

Minor cracks and some spalls are noted along construction joints. Cracking, scaling and some rust stains are noted at the barriers.

Stringers, Bearing and Diaphragms

Most of the beam-ends display major cracking and spalls, rust and/or efflorescence stains, and exposed shear reinforcement. An example of the most severe deterioration of a beam-end and pier cap is shown in Photo 3-10:

Photo 3-10. Beam-end and pier cap deterioration

Some of the sole plates are corroded and neoprene pads deformed with the ends curling. Some diaphragms have cracks, spalls and delaminations. The concrete diaphragm on pier W1 between beams S2 and S3 shows spalls with exposed shear reinforcement (see Photo 3-11).

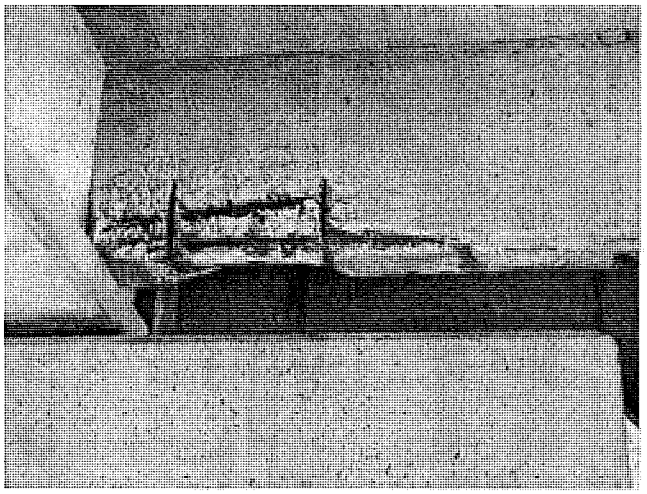

Photo 3-11. Spall with exposed reinforcement at diaphragm

3.7.1.4 *NBI No: 41027 S060*

The bridge was inspected on July 14, 2001. The inspection took 11 hours and 30 minutes between 7:00 a.m. and 6:30 p.m.

General Bridge Information

The bridge is located in Kent County. Constructed in 1963 the bridge carries US-131NB over 6th Avenue in Grand Rapids.

Bridge Geometry

The bridge is 138.7-ft long, 69.2 ft wide and carries 5 lanes of traffic with 4.6-ft wide sidewalks. The bridge orientation is North-South. This is a non-skewed three span bridge with twelve beams per span. The beam lengths are: 58.8-ft at the central span and 37.70-ft at the side spans. Side spans beam types are II, and center span beam type is III.

Abutments, Pier, Deck and Joints

The north abutment has vertical cracks through all abutment depth, spalls and rust stains. East side of the abutment has exposed reinforcement at wing wall. The south abutment has minor hairline vertical cracks.

Pier S1 has rust stain, delamination, spalls and rusty cracks. The north fascia of the pier is spalled with exposed reinforcement as shown in Photo 3-12.

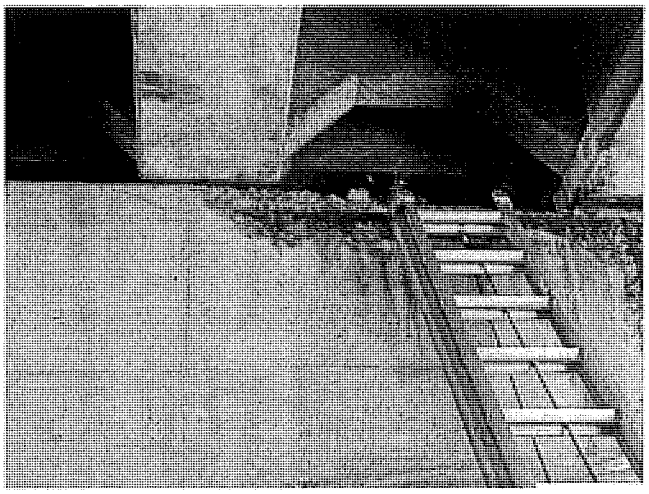

Photo 3-12. Spall at the North fascia of pier S1

Pier S2 has random cracks, spalls, rust and water stains, and delaminations. The south and north fascias of pier S2 have exposed shear reinforcement.

The deck has few patches, spalls, and a wide crack at the construction joint S1. Vertical cracks, spalls, efflorescence and rust stains are noted at both barriers.

Stringers, Bearing and Diaphragms

The beam-ends display cracks and spalls of various scales with rust and efflorescence stains.

Some of the concrete diaphragms on the South and North sides of pier S2 are cracked, delaminated and showed efflorescence and rusted stains. Concrete diaphragms on the North side of pier S1 are delaminated and exhibit efflorescence stains. The concrete diaphragms on the South side of pier S1 are in good condition.

Most of the sole plates are corroded and neoprene pads appear to have lost flexibility and deformed with ends curling.

3.7.1.5 *NBI No: 41025 S070*

The bridge was inspected on July 15, 2001. The inspection took 6 hours between 7:00 a.m. and 1:00 p.m.

General Bridge Information

The bridge is located in Kent County. Constructed in 1961 the bridge carries Knapp Street over I-96 in Grand Rapids.

Bridge Geometry

The bridge is 210.9-ft long, 32.8-ft wide and carries 2 lanes of traffic with 4.4-ft wide sidewalks. The bridge orientation is East-West. This is a non-skewed four span bridge with six beams per span. The beam lengths are 70.00-ft at the central spans and 35.00-ft at the side spans. The beam types of the two side spans are types II and III, and the beam type of the two center spans is type III.

Abutments, Pier, Deck and Joints

The west abutment has minor cracks, delamination and small areas of rust and water stains. The North side of West abutment is partially spalled with exposed reinforcement.

The east abutment has some vertical and horizontal cracks, delamination, and rust, water and efflorescence stains. The sole plates are corroded. The severe condition on the east abutment and delamination at the end of beam S3 are shown in Photo 3-13.

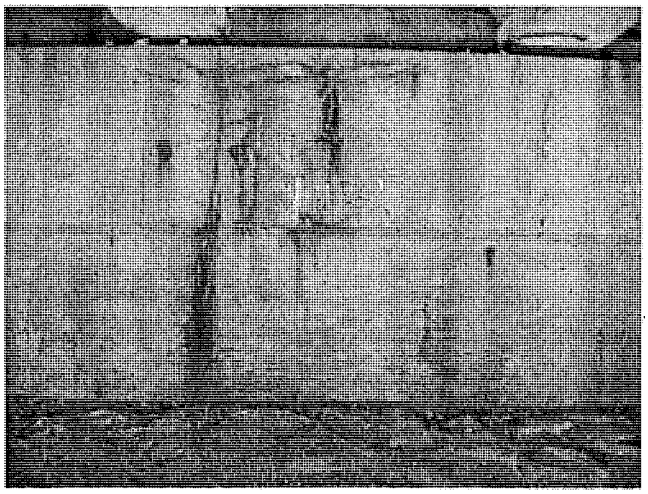

Photo 3-13. Condition of east abutment

Minor spalls, efflorescence, rust stains, and visible cracks are noted at West fascia of pier W1. The East fascia of pier cap of pier W1 is in good condition. Cracks, delamination, spalls, rust, and efflorescence stains are noted at the bottom of columns of pier W1.

Minor areas of spall, delamination, efflorescence and rust stains are noted at West fascia of the pier W2. Delamination, rust, water stains, and spalls are noted at the East fascia of pier W2. Efflorescence, rust, water stains, delaminations, spalls, and cracks are noted at both fascias of pier W3.

Cracks and potholes are noted between the deck and approaches. The deck shoulders are covered with sand and debris. Minor cracks and some spalls are noted along construction joints. Some joints are sealed. Multiple cracks, rust, and efflorescence stains are noticed at the barriers. The drainages are all clean and operable.

Stringers, Bearing and Diaphragms

Most of the beam-ends display cracks, spalls, water stains, rust and efflorescence. A few of the beams have exposed shear reinforcement. The sole plates are rusted and pads appear to have lost flexibility and are deformed with the ends curling.

The diaphragms at pier W1 are patched and have delamination, rust stains, and exposed reinforcement. The diaphragms at pier W2 show cracks, exposed reinforcement, and rust. The diaphragms at pier W3 are in good condition with minor areas of delamination at the bottom.

The example of the most severe deterioration of beam-end and diaphragm is shown in Photo 3-14.

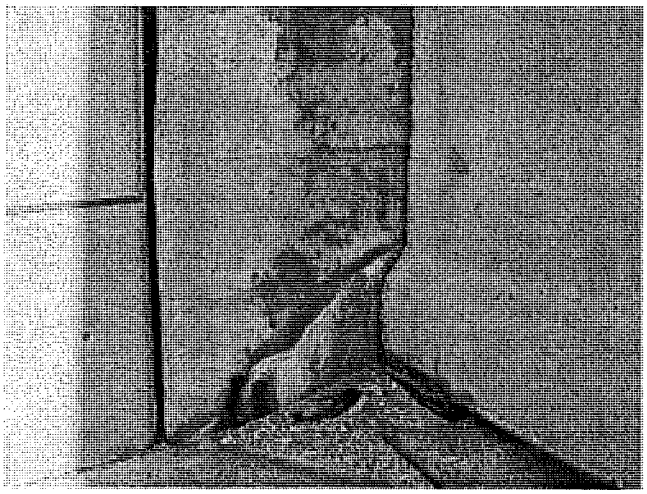

Photo 3-14. Beam-end and diaphragm condition

3.7.2 North Region

3.7.2.1 *NBI No: 67016 S090*

The bridge was inspected on July 18, 2001. The inspection took 3 hours between 9:00 a.m. and noon.

General Bridge Information

The bridge is located in Oceola County. It was constructed in 1984, and the bridge carries US-131 NB over US-10 in Reed City.

Bridge Geometry

The bridge is 111.0-ft long, 47.3-ft wide and carries 3 lanes of traffic with one 8-ft wide shoulder. The bridge orientation is North-South. This is a non-skewed one span bridge with six beams. The beam length is 111.00-ft and the beam type is Wisconsin 70" prestressed concrete I-beams.

Abutments, Deck and Joints

Both abutments have a few hairline vertical cracks through all retaining walls. Rust and efflorescence stains, spall and delamination noted. Efflorescence stain is noted at the bottom of the deck next to abutment as shown in Photo 3-15.

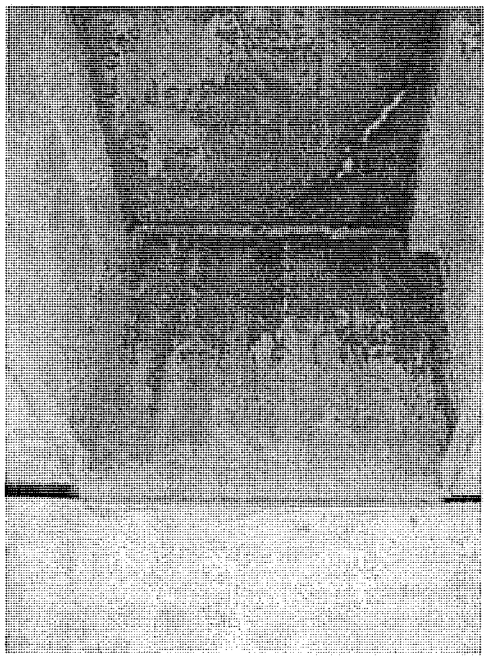

Photo 3-15. Rust and efflorescence stain on the deck

Next to the bearings there are water and rust stains. Some of the sole plates are partially rusted. Both embankments are in good condition. There is some vegetation on the slope.

The deck is new, and the drainage system is clean. Shoulders are covered with debris and some water stains are noted. The approaches are cracked and patched by asphalt. Minor cracks and some potholes are noted along construction joints.

Stringers and Diaphragms

Most of the beam-ends display minor cracking, spalls and rust stains. The common crack pattern is as shown in Photo 3-16.

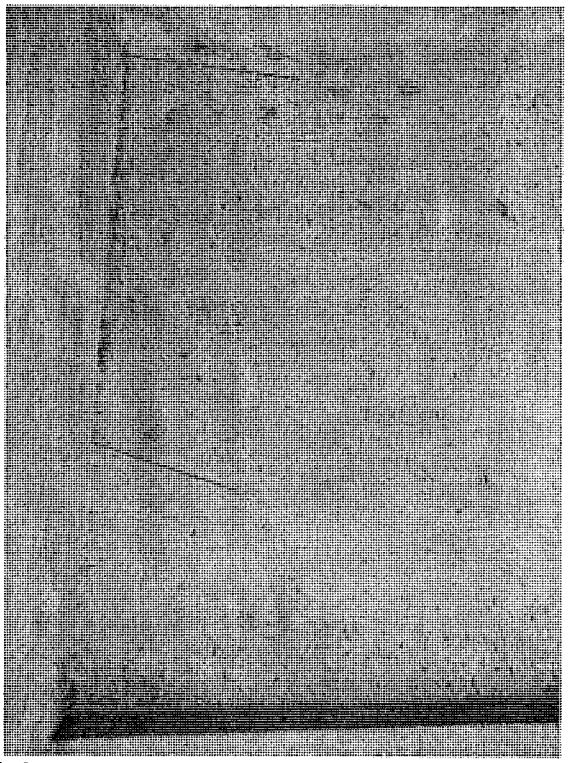

Photo 3-16. Beam-end common crack pattern (cracks outlined in blue)

The diaphragms located at the south abutment are in good condition. The team did not have equipment to check the diaphragms located at the middle of the span.

3.7.2.2 *NBI No: 67016 S100*

The bridge was inspected on July 18, 2001. The inspection took 3 hours and 30 minutes between 1:00 p.m. and 4:30 p.m.

General Bridge Information

The bridge is located in Oceola County. Constructed in 1984 the bridge carries US-131 SB over US-10 in Reed City.

Bridge Geometry

The bridge is 108-ft long, 53.1-ft wide and carries 3 lanes of traffic with 8-ft wide shoulders. The bridge orientation is North-South. This is a non-skewed one span bridge with seven beams. The beam length is 108.00-ft and the beam's type is Wisconsin 70" prestressed concrete I-beams.

Abutments, Deck and Joints

Both abutments have vertical cracks through all retaining walls, rust and water stains. Neoprene pads are in good condition. Sole plates have some rust. Both embankments are in good condition.

The deck is concrete. Expansion joints are full of sand and have rust stains and spall. Sand and water stains are noted at the shoulders. West concrete barrier has spall at South end of the deck. The approaches have some potholes and asphalt patches.

Stringers and Diaphragms

Most of the beam-ends display minor cracking, spalls, rust and water stains next to the bearings. The common crack pattern is as shown in Photo 3-17.

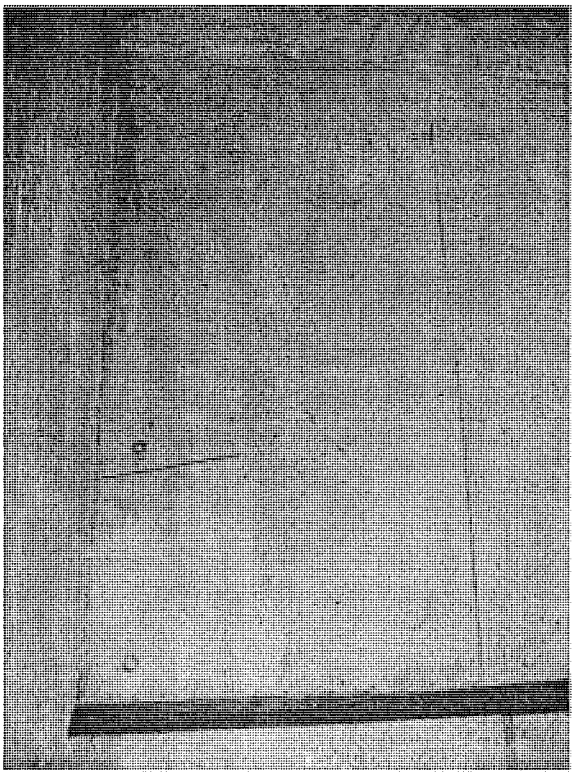

Photo 3-17. Beam-end common crack pattern (cracks outlined in blue)

The diaphragms located on the South abutment are in good condition. The team did not have equipment to check the diaphragms located at the middle of the span.

3.7.2.3 *NBI No: 53034 S050*

The bridge was inspected on July 19, 2001. The inspection took 7 hours between 7:00 a.m. and 2:00 p.m.

General Bridge Information

The bridge is located in Mason County. Constructed in 1986 the bridge carries Chauvez Road over US-31 in Ludington.

Bridge Geometry

The bridge is 305.77-ft long, 41.00-ft wide and carries 2 lanes of traffic with 7.4-ft wide shoulders. The bridge orientation is West-East. This is a skewed four span bridge with six beams per span.

The beam lengths are: 108.10-ft at two central spans W2 and W3, 37.70-ft at span W1 and 44.7-ft at span W4. The center spans beam type is Wisconsin 70" prestressed concrete I-beam. Side spans beams are 28" prestressed concrete I-beams for the interior beams and Wisconsin 70" prestressed concrete I-beams for fascia beams.

Abutments, Pier, Deck and Joints

The West abutment has a vertical hairline crack through all of the retaining wall. Both abutments have a few vertical cracks and minor rust, efflorescence and water stains. The sole plates have some rust.

Cracks, efflorescence, rust and water stains are noted at the piers caps. All pier caps are sealed with resin. The pier columns do not display any kind of deterioration. The common pier condition is shown in Photo 3-18.

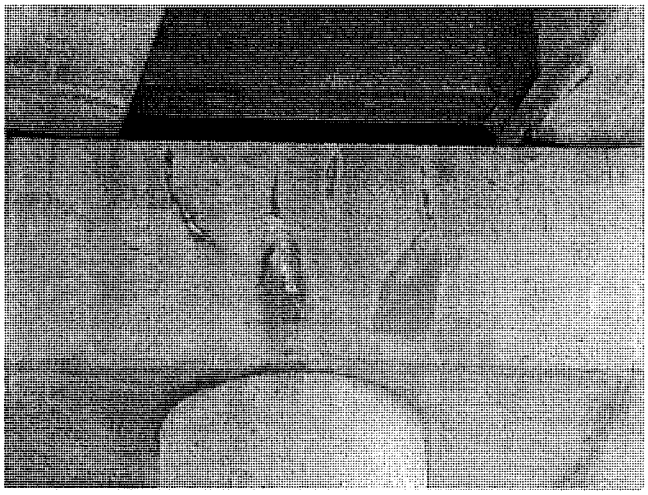

Photo 3-18. Pier condition with leaching from stress cracks

The bottom of the deck has some efflorescence staining mostly near the back wall as shown in Photo 3-19.

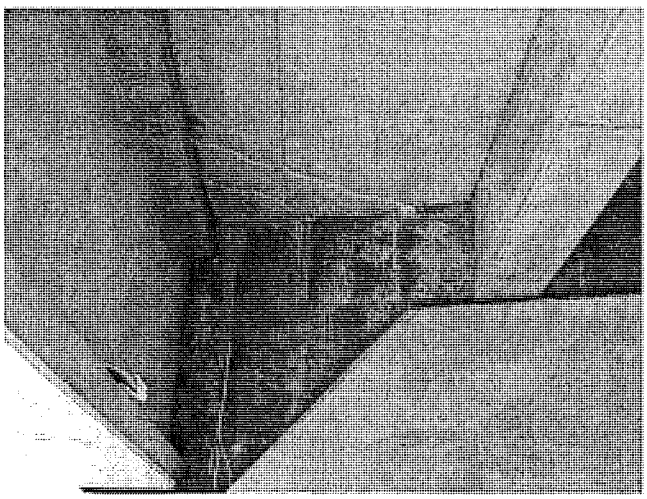

Photo 3-19. Efflorescence stain at bottom of the deck

The expansion joints are cracked and filled with sand. Sand is noted in the construction joints. The surface of deck has small potholes. The spalls are patched with epoxy. The concrete barrier has efflorescence stains and cracks.

Stringers, Bearings and Diaphragms

Most of the beam-ends display minor water and rust stains and micro and hairline cracks. The example of map cracking is shown in Photo 3-20.

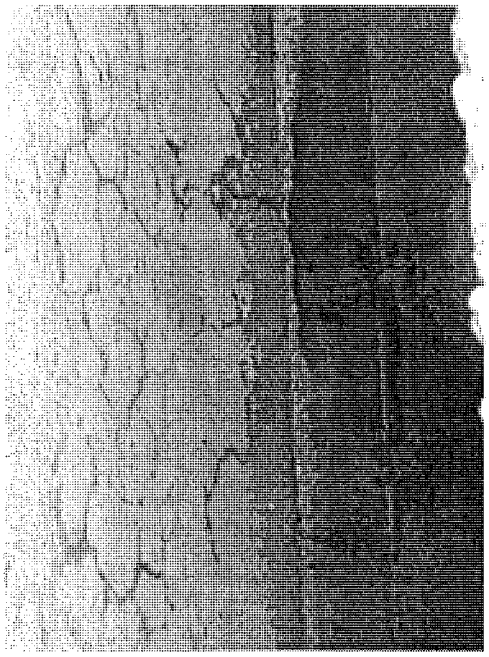

Photo 3-20. Example of map cracking at a beam-end

Some of the beam-ends are patched. Some of the sole plates are partially or completely rusted. Several neoprene pads are discolored. Hairline cracks are noted at some of the diaphragms, but most of them do not show any deterioration.

3.7.2.4 *NBI No: 83033 S060*

The bridge was inspected on July 19 and July 20, 2001. The inspection took 6 hours between 4:00 p.m. and 6:30 p.m. on July 19 and between 7:00 a.m. and 10:30 a.m. on July 20.

General Bridge Information

The bridge is located in Wexford County. Constructed in 1997 the bridge carries No. 36 Road over US-131 in Cadillac (Sec. 27 and 34 Haring TWP).

Bridge Geometry

The bridge is 146.00-ft long, 47.2-ft wide and carries 2 lanes of traffic with 10-ft wide shoulders. The bridge orientation is West-East. This is a non-skewed one span bridge with eight beams. The beam length is 142.6 ft and the beam type is Michigan 1800 beam.

Abutments, Deck and Joints

The West abutment has vertical cracks through the retaining wall. Spalls and delaminations are noted at wall top corners. The East abutment has vertical cracks through the entire retaining wall and light rust stains at both, North and South, sides.

The deck is new. A crack with efflorescence is noted at the bottom near the West abutment between beams S3 and S4. Sand and stones are accumulated on the shoulders and joints.

Stringers, Bearings and Diaphragms

Most of the beam-ends display hairline cracks. The examples of hairline cracks are shown in Photo 3-21 and Photo 3-22 (The crack is traced with purple chalk).

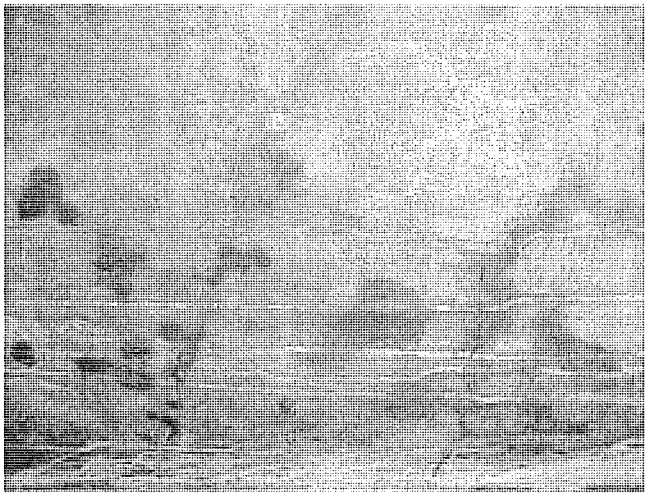

Photo 3-21. Example of hairline cracks

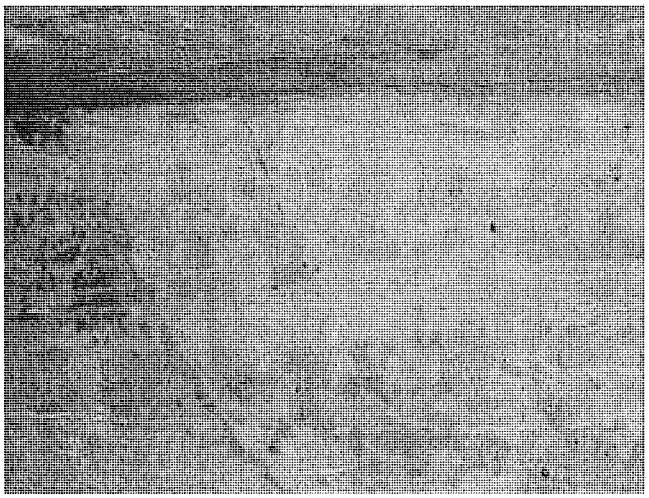

Photo 3-22. Example of hairline cracks

Some of the beam-ends are patched. Some of the sole plates are missing. Neoprene pads are deformed, dried out, or discolored.

3.7.2.5 *NBI No: 83033 S050*

The bridge was inspected on July 20, 2001. The inspection took 4 hours between 11:00 a.m. and 3:00 p.m.

General Bridge Information

The bridge is located in Wexford County. Constructed in 1998, the bridge carries Whaley Road over US-131 Reloc. in Cadillac.

Bridge Geometry

The bridge is 237.5-ft long, 47.2-ft wide and carries 2 lanes of traffic with 1.75-ft wide sidewalk. The bridge orientation is West-East. This is a skewed two span bridge with four beams per span. The beam length is 124.8-ft for the first span and 112.9-ft for second span. The beam type is Wisconsin 70" prestressed concrete I-beam.

Abutments, Pier, Deck and Joints

The West abutment has a few vertical hairline cracks through the retaining wall. The East abutment has few vertical and diagonal hairline cracks. On the back walls of both abutments vertical cracks, efflorescence, and rust stains are noted.

Water stain and few patches are noted on both the West and East fascias at the caps of the middle pier. Several pier columns have water stain (see Photo 3-23).

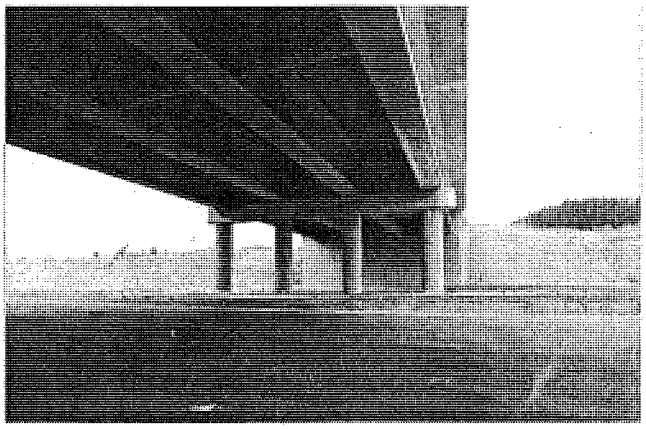

Photo 3-23. Water stain on the piers and caps

The bottom of the deck has efflorescence stain at the South corner of the West abutment and the North corner of the East abutment (see Photo 3-24).

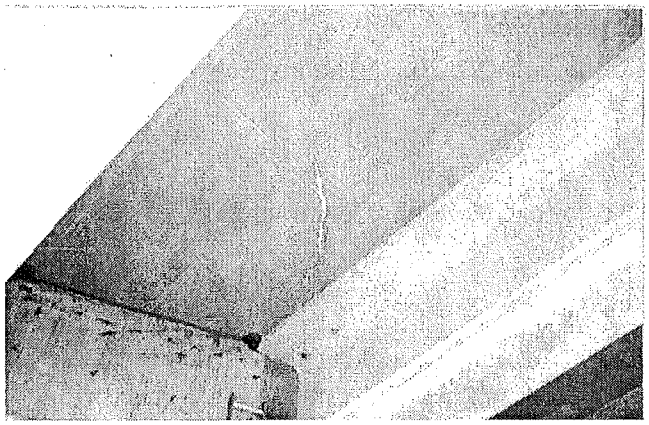

Photo 3-24. Efflorescence stain at South corner of West abutment and deck

The construction joints are cracked and filled with sand. An example of a control joint with hot-pour joint sealant is seen in Photo 3-25.

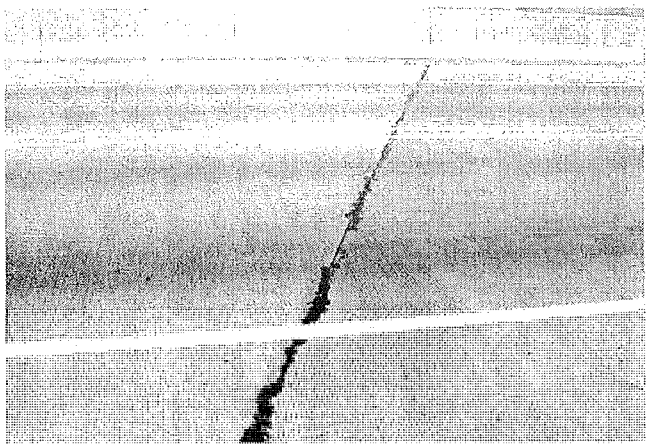

Photo 3-25. Condition of Deck Control joint

The sidewalks are covered with sand and gravel. The concrete barriers have a few cracks, rust, and efflorescence stains.

Stringers, Bearings and Diaphragms

Most of the beam-ends display microscopic and hairline cracks as shown in Photo 3-26.

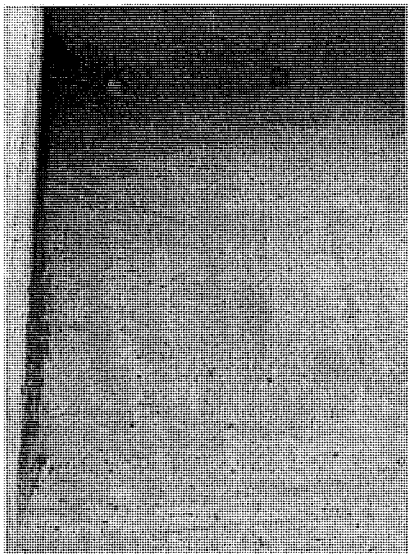

Photo 3-26. Hairline cracks at beam-end

Some of the beam-ends have incipient spalls as shown in Photo 3-27.

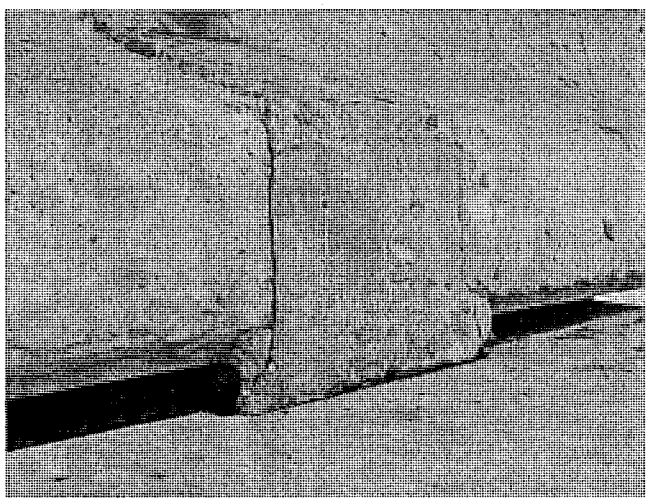

Photo 3-27. Beam-end restraint detail

Elastomeric bearings do not show any kind of deterioration. Few diaphragms at the middle pier have minor efflorescence and water stains. One diaphragm between beams S3 and S4 is patched. Diaphragm on the East abutment, North corner has crack and efflorescence stain.

3.7.3 Bay Region

3.7.3.1 *NBI No: 25042 S124*

The bridge was inspected on July 23 and July 24, 2001. The inspection took 5 hours between 7:30 a.m. and 10:00 a.m. on July 23 and July 24.

General Bridge Information

The bridge is located in Genesee County. Constructed in 1969 the bridge carries I-69 WB over I-75.

Bridge Geometry

The bridge is 210.0-ft long, 43.0-ft wide and carries 2 lanes of traffic with 18.0-ft wide shoulders and curbs. The bridge orientation is West-East. This is a skewed four span bridge with seven beams per the two center spans and four beams per the two side spans. The beam lengths are: 65.5-ft for two central spans W2 and W3, 38.5-ft for span W1 and 34.4-ft for span W4. The side and center spans beam type is III.

Abutments, Pier and Deck

The West abutment has several vertical cracks with water and rust stains (see Photo 3-28).

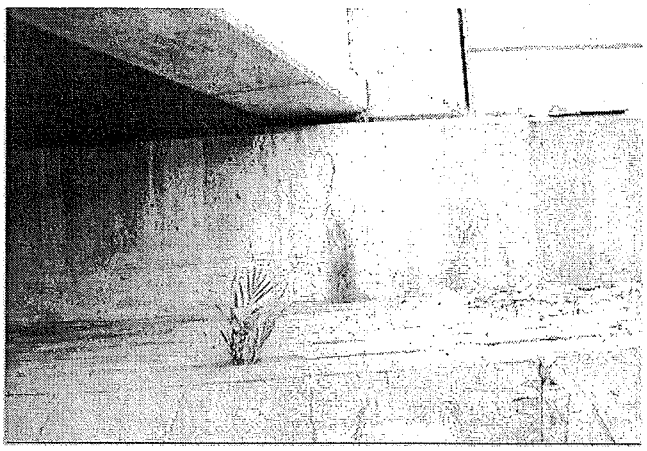

Photo 3-28. Vertical crack with moisture and rust stain at West abutment

The East abutment has a few vertical cracks, rust and water satins, and efflorescence stain at the North side of the abutment.

The pier caps have rust and water stain, and delamination. An efflorescence stain is noted at pier W3. The bottom of the cap of pier W2 is spalled and showing exposed reinforcement.

An efflorescence stain is noted at the bottom of the deck next to the East abutment. The surface of the deck was not inspected due to the time limit.

Stringers, Bearing and Diaphragms

Most of the beam-ends are delaminated, cracked, spalled and some exhibit exposed shear reinforcement as shown in Photo 3-29 and Photo 3-30 (at pier W1, beam S1; at pier W2, beams S1, S2, S4 and S6; at pier W3, beams S2 and S6).

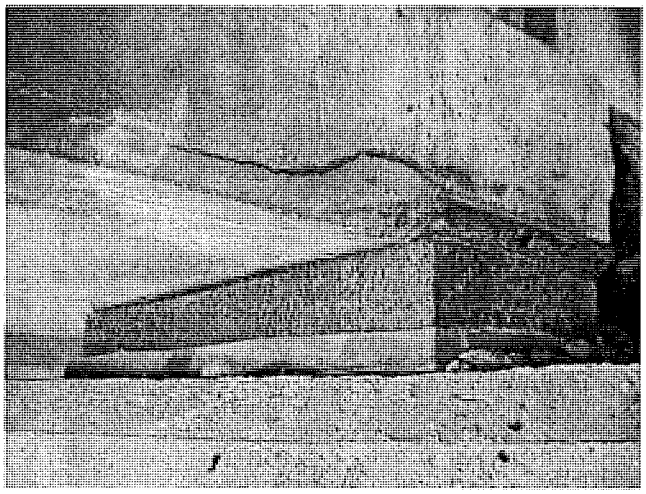

Photo 3-29. Delamination at the beam-end and bearing with sole plate

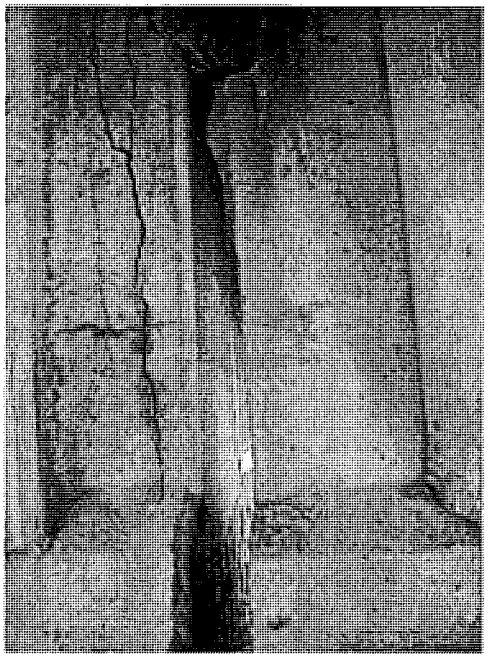

Photo 3-30. Beam-end cracking

Efflorescence stains are noted at some beam-ends. The beam-ends at the abutments have hairline cracks with some rust and water stain. Bearing plates are rusted and pads appear to have lost flexibility and deformed with ends curling.

Several diaphragms are cracked and delaminated. The diaphragms at pier W3 between beams S4 and S5 and pier W1 between beams S2 and S3 are spalled showing exposed shear reinforcement.

3.7.3.2 *NBI No: 25042 S123*

The bridge was inspected on July 23 and July 24, 2001. The inspection took 5 hours between 10:00 a.m. and 12:30 p.m. on July 23 and July 24.

General Bridge Information

The bridge is located in Genesee County. Constructed in 1969 the bridge carries I-69 EB over I-75.

Bridge Geometry

The bridge is 210.0-ft long, 43.0-ft wide and carries 2 lanes of traffic with 18.0-ft wide shoulders and curbs. The bridge orientation is West-East. This is a skewed four span bridge with seven beams per the two center spans and four beams per the two side spans. The beam lengths are: 65.5-ft for the two central spans W2 and W 3, 38.5-ft for span W1 and 34.4-ft for span W4. The side and center spans beam type is III.

Abutments, Pier and Deck

The east abutment has three vertical cracks through the entire abutment. Rust stain noted at one of the cracks located at the center of the abutment. A water stain is noted next to beam S1, and an efflorescence stain is noted next to beam S2. The West abutment has several vertical cracks with water and rust stains.

All of the pier caps have rust and water stains. Column S3 of pier W3 has multiple cracks. The cap of pier W1, N-end, has delamination and spall, and exposed reinforcement at the bottom. Pier W2, S-end, E-fascia has delamination.

An efflorescence stain is noted at the North corner at the bottom of the deck next to East abutment. The surface of the deck was not inspected due to the time limit.

Stringers, Bearing and Diaphragms

The beam-ends are cracked, delaminated, and spalled. Also, there is evidence of rust, water and efflorescence stains. The beam-ends of eight beams out of 22 are spalled with exposed shear reinforcement evident. The beam-ends at the abutment have hairline cracks with some rust and water stain. The sole plates are rusted and the pads appear to have lost flexibility and are deformed. The diaphragms between beams S5, S6 and S7 at pier W1 are delaminated. The diaphragm between beams S1 and S2 at pier W3 is delaminated at the bottom and partially spalled with exposed reinforcement. The condition at the beam-ends at the pier caps is shown in Photo 3-31.

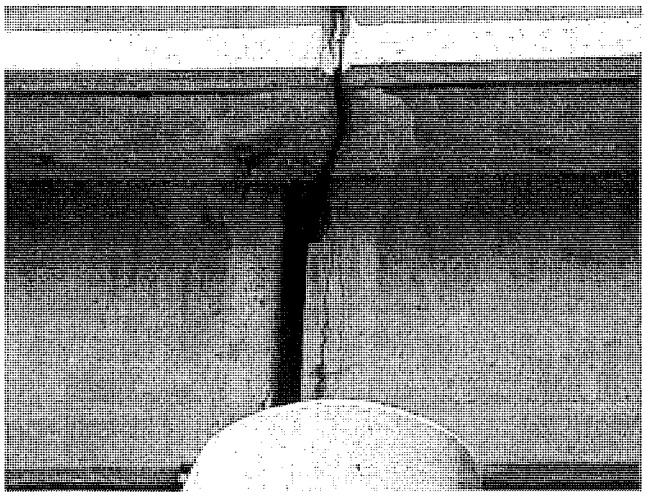

Photo 3-31. Condition at the beam-ends at the pier

3.7.3.3 *NBI No: 25042 S128*

The bridge was inspected on July 23 and July 24, 2001. The inspection took 4 hours between 12:30 p.m. and 2:30 p.m. on July 23 and July 24.

General Bridge Information

The bridge is located in Genesee County. Constructed in 1967 the bridge carries I-69 Ramp F over I-75.

Bridge Geometry

The bridge is 210.0-ft long, 27.0-ft wide and carries 1 lane of traffic with curbs. The bridge orientation is West-East. This is a skewed four span bridge with five beams per the two center spans and three beams per the two side spans. The beam lengths are: 65.5-ft for two central spans W2 and W3, 38.5-ft for span W1 and 34.4 ft for span W4. The side and center spans beam type is III.

Abutments, Pier and Deck

The East abutment has one vertical crack and a water stain all over the abutment. The West abutment has wide vertical cracks thought the entire wall at the South and North sides of the abutment. Several vertical cracks, water stain, and delamination are noted between beams S1 and S3.

All of the pier caps have water and rust stains. Delamination, cracks, and rust stains are noted at the fascia and bottom of all pier caps (see Photo 3-32).

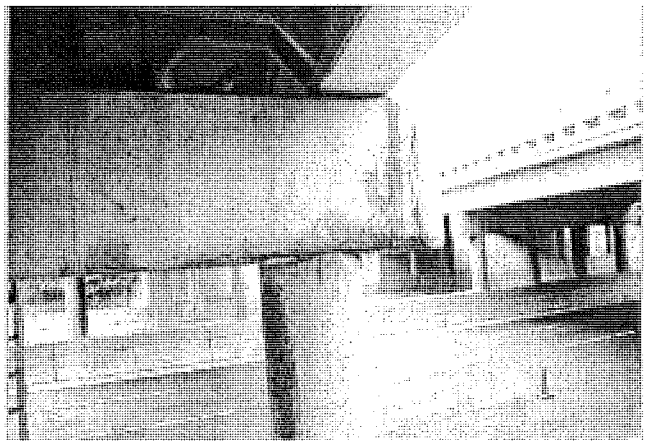

Photo 3-32. Delamination, cracks and rust stain at pier and pier cap

The bottom of pier W1 is spalled showing exposed reinforcement (see Photo 3-33).

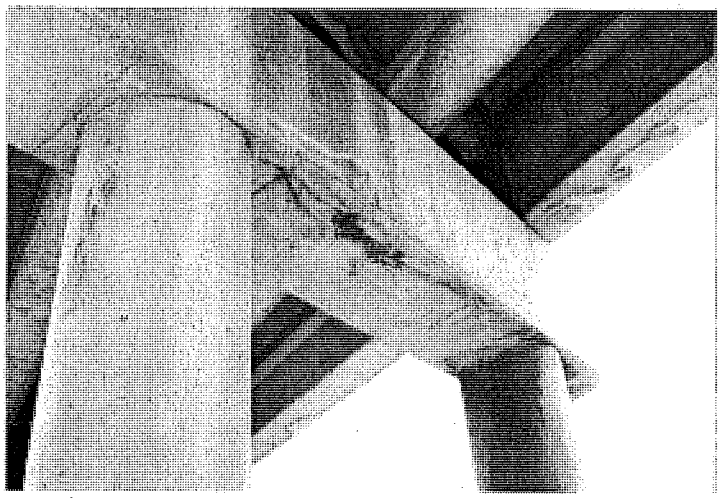

Photo 3-33. Exposed reinforcement at the bottom of the pier W1

No deterioration noted at the deck bottom. The surface of the deck was not inspected due to the time limit.

Stringers, Bearing and Diaphragms

All of the beam-ends are cracked. Many of the beam-ends have moisture leaching from the cracks. Some of the beam-ends are delaminated or spalled showing exposed shear reinforcement as shown in Photo 3-34.

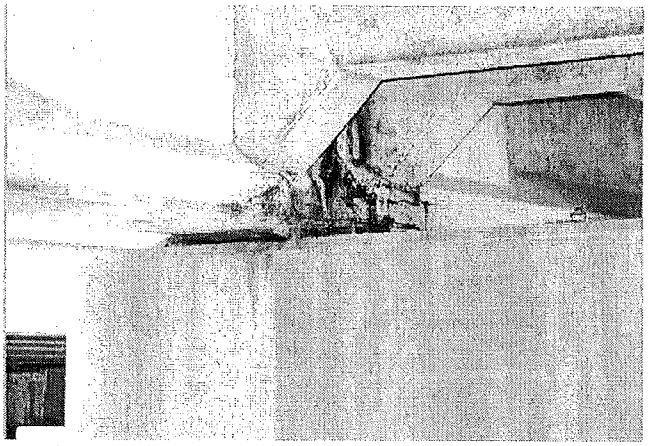

Photo 3-34. Deterioration at the beam-ends in between diaphragms

Some hairline cracks and small areas of water stain are noted at the beam-ends at the abutments. The sole plates are corroded, and the elastomeric pads are deformed. The diaphragms at pier W1 between beams S1 and S2 and S4 and S5 are cracked and delaminated and exhibit minor rust and efflorescence stains.

3.7.3.4 *NBI No: 25042 S127*

The bridge was inspected on July 23 and July 24, 2001. The inspection took 4 hours between 2:30 p.m. and 4:30 p.m. on July 23 and July 24.

General Bridge Information.

The bridge is located in Genesee County. Constructed in 1969 the bridge carries I-69 Ramp E over I-75.

Bridge Geometry.

The bridge is 210.0-ft long, 27.0-ft wide and carries 1 lane of traffic with curbs. The bridge orientation is West-East. This is a skewed four span bridge with five beams per the two center spans and three beams per the two side spans. The beam lengths are: 65.5-ft for two central spans W2 and W3, 38.5-ft for span W1, and 34.4-ft for span W4. The side and center spans beam type is III.

Abutments, Pier and Deck

The East abutment has vertical cracks through the abutment. The West abutment has vertical cracks thought the entire wall and rust and water stain.

Pier W1 has minor rust and water stain, spalls and cracks at both fascias (see Photo 3-35).

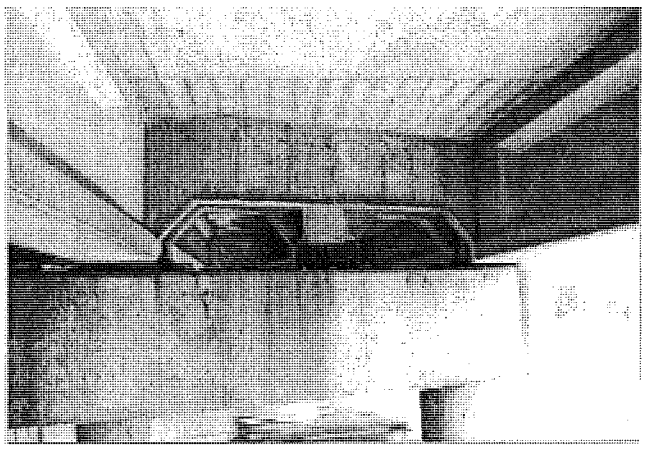

Photo 3-35. Rust and water stain, spalls and cracks at Pier W1

The East fascia of pier W1 has areas of delamination, cracks, and efflorescence stains. Piers W2 and W3 have water and rust stains. Pier W3 displays crack and delamination at the bottom of the pier cap (see Photo 3-36).

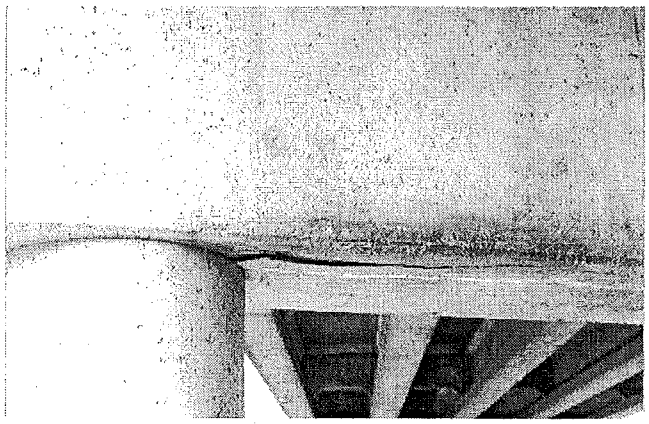

Photo 3-36. Crack and delamination at the bottom of the pier W3

Cracks and efflorescence stains are noted between piers W3 and W2 at the deck bottom. The surface of the deck was not inspected due to the time limit.

Stringers, Bearing and Diaphragms

The beam-ends at the piers are cracked, delaminated and spalled. Some of the beams have rust and efflorescence stain. Eleven beams out of twenty are spalled with exposed reinforcement. The beam-ends at the abutments have hairline cracks, water, and rust stains. The typical beam-end condition is shown in Photo 3-37.

Photo 3-37. Beam-end exhibiting significant deterioration

The exterior diaphragms at pier W1 are delaminated and display rust stains. The diaphragm between beams S2 and S3 has a diagonal crack. One exterior and two interior diaphragms at pier W3 are delaminated. The diaphragm between beams S2 and S3 exhibits spalling. The diaphragm between beams S1 and S2 has a large horizontal crack, rust, and efflorescence stain.

The sole plates are rusted, and the neoprene pads are deformed and discolored or dried out.

3.7.3.5 *NBI No: 06111 S11*

The bridge was inspected on July 25, 2001. The inspection took 11 hours and 30 minutes between 7:30 a.m. and 8:00 p.m.

General Bridge Information

The bridge is located in Arenac County. Constructed in 1968 the bridge carries M-33 over I-75 at 1.0 MI N of Alger.

Bridge Geometry

The bridge is 380.8-ft long, 48.2-ft wide and carries 4 lanes of traffic with narrow sidewalks. The bridge orientation is West-East. This is a skewed six span bridge with nine beams per span. The beam lengths are: 73.3-ft for the four central spans W2, W3, W4 and W 5, 37.0-ft for span W1 and 50.6-ft for span W6. The center spans beam type is III. Side span W1 beam types are II for fascia and I for interior. Side span W6 beam types are II for fascia and III for interior.

Abutments, Pier, Deck and Joints

The west abutment has several narrow cracks, light water stain, and minor area of spall and delamination. The East abutment has few narrow cracks at the North side and wide crack at the South side. Water and rust stains are noted along both abutments.

All pier caps have delamination, rust, and water stain. The worst condition at the piers is shown in Photo 3-38.

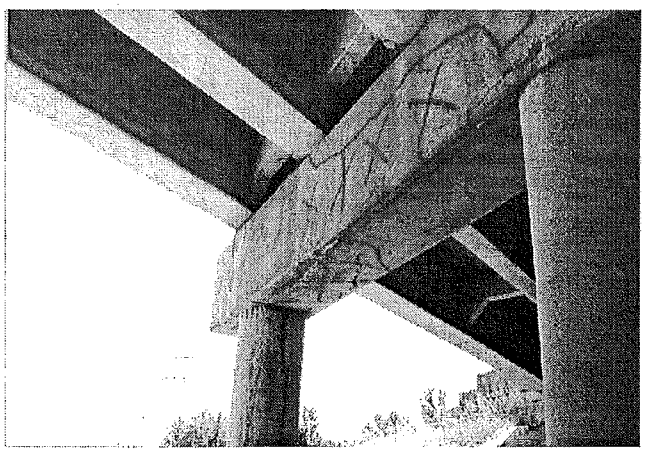

Photo 3-38. Condition of pier and pier cap

The corners of the pier caps at piers W4 and W5 are spalled and showing exposed reinforcement and efflorescence stains (see Photo 3-32). Some of the piers are cracked and patched. Most of the pier columns have water and rust stains. Column S4 of pier W1 has several wide vertical cracks thought all column height (see Photo 3-39).

Photo 3-39. Vertical cracks at column S4 of the pier W1

The surface of the concrete deck has many areas with cracks and efflorescence. The bottom of the deck is cracked with efflorescence and water stains next to both abutments. The deck sidewalks are covered with sand and gravel. Delamination, cracks, efflorescence, and rust are noted on the barriers. Some joints are filled with the sand. Several spalls and patches are noted along the joints. One joint has a spall with exposed reinforcement visible as shown in Photo 3-40.

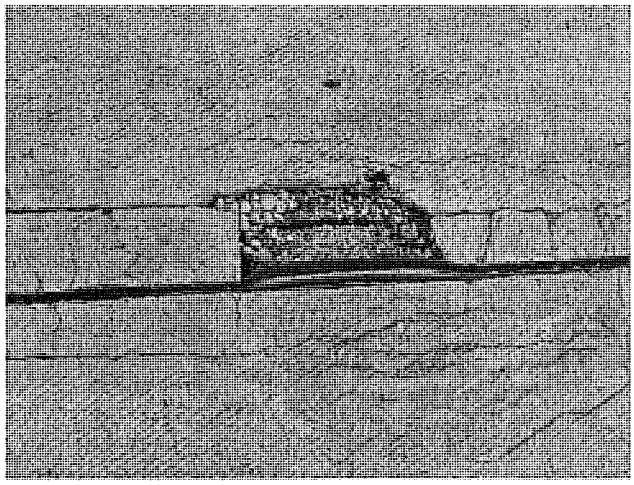

Photo 3-40. Spall with exposed reinforcement at the deck joint

Stringers, Bearing and Diaphragms

Vertical and horizontal cracks of various widths, from hairline to wide, are noted at the beam-ends (see Photo 3-41). Also, some beam-ends had been patched, but they were noted to have delaminations.

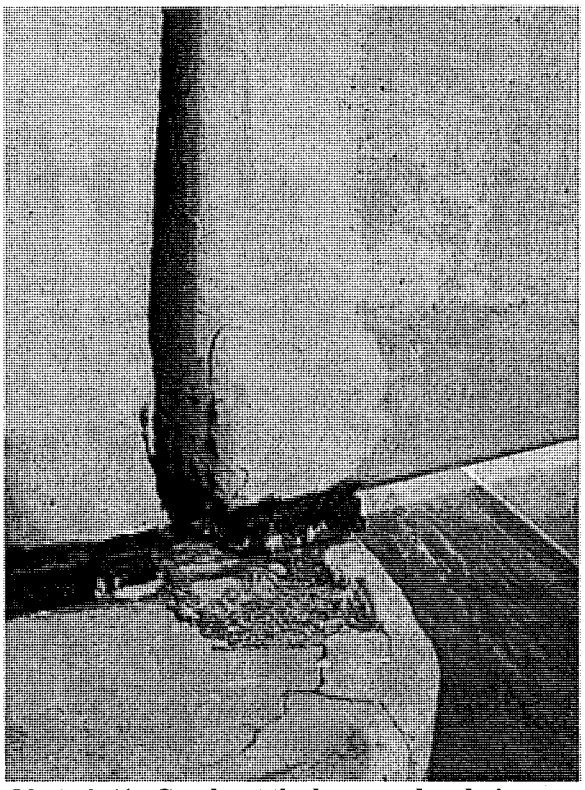

Photo 3-41. Cracks at the beam-end and pier cap

Some of the beam-ends have rust, water, and efflorescence stains and exhibit exposed shear reinforcement (see Photo 3-42). Sole plates are corroded. The diaphragms at the abutments are cracked. Most of the diaphragms at the piers are cracked and delaminated at their bottom and exhibit some rust stains and exposed reinforcement.

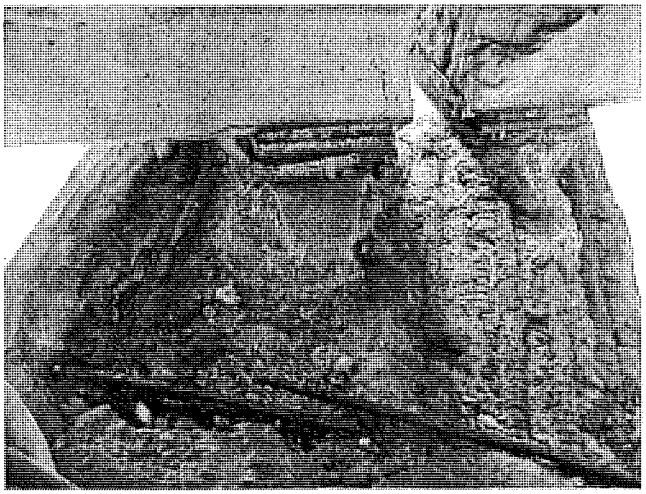

Photo 3-42. Delaminated beam-end and pier

3.7.3.6 *NBI No: 25132 S34*

The bridge was inspected on August 27, 2001. The inspection took 6 hours between 8:00 a.m. and 2:00 p.m.

General Bridge Information

The bridge is located in Genesee County. Constructed in 1971 the bridge carries I-475 over Clio Road at 1.5 MI E of N JCT I-75.

Bridge Geometry.

The bridge is 175.20-ft long, 51.51-ft wide and carries 2 lanes of traffic with variable shoulders width. The bridge orientation is West-East. This is a skewed four span bridge with six beams per span. The beam lengths are: 58.6-ft for the two central spans W2 and W3 and 29.0-ft for the two side spans W1 and W4. The two center spans beam type is III. Side span W1 and W4 beam types are II for fascia and I for interior.

Abutments, Pier, Deck and Joints.

Both abutments have several cracks through the entire wall. The West and East abutments have rust and water stains at the North and South corners. The North corner of East abutment spalled showing exposed reinforcement as shown on Photo 3-43.

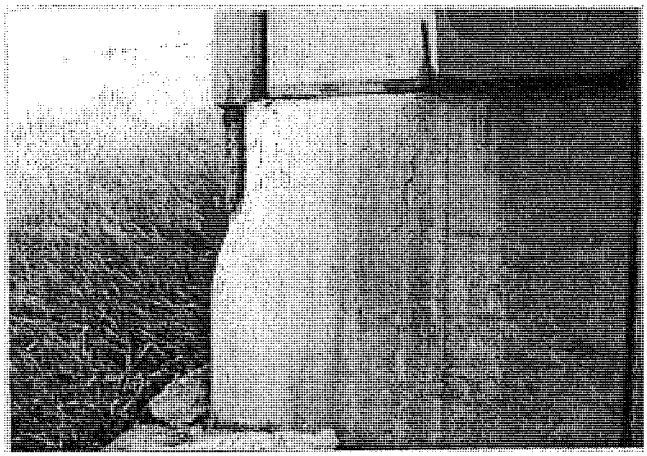

Photo 3-43. Spall at North corner of East abutment

The sole plates are partially rusted, and the neoprene pads are deformed, sometimes broken or displaced.

All piers show rust and water stains. Few cracks and some areas of delamination are noticed at the center pier W2.

The deck is under replacement. New concrete overlay is being placed on the East approach and main deck. Concrete on the West approach is removed up to the reinforcement. The shoulders are cracked. Cracks, some areas of water and efflorescence stains are noticed at the deck bottom. The concrete barriers are cracked at several locations. The hole through the entire width of the deck depth is noticed at the West approach (see Photo 3-44).

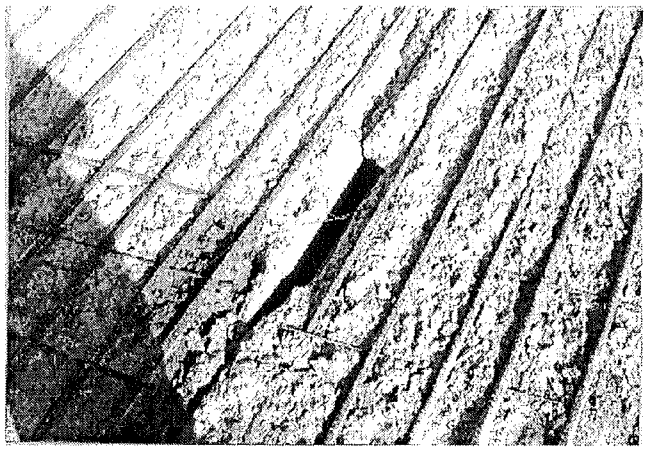

Photo 3-44. Hole at the deck West approach

Stringers, Bearing and Diaphragms

Major spall occurred at one of the beam-ends (Beam S5, Pier W3) and minor spalls are noticed at several others. Vertical and horizontal cracks are noted at the ends of beams. The typical beam-end condition is shown on Photo 3-45.

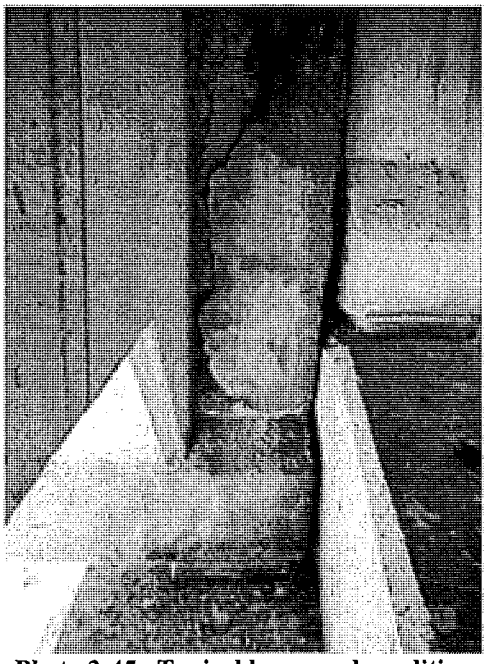

Photo 3-45. Typical beam-end condition

Spalls occurred at most of the beam-ends next to the bearings. The sole plates are rusted, and the neoprene pads are deformed and sometimes broken. An example of the beam-end condition is shown in Photo 3-46.

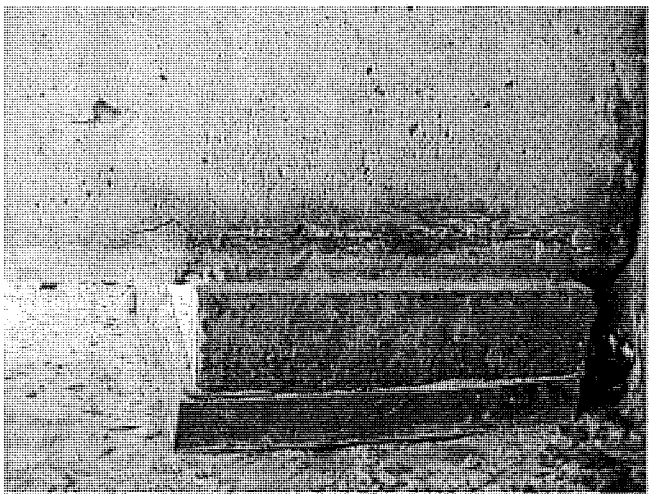

Photo 3-46. Rust crack at beam-end

The diaphragms at the abutments do not exhibit any kind of deterioration. Some of the diaphragms at the piers have cracks and small areas of delamination.

3.7.3.7 *NBI No: 29011 S03*

The bridge was inspected on August 27 and August 28, 2001. The inspection took 4 hours and 30 minutes between 4:00 p.m. and 6:30 p.m. on August 27 and between 7:00 a.m. and 9:00 a.m. on August 28.

General Bridge Information

The bridge is located in Gratiot County. Constructed in 1961 the bridge carries US-27 NB over US-27 BR (Polk Road) 2.0 MI N of Ithaca.

Bridge Geometry

The bridge is 113.9-ft long, 47.7 ft-wide and carries 2 lanes of traffic with 2.7-ft wide shoulders. The bridge orientation is North-South. This is a non-skewed three span bridge with nine beams per span. The beam lengths are: 43.9-ft for central span S2 and 35.0-ft for the two side spans S1 and S3. The center span beam type is II. The side spans S1 and S3 beam types are II for fascia and I for interior.

Abutments, Pier, Deck and Joints

The South abutment has horizontal and vertical cracks below beams W5 and W4, efflorescence, water and rust stains (see Photo 3-47).

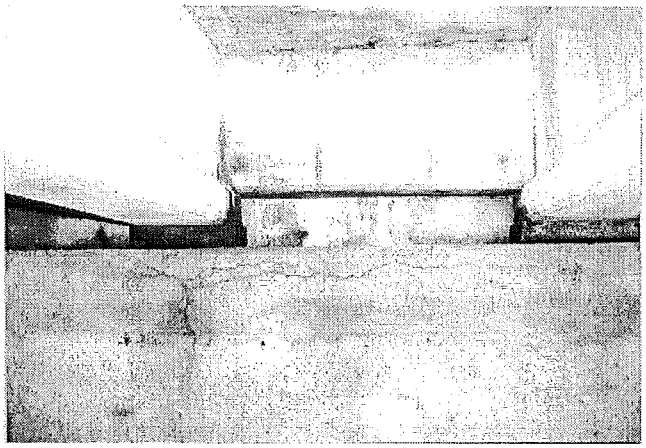

Photo 3-47. Condition of South abutment

The North abutment has water stains, heavy rust stains and areas of delamination and spall (see Photo 3-48).

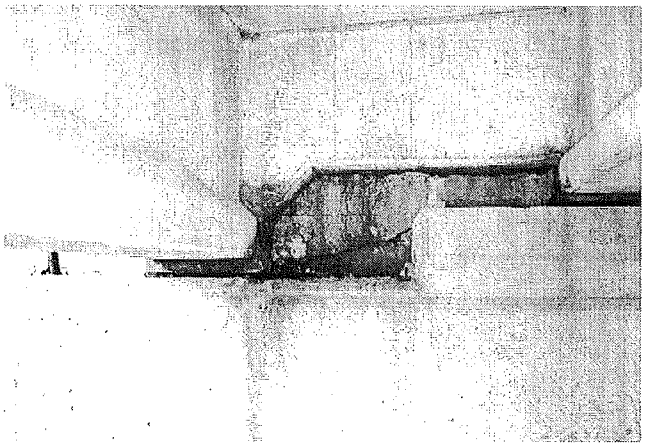

Photo 3-48. Condition of North abutment and diaphragm

Several vertical cracks are noticed thought out entire wall. Very wide diagonal crack noted at West side of the abutment. The sole plates are rusted. The elastomeric pads are in good condition. The pier caps have rust and water stains. Few cracks and some areas of delamination are noticed at pier W2 (see Photo 3-49).

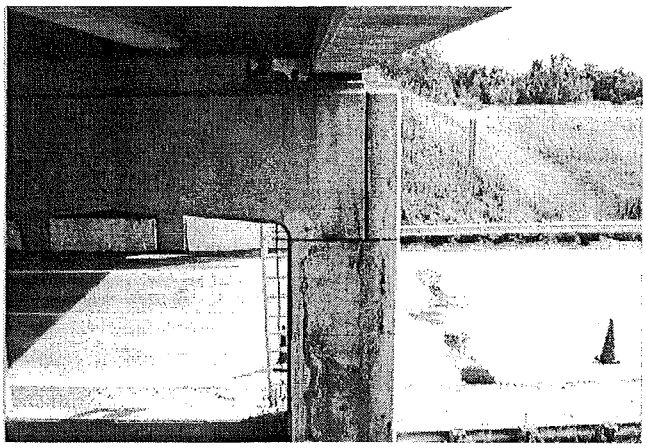

Photo 3-49. Deterioration observed at pier W2

Most of the columns are patched. Column W9, at pier S2 has cracks and water stains.

Several efflorescence and water stains are noted at the bottom of the deck. The concrete barriers have some cracks. The drains are clean and operable. Gravel and stone debris have accumulated on the shoulders. The joints are covered with an asphalt overlay. The overlay of the main deck and approach is new. The main deck has a new asphalt patch.

Stringers, Bearing and Diaphragms

Most of the beam-ends display cracks, some rusted, spalled and delaminated areas, and efflorescence and water stains (see Photo 3-50). The sole plates are discolored and deformed with ends curling. Some of the diaphragms at the piers are cracked and show rust and efflorescence stains. The diaphragms at the abutments have horizontal narrow cracks and small areas of rust and efflorescence stains.

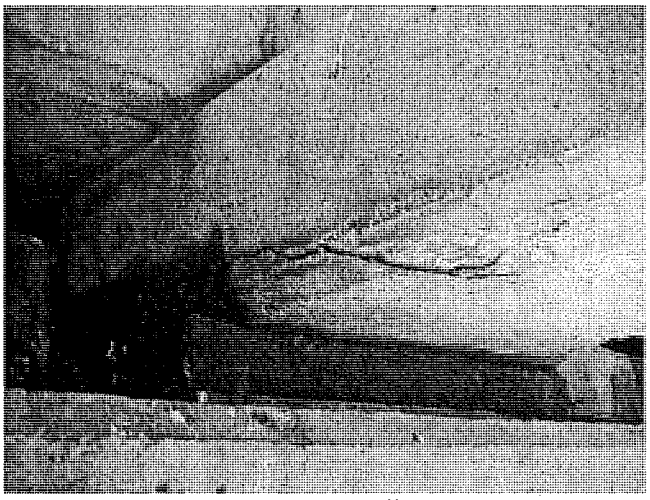

Photo 3-50. Rust and spall at beam-end

3.7.3.8 *NBI No: 06111 S04*

The bridge was inspected on August 28, 2001. The inspection took 5 hours between 10:30 a.m. and 3:30 p.m.

General Bridge Information

The bridge is located in Arenac County. Constructed in 1968 the bridge carries I-75 NB over M-61 at 4.0 MI W of Standish.

Bridge Geometry

The bridge is 111.8-ft long, 42.9-ft wide and carries 2 lanes of traffic with 9.45-ft wide shoulders. The bridge orientation is South-North. This is a non-skewed three span bridge with six beams per span. The beam lengths are: 49.0-ft at the central span S2 and 31.3-ft at the two side spans S1 and S3. The side spans beam types are III for fascia and I for interior, and center spans beam type is III.

Abutments, Pier, Deck and Joints

Both abutments have vertical crack through the center of the abutment and wet cracks with efflorescence stain at East and West corners. The North abutment has rust and water stains. The South fascia of pier S1 has heavy rust stains under beam W1. The North fascia of pier S1 has rust and water stains, delamination with spalls and exposed shear reinforcement. The worst condition observed was under beam W1 as shown in Photo 3-51.

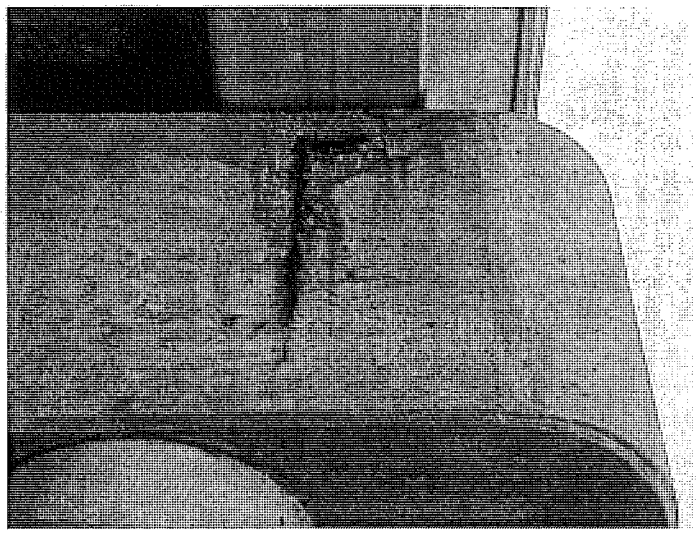

Photo 3-51. Spall with exposed reinforcement at pier S1 under beam W1

Both fascias of pier S2 have rust and water stain (see Photo 3-52).

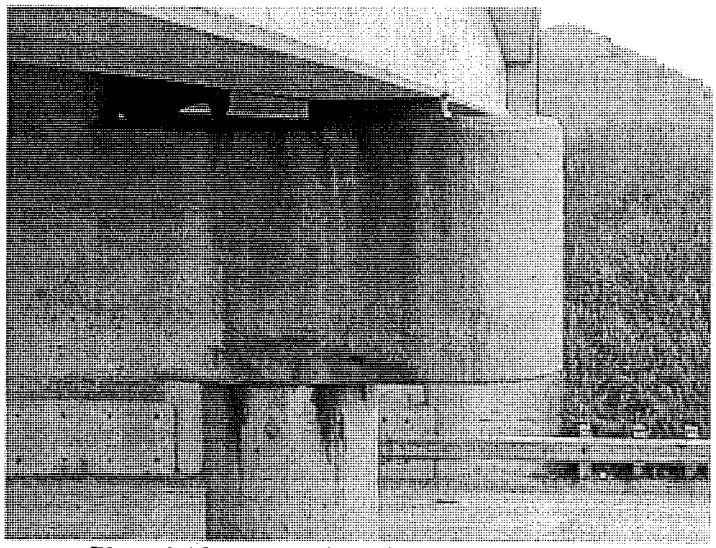

Photo 3-52. Rust stain and wet spots at pier S2

Efflorescence stains and a horizontal crack were noted under beam W6 at the pier cap, on the North fascia.

The deck has a new concrete overlay. Spalls at approaches and along joints were noted. At the South approach rusted cracks were noted. The joints are sealed with asphalt and are partially broken. The shoulders are patched and covered with sand, gravel and debris. The drainage system is clean and operable. The bottom of the deck displays multiple cracks and rust stains.

Stringers, Bearing and Diaphragms

The beam-ends at the piers display cracks, minor rust stain, and spall next to the bearings. Most of the sole plates are rusted and pads are deformed (see Photo 3-53).

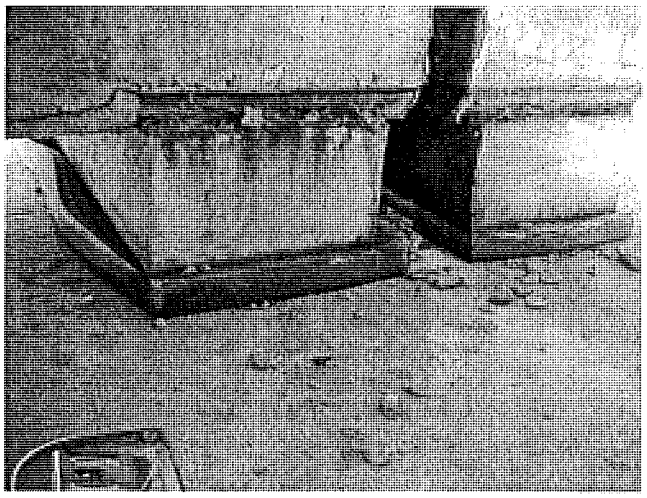

Photo 3-53. Condition of the bearings on pier

The diaphragms at the piers are in good condition. The diaphragms at the North abutment have small areas of delamination between beams W1 and W4 and exposed shear reinforcement

between beams W2 and W3. The diaphragms at the South abutment between beams S1 and S2 are cracked. The sole plates at the abutments are painted and slightly rusted.

Some of the neoprene pads appear to have lost flexibility, deformed and partially lost.

3.7.3.9 *NBI No: 06111 S05*

The bridge was inspected on August 29, 2001. The inspection took 5 hours and 30 minutes between 7:00 a.m. and 12:30 p.m.

General Bridge Information

The bridge is located in Arenac County. Constructed in 1968 the bridge carries Lincoln Road over I-75 SB in 2.4 MI South of Sterling.

Bridge Geometry

The bridge is 155.8-ft long, 32.2-ft wide and carries 2 lanes of traffic with 4.1-ft wide sidewalks. The bridge orientation is West-East. This is a skewed three span bridge with five beams per span. The beam lengths are: 54.80-ft at the central span W2, 33.6-ft at span W1 and 36.8-ft at span W3. The side spans beam types are III for fascia and II for interior, and center spans beam type is III.

Abutments, Pier, Deck and Joints

The west abutment has several hairline vertical cracks. The North side of the abutment has wet and leaching cracks (see Photo 3-54).

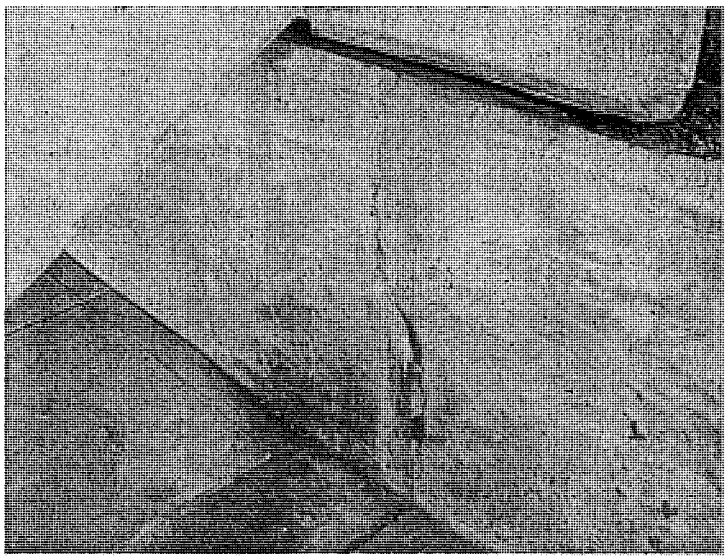

Photo 3-54. Leaching crack at the North side of West abutment

The East abutment has cracks between beams S2 and S4 and wet and leaching cracks at the South and North sides of the abutment.

Pier W1 has vertical and horizontal cracks, rust and water stains. Large area of delamination noted under beams S4 and S3 at the East fascia of pier W1. The West fascia of pier W1 exhibits

heavy rust stain and exposed reinforcement. Pier W2 has rust and water stain. Wet cracks, areas of exposed reinforcement and delamination noticed. The typical condition at the piers is shown in Photo 3-55:

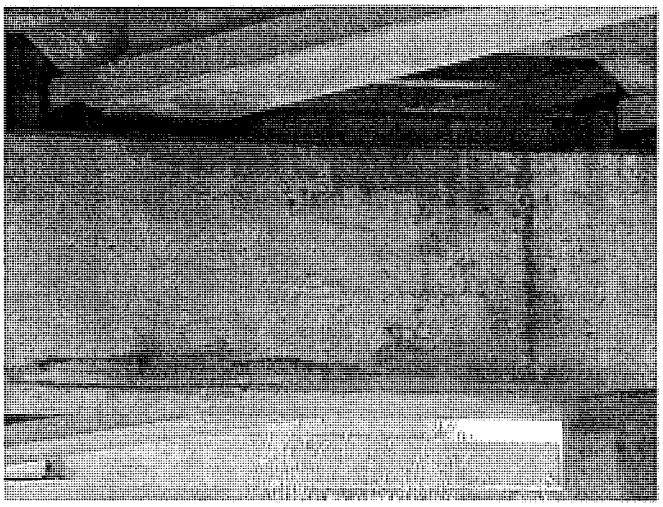

Photo 3-55. Typical pier cap beam condition

The concrete deck overlay is patched with the asphalt. The expansion and construction joints are broken and few asphalt patches noticed along the construction joints. Sand, gravel and debris accumulated along the sidewalks. The drain system is partially filled with debris. Cracks are noted at the deck bottom along East abutment and exposed reinforcement with rust stain around at bay S1. Efflorescence stain noted at bays S1 and S2 next to West abutment.

Stringers, Bearing and Diaphragms

The beam-ends display cracks, spalls, delamination, rust, water, and efflorescence stains (see Photo 3-56).

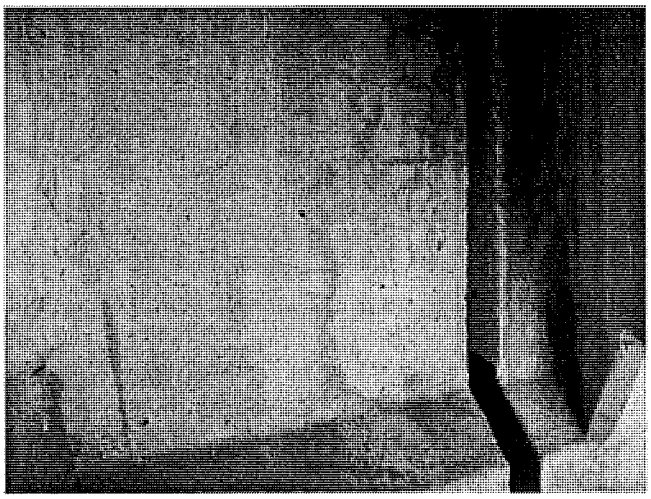

Photo 3-56. Cracks and water stain at the beam end

Some of the spalled beam-ends showed exposed reinforcement (see Photo 3-57).

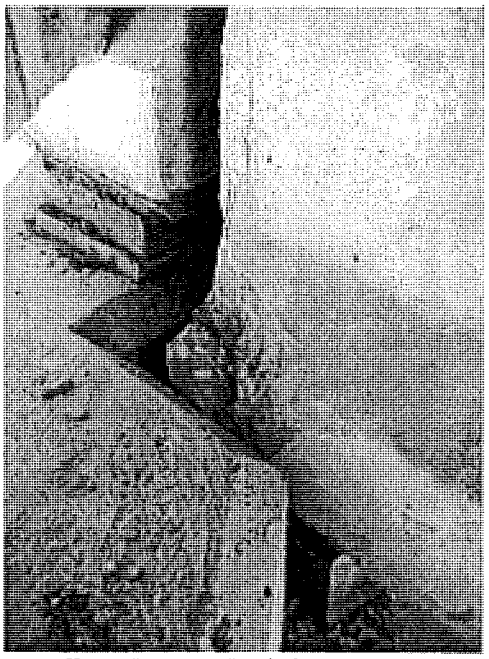

Photo 3-57. Cracks, spalls and exposed reinforcement at some of the beam-ends

The sole plates at the piers are rusted and bearing pads are deformed. The beam-ends at the abutments have hairline cracks, minor water and rust stains. The bearings at the abutments are painted but partially rusted. Some elastomeric pads are deformed with ends curling. Few diaphragms are cracked and have some rust and efflorescence stains.

3.7.3.10 *NBI No: 06111 S06*

The bridge was inspected on August 29, 2001. Inspection took 4 hours between 12:30 p.m. and 4:30 p.m.

General Bridge Information

The bridge is located in Arenac County. Constructed in 1968 the bridge carries Lincoln Road over I-75 NB in 2.4 MI South of Sterling.

Bridge Geometry

The bridge is 155.8-ft long, 32.2-ft wide and carries 2 lanes of traffic with 4.1-ft wide shoulders. The bridge orientation is West-East. This is a skewed three span bridge with five beams per span. The beam lengths are: 54.30-ft at the central span W2, 36.8-ft at span W1 and 33.6-ft at span W3. Side spans beam types are III for fascia and II for interiors, and center spans beam type is III.

Abutments, Pier, Deck and Joints

Both abutments have vertical hairline cracks through the walls and wet cracks, some with efflorescence stains, at South and North corners (see Photo 3-58).

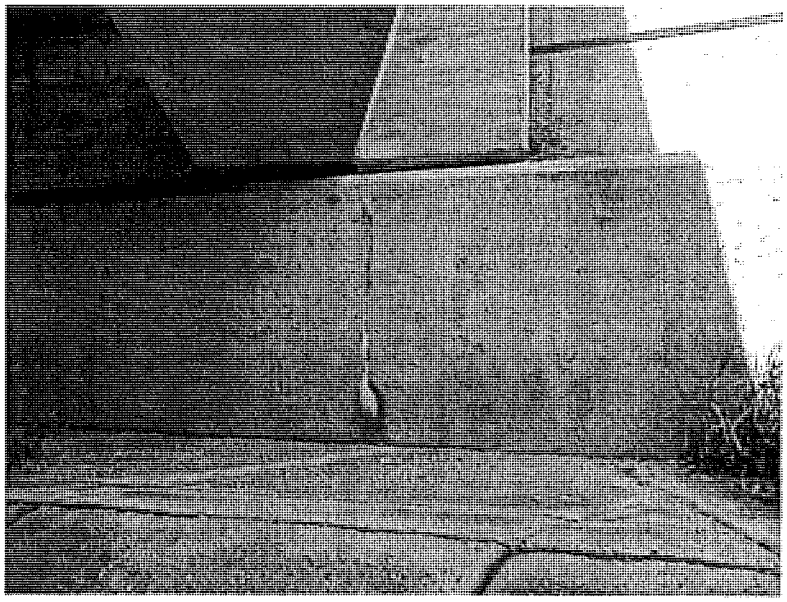

Photo 3-58. Cracks with evidence of moisture and efflorescence at the abutments

Next to the beam-ends some diaphragms at the abutments have minor spalls and water stains. The North side of the diaphragm at the East abutment is delaminated and the South side of the West abutment has exposed reinforcement and rust stains.

The piers have rust and water stain. The East fascia of pier W1 and the West fascia of pier W2 are cracked and delaminated. The West fascia of pier W2 displays exposed shear reinforcement, rust and efflorescence stains (see Photo 3-59).

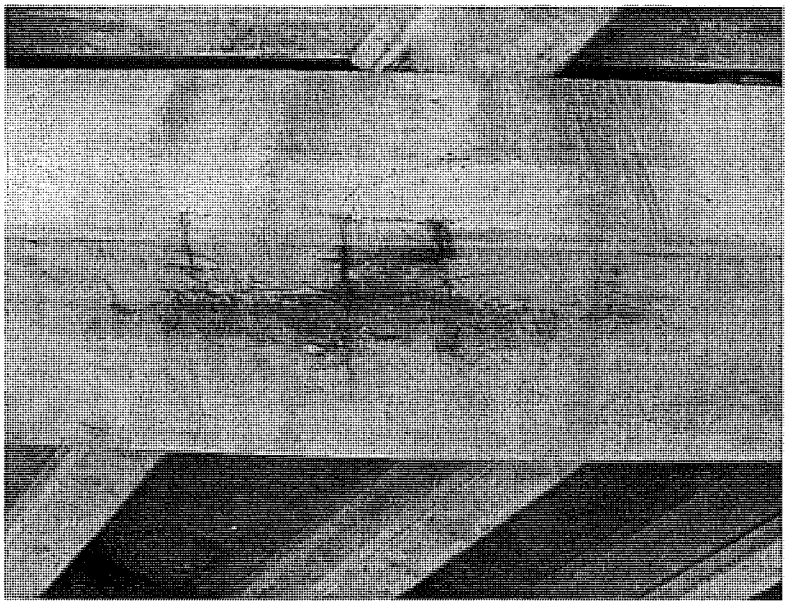

Photo 3-59. Exposed reinforcement, rust and efflorescence at W. fascia of pier cap beam W2

The concrete deck of the main span is in good condition. Both approaches have asphalt patches and potholes. The construction joints are partially broken as it shown in Photo 3-60.

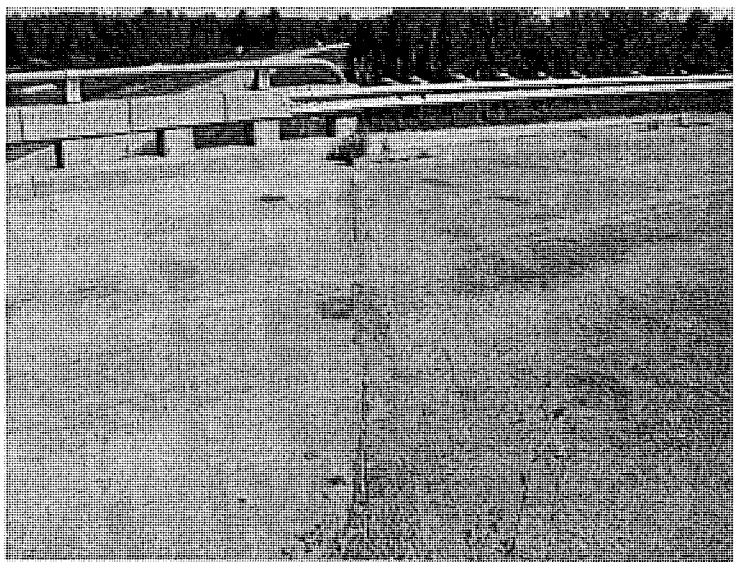

Photo 3-60. Construction joint between deck and approach

The shoulders are covered with gravel and debris. Drainage system is partially filled with debris. The bottom of the deck has cracks and efflorescence stains in the bays next to both abutments. Spalls with exposed reinforcement are noticed at bay S1 and bay S4 next to East abutment.

Stringers, Bearing and Diaphragms

The beam-ends at the piers are cracked and delaminated. At pier W2 beams S2 and S5 and at pier W1 beams S3 and S5 spalled and showing exposed shear reinforcement. The common beam-end condition is shown in Photo 3-61.

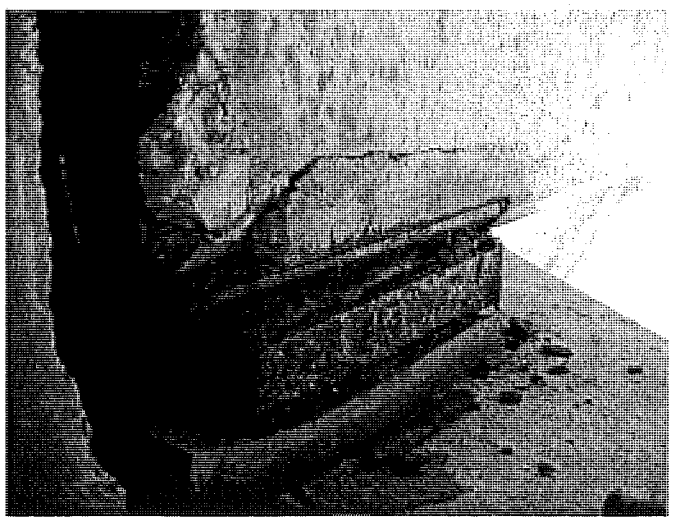

Photo 3-61. Common beam-end condition

At the abutments the beam-ends display some hairline cracks and some areas of water and rust stains.

Most of the diaphragms do not display any kind of deterioration. One diaphragm at pier W1 between beams S2 and S3 has a horizontal crack.

The sole plates are painted, some of them are slightly rusted. Some of the elastomeric pads are deformed with ends curling.

3.8 Data Organization

3.8.1 Condition Database

The data collected during the field investigation are organized in a Microsoft Access database. The organization of the database consists of several tables with links as shown in Figure 3-2. The first table of the hierarchy is the Inventory table. This table contains the inventory information on the 20 bridges that were inspected. The fields in this table are Pontis Bridge ID, County, Region, Year Built, Number of Spans, Maximum Span Length, Deck Width, Length, Clearance, Facility Carried, Feature Intersected, Deck Notes, Barrier Notes, Pier Notes, and Abutment Notes.

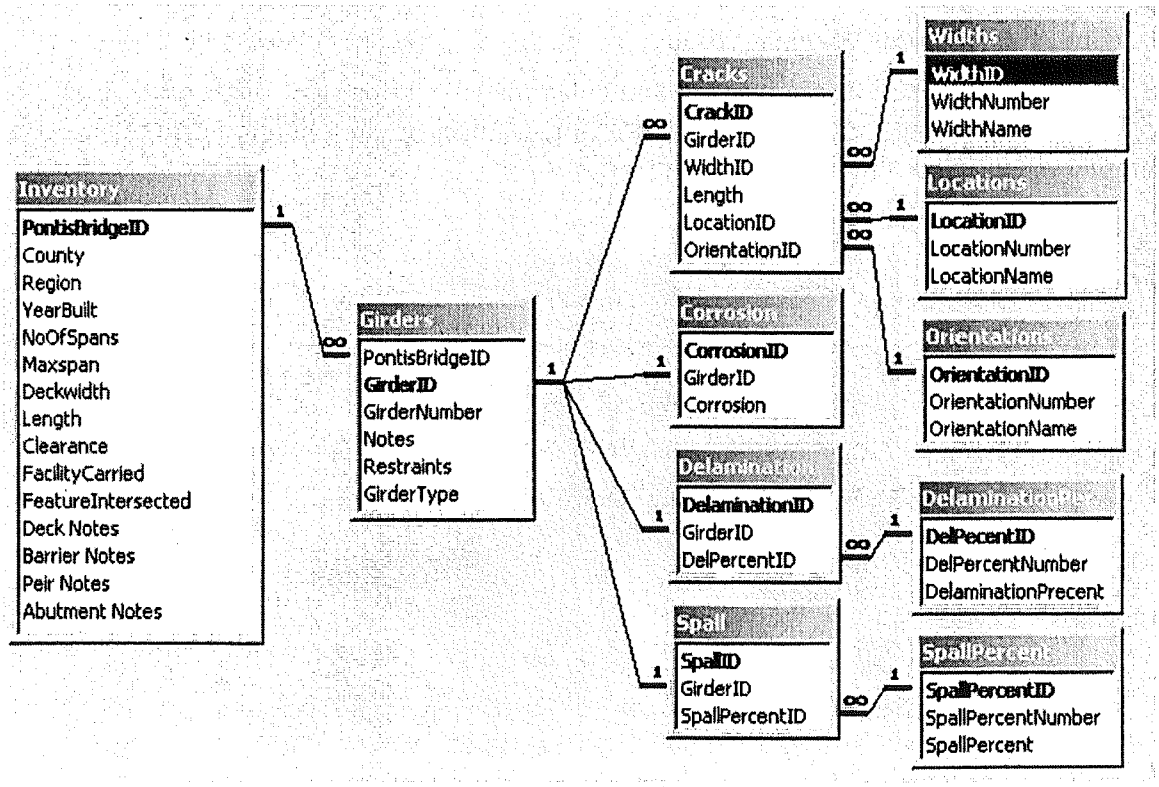

Figure 3-2. Data Base Relationships

The next table is titled Girders, and it has a "one to many" relationship with the Inventory table. "One to many" refers to the relationship where one field in a table can have many fields from another table related to that one. The fields in this table are Girder ID, Girder Number, Notes, Restraints, and Girder Type. The Girder ID field is an auto-numbering column used to create relationships to other tables. The Girder Number includes a span, a beam in the span, an end of that beam, and a face at that end. The first letter in the notation explains which direction to start counting the spans from (either S-south or E-east), and the number that follows is the span number. Next, is a letter denoting the direction for counting of the beams (either S-south or E-east), and the number that follows is the beam number. The following letter designates the end of the beam of interest (either {N-north or S-south} or {E-east or W-west}). The last letter designates one of the seven faces (either {N-north and S-south} or {E-east and W-west} U-underneath, R-rear end, B-bearing, I-interior diaphragm, X-exterior diaphragm). An example of a beam number for a bridge running north to south with three spans and seven beams in a span is S2-E5-N-W.

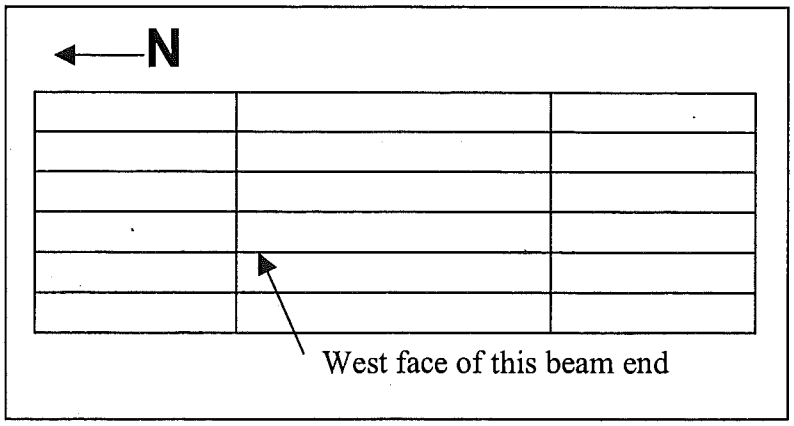

Figure 3-3. Example of How to Designate a Beam Number

This number reads: second span from the south, fifth beam from the east, north end, west face. The Notes field is for any comments on that particular Girder Number. A pictorial representation of where the girder-end is located can be seen in Figure 3-3. The Restraints field describes the beam-ends as either pinned or roller. The Girder Type only permits the four AASHTO types, Wisconsin 70" I-beam type, Michigan 1800 type, or no type (when the face is a diaphragm).

The Cracks table has a "one to many" relationship with the Girders table. The fields in this table are Crack ID, Girder ID, Width, Length, Location, and Orientation. The Crack ID and Girder ID are both auto-numbering columns used to create relationships to other tables. The Width field has an associated table named Width where the preset values for this field are kept; the relationship between Width field and Width table is a "many to one." The preset values in the Width table are Hairline, Moderate, Major. The number values designated to Hairline are ≤ .001 inch, Moderate are .002-.010 inch, and Major are > .010 inch. The Length field has the numeric values in inches of each crack length. The Location field has an associated table named Location

where the preset values for this field are kept; the relationship between Location field and Location table is a "many to one." The preset values in the Location table are Top Flange, Web, Bottom Flange, Bearing, Top Flange & Web, Web & Bottom Flange, Top & Web & Bottom, and Diaphragm. The Orientation field has an associated table named Orientation where the preset values for this field are kept; the relationship between Orientation field and Orientation table is a "many to one". "Many to one" refers to the relationship where one field in a table can have many of the same entries of a preset value in another table. The preset values in the Orientation table are Horizontal, Vertical, < 90, > 90, MUC (Multiply Ultra fine Cracks), and Mapping. < 90 and > 90 refer to diagonal cracks, and the convention is shown in Figure 3-4.

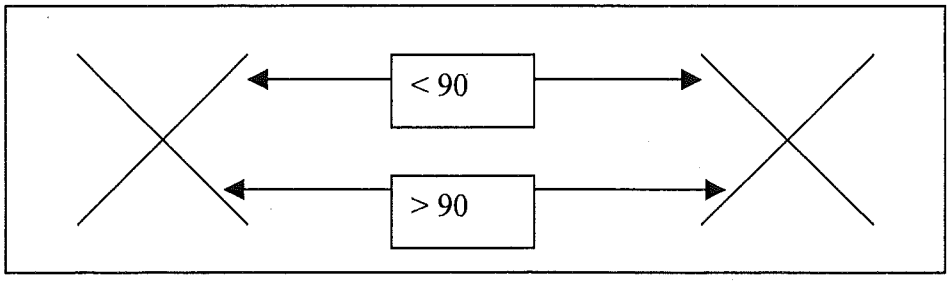

Figure 3-4. Diagonal Crack Convention

The Corrosion table has a "one to one" relationship with the Girders table; the fields in this table are Corrosion ID, Girder ID, and Corrosion. The Corrosion ID and Girder ID are both auto-numbering columns used to create relationships to other tables. The Corrosion field is a check box. If there was any sign of rust on that particular face then the box was checked.

The Delamination table has a "one to one" relationship with the Girder table; the fields in this table are Delamination ID, Girder ID, and DelPercent ID. Delamination ID and Girder ID are both auto-numbering columns used to create relationships to other tables. The DelPercent ID field has an associated table named Delamination Percent where the preset values for this field are kept; the relationship between DelPercent ID field and Delamination Percent table is a "many to one." The preset values in the Delamination Percent table are 0%, 25%, 50%, 75%, 100%. These percentages have a range meaning:

Table 3-9. Delamination Percent

Database Entry	Range
0%	0%,
25%	1%-25%,
50%	26%-50%,
75%	51%-75%
100%	76%-100%

The Spall table has the same format as the delamination table.

A data entry form was created in Microsoft Access to aid in the data entry process, which is shown in Figure 3-5.

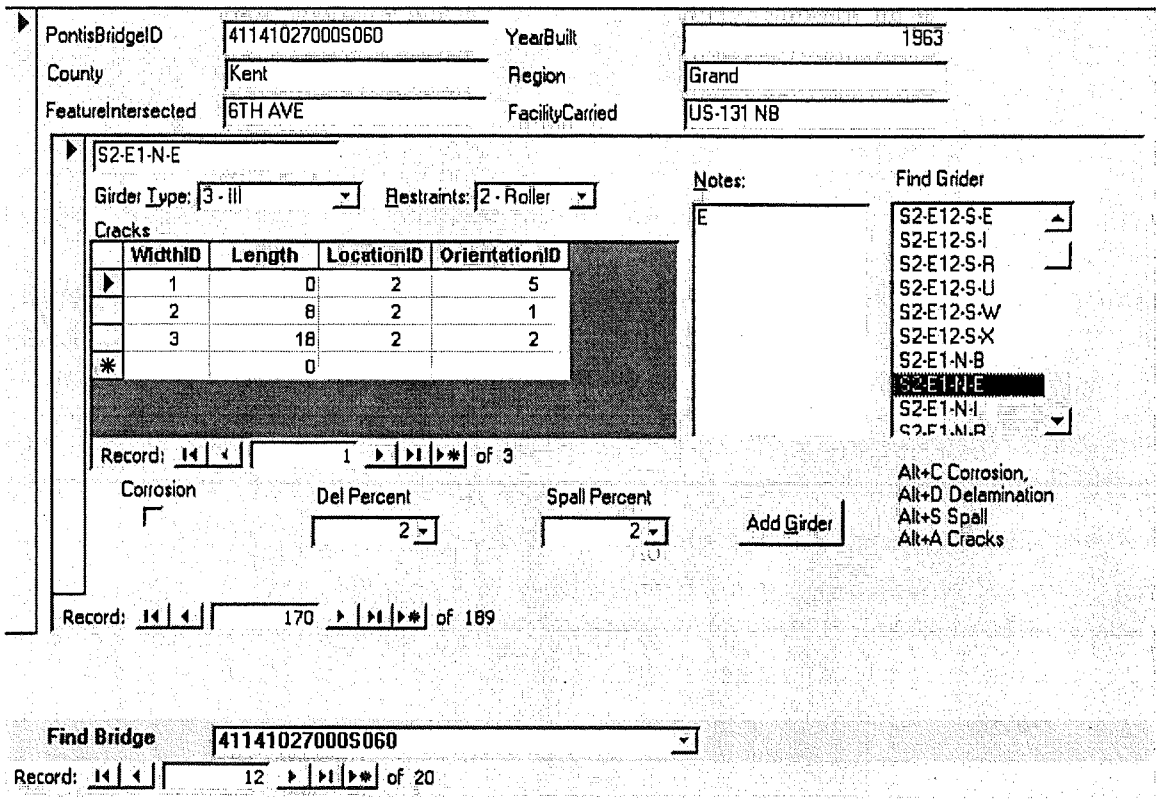

Figure 3-5. Inspection Data Entry Form

3.8.2 Inspection Photographs

The inspection photographs were organzined into a digital database that is located on the website, therefore it will be discussed in sub-section 8.3.1.

3.9 Summary

Field inspection of twenty prestressed concrete I-beam bridges was conducted. These bridges ranged from two to forty years old and were previously condition rated between four (poor) and eight (very good).

The field survey included a detailed visual inspection of the overall I-beam structure condition, including documenting the condition of each I-beam end.

As was expected the older structures exhibit more deterioration than the newer structures. The field survey shows that most of the older bridges suffer severe beam-end deterioration. Although

the bridge from 1968 located at Bay region, Arenac County, NBI No. 06111 S04 was found to be in excellent shape in comparison to its peers.

Two to seven year old beam-ends were found to be in good condition, although these bridges (1984-1999) already display some beam-end problems, such as vertical and diagonal cracks, and horizontal cracks along the flange.

The data collected during the field inspection was analyzed and compared with the information available in MDOT NBI inspection reports. The condition of abutments, piers and deck observed by the team does not differ significantly from NBI inspection comments for these items.

The main goal of the team was to collect precise information on the beam-end condition and thus very detailed information on location, size, and orientation of deterioration was obtained. This information could be obtained from the field notes and it is also available on the website. The issue of beam-end deterioration was difficult to compare with MDOT practice because most of the NBI inspection reports do not rate the condition of beam-ends. Some NBI reports mentioned beam-end deterioration under the item 59 "Stringer". There is a need to include end condition assessment in the inspection procedure. This will allow for inspectors to rate the condition and properly assign a protective strategy prior to severe deterioration.

The analysis for the inspection data can be found in section 4.3.

4.0 Identification of Bridges Prone to Deterioration (Task 3)

4.1 Introduction

The objective of Task 3 was to identify bridges that are vulnerable to end distress. Bridge management in Michigan is performed using a relational database integrated under a software program called "Pontis." Pontis data that has been collected by MDOT bridge inspectors was analyzed along with the data collected from the research team's field investigation. A cursory inspection of recent I-girders as well as a visit to the precast plant showed that the girder ends are often cracked. The primary objective of the Pontis data analysis is to evaluate the impact of early age cracking on girders durability. The methodology and results of the analysis are described in this chapter.

4.2 Pontis Data Analysis

Pontis data as of May 2001 indicates that there are 5902 bridges under MDOT's responsibility. Out of this total, there is in excess of 2600 prestressed concrete bridges with the design types of I-beam, box beam, or spread box beam. Further analysis of Pontis data indicates that there are about 750 prestressed concrete I-beam bridges under MDOT's responsibility. Further investigation of the Pontis data showed that there are approximately 50 duplicate entries of the prestressed concrete I-beam bridges. In this report the research team ignored the duplicates and used the sample space as 750. Figure 4-1 shows the fleet parameters of prestressed concrete I-beam bridges.

The Michigan Design Manual, Bridge Design Section 7.02.03 discusses beam material selection. This manual provides a guide for beam material selection. Prestressed concrete box beams can be used up to a span of 140-feet. AASHTO type prestressed concrete I-beams can be used up to a span of 105 feet, and Michigan 1800 I-beams up to a span of 150 feet. It is stated that concrete beams are preferable in freeway bridges subjected to severe exposure conditions.

The changes to the prestressed concrete bridge stock were investigated by querying the reconstructed bridges in Pontis. Table 4-1 summarizes the results. Also, Figure 4-2 shows the percentages of where the prestressed concrete I-beam bridges are located by region, and county. County numbers shown in Figure 4-2 are correlated to County names in Table 4-2.

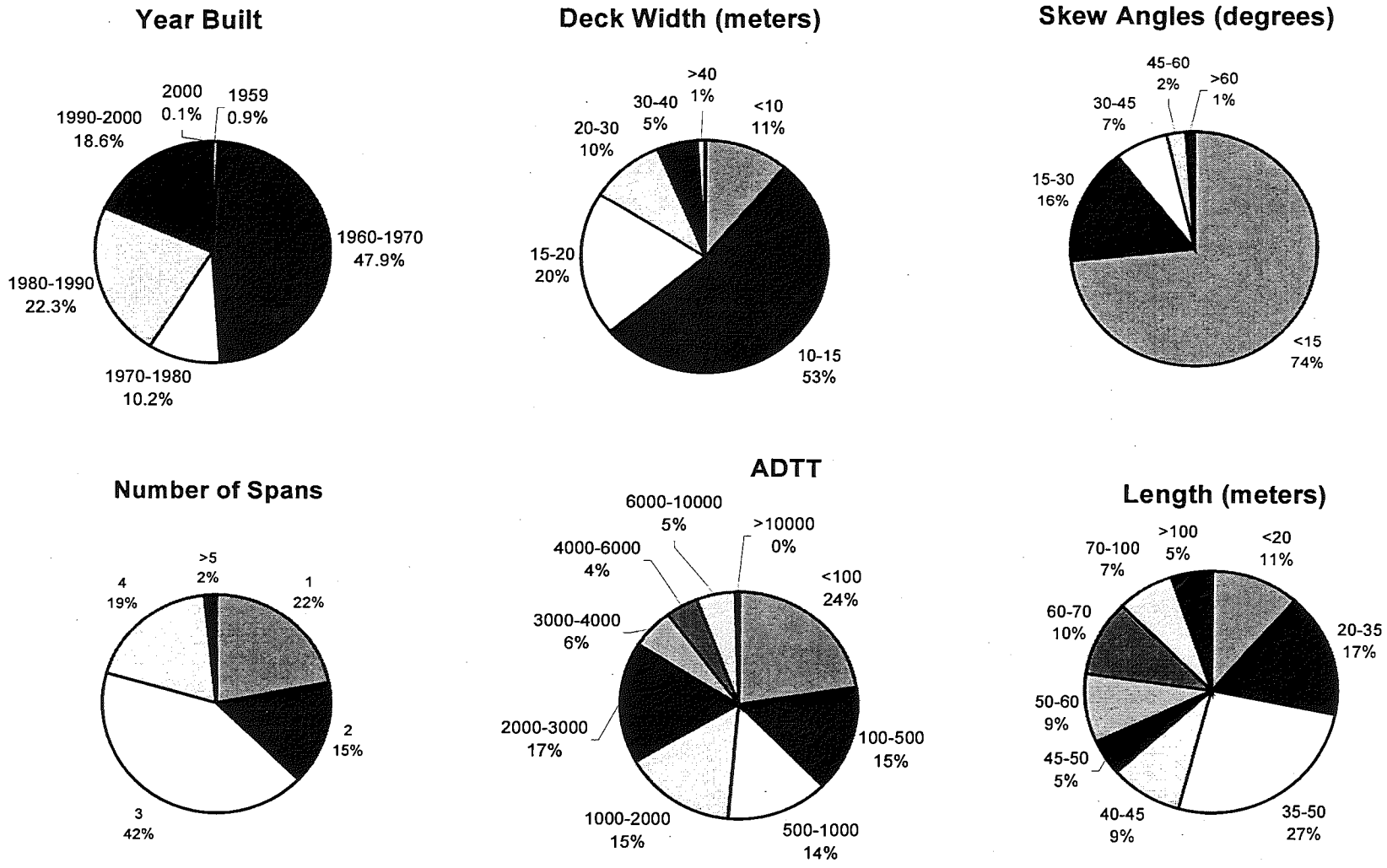

ADTT: Average Daily Truck Traffic

Figure 4-1. Fleet Parameters of Prestressed Concrete I-Beam Bridges

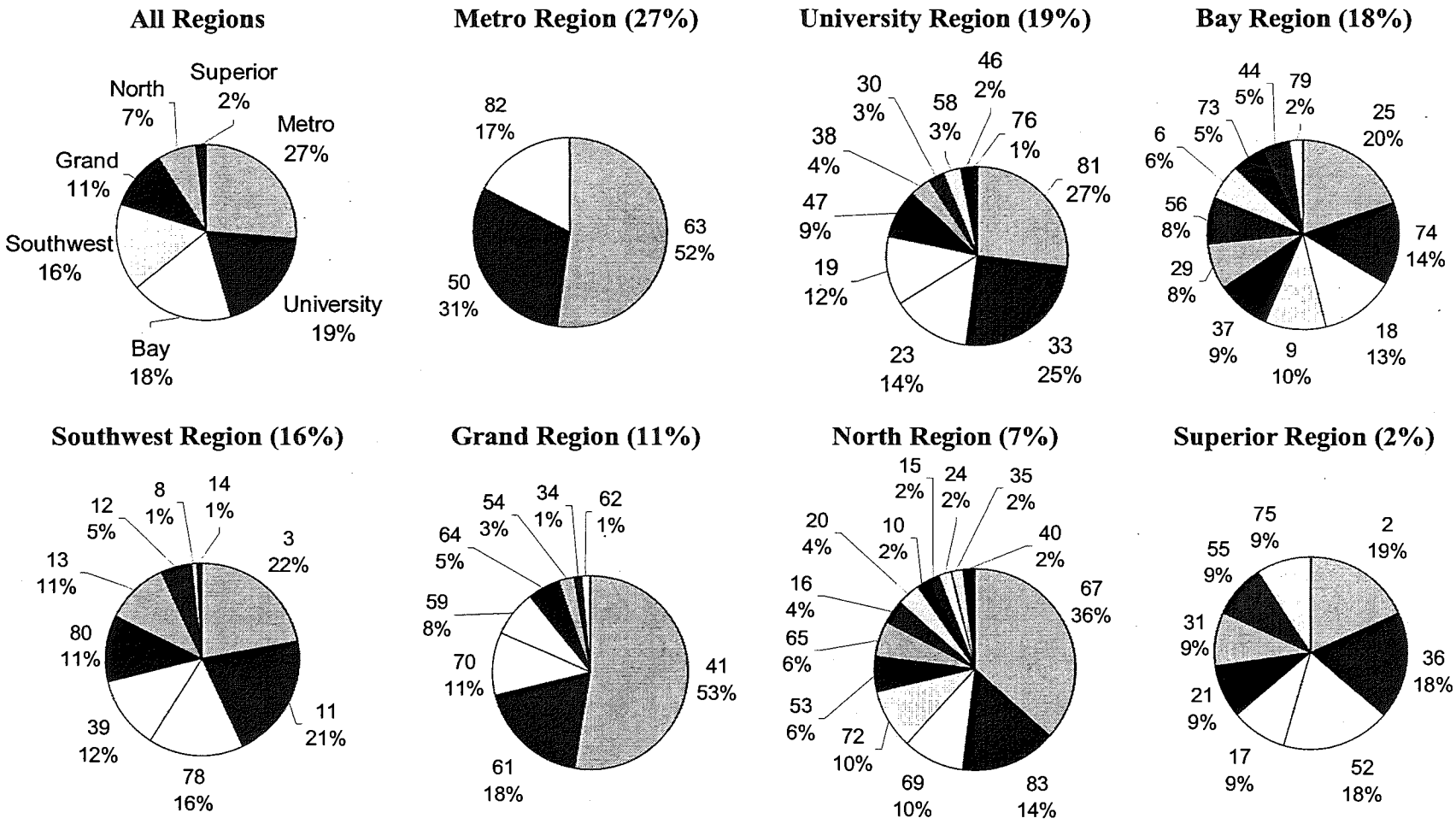

Figure 4-2. Fleet Location by Region of Prestressed Concrete I-girder Bridges

Table 4-1. Material Selection in Reconstructed Bridges

Years	Total Replaced	PC I-Beam	Box Beam	Spread Box Beam
1960-70	69	2	2	-
1970-80	127	4	9	-
1980-90	161	18	6	-
1990-00	261	51	24	18

Table 4-2. County Numbers as given by MDOT

#	Counties	Region		#	Counties	Region
1	ALCONA	NOR		43	LAKE	NOR
2	ALGER	SUP		44	LAPEER	BAY
3	ALLEGAN	SWR		45	LEELANAU	NOR
4	ALPENA	NOR		46	LENEWEE	UNIV
5	ANTRIM	NOR		47	LIVINGSTON	UNIV
6	ARENAC	BAY		48	LUCE	SUP
7	BARAGA	SUP		49	MACKINAC	SUP
8	BARRY	SWR		50	MACOMB	METRO
9	BAY	BAY		51	MANISTEE	NOR
10	BENZIE	NOR		52	MARQUETTE	SUP
11	BERRIEN	SWR		53	MASON	NOR
12	BRANCH	SWR		54	MECOSTA	GR
13	CALHOUN	SWR		55	MENOMINEE	SUP
14	CASS	SWR		56	MIDLAND	BAY
15	CHARLEVOIX	NOR		57	MISSAUKEE	NOR
16	CHEBOYGAN	NOR		58	MONROE	UNIV
17	CHIPPEWA	SUP		59	MONTCALM	GR
18	CLARE	BAY		60	MONTMORENCY	NOR
19	CLINTON	UNIV		61	MUSKEGON	GR
20	CRAWFORD	NOR		62	NEWAYGO	GR
21	DELTA	SUP		63	OAKLAND	METRO
22	DICKINSON	SUP		64	OCEANA	GR
23	EATON	UNIV		65	OGEMAW	NOR
24	EMMET	NOR		66	ONTONAGON	SUP
25	GENESEE	BAY		67	OCEOLA	NOR
26	GLADWIN	BAY		68	OSCODA	NOR
27	GOGEBIC	SUP		69	OTSEGO	NOR
28	GD. TRAVERSE	NOR		70	OTTAWA	GR
29	GRATIOT	BAY		71	PRESQUE ISLE	NOR
30	HILLSDALE	UNIV		72	ROSCOMMON	NOR
31	HOUGHTON	SUP		73	SAGINAW	BAY
32	HURON	BAY		74	SANILAC	BAY
33	INGHAM	UNIV		75	SCHOOLCRAFT	SUP
34	IONIA	GR		76	SHIAWASSEE	UNIV
35	IOSCO	NOR		77	ST. CLAIR	METRO
36	IRON	SUP		78	ST. JOSEPH	SWR
37	ISABELLA	BAY		79	TUSCOLA	BAY
38	JACKSON	UNIV		80	VAN BUREN	SWR
39	KALAMAZOO	SWR		81	WASHTENAW	UNIV
40	KALKASKA	NOR		82	WAYNE	METRO
41	KENT	GR		83	WEXFORD	NOR
42	KEWEENAW	SUP				

According to MDOT terminology a bridge is termed reconstructed even when the project activity is limited to deck replacement, consequently in Table 4-1 'Total Replaced' also includes deck replacement projects. In other words, the difference between the numbers of "Total Replaced" and total of prestressed concrete beams does not necessarily indicate the use of steel girders. Simple analysis of the data in the table shows that during the last decade an average of ten bridges per year are being replaced using prestressed concrete girders (PC I-Beam, Box Beam, or Spread Box Beam). These reconstructed prestressed concrete bridges are predominantly being rebuilt using prestressed concrete I-beams (51 of 93).

The Pontis data was further analyzed specifically for evaluating the condition of I-beams. Inspection reports prepared by an MDOT inspector are documented in Pontis. A total of 499 reports were analyzed by reviewing each record and counting the occurrences of the following specific terms: cracking (denoted by C), corrosion or rust (R), delamination (D) and spalling (S). Data processing revealed that the delamination term is redundant because this phenomenon is always accompanied with spalling. Therefore, the analysis was focused on inspector reports containing the terms of rusting and spalling. In order to see the influence of cracking on the beams, the data was analyzed with respect to numbers of bridges with beams with cracks and without cracks.

The total number of 499 records was obtained from Pontis for prestressed concrete I-beam bridges with available inspection reports. The histogram of these bridges built between 1960 and 2000 is shown in Figure 4-3. Out of this total of 499 bridges, 55 records contained duplicate Bridge ID numbers but different inspection comments.

The histogram of cracked and uncracked prestressed concrete I-beams showing rust are shown in Figure 4-4. Using all 499 inspector comment records, the number of bridges with notes indicating cracked prestressed concrete I-beams was counted as 263, leaving 236 records for the bridges with no mention of beam cracking. Further review of inspector comments showed that 109 bridge beams include "cracks and rusting or corrosion," whereas 40 comments were found for the beams that only indicate "corrosion or rusting" but with no mention of cracking. When both "rusting or corrosion" and "spalling" are searched in the inspector comments, the numbers reported with cracked beams was 87, and 23 for the beams with no mention of cracks.

The influence of cracking on prestressed concrete I-beam durability is depicted in Figure 4-4. Taking beam corrosion as the primary parameter, the ratio of bridges with prestressed concrete I-beams showing signs of corrosion to the total number of cracked and uncracked beams document the importance of cracking in beam durability. The ratio of the number of bridges with observed signs of corrosion to the total number bridges with cracked beams is 0.41 whereas this ratio decreases to 0.17 for the bridges with beams where inspectors did not indicate any cracks.

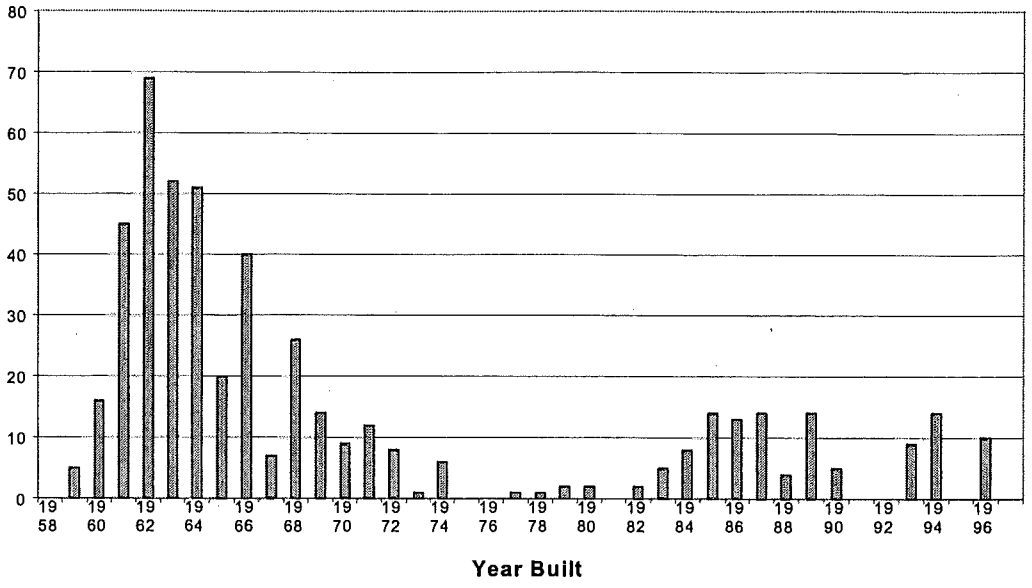

Figure 4-3. Prestressed Concrete I-Beam Bridges Constructed Since 1960

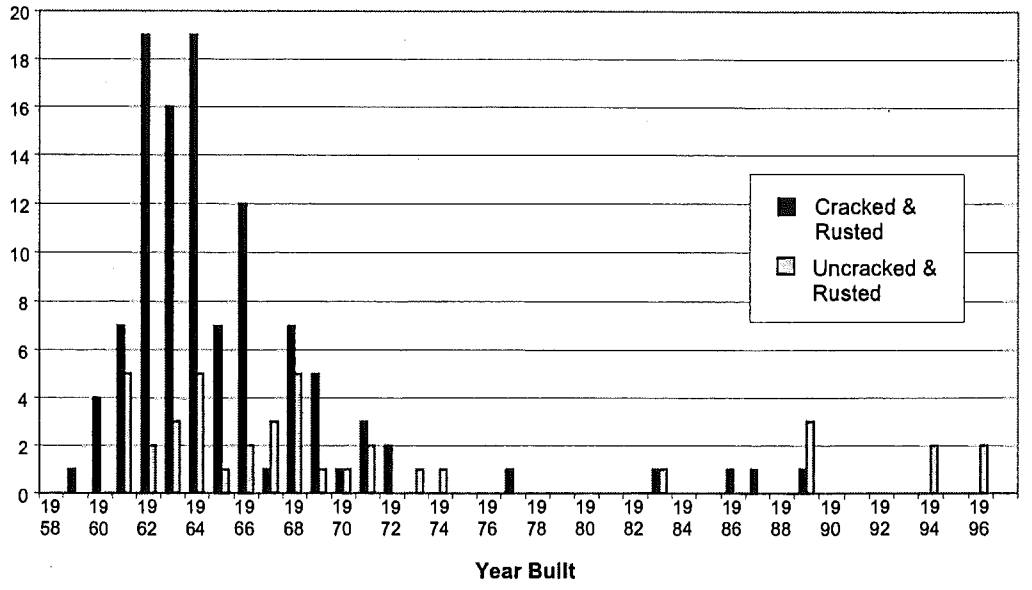

Figure 4-4. Corrosion Comparison in Cracked and Uncracked Prestressed Concrete I-Beam Bridges showing rust

4.3 Field Inspection Data Analysis

The field investigation data was collected on template forms. The template includes the bridge ID on the top left of the sheet and the beam layout on the top right of the sheet. The inspector designated the specific beam being inspected on the beam layout and completed the condition information on the beams and diaphragms.

During field visits, all faces of the beam-ends were inspected and signs of distress/deterioration were entered onto the form. Cracks were drawn to a rough approximation with respect to their length, location, and orientation. For each crack the length was measured and the width was estimated sometimes using crack gages. Corrosion, delamination, spall, water stain, efflorescence, and exposed rebar were carefully sketched onto the form to show approximate areas and locations. Figure 4-6 is an example of one of the field investigation forms with data sketched from the field. The data presented on all the field investigation forms is qualitative information, therefore a database was created to transform that data into quantitative information so it could be analyzed. The beam condition data was entered into a custom made Microsoft Access database that was described in Section 3.8.1.

As seen in Figure 4-6 there are six faces to a beam-end and the seventh face is the bearing. There are a total of 5364 faces in the database for the 20 bridges that were investigated. On those faces there are 5041 cracks for which four items of data was entered (width, length, location, and orientation). Additionally, the corrosion, delamination, and/or spall evidence on each face was entered. Sometimes for a face "notes" were entered describing the moisture stains, exposed rebar, efflorescence, and any other indicators of distress.

The Pontis analysis conducted on the "Inspector Notes" documented the influence of early age cracks on prestressed concrete I-beam end durability. For this purpose, the hypothesis developed for the analysis of inspection data was related to the influence of cracking. The hypothesis of beam end deterioration for prestressed concrete I-beams is that cracks in the early part of a bridge's life results to more rapid progression of rebar and tendon corrosion. To verify this hypothesis a statistical analysis was conducted on the field inspection data.

First, 12 queries were performed to yield all the primary faces of interest. The inspection data is organized for each face of the girder-end. These faces are the north and south elevation, or east and west elevation (dependent upon orientation of the bridge), bottom, and side faces of all 20 bridges with a total of 3000 faces. The remaining 2364 faces are the two diaphragm faces and bearing. The results from the 12 queries are given in Table 4-3. (In all of the following tables of this section "Corr" is an abbreviation of corrosion and "Del" is an abbreviation of delamination.)

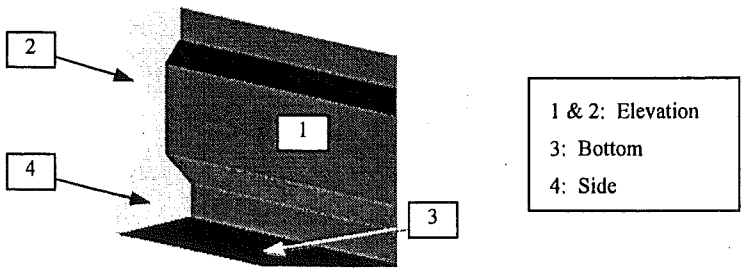

Figure 4-5: Primary Faces of Girder-end

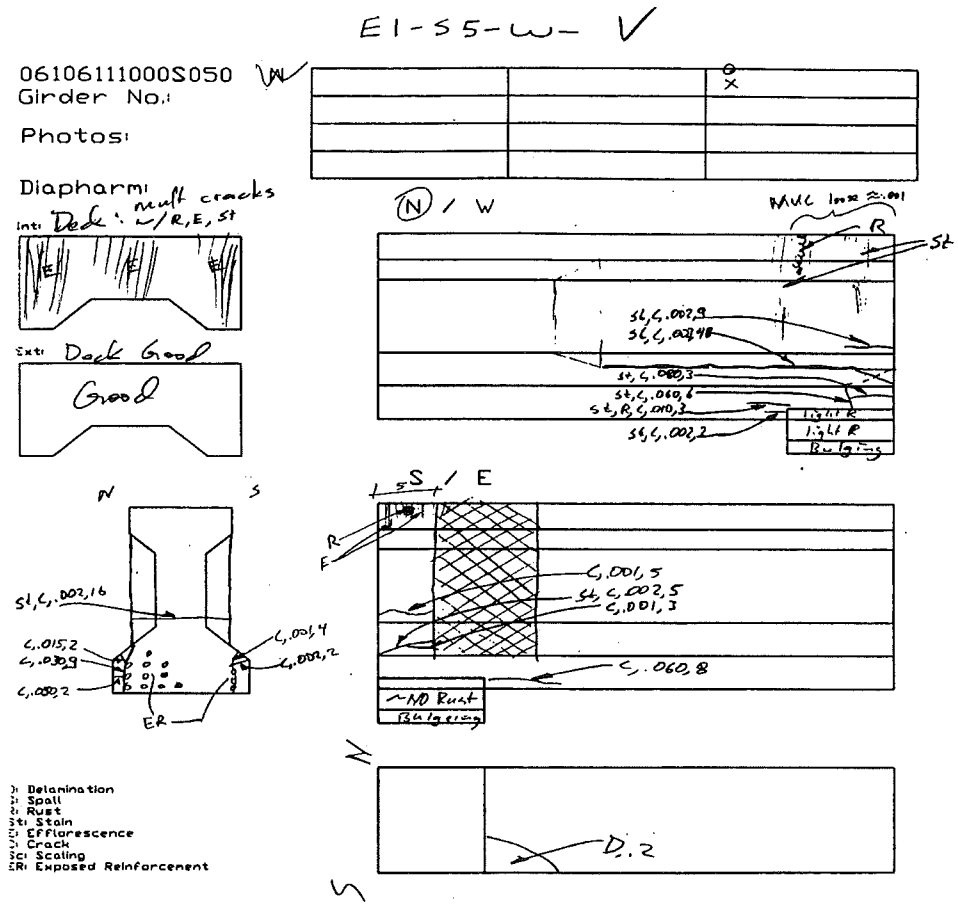

Figure 4-6. Example of Field Investigation Template Form

The girder-end condition database contains information on cracked, corroded, delaminated, and spalled states. The information is recorded for each one of the four girder-end faces. The direct query using a specific condition state provided the data given in Table 4-3. The data in Table 4-3 was further processed to obtain the bridge and girder-end specific data as tabulated in Table 4-4 as frequencies and Table 4-5 as percentages. The data in Table 4-5 is represented in Figure 4-7 temporally by year built in terms of distress frequencies. The deterioration against bridge age is observed in Figure 4-7. The relation between cracking and deterioration cannot be observed because of linked samples of uncracked girders.

Table 4-3. Queries from Condition Database of Faces Inspected

	Total Faces	Cracked Faces	Crack & Corr Faces	Corr Faces
Total	3000	1515	704	888
Delamination	990	602	350	420
Spall	674	477	328	405
Spall & Del	399	293	200	237

Table 4-4. Summary of Result from Condition Database with respect to Each Bridge and Beam-ends

Bridge ID	County	Region	Year Built	No. of Spans	No. of Girders	Total No. of Beam-ends Inspected	Beam-ends w/ No Cracks & No Corr	Beam-ends w/ Cracks	Beam-ends w/ Cracks & Corr	Beam-ends w/ Del	Beam-ends w/ Spall	Sum
29011 S03	Gratiot	Bay	1961	3	27	54	0	0	15	21	18	54
06111 S04	Arenac	Bay	1968	3	18	35	0	9	9	6	11	35
06111 S05	Arenac	Bay	1968	3	15	30	0	2	10	9	9	30
06111 S06	Arenac	Bay	1968	3	15	30	0	1	10	8	11	30
06111 S11	Arenac	Bay	1968	6	54	62	0	12	3	6	41	62
25042 S12-8	Genesee	Bay	1969	4	16	28	1	1	5	4	17	28
25042 S12-3	Genesee	Bay	1969	4	22	44	0	0	4	5	35	44
25042 S12-4	Genesee	Bay	1969	4	22	43	0	0	3	5	35	43
25042 S12-7	Genesee	Bay	1969	4	16	32	0	0	4	5	23	32
25132 S34	Genesee	Bay	1971	4	24	48	0	10	10	17	11	48
41025 S07	Kent	Grand	1961	4	24	47	0	2	10	16	19	47
41027 S06	Kent	Grand	1963	3	36	71	0	12	11	12	36	71
41029 S16-3	Kent	Grand	1964	3	24	46	0	1	8	6	31	46
41029 S16-4	Kent	Grand	1964	3	24	48	0	7	9	15	17	48
41029 S23	Kent	Grand	1972	3	24	48	0	28	3	5	12	48
67016 S09	Oceola	North	1984	1	6	11	0	2	2	6	1	11
67016 S10	Oceola	North	1984	1	7	14	0	9	2	1	2	14
53034 S05	Mason	North	1986	4	24	27	0	5	14	6	2	27
83033 S06	Wexford	North	1997	1	8	16	0	15	1	0	0	16
83033 S05	Wexford	North	1998	2	8	16	2	13	1	0	0	16
Total					414	750	3	129	134	153	331	750

Table 4-5. Percentages of Summary of Result from Condition Database with respect to Each Bridge and Beam-end

Bridge ID	County	Region	Year Built	No. of Spans	No. of Girders	Total No. of Beam-ends Inspected	Beam-ends w/ No Cracks & No Corr (%)	Beam-ends w/ Cracks (%)	Beam-ends w/ Cracks & Corr (%)	Beam-ends w/ Del (%)	Beam-ends w/ Spall (%)	Sum (%)
29011 S03	Gratiot	Bay	1961	3	27	54	0	0	28	39	33	100
06111 S04	Arenac	Bay	1968	3	18	35	0	4	21	34	40	100
06111 S05	Arenac	Bay	1968	3	15	30	0	17	16	17	51	100
06111 S06	Arenac	Bay	1968	3	15	30	0	2	17	13	67	100
06111 S11	Arenac	Bay	1968	6	54	62	0	15	19	31	35	100
25042 S12-8	Genesee	Bay	1969	4	16	28	0	26	26	17	31	100
25042 S12-3	Genesee	Bay	1969	4	22	44	0	7	33	30	30	100
25042 S12-4	Genesee	Bay	1969	4	22	43	0	3	33	27	37	100
25042 S12-7	Genesee	Bay	1969	4	16	32	0	19	5	10	66	100
25132 S34	Genesee	Bay	1971	4	24	48	4	4	18	14	61	100
41025 S07	Kent	Grand	1961	4	24	47	0	0	9	11	80	100
41027 S06	Kent	Grand	1963	3	36	71	0	0	7	12	81	100
41029 S16-3	Kent	Grand	1964	3	24	46	0	0	13	16	72	100
41029 S16-4	Kent	Grand	1964	3	24	48	0	21	21	35	23	100
41029 S23	Kent	Grand	1972	3	24	48	0	58	6	10	25	100
67016 S09	Oceola	North	1984	1	6	11	0	18	18	55	9	100
67016 S10	Oceola	North	1984	1	7	14	0	64	14	7	14	100
53034 S05	Mason	North	1986	4	24	27	0	19	52	22	7	100
83033 S06	Wexford	North	1997	1	8	16	0	94	6	0	0	100
83033 S05	Wexford	North	1998	2	8	16	13	81	6	0	0	100
Total					414	750	0	17	18	20	44	100

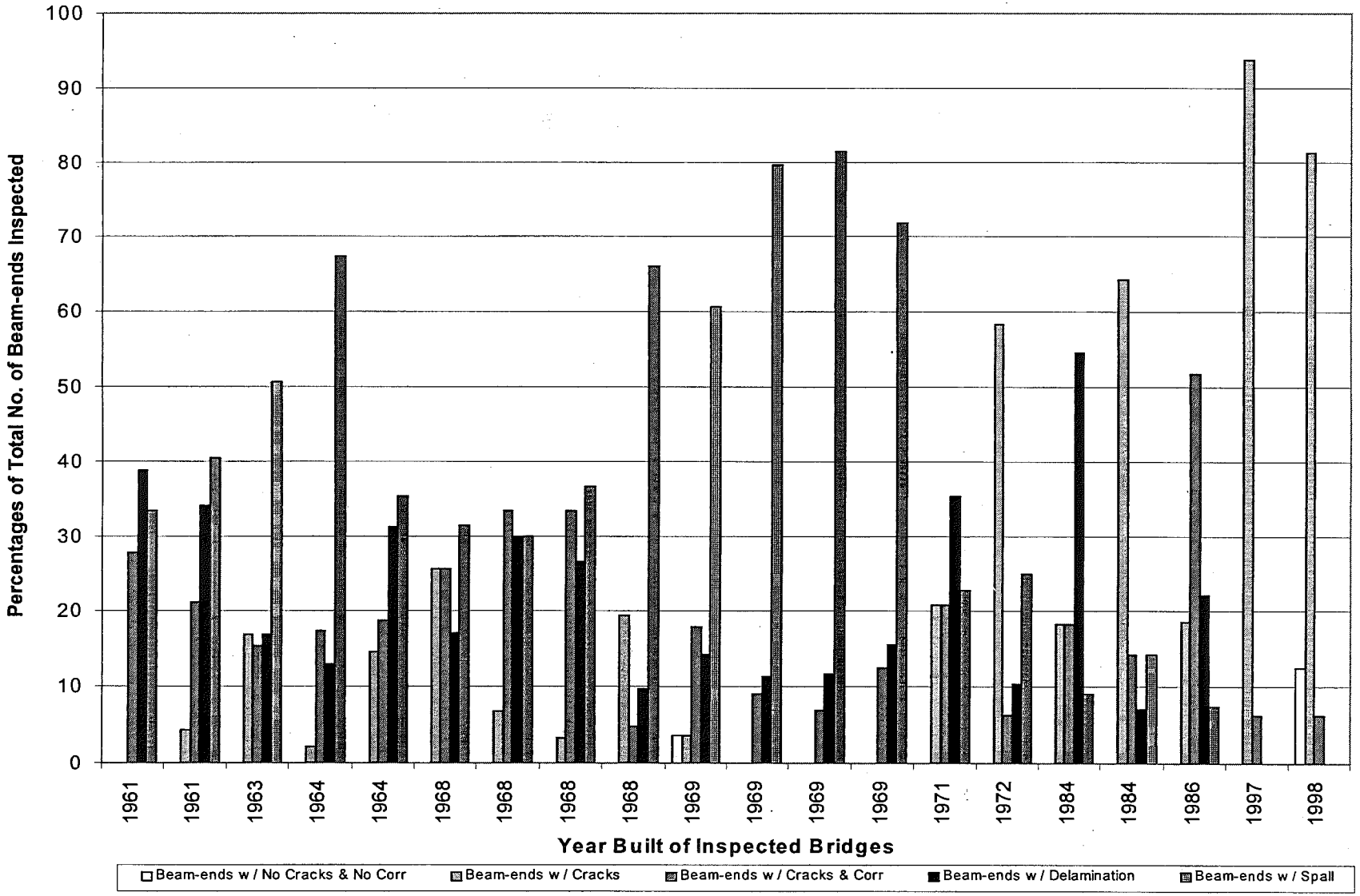

Figure 4-7. Percentages of Summary of Result from Condition Database with respect to Each Bridge & Beam-ends

An observation from the pontis data analysis and the research team's field data is the count of delaminated beam-ends. The research team's approach of checking delaminations at the beam-ends and diaphragms is by sounding across the entire surface area. The data in Table 4-6 came from 20 bridges inspected by the research team. The column titled "Inspector's Comment on Delaminated Stringers" came from the comments regarding stringers from the Safety Inspection Reports completed for those bridges by MDOT bridge inspectors as seen in Figure 4-8. If the inspector's comments included delaminations on any stringer, then "Yes" is entered into that cell. The column titled "Research Team's Comments on Delaminated Stringers" is based on the research team's inspection forms indicating delaminations on any stringer. For the 20 bridges investigated in this research, the stringers comments field in the MDOT Inspection Reports indicating delaminations show only 3 bridges versus 17 bridges determined by the research team. With all fairness the amount of man-hours it took the research team to complete an inspection was well above the inspector could afford to spend. In any case, these data indicate that delaminations are difficult to check during inspection.

Table 4-6. Findings on Evidence of PCI Girder-end Delaminations

PontisBridgeID	County	Region	Year Built	Inspector's Comment on Delaminated Stringers	Research Team's Comments on Delaminated Stringers
29011 S03	Arenac	Bay	1968	No	Yes
06111 S04	Arenac	Bay	1968	No	Yes
06111 S05	Arenac	Bay	1968	Yes	Yes
06111 S06	Arenac	Bay	1968	No	Yes
06111 S11	Genesee	Bay	1969	Yes	Yes
25042 S12-8	Genesee	Bay	1969	No	Yes
25042 S12-3	Genesee	Bay	1969	No	Yes
25042 S12-4	Genesee	Bay	1960	No	Yes
25042 S12-7	Genesee	Bay	1971	No	Yes
25132 S34	Gratiot	Bay	1961	No	Yes
41025 S07	Kent	Grand	1961	Yes	Yes
41027 S06	Kent	Grand	1963	No	Yes
41029 S16-3	Kent	Grand	1964	No	Yes
41029 S16-4	Kent	Grand	1964	No	Yes
41029 S23	Kent	Grand	1972	No	Yes
67016 S09	Mason	North	1986	No	Yes
67016 S10	Oceola	North	1984	No	Yes
53034 S05	Oceola	North	1984	No	No
83033 S06	Wexford	North	1998	No	No
83033 S05	Wexford	North	1997	No	No

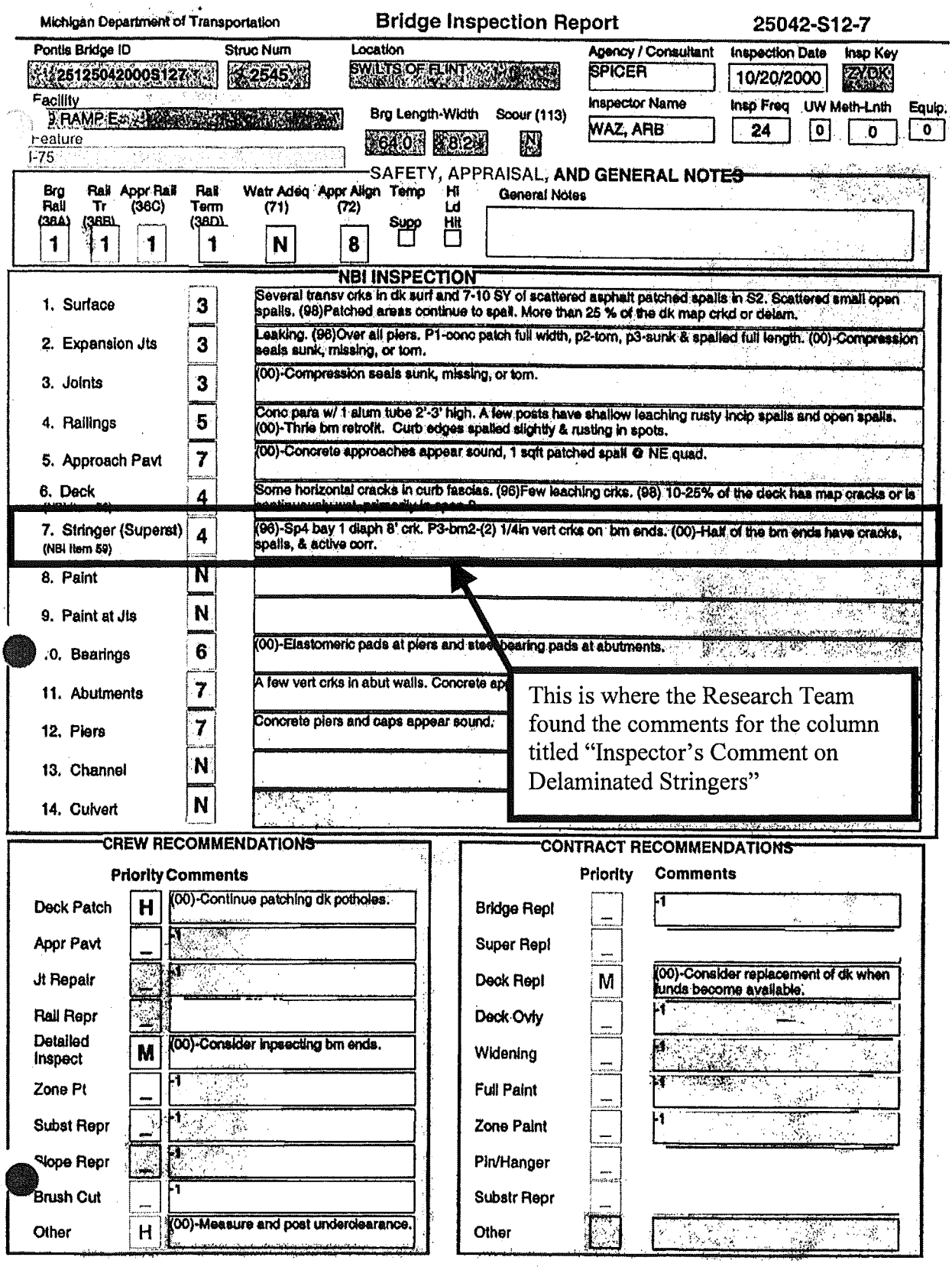

Michigan Department of Transportation — Bridge Inspection Report — 25042-S12-7

Pontis Bridge ID	Struc Num	Location	Agency / Consultant	Inspection Date	Insp Key
25125042000S127	2545	SWLTS OF FLINT	SPICER	10/20/2000	ZYDK

Facility: RAMP E
Feature: I-75

Brg Length-Width	Scour (113)	Inspector Name	Insp Freq	UW Meth-Lnth	Equip.
64.0 8.2	N	WAZ, ARB	24	0 0	0

SAFETY, APPRAISAL, AND GENERAL NOTES

Brg Rail (36A)	Rail Tr (36B)	Appr Rail (36C)	Rail Term (36D)	Watr Adeq (71)	Appr Align (72)	Temp Supp	Hi Ld Hit	General Notes
1	1	1	1	N	8	☐	☐	

NBI INSPECTION

1. Surface	3	Several transv crks in dk surf and 7-10 SY of scattered asphalt patched spalls in S2. Scattered small open spalls. (98)Patched areas continue to spall. More than 25 % of the dk map crkd or delam.
2. Expansion Jts	3	Leaking. (96)Over all piers. P1-conc patch full width, p2-torn, p3-sunk & spalled full length. (00)-Compression seals sunk, missing, or torn.
3. Joints	3	(00)-Compression seals sunk, missing, or torn.
4. Railings	5	Conc para w/ 1 alum tube 2'-3' high. A few posts have shallow leaching rusty incip spalls and open spalls. (00)-Thrie bm retrofit. Curb edges spalled slightly & rusting in spots.
5. Approach Pavt	7	(00)-Concrete approaches appear sound, 1 sqft patched spall @ NE quad.
6. Deck	4	Some horizontal cracks in curb fascias. (96)Few leaching crks. (98) 10-25% of the deck has map cracks or is
7. Stringer (Superst) (NBI Item 59)	4	(96)-Sp4 bay 1 diaph 8' crk. P3-bm2-(2) 1/4in vert crks on bm ends. (00)-Half of the bm ends have cracks, spalls, & active corr.
8. Paint	N	
9. Paint at Jts	N	
10. Bearings	6	(00)-Elastomeric pads at piers and steel bearing pads at abutments.
11. Abutments	7	A few vert crks in abut walls. Concrete ap
12. Piers	7	Concrete piers and caps appear sound.
13. Channel	N	
14. Culvert	N	

This is where the Research Team found the comments for the column titled "Inspector's Comment on Delaminated Stringers"

CREW RECOMMENDATIONS

	Priority	Comments
Deck Patch	H	(00)-Continue patching dk potholes.
Appr Pavt	_	-1
Jt Repair	_	-1
Rail Repr	_	
Detailed Inspect	M	(00)-Consider inpsecting bm ends.
Zone Pt	_	-1
Subst Repr	_	-1
Slope Repr	_	-1
Brush Cut	_	-1
Other	H	(00)-Measure and post underclearance.

CONTRACT RECOMMENDATIONS

	Priority	Comments
Bridge Repl	_	-1
Super Repl	_	
Deck Repl	M	(00)-Consider replacement of dk when funds become available.
Deck Ovly	_	-1
Widening	_	-1
Full Paint	_	-1
Zone Paint	_	-1
Pin/Hanger	_	
Substr Repr	_	
Other	_	

Figure 4-8. Example of a MDOT Safety Bridge Inspection Report

4.4 Indicators of Beam-End Vulnerability

Upon completing the inspection of 20 bridges it appeared clear that the vulnerable areas of a prestressed concrete bridge are: (1) beam-ends on piers, (2) beam-ends on abutments and (3) beam under-side near bearing pad/sole plate. These areas will be the first to exhibit the early signs of beam-end deterioration. Thus the inspection of these particular areas is recommended for vulnerability assessment as a part of maintenance inspection.

Specifically it is recommended that at the time of the inspection:

(1) The inspection of beam-ends on piers should focus on a 5.0-6.5 ft portion of the beam-end along the web and flange of the beam. Any cracks (especially hairline cracks in excess of 0.001 inch) and wet stains need to be documented. Such fine cracks should be visible using a water spray within arms length of inspection. Also, any moisture stain/leakage on the pier caps under the beam-ends should be noted. Special effort is required for the inspection of the beam-end back face at the piers. To be able to inspect the beam-end back face, one needs to get in between diaphragms and use a flashlight.

(2) The inspection of beam-ends at the abutments should focus on a 5.0-6.5 ft portion of that beam-end which extends from the edge of the abutment. The presence of hairline cracks and minor water stains is especially useful for vulnerability assessment. It is a concern sometimes the beam-end back face is encased in a diaphragm and cannot be inspected.

(3) The condition of elastomeric bearing pad, bearing plate, and sole plate should be noted. The elastomeric pad condition may be of corners curling, crack, delaminated. Bearing plate and sole plate may have corrosion.

Inspection shows the following in the proposed vulnerability assessment procedure the beam can be considered "not vulnerable" (see Photo 4-1).

- No cracks or hairline cracks (≤ 0.001 inch) at the girder end,
- Joint intact (not leaking),
- Sole plate clean free of rust,
- Functional elastomeric bearing pad,
- Beam faces and pier caps are dry.

It is the opinion of the research team that the possibility of water infiltration and freeze thaw mechanism has a small chance of affecting the intended design of the air entraiment system. Therefore, the criterion of less than 0.001 inch for "not vulnerable" is considered as a small value.

The following conditions should be considered as the first signs of beam-end problem:

- Moderate cracks (0.002-0.01 inch) at the girder end,
- Corroding sole plate,
- Moisture staining or leaking joint,
- Non-functional elastomeric bearing pad,
- Beam faces and pier caps show moisture staining.

If the inspection indicates any one of the above conditions, the beam is considered as "vulnerable" to end deterioration (see Photo 4-2).

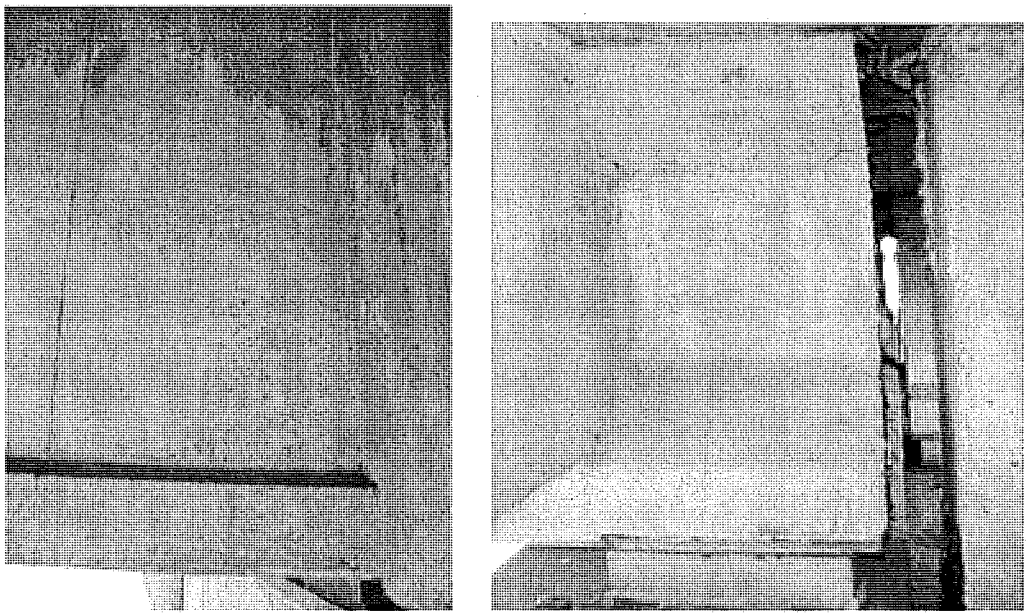

Photo 4-1. "Not vulnerable" Prestressed Concrete I-Beam

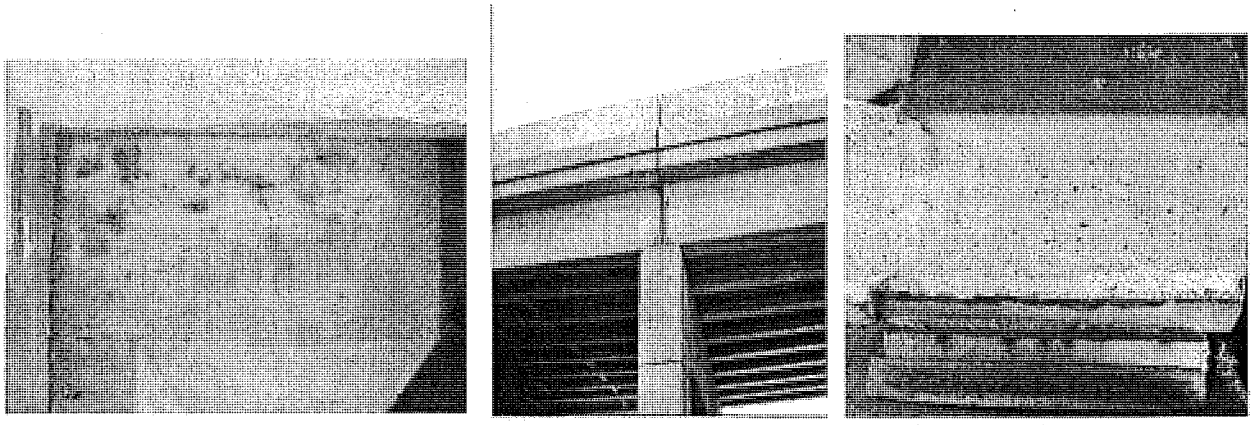

Photo 4-2. (Left and Middle) Wet stain at beam-end (Right) Sole plate corrosion

Additionally, if two or more of the conditions below are observed during inspection, the beam is considered as "highly vulnerable" to end deterioration (see Photo 4-3).

- Major cracks (> 0.01 inch) at the girder end,
- Leaking joint,
- Corroding sole plate, bearing plate
- Non-functional elastomeric bearing pad,
- Beam faces and pier caps are moist.

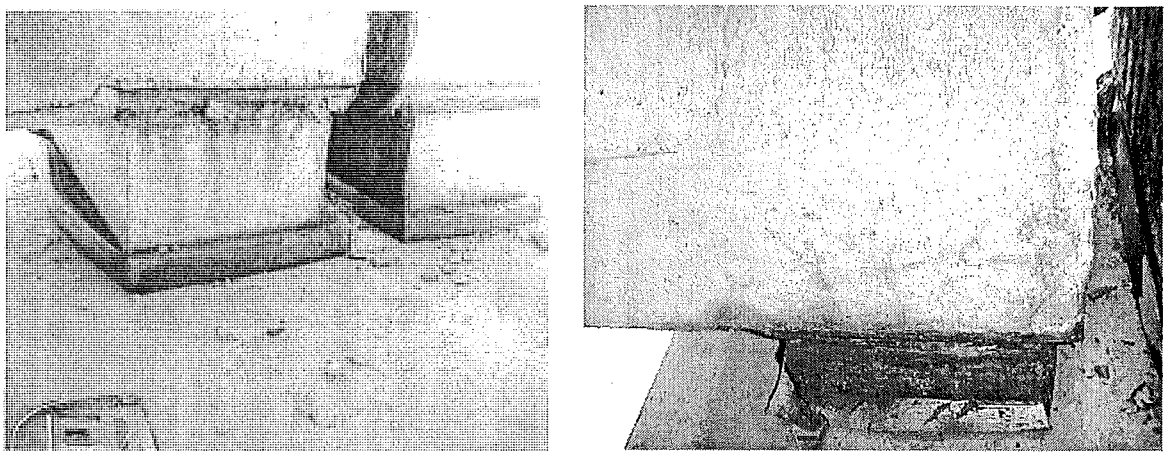

Photo 4-3. (Left) Sole plate corrosion and bulging at the sides of bearing pad, (Right) Sole plate corrosion and splitting, tearing and bulging at bearing pad

4.5 Summary

In this chapter, the prestressed concrete I-beam vulnerability to deterioration is defined based on the distress observed at the girder ends. A reason aggravating the beam-end distress is the expansion joint and/or the drainage system failure. As a result, the surface water together with dissolved deicing salts drain over the girder ends. With sufficient time deicing salts reach and initiate corrosion of the reinforcement and the tendons.

After performing the inspection and reviewing the inspection data consisting of 750 beam-ends and an equal number of bearings and sole plates, a pattern of deterioration was identified and a vulnerability assessment measure was proposed. The vulnerability assessment measure is based on the state of girder-end cracking in excess of 0.001 inches, expansion joint condition, functionality of the bearing pads and the state of corrosion of the sole-plate and bearing plate. The vulnerability can directly be assessed from the biennial visual inspection reports.

Five of the bridges inspected were of more recent vintage incorporating the continuous joint detail cast monolithically with the diaphragm and deck. The behavior of newer bridges is significantly different due to the lack of water infiltration (no leaky joint) and lack of subsequent restraint at the pier and abutment reduce sole plate corrosion.

The field survey of twenty prestressed concrete I-beam bridges included detailed visual inspection of the overall I-beam structure condition, including end deterioration for each I-beam. Beam-ends aging from two to ten years old were in very good condition, while older structures exhibited a greater amount of deterioration. Joint details in this bridge group vary with age and are likely the source of deterioration (high volumes of de-icing salts through leaky joints cause end deterioration of the I-beams). There is a need to include end condition assessment in the inspection procedure. This will allow for inspectors to rate the condition and properly assign a protective strategy prior to severe deterioration.

5.0 Multi-State Survey (Task 4)

5.1 Introduction

Having already obtained some Michigan data on the inspection, preventive maintenance and repair of prestressed concrete I-beams with the literature review and field inspections, it was imperative to know whether other states may be experiencing beam-end durability problems. To understand potential problems in other states, the research team developed, issued, and reviewed the feedback from a technical survey. With well-structured questions and an adequate response, a survey can be an effective tool for quickly interviewing a wide range or set group of respondents. The use of surveys is not a new concept in research. The durability and deterioration of prestressed concrete bridges has been investigated using surveys of state transportation departments in at least three past projects (Moore et al, 1970; Shanafelt and Horn, 1980; Rolander et al, 2001).

5.2 Objectives and Approach

Objectives of the survey included determining practices that are used for inspecting and repairing prestressed concrete I-beam ends, and identifying reports relating to the evaluation or repair of prestressed concrete I-beam ends. Specifically, five objectives were identified when preparing questions for the survey and they included:

1. Obtain a nationwide response rate of 20%; 100% from WI, IN, OH, MN, and IL.
2. Identify contacts for specialized areas of bridge engineering.
3. Locate potential sources of overall bridge condition and detailed beam end survey data.
4. Determine what practices are being used for evaluating and repairing prestressed concrete I-beam ends.
5. Identify reports relating to the evaluation or repair of prestressed concrete I-beam ends.

A section in the survey was also included for additional comments where recipients could clarify their overall opinions or comments relating to prestressed concrete I-beam evaluation and repair.

The survey was constructed to obtain as much information as possible from the respondents with as little effort on their part as possible. However, because of the unique information to be

gathered from each respondent, some questions request document information and most questions provide space for a contact name and telephone number. Where possible, the questions were structured with established answers (yes/no, or multiple choice). A copy of the survey and an accompanying cover letter is included in Appendix G-1: Survey Sent to State Departments of Transportation and Appendix G-2: Cover Letter for Multi-State Survey Instrument.

Several options were available for distributing and receiving survey responses. These formats consisted of:

1. Hardcopy (with U.S. Mail or fax return)
2. Response inside of e-mail text
3. Response inside of an e-mail attachment
4. On-line at the project or other website

Mr. Roger Till of MDOT Construction and Technology Division suggested that based on his experience, more responses would be generated if the survey was structured in a hardcopy or e-mail text format. To better satisfy the survey objectives, reference to completion and return of the survey on hardcopy or through the e-mail text was included in the survey cover letter.

The survey was distributed via email to the state bridge engineer, at each state's department of transportation, on June 27, 2001 by Mr. Till. The survey was accompanied by a cover letter, which is included in Appendix G-2: Cover Letter for Multi-state Survey Instrument. Email addresses for these engineers are contained in the MDOT list-serve database. Surveys were collected by Mr. Till and forwarded to Dr. Tess Ahlborn at Michigan Tech in order to centralize, review, and sort the survey data. Responses to MDOT were received between June and August 2001. The survey responses are tabulated in Appendix H and results discussed below.

5.3 Findings

Objectives for the multi-state technical survey were partially to fully met. A survey return-rate of 40 percent was achieved with 20 states responding. Responding states were located across the country and are shown as darkened states in Figure 5-1.

Two of Michigan's five neighboring states responded to the survey by the requested date and follow-up with non-responding states generated one additional survey response. One survey respondent indicated that the state did not have a prestressed concrete I-beam end deterioration problem and did not include a completed survey. This state was eliminated for the purposes of discussing the remainder of the results, leaving a base of 19 respondents.

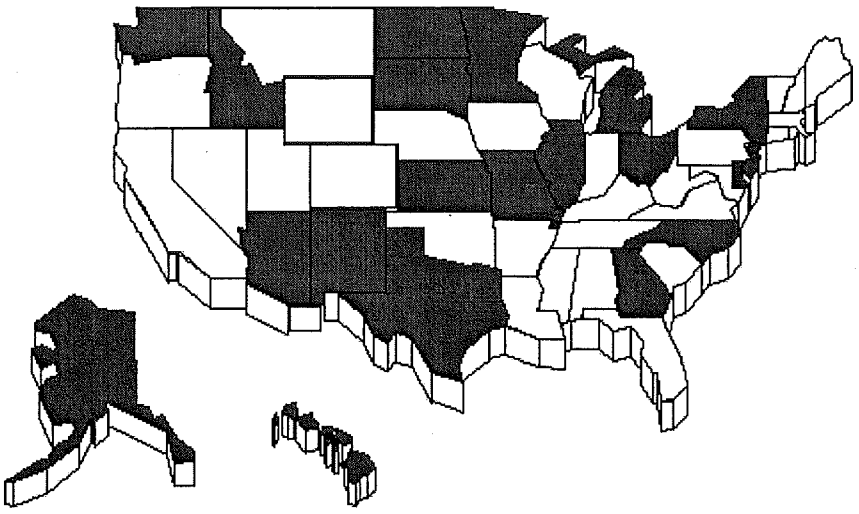

Figure 5-1. States Responding to the E-mail Survey

5.3.1 Inspection-Bridge Management Practices

Over 70 percent of the respondents indicated that they use some unique internal software for management of their state's bridge structural / safety data. All respondents indicated they do not gather specific inspection data on prestressed concrete beam end conditions. In regard to bridge inspection, all respondents indicated that the *FHWA Bridge Inspector's Training Manual / 90* (Hartle et al, 1990) is being used by their agency. The *AASHTO Manual for Condition Evaluation of Bridges* (AASHTO, 2000) was reported as being used by 74 percent of those responding. Nearly half (9 of 19) of those responding indicated that they also used some type of separate state-created document for inspecting bridges.

Illinois indicated having an inspection or assessment guideline, Illinois System Structure Information and Procedure Manual, (ISSIPM) which specifically addressed prestressed concrete I-beams. However, subsequent conversations with the Illinois Bridge Investigations and Repair Plans Unit Chief, Mr. Carl Puzey, indicated that the ISSIPM is only the Illinois version of how ratings for the NBIS should be taken (Puzey, 2001). The ISSIPM is largely based on the FHWA Recording and Coding Guide, according to Mr. Puzey (Puzey, 2001). Specific data on beam end conditions is not recorded and the ISSIPM is not intended to have the inspector pay closer attention to any one (bridge) item, according to Mr. Puzey.

Texas and Washington responded that non-destructive testing equipment (impact echo, detachable mechanical strain gauge, and fiber optic camera) was being used for inspection and assessment of their prestressed concrete I-beams. Follow-up with Mr. Randy Cox, Texas Department of Transportation Field Operations Section Director, indicated that bridge inspectors are not using impact echo and DEMEC gauges as part of routine bridge inspections (Cox, 2001). According to Mr. Cox, these tools are being used in special circumstances to investigate alkali-silica reaction (ASR) and delayed ettringite formation (DEF) deterioration of about 40 prestressed concrete I-beam bridges in Texas. Further, according to Mr. Cox, the DEMEC gauges are used to measure crack widths rather than strain in the members.

The remaining states indicated that their review of prestressed I-beams is limited to visual inspection and hammer sounding techniques.

5.3.2 Preventive Maintenance Practices

It was unclear from the survey responses if any states are using existing documentation (reports, etc.) to aid in the preventive maintenance of prestressed concrete I-beams.

Illinois was the only responding state that indicated they had documented prestressed concrete I-beam end preventive maintenance projects in their state. 3M's Zinc-Hydrogel Anode 4727 was applied to beam-ends as a preventive maintenance measure according to Illinois' survey response. Follow-up with Mr. Mark Gawedzinski of the Illinois Department of Transportation generated an IDOT report on Illinois' experience with the anode (Gawedzinski, 2001). According to this report, select I-beam ends of four structures were chosen for anode application in Illinois (IDOT, 2001). Both fascia and interior beams were selected (IDOT, 2001). The anodes were evaluated over a period of approximately three years for conformance with National Association of Corrosion Engineers (NACE) Standard 290-90 "Standard Recommended Practice for Cathodic Protection of Reinforcing Steel in Atmospherically Exposed Concrete Structures" (IDOT, 2001).

Although the 3M Zinc-Hydrogel Anode 4727 showed initial promise by conforming to the NACE Standard performance requirements, subsequent review of the anodes in 2000 revealed anode separation from the substrate and degradation of the hydrogel adhesive (IDOT, 2001). In addition, test procedures that were used to determine conformance to the Standard were suspected of not being representative of actual conditions. Consequently, Illinois rejected the 3M Zinc-Hydrogel Anode 4727 as a cathodic protection system.

On Texas' prestressed concrete I-beams affected by ASR and DEF, distresses are both local and widespread (Cox, 2001). Mr. Cox stated that some distresses are occurring at beam-ends where there are open joints (and water infiltration). Conversations with Mr. Cox, TxDOT, revealed that TxDOT applied a silane / paint treatment roughly 8 years ago to some prestressed concrete I-beams to try to mitigate ASR and DEF damage. Although no report was available on the study, Mr. Cox indicated that some additional distress has occurred to beam-ends since the treatment was first applied. Future distress of ASR and DEF damaged prestressed concrete I-beam bridges in Texas is anticipated to be so severe in the future that full replacement will be required, per Mr. Cox. Texas Special Specification 4421, Penetrating Concrete Surface Treatment, was cited by Mr. Cox as a specification that may be used in the preventive maintenance of prestressed concrete I-beams.

5.3.3 Repair Practices

While most states have not repaired prestressed I-beams for end deterioration, roughly 50 percent of the respondents indicated that their state's DOT specifications would be used in the rehabilitation of prestressed concrete I-beam ends. With the exception of Michigan, all states were contacted that indicated the potential use of their state's DOT specifications in beam repair. The reason for the follow-up was to obtain specific applicable section numbers that would govern the work. Hawaii and New Jersey engineers replied to the follow-up by indicating that, in contrast to their earlier response, a DOT specification did not exist that would govern prestressed concrete I-beam end repair. Both states indicated either a special provision or new specification section would need to be prepared to perform the work. Additional information was also obtained from three other states that indicated DOT specifications were available (Texas, New Mexico, and Illinois).

Texas Standard Specification Item 429, Concrete Structure Repair governs the repair of spalled and chipped areas of concrete structures. Epoxy mortar, portland cement concrete, and pneumatically placed concrete materials are permissible concrete repair materials in Texas per Item 429. Item 429 also includes recommended concrete removal, repair preparation, repair anchorage, and repair curing. Texas Special Specification 4421, Repair of Impact Damaged Prestressed Concrete Beams, was also cited by Mr. Cox as a potential document of interest to this project.

Mr. Puzey, IDOT, indicated that their Guide Bridge Special Provisions on Formed Concrete Repair, High Performance Shotcrete, and Polymer Modified Portland Cement Mortar could be followed for prestressed concrete I-beam end repairs in Illinois (Puzey, 2001). He indicated that Illinois had not found much success with epoxy mortars in repair. Other specifications are generated on a project specific basis.

Texas was the only state that cited the use of the *ACI Concrete Repair Manual* and *ICRI Repair Guidelines* for repairs. One initiative of the government funded SHRP was to develop concrete assessment and rehabilitation technologies (TTI, 1998). Although not mentioned in the survey, SHRP documents were not indicated as being used by any states.

Missouri was the only responding state that indicated using FRP repairs for the repair of damaged beams, however the respondent indicated that these repairs were not applied to beam ends.

Michigan has developed an overcasting repair procedure for prestressed concrete I-beams with end distress (Needham, 1999). Prior to encasing the beam end, the Michigan procedure specifies removal of deteriorated web and flange concrete. The overcast section on the beam end is also integrated with a new diaphragm. Repair concrete for this design is MDOT Grade D polymer (latex) modified concrete. MDOT plans were prepared detailing an end repair method for prestressed concrete I-beams with and without end blocks. This repair technique was executed in 1999 in Lower Michigan (Needham, 2000). Although numerous problems were encountered in the field repairs, they appeared to be attributed to contractor/engineer miscommunication and not necessarily the design details. According to MDOT, the cost of repairing prestressed concrete I-beam ends using this procedure was found to be 35 to 69 percent of full-replacement cost.

5.4 Summary

The survey was successful in showing that only a few states have addressed prestressed concrete I-beam end deterioration from an inspection, preventive maintenance, or repair point of view.

All states responding to the survey indicated that *FHWA Manual 90* was used as a guideline for the inspection of their bridges. Most states also use the *AASHTO Manual for Condition Evaluation of Bridges (2000)*. No states appear to be using non-destructive testing, other than acoustic emission testing, as part of routine bridge inspections, nor is any state paying particular attention to prestressed concrete I-beam ends during their inspections.

Preventive maintenance techniques that are currently in use include passive cathodic protection and sealers. According to the survey, Michigan is the only state that has attempted beam-end repair. Half of the responding states indicated that if beam-end repair was needed, that their state's standard specifications would govern the work.

6.0 Survey of Inspection Techniques (Task 5)

6.1 Introduction

The primary goal of this task was to develop an inspection procedure for early identification of prestressed concrete I-beam ends prone to deterioration. Due to field constraints it is desirable to limit the inspection techniques to visual (at an arms length). The techniques presented here are based on the literature review and the field inspection conducted during this project. The research team inspected 20 bridges and performed casual drive by inspections of numerous other prestressed concrete I-beam bridges. Afterwards the expectations from the inspection procedure were defined as to identify the symptoms related to: 1) material distress, 2) structural behavior, loading distress and 3) distress resulting from deferred maintenance. In some cases the symptoms related to the distress may overlap.

In reviewing the observations and data obtained during the inspections there are three inspection items of importance that directly impact I-beam end deterioration. These items are:

1. Presence of beam end cracking,
2. Bearing condition and their influence on beam end restraints, and
3. Drainage and expansion joint condition.

The presence of beam end cracks was observed as early as during production. Additional causes of beam end cracking may be due to loading and end restraints. Beam end restraints are controlled by the bearings, diaphragms and the deck if cast continuously. The effects of the restraints to beam behavior is investigated and described in Chapter 10.

Aside from the maintenance and structural behavior related distress, the material related distress is observed as cracking around the beam-end forming at the time of production. It is the research team's opinion that these cracks contribute significantly to premature end deterioration. Field inspection data showed that these cracks are widened with moisture ingress and freezing action. Later the ingress of chlorides further widens cracks during the shear reinforcement and tendon corrosion process. The initial crack widths are often around 0.001 inch and detection during inspection is difficult. (The cracking was observed using a water spray bottle and a magnifying crack gage). However, identification of cracks during early ages and including those beams in a preventive maintenance program with an appropriate sealant will prolong beam life.

Another inspection item identified during the field inspection was the sole plate and bearing plate assembly. Sole plate corrosion causes cracking of the beam near the base of the bottom flange. This cracking is perhaps initiated by the corrosion progressing to the sole plate anchors. Also,

this cracking propagates parallel to the bottom flange as corrosion progresses. Corrosion to the sole plate should be prevented either during design by the use of a non-corrosive plate or by maintenance. For existing bridges, maintenance solutions to the sole plate corrosion issue need identification. Sole plate corrosion is different from bearing plate corrosion by the fact that the sole plate is directly in contact with the beam and generates stresses in concrete unlike bearing plate corrosion which only effects the integrity of the bearing plate and elastomeric bearing pad.

6.2 Common States of I-Beam End Deterioration

This section reviews the current standards for the condition assessment of prestressed concrete beams and proposes condition states specifically for beam end deterioration.

6.2.1 Standards for Condition Assessment in Michigan

There are two current standards in Michigan for assessing the amount of deterioration to prestressed concrete I-beams. First, certified bridge inspectors for the State of Michigan are trained to assigned condition state numbers to each component of the bridge such as the deck, stringers, piers, and abutments, according to the Federal Highway Administration guidelines listed in the *FHWA Bridge Inspector's Manual / 90* (1991, revised 1995). These eleven condition states are given in Table 6-1.

Table 6-1. Federal Highway Administration condition ratings

Rating	Description
N	NOT APPLICABLE
9	EXCELLENT CONDITION
8	VERY GOOD CONDITON – no problems noted
7	GOOD CONDITION – some minor problems
6	SATISFACTORY CONDITION – structural elements show some minor deterioration.
5	FAIR CONDITION – all primary structural elements are sound but may have minor section loss, cracking, spalling, or scour.
4	POOR CONDITION – advanced section loss, deterioration, spalling, or scour.
3	SERIOUS CONDITION – loss of section, deterioration, spalling, or scour have seriously affected primary structural components. Local failures are possible. Fatigue cracks in steel or shear cracks in concrete may be present.
2	CRITICAL CONDITION – advanced deterioration of primary structural elements. Fatigue cracks in steel or shear cracks in concrete may be present or scour may have removed substructure support. Unless closely monitored it may be necessary to close the bridge until corrective action is taken.
1	"IMMINENT" FAILURE CONDITION – major deterioration or section loss present in critical structural components, or obvious vertical or horizontal movement affecting structure stability. Bridge is closed to traffic but corrective action may put bridge back in light service.
0	FAILED CONDITION – out of service; beyond corrective action

Certified bridge inspectors also assign a Pontis Condition State using the Pontis Bridge Inspection Manual (MDOT Lansing Maintenance Division, 1999). The manual illustrates four condition states for prestressed concrete I-beams; see Figure 6-1.

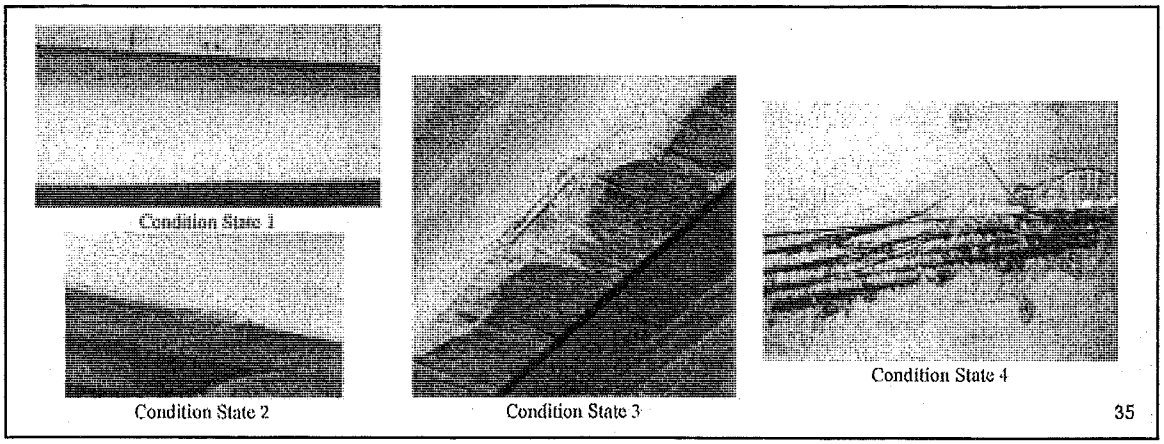

Figure 6-1. Pontis Bridge Inspection Condition State

While both inspection documents noted above are well known and highly used, neither is specifically written for inspection of prestressed concrete I-beam end deterioration.

6.2.2 Condition States

An accurate condition assessment of prestressed concrete beam-end deterioration is necessary to determine that level of distress and an appropriate preventative maintenance or repair technique. Condition states for a prestressed concrete I-beam should describe the level of distress at the beam-end that progresses with time. The following information has been assembled to assist an inspection crew with accurately assessing the condition of a beam-end. Twelve condition states have been developed (Table 6-2) utilizing the inspection data compiled during a field investigation of twenty prestressed concrete bridges in Michigan ranging in age from 2 to 40 years old (see Chapter 3). These condition states are only applicable to the beam-end and are meant to refine the FHWA Condition Ratings 9-4 and Pontis Condition States 1-3 reviewed above. In Table 6-2, hairline, moderate, and major crack widths are the same ranges as described in section 3.8.1-Condition Database.

Table 6-2. Condition States of Prestressed Concrete I-Beam Ends

Rating	Condition State
1	No cracks observed, no staining
2	Efflorescence, water-stains, and/or corrosion
3	Hairline Cracks. They can be horizontal, vertical, and/or diagonal
4	Map Cracks
5	Hairline Cracks with efflorescence, water-stains, and/or corrosion with a horizontal crack propagating from the sole plate
6	Cracked and Deformed Neoprene Pad, probably non-functional
7	Moderate Cracks
8	Moderate Cracks with efflorescence, water-stains, and/or corrosion
9	Major Cracks with efflorescence, water-stains, and/or corrosion
10	Delamination with Moderate and/or Major Cracks
11	Spall, Delamination, Corrosion, and Cracks
12	Spall, Exposed Reinforcement, and Corrosion

All photographs taken during the field inspection were grouped into respective condition states folders based on the distress demonstrated in the photo and the information obtain from the inspection form. The most distressed beam-end condition that was seen in the photo and on the inspection form defines the condition state for that beam-end. For example, if a photo of a beam-end only showed moderate cracks, and the inspection form also noted an area of delaminated concrete then the inspection form data will define the condition state and the assigned rating would be 10 and not 7. Two examples of every condition state are given in Photo 6-1 through Photo 6-12; photo name and bridge inventory number are also provided for each photo. The photo file convention is described in section 8.3.2.1-Bridge Inspection Photo Database. Photos are also tabulated to assist the inspector in defining condition states (Table 6-3).

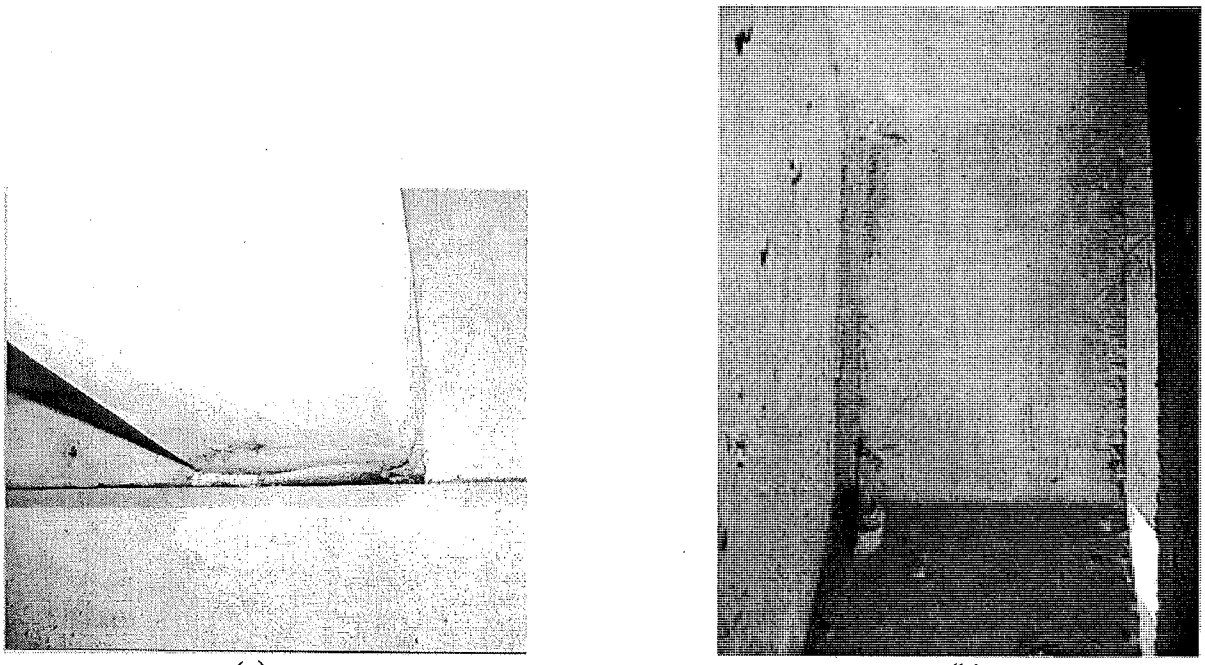

(a) (b)

Photo 6-1. Condition State 1—No cracks observed, no staining (a) E1-S4-E-U from 25132 S34 and (b) S1-E2-N-E.2 from 06111 S04

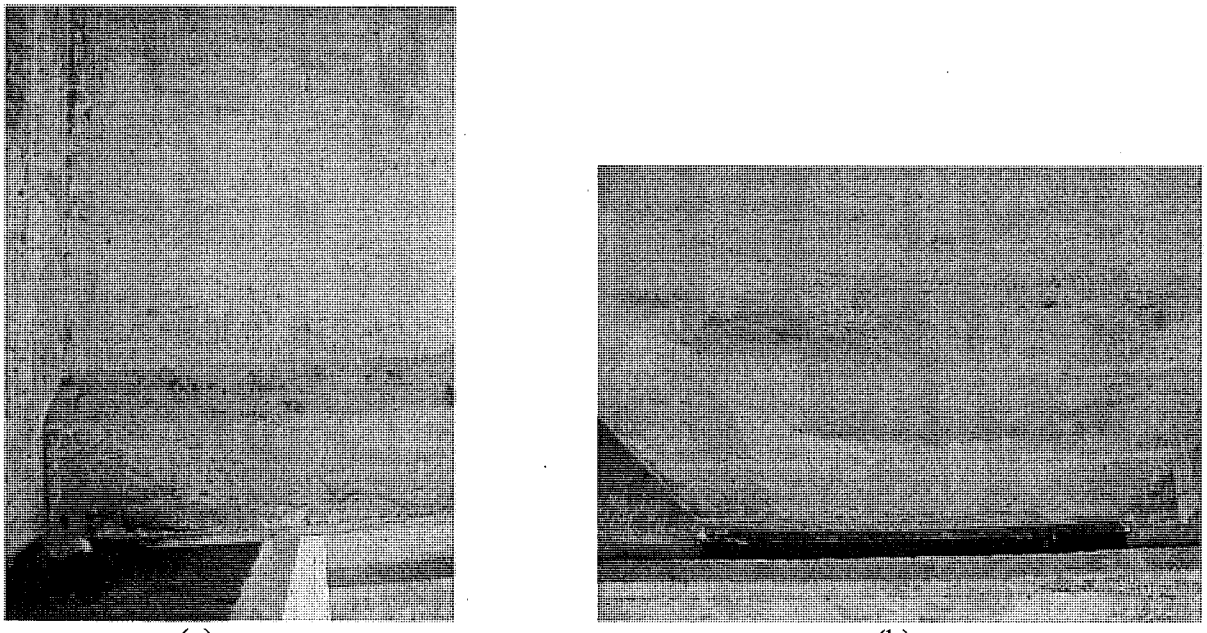

(a) (b)

Photo 6-2. Condition State 2—Efflorescence, water-stains, and/or corrosion (a) E4-S5-W-B from 53034 S05 and (b) S1-E2-N-U from 67016 S09

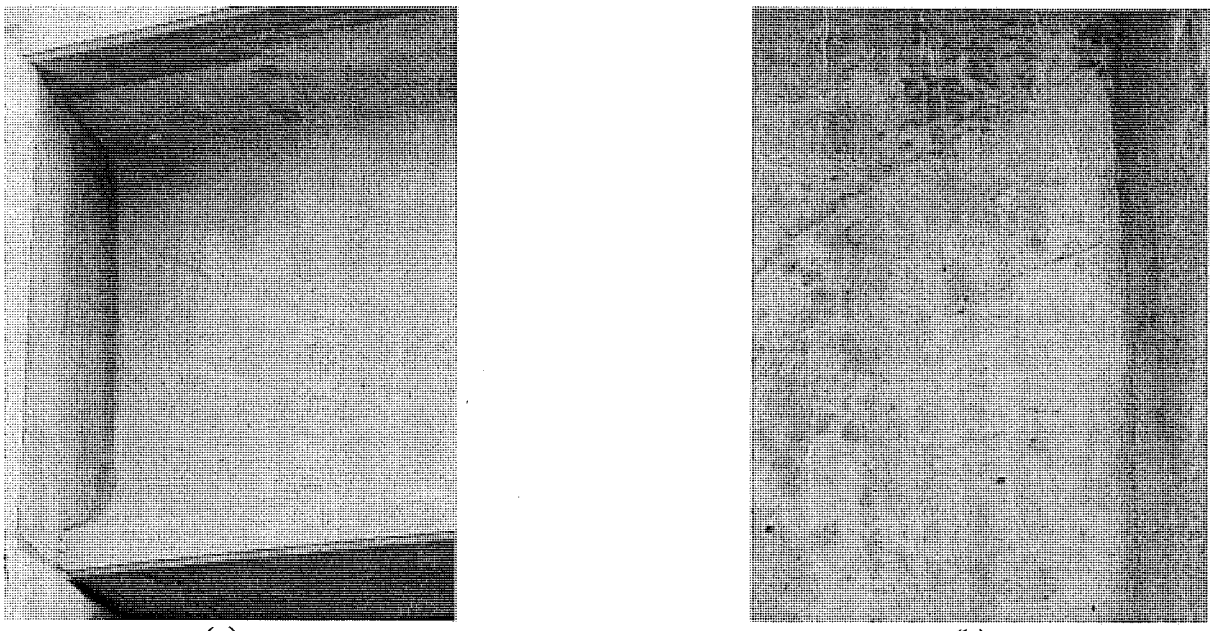

(a) (b)

Photo 6-3. Condition State 3—Hairline Cracks. They can be horizontal, vertical, and/or diagonal (a) E1-S1-W-S.3 from 83033 S06 and (b) E1-S8-W-N.2 from 83033 S06

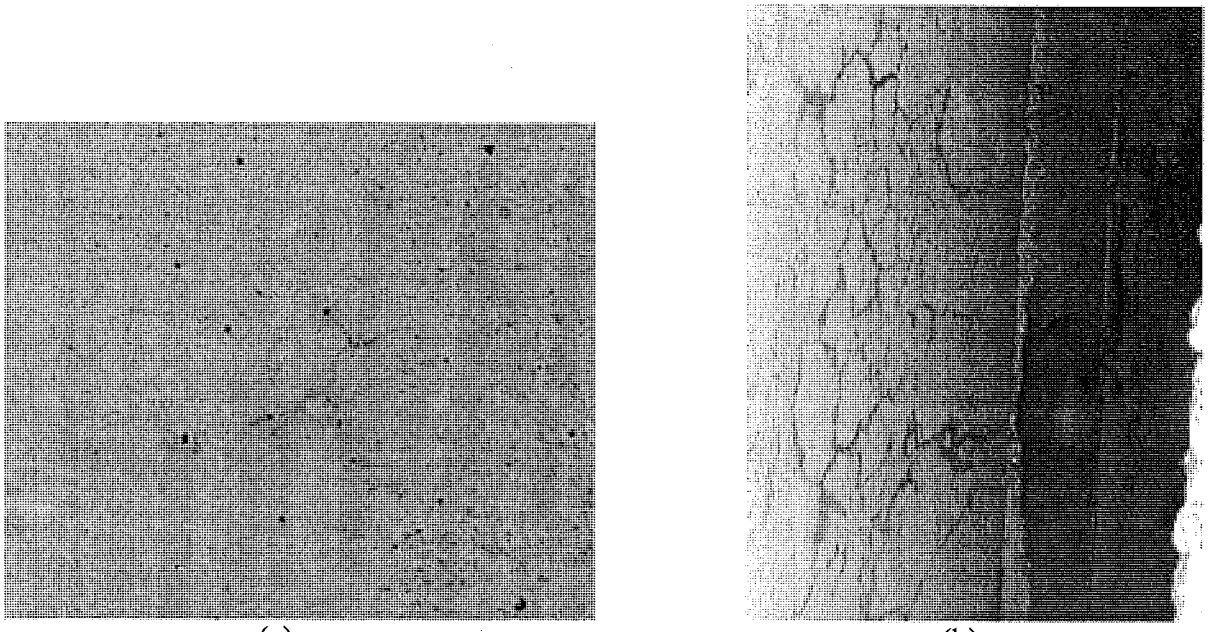

(a) (b)

Photo 6-4. Condition State 4—Map Cracks (a) E2-S3-E-S from 25132 S34 and (b) E4-S1-E-R from 53034 S05

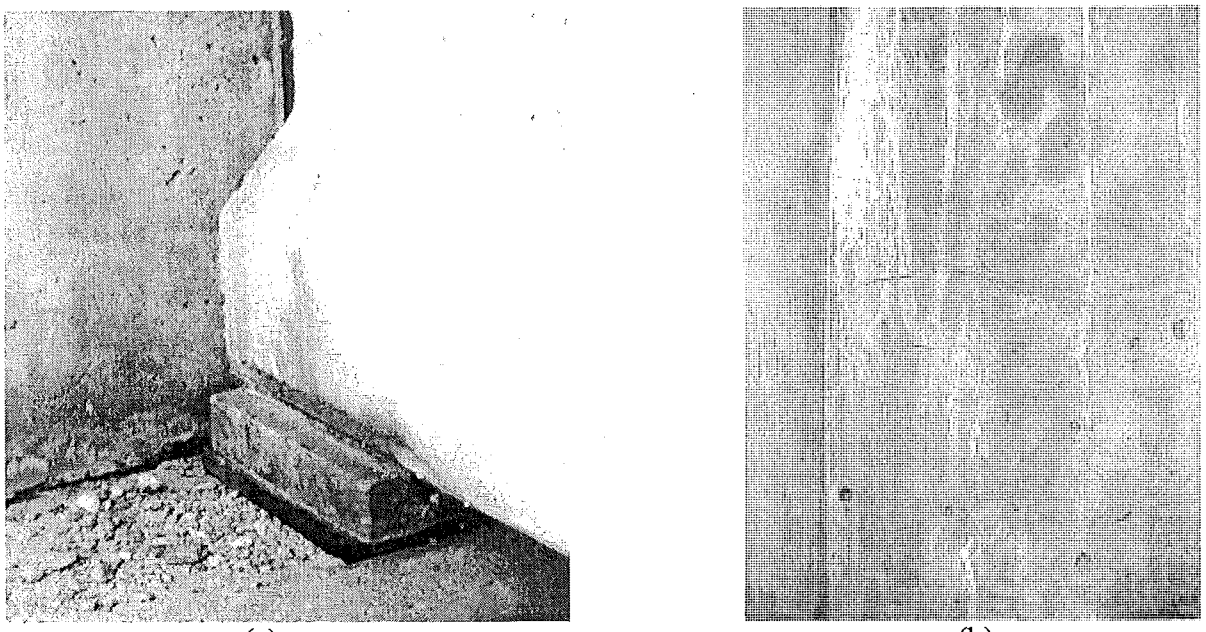

(a) (b)

Photo 6-5. Condition State 5—Hairline Cracks with efflorescence, water-stains, and/or corrosion with a horizontal crack propagating from the sole plate (a) S3-E9-N-E.1 from 29011 S03 and (b) E1-S8-W-S.1 from 83033 S06

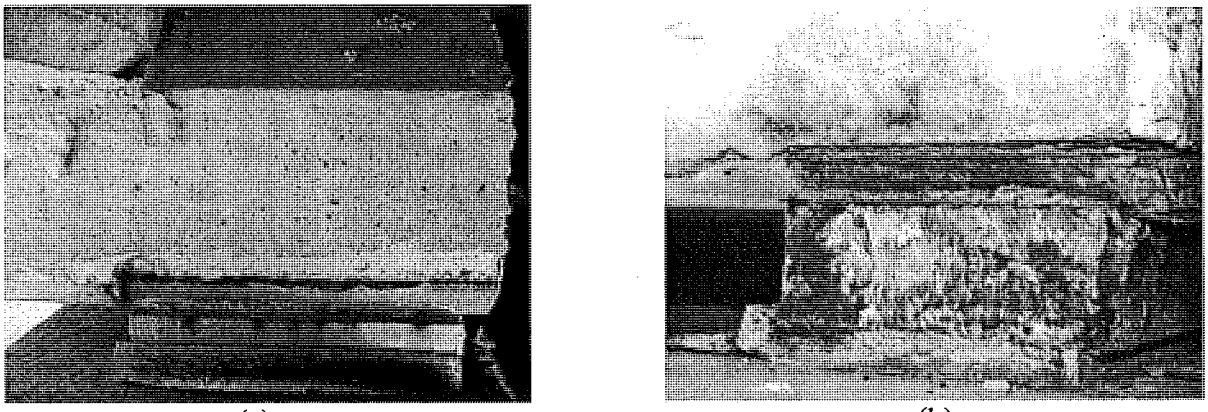

(a) (b)

Photo 6-6. Condition State 6—Cracked and Deformed Neoprene Pad, probably non-functional (a) S1-E2-N-B from 06111 S04 and (b) E1-S2-W-N from 41029 S16-3

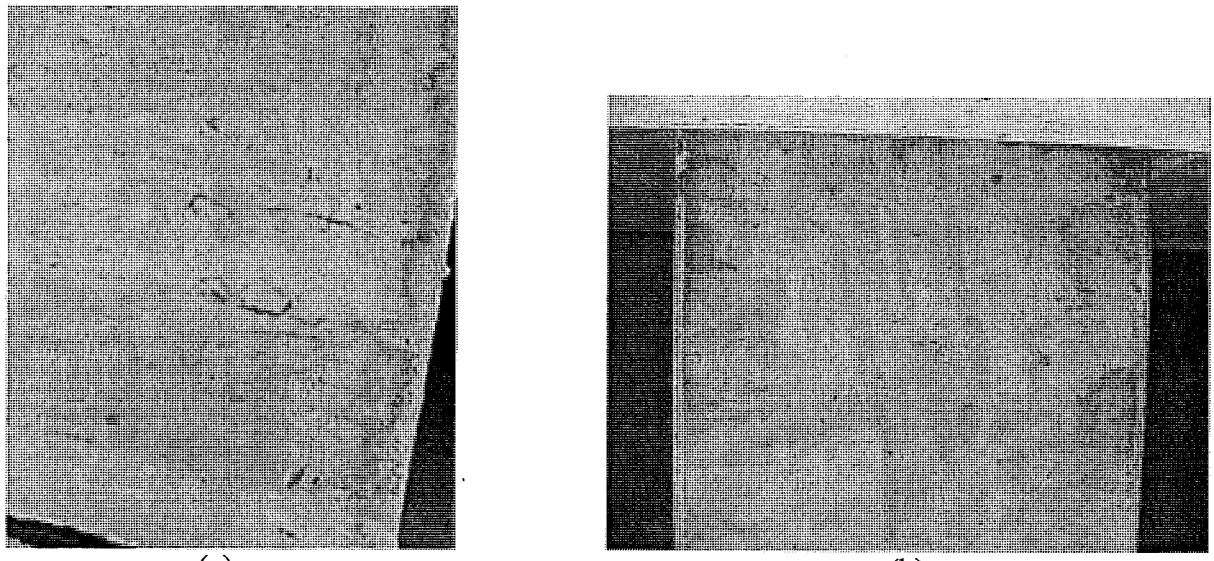

(a) (b)

Photo 6-7. Condition State 7—Moderate Cracks (a) E4-S1-E-S from 53034 S05 and (b) S1-E3-N-U from 67016 S09

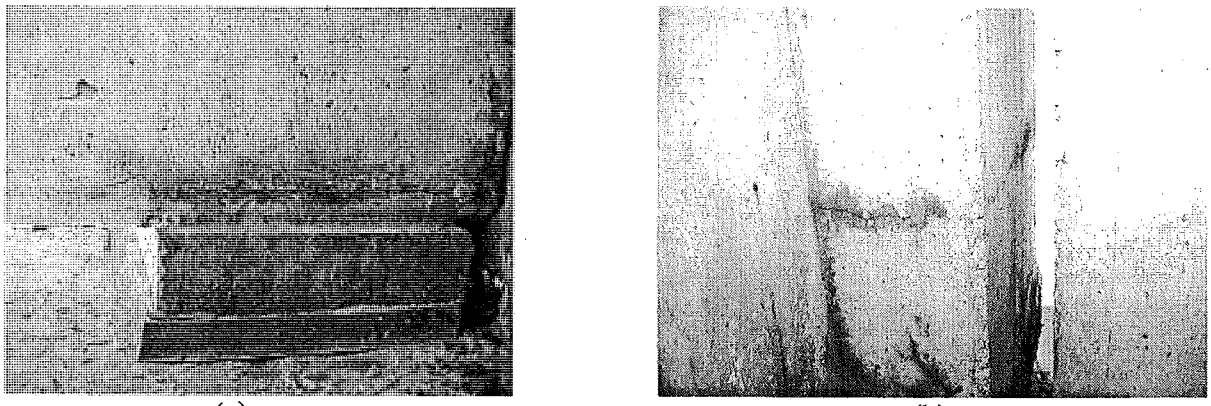

(a) (b)

Photo 6-8. Condition State 8—Moderate Cracks with efflorescence, water-stains, and/or corrosion (a) E2-S3-E-B from 25132 S34 and (b) E2-S8-E-S.2 from 41029 S16-4

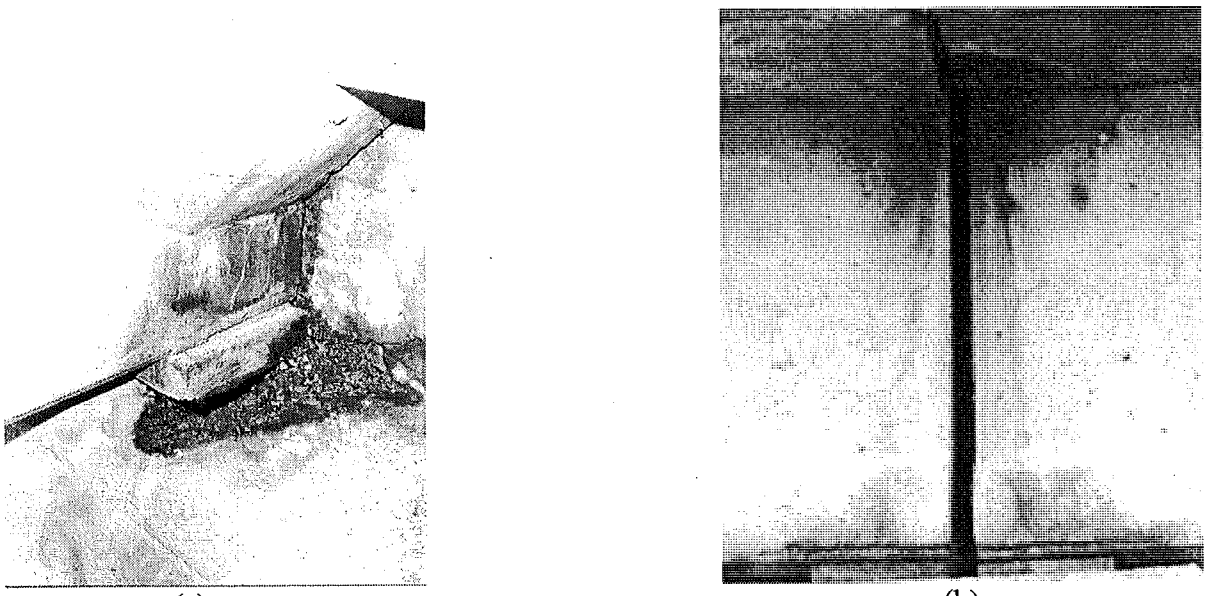

(a) (b)

Photo 6-9. Condition State 9—Major Cracks with efflorescence, water-stains, and/or corrosion (a) S3-E9-N-W.2 from 29011 S03 and (b) S2-E9-N-W from 29011 S03

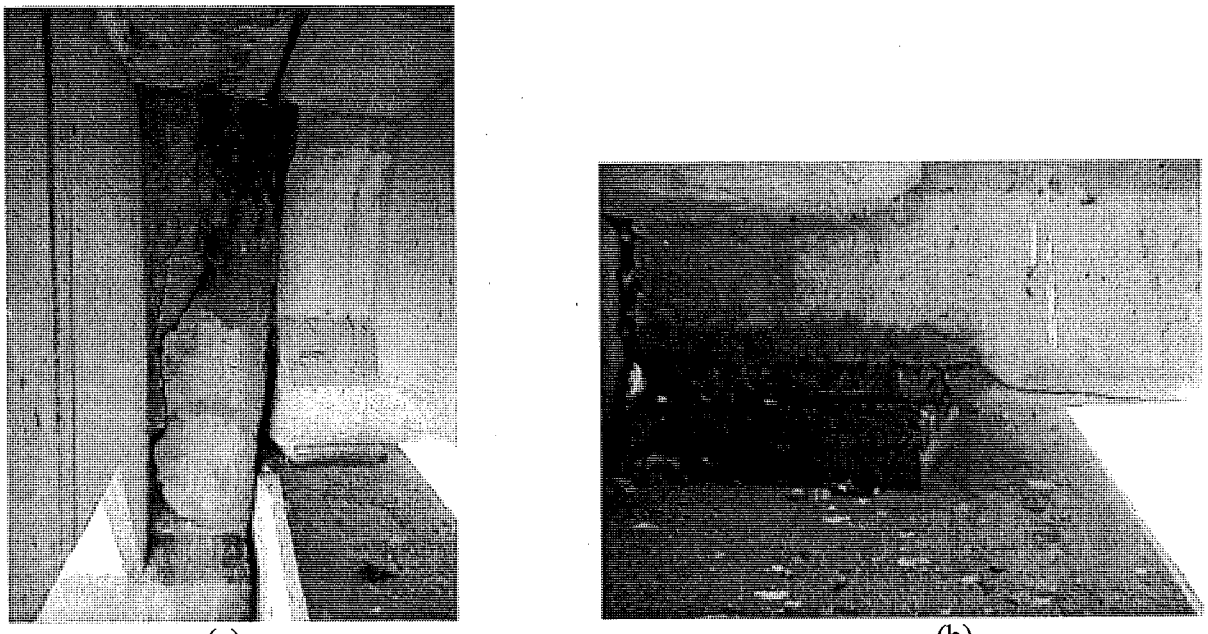

(a) (b)

Photo 6-10. Condition State 10—Delamination with Moderate and/or Major Cracks (a) E2-S5-E-S.1 from 25132 S34 and (b) S2-E8-N-W from 29011 S03

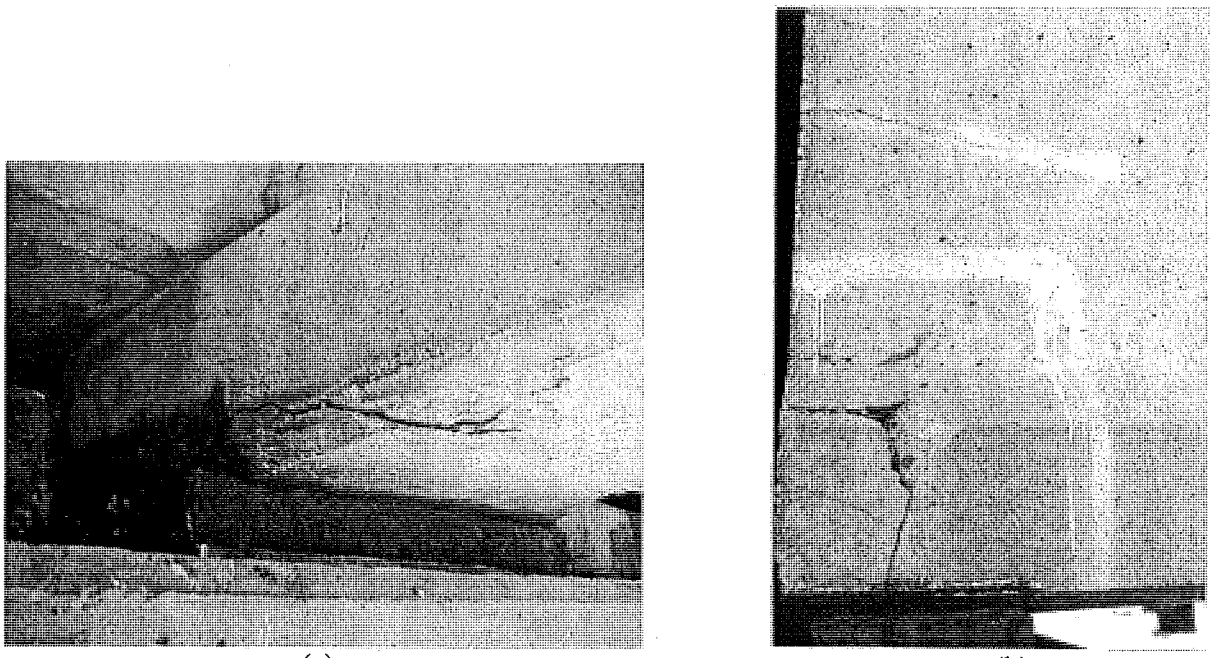

(a) (b)

Photo 6-11. Condition State 11—Spall, Delamination, Corrosion, and Cracks (a) S2-E7-N-U from 29011 S03 and (b) E2-S8-E-N.6 from 41029 S16-4

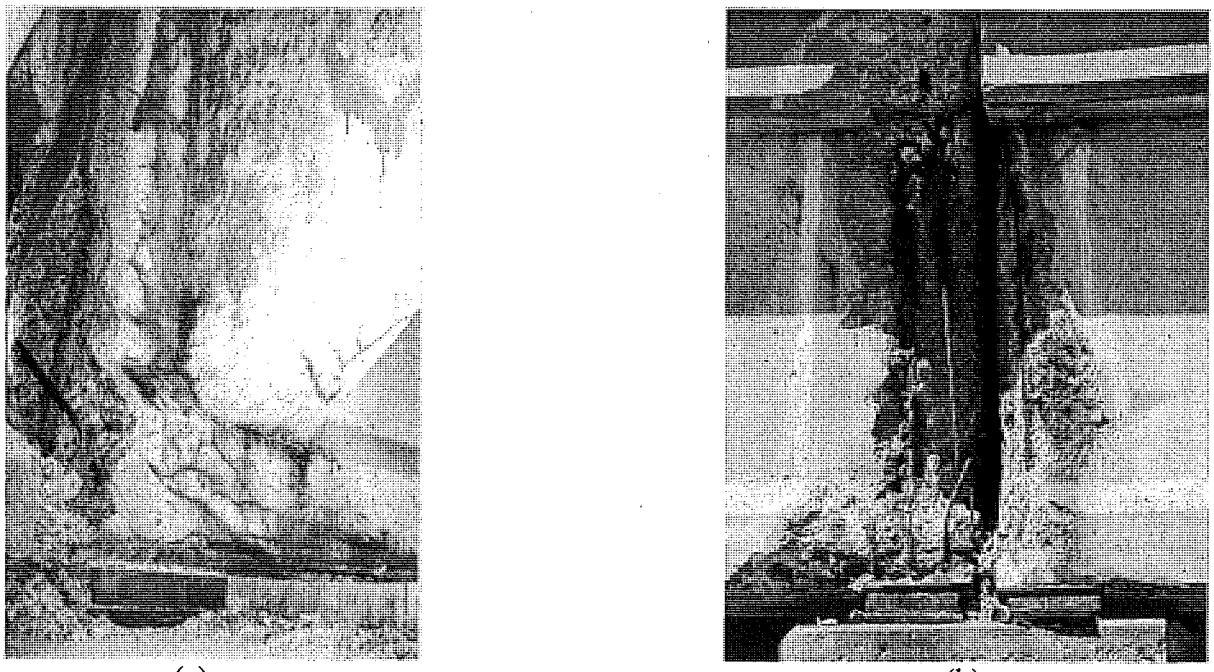

(a) (b)

Photo 6-12. Condition State 12— Spall, Exposed Reinforcement, and Corrosion (a) E3-S1-E-N.2 from 41029 S16-4 and (b) E2-S1-W-S.3 from 41029 S16-4

Table 6-3. Condition States Photographs

Condition State	Photos Demonstrating the Condition States
1) No cracks observed, no staining	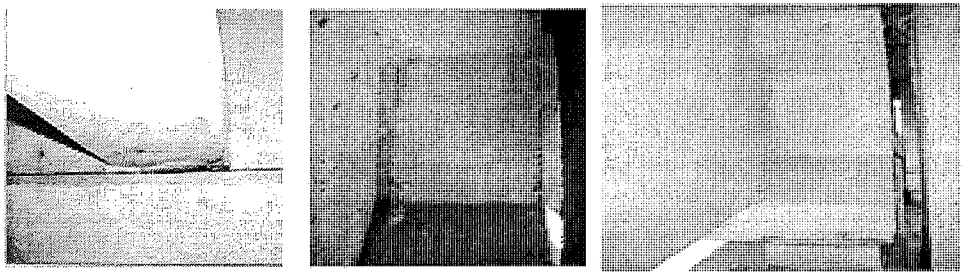
2) Efflorescence, water-stains, and/or corrosion	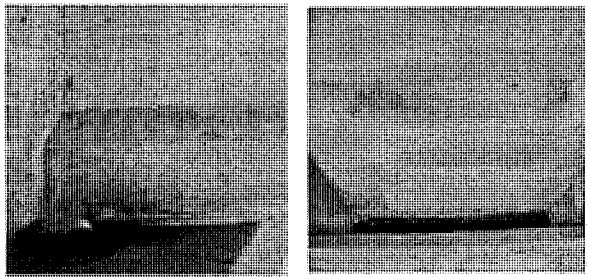
3) Hairline Cracks. They can be horizontal, vertical, and/or diagonal	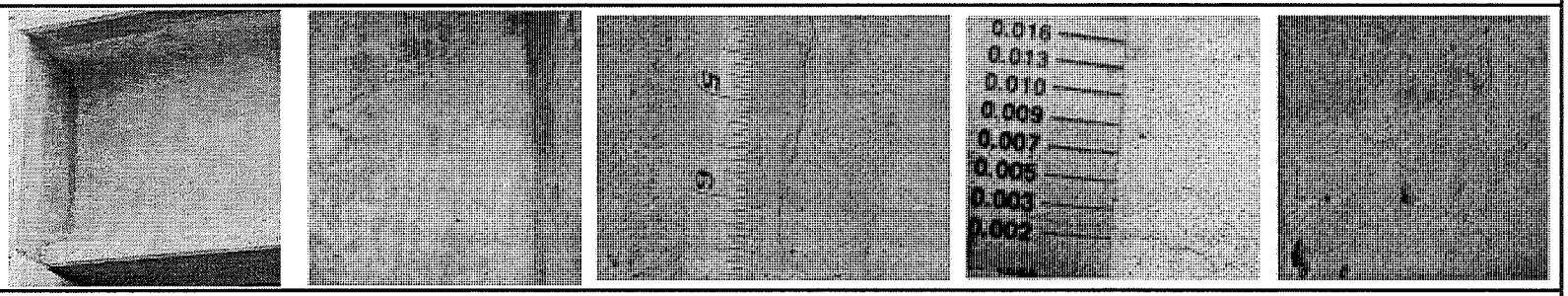
4) Map Cracks	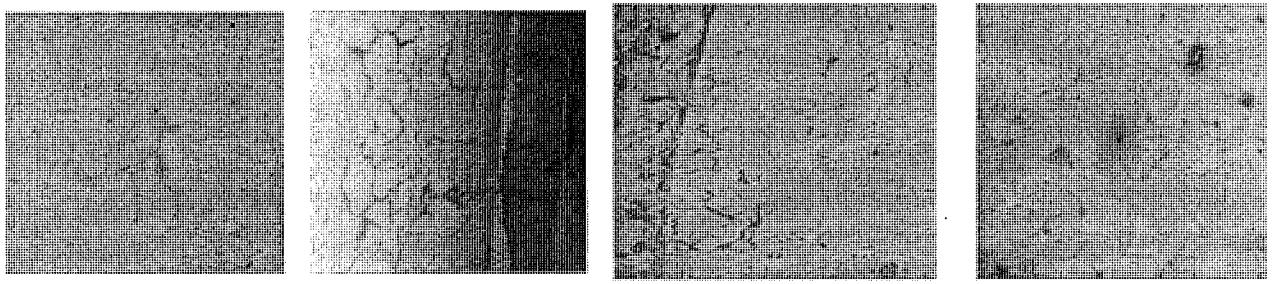

5) Hairline Cracks with efflorescence, water-stains, and/or corrosion with a horizontal crack propagating from the sole plate	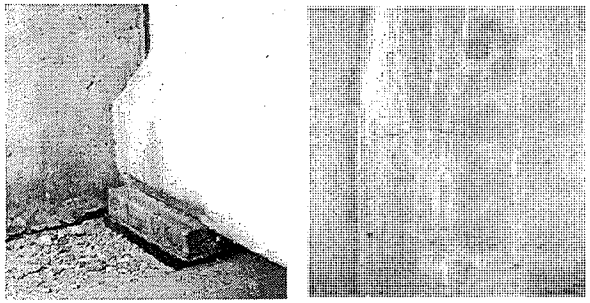
6) Cracked and Deformed Neoprene Pad, probably non-functional	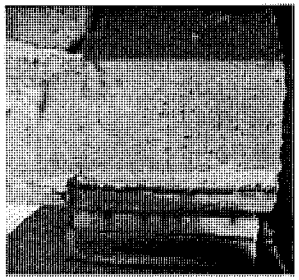 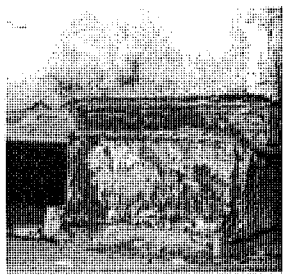 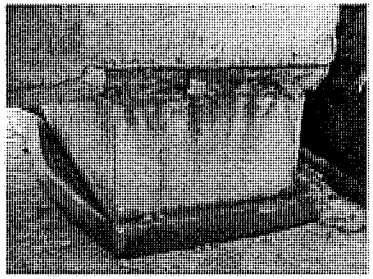
7) Moderate Cracks	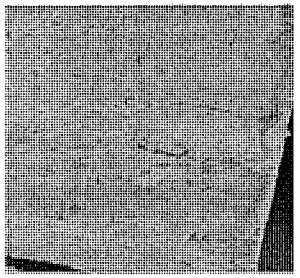 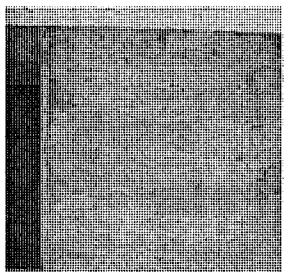 
8) Moderate Cracks with efflorescence, water-stains, and/or corrosion	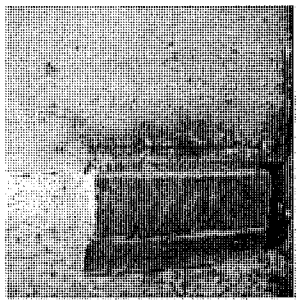 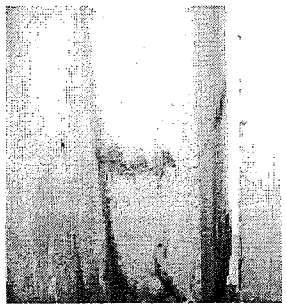  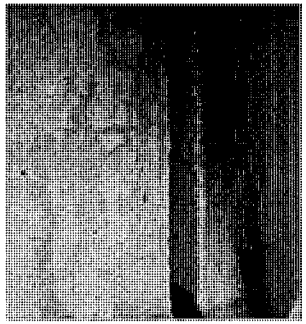 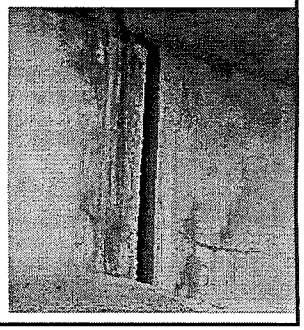

9) Major Cracks with efflorescence, water-stains, and/or corrosion

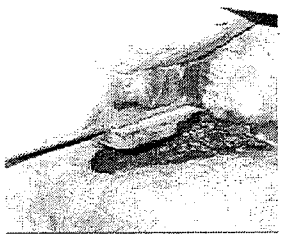
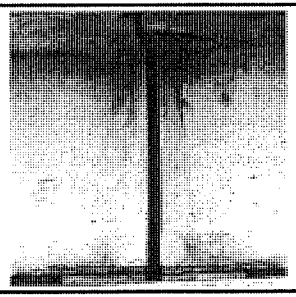
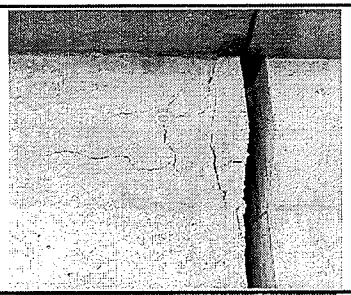

10) Delamination with Moderate and/or Major Cracks




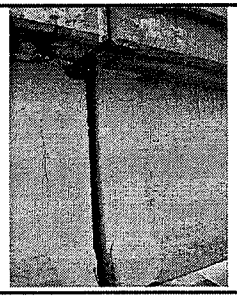
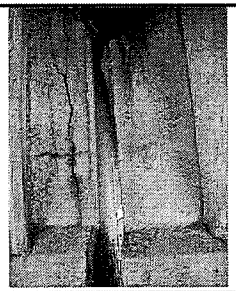

11) Spall, Delamination, Corrosion, and Cracks

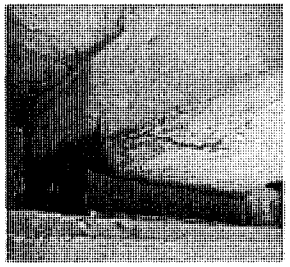
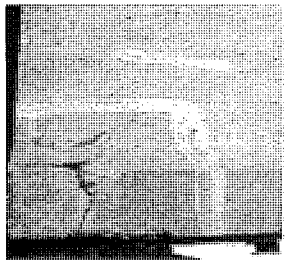
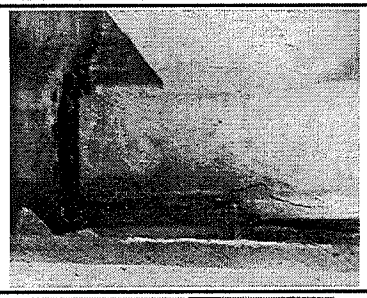
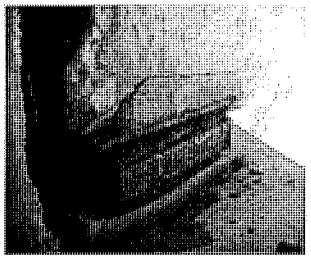
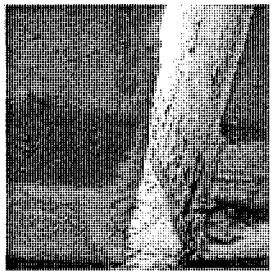

12) Spall, Exposed Reinforcement and Corrosion

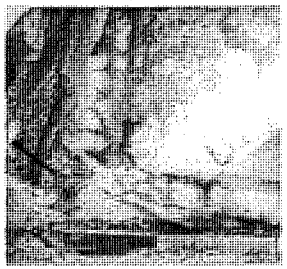

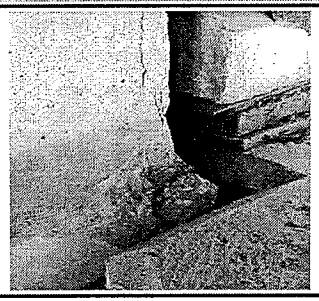
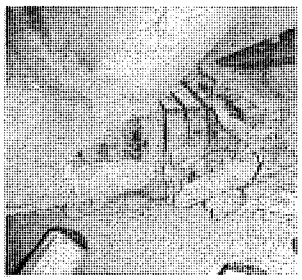


6.3 Summary

Accurate condition assessment of prestressed concrete I-beam ends is essential for the decision related to providing adequate preventative maintenance and repairs. Table 6-2 and Table 6-3 will assist the inspectors with accurate assessment. Later in Chapter 12, Table 6-3 is further linked to suggestions for preventative maintenance and repair.

7.0 Preventive Maintenance Techniques for End Deterioration (Task 6)

7.1 Introduction

This study identified four major families of preventive maintenance approaches that can be applied to beam-ends. These techniques were:

- Structure Modifications,
- Surface Insulating Methods,
- Electrical Control Methods, and
- Environment Modifying Methods.

These families of techniques were discussed in detail in Section 2.4.2 and are also presented in Appendix J. Advantages and disadvantages were also discussed in Section 2.4.2. As shown in Appendix J, several techniques are available for use. However, the research team found that silanes, siloxanes, and sacrificial anode cathodic protection are currently being used by other states for preventive maintenance purposes.

7.2 Analysis Tools

The research team has identified and developed analysis tools that can be used by MDOT to classify the severity of end-distress and determine which techniques may be most effective in preventing corrosion-induced deterioration of beam-ends. These tools are discussed in the following sections and apply to both preventive maintenance and repair type work.

7.2.1 Distress Severity Classification

To arrive at or decide upon an appropriate preventive maintenance or repair approach, say during a bridge scoping or as a prelude to a structural analysis, information on the condition of a deteriorated beam-end would need to be obtained. To this end, several different observations or tests can be performed to assess the condition of a beam-end. The research team has identified tests applicable to corrosion-induced deterioration that could be performed by MDOT to assist in classifying the severity of end distress. These tests are listed in Table 7-1. Engineering

judgment was largely used to establish severity levels based on a test result. However some references provided insight in setting each level. These references are included in Table 7-1.

Table 7-1. Testing Procedures and Distress Severity Criteria for Prestressed Concrete I-Beam End Deterioration

Test	Testing Performed In	End Distress Severity (references)			Notes
		Low	Moderate	High	
Air Content	Lab	≥ 6.0% (Kosmatka et al, 2002; ACI, 1999; ACI, 1992)	< 6.0%	< 6.0%	Deicer environment. Assuming a nominal maximum aggregate size of 3/4-inch (severe exposure)
		≥ 5.0% (ACI, 1992; AASHTO, 1996)	< 5.0%	< 5.0%	Non-deicer environment (moderate exposure)
Carbonation	Field / Lab	< 1-inch	≥ 1-inch and < 1.5-inches	≥ 1.5-inches	All conditions
Chloride Ion Content	Field / Lab	< 0.06% by wt. cement, water soluble (ACI, 1992; ACI, 1999)	≥ 0.06% and < 0.12% by wt. cement	≥ 0.12% by wt. cement	For all conditions, as measured at reinforcement.
Concrete Cover	Field	≥ 2-inches (ACI, 1999)	< 2-inches and ≥ 1-inch	< 1-inch	Deicer environment, tension less than $6(f'ci)^{0.5}$ (ACI, 1999)
		≥ 1.5-inches (ACI, 1999)	< 1.5-inches and ≥ 1-inch	< 1-inch	Non-deicer environment
Concrete Loss (Delamination and Spalling)	Field	No Concrete Loss	< 10% of end or any one side surface area	> 10% of end or any one side surface area	All conditions
Corrosion Potential	Field	more + than -200mV (ASTM, 1991)	more - than -350mV (ASTM, 1991)	more - than -350mV (ASTM, 1991)	All conditions
Corrosion Current Density	Field	≤ 0.2-mA/sf (Clear, 1989)	> 0.2-mA/sf and ≤ 1-mA/sf	> 1-mA/sf	All conditions
Crack Size (non-delamination)	Field	≤ 4-mils (Moore et al, 1970)	> 4-mils and ≤ 7-mils	> 7-mils	Deicer environment.
		≤ 7-mils (PCI, 1999)	> 7-mils and ≤ 10-mils	> 10-mils	Non-deicer environment.
Crack Type	Field	Non-structural	Non-structural	Structural	All conditions
Crack Length	Field	No criteria established			
Crack Direction	Field	No criteria established			
Staining	Field	No Evidence	Any Evidence	Any Evidence	All conditions

Test	Testing Performed In	End Distress Severity (references)			Notes
		Low	Moderate	High	
Water / Cement Ratio	Lab	≤ 0.40 (Kosmatka et al, 2002; ACI, 1999)	> 0.40 and ≤ 0.45	> 0.45	Deicer environment
		≤ 0.50 (Kosmatka et al, 2002; ACI, 1999)	> 0.50	> 0.5	Non-deicer environment Note: Criteria assumes air-entrained concrete

Some tests listed in Table 7-1 cannot be performed rapidly in the field or by inexperienced staff. These tests are generally more costly to perform and inherently less preferable to less intensive or advanced procedures. In addition, some tests hold more worth in assessing the condition of a beam-end compared to other tests. For example, the amount of concrete loss is, even to the casual observer, more influential in determining the condition of a beam-end than say air content. To effectively use Table 7-1, MDOT would need to first identify which tests or observations to perform and second, assign weighted importance to the tests themselves. Lastly, a procedure would need to be developed to sum the results of all tests performed to determine the distress severity. Recommendations for accomplishing the effective use of Table 7-1 are included in Section 14.4 of this report.

7.2.2 Distress Cause and Recommended Follow-up Techniques

Determining the level of distress severity is one step towards selecting a preventive maintenance or repair technique to use on a beam-end. In order for a preventive maintenance or repair technique to be effective, the cause of the distress must be known and technique selected to properly address the cause. Table 7-2 presents several cause-evidence relationships that field personnel can use to identify the cause of beam-end distress. It should be noted that although beam-end distress in Michigan I-beam bridges appears to be corrosion induced deterioration, other forms of deterioration might surface in the future. Therefore, several cause-evidence relationships are listed.

A natural progression of Table 7-2 is to identify preventive maintenance or repair techniques that can be used for a particular cause-evidence (effect) relationship. At a basic level, a subjective approach can be used to say that one technique for one or multiple distress severities (e.g., use passive cathodic protection for low and moderate severity beam-end distress). It is imperative to understand that while each cause of distress can be linked to a preventative maintenance or repair technique, every case must be considered on an individual basis. For example, for a case where the primary cause of distress is leaking expansion joints the immediate solution appears to be repairing the joint. However, corrosion must be halted so that continued degradation does not occur. Depending on the level of distress, chloride ion extraction may be necessary in conjunction with cathodic protection and additional sealers. MDOT can use and extend this approach to future work as another means of obtaining desirable results.

Table 7-2 attempts to list preventative maintenance (PM) and repair techniques for low, moderate and high severity levels of distress. For distresses directly linked to corrosion-induced deterioration, methods from Appendix J have been subjectively assigned to varying distress levels. For non-corrosion induced distress, such as thermal-induced movements, no techniques

have been listed at this time. Rather a note has been added stating "Identify and Subjectively Assign Techniques" and should be addressed through future work.

Table 7-2. Cause-Evidence Relationships for Beam-End Distress

Primary Cause of Distress	Secondary Cause of Distress	Beam-End Evidence	PM / Repair Technique		
			Low Severity Distress	Moderate Severity Distress	High Severity Distress
Leaking expansion joints	Chloride-induced corrosion	• Failed joint (look between diaphragm pairs). Fine debris (sand, cigarette butts) will be present on the top of the pier (investigators observations). • Top or sides of pier may show deterioration. • Elevated levels of chloride ion may be present with corrosive staining. • Spalled, cracked, or delmainated concrete may be present (investigators observations). • Vertical cracks may be present.	see App. J 1.0 2.0	 1.0 3.0 4.0 5.0	 1.0 4.0 5.0
Wet or moist service environment	Frozen, corroded bearings	• Localized spalling at the bearings with little to no signs of reinforcement corrosion • Steel bearing plates would show complete corrosion	Identify and Subjectively Assign Techniques		
	Freeze-thaw deterioration	• Surface scale, cracking, or crumbling of the beam end will be evident. • Of these distresses, scaling will likely give the greatest indication that the distress is freeze-thaw related. • Low air content of concrete.	Identify and Subjectively Assign Techniques		

Primary Cause of Distress	Secondary Cause of Distress	Beam-End Evidence	PM / Repair Technique		
			Low Severity Distress	Moderate Severity Distress	High Severity Distress
Acidic service environment	Carbonation-induced corrosion	• High *w/c*. • Older structures may be affected to a greater degree. • Distress may extend to the entire member. • Some source of moisture would need to be present; a high humidity environment may be sufficient. • Vertical cracks may be present.	see App. J 2.0 4.0	4.0	4.0 5.0
Inadequate concrete cover	Carbonation-induced corrosion	• Cover to reinforcement may be less than indicated on the design drawings or less than current design requirements. • High *w/c*. • Older structures may be affected to a greater degree. • Distress may extend to the entire member. • Some source of moisture would need to be present; a high humidity environment may be sufficient. • Vertical cracks may be present.	see App. J 1.0 2.0	1.0 2.0 5.0	1.0 5.0
	Chloride-induced corrosion	• Cover to reinforcement may be less than indicated on the design drawings or less than current design requirements. • Elevated levels of chloride ion will be present with corrosive staining, spalled, cracked, or delmainated concrete. • Vertical cracks may be present.	see App. J 1.0	1.0 3.0 4.0 5.0	1.0 3.0 4.0 5.0
Thermal-induced movements	None identified	• Twisting or other distortion of the member, possibly in the weak axis.	Identify and Subjectively Assign Techniques		
Diaphragm bonding	None identified	• Horizontal cracking may be present.			

Primary Cause of Distress	Secondary Cause of Distress	Beam-End Evidence	PM* / Repair Technique		
			Low Severity Distress	Moderate Severity Distress	High Severity Distress
Overloading or impact of the element	None identified	• Diagonal cracking may be present.	Identify and Subjectively Assign Techniques		
Improper cutting of prestressing strands	None identified	• Horizontal, diagonal, or frown cracking may be present.			
Location of un-bonded strands	None identified	• Longitudinal flange cracking may be present.			
Insufficient reinforcement	None identified	• Diagonal or map cracking may be present.			

*PM is an Abbreviation for Preventative Maintenance

7.2.3 Performance Matrix

If it is desired to use preventive maintenance to prolong beam life, a performance matrix may aid in selecting the most effective approach between multiple suitable approaches. For this study, an example matrix was developed specifically for distresses attributed to corrosion-induced deterioration from leaking transverse deck joints. Similar tables may be developed for other cause-effect scenarios, however this relationship appears to govern a majority of the time.

In order to develop a performance matrix, technical requirements for the preventive maintenance approach need to be identified. For this study, technical requirements were selected as those having the greatest impact on prestressed concrete I-beams in Michigan. MDOT will ultimately need to identify which technical requirements are most important, however, as a starting point, MDOT may want to consider the:

- Effectiveness to control reinforcement corrosion.
- Durability of the technique.
- Infrastructure requirements of the technique.
- Service life of the technique.

In Table 7-3, each preventive maintenance approach is evaluated for meeting the technical requirements. The research team attempted to identify a consistent procedure that could be used to assign a score to a technical requirement. At a basic level, a technical requirement score could be determined by review of independent or vendor provided literature, and conclusions can be made for products either meeting, not meeting, or inconclusively meeting the technical requirements.

Table 7-3. Example Performance Matrix for Preventive Maintenance Techniques

Approach **All approaches are not listed.**	Technical Requirement	Effectiveness	Durability	Infrastructure	Service Life	**Total Score (60 max)**
	Weighted Importance	10	7	8	5	
	Impact Definition	0 = Not effective 1 = Inconclusive 2 = Effective	0 = Not durable 1 =Inconclusive 2 = Durable	0 = Required 1 = Inconclusive 2 = Not required	0 = < 4 years 1 =Inconclusive 2 = ≥ 4 years	
Transverse Deck Joint Maintenance	Weighted Score (weighted importance x impact definition)	20	7	16	10	**53**
Sacrificial Anode Cathodic Protection, SACP		10	7	16	5	**38**
Penetrating Sealers		0	7	16	5	**28**
Surface Sealers		0	7	16	5	**28**
Surface Coatings		10	14	16	10	**40**
Surface Applied Corrosion Inhibitors		10	7	16	5	**38**
Crack Treatment for Beams		10 [a]	7	16	5	**38**
Impressed Current Cathodic Protection		20	0	0	10	**30**

[a] No data available, therefore an inconclusive impact definition was assigned

Table 7-3 is an example of what a completed performance matrix may look like. In Table 7-3, the importance of each requirement was viewed relative to one another and assigned weights using a point scale of 1 to 10. A high score in the matrix does not necessarily mean a technique is appropriate for a certain level of distress, but does establish preference among the available options. MDOT can refine this matrix or develop new matrices based on specific input from their personnel. Additionally, ideas for future development of this performance matrix are given in Chapter 14 – Recommendations for Future Work.

7.3 Summary

Four families of preventative maintenance techniques were identified and can be applied for beam-end deterioration. Several test procedures are identified for inspectors and field personnel to assist in categorizing the level of distress (low, moderate, high). While determining the level of distress is important in selecting a preventative maintenance technique, the cause of distress must be known (usually through beam-end evidence) so that technique can properly address the cause. Therefore, several cause-evidence relationships were identified, including those forms of deterioration beyond corrosion-induced deterioration. Each distress cause and its beam-end evidence has been linked to several preventative maintenance and repair techniques for varying levels of distress. It is important to understand that while each distress cause can be linked to a preventative maintenance technique, every case must be considered on an individual basis.

8.0 Project Website (Task 7)

8.1 Introduction

The Center for Structural Durability's website provides information on completed and current projects activities. The project website is regularly being updated and modified as new and old projects are started and completed. The website is located at Wayne State University in accordance with Task 7 description. Figure 8-1 shows the Homepage of the project website. The current website address is:

http://webpages.eng.wayne.edu/durabilitycenter

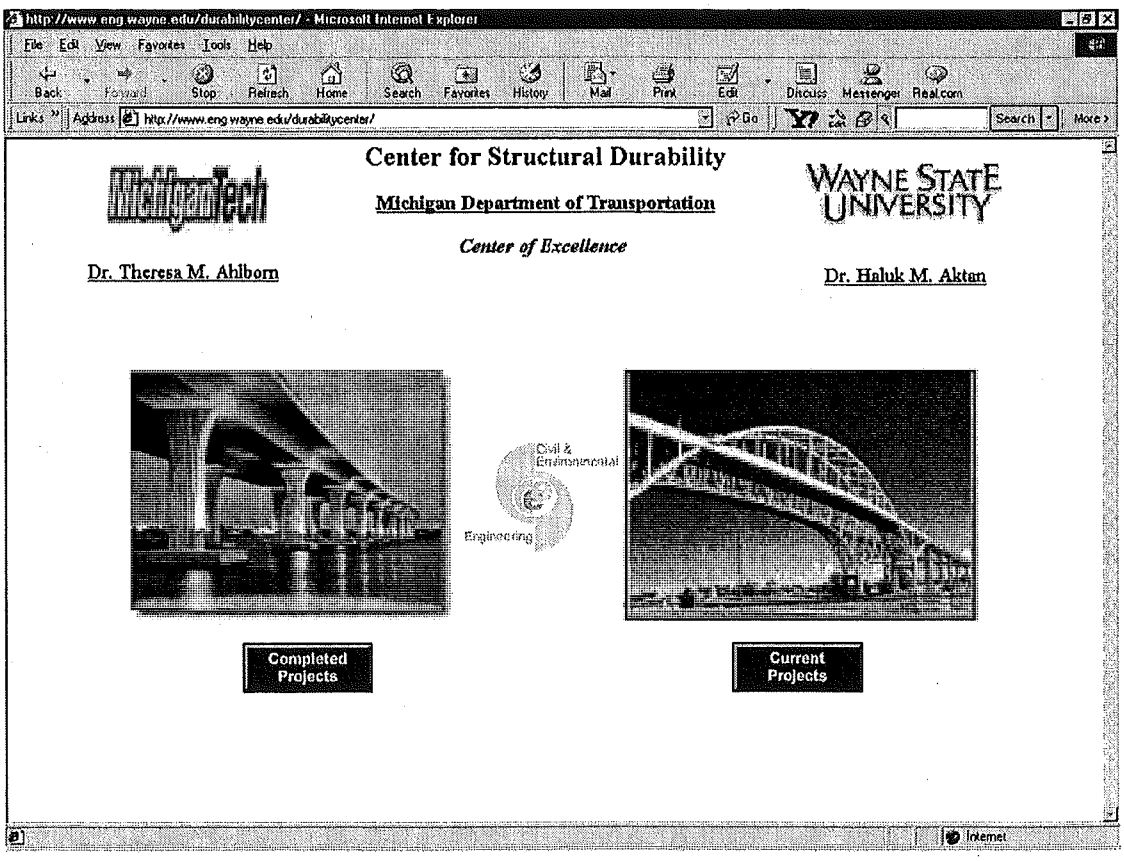

Figure 8-1. Durability Center's Homepage

8.2 Site Map

The site map provides a visual overview of how the web pages are connected through hyperlinks. Figure 8-2 depicts the main pages of the Center for Durability's website.

A. Homepage of Center for Durability
B. List of Completed Projects
C. Project Homepage of Evaluation of Concrete Permeability by Ultrasonic Techniques
D. List of Current Projects
E. Project Homepage of Causes & Cures of PC I-Beam End Deterioration
F. Project Homepage of Criteria and Benefits of Penetrating Sealants for Bridge Decks

As projects are completed, they will move to the List of Completed Projects.

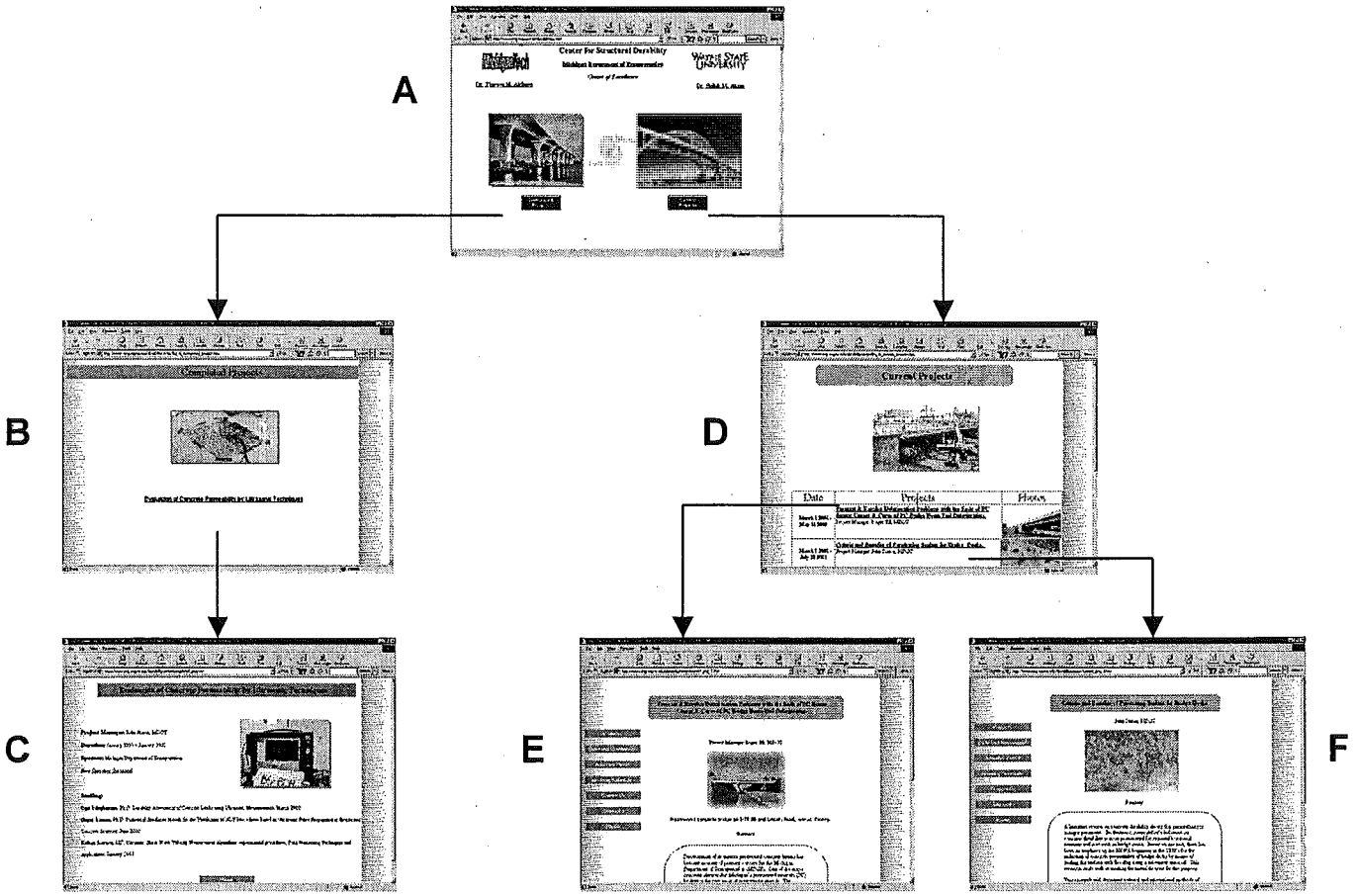

Figure 8-2. General Site Map of Durability Center Website

8.3 Project Homepage of Causes & Cures for Prestressed Concrete I-Beam End Deterioration

The project home page is an active site. The web site contains two areas: one area is limited to the project group, and the other area is open for public access. The ID's and Passwords were transmitted to the project participants during July 2001. The public part of the website contains overview information on the ongoing status of the Causes & Cures for Prestressed Concrete I-Beam End project.

8.3.1 Password Protected Portion

The password-protected portion of the website is for use by the project staff as a communication medium. Two features are currently implemented. One feature is for compiling all the references reviewed to date, including abstracts. This feature allows coordination of the literature review between Michigan Tech and Wayne State. Its primary purpose is to avoid duplication of work by the project participants located at the two institutions. An additional purpose is to provide information to the research advisory panel in terms of the extent of work being performed.

The second feature of the password-protected portion is for report preparation. This feature of the site allows the research team to develop report outlines and enter report text. This site will also give information to the research advisory panel about the development of the reports.

8.3.2 Public Access Portion

This portion of the site contains general information regarding the project. Data and Documents, Advisory Panel, Meeting Schedule, Contact Us, and Site Links are the buttons that a user can choose to access information. The Data and Documents link contains data, abstracts, papers, and reports completed to date. The Advisory Panel link contains a list of the research advisory panel members with email addresses and some telephone numbers. The Meeting Schedule link contains the schedule of meeting, meeting minutes, and handouts. The Contact Us button contains email addresses and telephone numbers of the people responsible for this project. The Site Links button contains links to the two universities' civil engineering homepages and links to other organizations. The bridge inspection picture database (which is part of Data and Documents) will be discussed in the following subsection.

8.3.2.1 *Bridge Inspection Photo Database*

During the field investigation, digital pictures and photographs were taken of a fraction of the beam-ends and of the overall structure as the research team completed their field investigation forms. Pictures of the beam-ends were taken when the research team members saw repetitive deterioration features such as mapping cracks or horizontal hairline cracks at the web. The pictures of the research team's field investigation are displayed on the Center of Durability's website (http://www.eng.wayne.edu/durabilitycenter). Access the site by "Current Projects," they by "Causes & Cures for Prestressed Concrete I-Beam End Deterioration," next by "Data and Documents," then the hyperlink Bridge Inspection Picture Database. These actions will display the image depicted in Figure 8-3. Once this page is reached access to the bridge file is by the bridge's ID number.

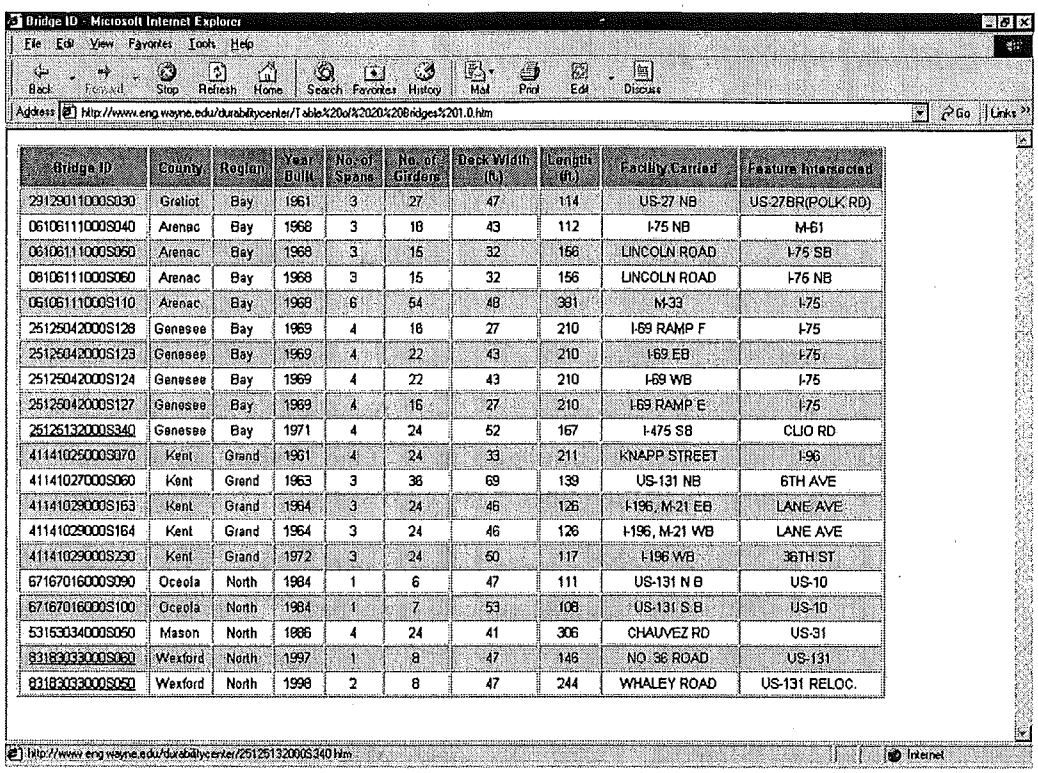

Bridge ID	County	Region	Year Built	No. of Spans	No. of Girders	Deck Width (ft.)	Length (ft.)	Facility Carried	Feature Intersected
29129011000S030	Gratiot	Bay	1961	3	27	47	114	US-27 NB	US-27BR(POLK RD)
06106111000S040	Arenac	Bay	1968	3	18	43	112	I-75 NB	M-61
06106111000S050	Arenac	Bay	1968	3	15	32	166	LINCOLN ROAD	I-75 SB
06106111000S060	Arenac	Bay	1968	3	15	32	156	LINCOLN ROAD	I-75 NB
06106111000S110	Arenac	Bay	1968	6	54	48	381	M-33	I-75
25125042000S128	Genesee	Bay	1969	4	18	27	210	I-69 RAMP F	I-75
25125042000S123	Genesee	Bay	1969	4	22	43	210	I-69 EB	I-75
25125042000S124	Genesee	Bay	1969	4	22	43	210	I-69 WB	I-75
25125042000S127	Genesee	Bay	1969	4	18	27	210	I-69 RAMP E	I-75
25125132000S340	Genesee	Bay	1971	4	24	52	167	I-475 SB	CLIO RD
41141025000S070	Kent	Grand	1961	4	24	33	211	KNAPP STREET	I-96
41141027000S060	Kent	Grand	1963	3	38	69	139	US-131 NB	6TH AVE
41141029000S163	Kent	Grand	1964	3	24	46	126	I-196, M-21 EB	LANE AVE
41141029000S164	Kent	Grand	1964	3	24	46	126	I-196, M-21 WB	LANE AVE
41141029000S230	Kent	Grand	1972	3	24	60	117	I-196 WB	36TH ST
67167016000S090	Oceola	North	1984	1	6	47	111	US-131 N B	US-10
67167016000S100	Oceola	North	1984	1	7	53	108	US-131 S B	US-10
53153034000S050	Mason	North	1986	4	24	41	306	CHAUVEZ RD	US-31
83183033000S060	Wexford	North	1997	1	8	47	146	NO. 36 ROAD	US-131
83183033000S050	Wexford	North	1998	2	8	47	244	WHALEY ROAD	US-131 RELOC.

Figure 8-3. Table of 20 Inspected Bridges, which is located on the Website

For example access by bridge ID "25125132000S340" will display Figure 8-4. This is a schematic representation of this bridge's primary elements to show the location of the pictures. The name of each picture will access display that particular picture. For example the name E2-S5-E-S.1 will access Photo 8-1. The name of the picture also denotes the location of that picture. The picture file convention was developed to give each picture a name that relates the contents of the picture to a position on the bridge (see Figure 8-5). A complete explanation of the picture file convention is provided in this sub-section.

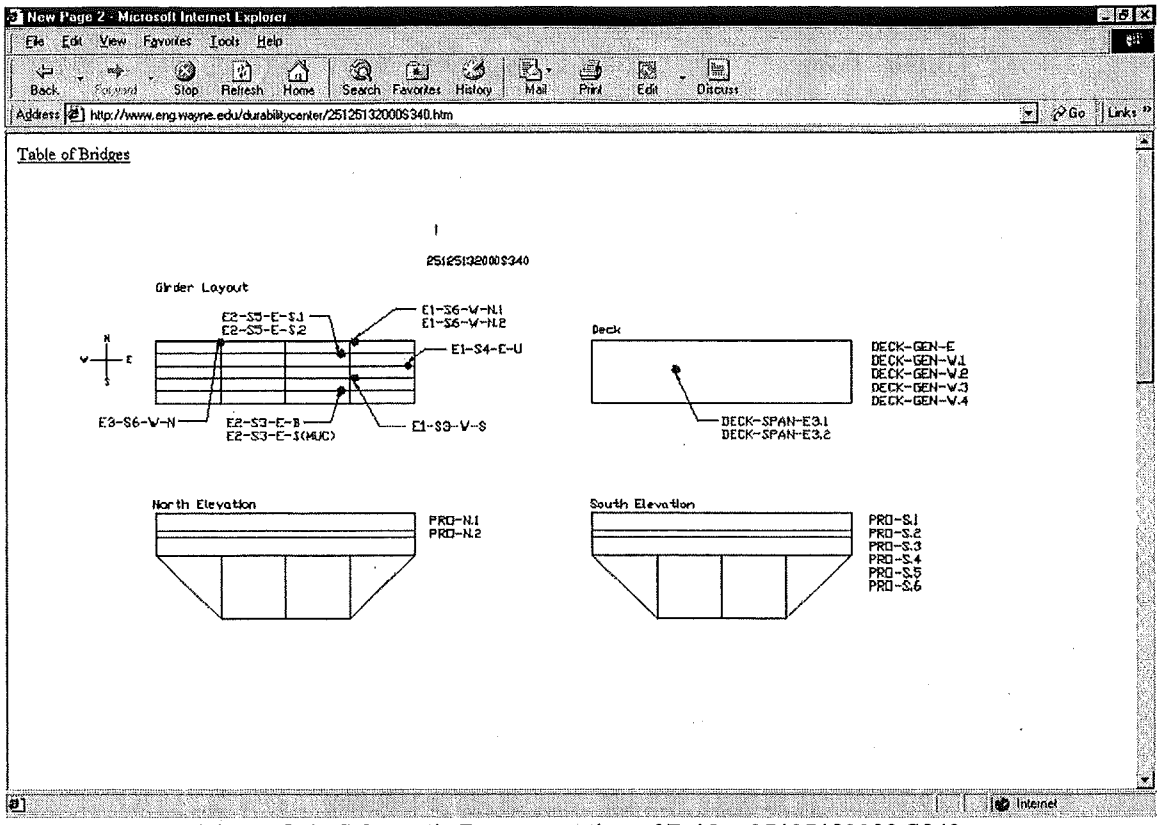

Figure 8-4. Schematic Representation of Bridge 25125132000 S340

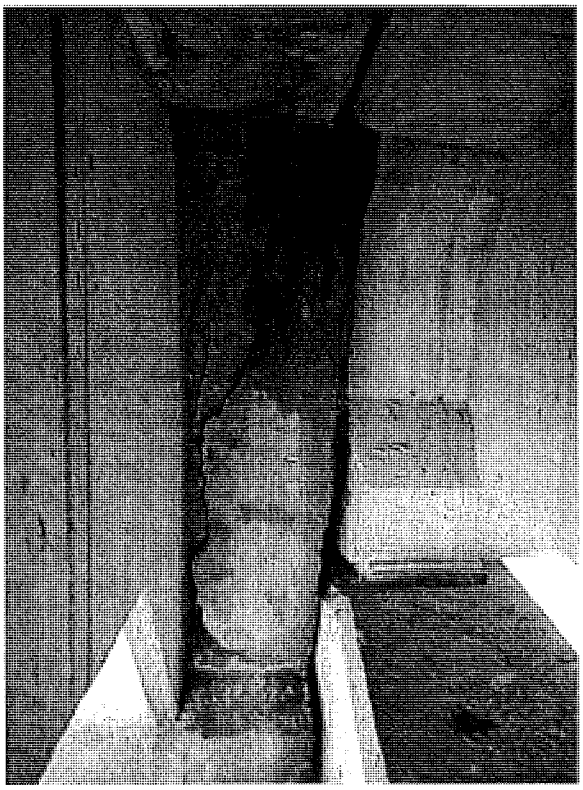

Photo 8-1. E2-S5-E-S.1 from 25125132000 S340

- Girder Photo: (span; S#, E#)-(girder; S#, E#)-(end; N,S,E,W)-(face; N,S,E,W,R,U,B,X,I). # in set
- Profile Photo: PRO-(face of bridge shown; N,S,E,W). # in set
- Abutment Photo: ABUT-(end; N,S,E,W)-(face N,S,E,W)-(nearest girder; S#, E#, GEN). # in set
- Pier Photo: PIER-(pier; S#, E#)-(column; S#, E#, GEN)-(face; N,S,E,W). # in set
- Deck Photo: DECK-(type; GEN, APP, JOINT, SPAN, UNDER)-(if GEN then looking direction; N,S,E,W / if APP then approach; N,S,E,W / if JOINT or SPAN then ; S#, E# / if UNDER then SPAN; S#, E#). # in set

Figure 8-5. Photo File Convention

- **Girders Photos** are named using the same convention used in designating the Girder Numbers in the database. The girder photo file name includes a span, a beam in the span, a beam-end, a face of the beam-end, and a photo index number in that set. The first letter in the notation describes which direction to index the spans from (either S-south or E-east), and the number that follows is the span index. Next is a letter denoting which direction to start counting from for the beams (either S-south or E-east), and the number that follows is the beam index. The following letter determines the end of the beam of interest on (either {N-north or S-south} or {E-east or W-west}). The last letter designates one of the seven faces (either {N-north and S-south} or {E-east and W-west}, U-underneath, R-rear end, B-bearing, I-interior diaphragm, X-exterior diaphragm). The last number in the convention gives the photo index in that set. An example of a girder photo file for a bridge orientation of north to south with three spans and seven girders in a span is S2-E5-N-W.2. Such an example defines the second span from the south, fifth beam from the east, north end, west face, and second photo in this set.
- **Profile Photos** convention all begin with the designation PRO followed by a letter that denotes the face of the bridge shown in the photo (either {N-north or S-south} or {E-east or W-west}). The last number in the convention gives the photo index in that set. An example of a profile photo file is PRO-N.3. Such an example defines the north face profile of a bridge and the third photo in that set.
- **Abutment Photos** convention all begin with the designation ABUT followed by a letter that denotes one of the two abutments of the bridge that is shown in the photo (either {N-north or S-south} or {E-east or W-west}). The following letter in the photo file gives the primary face of the abutment shown in the photo (either N-north, E-east, S-south, W-west). The third letter denotes which direction to index the nearest girder shown in the photo—or, if it is a general view, then GEN is used (either S-south or E-east)—and the number that follows is the girder index. The last number in the convention gives the photo index in that set. An example of an abutment photo

file is ABUT-W-N-S8.2. Such an example reads abutment photo, west abutment of bridge, north face, nearest girder is eighth from the south, and second photo in this set.

- **Pier Photos** convention all begins with the designation PIER. The first letter in the notation explains which direction to index the piers from (either S-south or E-east), and the number that follows is the pier index. Next, is a letter denoting which direction to index the columns, and if it is a general view then GEN is used (either S-south or E-east), and the number that follows is the column index. The last letter designates the face shown in the photo (either {N-north or S-south} or {E-east or W-west}). The last number in the convention gives the photo index in that set. An example of a pier photo file is PIER-S2-GEN-N.2. Therefore this example of a pier photo file reads the second pier from the south, general view of all columns, north face, and second photo in this set.
- **Deck Photos** convention all begins with the designation DECK. Then the following group of letters in the notation denotes the type of the deck photo general view, approach, joint, span, or underneath the deck (either GEN, APP, JOINT, SPAN, UNDER). If the type is GEN then the following letter will represent the looking direction in the photo (either N, S, E,W). If the type is APP then the following letter will represent an approach (either N, S, E,W). If the type is JOINT or SPAN then following letter will represent which direction to index the joints or spans respectively (either S-south or E-east), and the number that follows is the joint or span index respectively. The last number in the convention gives the photo index in that set. An example of a deck photo file is DECK-JOINT-E3.1. Therefore this example of a deck photo file reads deck photo, joint of bridge, third joint from the east, and first photo in this set.

8.4 Summary

Overall, the Center for Structural Durability's website is a useful tool that provides easy to access information to the research advisory panel and the research team. The site map shows an overview of how to navigate to a project homepage. The password and public access portions of the project homepage supply a balance of protected and accessible information. The bridge inspection photo database displays a set of organized web-based images of bridge photographs, and shows potential for further growth in digital organization of bridge management.

9.0 Repair Techniques for Beam-End Deterioration (Task 9)

9.1 Introduction

This study identified four major families of repair approaches that can be applied to deteriorated prestressed concrete I-beam ends. These techniques are:

- Structure Modifications,
- Surface Insulating Methods,
- Electrical Control Methods, and
- Environment Modifying Methods.

These techniques are discussed in detail in Section 2.4.2 of this report and are combined with preventative-maintenance techniques. The discussion also includes the advantages and disadvantages of each group. A corresponding detailed list of preventative maintenance and repair techniques is included in Appendix J. This study found that very few individual techniques have been attempted in the concrete-repair field on general concrete structures as well as by state transportation departments on deteriorated prestressed concrete I-beam ends. Repair alternatives that have been implemented on prestressed concrete beam-ends include partial depth repair, the MDOT "chip and overcast procedure" (MDOT R-1373, 1999) and complete beam replacement. Results from all but the latest techniques, for which long-term performance data is not available, generally suggest that no repair or preventive-maintenance strategy (excluding beam replacement) can restore the member to an original level of service.

9.2 Analysis Tools

For this study, the research team searched for ways to move from identifying the extent of beam-end deterioration to selecting an appropriate preventive-maintenance or repair technique. These efforts were discussed in *7.2 Analysis Tools* for both preventive-maintenance and repair techniques. In summary three analysis tools have been developed and were included:

- Table 7-1. Testing Procedures and Distress Severity Criteria for Prestressed Concrete I-Beam End Deterioration (This table listed several tests applicable to corrosion-induced deterioration that could be performed by MDOT to assist in classifying the severity of end distress.)

- Table 7-2. Cause-Evidence Relationships for Beam-End Distress (This list suggested preventative-maintenance and repair techniques for low-, moderate- and high-severity levels of distress for various causes of distress.)

- Table 7-3. Example Performance Matrix for Preventive Maintenance Techniques (This matrix was initialized to aid in the selection of an appropriate preventative-maintenance technique. A similar concept can be used for selection of appropriate repair techniques. Ideas for future refinement of this matrix are given in Chapter 14 – Future Life-Cycle-Cost-Benefit Optimization Studies.)

Accurate assessment of I-beam end conditions is necessary for providing adequate preventative maintenance and repairs. Condition states developed from field inspections (Table 6-2) and photo collection (Table 6-3) will assist inspectors with accurate assessment. Chapter 12 links these condition states to preventative-maintenance and repair techniques.

9.3 Basics of Beam Repair

Repair of a deteriorated beam-end can range from a simple solution to a complex long-term process. It is imperative to understand that, while the simple solution may be to employ a one-fix-cures-all approach, every case must be considered on an individual basis. For example, a carbonation test (from Table 7-1) may show a moderate level of deterioration at the reinforcement level. However, the moderate level is only at that isolated location or locations where sampling has been conducted. The true extent of deterioration may turn out to be different as the concrete-removal process takes place. A few basic issues related to beam-end repair are listed here for consideration.

1. The *1996 MDOT Specifications for Construction, Section 712, Bridge Rehabilitation – Concrete* provides information regarding the removal of concrete and patching. However, no attention is given for prestressed concrete I-beam repairs, and little direction is given for vertical repair work.

2. The *MDOT Special Provision – Vertical and Overhead Structure Repairs* should consider two additional acceptance criteria: maximum crack-width criterion of 6 mils and a bond-tensile-strength criterion other than simple delaminations (see Chapter 11).

3. All concrete-removal processes in the beam-end region should list provisions for temporary shoring of the beams. The true depth of deterioration often cannot be known until the removal process progresses. Safety of the structure and personnel dictates that temporary shoring be provided for all repair procedures where concrete removal is needed.

4. Corroded steel must be cleaned during any repair process. To reduce or eliminate further corrosion, a non-corrosive environment must be provided and/or a sacrificial anode system should be incorporated. Placing sacrificial anodes around the patch perimeter can reduce the "ring" effect, an area of accelerated deterioration due to chloride imbalance.

5. All unsound or contaminated concrete must be removed to effectively halt further deterioration. Placing patches over material such as chloride-contaminated concrete will accelerate deterioration near the patch, rendering the patch ineffective. In addition, patching over unsound concrete will not be effective in holding the unsound concrete in place for long-term conditions.

9.4 Summary

As in Chapter 7, we have identifified several families of repair techniques that can be applied for beam-end deterioration. Testing procedures and distress-severity criteria applicable to corrosion-induced deterioration are appropriate for classification of beam-end distress as noted throughout this document. A list of repair techniques has been developed for low-, moderate-, and high-distress severity. And a concept of a performance matrix was developed to assist in selecting the most effective technique for a given situation. In addition, suggestions for beam-end repair and clarifications to MDOT standard practices have been documented for consideration.

10.0 Analytical Modeling of a PC I-Beam Bridge (Task 10)

10.1 Introduction

Inspection and evaluation of the conditions of the inspected bridges revealed the possibility of design and manufacture related factors aggregated to the aggressive environmental effects causing the end deterioration in PC I-beams (see Chapter 3 for the inspection results). In order to investigate the stress states near the beam-ends, analytical studies are performed under the load effects during manufacture, construction, and operation. The analyses are completed in two main phases. First, the finite element modeling of a PC I-beam is performed to identify the effects of prestressing loads and the design changes in tendon geometry and arrangement. Second, the behavior of a PC I-beam bridge is modeled and analyzed under dead and live loads and environmental conditions to evaluate the diaphragm impact on beam-ends and load distribution in the bridge.

The essential parts and goals of the analyses included:

1. Assessing the prestressing force effects on the stresses at PC I-beam ends.
2. Evaluating the effects of bearing condition on the life span of the beams.
3. Evaluating the load paths on a PC I-beam with non-functional bearing pad near beam-ends under dead and live loads.
4. Assessing the structural behavior of a PC I-beam bridge.
5. Evaluating the effect of the diaphragms material and geometry on the structural behavior of bridges.
6. Attaining a better geometry and a type of diaphragm that will enable the inspectors to examine the conditions of the beam-ends efficiently.

10.2 Programs Utilized

10.2.1 HyperMesh

HyperMesh is used as pre and post processor in structural modeling. It also includes a linear and non-linear finite element analysis program, which was not utilized in this research. The pre- and post-processor helps to generate the finite element models for simulation and analysis (HyperMesh 2.0 Documentation, 1995). HyperMesh pre-processor provides extensive finite

element analysis assistance for generating models and advanced post-processing capabilities for in-depth visualization of simulations.

10.2.1.1 *Pre-processing*

One of the main advantages in using HyperMesh, as a pre-processor, is its ability to create compatible input files for the structural analysis programs. Its library is large enough to generate input files, including model data to be analyzed, for many other programs such as ABAQUS, Ansys, Ls-Dyna3d, Madymo, Nastran, and Radioss.

The pre-processing consists of the following steps (HyperMesh 4.0 Documentation, 2000):

1. The geometry of the structural element is generated by creating the geometric properties and the form of the structure.
2. Based on the geometry of the structure, finite element discretization is performed.
3. The completed finite element representation of the geometry is checked for continuity and element quality by using fundamental relations of structural analysis.
4. Boundary conditions such as loads and constraints are described.
5. Material properties and other properties are defined.
6. The finite element description of the model is exported in the format suitable for the analysis code.

10.2.1.2 *Post-processing*

In post-processing, the analysis results are interpreted by completing the following tasks (HyperMesh 4.0 Documentation, 2000):

1. Translating the results from the ABAQUS's output format into HyperMesh's own format.
2. Reviewing and animating the model with deformed shapes.
3. Reviewing color contours of the element and nodal data (stress, strain, or displacement) displayed on the finite element model.
4. Generating plots and stress contours for reporting and documenting the analyses results.

10.2.2 ABAQUS

ABAQUS is an engineering simulation program. It is based on the finite element method and designed specifically for advanced analysis applications. The program capabilities are described by its element library, material models, and analysis procedures. The program is developed with a very extensive library of elements that can be used for modeling different structures virtually and geometrically. The material library includes many engineering materials, such as metals, rubber, polymers, composites, reinforced concrete, crushable and resilient foams, and geotechnical materials (ABAQUS / Standard Version 5.8 Manual, 1998). The material response for each of these models may be highly nonlinear. General elastic, elastic-plastic, and elastic-viscoplastic behaviors are provided. Both isotropic and anisotropic behavior can be modeled. User-defined materials can also be created with a subroutine interface.

ABAQUS provides various time- and frequency-domain analysis procedures. These procedures are divided into two groups:

General Analyses: In this case the response may be linear or nonlinear.

- Static stress/displacement analysis
- Viscoelastic / viscoplastic response
- Transient dynamic stress/displacement analysis
- Transient or steady state heat-transfer analysis
- Transient or steady state mass-diffusion analysis
- Steady-state transport analysis
- Coupled problems
- Thermo-mechanical (sequentially or fully coupled)
- Thermo-electrical
- Pore fluid flow-mechanical
- Stress-mass diffusion (sequentially coupled)
- Piezoelectric (linear only)
- Acoustic-mechanical (linear only)

Linear Perturbation Analyses: In this case linear response is computed about a general, possibly nonlinear, base state.

- Static stress/displacement analysis
- Linear static stress/displacement analysis
- Eigenvalue buckling-load prediction
- Dynamic stress/displacement analysis
- Determination of natural modes and frequencies
- Transient response via modal superposition
- Steady-state response resulting from harmonic loading
- Response spectrum analysis
- Dynamic response resulting from random loading

10.3 Overview of Analytical Modeling

Finite element (FE) analysis method is a useful tool to determine the behavior of structures. It is the highly improved form of structural analyses commonly used for research and development purposes. In FE analysis, a structure is divided into finite elements, and their behaviors are investigated. In this way the mechanisms within the structure, the load response of each finite element, and behavior of the entire structure are studied.

Bridge inspection results on beam-ends conditions and a visit to the PC plant revealed the possibility that some of the beam-end cracking is formed at the plant. Inspection data showed that cracks are common in almost all PC I-beams near the bottom flange and web-transition zone and at the mid-web. Literature also indicated that there are various mechanisms causing beam-end cracking. Some of these mechanisms are initiated as soon as the girders are cast and the tendons are released (Buckner, 1995; Russell and Burns, 1996; Kannel et al, 1997; Russell and Burns, 1997; Leonhardt, 1964, Sozen, 1965 and 1967). The cracking during fabrication leads to further and rapid deterioration of the girders. The initial cracking, therefore, should be reduced

in order to extend service life of PC I-girders. In order to develop reliable remedies for the structures in distress and to provide necessary precautions for new girder and bridge designs, analytical modeling is a useful tool for generating the realistic stress state for comparisons to nominal stresses assumed in design. Detailed inspection of PC I-beam bridges also revealed that non-functional elastomeric bearing pads and rigid concrete diaphragms might also contribute to girder-end distress. Finite element analysis method is applied to investigate the causes for initial cracking, the impact of non-functional bearings, structural behavior in a bridge, and diaphragm impact on the girder-ends.

The main goals of the analyses are summarized as below:

1. Assessing the shear and flexural stresses near I beam-ends due to prestressing force transfer length, strand debonding, and strand draping.
2. Quantifying the cracking potential near the beam-ends.
3. Evaluating the load paths near beam-ends under dead and live loads.
4. Evaluating the influence of bearing conditions on the beam-end stresses.
5. Investigating the full bridge behavior under live and dead loads.
    a. Diaphragm restraining effects on girder-ends.
    b. Effects of various diaphragm types on girder-end stresses.
    c. Temperature effects on a bridge, considering functional and non-functional elastomeric bearing pads.

The beam cross-section and tendon geometry affect the structural behavior and performance. Single girder analyses are grouped according to the cross-section and tendon geometry, design of the beam, bond properties of the co ete, and loading cases to identify the significance of each parameter independently. The first rameter is the cross-section and tendon geometry of AASHTO I-beams. Therefore, the gir s with the following tendon geometries are studied to document the geometry effects.

1. Beams with Straight Tendons
2. Beams with Draped Tendons
3. Beams with Bond-Breakers (Sheathed Tendon

The concrete quality may vary due to several re is such as admixtures, placing, and curing procedures and conditions that, in turn, affect the ality of bond between the tendon and the concrete. Therefore, as another parameter, the conc te quality effect is studied to evaluate its impact on the stress pattern and transfer length near the beam-end. Three bond qualities are assumed; good bond quality (high estimate), average bond quality (best estimate), and poor bond quality (low estimate).

The finite element analyses are further expanded by evaluating the stresses and deformations generated in three stages of a PC I-beam during its lifespan, the manufacture, the construction, and the service. Loading conditions are based on these stages. Accordingly, the following loading cases are considered in the model.

1. Prestressing Load
2. Dead Load
3. Live Load

The dead and live load analyses are performed to verify the effect of the non-functional bearing on the beam-end stresses and on the load path from deck to the supports.

Additionally, the structural behavior of the full bridge and restraining effects of the diaphragms are analyzed in a PC I-beam bridge model. The model is developed from the structural components. In the analyses, the significance of the concrete diaphragms, their geometry effects are assessed and compared to steel bracings as a potential replacement to concrete diaphragms. The thermal effects on the girder-ends and load distribution induced by temperature deviations are also investigated.

Analytical modeling steps are summarized in Figure 10-1.

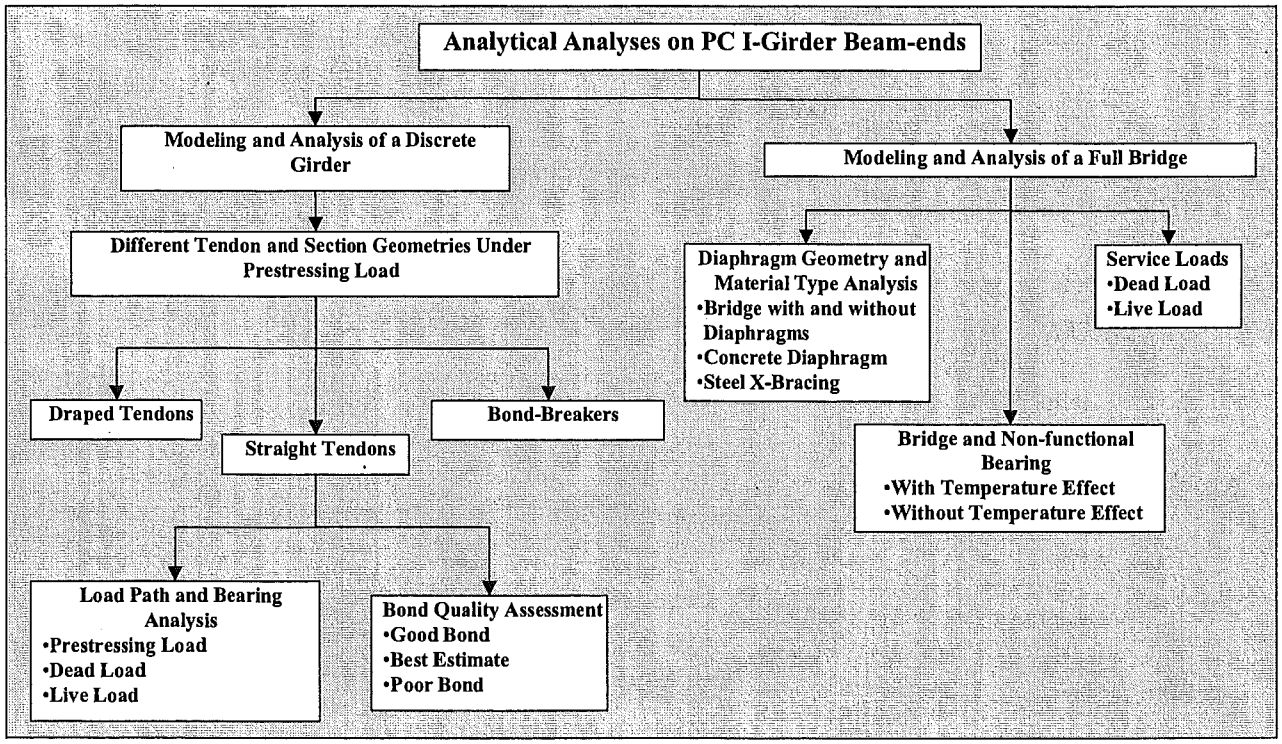

Figure 10-1. Steps of Analytical Modeling

10.4 Cracking Potential of a Prestressed Concrete I-Beam

Previous research and field inspection results has identified the presence of cracks near the beam-ends as one of the significant parameters in the girder service life. Prestressing tendons corroding due to the presence of oxygen and the infiltration of moisture through cracks is the most common distress mechanism seen near the I-beam ends. Field studies showed that PC I-beam end cracks form as early as in the precast plant as shown in Figure 10-2-a and -b. The cracked girders exposed to aggressive environmental conditions deteriorate rapidly. The moisture ingress increases in a cracked girder, and freezing action widens the cracks as seen Figure 10-2-c and -d. The moisture carries aggressive agents, which further aggravate the deterioration and feed back moisture ingression. Aggressive agent exposure generates

delamination, Figure 10-2-e, and spall of concrete cover, Figure 10-2-f, reducing the durability of the girder by a significant amount. Consequently, cracking prevention or reduction during manufacture, construction, and operation is the proper way to increase the durability and the lifetime of the PC I-beams.

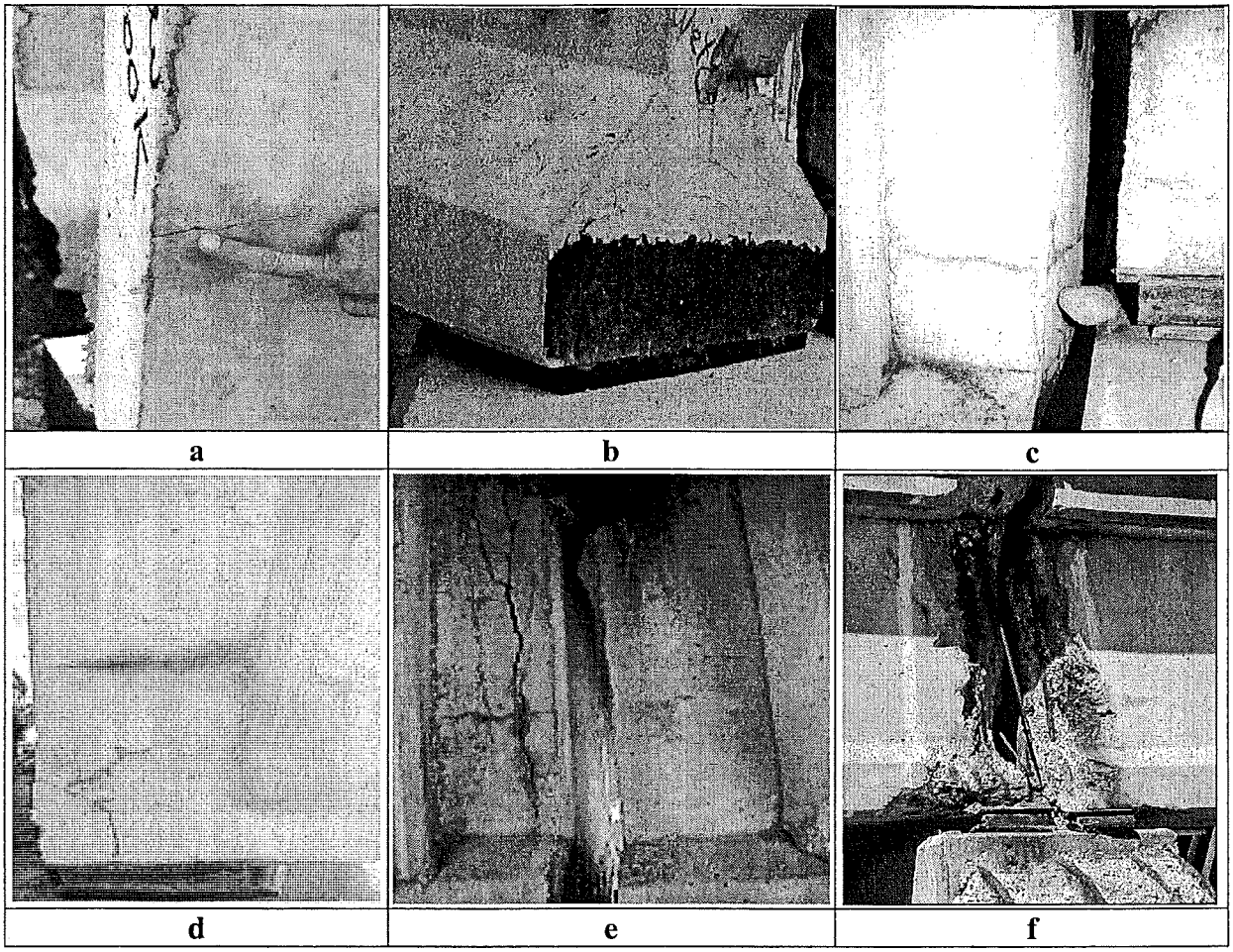

Figure 10-2. (a) Cracking at the Web Zone at the Precast Plant; (b) Cracking within the Proximity of Bottom Flange of a Girder in a Bridge under Construction; (c) Cracking Observed on the Web and Around the Bottom Flange of Girders in-Service; (d) Moisture Presence Around Cracking on the Web; (e) Delamination and Spalling on a Girder; (f) Spalling of Cover Concrete and Exposed Rebar

Detailed structural analyses of the PC I-beams are necessary to clearly verify and identify the cracking mechanisms, their causes, and the significance of the load stages and the environmental factors. Finite element analyses are performed to identify the cracking potential and vulnerability of girders to cracking. By using the results of the finite element analysis, better reinforcement details for beam-ends can be developed for crack width and length minimization. Finite element models are generated utilizing the existing geometrical, environmental, and load conditions to simulate the real structural behavior as much as the theoretical assumptions allow. In modeling the girder for FE analysis, certain assumptions are necessary. Some of these assumptions are behavioral and others are for incorporating some mechanisms into FE model of the girder.

Behavioral assumptions are as follows:

1. Statical analysis is performed, excluding the dynamic effects.
2. Small deformations are considered; therefore, second order effects are not incorporated.
3. Materials, steel for the tendons and concrete for the girder, are assumed to remain in their elastic state.
4. Prestressing losses due to creep and shrinkage is ignored in evaluating early age load effects.
5. Symmetrical tendon-cutting pattern is assumed. Thus, moments generated by unbalanced tendon forces are not included.
6. To identify only the early age effects that occur during manufacturing on a PC I-beam, the initial prestressing forces before concrete shrinkage losses are not applied. Only losses due to elastic shortening of the beam are included.
7. Shrinkage effects of the deck on the girder are not incorporated. Deck is only regarded as dead load.
8. The boundary conditions at the both ends are assumed free.

The FE modeling related assumptions are as follows:

1. The deformations are calculated only at the nodes. The variations between the nodes are assumed linear.
2. The bond properties between the tendons and concrete are modeled using the flexible springs as connection elements.
3. The tendons are attached to the concrete only at the nodes through flexible springs.
4. Tendons are assumed to have only axial stiffness and modeled as linear truss elements with no change in cross-sectional geometry under prestressing forces.

The finite element analyses are performed on models based on three types of I-beams taken from existing bridges in Michigan, considering girder tendon and section geometries as main parameters. AASHTO I-beam types, Michigan 1800, and Wisconsin-70 (WI-70) are used in Michigan. Their use according to years is summarized in Table 10-1; AASHTO I-IV were first utilized in 1958, then in 1977 WI 70-inch, and in 1997 MI 1800 were introduced.

Table 10-1. PC I-Beam Types Used in Michigan According to Years and Maximum Span Lengths

Beam Types	AASHTO I-IV	AASHTO I-IV	AASHTO I-IV	AASHTO I-IV	WI 70	AASHTO I-IV	AASHTO I-IV MI 1800
Years	1958	1959	1964	1975	1977	1989	1997
Span Length (ft)	80	100	90	100	90-150	100	90-150

The first analysis model describes an AASHTO girder with straight tendons as shown in Figure 10-3.

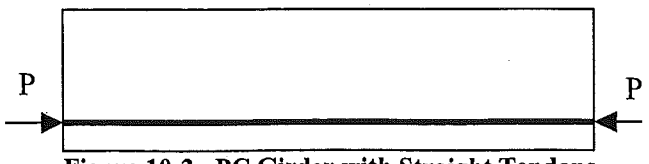

Figure 10-3. PC Girder with Straight Tendons

The second model is a Wisconsin type girder with bond-breakers, as shown in Figure 10-4, which is the recent tendon design form. In this type, bond-breakers (sheathing) are used around the tendons at the beam-ends.

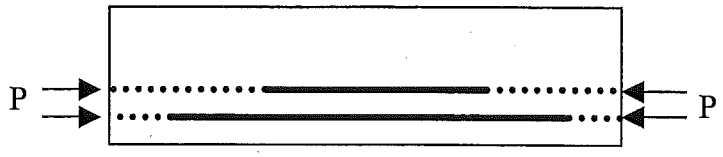

Figure 10-4. PC Girder with Sheathed Tendons

The third model shown in Figure 10-5 is an AASHTO cross-section with draped tendons. In draped girders, end blocks are incorporated to accommodate the anchoring of the tendon on the web.

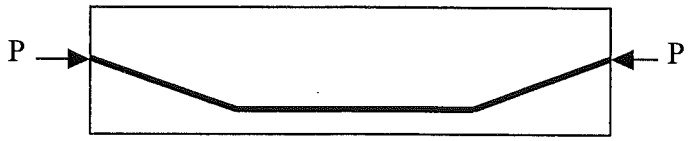

Figure 10-5. PC Girder with Draped Tendons

The design assumptions and the real behavior of the PC girders should be compared to provide more realistic and accurate design procedures. The structural behavior and the stress distribution mechanisms in the girder may be different from what is projected. The main issue here is to improve the assumptions and features to improve design reliability. In order to describe the design approach, a girder with straight tendons will be used as an example. In this case, uniform flexural and axial stresses are created by using straight tendons. The axial stress is regarded as proportional to the applied prestressing load, and inversely proportional to the cross-sectional area of the beam. The nominal stress distribution under prestressing forces is shown in Figure 10-6. The compressive stress considered in the PC girder design is the summation of flexural stresses with axial stresses calculated at the bottom fiber as shown in Equation 10-1. The total axial stress in Equation 10-1 is assumed linear on the beam cross-section and uniform along the beam. This total axial stress is used during design of the PC structures.

In a real girder, the structural behavior is different near the beam-ends from what is considered in the design. The prestressing load is not directly transferred from the tendons to concrete precisely at the girder-end. In prestressed girder, the tendons are eccentrically arranged with respect to the beam centroid. The prestressing load is gradually transferred along the girder at a distance termed as transfer length. As the prestressing force is transferred to the member, the axial load and the flexural stresses gradually develop within the transfer length. During this force transfer, the axial force within the force transfer zone varies as depicted in Figure 10-7.

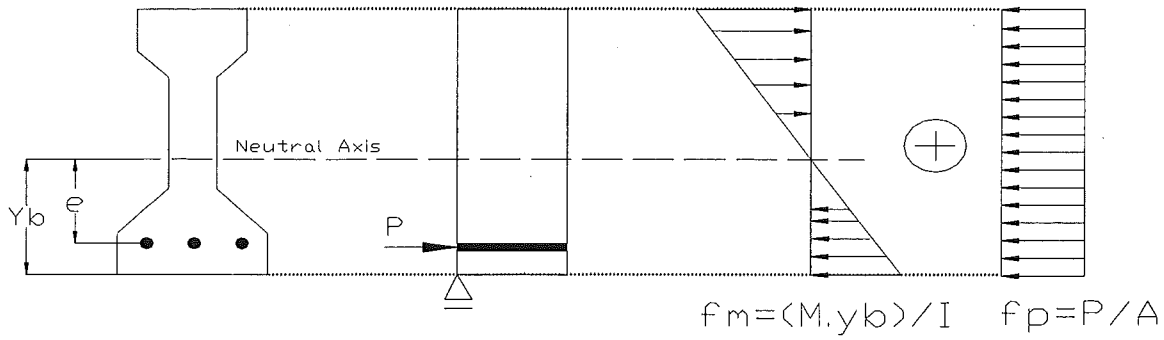

Figure 10-6. Axial Stresses Forming due to Prestressing Load

$$f_b = \frac{M \cdot y_b}{I} + \frac{P}{A}$$ **Equation 10-1**

where

A = Cross-sectional area of the girder
e = The eccentricity of prestressing load measured from neutral axis
f_b = Total axial stress at the extreme bottom fiber
f_m = Flexural stress due to eccentric prestressing force
f_p = Axial stress due to prestressing
I = Moment inertia of the section
M = Bending moment due to prestressing load; M= P·e
P = Prestressing force
y_b = Distance of neutral axis to the extreme bottom fiber

Considering an incremental element within the transfer length, the stress at each side of the element will be unequal (Russel et al, 1997). Thus, shear stress is generated. This change in nominal stresses near beam-end and equilibrium is described on an isolated incremental element as shown in Figure 10-8. Equation 10-2 describes the static equilibrium condition of the incremental element. Beyond the transfer length, the prestressing force remains constant. Therefore, the resultant shear stress shown in Figure 10-8 diminishes. The shear stress can also be explained by the Poisson's effect. By the changing uniaxial stresses, two incremental elements next to each other deform differently due to Poisson's effect. The preceding element lateral deformation is less than the succeeding element within the transfer length zone. Due to this difference in deformations between the elements, shear stresses are generated. Considering the shear stress generation within the transfer length, FE model of the PC I-girder is developed based on the description of force transfer from the tendon to the concrete medium.

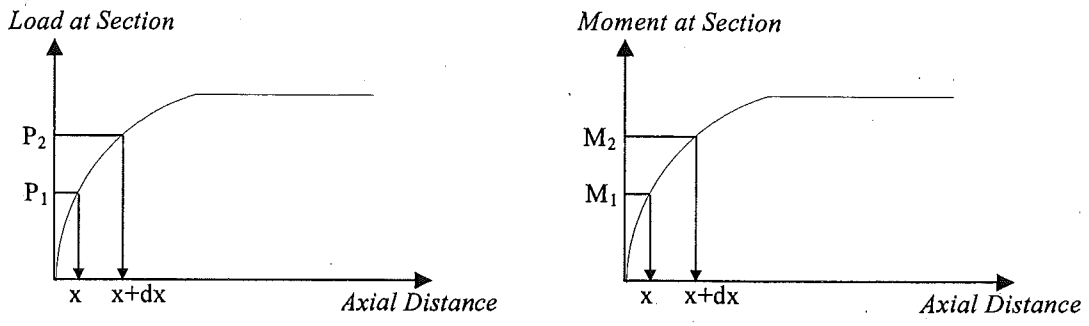

Figure 10-7. Axial Stresses on an Incremental Element

The differences between the approaches in the design and in reality are explained above. It is clearly seen that the design procedure does not address the structural behavior within the transfer length. The significance of the shear stresses generated near the girder-ends will be explained in more detail in the next section titled "Discrete Girder Analysis" on existing girders under prestressing load only so that the analysis may help to judge the accuracy of the design assumptions.

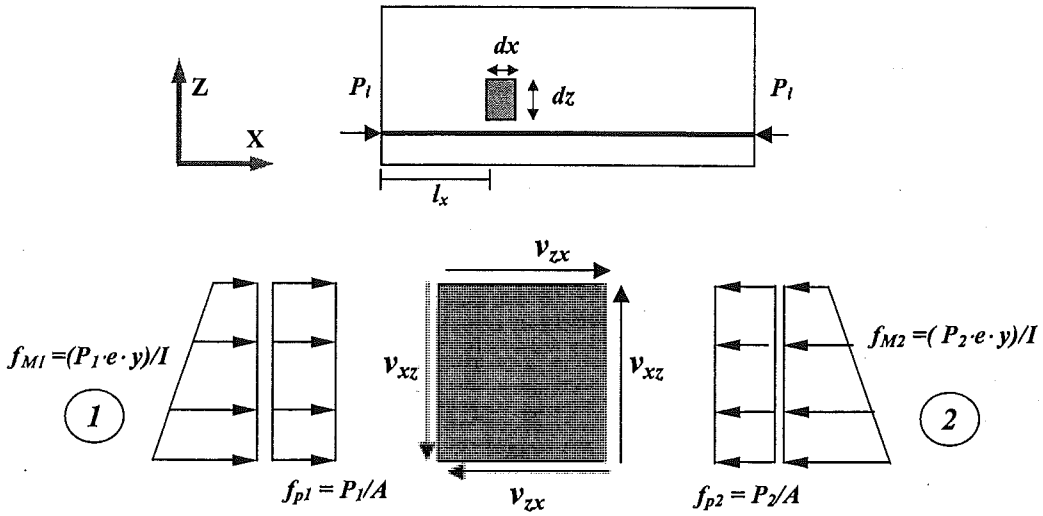

Figure 10-8. Stress Equilibrium of an Infinitesimal Element

$$v = f_{b1} + f_{b2} = \Delta f_m + \Delta f_p$$

$$v = \frac{(M_1 - M_2)y}{I} + \frac{(P_1 - P_2)}{A}$$

$$v = \frac{\Delta M \cdot y}{I} + \frac{\Delta P}{A}$$

Equation 10-2

where

v = Shear stress
y = Distance of neutral axis to a fiber on bottom of the section
f_{b1} = Axial stress at the extreme bottom fiber of the section at side 1
f_{b2} = Axial stress at the extreme bottom fiber of the section at side 2

10.5 Discrete Girder Analyses

The discrete girder analyses included three PC AASHTO I-beam types as mentioned in the overview. These types are girder with straight tendons, girder with draped tendons, and girder with bond breakers. The models generated for each girder are based on the design drawings. In other words, manufacture related errors are not incorporated.

The concrete properties used during manufacture may vary. These parameters and their significance are out of the scope for this project. However, to incorporate the existing conditions in reality, the concrete quality should be taken as a factor affecting the girder behavior. Therefore, the bond quality effect on the load configuration and transfer length at the beam-end zones are included in the FE analysis. The bond quality of concrete is taken proportional to its modulus of elasticity (Leonhardt, 1964). Here the assumption refers to the bond stiffness, not the bond strength. Assuming strain compatibility between the tendon and the surrounding concrete, the amount of stress developed in concrete will be proportional to the strain. The proportionality constant in this case will be the modulus of elasticity of concrete. The assumed variation is between twice the elasticity modulus as upper bound and one half as lower bound. These bounds are hypothetical, but they will provide an assessment on the sensitivity of the transfer length, and therefore, shear stresses to bond quality.

The load path due to dead and service loads in a girder is important and, therefore, to assess the cracking and the significance of the deterioration. The results of this analysis will help the inspectors to evaluate the safety of the deteriorated girders. Therefore, load path analyses are performed by applying the dead and live loads on a girder to evaluate the vulnerability of a girder with deteriorated ends. In other words, if the load path is clearly described, any girder-end deterioration within the zone of low stress will not necessarily jeopardize girder capacity. However, if deterioration is within high stress zones, girder capacity will be affected. In the load path analyses, one of the girders analyzed under only prestressing load is also analyzed under dead and live loads to document the load path through beam-end onto the support.

10.5.1 Girder with Straight Prestressing Tendons under Prestressing Load

The beam modeled is from a bridge in the Bay Region with inventory ID number S04 of 06111, built in 1968. The bridge description was given in Section 3.3.3. Two standard I-beams according to AASHTO prestressed concrete I-beams standards are used in the bridge. The beam used in the analysis is Type-III, a girder located within the mid-span of the bridge, with a 48 ft length. The material properties for concrete used in the analysis are the modulus of elasticity and Poisson's ratio. The modulus is calculated from design concrete compressive strength of 5,000 psi, using the formulation given in ACI 318-02 as $E_c=57{,}000\cdot\sqrt{f'_c}$, where E_c is modulus of elasticity of concrete and f'_c is compressive strength of concrete. The elasticity modulus of prestressing steel is the only property described in the model. The modulus for the Grade 250 7-wire strand bundle is assumed equal to the steel modulus of 29,000 ksi. It needs to be emphasized that the modulus is in reality the tangent modulus at the initial prestressing force of 24.5 kips. The beam cross-section and tendon geometry are shown in Figure 10-9.

Mark	Type	NUMBER OF 1/2 - 7WIRE STRANDS IN INDICATED ROW																			Total No.	Initial Prestressing Force, Pi (kips)
		MIDSPAN (Section B - B)							END (Section A - A)													
		BOTTOM							BOTTOM							TOP						
		1	2	3	4	5	6	7	1	2	3	4	5	6	7	1	2	3	4	5	6	
1-I	I	-	6	4	2	-	2	-	-	6	4	2	-	2	-	-	-	-	-			14	24,200
2-I	I	-	6	4	2	-	2	-	-	6	4	2	-	2	-	-	-	-	-			14	24,200
1-III	III	-	8	4	-	-	-	-	-	8	4	-	-	-	-	-	-	-	-			12	24,500
2-III	III	-	6	4	4	4	-	-	-	6	4	4	4	-	-	-	-	-	-			18	24,500
3-III	III	-	8	4	-	-	-	-	-	8	4	-	-	-	-	-	-	-	-			12	24,500

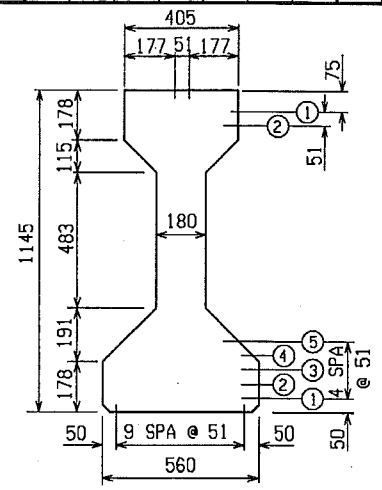

Figure 10-9. Tendon Arrangement and Cross-sectional Geometry of the I-Beam Modeled

Using symmetry, one half of the beam is modeled. Only the prestressing load is taken into account. The self-weight of the beam is not included to evaluate the beam-end stresses under only the prestressing load. In other words, the beam is isolated from other forces just to evaluate the prestressing force impact. The boundary conditions are described as the support at the end zone, roller in longitudinal direction, and the mid-point of the beam, roller in vertical direction, as defined by the symmetry constraints shown in Figure 10-10.

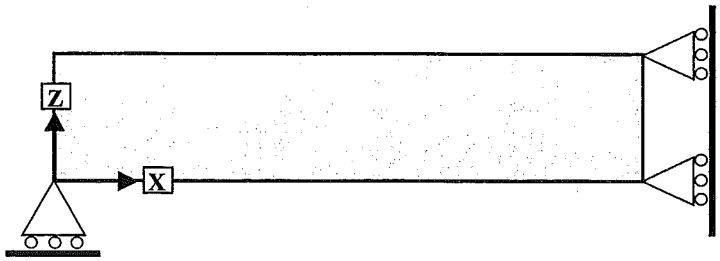

Figure 10-10. Boundary Conditions Described in the FE Model

The FE models are generated by using a finite element pre-processor and post-processor program, HyperMesh, and analyzed by a finite element analyzer program, ABAQUS. The finite element mesh and element selection is formed according to the options and analyzing procedures defined by the programs. The FE model of the girder, shown in Figure 10-11, includes 2185 solid continuum elements with 8 nodes, 342 truss elements with 2 nodes, 342 spring elements with 2 nodes, and 342 kinematic coupling elements with 2 nodes for a total of 24,688 degrees of

freedom. Continuum elements are used to define the concrete medium. The truss elements defining the prestressing tendons are prestressed as an initial condition. The spring members are utilized for the transfer of prestressing force from the truss elements used for tendons to the continuum elements used for concrete girder. The kinematic coupling elements are utilized due to modeling requirements in ABAQUS. They are used as intermediate agents to provide composite action between the spring and truss elements.

The geometry used in the model is identical to that of the real I-beam. The FE mesh is further refined near the beam-end. The length of the finite concrete elements is 4 inches at the beam-end for the first 8 inches, then 6.5 inches for the following 52 inches, and 26 inches for the remaining 234 inches, as shown in Figure 10-11.

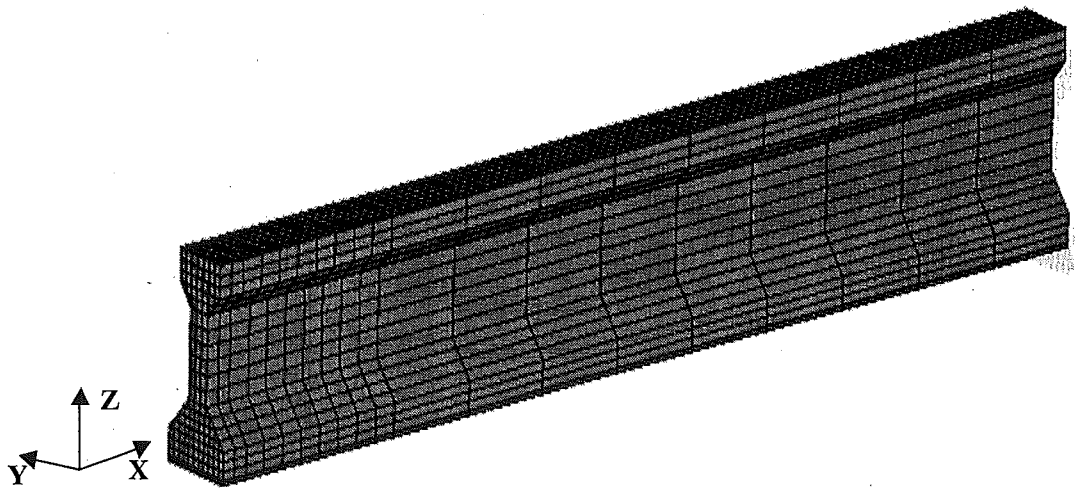

Figure 10-11. The Girder with Straight Tendons

The work performed prior to conducting the analysis dealt with the tuning of bond springs for achieving the theoretical transfer length of 26.7 inches for 7-wire strands with ½ in nominal diameter. The transfer length is calculated by using $l_d=(f_{se}/3)\cdot d_b$, where f_{se} is the effective stress in prestressing steel after losses and d_b is the nominal diameter of the strand (AASHTO, 1998). The tuning of springs stiffness is not within the focus of this report and will not be described here.

The analysis results are presented as contours of various stress components. To help the reader to evaluate the stresses and their variations within the girder-end, a description and coordinate designation of the 3-dimensional state of stress is given in Figure 10-12. On this element, the variation between the axial stresses on each side of the element generates shear stresses. In forming an analogy with the two-dimensional beam model used in design, f_{xx} is the uniaxial, axial and flexural combined, stress, and f_{xz} is the shear stress. The shear stresses at opposite faces are equal i.e. $f_{xz} = f_{zx}$, $f_{xy} = f_{yx}$, and $f_{yz} = f_{zy}$.

First, the analysis results using an average bond quality are described. The axial stress variation near the beam-end is shown in Figure 10-13 and Figure 10-14. As seen in the figures, near the end zone the axial stress gradually redistributes until its contours become uniform at about transfer length distance, between 27.5 and 34 inches from the end. Specifically, Figure 10-14 shows the variation along the beam axis on the x-z plane. It should be noted that the high stress

zone near the tendons at the beam-end gradually redistributes until a uniform stress contour is achieved. In this uniform zone, the maximum compressive stress is around 1,500 psi at the bottom fiber and the stress at the top fiber is tensile at about 100 psi.

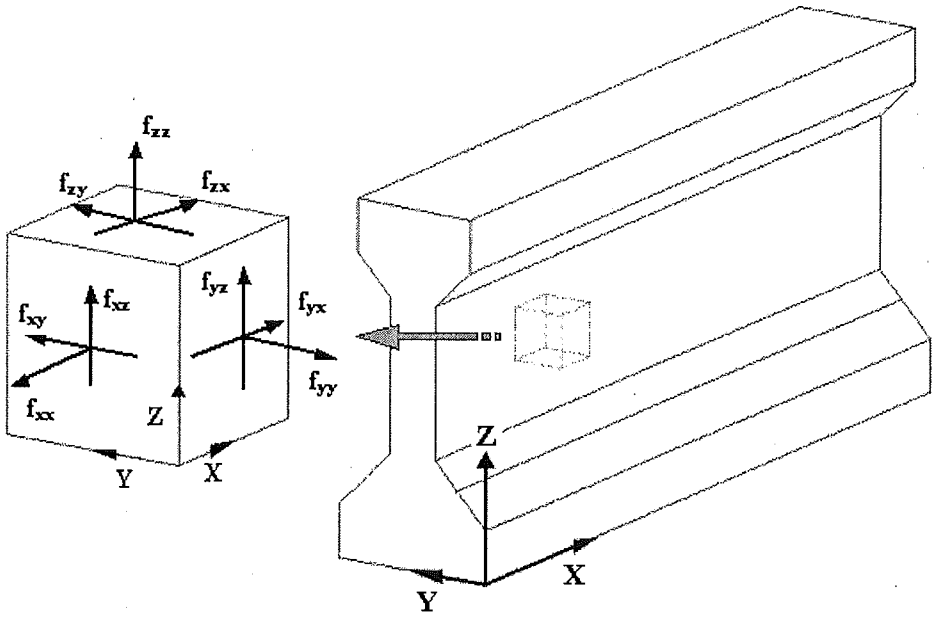

Figure 10-12. Stresses and Coordinate System used in the Model for the Infinitesimal Element

The axial stress distributions in the z and y directions are shown in Figure 10-15-a and Figure 10-15-b, respectively. In Figure 10-15-a and Figure 10-15-b, the zones under tensile stress may initiate cracking. Level of tensile stress that is of significance is only seen in Figure 10-15-a within the web zone, around 390 psi. During field inspection and plant visit, web cracking at the same location was observed (see Figure 10-2-a, -b, -c, and -d).

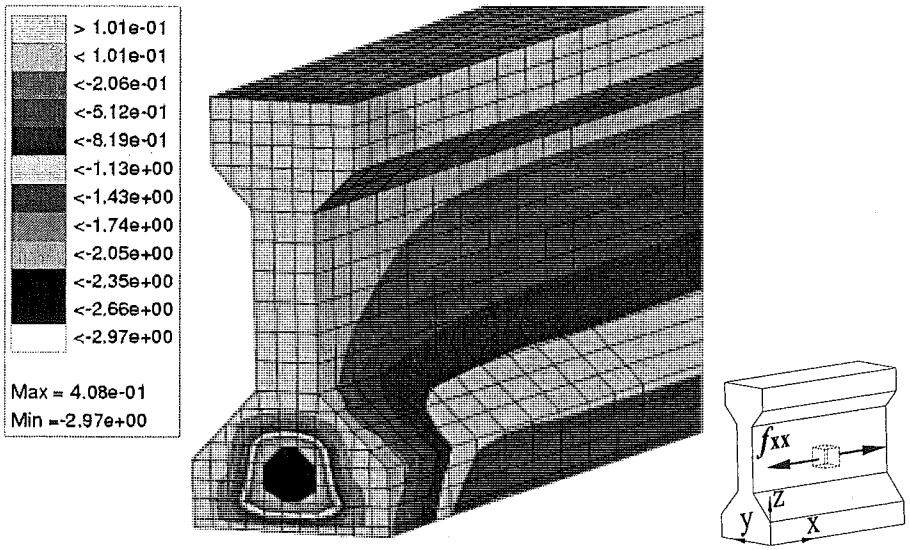

Figure 10-13. Axial Stress near the Beam-end (ksi), in X-Direction

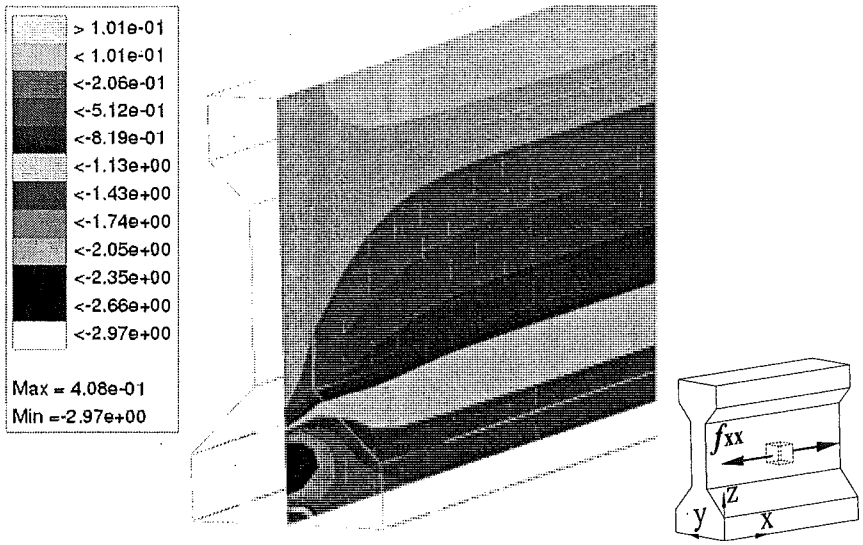

Figure 10-14. Axial Stress (ksi) Trajectory in X-Direction near the Beam-end

The shear stress magnitudes on x-z plane shown in Figure 10-15-c are significant. The maximum values are at the bottom flange, within the proximity of the web. The shear stresses on x-y plane seen in Figure 10-15-d are not significantly lower than the shear stresses on the x-z plane.

The shear stress development on x-z plane is also studied at selected sections along the beam axis as shown in Figure 10-16. In the figure, "Distance Along Z Axis" is along the depth of the beam. Figure 10-16-a to Figure 10-16-i shows the changes in shear stress distribution at sections along the beam starting from the beam-end. The section locations are also defined in the figures by the numerical value of "Distance Along Z Axis." In Figure 10-16, the distance from the beam-end to the location where the shear stress fully diminishes is 47 inches. A closer inspection shows that shear stress is insignificant starting at a distance from the beam-end just beyond 27.5 inches, which designates the point at which the prestressing forces in the tendons are fully developed. It is also important to specify the length at which shear stress remains in excess of allowable. The zones where the shear stress is in excess of $3.5 \cdot \sqrt{f_c'}$ or 247 psi will define the portions of the beam with high cracking potential by ACI (ACI, 2002). However, this does not mean that the zones with high shear stress crack. This information can be useful to define the critical zones. In Figure 10-16, shear stress is in excess of 500 psi on the section 8 inches from beam-end, which is significantly high. In Figure 10-17, the axial stress (flexural stress) variation in the x-direction shows non-uniformity similar to the shear stress distribution seen in Figure 10-16.

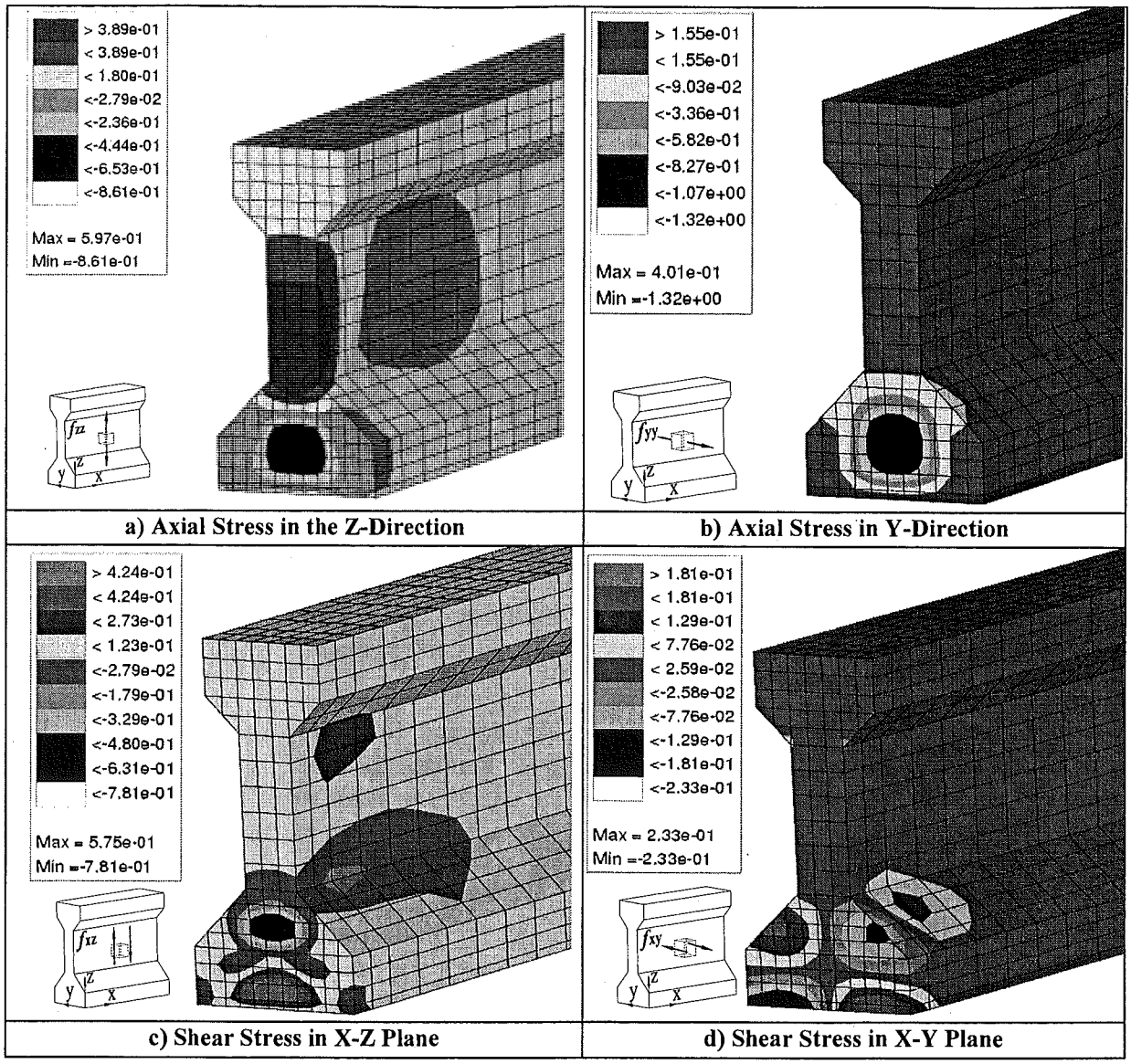

a) Axial Stress in the Z-Direction

b) Axial Stress in Y-Direction

c) Shear Stress in X-Z Plane

d) Shear Stress in X-Y Plane

Figure 10-15. Stresses (ksi) Observed near the End of the Girder with Straight Tendons

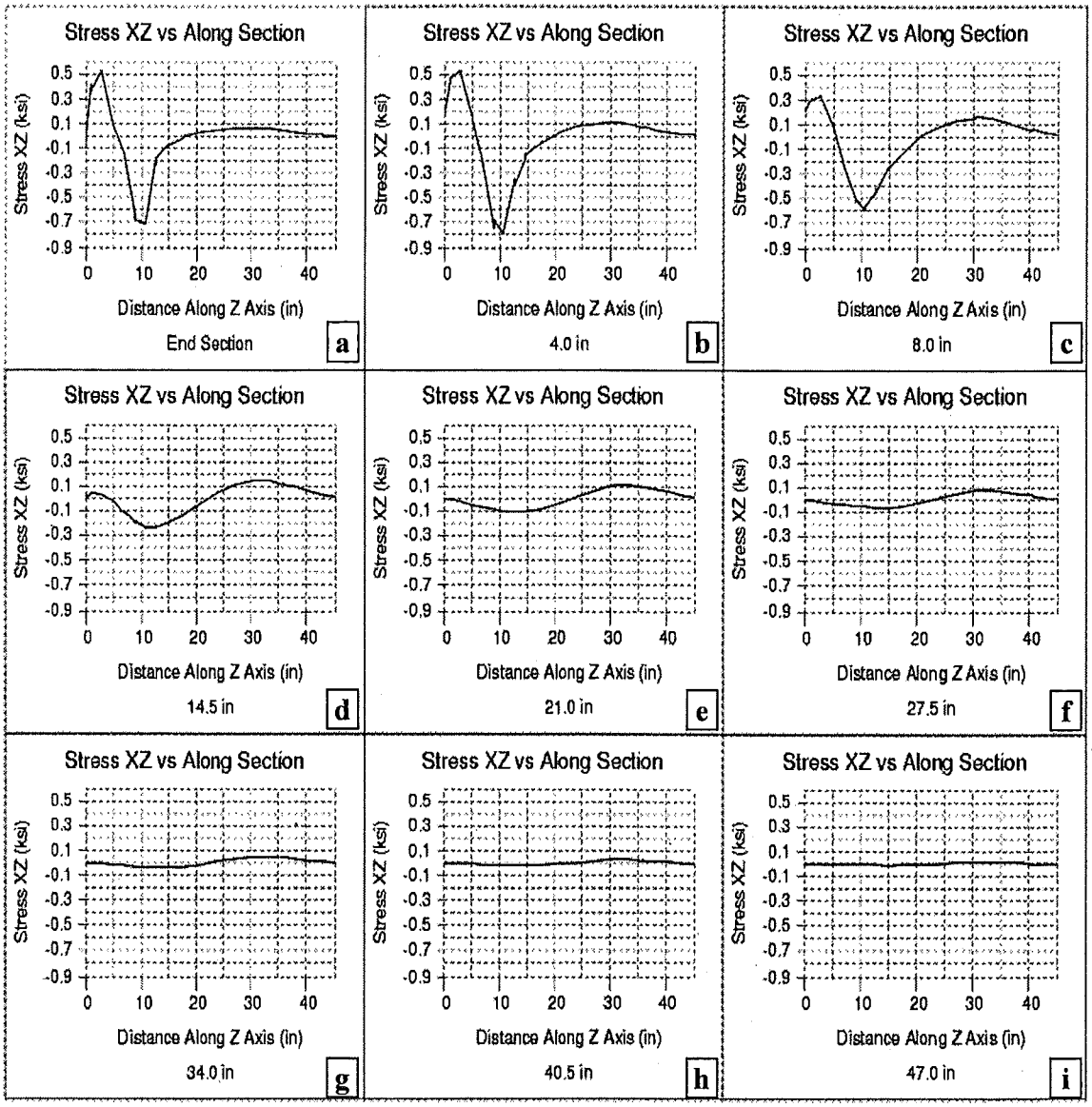

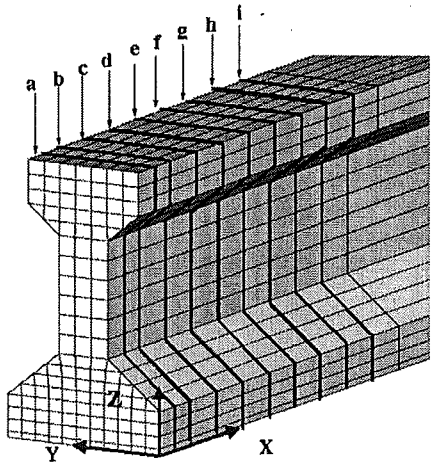

Figure 10-16. Shear Stress Distribution within the Web Projection at Selected Sections near the End Zone under Prestressing Loads

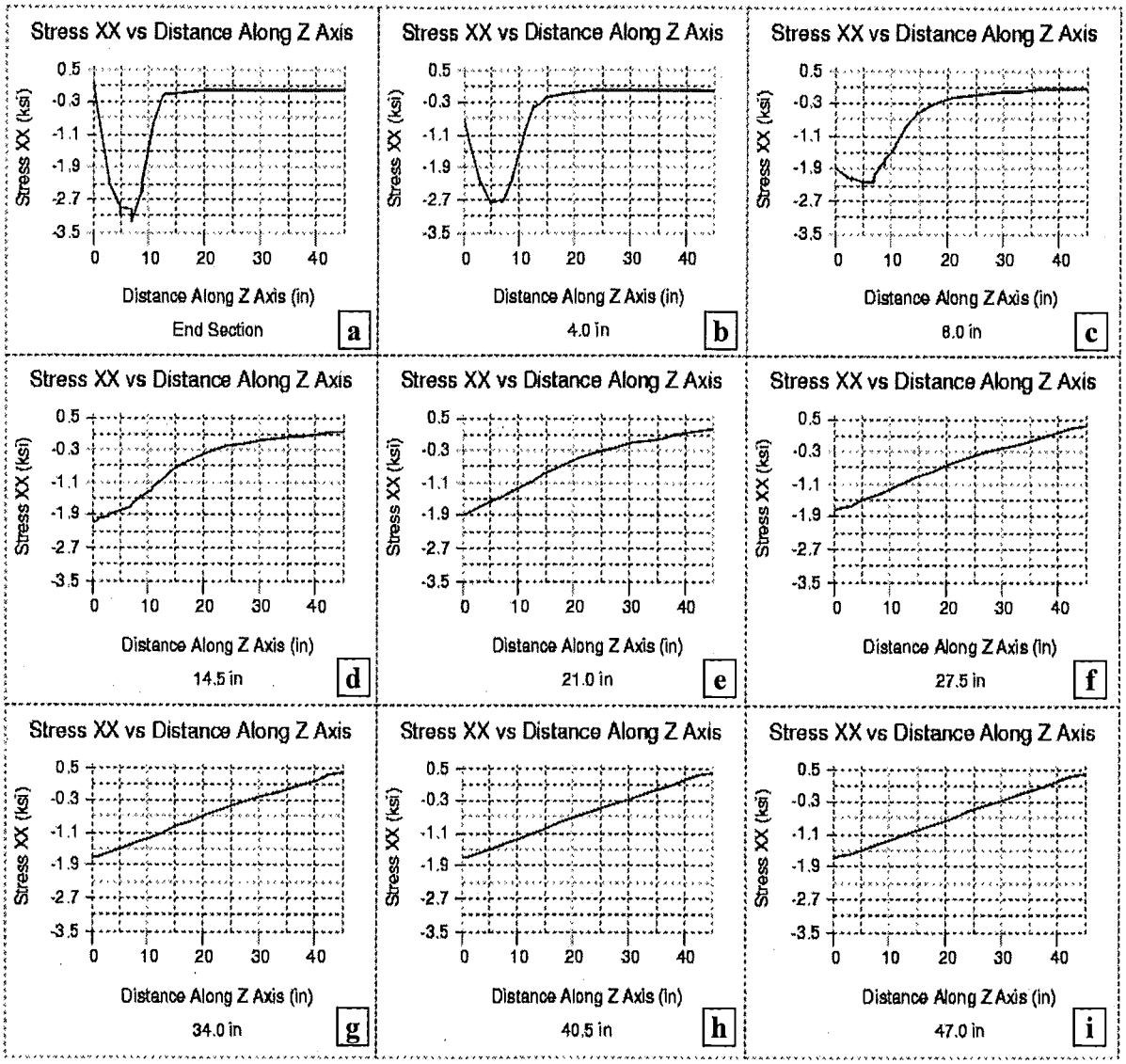

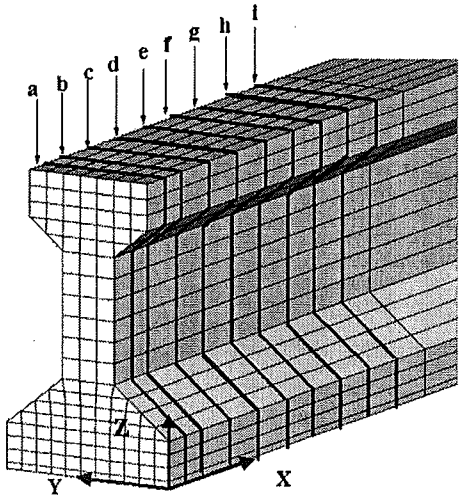

Figure 10-17. Axial Stress Distribution within the Web Projection at Selected Sections near the End Zone under Prestressing Loads

The cracking potential in the end zone is also described by using the principal stress contours. The principal stresses are calculated by rotating the x-y-z coordinates until the shear stress diminishes. In Figure 10-18, the principal stresses on the x-z plane are depicted by rotating the y-z coordinates through and angle "θ" about x-axis. The principal stresses of interest are noted by $f_{\theta 1}$ and $f_{\theta 3}$. $f_{\theta 1}$ and $f_{\theta 3}$ are the maximum and the minimum principal stresses, respectively. The principal stress $f_{\theta 2}$ is not significant for beam elements.

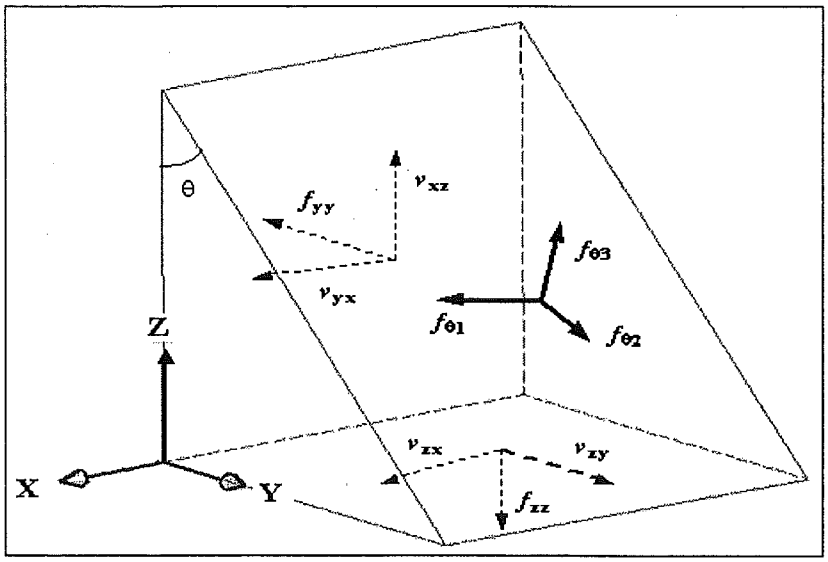

Figure 10-18. Principal Stresses on a Finite Element

The sign convention for the principal stresses is defined such that compressive stress is negative and tensile stress is positive. Principal stress (compressive) contour for $f_{\theta 1}$ is shown in Figure 10-19-a, with a magnitude of reaching a compressive stress of 3000 psi. Principal stress (tensile) $f_{\theta 3}$ shown in Figure 10-19-b is of significance to cracking. The maximum tensile stress magnitude reaches 400 psi near the beam-end on the web. The critical region seen in the principal stress analysis is the web to bottom flange transition area. The region from the bottom flange to the top flange through web, diagonally decreasing towards the end of the transfer length, is under relatively lower stresses (see Figure 10-19-a). The $f_{\theta 3}$ distribution indicates the vulnerability of the mid-web zone to cracking as shown in Figure 10-19-b.

The effects of bond quality on the transfer length and beam-end stresses are analyzed using two limiting values for bond stiffness. For good bond quality, the modulus of elasticity is assumed to be two times the best estimate ($2 \cdot E_c$). For poor bond quality, the modulus of elasticity is taken as half the best estimate ($E_c/2$). The spring stiffness used for modeling the bond between the tendon and concrete is modified to represent these two bounds. In Figure 10-20 and Figure 10-21, the axial and shear stresses for good and poor bond are compared. As the results are investigated, it is seen that the bond stress directly affects the stress intensity within the girder and their magnitude. Bond quality affects the axial and shear stresses near the beam-end as seen in Figure 10-20 and Figure 10-21. The shear and axial stresses increase as the bond quality increases, because the tendon slip decreases.

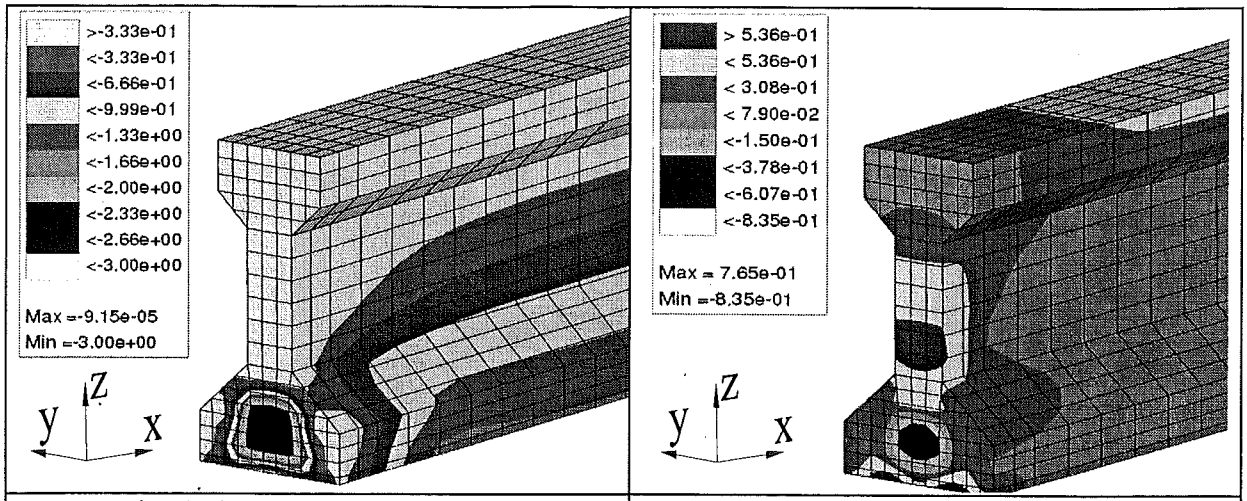

a) Principal Stress–1 Distribution | **b) Principal Stress–3 Distribution**

Figure 10-19. Principal Stresses (ksi) near the Girder-end under Prestressing Load

The good bond quality effect on transfer length is not as significant as the effect of poor bond quality. The transfer length in average bond case is around 30 inches; in the bad bond case, it is around 47 inches; and in the good bond case, it is around 27 inches.

The bond quality analyses are performed only on the girder with straight tendons. The main aim is to identify the impact of bond quality on the behavior of the girder. The results obtained are basic and will be the same on the other girders with different geometry and tendon configurations. Therefore, this analysis is not repeated on the other girders with bond-breakers and draped tendons.

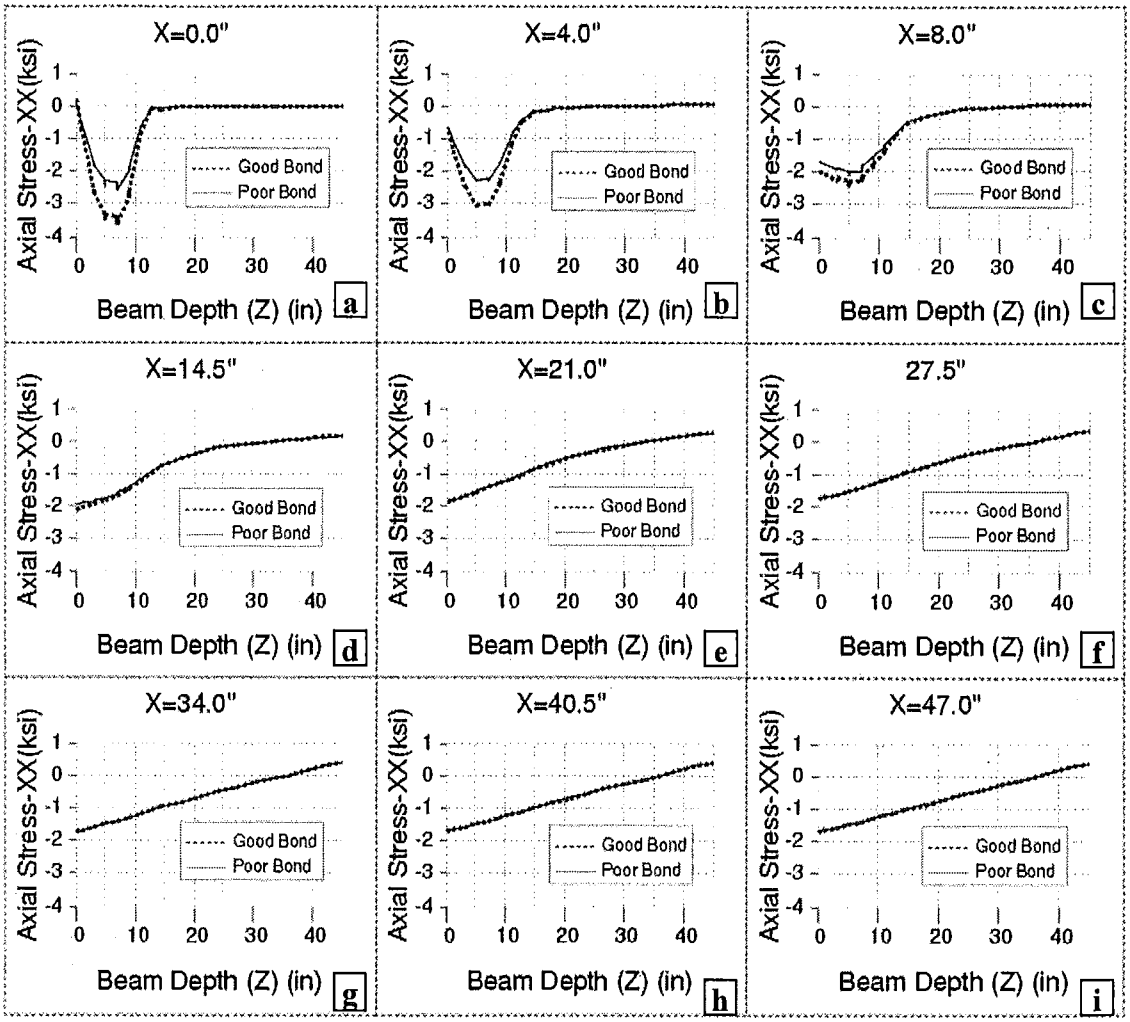

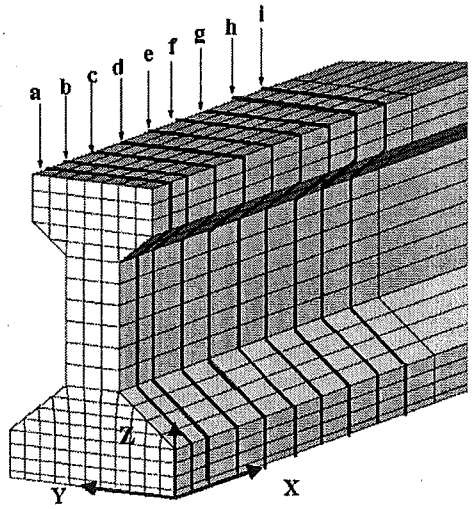

Figure 10-20. Axial Stress Distribution within the Web Projection at Selected Sections near the End Zone under Prestressing Loads with Good and Poor Bond Qualities

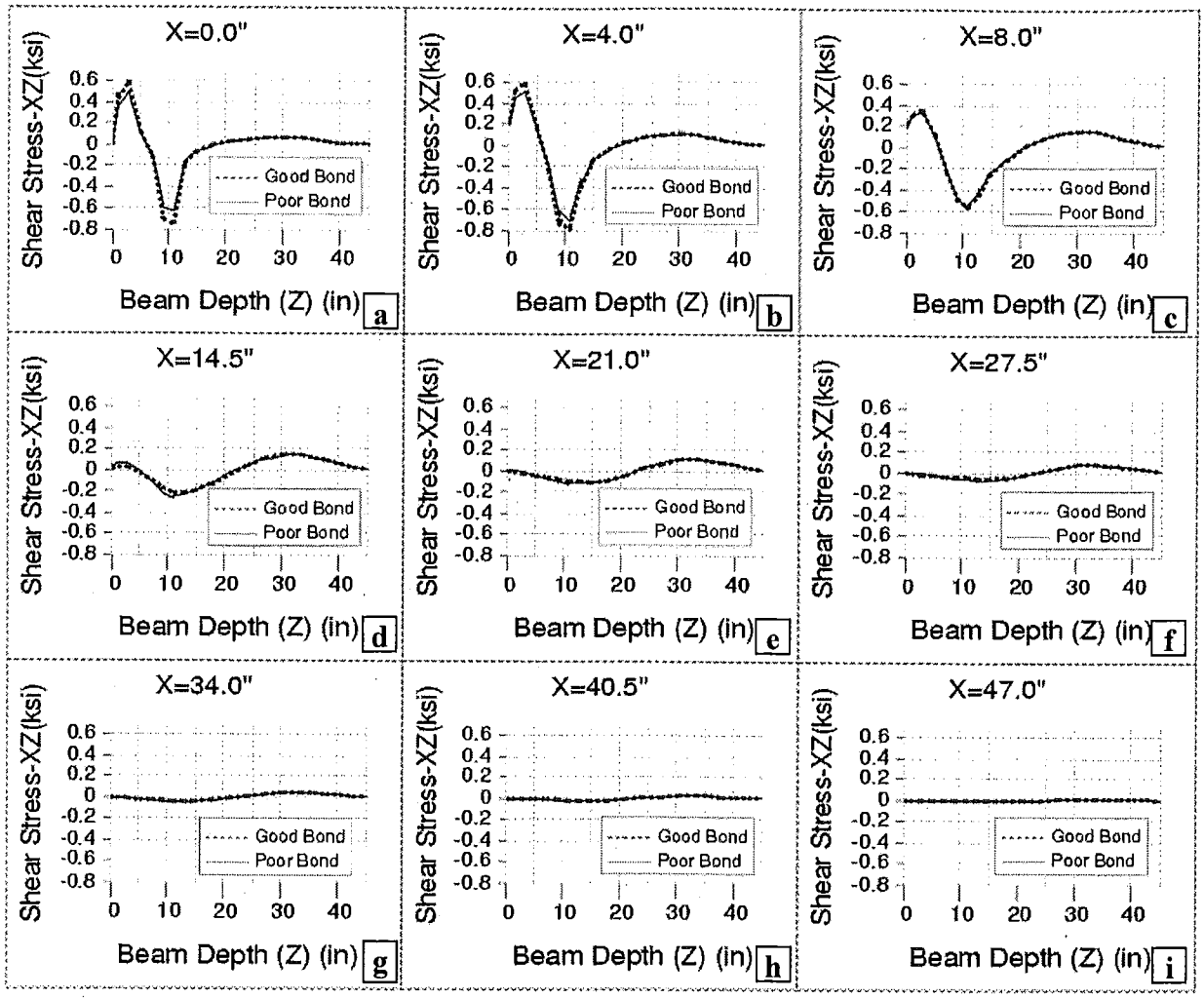

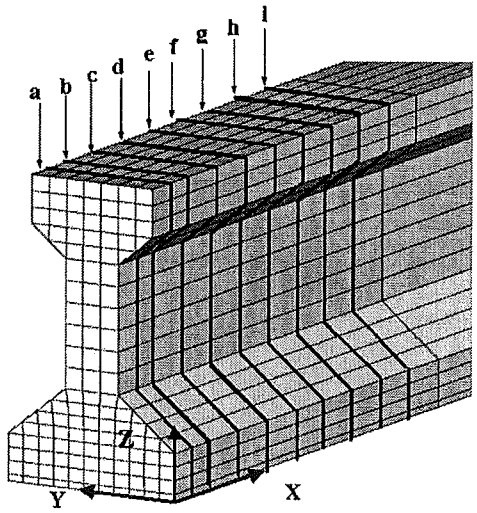

Figure 10-21. Shear Stress Distribution within the Web Projection at Selected Sections near the End Zone under Prestressing Loads with Good and Poor Bond Qualities

10.5.2 Analysis of Prestressed Girders with Bond-Breakers under Prestressing Load

The bond-breakers are employed around the tendons to reduce the concrete stresses near the beam-end. The tendons having bond-breakers are sometimes called sheathed tendons. Some of the strands with bond-breakers are debonded for a length near the beam-ends while the others are retained without bond-breakers. These types of beams were designed more recent than the straight and draped tendons. The year in which these beams are first utilized is seen in Table 10-1 as Michigan 1800 and Wisconsin 70. Using the finite element model (see Figure 10-22), the impact of the bond-breakers is studied. First, the beam is analyzed with straight (uniform) strands and then with bond-breakers. The analyses are compared for stresses and cracking potential, as shown in figures from Figure 10-23 to Figure 10-26.

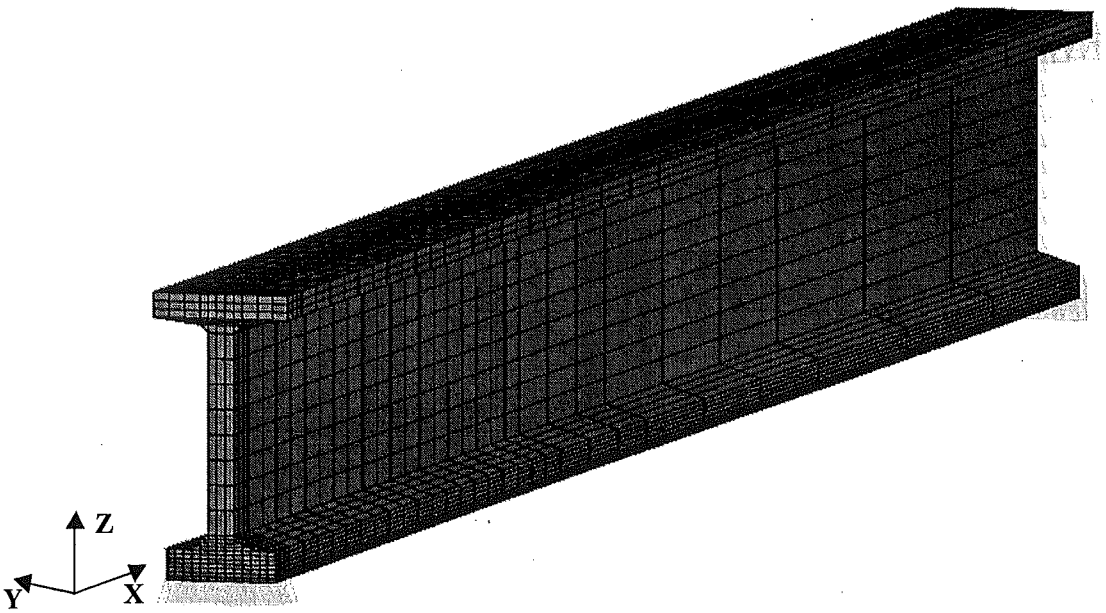

Figure 10-22. General View of the I-Beam with Bond-breakers

The beam modeled is selected from the bridge with the inventory ID of S05 of 53034, a three-span bridge, with skew of 14° 30'. The beam length is 111.5 feet. The total number of the strands is 34 with ½-inch nominal diameter. The strands are 7-wire low-relaxation steel having 270 ksi strength. Ten of these strands are sheathed for 8 feet, and another ten for 15 feet. The beam cross-sectional geometry is Wisconsin 70 with a height of 70 inches, and flange thickness is 6 inches at the top flange and 7.5 inches at the bottom flange. The initial prestressing force in each tendon is 31 kips. The design compressive strength for concrete is 5,000 psi.

In girders without bond-breakers, axial stress achieves a uniform distribution after prestressing transfer is complete as shown in Figure 10-23. However, in the case of girders with bond-breakers at locations where the strands are released, changes in axial stresses are observed as shown in Figure 10-27. The axial stress magnitude, which is not shown here, in the beam without bond-breakers (7.4 ksi maximum) is higher than in the beam with bond-breakers (5.35 ksi maximum). The shear stress distributions in x-z plane are similar for beams with and without bond-breakers. One minor difference is the presence of shear stress near the tendons' release

points. The shear stress magnitude, however, is approximately 30% lower in the girder with bond-breakers. The maximum shear stress on the web in the beam without bond-breakers is around 1.5 ksi, while in the beam with bond-breakers it's around 1.0 ksi (see Figure 10-24-a and Figure 10-26-a).

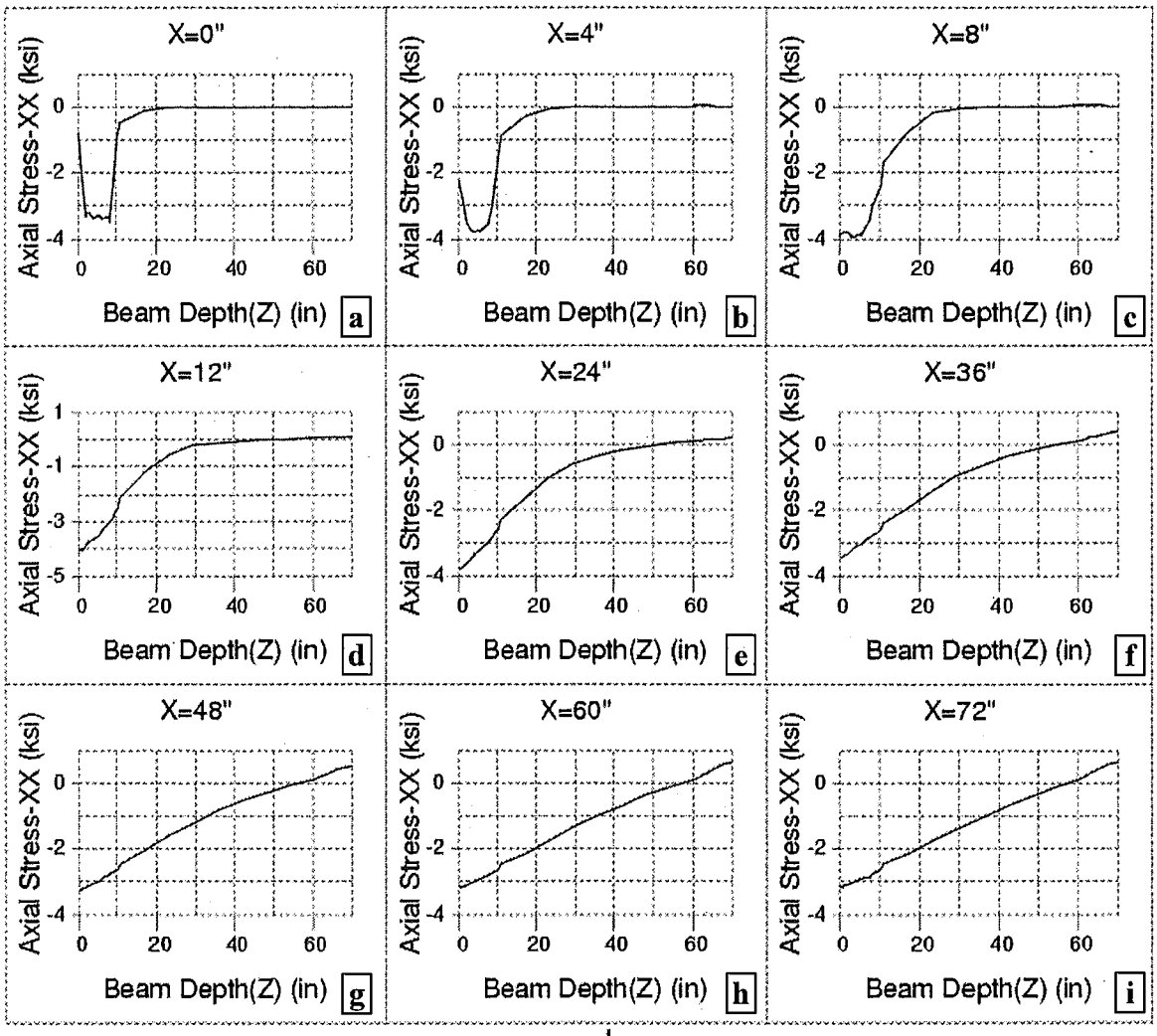

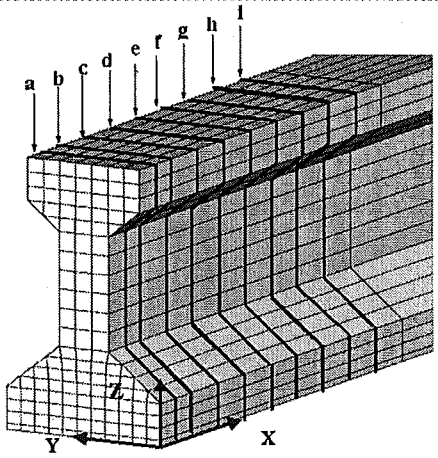

Figure 10-23. Axial Stress Distribution within the Web Projection at Selected Sections near the End Zone under Prestressing Loads on the Girder without Bond-Breakers

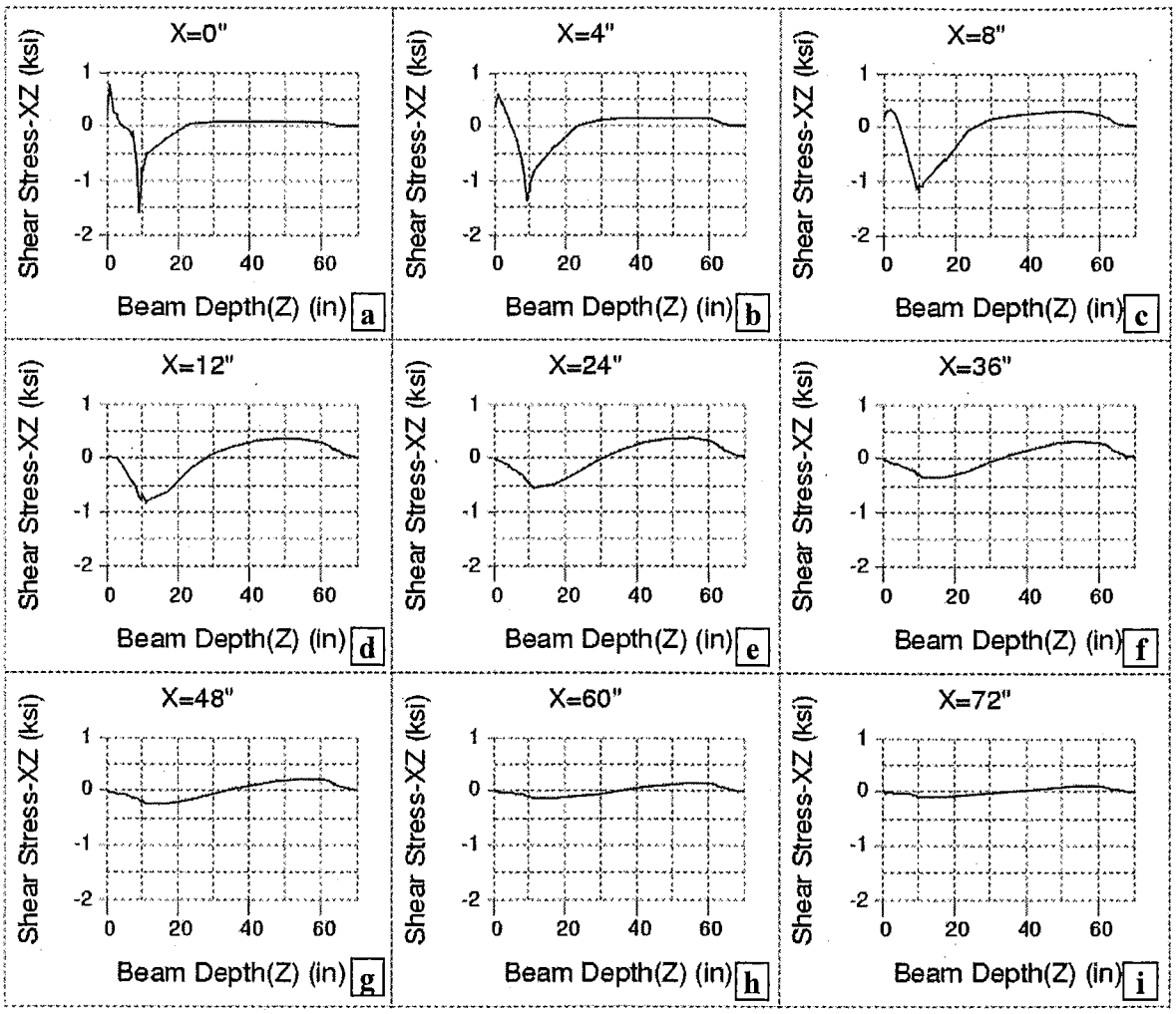

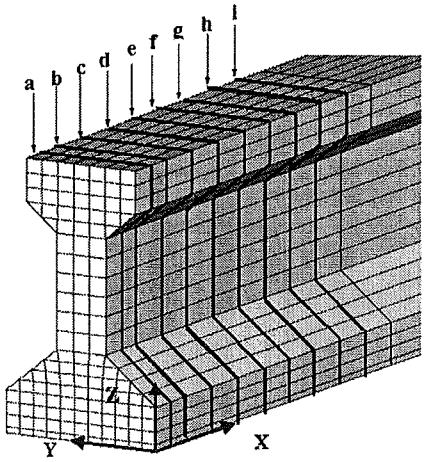

Figure 10-24. Shear Stress Distribution within the Web Projection at Selected Sections near the End Zone under Prestressing Loads on the Girder without Bond-Breakers

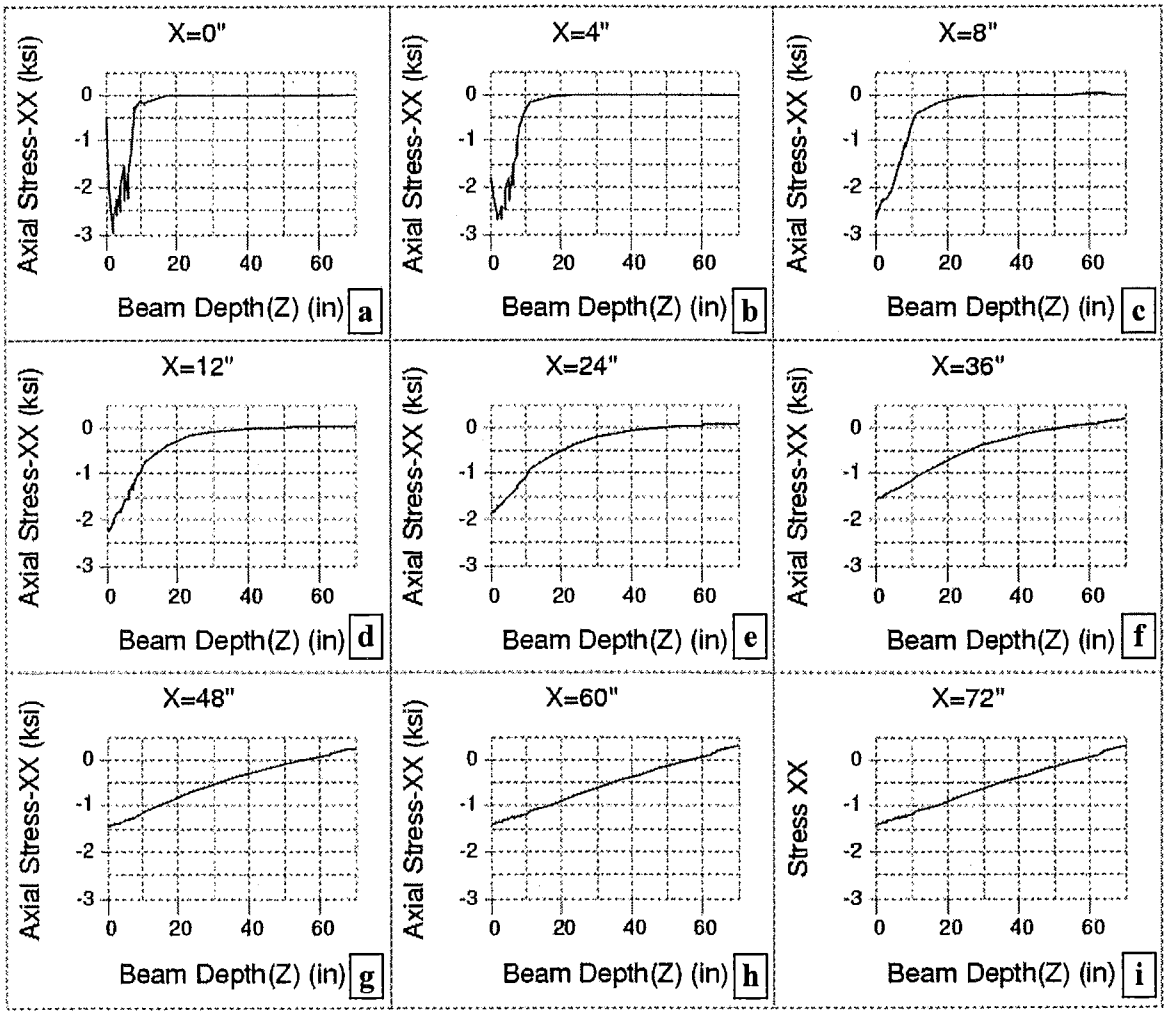

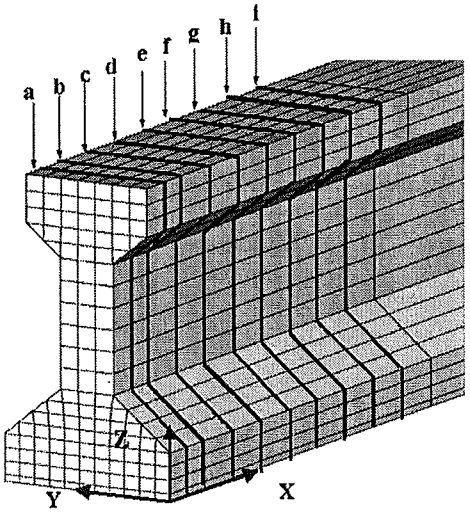

Figure 10-25. Axial Stress Distribution within the Web Projection at Selected Sections near the End Zone under Prestressing Loads on the Girder with Bond-Breakers

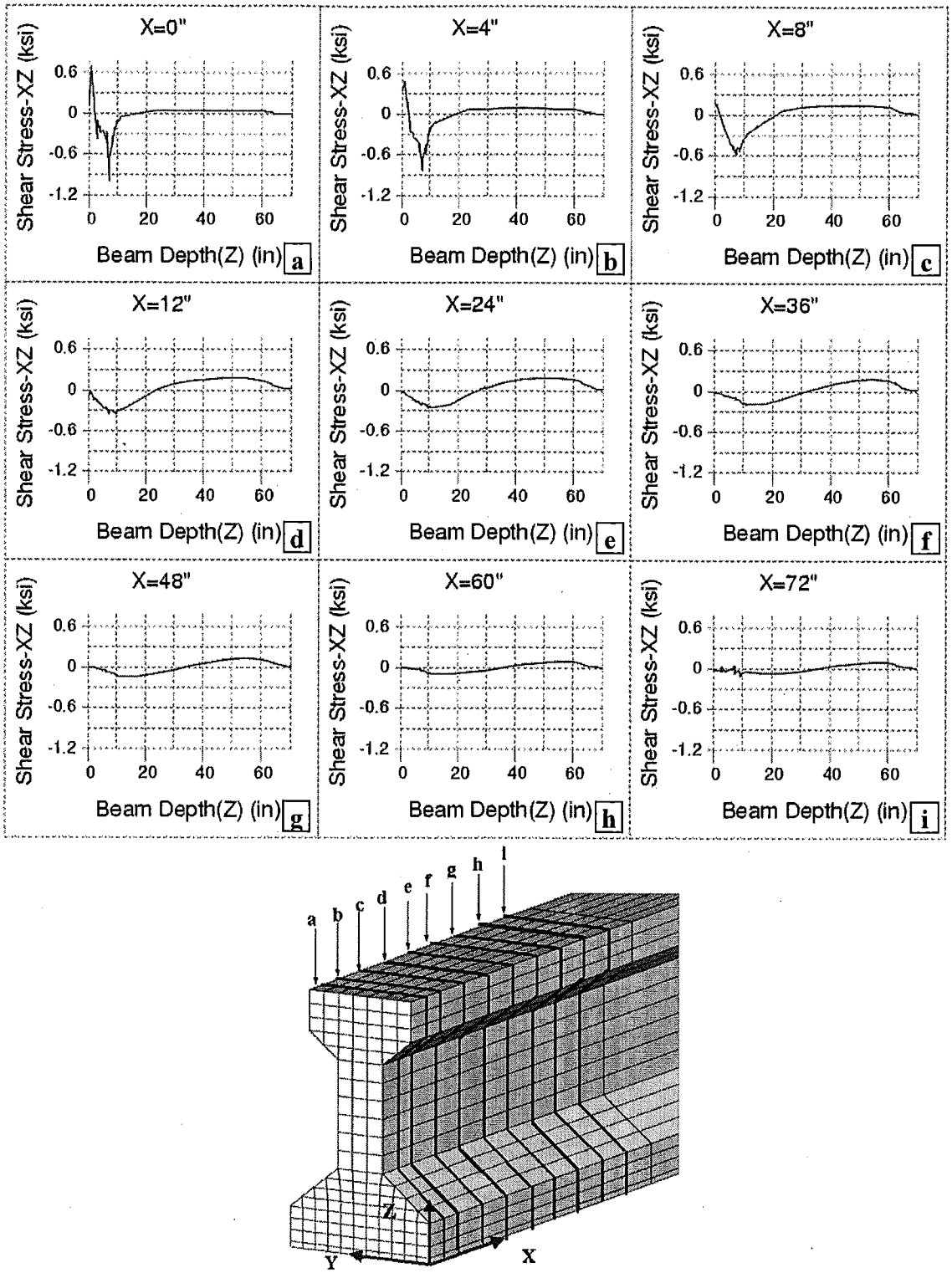

Figure 10-26. Shear Stress Distribution within the Web Projection at Selected Sections near the End Zone under Prestressing Loads on the Girder with Bond-Breakers

Axial and shear stress distribution at sections around the debonding locations are shown in Figure 10-27 and Figure 10-28. Small deviations are observed in both axial and shear stresses on

the girder within 24 inches, where debonding ends. The maximum shear stress is calculated as around 500 psi at the first release point as shown in Figure 10-28-a. Deviation of the axial stress between Figure 10-27-b and Figure 10-27-c is not significant.

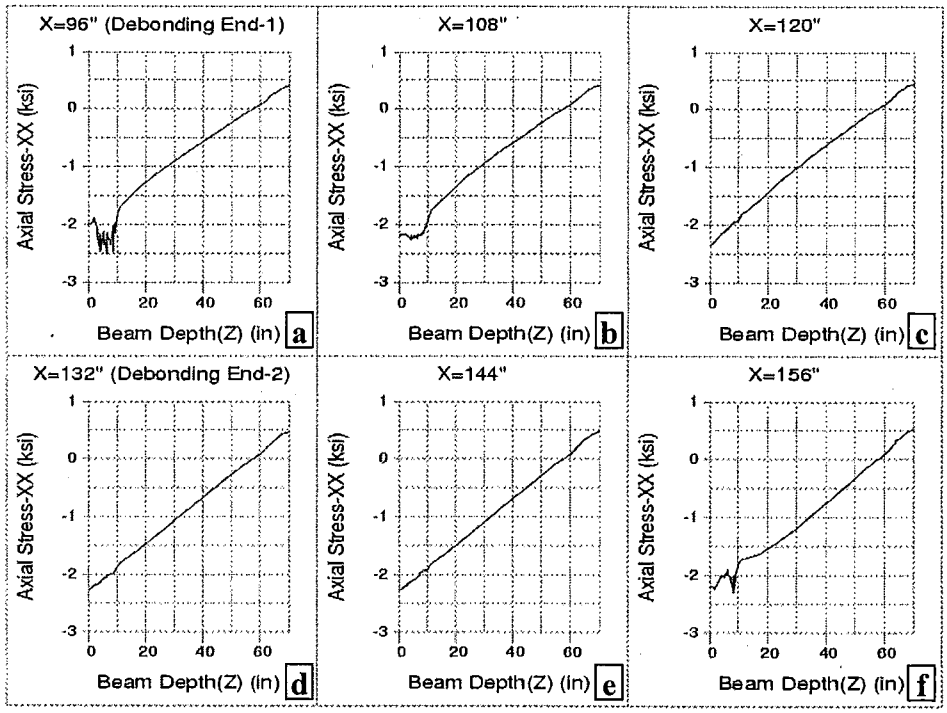

Figure 10-27. Axial Stress Distribution within the Web Projection at Selected Sections near the Release Points on the Girder with Bond-Breakers under Prestressing Loads

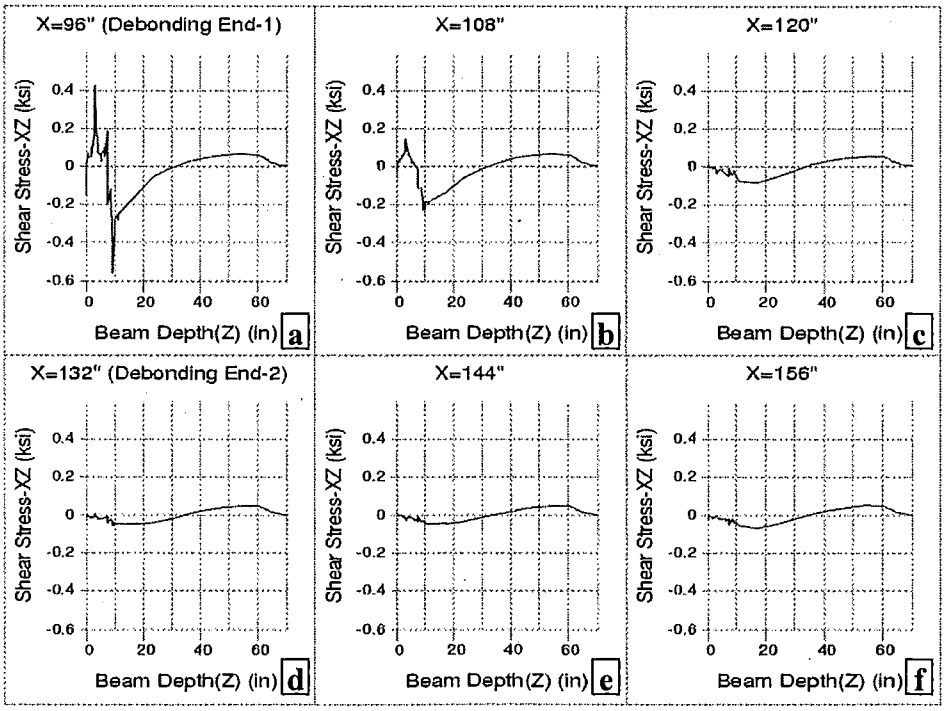

Figure 10-28. Shear Stress Distribution within the Web Projection at Selected Sections near the Release Points on the Girder with Bond-Breakers under Prestressing Loads

The shear stress cracking pattern may be described by the principal stresses. The maximum and minimum principal stresses for the beam with bond breakers are shown in Figure 29-a and -b. The maximum principle stress is 3.6 ksi around the tendons and the ends of debonding as shown in Figure 29-a. This stress is compressive and well below the compressive strength of concrete. The minimum principle stress, shown in Figure 29-b, is around 1.2 ksi. This tensile stress may be the main reason for the shear cracking. Because the stress value found exceeds the tensile strength of concrete, which is 424 psi. As it is seen in Figure 29-b, the web zone is prone to cracking due to excessive tensile stress.

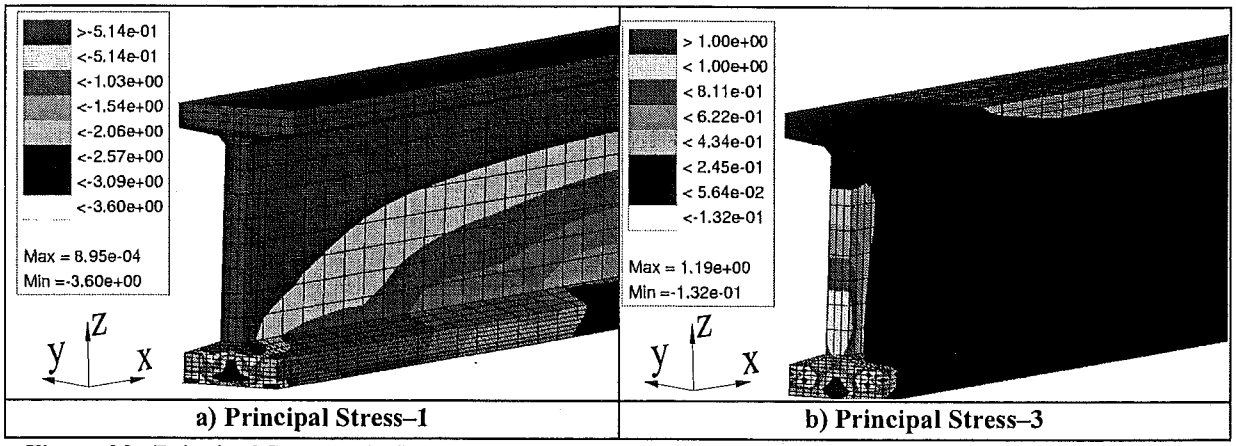

a) Principal Stress–1 **b) Principal Stress–3**

Figure 29. Principal Stresses (ksi) near the Beam-end under Prestressing Load for the Beam with Bond-breakers

10.5.3 Analysis of Girders with Draped Tendons under Prestressing Load

The third type of girder analyzed under prestressing load is the girder with draped tendons. In draping, the tendons are anchored at about the one-third points of the beam and pulled towards the top flange of the beam. In this girder type, end blocks are incorporated in order to accommodate the anchoring of the tendons near the girder-ends. Draped tendons with end blocks are commonly seen in earlier bridges, and they appear to be rare in recent bridges. Because there are many bridges built with draped beams suffering from end distress, it is important to analyze and discuss the effects of draping and the effect of the end block on stresses near the beam-ends.

The draped beam model is selected from the bridge with inventory ID S06 of 41027, with a length of 65 feet and 6 inches. The total number of strands used is 36, 28 strands are kept straight and 8 strands are raised near the beam-ends. The nominal diameter of the 7-wire strands is 7/16 inches. Initial prestressing load is 19.05 kips on each tendon, which has an ultimate strength (f_{pu}) of 250 ksi. The concrete design compressive strength is defined as 5,000 psi.

As described earlier in the straight tendon case, the change in the effective prestressing load transferred to the beam generates the change in axial stress distribution along the beam's longitudinal axis that in turn generates the shear stresses. In the beams with draped tendons, there are three parameters affecting change in the axial stress distribution. These are prestressing

force transfer between the tendon and concrete, angle of inclination of the draped prestressing tendons, and the change in the cross-sectional area due to the transition to the end block.

The FE model and mesh for the girder with draped strands shown in Figure 10-30 is significantly different than the other two tendon arrangements analyzed earlier. In this mesh, some of the elements are inclined in order to accommodate the inclined tendon and the end-block, where the web is gradually make thicker towards the beam-end.

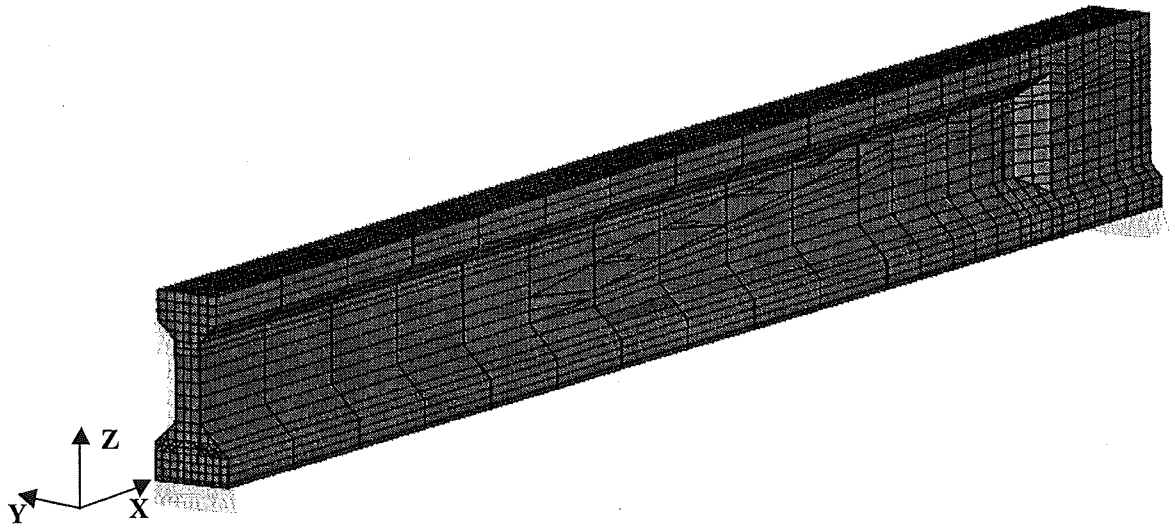

Figure 10-30. One Half of a Beam with Draped Tendons and End Block

The axial stress distribution in x-axis is shown in Figure 10-31 and the shear stress distribution on the x-z plane is shown in Figure 10-32. As seen in Figure 10-32, the change in effective prestressing force within the transfer length results in shear stresses generated near the top flange within the end block and near the zone where the end block is gradually discontinued. The shears stress near the girder-end exceeding 600 psi shows the vulnerability of these girders to cracking. The shear strength of the concrete is around 247 psi, according to AASHTO (AASHTO, 1998)

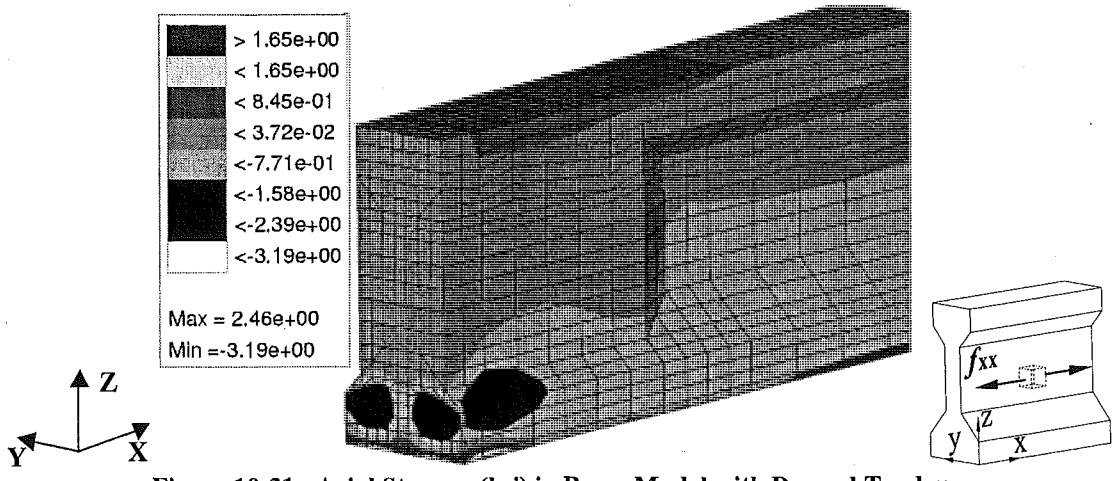

Figure 10-31. Axial Stresses (ksi) in Beam Model with Draped Tendons

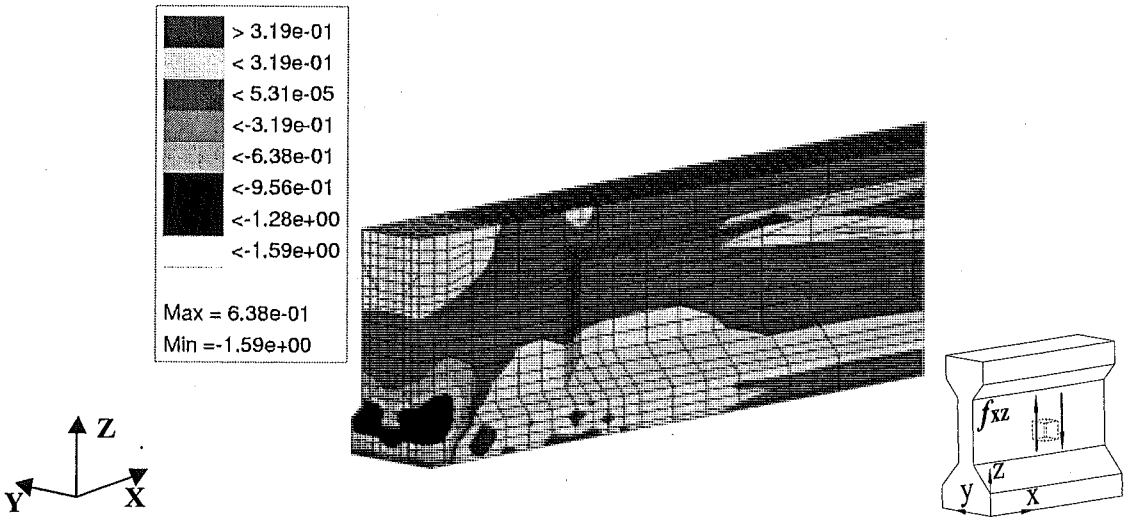

Figure 10-32. Shear Stresses (ksi) in Beam Model with Draped Tendons on X-Z Plane

10.5.4 Load Path Analysis

Load path analysis is performed to establish the portions of the beam-end that are within the load path under the combined action of dead, service, and prestressing loads. The purpose is to provide a means of evaluating the beam-end deterioration impact to its "load transfer" capacity. In other words, the beam-end evaluation is based on whether the zones with section loss interfere with the load path.

The bridge inspection revealed that significant numbers of elastomeric bearing pads appear to have lost their deformability. Similar conditions are observed from other inspections stated in the literature (Yazdani et al, 2000). The main reasons are stated as cold temperatures and aging. The analysis is performed under dead and live loads to establish the load path within the beam-end zone, including non-functional elastomeric bearing pads to simulate the realistic constraints at the girder-end. The non-functional bearings are modeled by modifying girder support restraints to adapt for this condition.

The diaphragms are employed to control the relative movement between the girders, and to help in maintaining the load transfer from the deck to the girders. In other words, diaphragm stiffness properties and location control the live load distribution to individual girders. In this case, the diaphragms are not included in the analysis model, and it is assumed that the girder load distribution factors given by AASHTO are applicable. Further information on the diaphragms is provided in the full bridge modeling section of this report.

The load path analysis is performed on a single girder, utilizing the same model developed in "Girder with Straight Prestressing Tendons under Prestressing Load" analyses (see section 10.5.1). The effects imposed on the girders by the diaphragms and the decks are not incorporated here.

The deck, the wearing surface, the barriers, and the girder are included in the dead load estimation. With a concrete unit weight of 0.150 k/ft^3 the dead load estimated for a girder is

0.583 k/ft. The deck dead load with an effective width of 45.5 inches and 8 inches of thickness is 0.379 k/ft. For the haunch with 1-inch thickness, the dead load is 0.017 k/ft. The barriers with an area of 2.61 ft^2 and 0.131 k/ft weight are described as superimposed dead load. The wearing surface with 2.5 inches of thickness adds 0.204 k/ft to superimposed dead load. AASHTO HS20-44 truck load (AASHTO, 1998) is used for the live load and applied at a position to generate the maximum flexural stress at the mid-span. The truck load used is for a gross truck weight of 72,000 lb, which is an approximated load amount for simulating the largest stress. For live load effect on a single girder, the distribution factors as given in the AASHTO codes are used. The girder spacing is 91 inches on center. Therefore, the live load distribution factor is calculated as 1.379 by using the formula given in AASHTO (AASHTO, 1998) as DF=S/5.5, where DF is the distribution factor and S is the girder spacing. The dead, superimposed dead, loads are distributed longitudinally uniform over the top surface. The live loads are distributed transversely uniform at the wheel locations at the top surface of the beam.

Influence of the bearing on the load path is an important parameter contributing to the stresses at the beam-end. The elastomeric bearing pad sits under a steel bearing plate. The concrete beam and the bearing plate are assumed in composite behavior, when the elastomeric bearing pads are deformable. However, when the elastomeric pad becomes non-functional, as shown in Figure 10-33-a, differential deformations between the bearing plate and the girder are observed. As the beam deforms under bending, the bearing without any deformability rocks on the pier cap. The effective support area is thus reduced. The exaggerated deformation is shown in Figure 10-33-b. Therefore, these differential deformations make the girder vulnerable to cracking, as shown in Figure 10-33-c.

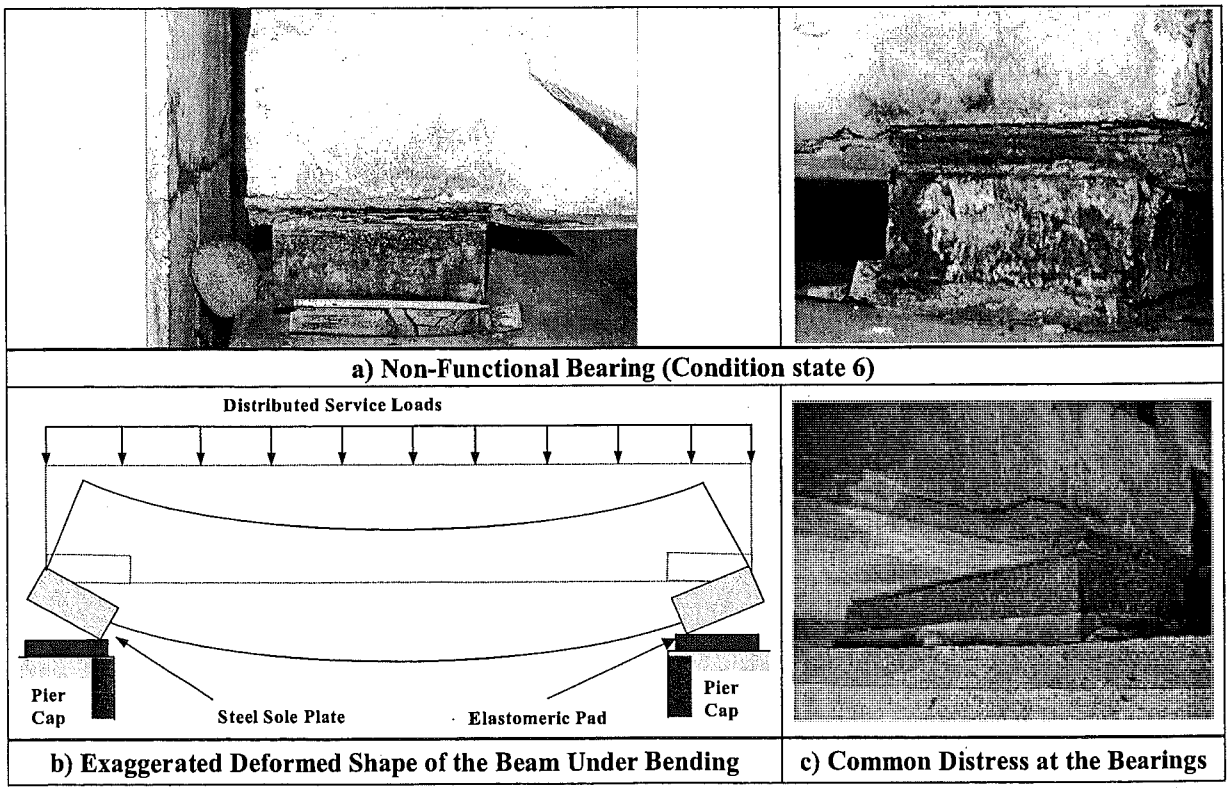

Figure 10-33. a) Condition of the Elastomeric Bearing Pads; b) the Exaggerated Deformed Shape of a Girder under Flexural Bending; c) Common Distress Observed at the Bearings

The beam model under dead load is shown in Figure 10-34-a with the modified support to simulate the rocking of the bearing plate over the non-functional bearing under bending. The beam under dead load is also analyzed for truck load that is live load (see Figure 10-34-b).

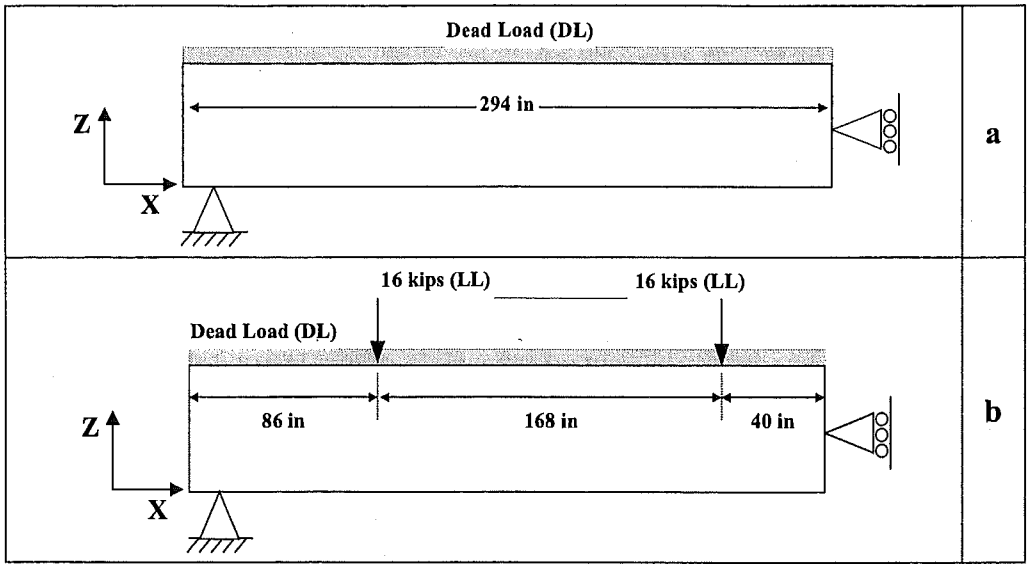

Figure 10-34. a) Beam FE Model and Loading under Dead Load; b) Live Load Distribution on the Girder

Figure 10-35 shows the axial stress distribution under prestressing and dead loads. It is seen that the tensile stresses are increased at the top flange due to reduction in support area. Negative moment is seen at the top of the support because the beam-end now hangs over the support as a cantilever beam. However, the maximum tensile stress, calculated as 290 psi, is less than the concrete tensile strength, which is 424 psi according to AASHTO given as $6 \cdot \sqrt{f_c'}$. Another important result is the stress pattern that describes the load path. The zone on the girder with the stress value of around 740 psi and above compressive stress defines the load path under dead load only. When the live load is included, a similar stress pattern and load path is observed near the end zone. In this case, the load path is defined by the zones of compressive stress of 760 psi and greater (see Figure 10-36). Tensile stresses develop at the beam-end under live load. The accuracy of the stress value is questionable because the deck contribution to load capacity of the beam is not considered in the analytical model.

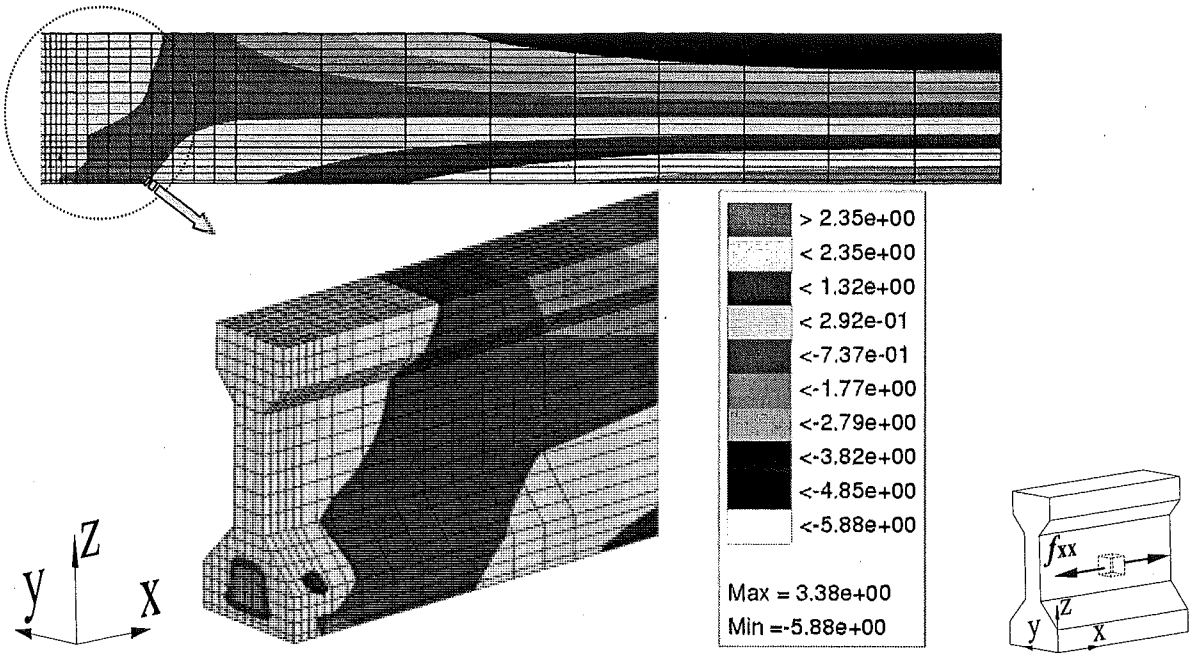

Figure 10-35. Axial Stress (ksi) in the Beam under Prestressing and Dead Load

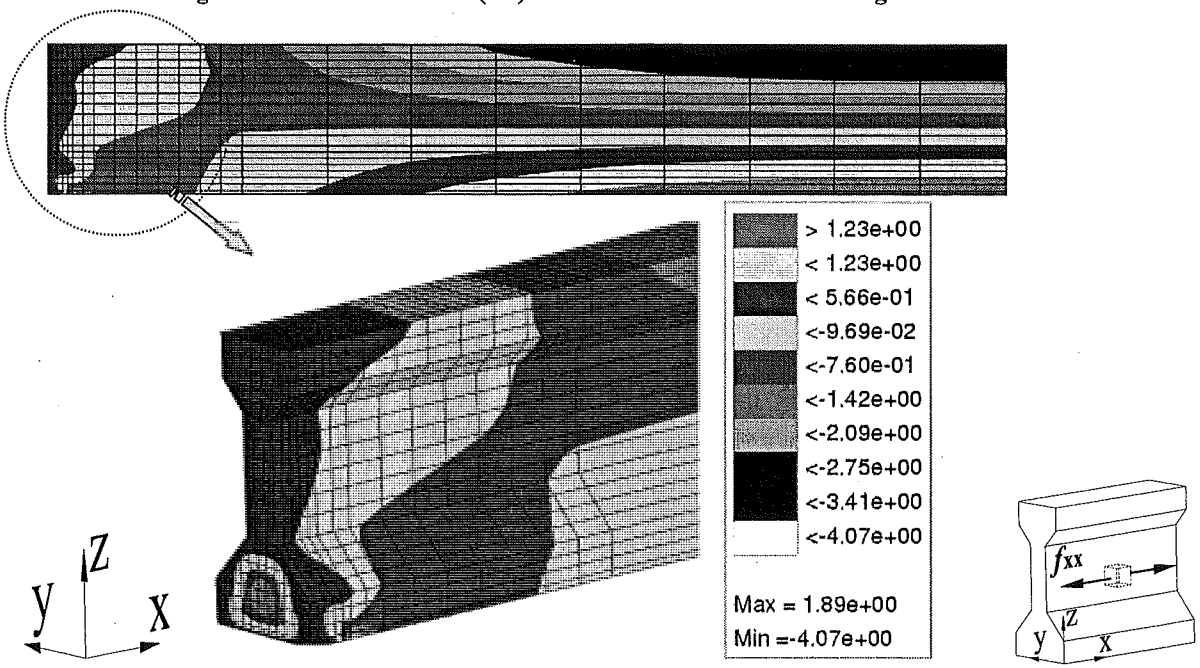

Figure 10-36. Axial Stress (ksi) in the Beam under Prestressing, Dead, and Live Loads

The shear stress distributions shown in Figure 10-37 under dead load and Figure 10-38 under dead and live loads are useful to document stress state near the beam-end. These figures are provided for documentation purposes, and evaluations will not be provided.

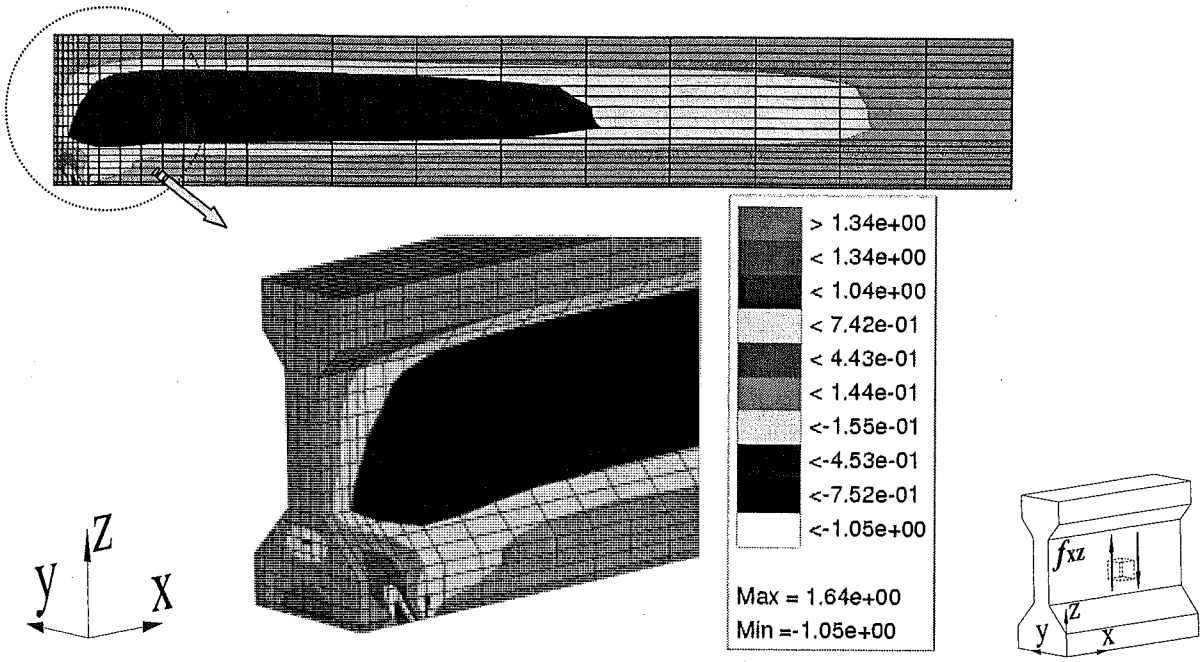

Figure 10-37. Shear Stress (ksi) under Prestressing and Dead Loads

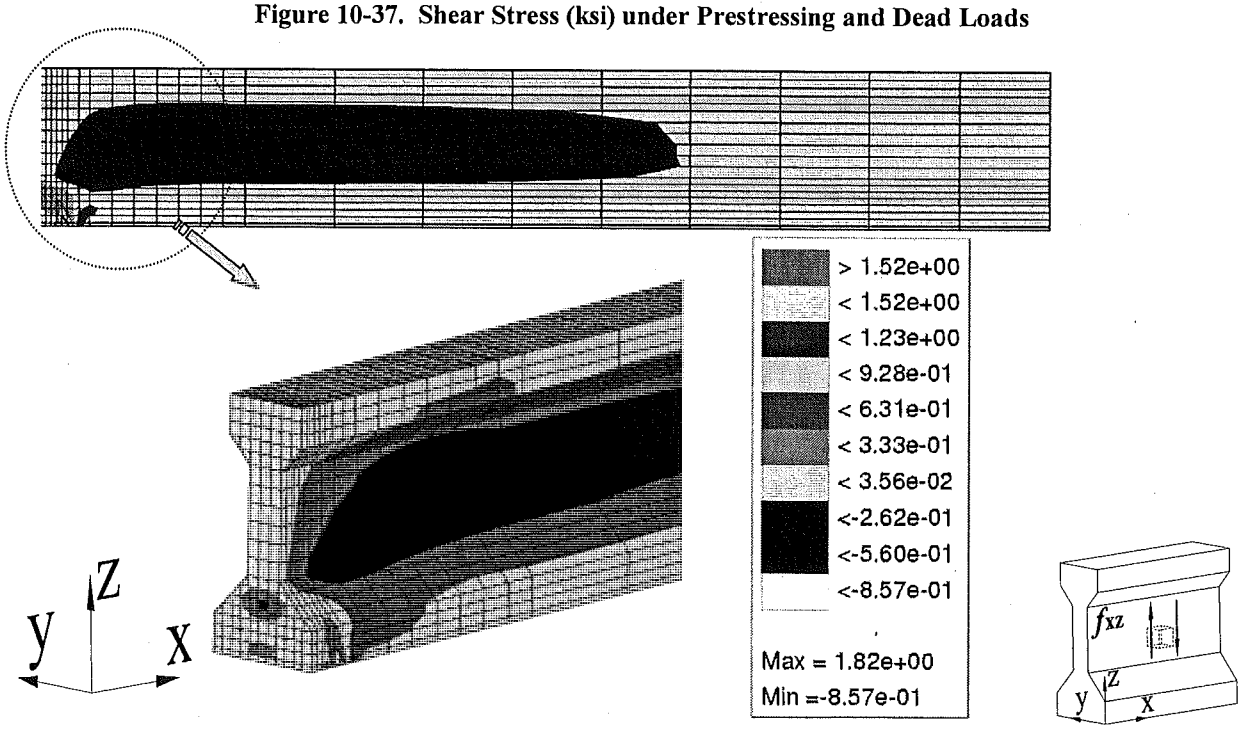

Figure 10-38. Shear Stress under Prestressing (ksi), Dead, and Live Loads

The axial and shear stress comparisons under dead and live loads at selected sections near the beam-end are shown in Figure 10-39 and Figure 10-40. The impact of the non-functional elastomeric bearing is also depicted in the figures. As the support area is reduced due to rocking of the bearing plate, consequently the stress intensities are increased. The dead and live loads give similar stress distributions around the support. The beam-end portion near the support under shear stress intensities exceeding 1.2 ksi is vulnerable to cracking as seen in Figure 10-40-f.

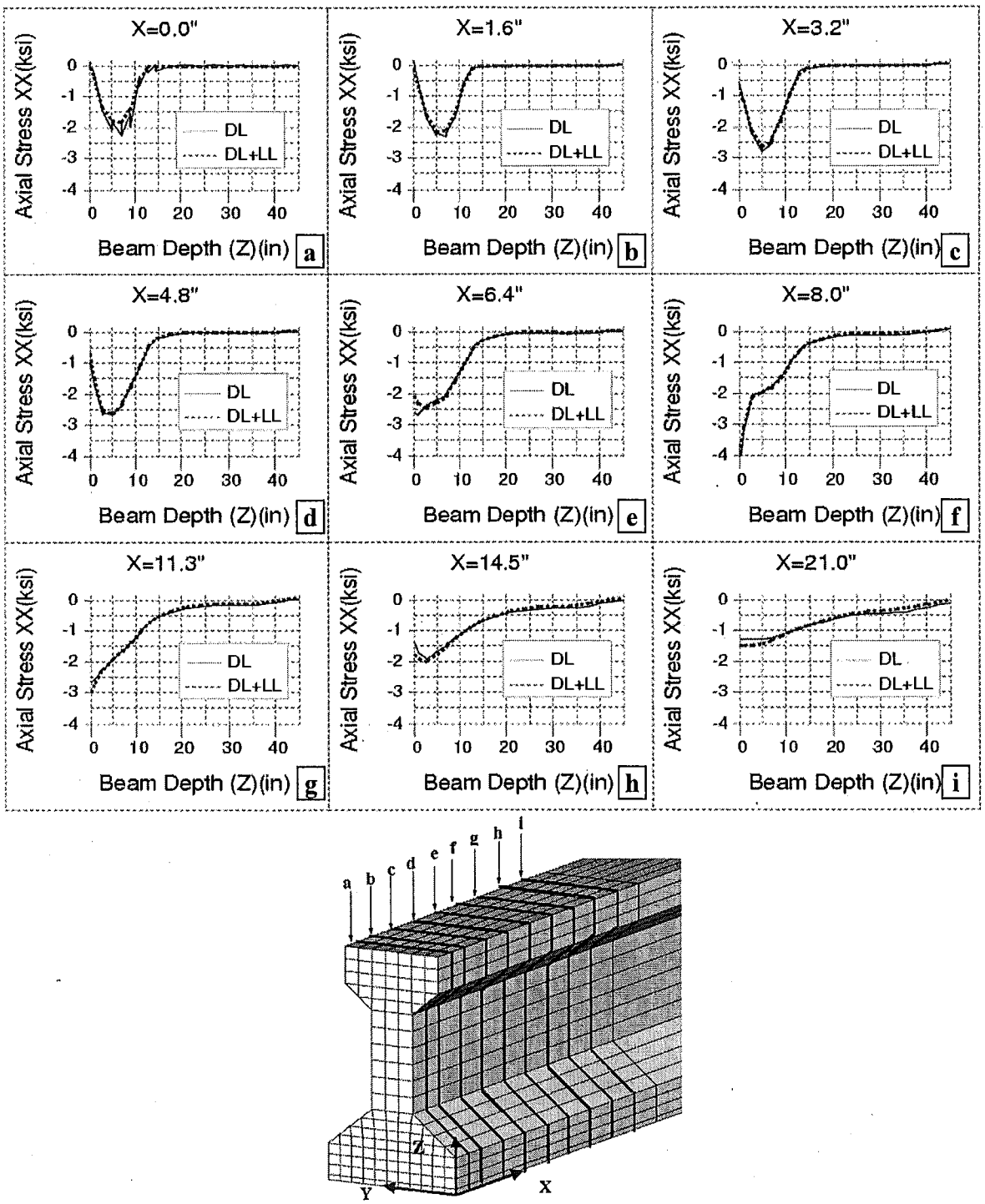

Figure 10-39. Axial Stress Distribution within the Web Projection at Selected Sections near the End Zone under Prestressing, Dead, and Live Loads

The principal stresses generated near the beam-end due to non-functional elastomeric bearing pads are shown in Figure 10-41-a and Figure 10-41-b. As shown in the figures, the stress intensity at the bottom flange is high. In particular, the principal stress intensity around the bearing is significant. The maximum compressive stresses observed under dead and live loads

are 7.84 ksi and 8.09 ksi, respectively. Considering the compressive strength of the concrete described, 5 ksi, principal stress, $f_{\theta l}$, is significant and higher than the compressive strength of concrete.

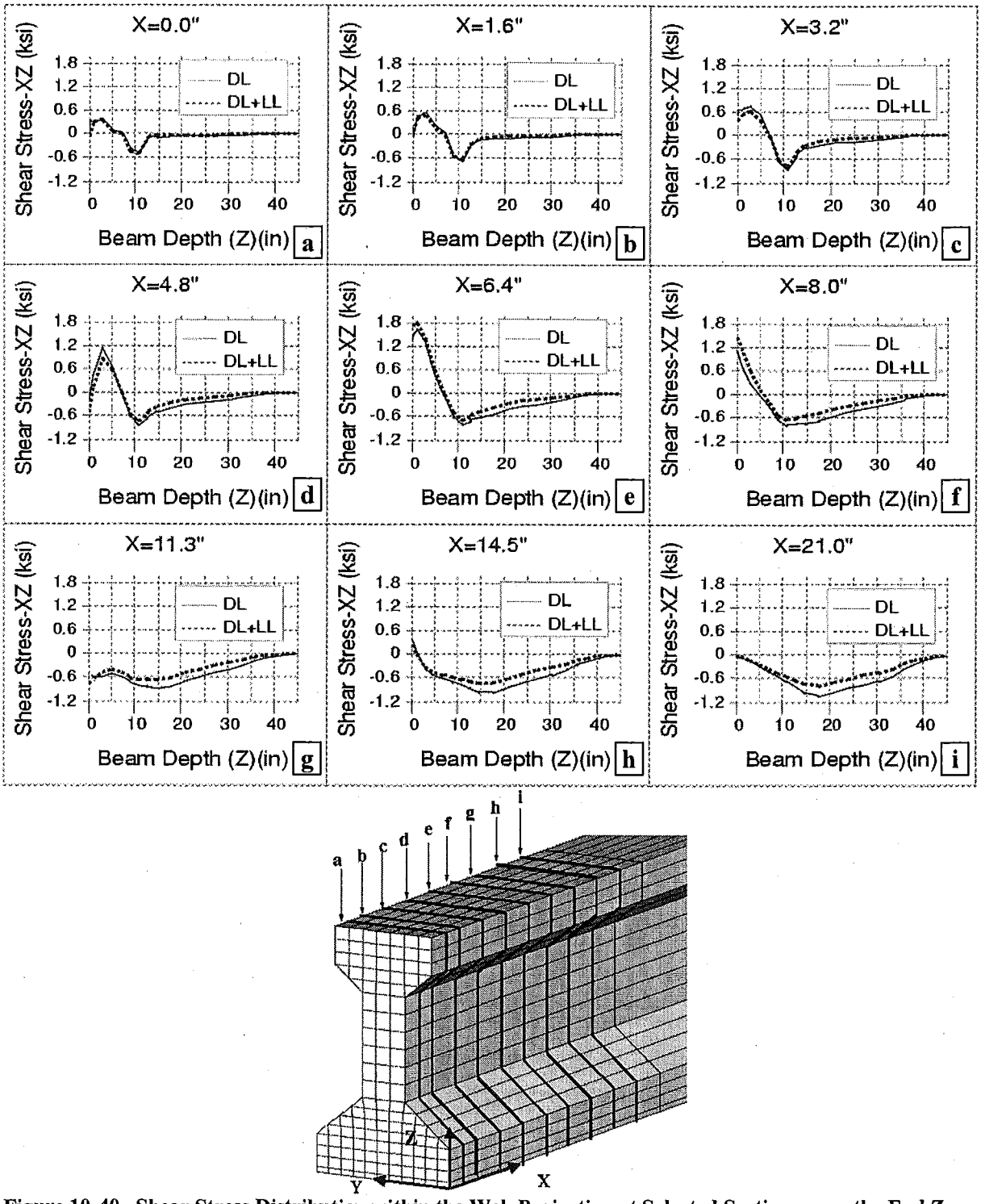

Figure 10-40. Shear Stress Distribution within the Web Projection at Selected Sections near the End Zone under Prestressing, Dead, and Live Loads

The load path in the girder is also investigated to identify the critical zones at the girder-ends. Von Misses stresses in Figure 10-42-a and Figure 10-42-b are utilized for describing the load path near the beam-end. The zones of the beam-end that is within stress contour of 1,920 psi under dead load and 2,400 psi under live load are defined as the load path and shown in Figure 10-42-c and Figure 10-42-d, respectively. The concrete zone shown in Figure 10-42-c defines the load path near the beam-end with non-functional bearing. Any deterioration that intrudes into the load path increases the vulnerability of the beam-end and its load carrying capacity. The beam-end condition may be assessed according to the intrusion of deterioration into the load path. Any kind of deterioration, such as delamination and spall that are not within this diagonal region or reaching the load path, can be repaired using the repair techniques described for condition states of "10" and "11" as given in Table 12-2 in Chapter 12 of this report.

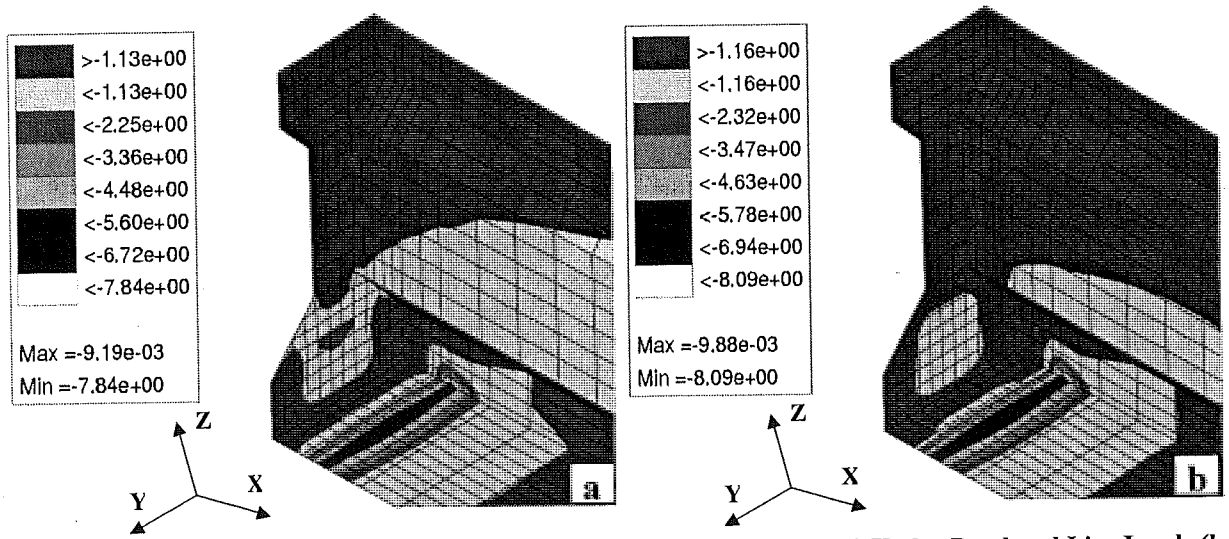

Figure 10-41. Principal Stress (Compressive), a) Under Dead Load (ksi); b) Under Dead and Live Loads (ksi)

The non-critical zones shown in Figure 10-42-c are removed for Figure 10-42-d, to generate a template for the inspectors to assess the significance of the deterioration at the beam-ends. Any deterioration on the regions shown in Figure 10-42-d is considered at risk.

The analysis results are shown only at the beam-end, specifically, for describing the load path. In this analysis the deck is not included as part of the load transfer medium. The model should include the deck for more realistic assessment of the load path.

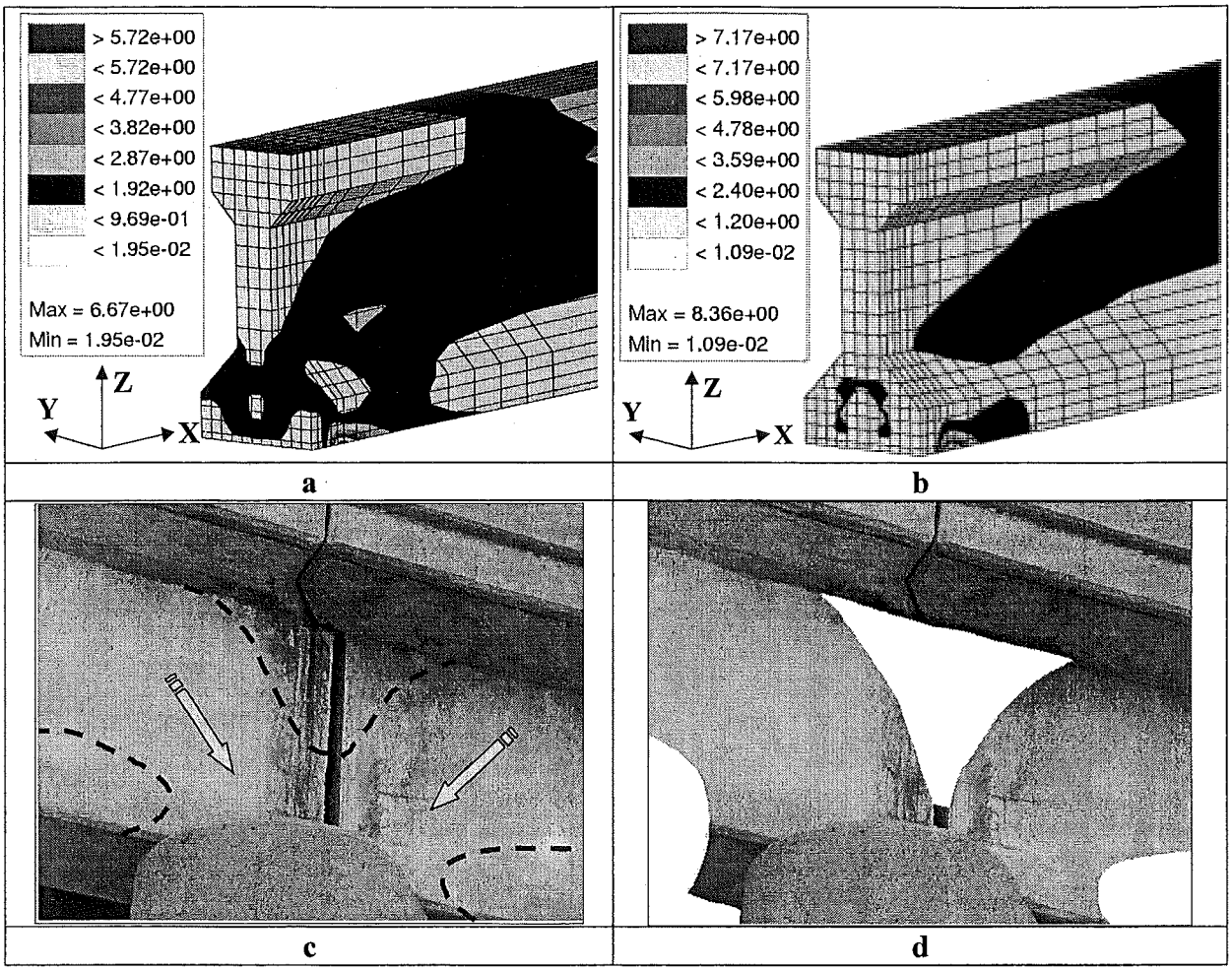

Figure 10-42. a) Von Misses Stress for Dead Load (ksi); b) Von Misses Stress for Dead and Live Loads (ksi); c) Load Path on a Girder; d) Critical Regions on Load Path

10.5.5 Shear Reinforcement Effects on Crack Reduction near Beam-end

The beam-end cracking due to combined high shear and flexural stresses near the beam-end can be controlled by providing confinement reinforcement. The confinement reinforcement primarily confines the zones of high axial stress with closed loops. As seen in Figure 10-43, triaxial stress application remarkably increases the strength of the concrete members. Elements under uniaxial loading show lateral deformation due to Poisson's effect. The lateral reinforcement generates passive pressure around the concrete inside the reinforcement by preventing the lateral deformations (Ersoy, 1997). Therefore, core concrete is loaded triaxial instead of uniaxial. Spiral and square hoop lateral confinements are shown in Figure 10-44. The reinforcement geometry and amount used influences the confining pressure supplied. The volume ratio of transverse steel to the volume of concrete member, the strength of the steel used, and reinforcement spacing is directly proportional to the confining pressure and therefore to the concrete strength (Park and Paulay, 1975). Spiral confinement is relatively more effective,

providing higher confinement. As it is seen in Figure 10-44, the section under lateral stress is larger inside the closed loop reinforcement.

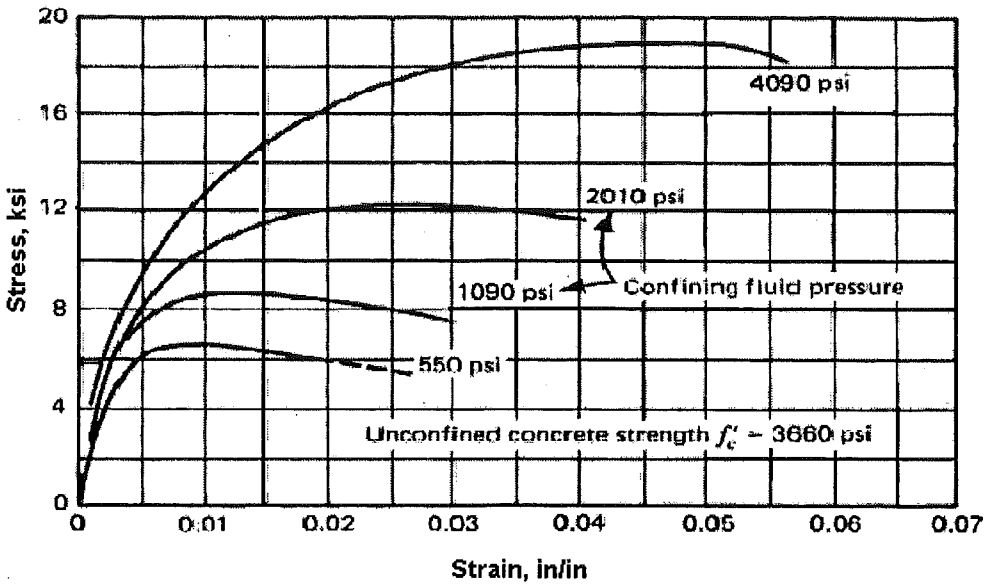

Figure 10-43. Axial Stress-Strain Curves from Triaxial Compression Tests on Concrete Cylinders (Park and Paulay, 1975)

Lateral confinement increases the member strength and provides greater shear capacity. For end stresses within transfer length due to prestressing transfer, if adequate reinforcement is supplied, the shear capacity of the member is improved and the crack width and length is reduced (Sozen, 1965 and Sozen, 1967).

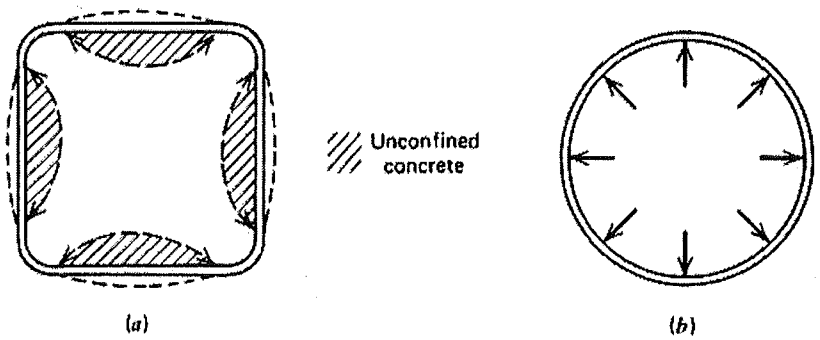

Figure 10-44. Confinement by a) Square Hoops and b) Spiral Hoops (Park and Paulay, 1975)

In the literature and the standards, member-end confinement is recommended as a remedy for bursting cracking. Vertical (lateral) reinforcement recommended for end stresses at transfer by PCI (PCI, 1999) is given in Equation 10-3. Further, the prestressing load effect creates temporary stresses at the time of transfer, and this reinforcement should not be in addition to shear and torsion reinforcement. Although the area needed can be estimated by the equation, the spacing and stirrup geometry is not described.

$$A_{vt} = \frac{0.021 P_o \, h}{f_s \, l_t}$$ **Equation 10-3**

Where
A_{vt} = Area of stirrups required at the end of a girder uniformly distributed over a length h/5 from the end.
f_s = Design stress in stirrups
h = Depth of the member
l_t = Strand transfer length
P_i = Initial prestressing force
P_0 = Prestress force at transfer ($0.9 \cdot P_i$)

Figure 10-45 shows the shear reinforcement used near the end zone of the girder. The shear capacity of Type III girders calculated accordingly is much higher than the maximum shear stress estimated in the discrete girder model. The shear reinforcement recommended by PCI (PCI, 1999) for the PC members under service loading and reinforcement stated in Equation 10-3 by PCI (PCI, 1999) for end zone is calculated. This formulation is not given in AASHTO. It is seen from the design drawings that the shear reinforcement supplied in existing beams is often more than required (see Figure 10-45). However, the shear reinforcements are not closed and they cannot provide the lateral confinement as described earlier. However, these stirrups will increase the shear capacity of the member and perhaps can reduce the crack width and propagation to some extend. The spacing for shear reinforcement specified in the design is 3 inches, which creates significant congestion.

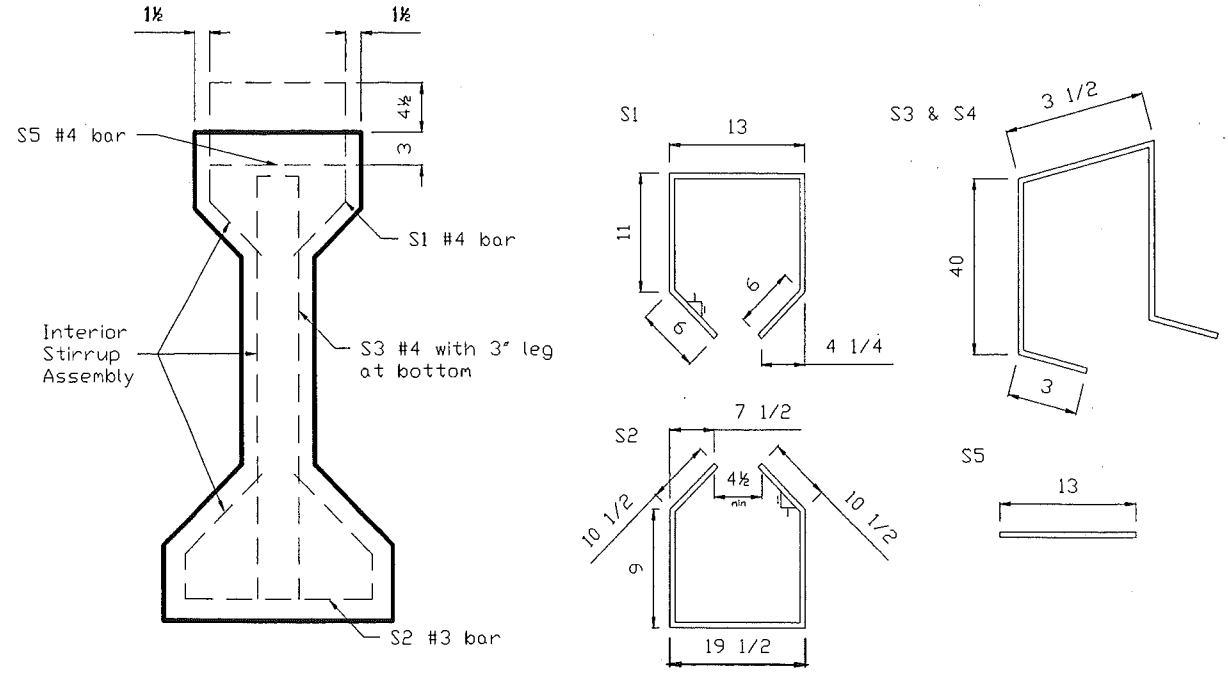

Figure 10-45. Shear Reinforcement used in the Girder Described in the Analytical Model (MDOT PC I-Beam Details)

MDOT Bridge Design Guides (MDOT, 2001) shows that confinement reinforcement is used in newly manufactured girders as seen in Figure 10-46-a, -b, and -c. From these drawings, it is observed that closed hoops are utilized as the shear reinforcement replacing the open hoops used in earlier designs. The purpose for the crack prevention and crack width reduction is noticed from these closed hoop confinement. In the field inspection, it is seen that the girders manufactured according to new shear reinforcement details also show of initial bursting cracking (see Figure 10-46-d). The reason may be concluded that the confinement reinforcement may not be sufficient to eliminate or reduce the width of initial cracks. Earlier studies state that the cracking is due to the transverse stresses in I-girders within the anchorage zone (Sozen, 1965 and Sozen, 1967). Sozen indicates that the reinforcement provided does not prevent cracking. The reinforcement provided becomes effective after the cracking takes place and therefore, confinement reinforcement may only reduce the width and length of cracks. The adequacy of the reinforcement should be studied in detail to assess the confinement effects. The reinforcement analysis is not provided here. The subject may be included as a further research project.

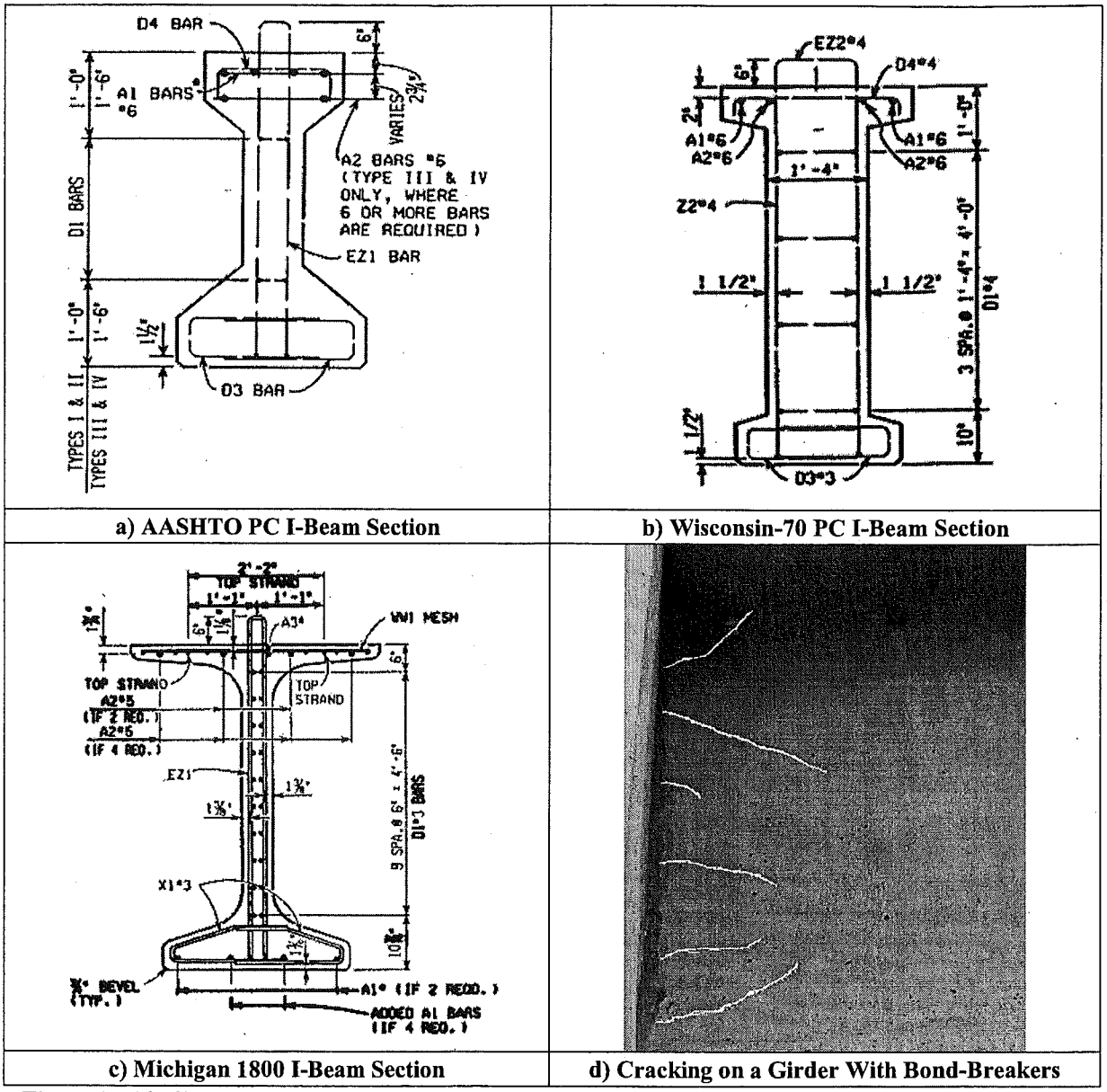

Figure 10-46. Shear Reinforcement used in Newly Manufactured Girders and Web Cracking Observed during Field Inspection on a PC I-Beam with Bond-Breakers

10.6 Modeling and Analysis of a Full Bridge

10.6.1 Overview and the Finite Element Model of a Prestressed Concrete I-Beam Bridge

Concrete diaphragms utilized in the PC I-beam bridges have a typical thickness of 8 inches. The concrete diaphragms have some disadvantages as far as the girder-end inspectability, maintenance performance, and the durability of the girders are concerned. The concrete diaphragms are placed between the girders in such a way that the beam-ends are not visible for the inspectors. The quality of the inspection will be impacted if the beam-ends are difficult to inspect. The beam-ends blocked with concrete diaphragms are also cumbersome to examine for cracking and deterioration.

Another disadvantage of concrete diaphragm is their influence on beam-end maintenance and durability. Concrete diaphragms make the beam-ends inaccessible so that maintenance cannot be performed. Small, inaccessible openings formed by the diaphragms around the beam-end cannot ventilate, hence, moisture accumulates. In some bridges, these also become bird-nesting areas, also affecting durability. Consequently, alternative diaphragm geometries and materials should be explored to replace the standard concrete diaphragms.

The analytical modeling is performed on the bridge with inventory ID S04 of 06111, also described in the discrete girder analysis. The three-span bridge has exterior spans of 31 feet 3 inches in length and a mid-span of 49 feet in length. The bridge deck has a uniform width of 43 feet 2 inches with two lanes. The minimum deck thickness is 8 inches. The drawing in Figure 10-47 shows the general view of the bridge.

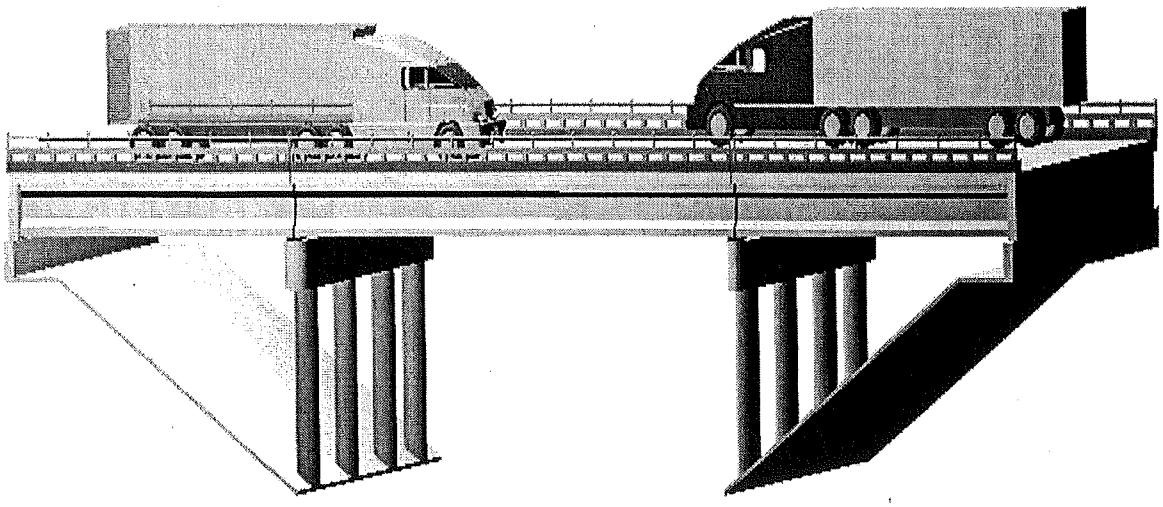

Figure 10-47. Drawing of the PC I-Beam Bridge Modeled

In bridge design, the purpose of diaphragms is to provide the girder with lateral support, and help with live load distribution. The diaphragm types provide different girder constraints due to the differences in cross-sectional geometries and material properties. The diaphragm is modeled with a spring group, each spring representing the shear, bending, and torsional properties. Different diaphragm types seen in the bridge are analyzed independently to calculate their stiffnesses that are incorporated in the model.

The diaphragm types employed between Type-III girders are Type-A on the pier cap as end-diaphragms and Type-G at mid-span as intermediate diaphragms. Between Type-I and Type-III girders, Type-J diaphragms are used. Type-B diaphragms are incorporated between two Type-I girders. All diaphragm types observed on PC I-beam bridges are shown in Appendix-I. Diaphragm and beam arrangement is shown in Figure 10-48. The representation of the girders and diaphragms in the FE model is shown in Figure 10-49. In the figure, the supports are at beam-ends, and the diaphragms are connected to the beams near the beam-end and geometrically aligned with the centerline of the physical diaphragms.

In addition to concrete diaphragms, steel X-bracings are also utilized as diaphragms in the U.S. for reducing the effects of lateral-impact loads from high load hits (HLH). Iowa State University (http://www.ctre.iastate.edu) is carrying out a project on steel-bracing diaphragms for the Iowa Department of Transportation in order to reduce the HLH effects. During HLH with the use of concrete diaphragms, the interior beams are also subjected to significant loads in addition to fascia beams. The approach is to protect the interior beams from the impact loads. Additionally, with steel diaphragms, beams and especially with open beam-ends, better ventilation is developed and conditions are less favorable for bird nesting. It is the consensus of concrete durability researches that, if animal intrusions and moisture effects are minimized, durability improves. In this project, steel diaphragms are being compared and their features are being compared to concrete counterparts for structural effectiveness. It is proposed that the intermediate steel bracing will provide the same efficiency as concrete diaphragms. The general appearance of the X-bracing is shown in Figure 10-50.

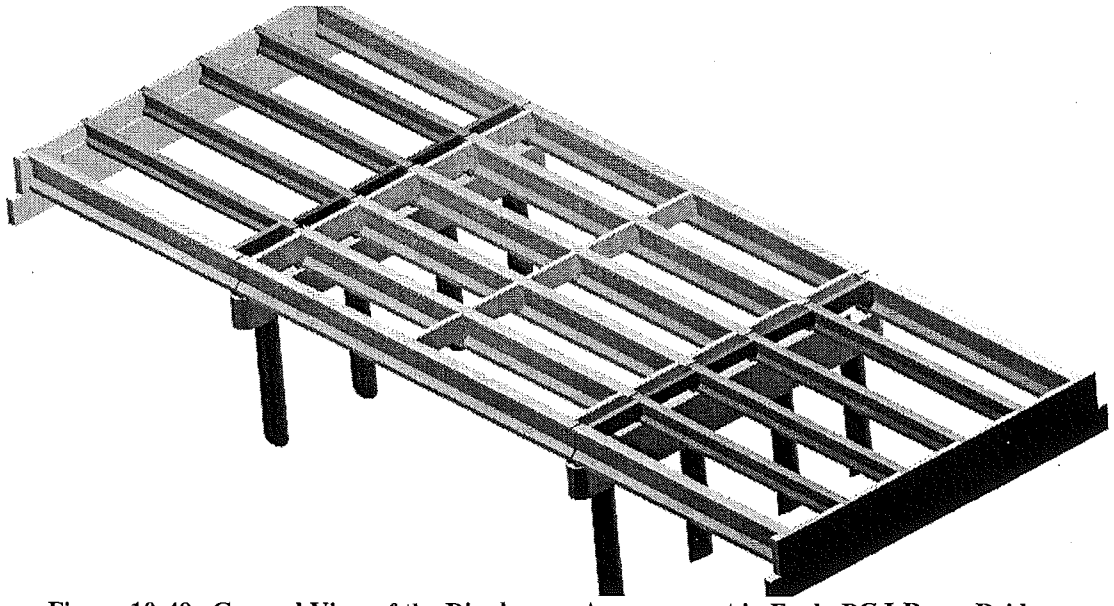

Figure 10-48. General View of the Diaphragm Arrangement in Early PC I-Beam Bridges

The beams are designed as simply supported, and bending moments are assumed to vanish at the supports. However, under service loads due to constraining effects of the diaphragms, bending stresses may generate near the beam-ends. The effect of diaphragm restraint to the beam under bending and torsion is investigated using the FE model.

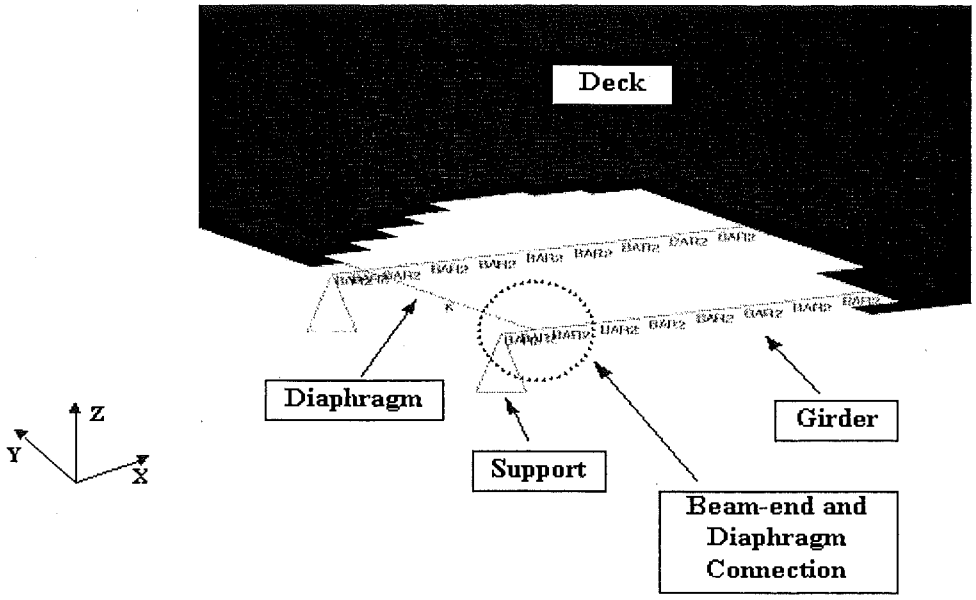

Figure 10-49. Diaphragms, Deck, and Beams in the Model

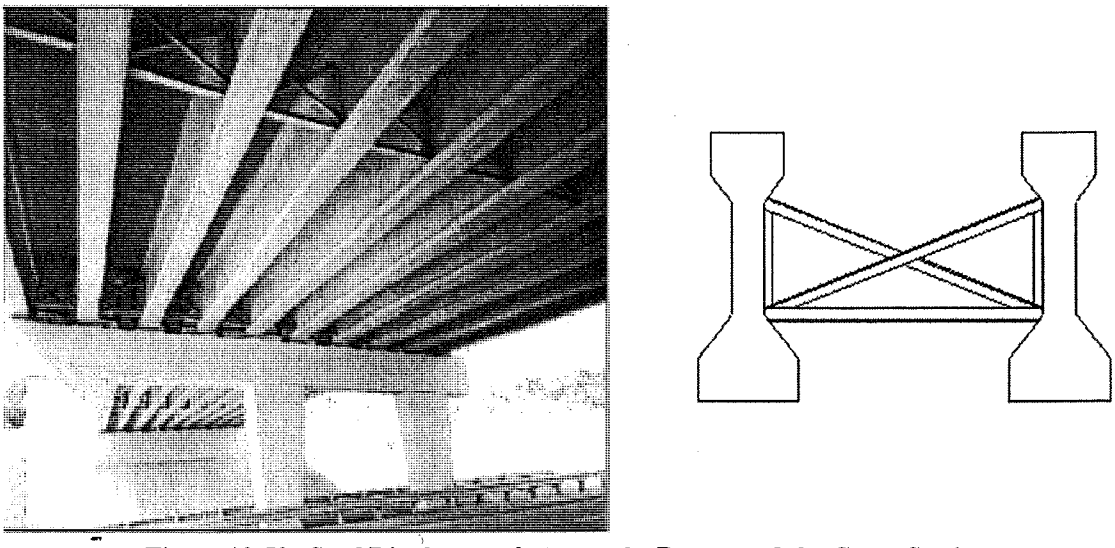

Figure 10-50. Steel Diaphragms between the Beams and the Cross-Section

The behavior of the bridge under temperature effects is also studied to evaluate the impact of non-functional elastomeric bearings. The bearings are assumed as roller supports in design, allowing the beam to bend and move in the axial direction (Yazdani et al, 2000). Deteriorated bearings restrain the beam in the axial direction, creating additional stresses near the beam-end. This restrains the elongation or shortening under temperature effects. Using the FE model, the

behavior of the bridge is investigated with pinned supports in order to simulate the deteriorated bearing condition under differential thermal loads.

The primary assumptions utilized in developing the FE analyses model are:

1. Ideal composite action between diaphragms, deck, and beams is assumed.
2. Secondary stresses due to deformation are ignored.
3. The members are described in their original condition.
4. The analyses are performed in the elastic region, and the material behavior is defined as elastic.

The bridge is modeled in three-dimensional domain using line elements; therefore, the cross-sections of structural members are simplified accordingly. The diaphragms are incorporated as springs, the beams as two dimensional bar elements, and the deck as thin shell. The bridge is modeled with the diaphragm restraining the beam in three directions: shear, bending, and torsion. For shear action axial (K_V), for bending (K_M) and torsion (K_T) rotational springs are employed (see Figure 10-51). The supports and bearings are placed at beam-ends as rollers in longitudinal and transverse directions, but restrained in the vertical direction.

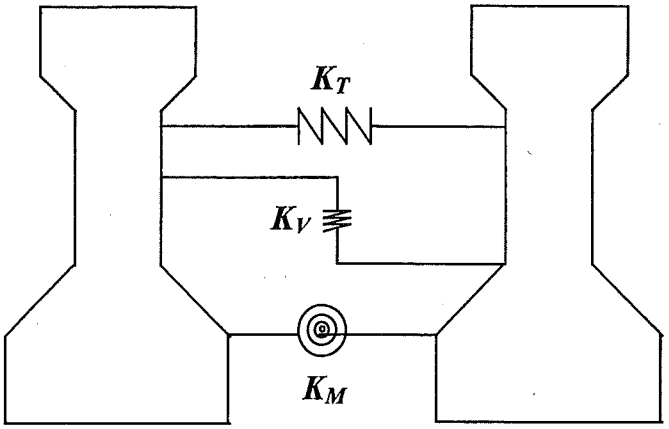

Figure 10-51. The Spring Representation of the Diaphragms

The diaphragm and the deck are sometimes monolithic, and in composite action. In this case, the spring stiffnesses for the diaphragms include the deck. The recommended effective width values are 48 inches by AASHTO and 64 inches by ACI. However, the length of deck on one side of the diaphragm is 10 inches. In that case, it is not possible to consider the diaphragms with the recommended effective width values. The cross-section of the diaphragm is estimated by adding an effective deck width of 10 inches on each side of the diaphragm. The spring stiffnesses representing the various diaphragm configurations are shown in Table 10-2.

The steel bracing can only develop shear stiffness. The shear stiffnesses of bracing with different geometries are given in Table 10-3. The main parameters considered in the stiffness calculations are the cross-section area (A), the modulus of elasticity of the bracing member, the girder spacing (S), and the angle of member inclination with the horizontal axis.

10.6.2 Finite Element Analyses Results of a Prestressed Concrete I-Beam Bridge

10.6.2.1 *The Finite Element Analyses of the Bridge under Dead Loads*

To document the influence of the diaphragms, the bridge is analyzed with and without the diaphragms. The first analysis is performed under dead load including the deck, the barriers, and the beams. In Figure 10-52 and Figure 10-53, bending moments on the interior beams and exterior beams are compared with and without diaphragms. The differences in bending moments are not significant. Effectively, the diaphragms increase the bending moment of the interior beams while reducing the bending moment of the exterior beams. Diaphragm effects are more pronounced when shear diagrams of the interior and the exterior girders are compared in Figure 10-54 and Figure 10-55. Additionally, torsion diagrams of interior and exterior girders are shown in Figure 10-56 and Figure 10-57.

In conclusion, the diaphragms' structural role in the bridge is to provide load distribution between the girders. The diaphragms increase bending moment, shear force, and torsional moment on the exterior girders while decreasing the load effects on the interior girder, thus equalizing the contribution of interior and exterior girders. The increase in shear forces reaching around 2 kips is significant in terms of increasing the cracking potential near the end of the exterior girder with diaphragms as shown in Figure 10-54 and Figure 10-55.

Table 10-2. Diaphragm Types and Equivalent Spring Stifnesses

Diaphragm Type	Diaphragm Type	Flexural Stiffness (K_M=E·I/L) (kips·in)	Shear Stiffness (K_V=G·A/L) (kips/in)	Torsional Stiffness (K_T=G·J/L) (kips·in/rad)
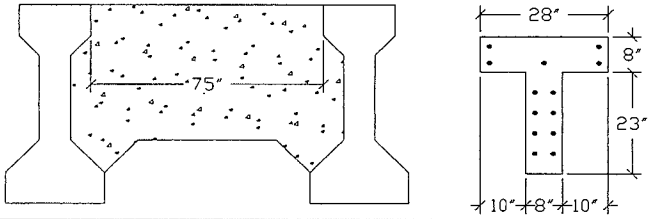	A	1,185,000	4,550	273,000
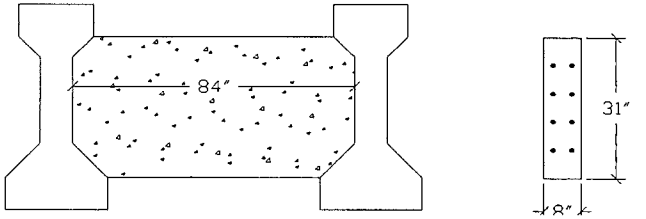	G	280,000	3,380	113,000
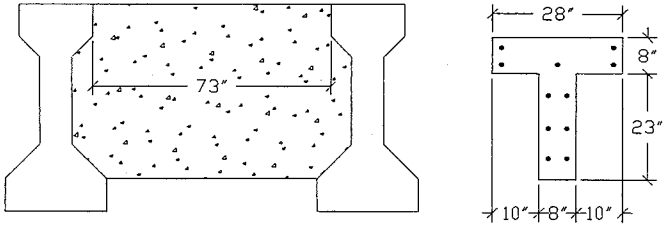	B	465,000	2,860	214,000
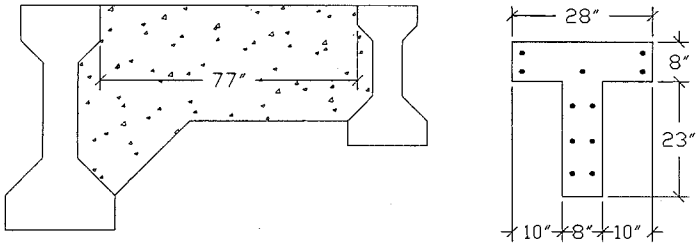	J	1,875,000	2,930	203,000

Table 10-3. Spring Stiffnesses to Represent Steel Diaphragms

Spring Stiffness for the Steel Diaphragms	Shear Stiffness (kips/in)
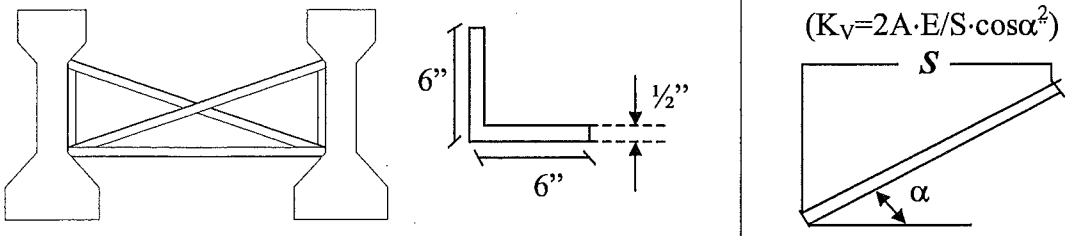	
Between two Type III	3,680
Between Type III and Type I	3,630
Between two Type I	3,880

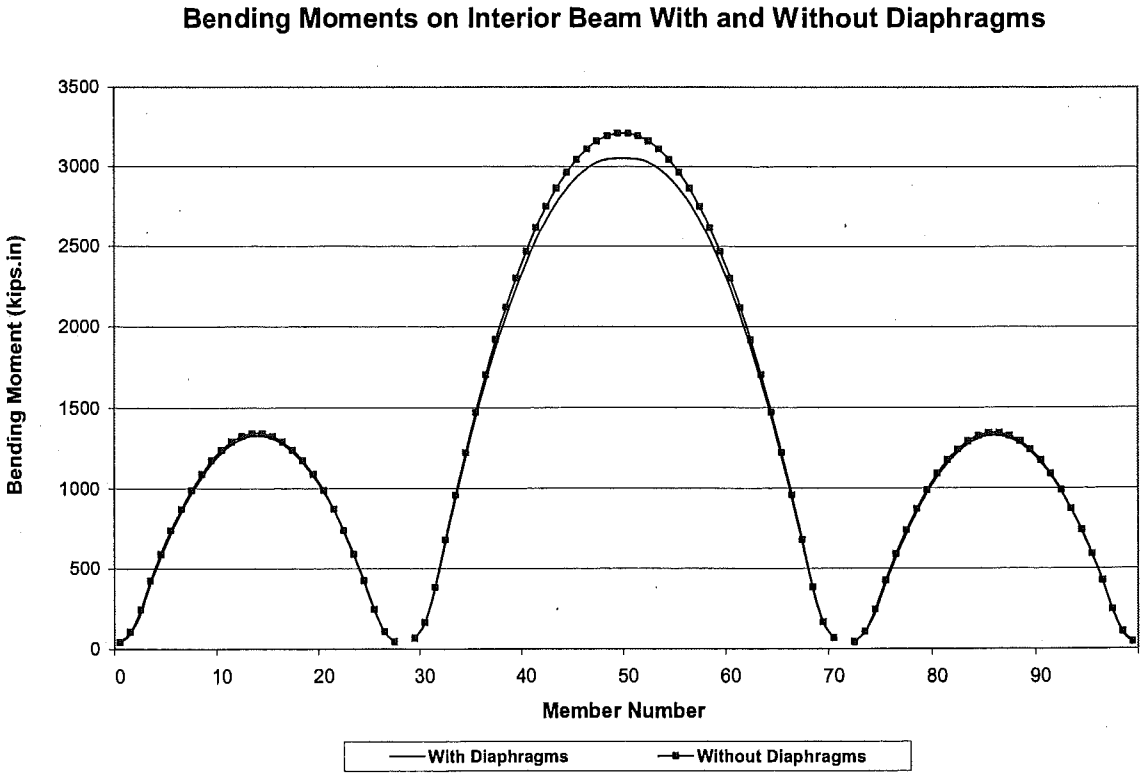

Figure 10-52. Bending Moment Diagram on the Interior Beams with and without Diaphragms

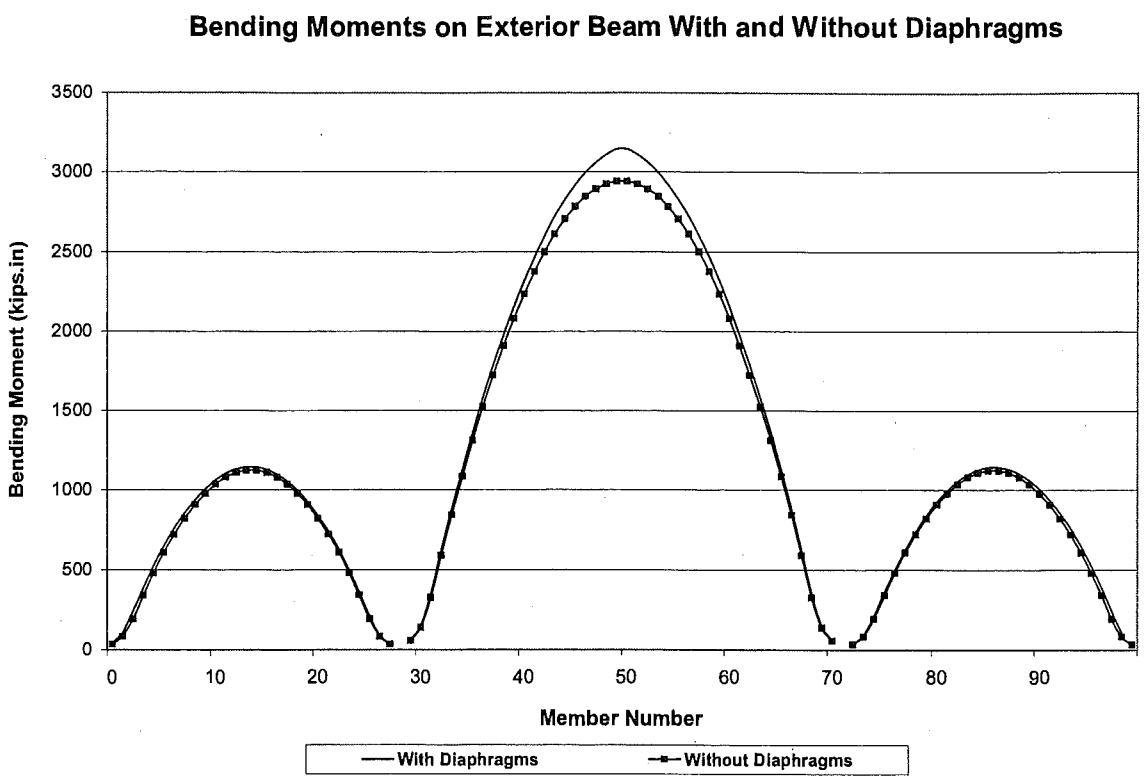

Figure 10-53. Bending Moment Diagram of the Exterior Beams with and without Diaphragms

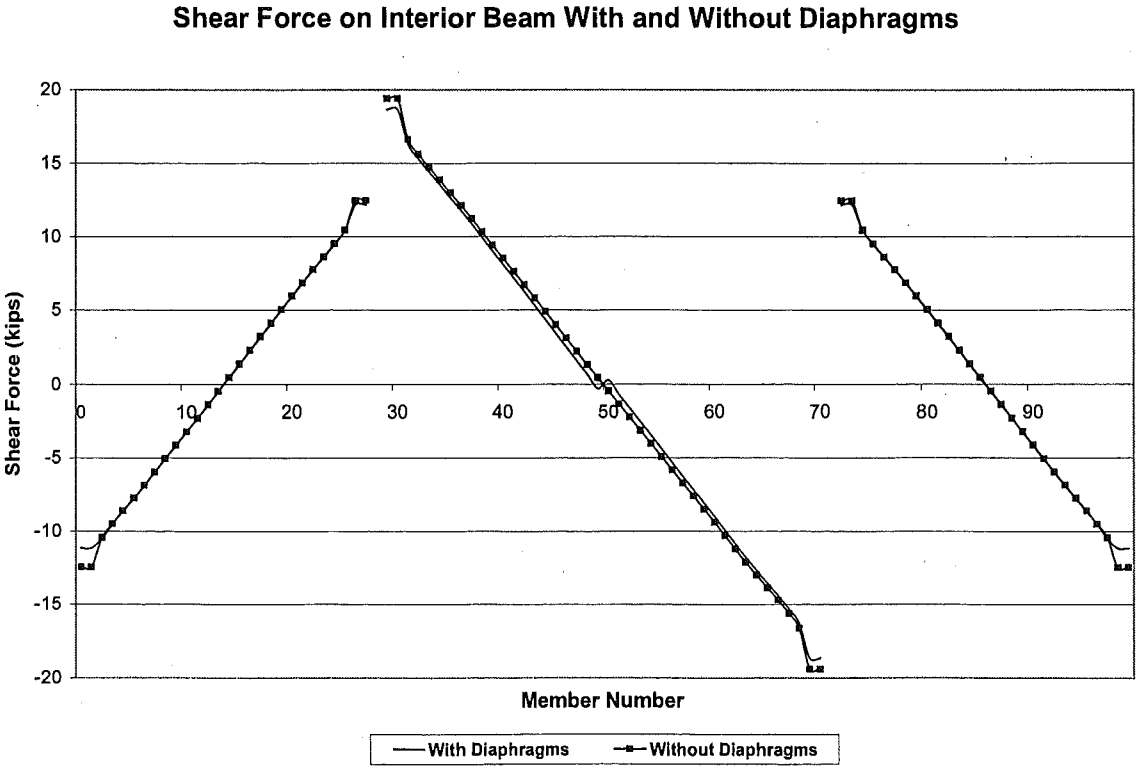

Figure 10-54. Shear Force Diagram of the Interior Beams with and without Diaphragms

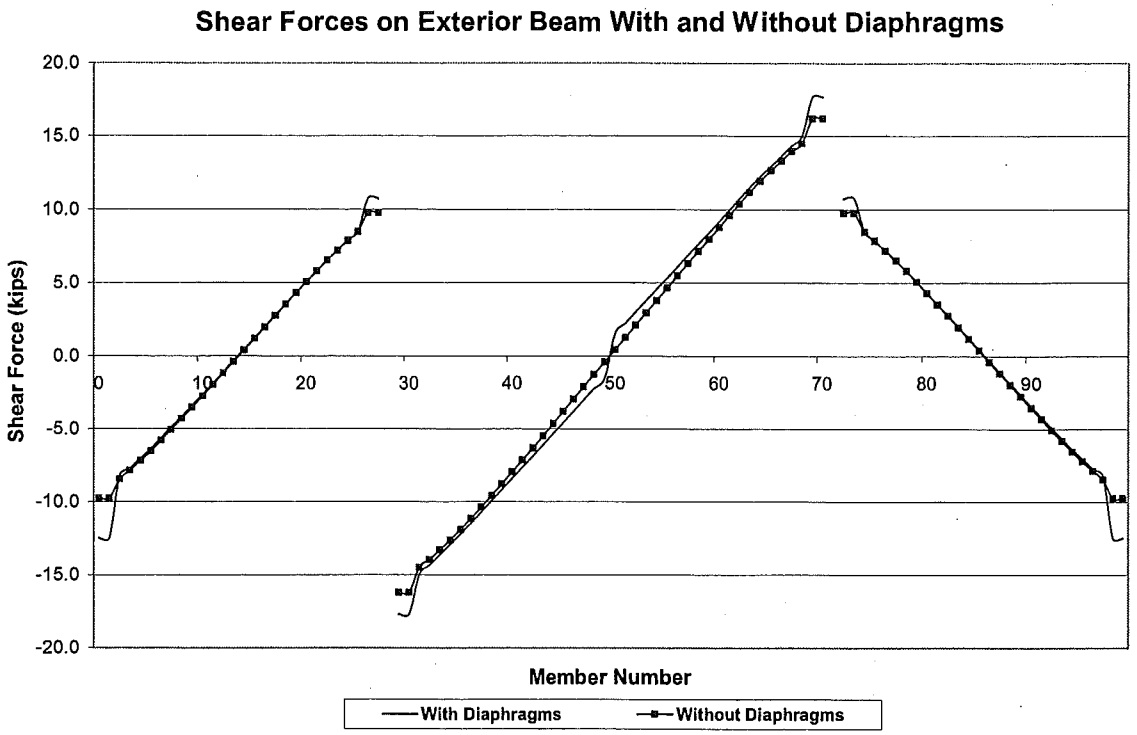

Figure 10-55. Shear Force Diagram of the Exterior Beams with and without Diaphragms

Torsion diagrams shown in Figure 10-56 of the interior girder and in Figure 10-57 of the exterior girder also demonstrate the diaphragm impact on the girders. The torsion observed on the interior girder is lower than on the exterior girder. The load is distributed symmetrically around the interior beam; consequently, torsion magnitudes are lower than those on the exterior beam. The shapes of the torsion diagrams are significantly different on girders with and without diaphragms. However, the magnitude of this difference is not significant.

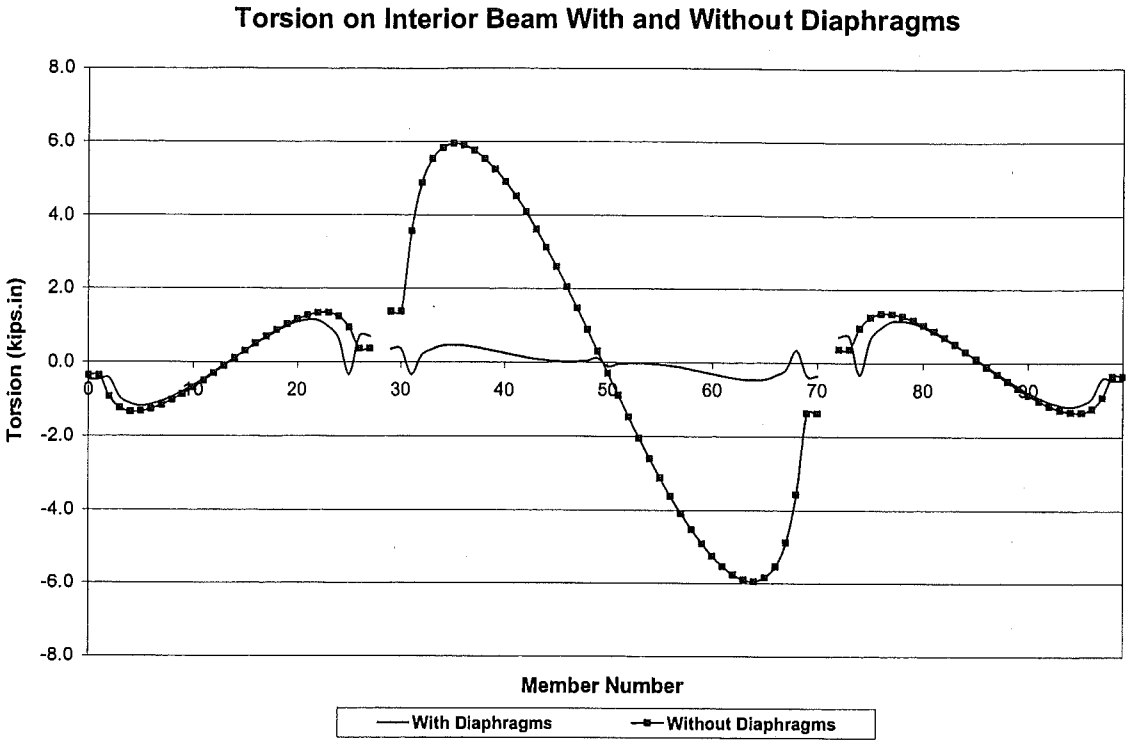

Figure 10-56. Torsion Diagram of the Interior Beams with and without Diaphragms

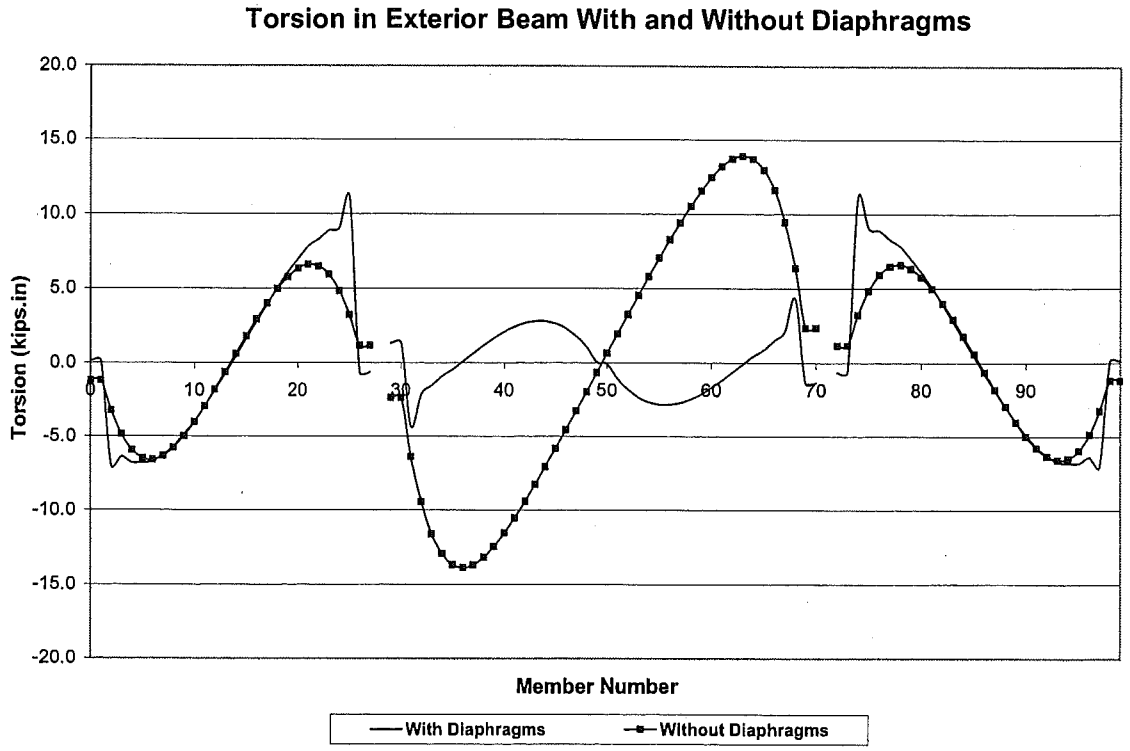

Figure 10-57. Torsion Diagram of the Exterior Beams with and without Diaphragms

10.6.2.2 *The Finite Element Analyses of the Bridge under Dead and Live Loads*

To evaluate the impact of the diaphragms on the exterior and the interior beams under live load, the bridge is analyzed with truck load in addition to dead load. The primary purpose is to evaluate the diaphragm effect on the girder load distribution. Later this analysis is compared to the girder load distribution when steel bracings are utilized instead of the concrete diaphragms. As live load, two trucks are placed on the bridge for maximum moment at the mid-span. The axle spacing used in bridge design is 14 feet according to AASHTO. However, in order not to change the mesh geometry of the deck and the girders, the axle spacing is altered to 13 feet 7 inches and 14 feet 4 inches to fit to the existing finite element mesh. The general orientation of the trucks on the FE model is shown in Figure 10-58 through Figure 10-60. Both trucks are located within a width of two lanes. The lateral spacing between the trucks is taken as 4 feet, as shown in Figure 10-59.

The analyses results are shown in Figure 10-61 through Figure 10-69. In these figures, the origin designated as "Member Number" axes is the beam-end on the abutment. The last point on the "Member Number" axes is the beam-end at the pier.

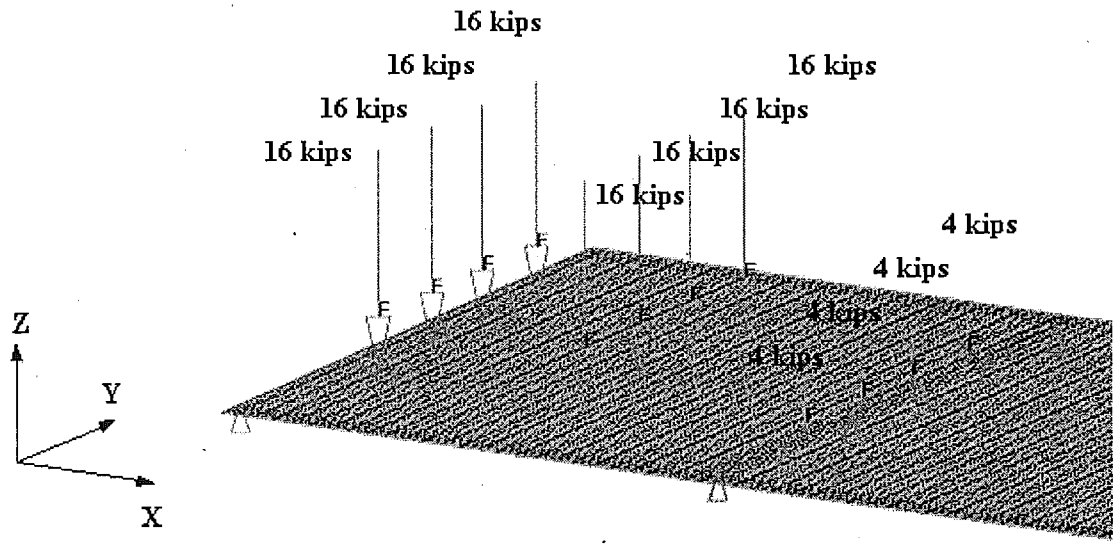

Figure 10-58. General View of Truck Load Distribution

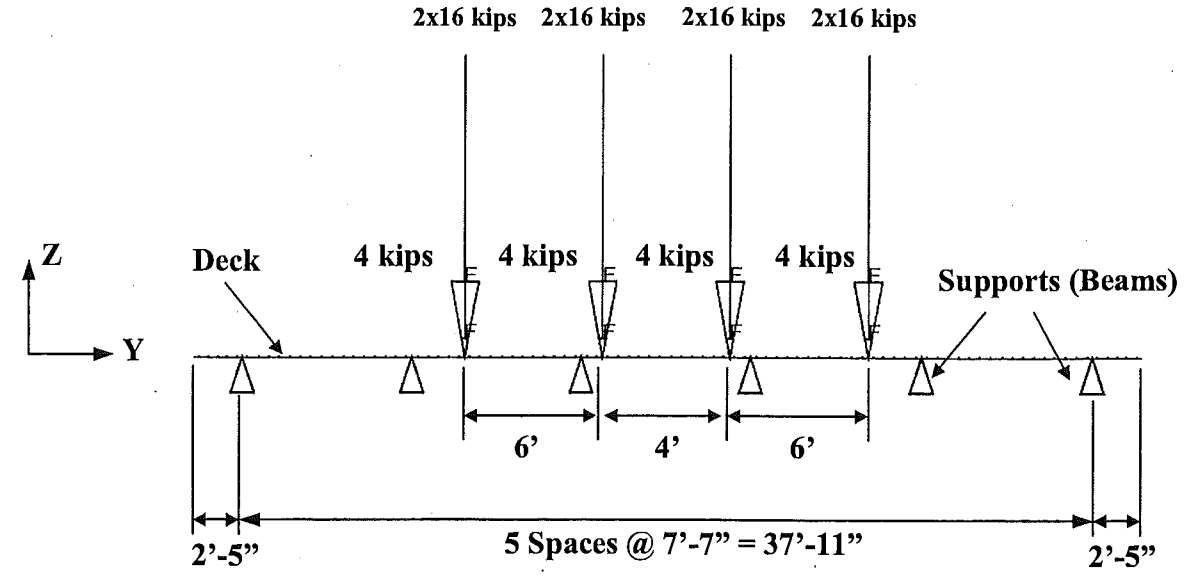

Figure 10-59. Transversal View of the Truck Load Distribution

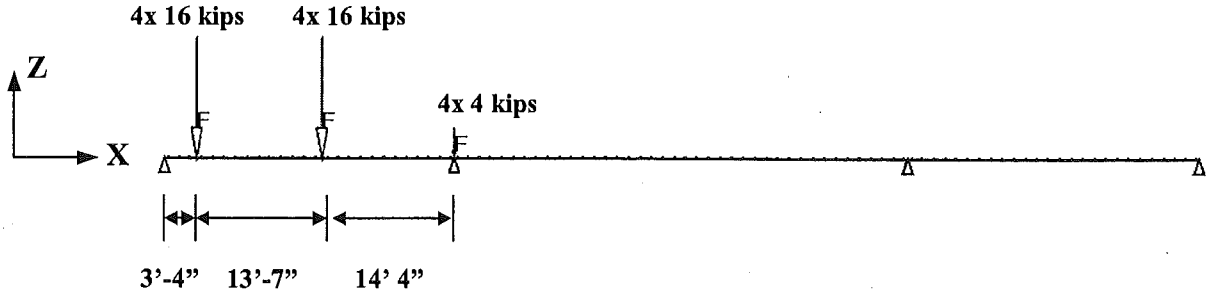

Figure 10-60. Longitudinal View of the Truck Load Distribution

The shear force diagram on one exterior and one interior beam on one of the exterior spans is shown in Figure 10-61. Shear force distribution on girders is affected by the truck axle locations. However, a dramatic difference is seen when the shear distributions on interior and exterior girders are compared. On both interior and exterior beams, the diaphragm effects on shear force are seen near the beam-ends. As seen in Figure 10-61, the diaphragms redistribute the shear force near the beam-ends by distributing the load. Consequently, the diaphragms increase the shear force on exterior girders, especially around 20 kips near the abutment where a Type A diaphragm is located. Another essential outcome of the analysis is the structural behavior difference observed at two ends of the girders due to differences in diaphragms with different shear stiffnesses. The diaphragms at the abutment are stiffer than the ones near the piers. Consequently, the diaphragm effect on the beam-end stresses is proportional to the diaphragm shear stiffness.

The bending moment diagrams for exterior and interior girders are shown in Figure 10-62. The diaphragm effect on moment transfer is negligible near the beam-ends.

The diaphragms influence the torsional moments near the beam-ends. The torsion diagrams for interior and exterior girders are shown in Figure 10-63. Increasing bending stiffness of the diaphragm reduces the torsional stresses near beam-ends. This is seen in Figure 10-63 when

torsion on interior and exterior girders is compared at both beam-ends. The torsion on girders is equal at the abutment end and diverges at the pier end. The load is distributed symmetrically around the interior beam; consequently, torsion magnitudes are lower than those on the exterior beam, as shown in Figure 10-63.

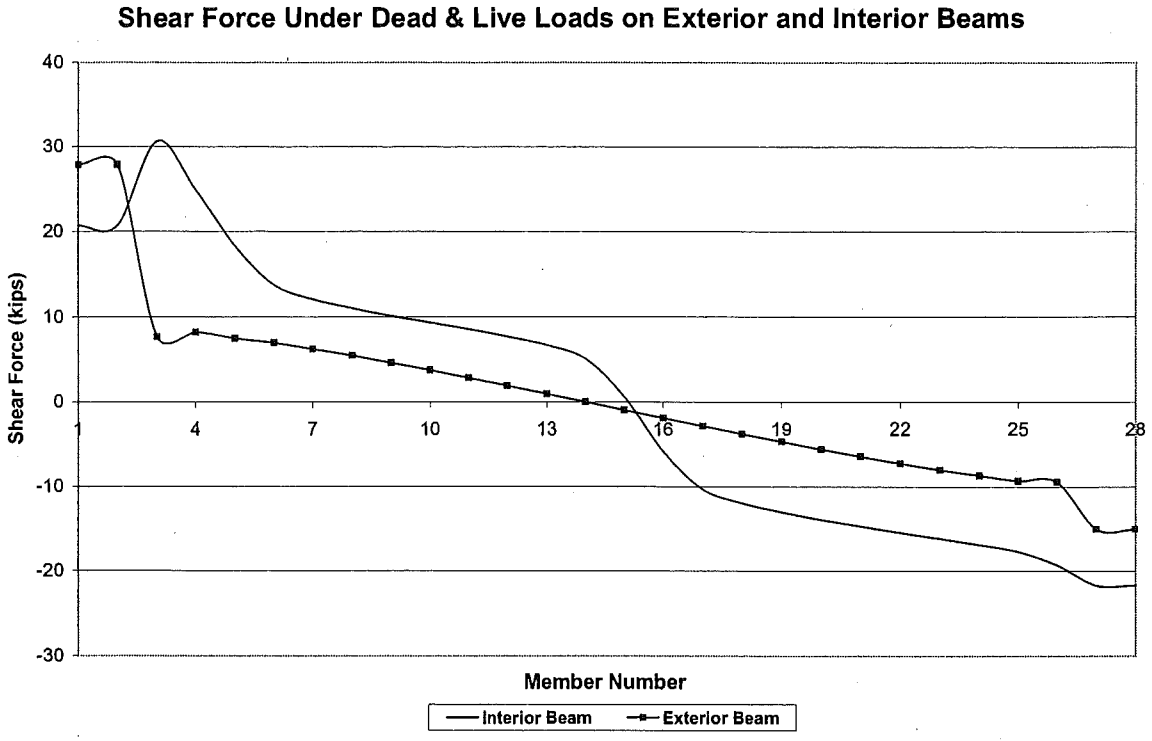

Figure 10-61. Starting from Abutment, Shear Force under Dead and Live Loads on Exterior and Interior Beams

The load distribution factor for the live load according to AASHTO is compared to the live load analysis. Distribution factor by AASHTO is calculated from the formula $DF = S/5.5$ for a PC I-beam bridge, where DF is the distribution factor, S is the girder spacing in feet, and 5.5 is a constant. Center to center girder spacing is 91 inches (7 feet 7 inches) giving a distribution factor of 1.38. From the shear diagram in Figure 10-61 for the interior beam, the distribution factor is calculated as approximately 0.50 for the beam-end at the abutment, and approximately 0.85 for the beam-end at the pier. These distribution factors correspond to a distribution factor of S/15.2 at the abutment end and S/9.1 at the pier end. The diaphragm stiffnesses at each beam-end are different; thus, corresponding distribution factors also differ. The distribution factor formulations for the interior girder is not comparable to the factors used in design. However, it demonstrates the diaphragm stiffness influence on the load distribution to the girders. In addition, a constant distribution factor is not realistic for obtaining the girder moments and shears.

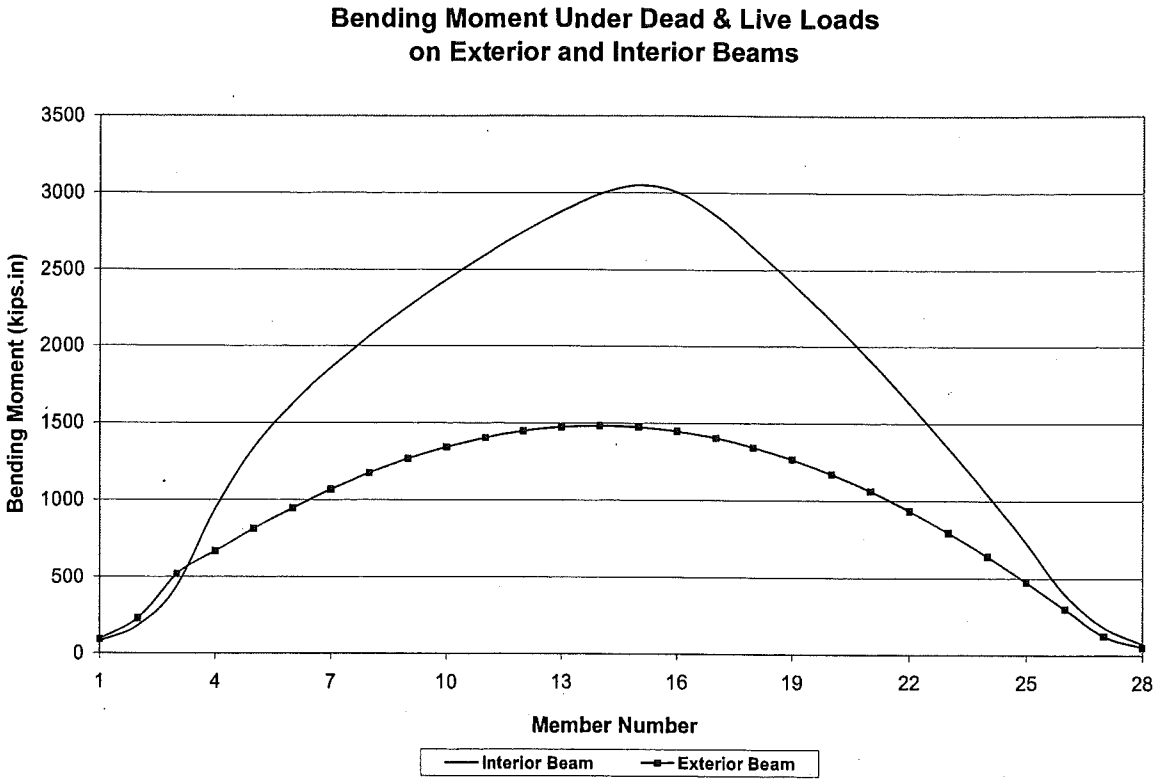

Figure 10-62. Starting from Abutment, Bending Moment under Dead and Live Loads on Exterior and Interior Beams

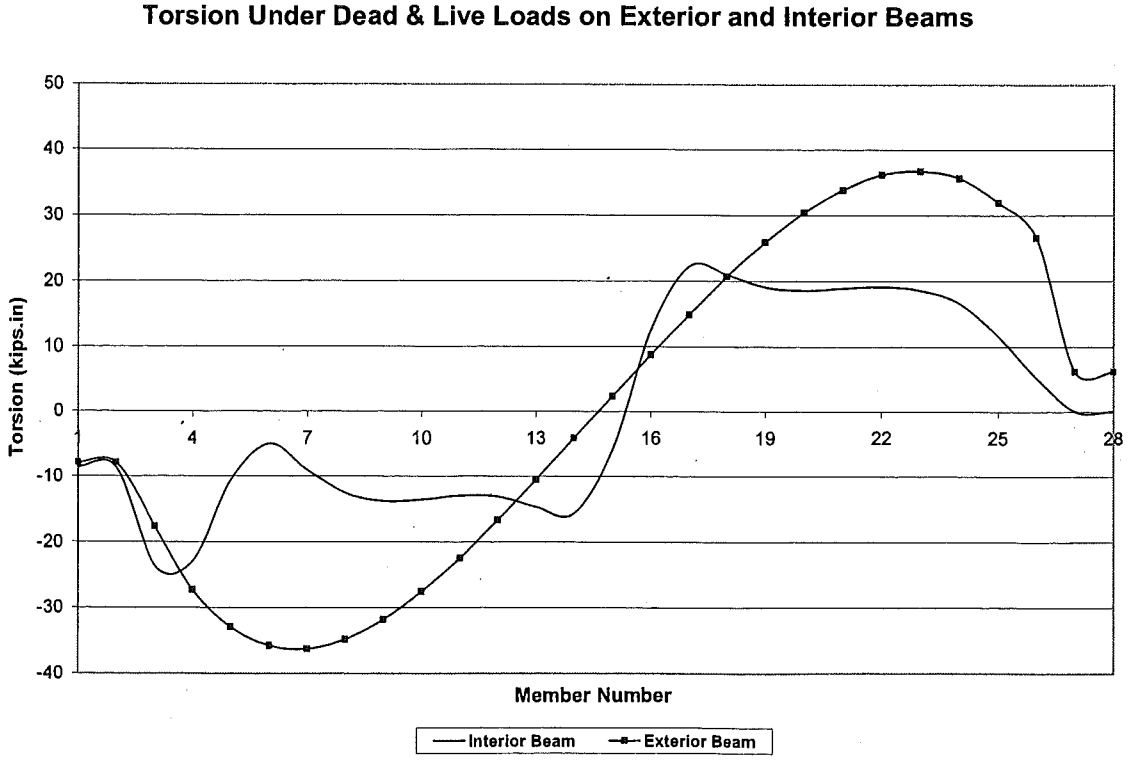

Figure 10-63. Starting from Abutment, Torsion under Dead and Live Loads on Interior and Exterior Beams

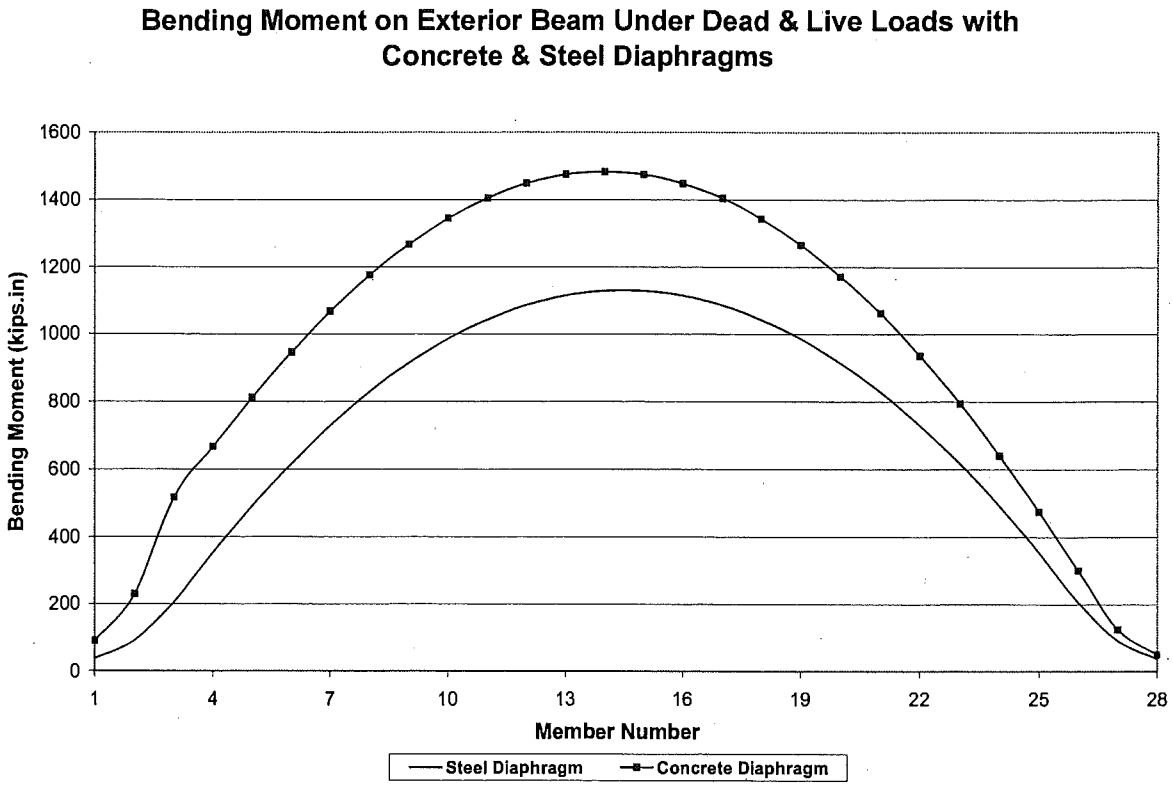

Figure 10-64. Starting from Abutment, Bending Moment on Exterior Beam under Dead and Live Loads with Concrete and Steel Diaphragms

10.6.2.3 *The Finite Element Analyses of the Bridge with Steel Bracings*

In order to evaluate the steel bracing as diaphragms, the bridge is further analyzed under dead and live loads after modifying the diaphragm stiffnesses. Bending and torsional stiffnesses of the steel bracings are zero, while its shear stiffness is higher than the concrete diaphragms (see Table 10-3). The bending moment diagrams for exterior and interior girders are shown in Figure 10-64 and Figure 10-65, respectively. These figures compare the influences of steel and concrete diaphragms on the girders. The material and the geometry influence on the bending moment magnitudes are negligible near the beam-ends. In other words, steel bracings do not change the bending moments at the beam-ends.

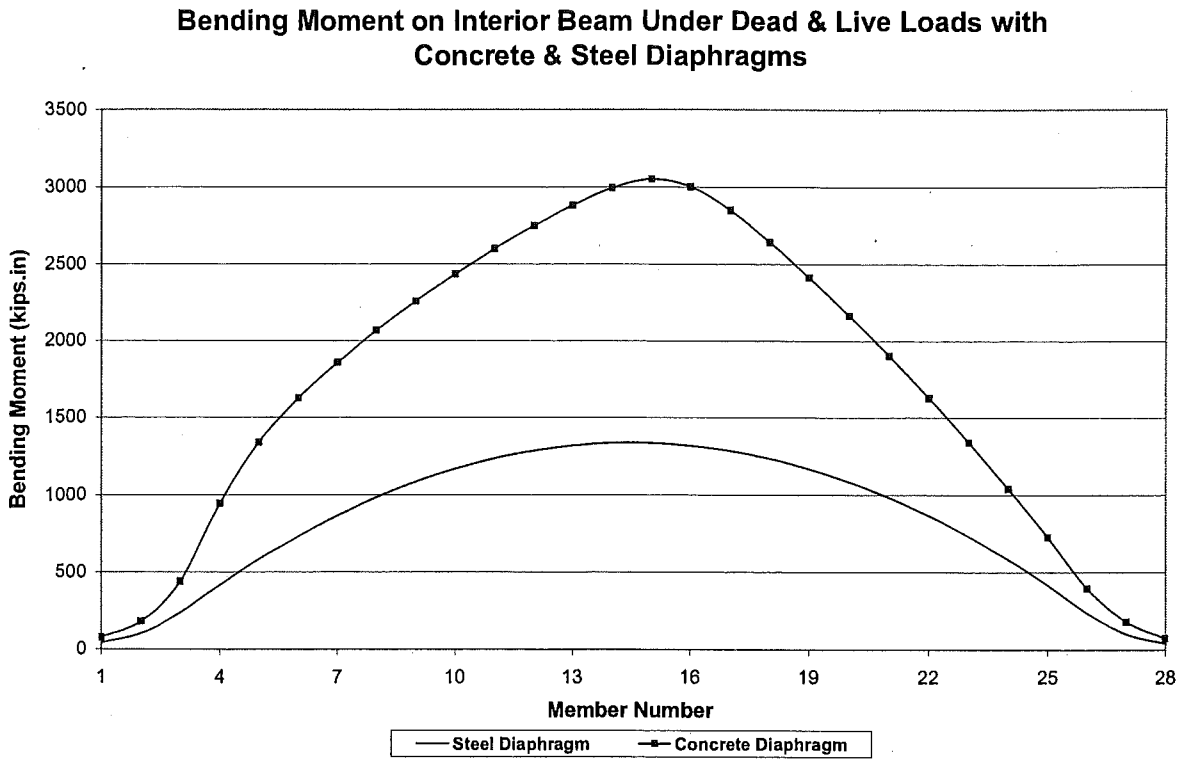

Figure 10-65. Starting from Abutment, Bending Moment on Interior Beam under Dead and Live Loads with Concrete and Steel Diaphragms

The torsion diagrams on exterior and interior girders are shown in Figure 10-66 and Figure 10-67, respectively. The figures show that the torsion on the girders with steel bracings is remarkably less than on the girders with concrete diaphragms. The magnitudes of torsion on both girders are not high; around 10 kips-in near the beam-end and 38 kips-in within the span on the girder with concrete diaphragms. The torsion on the girder vanishes when steel bracings are utilized as diaphragms. As observed in analyses results presented earlier, the diaphragm stiffness controls the load distribution near the beam-ends.

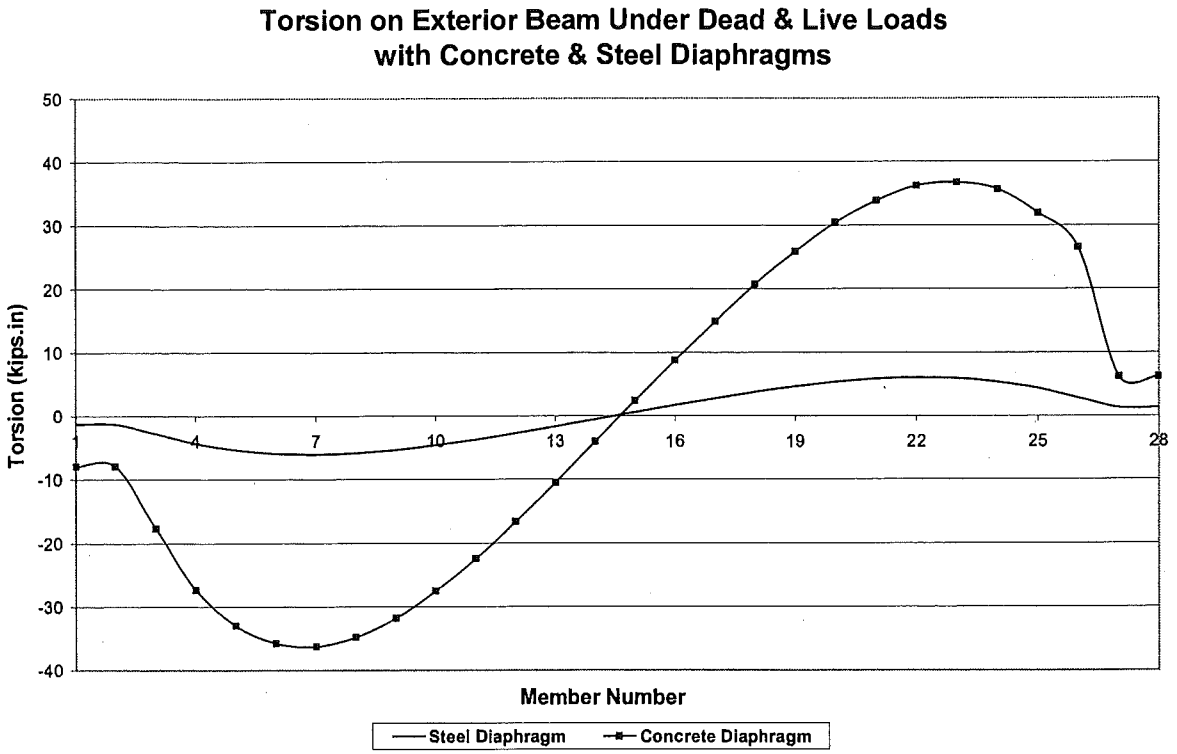

Figure 10-66. Starting from Abutment, Torsion on Exterior Beam under Dead and Live Loads with Concrete and Steel Diaphragms

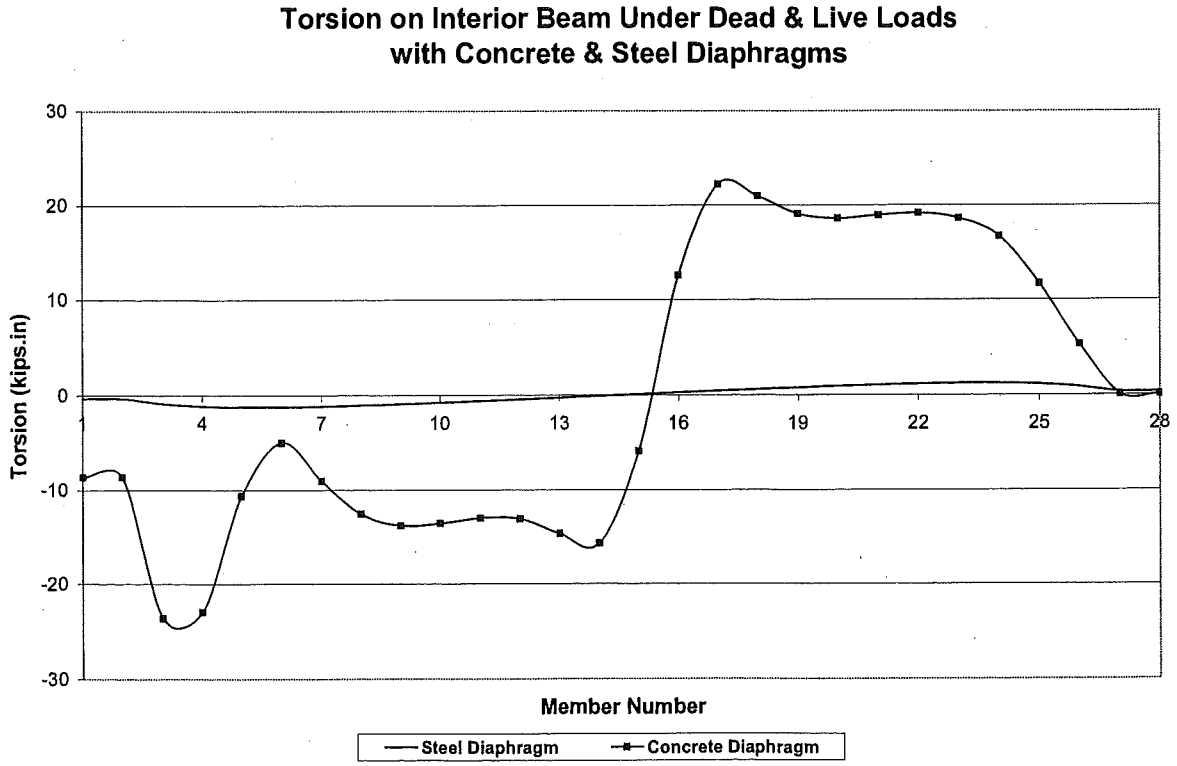

Figure 10-67. Starting from Abutment, Torsion on Interior Beam under Dead and Live Loads with Concrete and Steel Diaphragms

The shear force diagrams shown in Figure 10-68 on the exterior girder and in Figure 10-69 on the interior girder are used for comparing the steel bracings with concrete diaphragms. As seen in the figures, the beams have equal shears at the abutment and pier ends when steel diaphragms are used. The differential restraining effects of the diaphragms at the abutment and pier ends influence the internal force distribution when concrete diaphragms are used.

Use of steel diaphragms provides a uniform shear distribution among the girders as shown in Figure 10-68 and Figure 10-69. It should also be noted that lower values of shear force are calculated at the beam-ends when laterally supported with steel diaphragms. This will also positively impact by reducing the beam-end cracking potential.

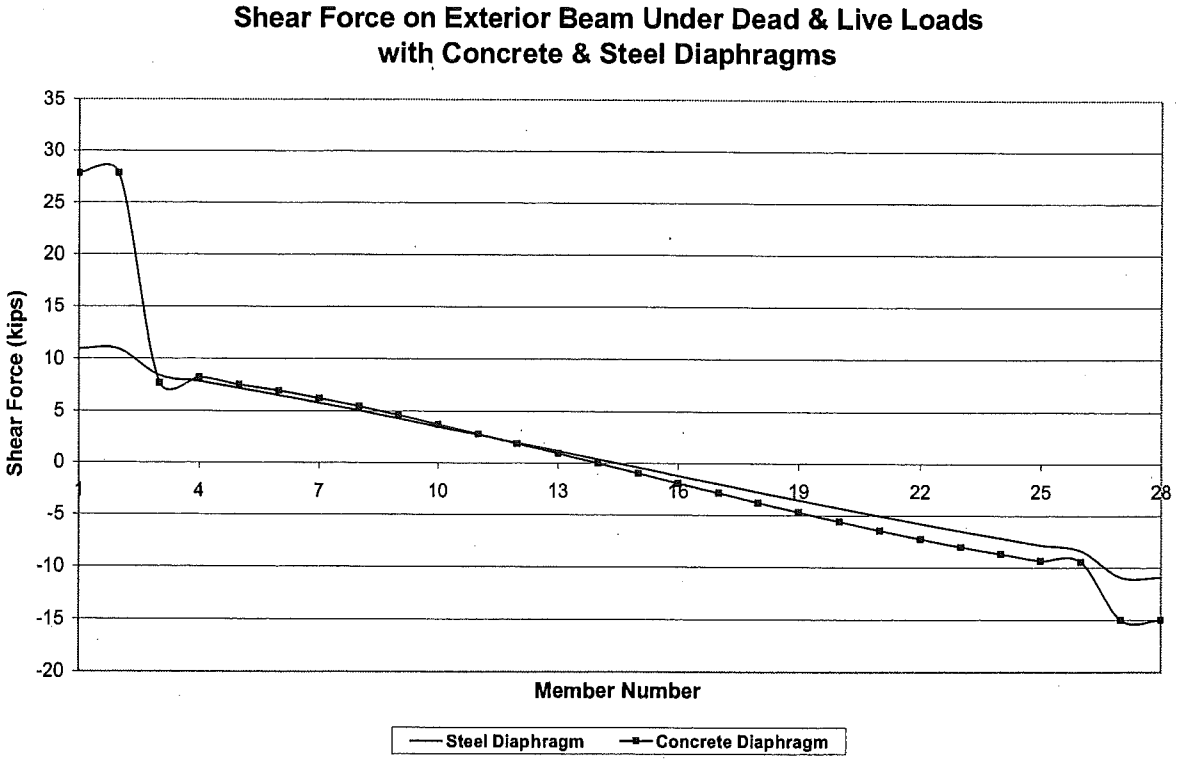

Figure 10-68. Starting from Abutment, Shear Force on Exterior Beam under Dead and Live Loads with Concrete and Steel Diaphragms

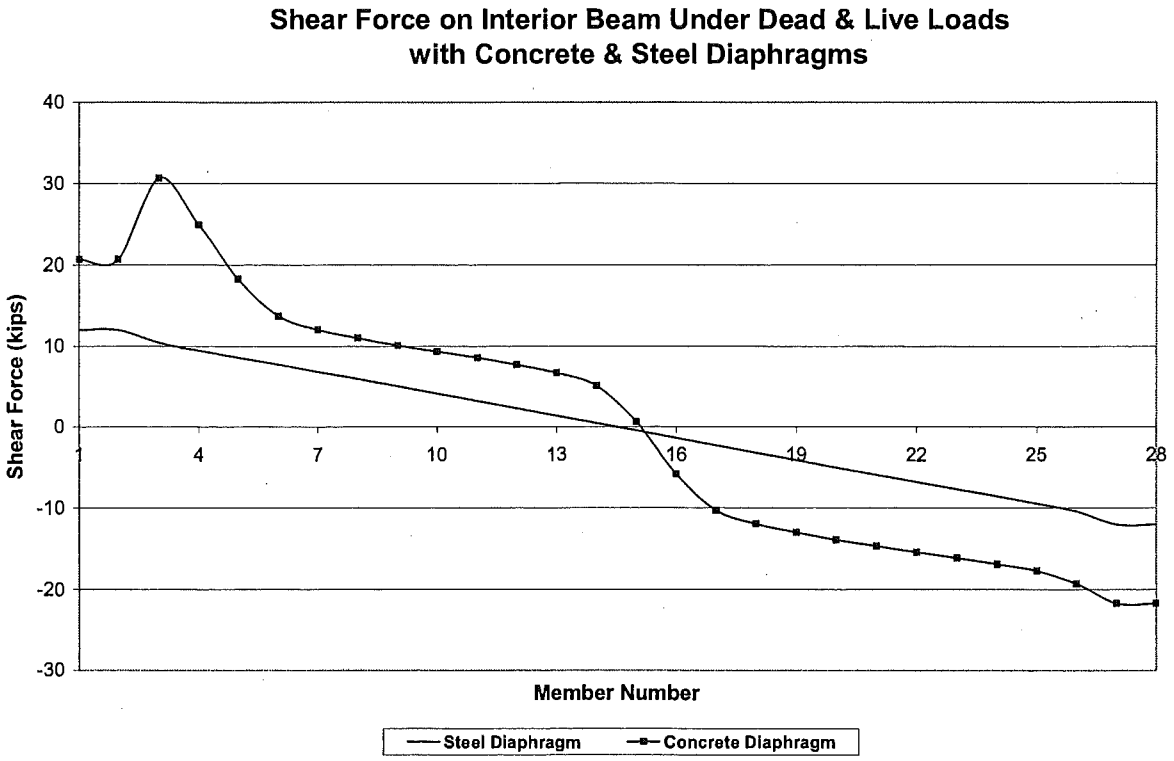

Figure 10-69. Starting from Abutment, Shear Force on Interior Beam under Dead and Live Loads with Concrete and Steel Diaphragms

The bridge model with concrete diaphragms is also analyzed under differential temperature effects. The hypothesis was that the differential temperature between the deck and the girder along on fascia beam would generate measurable stresses on the girders within the proximity of the diaphragms. These thermal stresses would be generated, because the diaphragms constraint the deformation of the girders. In the bridge model, non-functional bearings are also incorporated assuming that this will amplify the thermal effects. However, upon the analyses the stresses due to thermal effects are calculated to be insignificant. For this reason, the analysis results are not included here.

10.7 Summary

The finite element analyses are performed to evaluate the stresses near the beam-end, and to understand the structural behavior of a PC I-beam bridge. The analyses are performed for discrete I-beam analyses and complete bridge analyses under various load conditions.

A PC I-beam is modeled, and the distress in the transfer length region is investigated. The stresses near the beam-end and its impact on the cracking pattern are studied. Three types of I-beams with different tendon geometries are examined and compared (beams with straight tendons, with bond-breakers, and with draped tendons). The I-beams with straight tendons are also analyzed under varying bond quality between the tendon and concrete for the purposes of

evaluating the effects on stresses generating near the beam-end. The beams are representative of those used in existing bridges in Michigan.

The shear stresses observed in the prestressing load transfer region and this stress formation are compared for the three tendon configurations. Significance of high stress concentration near the beam-end is also evaluated. Overall, the analysis shows that the beams with draped tendons are more vulnerable to cracking due to end-block use and the tendon angle. The beams with bond-breakers are the least vulnerable to end cracking. The impact of the bond quality of concrete on the load transfer length and the stress pattern near the beam-end showed that good quality bond reduces the transfer length, and with poor bond quality, the elastic loss and shear stresses are increased.

The beam with straight tendons is further analyzed under service loads, to estimate the bearing effect and the load path near the beam-end. Significantly high stresses are calculated near the supports when the elastomeric bearing pads are non-functional.

A PC I-beam bridge is modeled and analyzed to evaluate the impact of the diaphragm and the deck on the beam-end stresses. The load distribution among the girders is also studied when the bridge is under combined dead and live loads. The analyses showed that the restraining effect of the diaphragms on the beam-ends is significant, which increased the shear and torsional stresses. The increase in stress is directly proportional to the stiffness of the employed diaphragms, which also can be different at each end of the beam. The steel bracing use as a lateral support is compared to the concrete diaphragms. The shear restraining effect of the steel bracing is more significant, but a more uniform shear force distribution among girders is obtained.

Finally, differential thermal effects are analyzed combined with the non-functional elastomeric bearing pads, and the effects on the beam-end stresses are found to be insignificant.

The analyses results are summarized first for the single girder analysis. The PC I-beam and load transfer induced stresses at PC I-beam ends are presented. The analytical modeling included three girder types and three bond qualities. The stresses were calculated for the load effects during manufacturing and under service loads. The shear and axial stresses near the beam-ends are presented in Table 10-4 and Table 10-5. The results in the tables clearly demonstrate that beam-end cracking is to be expected.

Full bridge is modeled and analyzed under dead load, live load, and thermal effects. Composite action between bridge members and the impact of diaphragm rigidity on beam-end forces are investigated.

The forces near the beam-ends from the full bridge analysis are shown in Table 10-6. The table is organized according to loads, diaphragm types, and force locations. The results are grouped under locations along the beam defined as outside the diaphragm (OD) and inside the diaphragm (ID) to show the diaphragm influence on the beam-end forces. The analyses results are presented only for the first span and the middle span. The beam-end forces are also shown in Table 10-6 for the exterior (fascia) and the interior girder.

Table 10-4. Stresses in Girders under Prestressing Load Only

Girder Type Tendons		Maximum Shear Stress (ksi)	Axial Stress (ksi)	
			Compression	Tension
Straight (Uniform) Tendon		0.8	3.0	0.4
Draped Tendon		1.5	3.2	$>f_{ct}$
Bond-breakers	With Bond-breakers	3.0	5.4	$>f_{ct}$ (424 psi)
	Without Bond-breakers	4.0	$>>f_c'$ (5,000 psi)	$>f_{ct}$ (424 psi)

Table 10-5. Bearing Analysis on the Beam with Uniform Tendons

Loading Case	Maximum Shear Stress (ksi)	Axial Stress (ksi)	
		Compression	Tension
Under Prestressing Load	0.8	3.0	0.4
Under Dead Load	2.0	$>>f_c'$ (5,000 psi)	$>f_{ct}$(424 psi)
Under Live Load	3.4	5.2	$>f_{ct}$ (424 psi)

The major conclusions derived from the analytical study are as follows:

1. High shear stress intensity is calculated near the beam-ends upon tendon release.
2. High tensile stresses are formed at the web near the beam-end upon tendon release.
3. High shear and tensile stresses will initiate cracks on the web and near the web transition to the bottom flange upon tendon release.
4. The shear reinforcement provided in the girders will not prevent end bursting and shear cracking. Shear confinement only controls the width and progression of the cracks. For the durability beam-ends should protected by external means such as coating and sealants.
5. End blocks and draping employed in draped beams increase the cracking vulnerability near the beam-ends by amplifying the shear stresses.
6. Bond-breakers decrease the shear stresses within transfer length induced by prestressing load transfer. Thus, they reduce shear stress intensity and cracking potential.
7. The bearing condition directly affects the load path and stress pattern near the beam-ends with non-functional bearings; the support area reduction by rocking of the bearing plate generates high stresses near the support.
8. Replacement of non-functional bearings should be included in the preventive maintenance program.
9. In full bridge analysis for girder design, the boundary conditions must include the restraining effect of the diaphragms on the beam-ends.
10. The steel bracing will be an effective replacement for concrete diaphragms.

Table 10-6. Full Bridge Analysis Results near the Beam-ends

Without Diaphragms			With Diaphragms						Steel Bracing						Loading			
Dead Load			Dead Load			Live Load			Dead Load			Live Load						
V (k)	M (in-k)	T (in-k)	V (k)	M (in-k)	T (in-k)	V (k)	M (in-k)	T (in-k)	V (k)	M (in-k)	T (in-k)	V (k)	M (in-k)	T (in-k)				
10	82	1	12	105	0	28	230	8	11	92	1	17	142	10	ID	A	Exterior	First Span Beams
8	193	3	8	242	7	8	518	18	8	206	3	9	282	26	OD			
8	193	3	8	211	11	9	301	27	8	206	3	9	275	23	OD	P		
10	82	1	11	91	1	15	126	6	11	92	1	16	136	9	ID			
12	106	0	11	95	0	21	181	9	12	102	0	30	253	10	ID	A	Interior	
10	243	1	11	221	0	31	440	24	10	238	1	30	625	26	OD			
10	243	1	10	237	0	19	397	5	10	238	1	20	413	5	OD	P		
12	106	0	12	103	1	22	182	0	12	102	0	21	172	1	ID			
16	137	2	18	150	1	NA	NA	NA	18	149	0	NA	NA	NA	ID	P	Exterior	Middle Span Beams
14	326	6	15	352	4	NA	NA	NA	15	347	1	NA	NA	NA	OD			
19	164	1	19	158	0	NA	NA	NA	19	158	0	NA	NA	NA	ID	P	Interior	
17	383	4	16	370	0	NA	NA	NA	16	372	0	NA	NA	NA	OD			

A: Abutment end
ID: Inside of Diaphragm (Span Side)
OD: Outside of Diaphragm (Beam-end Side)
M: Moment
NA: Not Available
P: Pier-cap end
T: Torsion
V: Shear Force

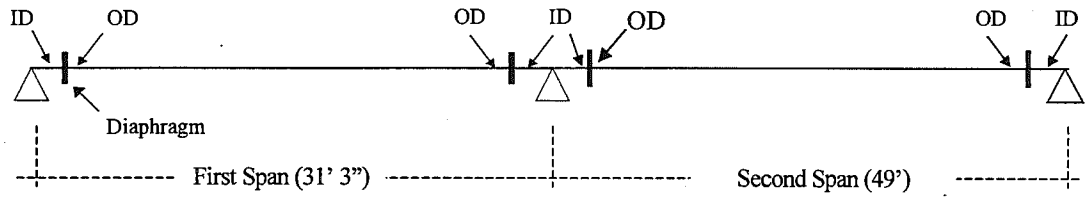

11.0 Performance Evaluation of Partial Depth Repair Materials (Task 11)

11.1 Introduction

Corrosion induced deterioration has been identified through field investigations as the major cause of beam end distress for I-beams in Michigan bridges. The resulting forms of distress include concrete spalling, delamination, cracking, and corrosion of reinforcement. The loss of concrete permits accelerated deterioration of reinforcing and prestressing steels, allows detensioning of prestressing steel, and increases the stress demand (bearing, shear, flexural) on the remaining section (see Photo 11-1).

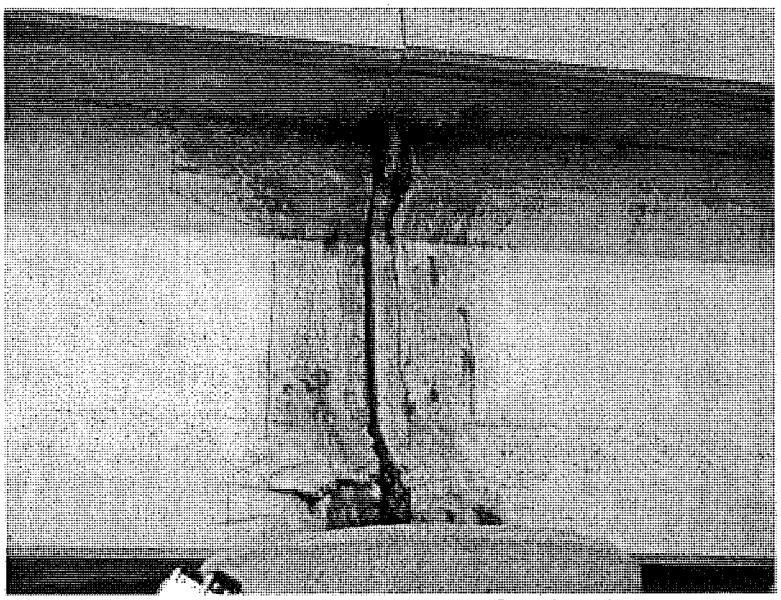

Photo 11-1. Typical beam-end deterioration

While complete replacement of the superstructure beam is an option, it is costly. If certain conditions are met, a more attractive alternative is to repair the deteriorated beam-end. At a minimum, a properly functioning repair can restore cover to reinforcing and prestressing steels and re-establish the original intended cross section of the concrete.

Briefly summarizing Chapter 2, several techniques exist for preventative maintenance and repair of concrete. These techniques may be subjectively categorized for low, moderate and high

11.0 Performance Evaluation of Partial Depth Repair Materials (Task 11)

11.1 Introduction

Corrosion induced deterioration has been identified through field investigations as the major cause of beam end distress for I-beams in Michigan bridges. The resulting forms of distress include concrete spalling, delamination, cracking, and corrosion of reinforcement. The loss of concrete permits accelerated deterioration of reinforcing and prestressing steels, allows detensioning of prestressing steel, and increases the stress demand (bearing, shear, flexural) on the remaining section (see Photo 11-1).

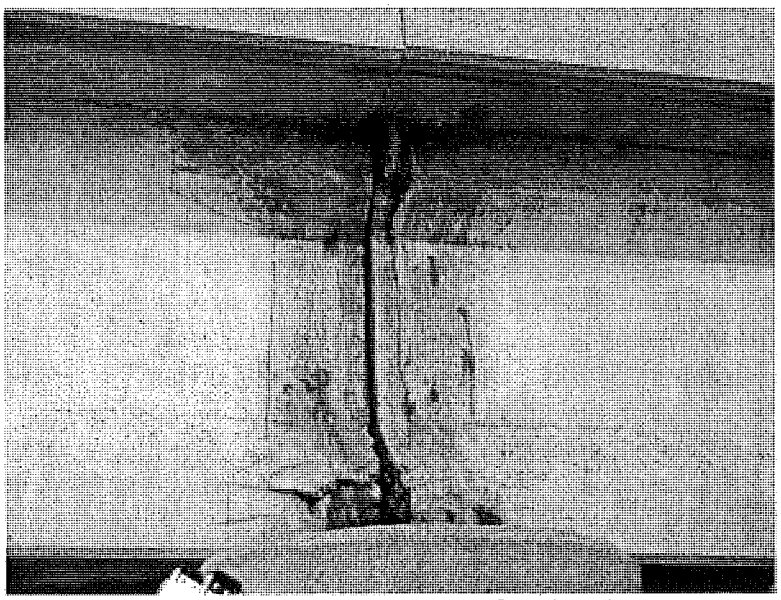

Photo 11-1. Typical beam-end deterioration

While complete replacement of the superstructure beam is an option, it is costly. If certain conditions are met, a more attractive alternative is to repair the deteriorated beam-end. At a minimum, a properly functioning repair can restore cover to reinforcing and prestressing steels and re-establish the original intended cross section of the concrete.

Briefly summarizing Chapter 2, several techniques exist for preventative maintenance and repair of concrete. These techniques may be subjectively categorized for low, moderate and high

severity distress levels. Some of these techniques include those listed in Table 11-1. Additional techniques are included in Appendix J.

Table 11-1. Preventive Maintenance and Repair Options for Deteriorated Beam-Ends

Low Severity Distress	Moderate Severity Distress	High Severity Distress
Sealers	Partial Depth Repair	Partial Depth Repair
Coatings	Cathodic Protection	Replacement
Do Nothing	Combined Sealers and Coatings	---

A partial depth repair procedure exists to perform prestressed concrete I-beam end repairs (Needham, 1999). This "chip and overcast" procedure could be applied to all levels of beam end distress, but is perhaps most effective for high and moderate severity conditions. It may therefore be a conservative approach if say less than 50-percent of the beam end surface area was damaged behind the diaphragm. For these situations, a less aggressive approach such as patching may be warranted. Other options such as sealers and coatings are specified by the MDOT and are useful for low distress levels. Current research through MDOT is underway regarding cathodic protection.

In addition to the specifications of Section 712 in the 1996 *MDOT Standard Specifications for Construction*, at least one MDOT special provision exists for "Vertical and Overhead Structure Repairs" (Staton, 2001; MDOT, 1996; MDOT, 2000). From a review of the 2001 MDOT Materials Source Guide, there are no products for vertical or overhead prepackaged patching materials listed on the MDOT Qualified Products List (MDOT, 2001c). According to MDOT, the three vertical and overhead patching materials listed as approved materials in the MDOT special provision were selected based on the manufacturers technical product literature (Staton, 2001). The three repair materials are Sika's Sika Top 126 Plus, ThoRoc's HB2, and Master Builder Technologies' Emaco R350-CI. These materials were chosen because of manufacturer tested bond strength and inclusion of corrosion inhibitors (Staton, 2001). However, at the project interim meeting of October 25, 2001, some MDOT personnel stated concerns with patching of I-beam ends, including adhesion problems, and the potential for a shrinkage differential between the patch material and the substrate that could allow future degradation of the materials through water infiltration.

From the above discussion, there is value to be gained in performing concrete repairs on prestressed concrete I-beam ends. However, the procedures and materials specified in the MDOT special provision for "Vertical and Overhead Structure Repairs" have not been subjected to substantial examination for their use in repair of deteriorated I-beam ends. Patches are typically referred to as 'shallow' for depths less than 1-in. and 'deep' for 1 to 3-in. Patch depths greater than 3-in are not recommended for the products listed in the special provision.

For a concrete repair to perform successfully in a relatively corrosive and high stress environment (such as a beam end when exposed to de-icing salts through leaking expansion joints and high bearing stresses) it must have several qualities. At a minimum the repair must:

- protect the reinforcing and prestressing steels. It cannot crack or shrink and allow rapid contaminant ingress at the patch edges, and it must
- develop sufficient bond / adhesion and compressive strength to assist the parent member in carrying loads. At a minimum it cannot debond from the substrate.

11.2 Experimental Program

11.2.1 Objective and Approach

The objective of the experimental testing was to verify that the repair materials referenced in the MDOT special provision perform at a minimum acceptable level of performance through the following assessments:

1. Evaluate the shrinkage and cracking of that materials with various repair depths compared to the surrounding concrete substrate.
2. Experimentally verify that repairs of various depths can develop sufficient tensile bond to the concrete substrate without mechanical anchorage when subjected to two environmental (thermal-cycle) scenarios.
3. Experimentally verify that each repair material can develop sufficient compressive strength to assist the substrate in carrying compressive loads.

In addition, a fourth objective could be assessed:

4. Determine whether or not performing vertical and overhead partial depth repairs is feasible.

11.2.2 Substrate specimens

An illustration of a typical specimen repaired in the vertical position is shown in Figure 11-1. In order to provide a host material for the repair materials, it was necessary to cast blank concrete specimens. Considerations and details on the construction of the substrate specimens follow.

11.2.2.1 *Formwork*

Individual single-use wood forms were constructed for fabrication of the substrate specimens. Pine boards having a 1-in nominal thickness were cut to 6-in width for the ends and bottom of the forms. The sides of the forms were constructed using 7/16-in OSB sheathing. Formwork pieces were cut such that the finished inside dimensions of the form were 6-in deep by 6-in wide by 21-in long. For ease of stripping, a release agent was applied to the inside of the forms approximately one-hour prior to the placement of concrete.

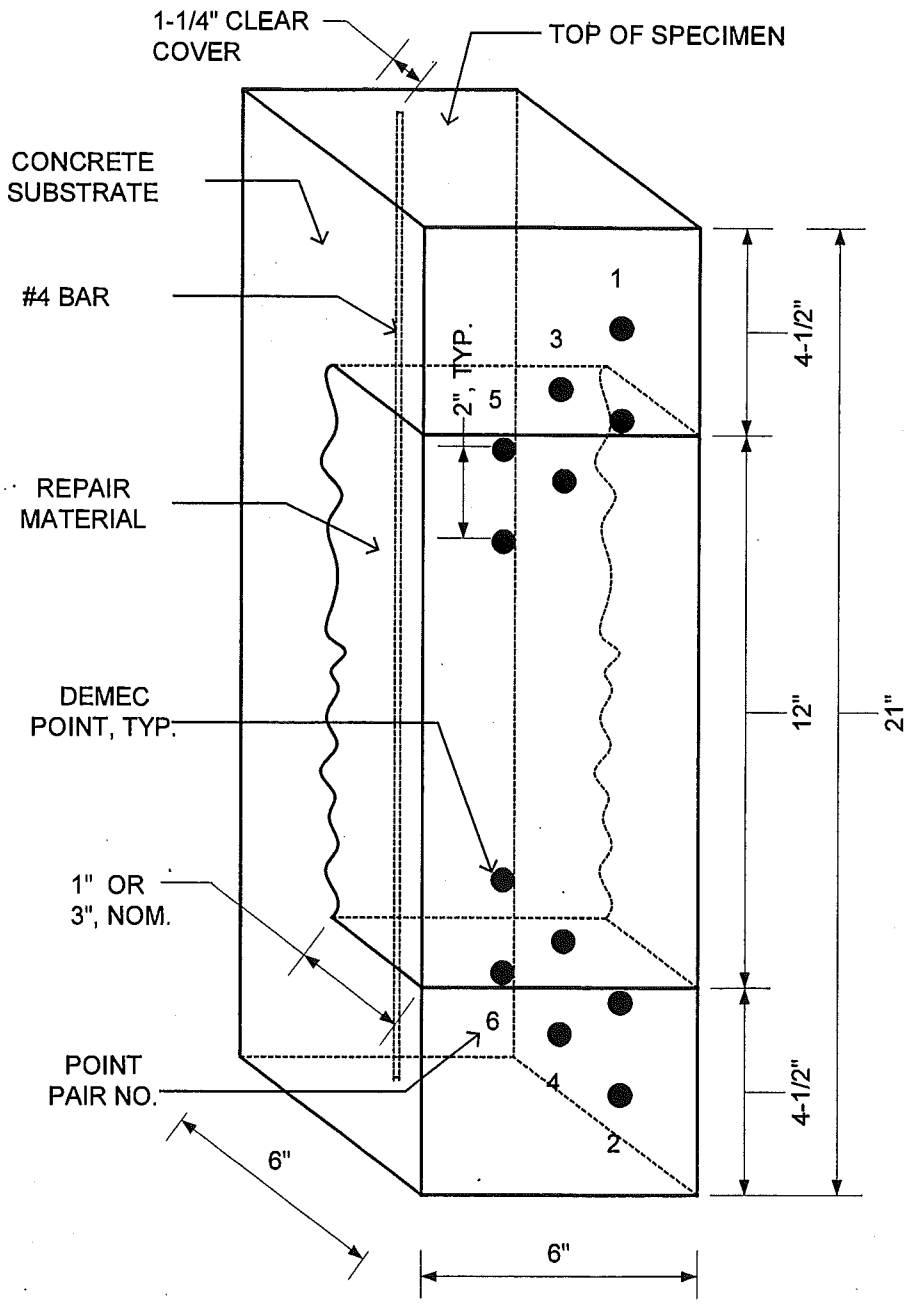

Figure 11-1. Typical Repair Specimen in Vertical Position

11.2.2.2 *Reinforcement*

Reinforcing bars were included in the fabrication of the substrate specimens for added ductility and strength. A single No. 4 bar 20-in long was selected for this purpose. After the forms had been oiled, the bars were set inside the formwork, supported on each end by polystyrene blocks. Once seated into the blocks, roughly 1 1/4-in of concrete cover was beneath the bars. Photo 11-2 shows a pallet of forms with bars in place.

Photo 11-2. Formwork coated with release agent and reinforcing bars in place

11.2.2.3 *Portland Cement Concrete*

It was desirable that the substrate specimens be as nearly identical as possible to that of concrete being used by Michigan I-beam precasters. Additionally, because bridges built in the 1960's are more likely to be susceptible to beam end deterioration (Ahlborn et al, 2001), a specimen having properties of this era would likely represent the type of substrate to which a repair material would be applied.

To this end, MDOT was able to provide a copy of the 1961 MDOT Specification and minutes from a 1957 plant trip to a Detroit precaster (Till, 2001c). It was decided to follow the guidance of the specification in setting the proportions for this project. A summary of the specification is shown in Table 11-2. The mix ordered for the project was the most representative mix relative to the 1961 mix based on aggregate classes, compressive strength, slump and air content that the local ready-mix supplier provided.

Table 11-2. Summary of Specified, Ordered, and As-Delivered Concrete Proportions and Properties

Mix	1961 Specification	Ordered for Project	As-Delivered
Cement	max. 705 lb/cy, Type I	658 lb/cy, Type I	657 lb/cy, Type I
Coarse Aggregate	see note, class 10B	1738 lb/cy, class 6A	1760 lb/cy, class 6A
Fine Aggregate	see note, class 2NS	1262 lb/cy, class 2NS	1413 lb/cy, class 2NS
Water	see note	28 - 29 gal/cy	12.7 gal/cy
Water Reducer	see note	26 oz/cy	26 oz/cy
Air Entrainment	see note	< 4 oz/cy	2.67 oz/cy
Compressive Strength (ASTM C39)	5000-psi at 28 days	5000-psi at 28 days	5070-psi at 24 days
Slump (ASTM C143	3-inches, max.	3-inches, max.	5-inches
Total Air Content (ASTM C231)	5.5 ± 1.5 percent	5.5 ± 1.5 percent	4.0 percent

Note: Proportion per manufacturer

11.2.2.4 *Substrate Fabrication*

Specimens were cast on January 8, 2002 on the heated Dillman Hall loading dock on the campus of Michigan Tech (see Photo 11-3). The concrete, supplied by Moyle Concrete of Houghton, MI, was batched in a mobile mixer with the proportions and properties noted in Table 11-2 under "As- Delivered".

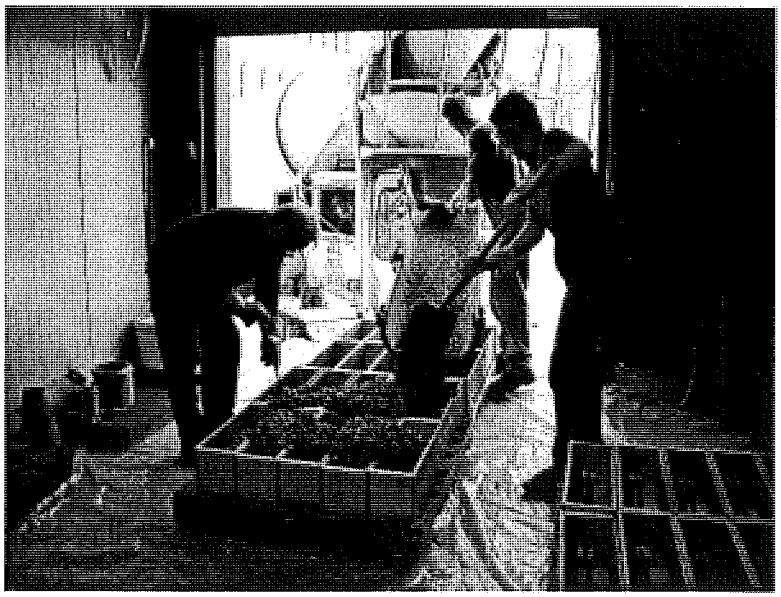

Photo 11-3. Placing concrete on the Dillman Hall loading dock

Tasks used in casting specimens included positioning forms, placing concrete, consolidating concrete, screeding specimens, inserting polystyrene blanks (top side), and performing field tests. The batch to final unload time was approximately one hour. Concrete consolidation was performed using a normal construction type hand-held concrete vibrator. The vibrator was inserted twice at roughly the third points of each specimen until the surface of the concrete was relatively smooth. Insertion points were offset from the specimen center to avoid contact with the substrate specimen reinforcement. Screeding of the specimens was accomplished with a wood straightedge. Multiple passes with the straightedge were performed to result in finished specimens with a consistent height.

Twenty-two of the thirty-nine specimens were fitted with 2-in polystyrene blanks over the middle 10-in of the specimen top (see Photo 11-4). The blanks served to reduce, but not eliminate, the need for concrete cutting during selective demolition of specimens to receive the 3-in deep patches. Blanks were inserted after screeding. The concrete was then finished around the blanks in the forms using the same floats.

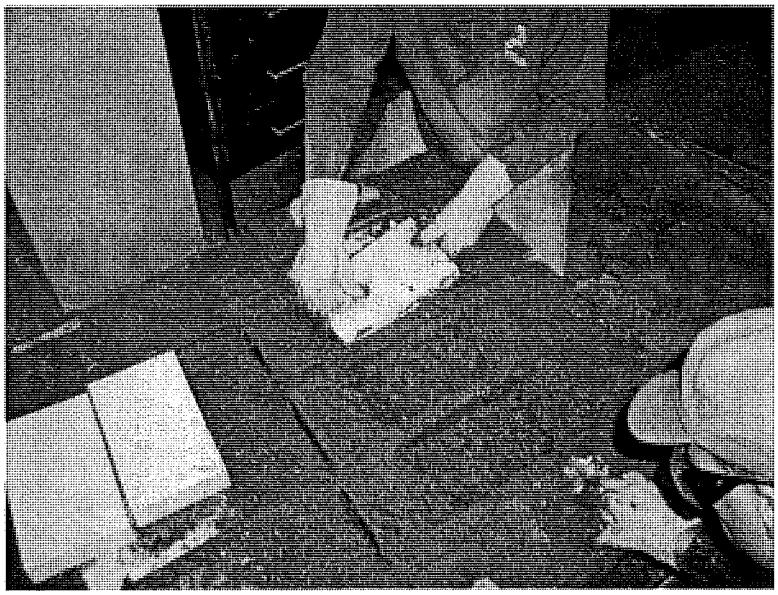

Photo 11-4. Inserting polystyrene blocks in deep repair specimens

11.2.2.5 *Laboratory Tests*

Properties of the freshly mixed concrete were determined at the time of concrete placement. Tests were performed under the direction of an ACI Field Testing Technician – Grade I. Consistency and air entrainment tests were performed in accordance with ASTM C143/C143M-00 and C231-97e1 respectively (ASTM, 2000, 1997). Slump and air content results of the "as-delivered" mix were listed previously in Table 11-2.

11.2.2.6 *Curing*

After casting, the specimens were immediately covered with multiple layers of polyethylene sheeting as shown in Photo 11-5. The sheeting was weighted with dimension lumber at the edges to trap moisture in the specimens. The sheeting remained in place for 22 hours before being transported from the loading dock to the curing laboratory with a pallet truck. Forms were stripped with hand tools and the specimens placed vertically in a pair of cure tanks (see Photo

11-6). Cure tank water was conditioned with Type S lime in accordance with ASTM C511-98 to prevent leaching of lime from the specimens (ASTM, 1998; Kosmatka et al 2002). Form removal and specimen placement in the tanks were completed in 4 hours with a 3-person team.

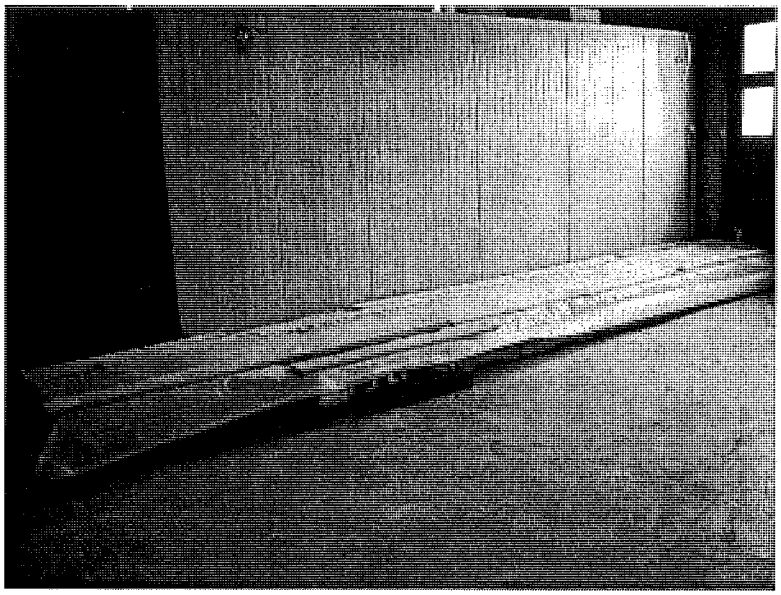

Photo 11-5. Short-term curing on the Dillman Hall loading dock

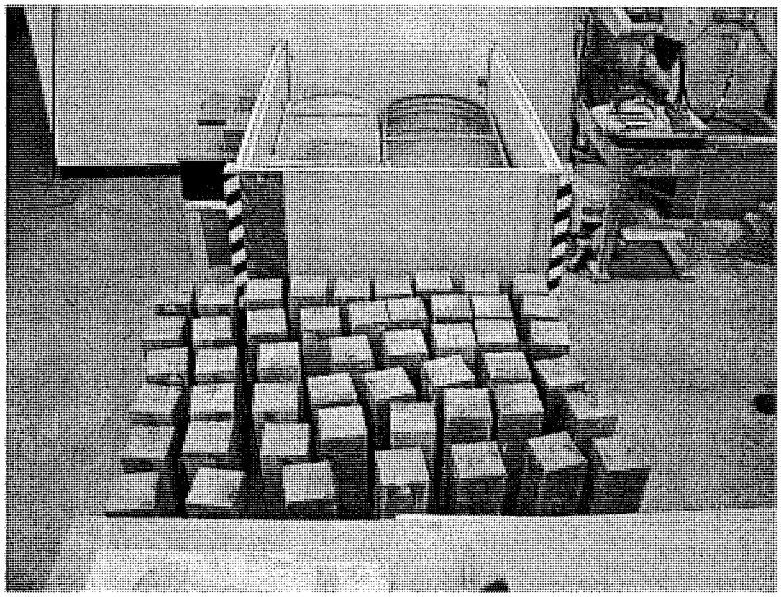

Photo 11-6. Substrate specimens stripped from forms and ready to be placed in cure tanks

The bath temperatures were maintained between 138 and 144 degrees Fahrenheit. The relatively high curing temperature and wet curing methods were selected to increase the degree of hydration within a short time period (Mindess and Young, 1981).

Tank water was heated and circulated in each tank with a Neslab Instruments, Inc. Model RTE-4 circulating bath. A temporary enclosure was constructed around the tanks using 2-inch

polystyrene insulation panels to assist the heaters in maintaining the desired tank temperatures and retain tank water. Cure tank temperatures and water depths were monitored daily using a Testo Model 925 digital thermometer and wooden yardstick. A completed temperature and depth log is located in Appendix D of Kasper's report (Kasper, 2002).

The specimens remained in the tanks for 7 days whereupon they were removed for selective demolition operations. The duration of room temperature/humidity curing prior to repair placement ranged from 7 days (January 16, 2002 to January 23, 2002) to 21 days (January 16, 2002 to February 5, 2002) depending on the specific specimen.

11.2.2.7 *Selective Demolition*

Concrete was removed from the top face (not confined by formwork) of the test substrate specimens using a concrete saw and rotary hammer. The saw selected for removal was a Champion Manufacturing Co. 20-inch stationary Blok Saw equipped with an 18-inch diamond tipped blade (shown in Photo 11-7). Due to the operational characteristics of this saw, it was necessary to cut the substrate specimens in the horizontal position. The dates that sawing was performed and the operator performing the work were documented and are included in Appendix E of Kasper's report (Kasper, 2002).

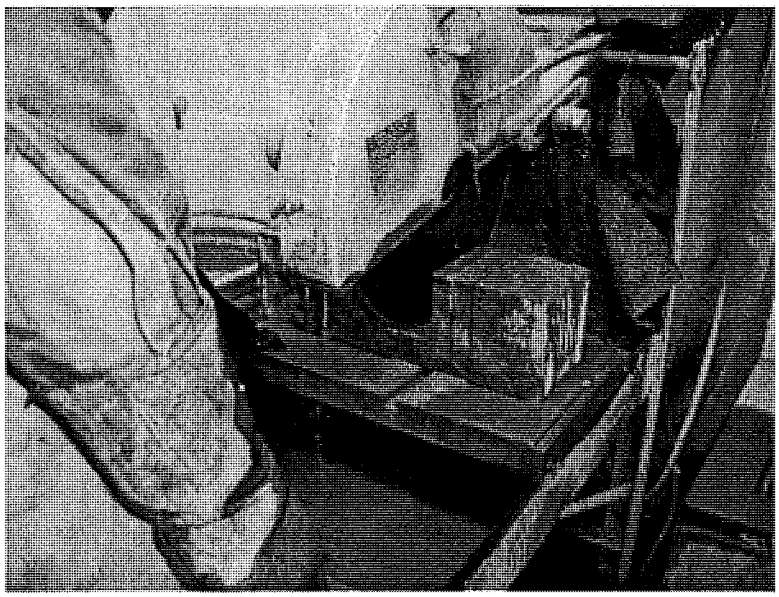

Photo 11-7. Passing the substrate specimen through the saw blade.

Saw cuts were spaced roughly one-inch apart across the face of the specimen by positioning the substrate specimens on the saw cart and passing the specimen through the blade. Saw depths of either 1-in or 3-in were made, based on whether or not the specimen was selected for a shallow or deep repair, respectively. For cuts made on the deep repair specimens, no effort was made to remove the polystyrene block prior to cutting. The above photo shows the saw at a depth of 3-in. An example of a fully sawn specimen is shown in Photo 11-8.

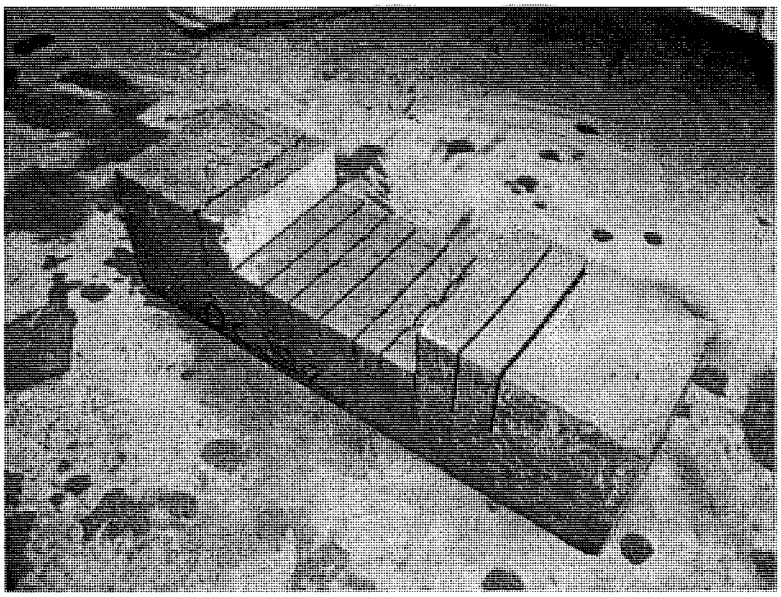

Photo 11-8. Fully cut substrate specimen. Polystyrene block has partially dislodged from void.

A Bosch 11219EVS rotary hammer fitted with a scaling chisel was used to break out sections of the concrete between the saw-cuts. As shown in Photo 11-9, break out was performed in the horizontal position on the laboratory floor. Typically the second section of concrete in from the outer edge of concrete to remain was removed first. With this section dislodged, removal efforts were directed to additional sections of scored concrete toward the center and eventually the opposite end of the specimen. Removal of an individual section was relatively easy when the chisel was oriented as close to parallel of the removal surface as possible.

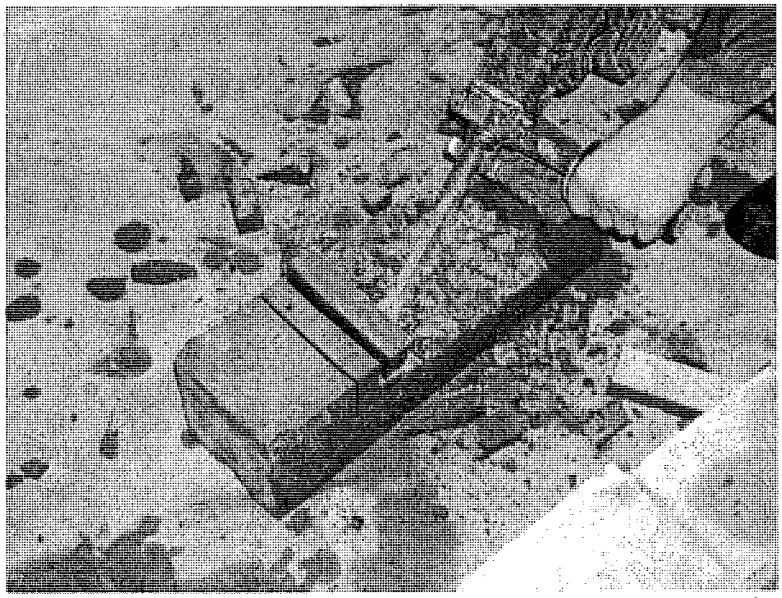

Photo 11-9. Concrete removal progressing across the substrate specimen

11.2.2.8 *Surface Preparation*

Two surface preparation techniques were evaluated. Repair practices commonly require that surface preparation techniques consist of high pressure water blasting or abrasive blasting. While these techniques are known to be effective, surface preparation consisting of brushing with a wire wheel could be another option that may be practical for small repair projects. For this project, testing was performed to determine whether or not an obvious difference existed between abrasive blasting and wire wheel preparation. To make this determination, one specimen was prepared using each method and then viewed under a microscope.

Abrasive blasting was performed on a deep repair specimen in an enclosed abrasive blasting cabinet in the foundry of the Mining and Materials Engineering building at Michigan Tech. Blasting media primarily consisted of 50-70-sieve sand with some similar sized steel shot intermixed in the media. Blasting was performed with the nozzle nearly perpendicular to the removal surface and continued for approximately 30 seconds until there was no noticeable change in the surface appearance. After abrasive blasting, the surface was blown with compressed air at roughly 60 psi until no further airborne debris was observed.

An electric angle grinder was fitted with a wire brush wheel to perform the second surface preparation method. Brushing was performed at full tool speed (approximately 10,000 RPM) and continued until there was no noticeable change in the surface appearance. After brushing, the surface was blown with compressed air at roughly 60 psi until no further airborne debris was observed.

Three surface locations were observed on each specimen using an Olympus SZH10 Zoom Stereo Microscope illuminated with directional lamps. Typically, two normally contoured and one depressed location was observed on each specimen. Photographs of each observation location were captured using an Optronics LX-750 3 CCD Video Camera System and Scion Corporation CG-7 RGB Color Frame Grabber capture card. Images were then downloaded to a Power Macintosh 9600/300 using Scion Image Version 1.62 software. Examples of the surface quality at 20x magnification for each specimen are shown in Photo 11-10 through Photo 11-13. Each photo, regardless of the preparation technique or relative depth on the specimen (depressed or non-depressed region) shows clean aggregate and air pockets within the cement matrix.

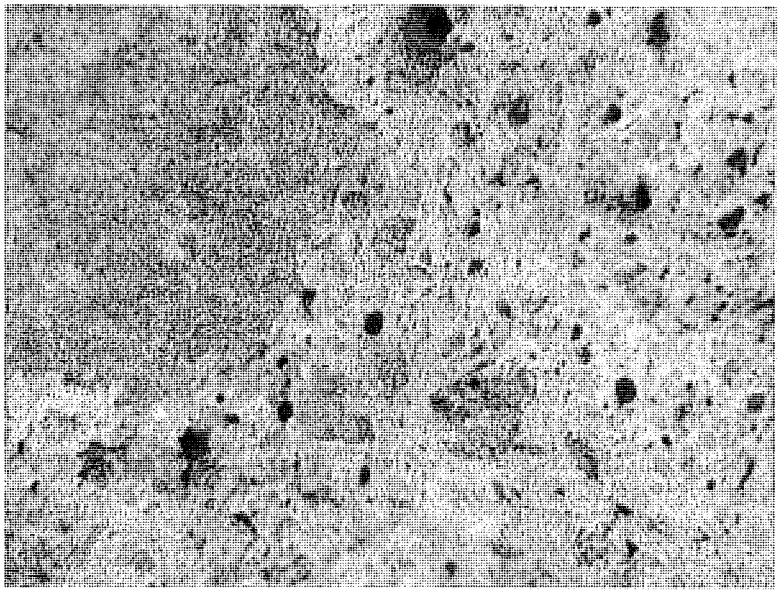

Photo 11-10. Sandblasted concrete surface at 20x magnification, non-depressed region

Photo 11-11. Wire brushed surface profile at 20x magnification, non-depressed region

Photo 11-12. Sandblasted surface profile at 20x magnification, depressed region

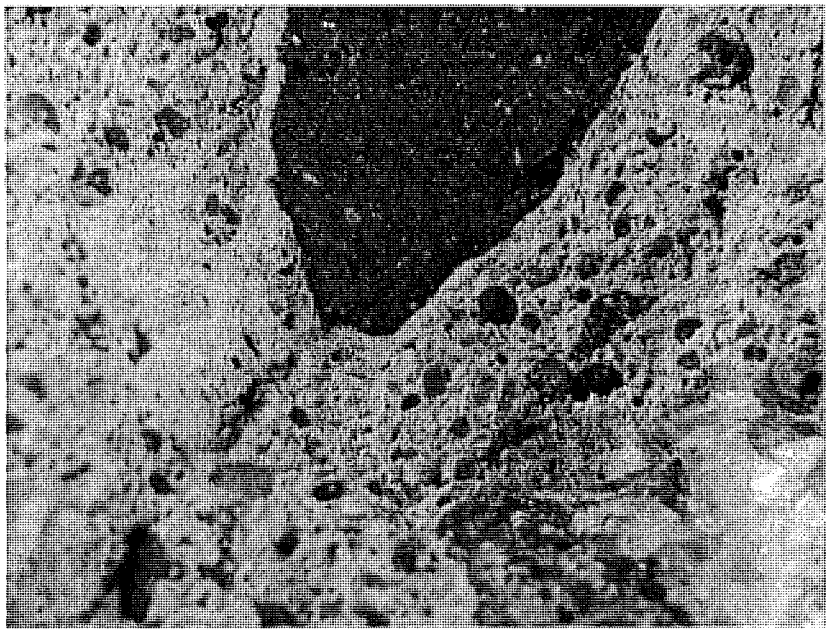

Photo 11-13. Wire brushed surface profile at 20x magnification, depressed region

Based on a visual review of Photo 11-10 through Photo 11-13, there was no obvious difference in the condition of the prepared surface between the sand blasted specimen and the wire brushed specimen. Michigan Tech research scientist Mr. Karl Peterson supported this opinion. Due to the similarity of preparation appearance and greater practicality, the wire brush method was selected to prepare the surface of all substrate specimens.

11.2.3 Repair of Substrate Specimens

Repair of the portland cement concrete specimens was performed in the Dillman Hall laboratories from January 23, 2002 to February 5, 2002. Repairs were typically performed at

room temperature using a two-person repair team. Details on the materials used and practices followed are summarized in the following sections. Thirty-nine specimens were repaired in accordance with Table 11-3.

Table 11-3. Number of Shallow and Deep Repair Specimens per Repair Material

Repair Material	No. of Shallow Repair Specimens	No. of Deep Repair Specimens
Brand X	6	6
Brand Y	6 + 2	6
Brand Z	6 + 1	6
Total No. of Specimens	**21**	**18**

11.2.3.1 *Specimen Naming*

A unique specimen identification system was created for the specimens. A four character alphanumeric designation for all of the repair specimens is shown in Table 11-4.

Table 11-4. Specimen Naming Convention for Vertical Repairs

Label	Description
First Digit: Repair Depth	D = Deep Repair S = Shallow Repair
Second Digit: Post-Curing Conditions	C = Cycled Temperatures A = Laboratory Ambient Temperatures
Third Digit: Repair Mortar Type	S = Brand X E = Brand Y T = Brand Z
Fourth Digit: Specimen No.	1 = Specimen No. 1 2 = Specimen No. 2 3, 4, etc = remaining specimens

As an example, the third shallow depth repair specimen repaired with Brand Y material and conditioned at laboratory ambient temperatures would be named "SAE3".

For accurate tracking, control and reserve specimens were also named. Reserve specimens were labeled with an "R" followed by the specimen number (e.g. R5). Control specimens without patch repairs were labeled with a "C" followed by an appropriate post-curing designation, "C" or "A", followed by the specimen number. For example, the second control sample that was seasoned under thermally cycled conditions would be "CC2".

11.2.3.2 *Formwork*

Individual multiple-use wood forms were used to form two edges for the repair of the substrate specimens. Pine boards having a 1-inch nominal thickness were selected for this purpose.

For ease of stripping, a release agent was applied to the inside of the forms. This release agent consisted of motor oil and was applied prior to clamping the forms to the sides of the substrate specimens.

11.2.3.3 *Repair Mortar*

For each repair, one of three prepackaged polymer-modified portland cement mortars was used, Sika Top 126 Plus, Emaco R350-CI, or Thoroc HB2. These products are intended for use in vertical and overhead applications where the thickness of the repair material is less than 1-in (overhead repair) to 3-in (vertical repair) (Sika USA, 2002; Chemrex 2002a, 2002b). Technical information on each of the mortars is presented in Table 11-5, based directly on information contained in manufacturer data sheets on each product (Sika USA, 2002; Chemrex 2002a, 2002b). While product information has been provided in this report, a blind study approach was used during testing and to compare results.

The layout of Table 11-5 is in conformance with the recommendations of other researchers in the concrete repair industry (McDonald et al, 2002). The table contains several rows of data for which information was not available, specifically with respect to the composition, physical properties, and performance properties of each material. However, past work has shown that these data are of interest to engineers when specifying repair materials (McDonald et al, 2002).

Table 11-5. Repair Material Data - All Manufacturers

Table 11-5 Repair Material Data - All Manufacturers			
Manufacturer	**Sika USA**	**Master Builder Technologies**	**ThoRoc**
Material	**Sika Top 126 Plus**	**Emaco R350 CI**	**HB2**
1. Repair Material Description			
Recommended Use	Use for fast repairs to overhead and vertical concrete or mortar surfaces on grade, above and below grade. Applicable for use as a repair material for building facades, parking structures, industrial plants, bridges, etc.	The product is ideally suited for patching and/or resurfacing distressed concrete. The lightweight nature of the product allows for excellent build without sagging. Emaco ® R350 CI repair mortar is designed for both interior and exterior use.	HB2 repair mortar can be used for vertical and overhead concrete repairs, around embedded steel reinforcement, where exceptional chloride and where carbon dioxide resistance is required. Product is suitable for interior or exterior use
Benefits	• Time/labor-saving material-application up to 3-in on vertical surfaces in one layer. • Application by hand or low-pressure wet-spray method. • Can be applied by hand or low- pressure wet spray equipment. • Factory proportioned packaging ensures constant quality. • High bond strength ensures excellent adhesion. • Good early and ultimate strength. • Increased freeze/thaw durability and resistance to deicing salts. • Enhanced with FerroGard 901, a penetrating corrosion inhibitor – reduces corrosion even in the adjacent concrete. • Low permeability provides protection against carbon dioxide and in water dissolved chlorides. • Compatible with coefficient of thermal • Expansion of concrete - Passes ASTM C884 modified. • Not a vapor barrier.	• Corrosion resistant - contains an integral corrosion inhibitor • One component - easy mixing and handling • Low permeability - resists moisture and chloride intrusion • Low modulus of elasticity - improved compatibility for surface renovation • Economical - excellent yield per bag, low unit weight	• Time/labor saving - can be applied up to 3-in on vertical and 1-1/2-in in overhead areas in one lift • Shrinkage compensated - minimizes shrinkage and stresses on the bond line • High bond strength - polymer component ensures excellent adhesion • Low permeability - provides protection against carbon dioxide and chloride intrusion • Durable - excellent freeze-thaw resistance • Compatible - coefficient of thermal expansion similar to concrete • Reliable - factory proportioned to overcome site-batched variations • Suitable for hand/trowel and low velocity wet spray applications

Table 11-5 Repair Material Data - All Manufacturers			
Manufacturer	**Sika USA**	**Master Builder Technologies**	**ThoRoc**
Material	**Sika Top 126 Plus**	**Emaco R350 CI**	**HB2**
Limitations	• Application thickness: Minimum: 1/8-in Maximum in one lift: 3-in vertical. 1-1/2-in overhead. • Minimum ambient and surface temperatures: 45F and rising at time of application. • Do not use solvent-based curing com-pounds. • Size, shape and depth of repair must be carefully considered and consistent with practices recommended by ACI. For additional information, contact Technical Service. • For additional information on substrate preparation, refer to ICRI Guideline No. 03732. • If aggressive means of substrate preparation is employed, substrate strength should be tested in accordance with ACI 503 Appendix A prior to the repair application	• Do not mix partial bags. • Minimum ambient and surface temperatures should be 45°F and rising at the time of application. • Do not use solvent-based curing compounds. • Do not mix longer than 5 minutes. • Featheredging will result in reduced performance. • Do not use in horizontal applications where wheeled traffic is anticipated.	• Do not mix partial bags. • Do not use in horizontal areas subjected to vehicular traffic. • Do not expose to rain or moving water during application. • Exposure to heavy rainfall prior to the final set may result in surface scour. • In cold conditions down to 45°F, maintaining the ThoRoc Polymer Liquid at 80°F is advisable to accelerate strength development. Normal precautions for working with cementitious materials in the winter should then be adopted. Do not apply if the temperature is expected to fall below 45°F within 24 hours of application. • At ambient temperatures above 80°F, the materials should be stored in the shade. Cooling the ThoRoc Polymer Liquid to 60°F is recommended.
2. Composition Data			
Base Material(s)	Two-component, polymer-modified, cementitious ready-to-use repair mortar that contains FerroGard 901 penetrating corrosion inhibitor.	A low-density, one-component, polymer-modified, shrinkage-compensated lightweight renovation mortar that contains an integral corrosion inhibitor.	Two-component, polymer-modified, shrinkage-compensated high-build repair mortar
SO_3 %: ASTM C563	None Listed	None Listed	None Listed
Alkali Content (lb./cy.)	None Listed	None Listed	None Listed
pH	None Listed	None Listed	None Listed
Air Content	None Listed	None Listed	None Listed
3. Physical Properties			
Unit Weight (lb/cf^3)	None Listed	103 lb / cf	None Listed

Table 11-5 Repair Material Data - All Manufacturers									
Manufacturer	**Sika USA**			**Master Builder Technologies**			**ThoRoc**		
Material	**Sika Top 126 Plus**			**Emaco R350 CI**			**HB2**		
Wet Density – ASTM C138	106 lb/cf			None Listed			105 lb / cf		
Strengths (psi):	Test Age (days)			Test Age (days)			Test Age (days)		
	1	7	28	1	7	28	1	7	28
Compressive: ASTM C109	2,500	3,500	5,500	1,500	3,500	5,000	2,300	4,500	5,800
Flexural: ASTM C348	650 (ASTM C496)	None Listed	1,600 (ASTM C496)	250	700	900	None Listed	None Listed	1,000
Tensile: ASTM C496	None Listed	None Listed	700	200	300	600	None Listed	300	500
Modulus: ASTM C469	None Listed			2.0 x 10^6 psi at 28 days			2.0 x 10^6 psi		
4. Performance Properties									
Drying Shrinkage: ASTM C157 (Mod.)	None Listed			None Listed			350 micro strain at 28 days		
Coefficient of Thermal Exp. CRD C 39-81	None Listed			None Listed			4.5 x 10^{-6} in/in/°F		
F-T Resistance: ASTM C666A	None Listed			100% relative dynamic modulus			100% relative dynamic modulus at 300 cycles		
Comp. Creep: ASTM C512	None Listed			None Listed			None Listed		
Rapid Chloride Permeability: ASTM C1202	Less than 500 coulombs at 28 days, per AASHTO T-277, modified			300 coulombs			941 coulombs		
Sulfate Resistance: ASTM C1012	None Listed			None Listed			None Listed		
Cracking Resistance: Ring Test	None Listed			None Listed			None Listed		
First Crack Age	None Listed			None Listed			None Listed		
Implied Strain	None Listed			None Listed			None Listed		
End of Test Age	None Listed			None Listed			None Listed		

Table 11-5 Repair Material Data - All Manufacturers			
Manufacturer	**Sika USA**	**Master Builder Technologies**	**ThoRoc**
Material	**Sika Top 126 Plus**	**Emaco R350 CI**	**HB2**
Cracking Resistance: German Angle	None Listed	None Listed	None Listed
5. Packaging, Storage			
Packaging	Component A: 1-gal. plastic jug; 4/carton. Component B: 53-lb. multi-wall bag.	55-lb. moisture-resistant bags	45 or 225-lb bags for dry component and 1 or 5-gallon containers for liquid component
Volume Yield	0.58 cubic feet / unit	0.61 cubic feet / unit	0.50 cubic feet / unit or 2.50 cubic feet / unit
Shelf Life	12 months	12 months	12 months
Storage Requirements	Store dry at 40 to 95 F. Condition material to 65 to 75 F before using. Protect Component A from freezing. If frozen, discard.	Store under cover in dry conditions between 45 and 90 F.	Transport and store in cool, dry conditions between 40°F and 85°F in the original, unopened containers.
6. How the Material Works			
Description	None Listed	None Listed	None Listed

Table 11-5 Repair Material Data - All Manufacturers			
Manufacturer	**Sika USA**	**Master Builder Technologies**	**ThoRoc**
Material	**Sika Top 126 Plus**	**Emaco R350 CI**	**HB2**
7. How to Use the Material			
Concrete Surface Preparation	Remove all deteriorated concrete, dirt, oil, grease, and all bond-inhibiting materials from surface. Be sure repair area is not less than 1/8-in. depth. Preparation work should be done by high-pressure water blast, scabbler, or other appropriate mechanical means to obtain an exposed aggregate surface with a minimum surface profile of ±1/16-in. (CSP-5). Saturate surface with clean water. Substrate should be saturated surface dry (SSD) with no standing water during application.	Perform surface preparation in compliance with ICRI Technical Guideline No. 03730 "Guide for Surface Preparation for the Repair of Deteriorated Concrete Resulting from Reinforcing Steel Corrosion." Square cut or undercut the perimeter of the area to be patched to a minimum depth of 1/8-in to prevent featheredges. Do not cut reinforcement. Chip and remove unsound and delaminated concrete within the area to be repaired to a depth of 1/8-in or to whatever additional depth is necessary to reach sound concrete. Limit the size of chipping hammers to 15-lbs. to reduce micro fractures. Hydrodemolition may be used. Remove areas that have been saturated with oil or grease. Remove 3/4-in of concrete behind the corroded reinforcing steel to provide adequate space for preparation and material placement. After concrete removal, thoroughly abrade the roughened surface and exposed reinforcement to remove all bond-inhibiting materials such as rust, dirt, loose chips, and dust.	Concrete substrate must be structurally sound. Loose or unsound concrete should be hammered out. Saw cut the edges of the repair locations to a depth of at least 3/8-in to avoid featheredging and to provide a square edge. Break out the complete repair area to a minimum depth of 3/8-in up to the sawn edge. Clean the surface by removing any dust, unsound or contaminated material, plaster, oil, paint, greases, corrosion deposits or algae. Where breaking out is not required, roughen the surface and remove any laitance by mechanical means or high-pressure water wash. Oil and grease deposits, should be removed by steam cleaning, detergent scrubbing, or the use of a degreaser. To ensure optimum repair results, assess the effectiveness of decontamination by a pull-off test.

Table 11-5 Repair Material Data - All Manufacturers			
Manufacturer	**Sika USA**	**Master Builder Technologies**	**ThoRoc**
Material	**Sika Top 126 Plus**	**Emaco R350 CI**	**HB2**
Mixing	Pour Component A into the mixing container. Add Component B while mixing continuously. Mix mechanically with a low-speed drill (400 to 600-rpm) and mixing paddle or in an appropriate mortar mixer. Mix to a uniform consistency, maximum 3-minutes. Manual mixing can be tolerated only for less than a full unit. Thorough mixing and proper proportioning of the two components is necessary.	Mechanical mixing is recommended with use of a slow speed drill (400 to 600-rpm) and a Jiffy-type paddle, or in an appropriate size mortar mixer. Add 0.95 to 1.1-gallon of clean potable water per 55-lb. bag of Emaco ® R350 CI. Pour approximately 90 percent of the mix water into the mixing container, then charge the mixer with the bagged material. Add remaining mix water as required for vertical or overhead applications. Mix to a uniform consistency. Typical mixing time is 3 to 5-minutes. Do not mix longer than 5-minutes.	Ensure that ThoRoc " HB2 Repair Mortar is thoroughly mixed. A forced action mixer is essential. Mixing in a suitably sized container using an appropriate paddle and variable speed (400 to 500-rpm) heavy-duty drill is acceptable for the occasional one-bag mix. Free-fall mixers should not be used and mixing of partial bags is not recommended. The material should always be mixed in a clean container. For normal applications, place 3-quarts of ThoRoc Polymer Liquid into the clean mixer for each complete 45-lb. bag of HB2 Repair Mortar and mix for 3 to 5-minutes until fully homogeneous. Avoid over-mixing. Note that the powder should always be added to the liquid. Depending on the ambient temperature and the desired consistency, additional ThoRoc Polymer Liquid may be added up to a maximum liquid content of 1-gallon per 45-lb bag of HB2 Repair Mortar.

Table 11-5 Repair Material Data - All Manufacturers			
Manufacturer	**Sika USA**	**Master Builder Technologies**	**ThoRoc**
Material	**Sika Top 126 Plus**	**Emaco R350 CI**	**HB2**
Application and Finish	SikaTop 126 Plus must be scrubbed into the substrate filling all pores and voids. SikaTop 126 Plus can be applied either by hand or low-pressure wet spray process equipment. The mixed SikaTop 126 Plus must be worked well into the primed substrate, filling all pores and voids. Compact well. Force material against edge of repair, working towards the center. Thoroughly compact the mortar around ex-posed reinforcement. After filling repair, consolidate, then screed. Finish with steel, wood or plastic floats, or damp sponges, depending on the desired surface texture. Where multiple lifts are required, score top surface on each lift to produce a roughened substrate for next lift. Allow preceding lift to harden before applying fresh material. Saturate surface of the lift with clean water. If previous layers are over 48-hours old, mechanically prepare the substrate. Dampen and apply bonding agent or scrub coat prior to the mortar.	Remove excess water from the saturated surface dry (SSD) substrate and apply while taking proper consideration for compaction around reinforcing steel. Scrub a bond coat of Emaco ® R350 CI repair mortar into the prepared surface with a stiff bristle broom or brush. Emaco ® R350 CI repair mortar must be placed before the bond coat dries. When applying in multiple lifts, scratch the preliminary lift before initial set. Apply the next lift after the preliminary lift has reached final set. If the next lift is not to be immediately placed, keep the surface continually moist. Cut off or level as required to match the original concrete elevation. Maximum application thickness is 2-3/4-in. Where rapid drying conditions exist (e.g., hot, dry, windy conditions) use Confilm ® evaporation reducer. Finish the final surface as required.	Substrate should be SSD (saturated surface dry) with no standing water. Using a stiff brush, scrub a thin coat of the mixed material thoroughly into the surface to ensure sufficient bonding. Before bond coat dries, thoroughly compact the mortar onto the substrate and around the exposed reinforcement. HB2 Repair Mortar can be applied in sections up to a 3-in thickness in vertical locations and up to a 1-1/2-in thickness in overhead locations in a single lift and without the use of formwork. Thicker sections should be built up in layers, but are sometimes possible in a single application depending on the actual configuration of the repair area and the volume of exposed reinforcing steel. If sagging occurs during application, HB2 Repair Mortar should be completely removed and reapplied at a reduced thickness onto the correctly re-primed substrate. HB2 Repair Mortar is finished by striking off with a straight edge and closing with a steel float. Wooden or plastic floats or sponges may also be used to achieve the desired surface texture. The completed surface should not be overworked.

Table 11-5 Repair Material Data - All Manufacturers			
Manufacturer	**Sika USA**	**Master Builder Technologies**	**ThoRoc**
Material	**Sika Top 126 Plus**	**Emaco R350 CI**	**HB2**
Curing	As per ACI recommendations for portland cement concrete, curing is required. Moist cure with wet burlap and polyethylene, a fine mist of water or a water based*, compatible curing compound. Curing compounds adversely affect the adhesion of following lifts of mortar, leveling mortar or protective coatings. Moist curing should commence immediately after finishing. If necessary protect newly applied material from direct sunlight, wind, rain and frost. *Pre-testing of curing compound is recommended.	Proper curing is extremely important and should be conducted in accordance with ACI 308, "Standard Practice for Curing Concrete." Apply a curing compound which complies with the moisture retention requirements of ASTM C 309, such as Masterkure ® 100W or 200W curing compounds. Apply curing materials as soon as the surface cannot be marred by the application. Sheeting material, wet burlap, or fog spray may be used in lieu of curing compounds. Minimum curing time for wet curing is three days. Give mortar extra time for curing in temperatures below 50°F.	Proper curing is extremely important. HB2 Repair Mortar should be cured immediately after finishing in accordance with good concrete practice (ACI 308) to approach peak performance of the repair. Proper curing is of particular importance when ambient conditions may cause rapid moisture loss (high temperature, low humidity, or moderate to high winds). The use of ThoRoc Acrylic Modifier, or an appropriate ASTM C 309 compliant curing compound, sprayed on to the surface of the finished repair in a continuous film, is recommended. Large areas of greater than 5-sq. ft. should be cured as troweling progresses without waiting for completion of the entire area. Other curing options include a fine mist of water, application of wet burlap (burlap must be kept continuously moist), application of polyethylene sheeting taped down at the edges, or a combination of the above to keep the finished repair moist for a minimum of 7-days. In cold conditions, the finished repair must be protected from freezing. If doubts arise concerning proper curing procedures, consult ACI guidelines.

Table 11-5 Repair Material Data - All Manufacturers			
Manufacturer	**Sika USA**	**Master Builder Technologies**	**ThoRoc**
Material	**Sika Top 126 Plus**	**Emaco R350 CI**	**HB2**
Cleanup	In case of spillage, scoop or vacuum into appropriate container, and dispose of in accordance with current, applicable local, state and federal regulations. Keep container tightly closed and in an upright position to prevent spillage and leakage. Mixed components: Uncured material can be removed with water. Cured material can only be removed mechanically.	This product when discarded or disposed of is not listed as a hazardous waste in federal regulations. Dispose of in a landfill in accordance with local regulations. For additional information on personal protective equipment, first aid, and emergency procedures, refer to the product Material Safety Data Sheet (MSDS)	HB2 Repair Mortar should be removed from tools, equipment and mixers with clean water immediately after use. Cured material can only be removed mechanically. Clean hands and skin immediately with soap and water or industrial hand cleaner.

Table 11-5 Repair Material Data - All Manufacturers			
Manufacturer	**Sika USA**	**Master Builder Technologies**	**ThoRoc**
Material	**Sika Top 126 Plus**	**Emaco R350 CI**	**HB2**
Safety	Component A - Irritant - May cause skin/eye/respiratory irritation. Avoid breathing vapors. Use with adequate ventilation. Avoid skin and eye contact. Safety goggles and rubber gloves are recommended. Component B - Irritant; suspect carcinogen - Contains portland cement and sand (crystalline silica). Skin and eye irritant. Avoid contact. Dust may cause respiratory tract irritation. Avoid breathing dust. Use only with adequate ventilation. May cause delayed lung injury (silicosis). IARC lists crystalline silica as having sufficient evidence of carcinogenicity in laboratory animals and limited evidence of carcinogenicity in humans. NTP also lists crystalline silica as a suspect carcinogen. Use of safety goggles and chemical resistant gloves is recommended. If PELs are exceeded, an appropriate, NIOSH/MSHA approved respirator is required. Remove contaminated clothing. In case of skin contact, wash thoroughly with soap and water. For eye contact, flush immediately with plenty of water for at least 15 minutes, and contact a physician. For respiratory problems, remove person to fresh air.	Eye irritant. Skin irritant. Causes burns. Lung irritant. May cause delayed lung injury. Avoid contact with eyes. Wear suitable protective eyewear. Avoid prolonged or repeated contact with skin. Wear suitable gloves. Wear suitable protective clothing. Do not breathe dust. In case of insufficient ventilation, wear suitable respiratory equipment. Wash soiled clothing before reuse. Wash exposed skin with soap and water. Flush eyes with large quantities of water. If breathing is difficult, move person to fresh air.	Product is alkaline on contact with water and may cause injury to skin or eyes. Ingestion or inhalation of dust may cause irritation. Contains free respirable quartz, which has been listed as a suspected human carcinogen by NTP and IARC. Repeated or prolonged overexposure to free respirable quartz may cause silicosis or other serious and delayed lung injury. Precautions: Prevent contact with skin and eyes. Prevent inhalation of dust. Do not take internally. Use only with adequate ventilation. Use impervious gloves, eye protection and if the TLV is exceeded or used in a poorly ventilated area, use NIOSH/MSHA approved respiratory protection in accordance with applicable federal, state and local regulations. In case of eye contact, flush thoroughly with water for at least 15 minutes and seek immediate medical attention. In case of skin contact, wash affected areas with soap and water. If irritation persists, seek immediate medical attention. Remove and wash contaminated clothing. If inhalation causes physical discomfort, remove to fresh air. If discomfort persists or any breathing difficulty occurs or if swallowed, seek immediate medical attention.

11.2.3.4 *Repair Fabrication*

11.2.3.4.1 General Practices

Certain practices were followed during repair fabrication, regardless of the repair material, thickness, or orientation. All surfaces of the substrate specimen to receive the repair material were re-cleaned with compressed air at roughly 60-psi until no further airborne debris was observed. This cleaning often resulted in the noticeable removal of concrete dust and at times small (less than 1/4-in diameter) concrete chips. Specimen orientation, vertical or overhead, was maintained during the repair and curing processes.

Forms were secured to the sides of the specimen using adjustable clamps (see Photo 11-14). The repair area of the substrate specimens was then wetted to a near saturated surface dry (SSD) condition. Multiple applications of water mist from a garden hose or hand held spray bottle were used to maintain this state prior to the installing the repair material.

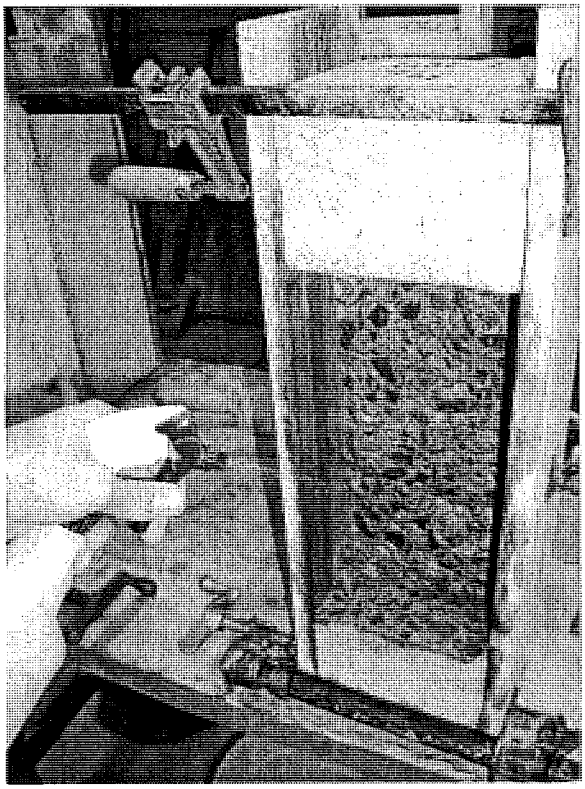

Photo 11-14. Formwork in place on a substrate specimen and wetting of prepared surface

Repair mortar was mixed in partial units in a Hobart Manufacturing Company Model N-50 variable speed stand mixer as shown in Photo 11-15. The quantities and limits of liquid component and dry component were pre-determined, measured with scales or graduated cylinders in clean containers, and added to the mixing bowl. Proportions used for each repair depth are presented in Table 11-6 through Table 11-8.

Table 11-6. Mixture Proportions for Brand X Repair Mortar

Brand X Component	Proportions for Shallow Repair	Proportions for Deep Repair
Dry Mortar	6.28-lb	16.34-lb
Polymer Liquid	15.2 oz	39.6 oz

Table 11-7. Mixture Proportions for Brand Y Repair Mortar

Brand Y Components	Proportions for Shallow Repair	Proportions for Deep Repair
Dry Mortar	6.22-lb	16.22-lb
Water	13.7 oz to 15.6 oz	35.7 oz to 40.7 oz

Table 11-8. Mixture Proportions for Brand Z Repair Mortar

Brand Z Components	Proportions for Shallow Repair	Proportions for Deep Repair
Dry Mortar	6.19-lb	16.11-lb
Polymer Liquid	13.0 oz to 17.7 oz	33.9 oz to 46.0 oz

For every batch of mortar mixed, the liquid component was always added prior to the dry component. The start of mixing was documented once the dry component was added to the mixing bowl. Mixing was performed with the mixer at low speed (agitator speed: 136 RPM, attachment speed: 60 rpm) for 3 (Brand X) or 5-minutes (Brand Y and Z). Mix times and batch quantities were documented and varied from batch to batch depending on the mortar manufacturer recommendations. After mixing, the fresh mortar was either transferred to stainless steel bowls or remained in the mixing bowl prior to placement. Repair material from each batch was placed within approximately 10 to 30 minutes after mixing.

Photo 11-15. Equipment used for preparing repair mortar

With the mortar freshly mixed, hand held stiff bristle brushes were used to scrub repair mortar into the SSD substrate (see Photo 11-16). Brush size and bristle stiffness varied, however a palm-sized plastic bristle brush was generally used for the bulk of the scrubbing and a toothbrush-sized steel bristle brush was used for corners and depressed areas.

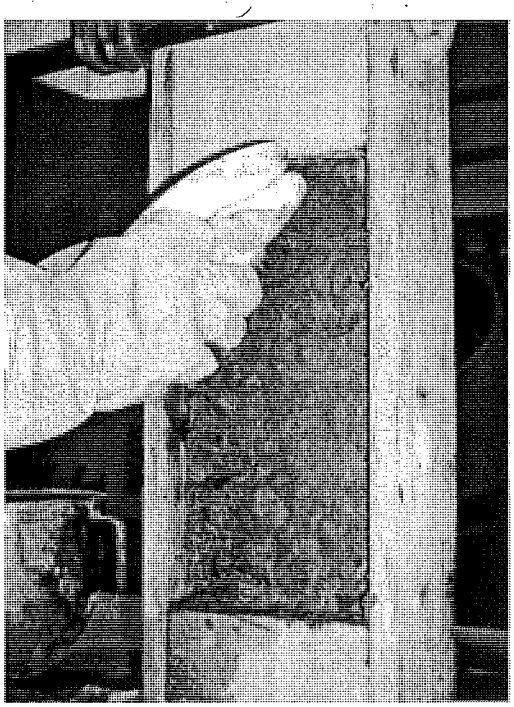

Photo 11-16. Scrubbing mortar into the prepared substrate surface

Several methods were attempted for placing the repair material into the void. These methods were by hand, putty knife, and steel trowel. A majority of the specimens were repaired by placing repair mortar with a 2-in steel putty knife (see Photo 11-17). The size of the knife alone required that small amounts of mortar be placed at a time.

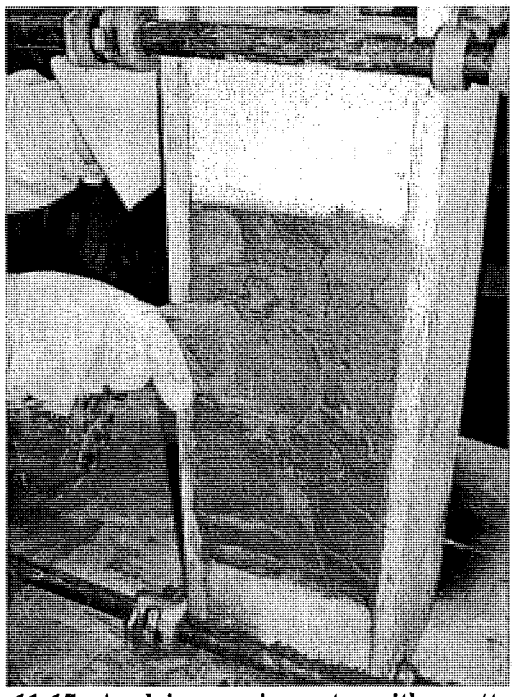

Photo 11-17. Applying repair mortar with a putty knife

The plastic repair material was consolidated in-place by a variety of methods. Tools used included fingers, round-nosed steel bars, flat steel bars, the pressure of the knife, and blunt-end bars. In general, a well-distributed pattern of penetration points was followed, regardless of the tool used, with the exception of the knife-pressure approach. Repair material placed for shallow repairs was generally consolidated once, after the full thickness of the repair had been achieved. Consolidation with tools having a large surface area (e.g. the flat side of a putty knife compared to a round-nosed rod) tended to produce the densest repairs. Deep repairs were generally consolidated twice, at the mid-depth thickness and again after the full thickness of the repair had been achieved. Applying additional mortar with the pressure of the knife closed depressions in the mortar that remained after consolidation.

Specimens were finished with a steel trowel as shown in Photo 11-18. Finishing operations were kept to a minimum, aiming to achieve surface uniformity without causing sagging of the repair material.

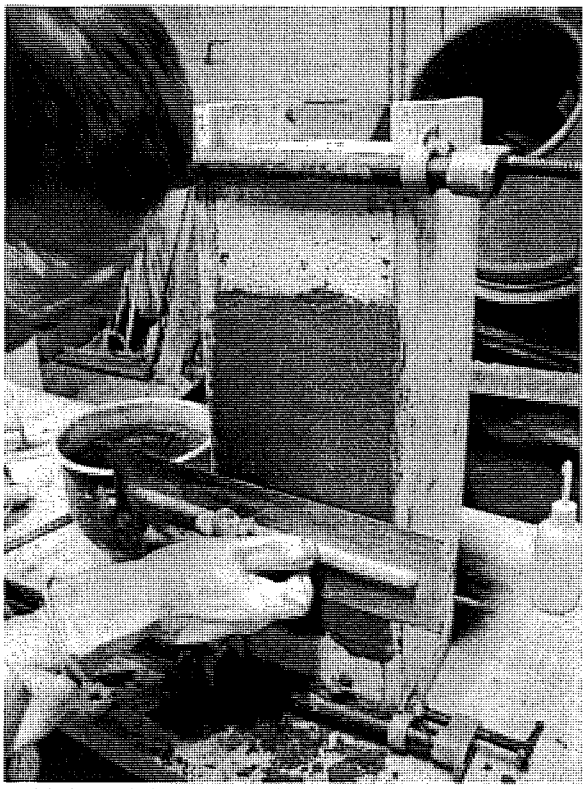

Photo 11-18. Finishing repair specimens with a steel trowel

11.2.3.4.2 Shallow Repair: Vertical Placement

Twenty-one shallow repairs cast in the vertical position were in general conformance with the procedures described above. The overall size of this repair type was 6-in by 12-in at a 1-in nominal repair depth. Substrate specimens were set atop a 3.5-ft high workbench to aid in placement of the mortar.

In general, mortar was placed first at the top of the specimen and progressed downward and outward to the finished surface. Specimens remained in the vertical position until initial set (approximately 30 minutes) whereby they were temporarily turned horizontal for setting of instrumentation points.

Due to bonding problems noticed during installation of repair material on one specimen, "SCE1", an additional specimen was fabricated. For this specimen, a reserve substrate specimen was prepared for a shallow depth repair and repaired using the Brand Y repair material in the vertical position. This specimen was thermally cycled after initial curing and was labeled "R1".

11.2.3.4.3 Shallow Repair: Overhead Placement

Two specimens were repaired in the overhead position, each using a different repair material. These specimens were in addition to the original 39 specimens cast for this experiment. As such, two of the reserve specimens, "R2" and "R5" were selected for the substrate specimens. The Brand Z and Brand Y materials were arbitrarily selected for the "R2" and "R5" specimens, respectively. Specimen "R2" was further designated to have post-curing thermal cycling while specimen "R5" was placed in a laboratory ambient post-curing environment.

The overall size of this repair type was 6-in by 12-in at a 1-in nominal repair depth. The intent of performing these repairs was to validate the feasibility and performance of a repair mortar applied in the overhead position.

In the laboratory, overhead repair specimens were set between two tables of equal height, approximately 3.5 feet off the floor of the laboratory (see Photo 11-19). Formwork application, surface preparation, mortar mixing, mortar placement, and mortar finishing then proceeded similarly to that for the vertical repair of shallow depth specimens with few exceptions. The most notable exception was that the mortar was not consolidated in-situ, other than with the consolidation provided by the pressure of the knife (see Photo 11-20).

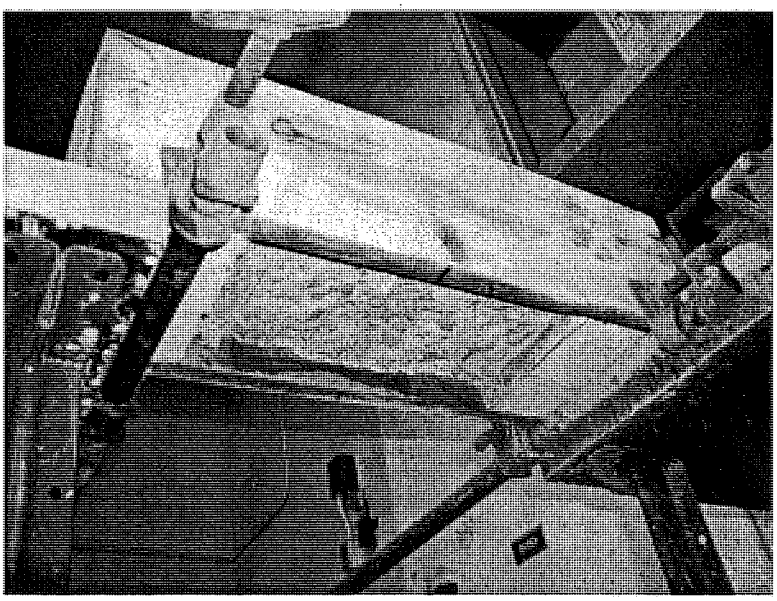

Photo 11-19. Specimen in the overhead position prior to initiating repairs

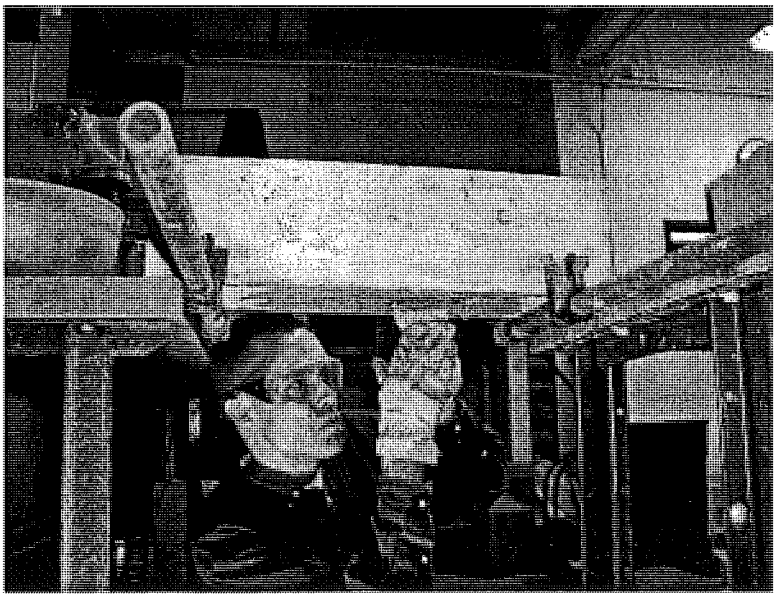

Photo 11-20. Placing repair material in the overhead position

Specimens remained in the overhead position until initial set (approximately 30 minutes) and were then temporarily turned upright for setting of instrumentation points.

11.2.3.4.4 Deep Repair: Vertical Placement

Eighteen deep repairs cast in the vertical position were in general conformance with the procedures described above. The overall size of this repair type was 6-in by 12-in at a 3-in nominal repair depth. Substrate specimens were set atop a 3.5-ft high workbench to aid in placement of the mortar.

Due to outward sagging of the repair material at a full-height placement of trial repairs, deep repair specimens needed to be repaired in two successive 6-in vertical lifts. In general, the lower mortar lift was first placed at the bottom of the specimen and progressed upward and outward to the finished surface. Edges of the formwork were clearly marked at the intended inter-lift height for reference during repair material placement. Typically, the lower lift was over-filled by one inch. After some hardening of the mortar, the excess was cut off with the knife to the inter-lift height. The top surface of the lower-lift mortar was then etched with an awl in a random pattern to improve bond between each lift.

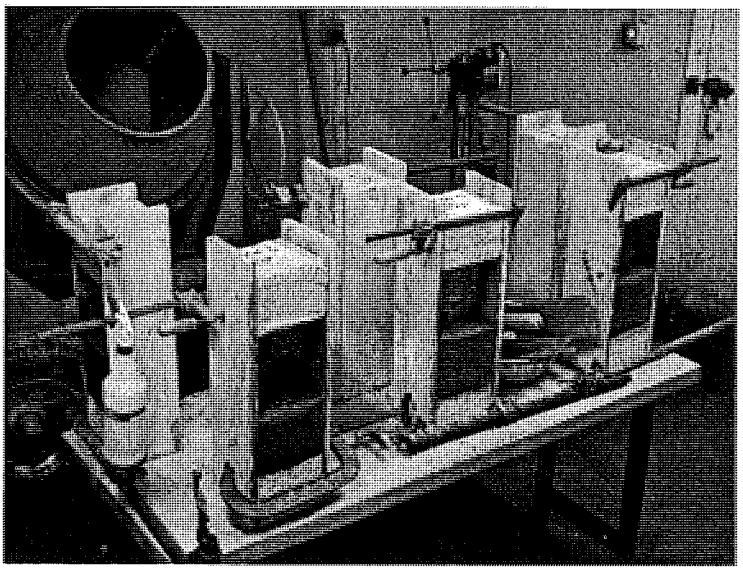

Photo 11-21. Deep repair specimens with the bottom lift in place

The upper lift of mortar was placed after the lower lift had hardened sufficiently to support the next lift (approximately 2-1/2 hours). Loose mortar that remained on the top surface of the lower lift was removed with compressed air prior to repair material placement. Repairs then proceeded in a similar fashion to those used for the shallow depth vertical specimens, including a mortar scrub of the top edge of the lower repair surface. After surface preparation, the void for the upper lift was filled from the top down, with the repair progressing downward and outward to the finished surface, in the opposite direction of the lower lift repair. These procedures were per the manufacturers technical support for deep repairs. These techniques would also be used for proper placement of repair mortar in the field.

Specimens remained in the vertical position until initial set of the upper lift (approximately 3 hours from start of lower lift) and were then temporarily turned horizontal for setting of instrumentation points.

11.2.3.5 *Instrumentation*

Each repair specimen was fitted with six pairs of DEtachable MEChanical (DEMEC) points after the last lift of repair material had achieved initial set. By measuring the change in distance between each pair of DEMEC points, shrinkage information of the mortar and substrate was to be gathered and assessed. The points were mounted on the surface of the specimen that received the repair mortar with the specimen in the horizontal position. Figure 11-1 previously illustrated the typical setting pattern used on each repair specimen.

Points were set in pools of Devcon 5-minute epoxy gel on the surface of each specimen and kept parallel to one another by steel bar stock spacer bars. Spacer bars were secured to each point pair with machine screws and removed from the pair within at least one day.

11.2.3.6 *Curing*

Moist curing methods were used to cure the repair materials selected for this study. Moist curing was selected as the curing method since it was appropriate for each of the three repair materials and could be performed in the field (Sika USA, 2002; Chemrex, 2002a; Chemrex, 2002b). In the field, moist curing of beam end repairs could be achieved with burlap blankets and intermittent water sprinkling.

Moist curing was initiated after the epoxy for the instrumentation points had set sufficiently (approximate set time of 15 minutes). With the epoxy set, the specimens were returned to the vertical or overhead position and transported to a moist cure room. The moist cure room used for this project was located on the ground level of Dillman Hall. This room is equipped with water misting nozzles at the ceiling, emitting spray on specimens set below. Specimen temperatures inside the cure room ranged between 55 to 60 degrees Fahrenheit.

Photo 11-22. Repair specimens undergoing initial curing in a moist cure room

Moist curing was conducted for 2 to 7 days inside the cure room, depending on the repair mortar manufacturer's minimum recommended curing time. At the conclusion of moist curing, the specimens were removed from the moist cure room and stored in Dillman Hall at laboratory ambient conditions. Specimens remained in laboratory ambient temperature and humidity conditions until one of the two designated starting dates for documenting post-curing conditions, February 7, 2002 (first 33 specimens repaired: lot 1), or February 13, 2002 (last 6 specimens repaired: lot 2). Specimens in lot 2 included R1, R2, R5, DCE3, DCT2, and DCT3. The time between removal from the curing room to the commencement of post-curing conditions for lot 1 specimens ranged from 7 to 12 days. Lot 2 specimens were in laboratory ambient temperature and humidity conditions for 1 to 6 days prior to commencement of post-curing conditions.

11.2.3.7 *Post-Curing Conditions*

Roughly half of the specimens were designated for laboratory ambient post-curing conditions with the other half reserved for thermally cycled conditions. The specimens designated for laboratory ambient post-curing conditions were stored in the vertical or overhead position until preparation for direct tension testing as described in Section 11.3.3.3. Specimens continually remained in their as-repaired position except when bi-weekly strain measurements were obtained.

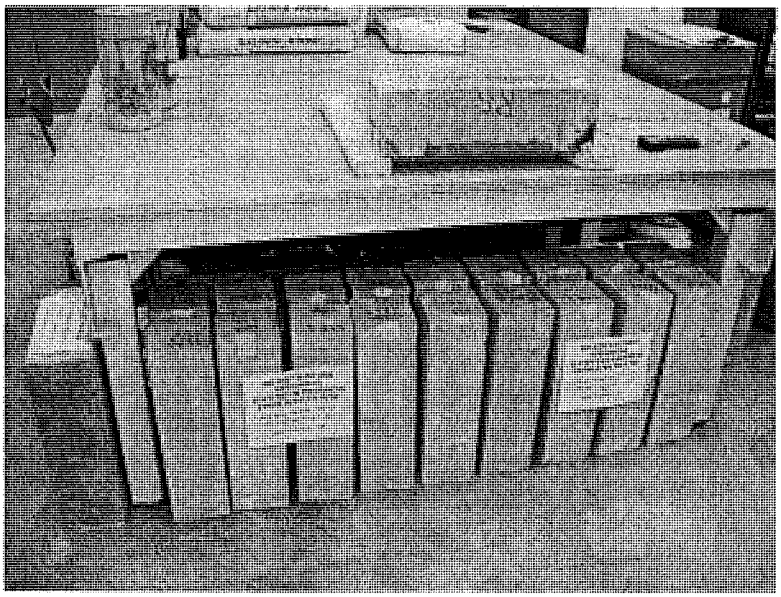

Photo 11-23. Storage of repair specimens undergoing laboratory ambient post-curing conditions

The remaining specimens were transported to a thermal chamber located in the Dow Environmental Science and Engineering Building. The thermal chamber used for this project was manufactured by Bally Refrigerated Boxes and equipped with a CAN-TROL Environmental Systems Ltd. control panel. Specimens were stored in the vertical or overhead

position until March 24, 2002 (lot 1) or March 30, 2002 (lot 2). Specimens continually remained in their as-repaired position except when bi-weekly strain measurements were obtained.

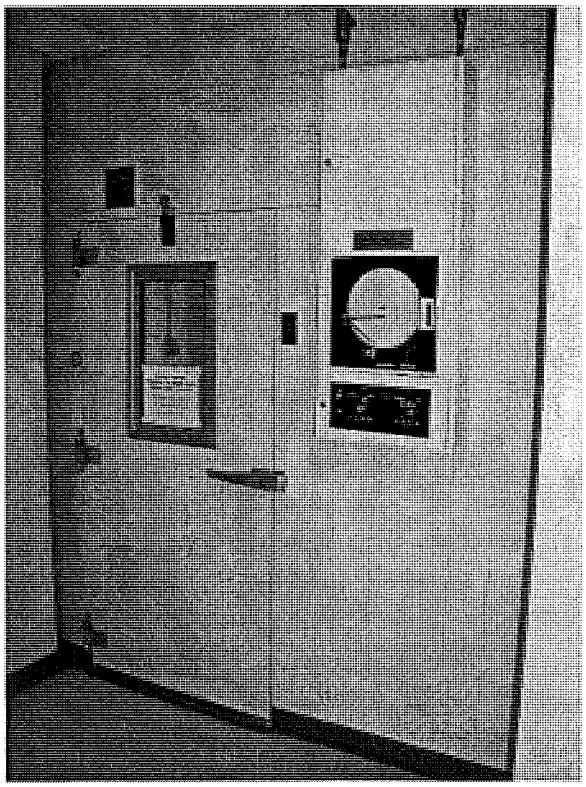

Photo 11-24. Exterior of thermal chamber

The features of the chamber control panel required that the temperatures be manually cycled on a daily basis. A log of the daily-programmed chamber temperature, previous chamber temperature, and previous chamber setting is included in Appendix G of Kasper's report (Kasper, 2002). Chamber temperatures were typically set at 32 or 95 degrees Fahrenheit. However, actual chamber temperatures ranged from 32 to 88 degrees Fahrenheit 24 hours after manually changing the chamber temperature.

Each specimen was in the chamber for 44 days. Because the chamber was not cycled for one weekend, the specimens were subjected to 21 high-low-high temperature cycles.

Specimens were subjected to visual inspection of repair surfaces (Section 11.3.2), strength evaluation (Section 11.3.3) including isolated material tests, and shrinkage evaluation (Section 11.3.4).

11.3 Experimental Results and Observations

In this section, the results of the experimental study conducted are presented. In addition to numerical data and analysis, a portion of this section includes observations made during fabrication and a discussion of the surface condition of the repairs at the conclusion of post-curing conditioning. Test procedures used in the study will be briefly described, along with the results and significance of the test data. Where testing procedures have deviated from established standards, the actual practices used have been described.

11.3.1 Fabrication Observations

11.3.1.1 *Substrate Specimens*

Fabrication of the substrate specimens followed engineering judgment and construction practice as previously described in this chapter. Substrate specimens generally exhibited sufficient consolidation, as evidenced by infrequent bugholes on the sides of the specimens. The addition of the No. 4 reinforcing bar opposite of the repaired face appeared to have provided sufficient ductility and durability to the substrate specimen, as no specimens were damaged during selective demolition. The surface finish of the substrate specimens was generally rough and at times, uneven. This finish and texture was difficult to match when placing repair material within the substrate specimen. The use of polystyrene blanks in the face of the substrate specimens did not adversely affect the casting of the substrate specimen and accelerated concrete removal operations.

Cutting concrete with a diamond saw blade was found to be a practical and effective method for sound concrete removal. Although the saw used for this study was a stationary unit, it is anticipated that similar results could be achieved with hand held equipment. Sawing provides a way of eliminating featheredges of repairs by providing a square edge at the limit of the repair. If in future work a more effective means of concrete removal is found, sawing may still be desirable to produce desired substrate edges at the limits of the repair. However, bond between the repair material and substrate at the smooth interface may be of concern. Bond at this location was not evaluated in this study.

A rotary hammer was proven to be a practical and effective tool for removing sound, scored concrete. The rotary hammer used for this study had an approximate weight of 14 pounds and generated 4.4 ft-lbs of impact energy (S-B Power Tool Company, 2002). Other rotary hammers are commercially available with a range of hammer weight and impact energy characteristics. These tools may also be suitable for concrete removal. However, based on the bond tensile strength results discussed later in the sections *Bond Tensile Strength of Repairs* and *Bond Tensile Strength of Substrate*, the use of the rotary hammer may have had an adverse effect on the bond of the repair material to the substrate. This is evidenced by the lower failure stress of those repair specimens that failed entirely within the concrete substrate compared to the failure stress of the control substrate-only specimens.

Surface preparation with a wire wheel brush may or may not be an effective method of preparing a concrete substrate prior to repair. This inconclusive observation is made because the preparation quality was sufficient to allow failure within the substrate in roughly 5-percent

of the bond tensile strength tests, but that over 75-percent of the repair bond tensile strength failures occurred at the repair-substrate interface.

11.3.1.2 *Repair Specimens*

Manufacturer installation instructions for each of the three prepackaged repair materials permitted user variation in repair mortar consistency (Sika USA, 2002; Chemrex, 2002a; Chemrex, 2002b). Placing mortars that were mixed at the lower range of recommended water or polymer to cement ratios (*w-p/c*) were difficult to place. This was evidenced by the installation of repair mortar in specimens SAT1 and SAT2. The liquid component for these repairs was at the lower limit of the *w-p/c* ratio of other specimens. The stiff consistency not only made for difficult material placement, but also was difficult to consolidate and finish.

Manufacturer installation instructions for each of the repair materials also suggest that the dry and liquid components of the repair mortar be mixed in "full-bag" portions (Sika USA, 2002; Chemrex, 2002a; Chemrex, 2002b). However, for this study, roughly 20 individual batches of repair mortar were produced from each full-bag of dry repair material. It was found that the individual batches were similar in terms of initial mortar consistency and workability based on observations during repair. In addition, it was observed that the repair mortars became difficult to work as the material was used during repair. Depending on the level of experience of the person or team working with the repair material, environmental conditions, repair geometry, and mixing equipment, partial bag mixing may be a more efficient use of repair material. If full bag batches are used, waste material can be expected due to the material attaining set prior to installation.

Sagging of plastic repair mortar can be a problem in shallow and deep repairs. Sagging is an outward progression of the repair mortar from the intended exterior limit of the repair. In general, mixes with a stiffer consistency were found to sag less than those mixes that exhibited greater flow. Sagging was reduced in shallow depth vertical repairs by placing the mortar at the top of the specimens first and progressing to the sides and bottom of the repair. Sagging was a significant problem in deep repairs, as evidenced by observations of the first deep repairs attempted in this study (DAT1, DAT2). A suggestion from the technical representatives at Chemrex to minimize sagging was to build the deep repairs from the bottom up with individual lifts of material. This approach worked marginally well when using two subsequent 6-in vertical lifts of repair mortar. The lower lift was typically allowed to set approximately 2-1/2-hours prior to placing the upper lift. However, sagging did occur in the lower lift of some specimens. Smaller lifts and/or longer times between successive lifts may have produced even less sagging and therefore better results, but the time required to make multiple lift repairs can make this approach undesirable.

Manufacturer installation instructions for each of the three prepackaged repair materials did not state how to achieve consolidation of the repair mortar. Numerous types of consolidation procedures for the repair mortar were attempted on the vertical repairs. Consolidation was attempted with a flat bar, by hand, putty knife pressure, round-nosed dowels, and blunt-ended bars. Using tools with a relatively large contact area such as a putty knife or blunt-ended bars worked the best for consolidating mortar into the repair area. However, excessive consolidation of the repair mortar, regardless of the tool used, resulted in sagging.

Each of the three repair materials generally finished well with the steel trowel. Repeated finishing in an effort to achieve maximum surface uniformity often contributed to sagging. It

was therefore desirable to finish the specimens with as little effort as possible. Finishing with a "dry" trowel tended to split or tear the exterior surface of the repairs, especially for repairs using polymer liquid components.

11.3.2 Visual Review of Repair Surfaces

A visual review of the repair surface for each specimen was conducted after obtaining final distance measurements between the DEMEC points and prior to performing bond tensile strength testing. The examination was performed to document obvious repair conditions such as the presence of cracking, sagging, spalling, finishing defects, and delaminations. Cracks were visually documented with the aid of a crack comparator and delaminations were located by tapping on the repair surface with a mason's hammer. Laboratory logs were completed for each set of three specimens cast for a particular material, repair depth, and post-curing condition and are included in Appendix H of Kasper's report (Kasper, 2002).

Observations were performed on March 26, 2002 (lot 1 specimens) and March 30, 2002 (lot 2 specimens). A discussion of observations follows, separated per repair material.

11.3.2.1 *Brand X Repaired Specimens*

Twelve specimens were repaired with Brand X. Two-thirds of these specimens exhibited cracking at the bottom repair-substrate joint for specimens in the vertical position. For deep repair specimens, crack widths were on the order of 2-mils. Three of the cracked shallow repair specimens had cracking at the bottom repair-substrate joint in the range of 2 to 13 mils in width, however two other shallow repair specimens exhibited cracking of greater widths. These specimens, SCS1 and SCS2, exhibited relatively wide cracking, possibly severe enough to be considered a void, at the bottom repair-substrate joint. This crack or void resembled a surface retreat of the mortar away from the substrate. The width of the cracking was on the order of 16 mils to 1/16-in and the depth of the crack was approximately 1/16-in.

Specimens SCS2, SAS1, SAS2 had signs of edge spalling along the length of the repairs (see Photo 11-25, note that the specimens have been drilled for bond tensile strength testing). Additionally, specimens SCS1, SCS3, SAS2, and DCS3 exhibited diagonal cracking along the long repair edge of the finished face. Both of these distresses are possibly due to early form removal and/or insufficient release agent on the repair formwork that was noticed after form removal.

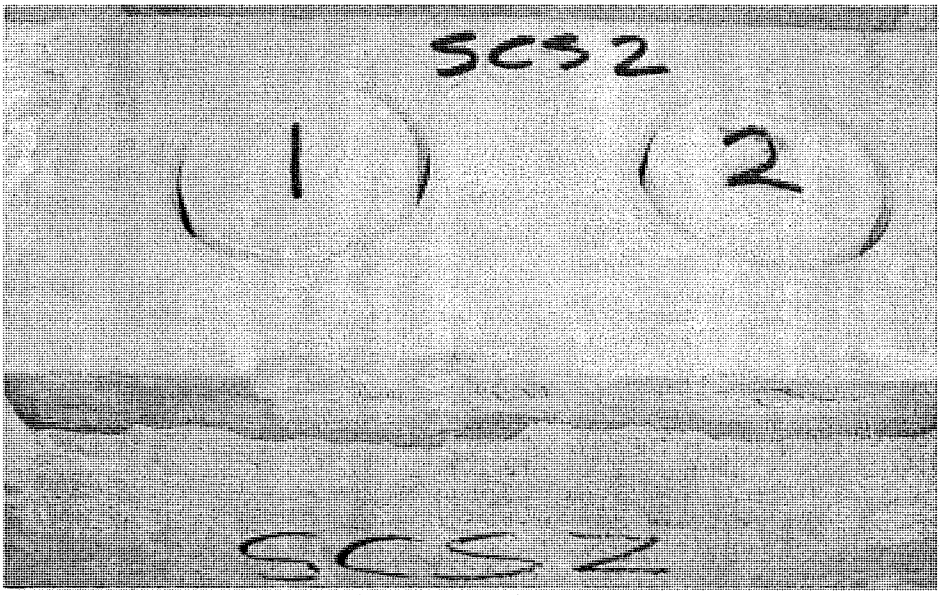

Photo 11-25. Typical edge spalling on repair specimens

Surface cracks that resembled a tearing of the surface were observed on specimens DAS3, DCS1, SAS3, and SCS1. Tearing cracks are suspected to be attributed to finishing the repair material after it had excessively hardened or excessive friction between the trowel and repair mortar.

Acoustic impact testing was performed to assess the presence of delamination between the repair mortar and concrete substrate. Testing was accomplished by tapping the surface of the repair mortar with a mason's hammer. The frequency and damping characteristics of the resulting sound gives an indication of the presence of defects (ACI, 1994). Delaminations were not detected in specimens repaired with Brand X material.

11.3.2.2 *Brand Y Repaired Specimens*

Thirteen specimens were repaired with Brand Y repair material. Most developed pattern cracking at roughly three weeks after installing the repair materials. Deep and shallow repairs made with the Brand Y material exhibited fine openings on the concrete surface that were generally parallel and normal to the length of the specimen (see Appendix H of Kasper, 2002, and Photo 11-26). Pattern cracking on the order of 2 to 3 mils in width was observed on 12 of the 13 specimens that were repaired with Brand Y material. Estimation of crack width was made using a hand-held crack comparator. An example of typical pattern cracking observed is shown in Photo 11-26. Cracks in Photo 11-26 were wetted with water to better show their presence. Reasons for pattern-cracking formation are not specifically known, however, mix proportions (dry to liquid component) and mixing time were similar between specimens that exhibited cracking and the specimen that did not crack.

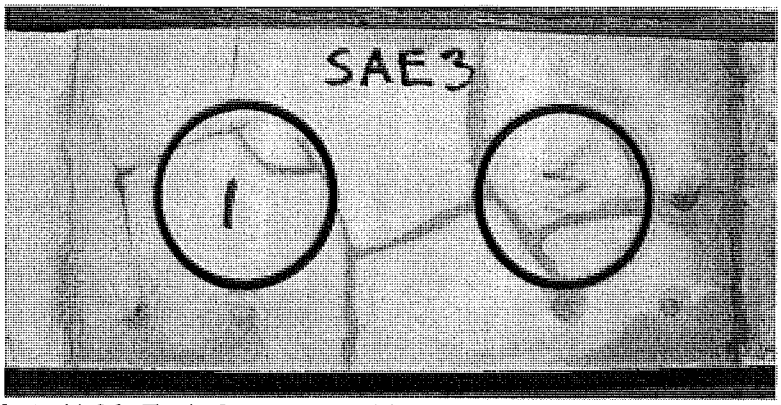

Photo 11-26. Typical pattern cracking observed on Brand Y specimens

Deep repair specimens exhibited an additional crack at the lift joint between the bottom and top halves of the repair area. Similar to the pattern cracking, the lift joint crack was documented to be on the order of 2 to 3 mils, as estimated by a crack comparator. This crack is due to shrinkage of one or both lifts of repair material. Cracks on the order of 2 to 3 mils were also present on 5 of the 6 of the deep repair specimens at the bottom repair-substrate joint of the vertical specimens.

Shallow depth repair specimens exhibited larger crack widths than did the deep repair specimens for the Brand Y repair material, especially at the bottom repair-substrate joint. Cracks at the bottom repair-substrate joint in the shallow repair vertical specimens were on the order of 10 to 60 mils in width for two-thirds of the specimens and less than 5 mils in width for the remaining two specimens. It is possible that the geometry of the shallow repairs influenced the more severe cracking compared to the deep repair specimens. One of the shallow repair specimens, SAE3, exhibited relatively wide cracking, possibly severe enough to be considered a void, at the bottom repair-substrate joint of the vertical specimen. This crack or void resembled a surface retreat of the mortar away from the substrate. The width of the cracking was roughly 50 mils and the depth of the crack was on the order of 1/16 to 1/8-in. The formation of this crack or void may be attributed to the placing the specimens too early in the curing room, before the material had sufficiently set to resist washout from curing moisture. Surface cracks that resembled a tearing of the surface were observed on specimen SAE2. Tearing cracks are likely attributed to finishing the repair material after it had excessively hardened or excessive friction between the trowel and repair mortar.

Mortar sagging near the lift joint was observed on 4 of the 6 deep repair specimens fabricated with Brand Y material. Sagging either extended on both sides of the lift joint or was present in the top lift only. The overall height of the sagging, as measured normal to the length of the specimen, was on the order of 1 to 3-in. Sagging is likely attributed to excessive weight of the plastic mortar on the lower regions of the repair, prior to these lower regions attaining sufficient set to support the plastic mortar above it.

Acoustic impact testing was performed to assess the presence of delamination between the repair mortar and concrete substrate. Delaminations were revealed through the testing on 2 of the 6 Brand Y material shallow repair specimens and are shown as hatched areas on Photo 11-27 and Photo 11-28.

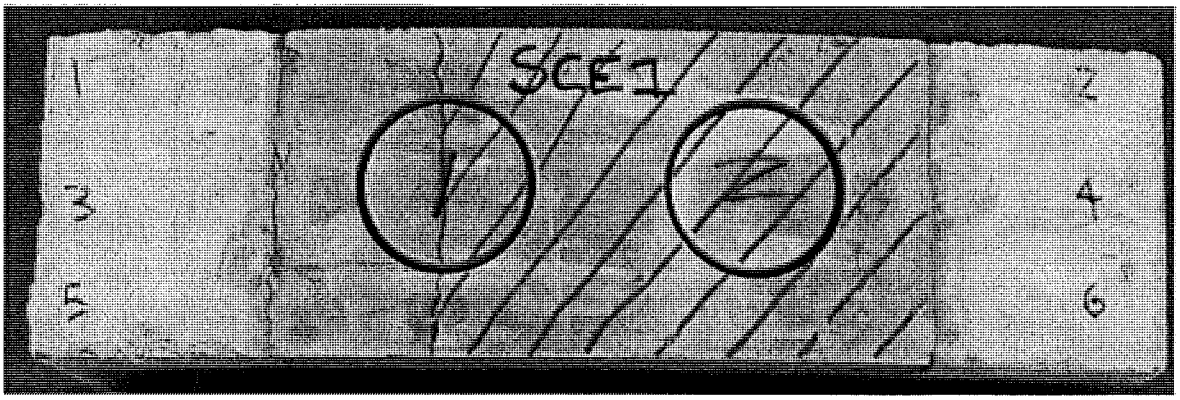

Photo 11-27. Hatched, delaminated region of specimen SCE1

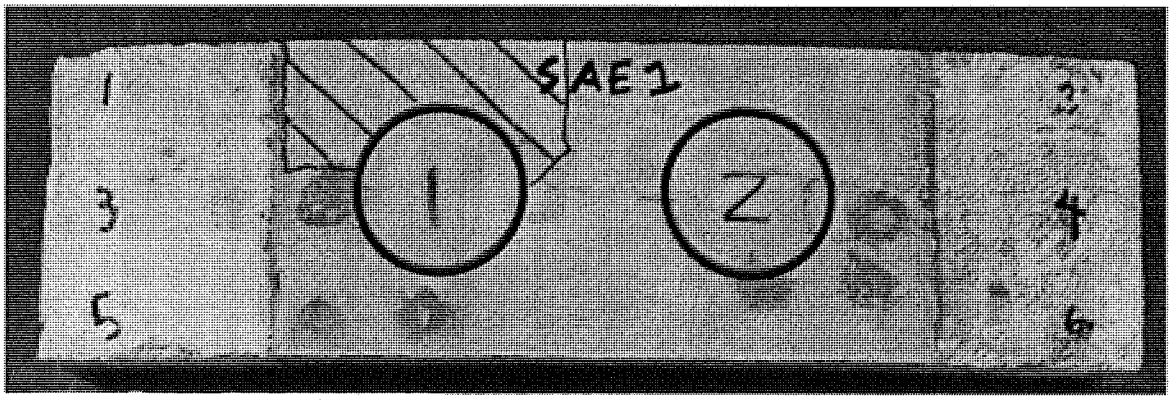

Photo 11-28. Hatched, delaminated region of specimen SAE1

Not shown in Photo 11-28 is a delaminated region of test location no. 1, which is roughly the top half (photo orientation) of core location no. 1. The potential for repair material delamination of specimen SCE1 was suspected during fabrication, as problems arose with the repair adhering to the substrate. It was suspected that the mortar scrub coat had dried on this specimen prior to application of the repair material.

11.3.2.3 *Brand Z Repaired Specimens*

Twelve specimens were repaired with Brand Z material. A condition unique to these specimens was a deposit of precipitate at the bottom repair-substrate joint of the vertical specimens. The precipitate was only present on shallow repair specimens and could be seen on 5 of the 6 shallow repair specimens. An example of the precipitate formation is shown in Photo 11-29. As shown in this photo, the precipitate tended to form trails toward the bottom of the specimen, possibly indicating that internal moisture was drawn out from the bottom joint. It is possible that the moisture then leaked down the side of the specimen assisted in creating the formations. It should be noted that the polymer liquid component used to mix the Brand Z repair material was white in color. While it is not suspected that presence of the precipitate has an immediate adverse effect on load carrying capacity, continual formation may degrade the overall integrity of the repair.

Similar to other repair materials, half of the Brand Z deep repair specimens exhibited sagging of the repair mortar. The bottom 4-in of repair area for specimens DAT 2 and DAT3 as well as the upper 4-1/2-in of the top half of the bottom lift of specimen DAT1 exhibited the sagging. Sagging is likely attributed to excessive weight of the plastic mortar on the lower regions of the repair, prior to these lower regions attaining sufficient set to support the plastic mortar above it.

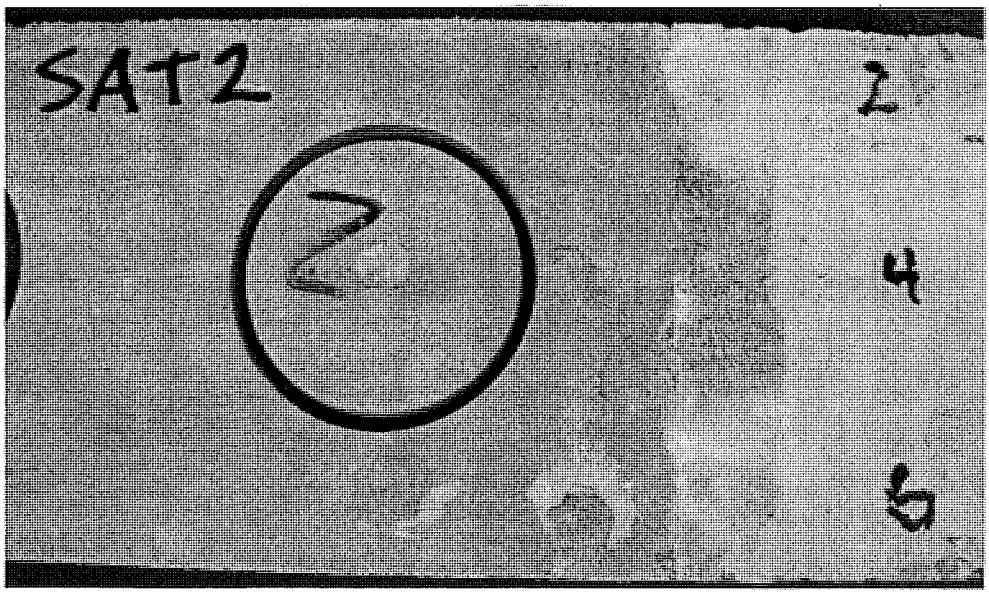

Photo 11-29. Typical white precipitate leaching from the bottom repair-substrate joint

Surface cracks that resembled a tearing of the surface mortar were observed on specimens DAT2, DAT3, SCT2, and SAT1. Tearing cracks were on the order of 2 to 16 mils in width and was likely attributed to finishing the repair material after it had excessively hardened or excessive friction between the trowel and repair mortar.

Perhaps of greater importance is the presence of wider cracking, possibly severe enough to be considered a void, at the lift joint and the bottom repair-substrate joint of some Brand Z vertical specimens. This crack or void resembled a surface retreat of the mortar away from the substrate, possibly resembling erosion of repair material at the affected location. Specimens affected by this condition included DCT2, DCT3, SAT3, and SCT3. The width of the cracking was on the order of 25 mils to 3/32-in and the depth of the cracking was roughly 1/16 to 1/8-in.

Lift joint locations were often difficult to visually distinguish on the finished surface of the Brand Z deep repair specimens. One of the six deep repair specimens exhibited cracking at the lift joint. The width of this crack was on the order of 16-mils, maximum.

Acoustic impact testing was performed to assess the presence of delamination between the repair mortar and concrete substrate. Delaminations were not detected on specimens repaired with the Brand Z repair material.

11.3.2.4 *Performance Evaluation Based on Visual Observations*

Probably of greatest interest is the formation of cracking and more specifically pattern and joint cracking. If a concrete member were free in space, it would expand and contract with changes in moisture and temperature (ACI, 1990). Expansion and contraction of the unrestrained member would occur without distress to the member and no stresses would be induced. However, if say two or more edges of the member were fixed (restrained), the member would develop tensile stresses. If the tensile stresses exceed the tensile strength of the material, cracking will occur. Cracks allow more rapid ingress of contaminants (e.g.: moisture, carbon dioxide, deicers) into the member, or in the case of this study, the repair.

ACI has suggested maximum crack widths for reinforced concrete structures, based on their service condition (ACI, 1990). These crack widths are summarized in Table 11-9.

Table 11-9. Suggested maximum crack widths for in-service structures (ACI, 1990)

Exposure Condition	Crack Width
Dry air, protective membrane	16 mils
Humidity, moist air, soil	12 mils
Deicing chemicals	7 mils
Seawater and seawater spray, wetting and drying	6 mils
Water retaining structures	4 mils

Beam-ends in locations of defective transverse deck joints could be considered to be in a wetting and drying environment. As such, a crack width of 6 mils is considered detrimental to the performance of repair materials, based on the ACI recommendations. This crack width also corresponds to a moderate crack from the vulnerability assessment in Chapter 4. Crack widths or voids greater than 6 mils were observed on 21 of the 39 repair specimens in this study (54 percent of samples), based on visual observations. Deep repair specimens exhibited cracking greater than 6 mils less frequently than shallow repair specimens based on a percentage of the total number of samples in each repair depth category. Deep repair specimens constituted 7 of the 21 specimens that had crack or void widths greater than 6 mils. These cracks are located within the repair itself and at the top and bottom of the vertical specimen. However, the expansion and contraction of the substrate impacts the repair performance in terms of cracking, including the repair-substrate joints. Not considering cracking or voids that were at the repair-substrate joints, surface cracks or voids were present on 14 of the 39 repair specimens fabricated (36 percent of samples). Cracks or voids on these specimens ranged from 7 to 60 mils in width. Comparing the quantity of specimens with cracks or voids in the region outside of the repair-substrate joints, one of the three materials clearly exhibited better performance than the others, as shown in Figure 11-2. However, the Brand Y repaired specimens had fine pattern cracking, as opposed to larger cracks. Fine pattern cracking may be detrimental to future performance if crack widths increase or the integrity of the repair is further reduced by the presence of the cracks.

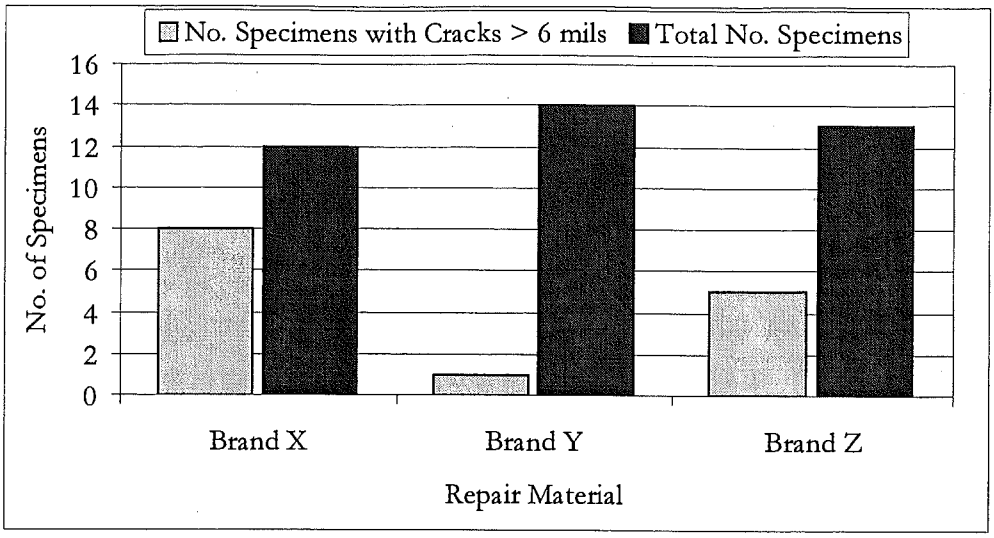

Figure 11-2. Number Of Specimens with Cracking Greater Than 6 mils Outside the Repair-Substrate Joint (Per Repair Material)

The depth of repair or type of post-curing environment appears to have little effect on the performance of the repairs, in terms of cracks greater than 6 mils in width. This is shown in Figure 11-3 and Figure 11-4.

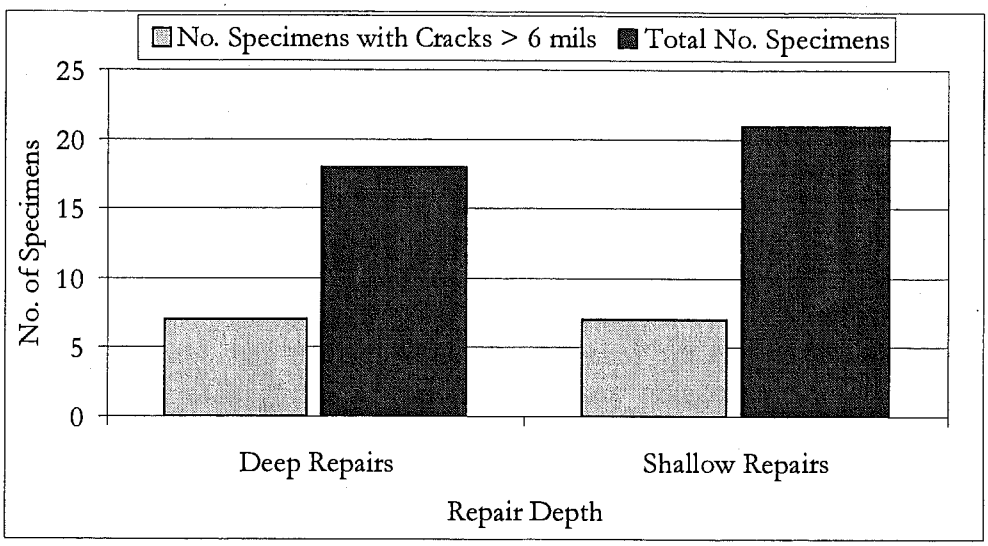

Figure 11-3. Number Of Specimens with Cracking Greater Than 6 mils Outside the Repair-Substrate Joint (Per Repair Depth)

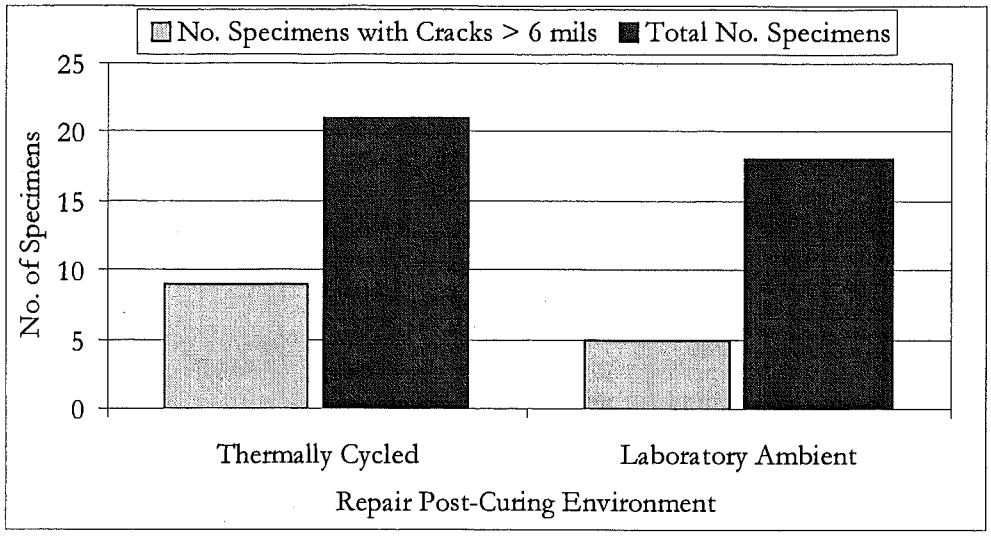

Figure 11-4. Number Of Specimens with Cracking Greater Than 6 mils Outside the Repair-Substrate Joint (Per Repair Post-Curing Environment)

General expectations of the repairs prior to application were that they not be cracked or delaminated from the substrate after the post-curing period. As evidenced in the previous discussion, cracking and delamination of many repairs did occur. If the repair adhered to the prepared substrate during patching, the repairs did not delaminate with exception of one specimen. From a finishing standpoint, it was expected that finishing would take place without damage to the repair. The development of tearing cracking and increased tendency for sagging with over-finishing indicates that the repair materials did not perform as expected.

11.3.3 Strength Evaluation

Three types of strength evaluations were performed for this study. Two evaluations were performed to assess compressive strength while a third test was performed to determine bond tensile strength. Compressive strength testing was performed on standard-sized concrete cylinders and repair mortar cubes in accordance with ASTM testing standards.

11.3.3.1 *Concrete Cylinders - Compressive Strength*

Testing of the freshly mixed concrete was performed during casting of the substrate specimens. Testing included casting sixteen test compressive strength specimens per ASTM C31/C31M-00e1 (ASTM, 2001). Specimens were cured similarly to the curing procedures used for the substrate concrete described earlier. The specimens were scheduled for testing as indicated in Table 11-10.

Table 11-10. Schedule for Testing Substrate Compressive Strength Specimens

No. of Cylinders to be Tested	Conditioning	Test Age
3 + 1 spare	Wet Cure + Ambient (repair installation) before thermal cycling	30 days
3 + 1 spare	Wet Cure + Ambient	28 days
3 + 1 spare	Wet Cure + Ambient (repair installation) + Thermal Cycling	75 days
3 + 1 spare	Wet Cure + Ambient (repair installation) + Ambient (companion to above)	75 days

Due to space restrictions in the wet curing environment, the spare compressive strength specimens could not experience the same initial curing as the other specimens and were therefore discarded. Compressive strength testing was performed in general conformance with ASTM C39-01 (ASTM, 2001). Testing was conducted using a Baldwin Materials Testing Equipment Model 300CT test machine located in the Dillman Hall Laboratory. Individual strength results of the 6-in by 12-in cylinders are shown in Table 11-11.

As shown in Table 11-11, the mean 24-day compressive strength was within 70-psi or 1.4 percent of the targeted compressive strength for the substrate mixture, i.e. 5,000-psi. The coefficient of variation, COV, is defined as the standard deviation divided by the mean, and is listed in the table as percent. The mean strength of the specimens that were thermally cycled after initial curing was 10-psi less than the mean strength of those specimens that were placed in laboratory ambient conditions after initial curing.

A t-test was performed to determine whether or not there was any reason to believe that the substrate concrete (i.e., "28-day" compressive strength from Table 11-11) came from a population having a mean other than 5000-psi (Ayyub and McCuen, 1997). The use of this test requires that the two samples under consideration be independent, and normally distributed. Both assumptions were made for statistical t-tests in this study. A level of significance of 5 percent was selected for the test. This represents the probability of making a Type I error. A Type I error occurs when the null hypothesis is rejected when in fact it is actually true. The significance level of 5 percent was chosen because this is typically an acceptable level for a Type I error. The null hypothesis was that the mean 28-day compressive strength was equal to the design compressive strength 5000-psi. The alternate hypothesis was that the 28-day compressive strength was not equal to the design compressive strength, i.e., a two-sided t-test. The result of the t-test indicated that there is no statistical reason to believe that the "28-day" compressive strength of the substrate was from a population with a mean other than 5000-psi.

A two-sided t-test was also performed to determine if there was any reason to believe that the mean compressive strengths were not equal between the "End of Post-Curing Compressive

Strength - Thermally Cycled" specimens and the "End of Post-Curing Compressive Strength – Laboratory Ambient" specimens (seeTable 11-11). Because no population variance data were available, a statistical F-test was performed first to determine if the sample means came from populations with unequal and unknown or equal and unknown variances. For the F-test a level of significance of 10-percent was used. The F-test indicated that there was no statistical reason to believe that the two samples came from populations with unequal variances. Therefore, it was assumed that the population variances were equal when performing the two-sided t-test of the means. For the t-test, a level of significance of 5-percent was again used. The result of the t-test indicated that there was no statistical reason to believe that the thermally cycled and laboratory ambient test cylinders came from populations with unequal means.

Table 11-11. Concrete Compressive Strength at Various Test Ages and Post-Curing Conditioning

Specimen No.	Cast	Test Date	Age (days)	Load (lb)	Stress (psi)	Mean (psi)	COV
		"28-Day" Compressive Strength					
C1	1/8/02	2/1/01	24	143000	5060	5070	0.23%
C2	1/8/02	2/1/01	24	143000	5060		
C3	1/8/02	2/1/01	24	143500	5080		
		Start of Post-Curing Compressive Strength					
C4	1/8/02	2/7/02	30	141500	5010	5020	0.30%
C5	1/8/02	2/7/02	30	142500	5040		
C6	1/8/02	2/7/02	30	142000	5020		
		End of Post-Curing Compressive Strength - Thermally Cycled					
C7	1/8/02	3/24/02	75	147000	5200	5170	1.35%
C8	1/8/02	3/24/02	75	144000	5090		
C9	1/8/02	3/24/02	75	147500	5220		
		End of Post-Curing Compressive Strength – Laboratory Ambient					
C10	1/8/02	3/24/02	75	149000	5270	5180	1.46%
C11	1/8/02	3/24/02	75	145000	5130		
C12	1/8/02	3/24/02	75	145500	5150		

Target Design Strength = 5000-psi

11.3.3.2 *Repair Mortar Cube Compressive Strength*

Compressive strength cubes were cast for each repair material used in the study. Cubes were cast in general conformance with ASTM C109/C109M-99 (ASTM, 1999). Curing of the mortar cubes consisted of a two to seven day moist curing period. Duration of moist curing was in conformance with each repair material manufacturer's recommendations, similar to the procedure used for the repair specimens. Moist curing was performed in the Dillman Hall moist curing room. After initial curing, mortar cubes were either placed in thermally cycled or laboratory ambient temperature conditions, similar to the conditions provided for the repair specimens. The temperature of the moist cure room was not formally documented for this portion of the work but was estimated to be on the order of 55 to 60 degrees Fahrenheit daily, based on measurements obtained for other portions of this study.

Strength testing of the cubes was in general conformance with ASTM C109/C109M-99 (ASTM, 1999). Load to the specimens was applied by an MTS 810 material test system.

Force and displacement data were obtained during the test by MTS Test Star II hardware and processed with MTS Test Ware SX software.

Dates when each of the repair mortars was cast, ages at testing, and compressive strength test results are indicated in Table 11-12 through Table 11-14. Shaded data in Table 11-12 through Table 11-14 had been eliminated from calculating the mean compressive strength in accordance with ASTM C109/C109M –99 because these tests fall outside the permitted range of test results (ASTM, 1999).

Table 11-12. Brand X Compressive Strength at Various Test Ages and Post-Curing Conditioning

Specimen No.	Cast	Test Date	Age (days)	Load (lbf)	Stress (psi)	Mean (psi)	COV
		"28-Day" Compressive Strength					
M1	2/7/02	3/7/02	28	28589	7150	7630	4.26%
M2	2/7/02	3/7/02	28	30966	7740		
M3	2/7/02	3/7/02	28	30948	7740		
M4	2/7/02	3/7/02	28	31517	7880		
		Start of Post-Curing Compressive Strength					
M5	2/7/02	2/13/02	6	11581	2900	4200	2.29%
M6	2/7/02	2/13/02	6	17164	4290		
M7	2/7/02	2/13/02	6	16887	4220		
M8	2/7/02	2/13/02	6	16397	4100		
		End of Post-Curing Compressive Strength - Thermally Cycled					
M9	2/7/02	3/30/02	51	31699	7920	7530	7.42%
M10	2/7/02	3/30/02	51	28503	7130		
M11	2/7/02	3/30/02	51	27088	6770		
M12	2/7/02	3/30/02	51	32768	8190		
		End of Post-Curing Compressive Strength – Laboratory Ambient					
M13	2/7/02	3/30/02	51	28858	7210	7720	6.48%
M14	2/7/02	3/30/02	51	30998	7750		
M15	2/7/02	3/30/02	51	32826	8210		

Target 28-day strength, cured per ASTM C109 = 5500-psi (per manufacturer)

Table 11-13. Brand Y Compressive Strength at Various Test Ages and Post-Curing Conditioning

Specimen No.	Cast	Test Date	Age (days)	Load (lbf)	Stress (psi)	Mean (psi)	COV
		"28-Day" Compressive Strength					
S1	2/11/02	3/11/02	28	25294	6320	6100	3.16%
S2	2/11/02	3/11/02	28	24622	6160		
S3	2/11/02	3/11/02	28	24235	6060		
S4	2/11/02	3/11/02	28	23446	5860		
		Start of Post-Curing Compressive Strength					
S5	2/11/02	2/13/02	2	10265	2570	2520	2.81%
S6	2/11/02	2/13/02	2	8743	2190		
S7	2/11/02	2/13/02	2	9888	2470		
S8	2/11/02	2/13/02	2	10954	2740		
		End of Post-Curing Compressive Strength - Thermally Cycled					
S9	2/11/02	3/30/02	47	24040	6010	6590	0.21%
S10	2/11/02	3/30/02	47	26407	6600		
S11	2/11/02	3/30/02	47	28680	7170		
S12	2/11/02	3/30/02	47	26334	6580		
		End of Post-Curing Compressive Strength – Laboratory Ambient					
S13	2/11/02	3/30/02	47	27892	6970	5050	0.98%
S14	2/11/02	3/30/02	47	20339	5080		
S15	2/11/02	3/30/02	47	20052	5010		

Target 28-day strength, cured per ASTM C109 = 5000-psi (per manufacturer)

Table 11-14. Brand Z Compressive Strength at Various Test Ages and Post-Curing Conditioning

Specimen No.	Cast	Test Date	Age (days)	Load (lbf)	Stress (psi)	Mean (psi)	COV
		"28-Day" Compressive Strength					
T1	2/5/02	3/5/02	28	29635	7410	7820	6.65%
T2	2/5/02	3/5/02	28	32110	8030		
T3	2/5/02	3/5/02	28	33800	8450		
T4	2/5/02	3/5/02	28	29460	7370		
		Start of Post-Curing Compressive Strength					
T5	2/5/02	2/13/02	8	19276	4820	4390	9.66%
T6	2/5/02	2/13/02	8	16000	4000		
T7	2/5/02	2/13/02	8	18744	4690		
T8	2/5/02	2/13/02	8	16361	4090		
		End of Post-Curing Compressive Strength - Thermally Cycled					
T9	2/5/02	3/30/02	53	27781	6950	8970	0.76%
T10	2/5/02	3/30/02	53	35689	8920		
T11	2/5/02	3/30/02	53	35816	8950		
T12	2/5/02	3/30/02	53	36213	9050		
		End of Post-Curing Compressive Strength – Laboratory Ambient					
T13	2/5/02	3/30/02	53	39031	9760	Retest Required	
T14	2/5/02	3/30/02	53	14621	3660		
T15	2/5/02	3/30/02	53	23583	5900		

Target 28-day strength, cured per ASTM C109 = 5800-psi (per manufacturer)

The mean 28-day compressive strength of each repair mortar exceeded the 28-day compressive strength stated on mortar manufacturer's technical data sheet (Sika USA, 2002; Chemrex 2002a; Chemrex 2002b) on the order of 600 to 2,200-psi. As with the concrete cylinders, F-tests and t-tests were performed for each repair material to determine if there was any statistical reason to believe that the 28-day repair mortar strengths were not representative of a population having a mean compressive strength as stated on the manufacturer data sheets (the null hypothesis). As before, F-tests were performed prior to performing the t-tests in order to determine, with a 10-percent level of significance, if the population variances can be assumed to be unknown and equal or unknown and not equal. The result of the F-test determined which t-test was to be performed (i.e., test with unknown and equal population variances or test with unknown and unequal population variances). The F-test indicated that there was no statistical reason to believe that the two samples came from populations with unequal variances. Therefore, it was assumed that the population variances were equal when performing the two-sided t-test of the means. Using a level of significance of 5-percent, the t-test indicated that for each repair material the null hypothesis should be rejected. In other words, for each repair material, there was reason to believe that the mean 28-day compressive strength was representative of a population with a mean different than that indicated on the repair manufacturer data sheet (see Appendix F of Kasper's report (Kasper, 2002)).

Depending on the repair material, the post-curing strength may be greater for the laboratory ambient or thermally cycled test cubes. The difference in mean compressive strength between the two post-curing environments ranged from 190 to 1540-psi depending on the repair material. It should be noted however that, as shown in Table 11-14, an end of laboratory ambient post-curing mean compressive strength for Brand Z material could not be calculated per ASTM C109/C109M. An insufficient amount of individual test results were available to determine a mean compressive strength if outlying test results are not considered.

As with the concrete cylinders, t-tests were performed to determine if, for each repair material, there was a statistical difference between the post-curing mean compressive strengths. These tests were performed on sample means based on the corrected strength data (see ASTM C109/C109M). As such, a t-test was not performed on the Brand Z material because one of the two means could not be calculated due to excessive outlying data.

For these tests, the alternate hypothesis was that the population means were not equal. As there was no information available on the population variance for each material, F-tests were performed first to determine if the samples were from populations with equal or unequal variances, again assuming a 10-percent level of significance. The results of the F-test indicated that there was no statistical reason to believe that the samples came from populations with different variances. With information known, the t-tests were performed. The statistical tests indicated that for the Brand Y material, there was no reason to believe that the mean post-curing compressive strengths were from populations having different means. However, the t-test performed for the Brand X material indicated that the null hypothesis should be rejected. In other words, there the samples come from populations with unequal means. As such, a conclusive relationship could not be established between post-curing thermal conditions and mortar compressive strength.

11.3.3.2.1 Performance Evaluation for Compressive Strength of Repair Mortars

One of the objectives of this study was to determine whether the repair materials could develop sufficient compressive strength to assist the substrate in carrying loads. Test results indicated that each of the 28-day repair mortar compressive strengths was in excess of the strength of the substrate, and presumably, therefore, of many in-service structures (see Table 2-3). It should be noted that although the test procedures used to cast the specimens were in accordance with ASTM standards, the specimen sizes and overall preparation methods were considerably different. No relationship is known that normalizes one test procedure to another, nor is it known if one is needed.

Therefore, based on compressive strength data alone, it is not possible to make a statement on how the strength of a material relates to repair performance. However, relationships may exist between compressive strength and other properties that can be better related to performance. This is examined in a future section of this report, *Bond Tensile Strength of Substrate.*

11.3.3.3 *Bond Tensile Strength of Repairs*

Bond tensile strength testing was performed on each of the repaired specimens and on four non-repaired control specimens. The practices recommended in British Standard 1881 : Part 207 (BSI) were followed to assess the bond tensile strength of either the repair material to the concrete substrate or the substrate itself (British Standard Institution, 1992). In general, the test involves predrilling the repair and substrate, preparing the testing surface, securing a steel disk to the repair, advancing a core around the disk into the repair and substrate, and applying a tensile load to the disk from a testing instrument.

For the purposes of this study two test locations were created on each repair specimen as shown in Figure 11-5.

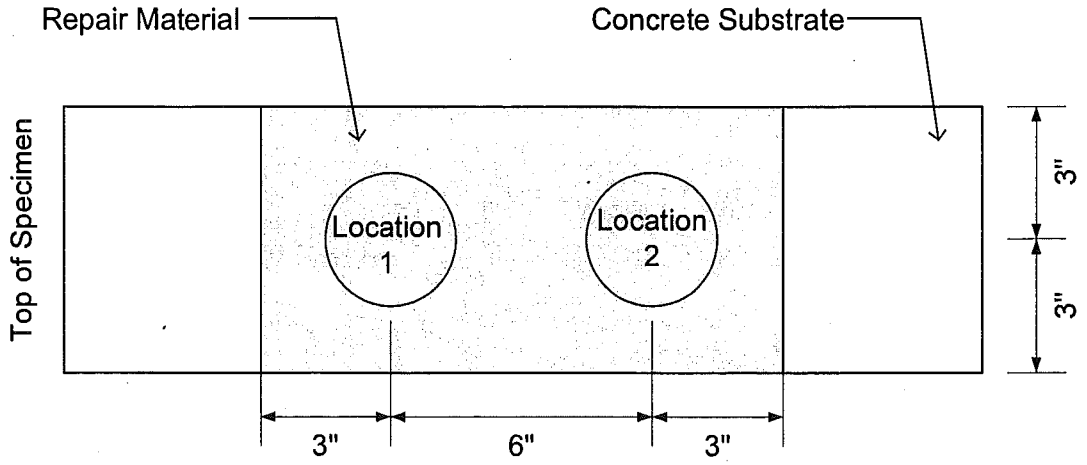

Figure 11-5. Repair Specimen Bond Tensile Strength Locations

For vertically repaired specimens, test location no. 1 was designated as the test location on the top half of the specimen. Test location no. 2 was located in the bottom half of the repair area. For specimens cast, cured, and conditioned in the overhead position, test location no. 1 was

positioned closest to the odd numbered DEMEC point locations, similar to the practice used for the vertical specimens.

For this study, coring of the specimen was performed first, followed by surface preparation, disk application, and load testing. In order to conduct the test, it was first necessary to drill through the repair material into the substrate. A 3-in inside diameter wet cut diamond core bit fitted on a 20-amp Milwaukee Diamond Coring motor attached to a Milwaukee Dymorig coring rig was used to advance the hole into the specimen. Along with the coring rig, a treated wood drilling platform and guide fence were fabricated, leveled, and bolted to the laboratory's concrete floor (see Photo 11-30). Leveling was performed using a torpedo level in an effort to produce a core with an axis perpendicular to that of the repair surface. With the specimens positioned on the drilling platform and core bit advanced to the repair surface, a guide stop was clamped to set the rig mast to the required drilling depth.

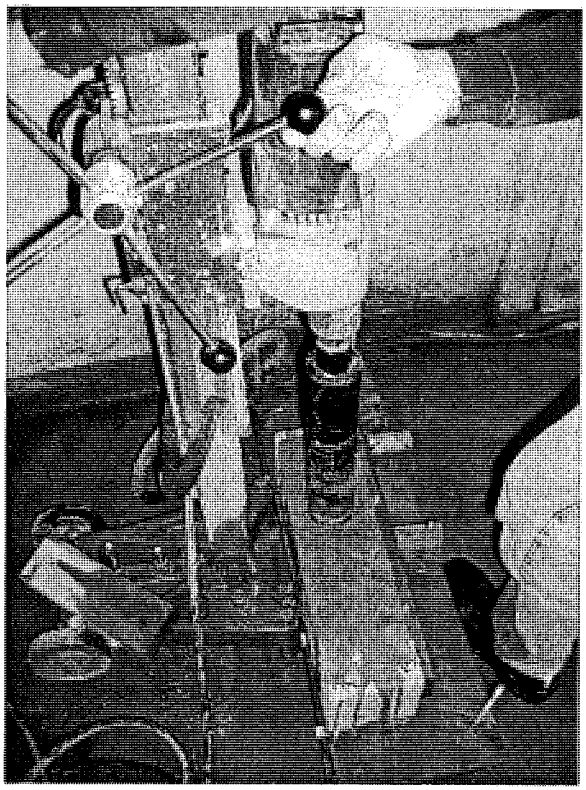

Photo 11-30. Drilling rig and platform used for the study

Nominal drilling depths were set to 4-in for deep repair specimens or 2-in for shallow repair specimens. These depths result in a nominal drilling depth of 1-in into the concrete substrate, which was the drilling depth used in the control specimens. BSI specifications require that the annulus of the core not be closer than the maximum nominal aggregate size from reinforcement (British Standards Institute, 1992). The BSI core depth requirement was exceeded for this study with the deep repair specimens, with the annulus approximately 1/4-in from the reinforcing steel. A distance of 1/2-in between the core annulus and the reinforcement would have met the BSI specification. In addition, other researchers have

suggested that the depth of drilling into the substrate should be 1-in or one-half the core diameter, whichever is larger (Vaysburd and McDonald, 1999).

Test locations on the specimen for this study also met the BSI specification for required geometry (British Standard Institution, 1992). BSI specifications require that the center of test locations be at least two core hole diameters apart. In addition, the specification states that the center of a test location should not be closer than one core diameter from an edge. Given that the cores for this study were 3-in in diameter, both geometry requirements of the specification were satisfied.

Surface preparation for the repair specimens consisted of first scrubbing the test surface with a wire brush and then blowing surface debris free with compressed air. The majority of repair specimens had a repair surface that was generally planar, however some specimens had surface irregularities (e.g. sagging) that were either ignored or partially remedied by filling depressions with adhesive. A plane surface, normal to that of the axis of the core, was desired to be able to apply a uniform axial load to the test location.

After the surface had been prepared, 3-in diameter, 1-in thick steel disks were adhered to the test surface using a fast-setting epoxy supplied by Germann Instruments, Evanston, Illinois. Generally, the adhesive was mixed to a fluid paste consistency and evenly distributed on the disk with a steel dowel (see Photo 11-31). Once placed on the test location, rotating the disk several times under pressure and then placing a weight on the top of the disk adequately seated the disks. Disk rotation during seating was performed to distribute the adhesive over the test location. Excess adhesive around the perimeter of the disk was removed with the steel dowel once seating was complete. Curing of the adhesive was accelerated by heating the adhesive and steel disk with a hot air gun for 10-minutes.

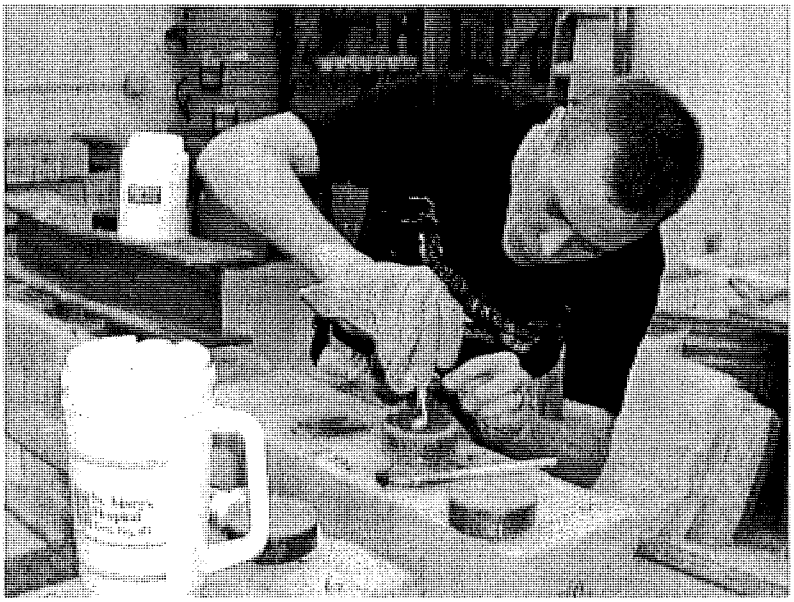

Photo 11-31. Application of adhesive to the steel disk

Test locations were loaded using a Germann Instruments BOND-TEST testing instrument. The instrument attached to the adhered disk through a pull bolt assembly (see Photo 11-32)

and applied load by reacting against the surrounding material via a counter pressure frame (see Photo 11-33).

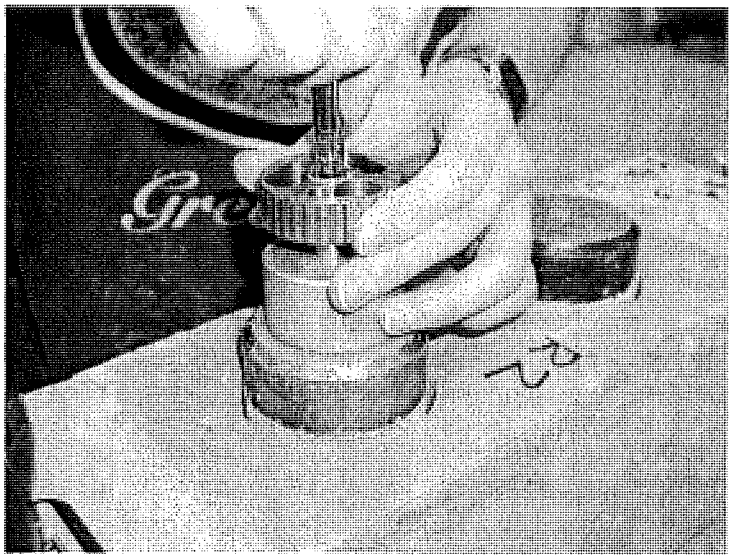

Photo 11-32. Securing the pull bolt to the steel disk

Test load was applied by hand at a rate of approximately 3-psi per second (0.1-kN per second per instrument display) until failure as shown in Photo 11-33. Specimens were air-dried at the time of testing. The rate of load application was in conformance with the BSI test specifications of 3 to 11-psi per second (British Standard Institution, 1992).

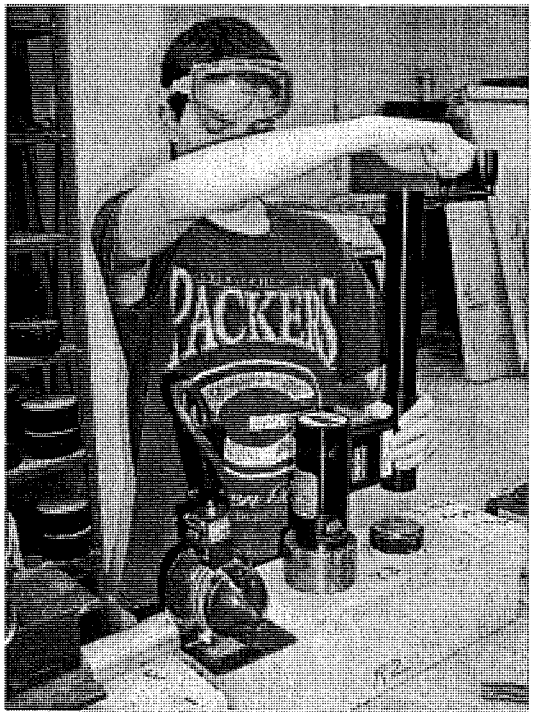

Photo 11-33. Bond tensile strength testing in progress

The failure stress was determined by matching the failure force to a stress calibration chart for the instrument. The calibration chart is included in Appendix I of Kasper's report (Kasper, 2002). Test results for each specimen, including information at various testing stages, failure loads, equivalent stresses, failure modes, and observations are included in Appendix J of Kasper's report (Kasper, 2002).

11.3.3.3.1 Failure Modes

When a direct tensile load is applied to a repair on a substrate, one of six potential failure modes is possible. These modes are:

Mode A. Bond failure at steel disk-repair interface,
Mode B. Cohesive failure of the repair mortar,
Mode C. Adhesive bond failure at the repair-substrate interface,
Mode D. Partial adhesive failure at the repair-substrate interface and cohesive failure of the repair mortar,
Mode E. Partial adhesive failure at the repair-substrate interface and cohesive failure of the substrate, and
Mode F. Cohesive failure of the substrate

Illustrations of each of these failure types are shown in Figure 11-6.

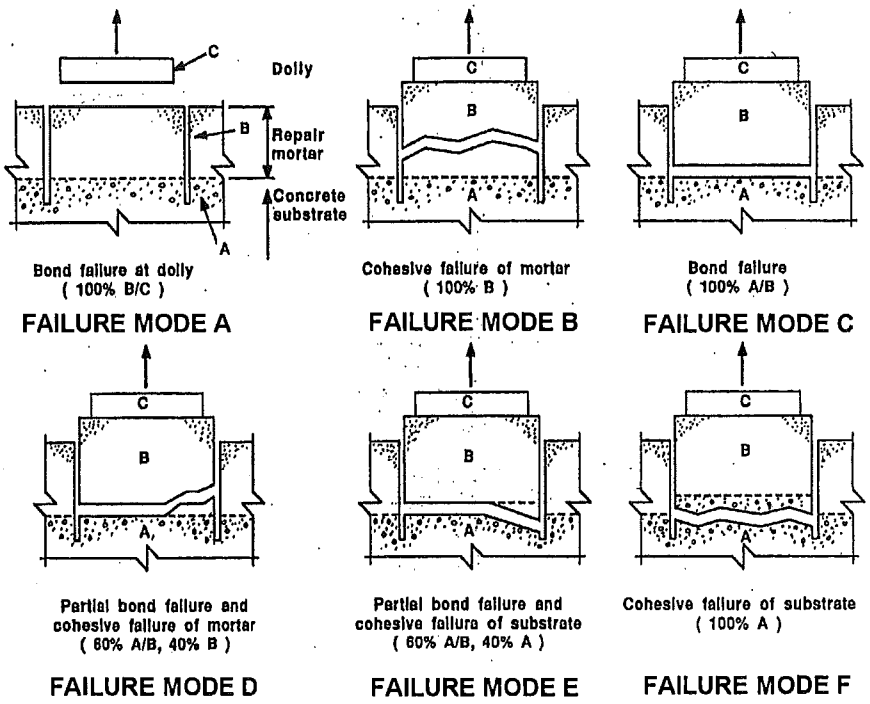

Figure 11-6. Bond Tensile Strength Test Failure Modes (Vaysburd and McDonald, 1992)

Figure 11-6 shows a smooth interface between the substrate (labeled A) and the repair mortar (labeled B). However, the actual interface for specimens in this study was rough, as would be expected in field repairs. Because of the texture at the repair-substrate interface, it was often

difficult to distinguish between failure modes C, D, and E. A common feature of failure modes C, D, and E is that each of the failures occurs near the interface of the repair and substrate. Therefore, for the purposes of comparing the test data, test failures corresponding to either a mode C, D, or E failure were designated as one mode: C-D-E. BSI as well as Vaysburd and McDonald have suggested that mode "A" failures not be included when calculating the mean bond tensile strength (British Standard Institution, 1992; Vaysburd and McDonald, 1999). Where disk-repair interface failures were encountered (mode A), efforts to perform at least one retest were made, with the exception of specimen SAS2, test location no. 2. As shown in the summary tables (Table 11-15 through Table 11-19), two of the test locations exhibited mode "A" failures at the conclusion of testing. Because the number of these failure types was relatively small, they were included when averaging the mean failure stress of a repair material per a given depth of repair and post-curing conditioning.

11.3.3.3.2 Bond Tensile Strength Test Results

Summary tables of the mean bond tensile strength tests are presented in Table 11-15 through Table 11-19. Table 11-15 includes tests results for all specimens, regardless of repair depth or type of post-curing environment. Individual test data are included in Appendix J of Kasper's report (Kasper, 2002).

Table 11-15. Summary of Bond Tensile Strength Test Statistics - All Depth and Post-Curing Specimens

Failure Mode	Statistic	Material			Total
		X	Y	Z	
A	No. Failures	1	-	1	2
	Mean (psi)	128		180	154
	COV	-		-	24%
B	No. Failures	-	8	4	11
	Mean (psi)		141	159	147
	COV		50%	84%	59%
C-D-E	No. Failures	22	18	16	56
	Mean (psi)	147	150	185	159
	COV	66%	47%	42%	53%
F	No. Failures	1	-	3	4
	Mean (psi)	226		297	279
	COV	-		7%	14%
All Modes	No. Failures	24	26	24	
	Mean (psi)	149	147	195	
	COV	63%	46%	46%	

Alternate ways of viewing the data presented in Table 11-15 are shown in Table 11-16 through Table 11-19. These tables examine the mean bond tensile strength test results when considering the four different repair and post-curing scenarios possible for this study.

Table 11-16. Summary of Bond Tensile Strength Test Statistics – Deep Repair, Thermally Cycled Post-Curing Specimens

Failure Mode	Statistic	Material			Total
		X	Y	Z	
A	No. Failures	-	-	1	1
	Mean (psi)			180	180
	COV			-	-
B	No. Failures	-	2	-	2
	Mean (psi)		105		105
	COV		71%		71%
C-D-E	No. Failures	6	4	2	12
	Mean (psi)	225	197	265	222
	COV	15%	18%	53%	26%
F	No. Failures	-	-	3	3
	Mean (psi)			297	297
	COV			7%	7%
All Modes	No. Failures	6	6	6	18
	Mean (psi)	166	225	267	219
	COV	39%	15%	30%	33%

Table 11-17. Summary of Bond Tensile Strength Test Statistics – Deep Repair, Ambient Post-Curing Specimens

Failure Mode	Statistic	Material			Total
		X	Y	Z	
A	No. Failures	-	-	-	0
	Mean (psi)				
	COV				
B	No. Failures	-	4	2	6
	Mean (psi)		187	173	182
	COV		23%	62%	32%
C-D-E	No. Failures	5	2	4	11
	Mean (psi)	169	162	238	193
	COV	24%	8%	25%	29%
F	No. Failures	1	-	-	1
	Mean (psi)	226			226
	COV	-			-
All Modes	No. Failures	6	6	6	18
	Mean (psi)	178	178	216	191
	COV	24%	20%	35%	28%

Table 11-18. Summary of Bond Tensile Strength Test Statistics – Shallow Repair, Thermally Cycled Post-Curing Specimens

Failure Mode	Statistic	Material			Total
		X	Y	Z	
A	No. Failures	-	-	-	0
	Mean (psi)				
	COV				
B	No. Failures	-	2	-	2
	Mean (psi)		87		87
	COV		37%		37%
C-D-E	No. Failures	6	6	6	18
	Mean (psi)	41	103	155	100
	COV	163%	76%	27%	77%
F	No. Failures	-	-	-	0
	Mean (psi)				
	COV				
All Modes	No. Failures	6	8	6	20
	Mean (psi)	41	99	155	98
	COV	163%	68%	27%	74%

Table 11-19. Summary of Bond Tensile Strength Test Statistics – Shallow Repair, Ambient Post-Curing Specimens

Failure Mode	Statistic	Material			Total
		X	Y	Z	
A	No. Failures	1	-	-	1
	Mean (psi)	128			128
	COV	-			-
B	No. Failures	-	-	2	2
	Mean (psi)			146	146
	COV			141%	141%
C-D-E	No. Failures	5	6	4	15
	Mean (psi)	157	163	138	154
	COV	75%	44%	46%	53%
F	No. Failures	-	-	-	0
	Mean (psi)				
	COV				
All Modes	No. Failures	6	6	6	18
	Mean (psi)	152	163	140	152
	COV	70%	44%	74%	59%

It should be noted that the mean failure stress for the two specimens repaired in the overhead position (R2 and R5) was 134-psi with a coefficient of variation (COV) of 57-percent. Three failures were at the repair interface (mode C-D-E) and one failure was observed within the repair material itself (mode B).

11.3.3.3.3 Discussion of Bond Tensile Strength Results

The relatively high COV indicates that there is a wide dispersion of test data about the calculated mean. Other researchers have experienced coefficients of variation on the order of 17 to 26 percent when performing bond tensile strength testing of concrete repair materials with this type of equipment (Vaysburd and McDonald, 1999). The higher COV's for this study are likely due to the large number of failures at the repair-substrate interface, and the variable results due to bond quality at this failure location. Examining the study by Vaysburd and McDonald (1999), it is seen that their work was performed on specimens in the horizontal position on relatively large slabs using repair mortars and concretes.

Bond tensile strength results for the repair specimens could not be compared to any existing data using the same materials and procedures. In addition, repair material manufacturers report different types of bond strength tests and not necessarily test results per the BSI test standard.

In light of the wide dispersion of test data, some statistical observations can be made. Of particular interest in this study are the effects of repair depth and post-curing conditioning. In

general, the mean bond tensile strength of deep repairs was greater than that of shallow repairs, regardless of the test material used. Depending on the material, the range of mean bond tensile strength difference was on the order of 15 to 126-psi between deep and shallow repairs for a given post curing conditioning.

To statistically examine the impact of these variables in the repair specimen bond tensile strengths, t-tests were performed at a significance level of 5-percent. When comparing repair materials of different depth and the same post-curing conditioning, an alternate hypothesis was selected such that the population mean of variable 1 was less than the population mean of variable 2 (i.e., H_A: $\mu_1<\mu_2$). However, when performing t-tests between repairs of similar depth and different post-curing conditioning, the alternate hypothesis was stated such that the population means were not equal (i.e., H_A: $\mu_1\neq\mu_2$). As before, F-tests were performed prior to performing the t-tests in order to determine, with a 10-percent level of significance, if the population variances can be assumed to be unknown and equal or unknown and not equal. The result of the F-test determined which t-test was to be performed (i.e., test with unknown and equal population variances or test with unknown and unequal population variances). The results of the F and t-tests are presented in Table 11-20 through Table 11-22.

Table 11-20. t-Test Results for Brand X Material

Material: Brand X			Variable 1			
Depth Comparison	*t-Test:*	H_O: $\mu_1=\mu_2$ H_A: $\mu_1<\mu_2$	Shallow Cycled		Shallow Ambient	
			F-test Result	*t-Test Result*	*F-test Result*	*t-Test Result*
	Variable 2	Deep Cycled	$\sigma_1^2=\sigma_2^2$	$\mu_1<\mu_2$		
		Deep Ambient			$\sigma_1^2\neq\sigma_2^2$	$\mu_1=\mu_2$
Post-Curing Comparison	*t-Test:*	H_O: $\mu_1=\mu_2$ H_A: $\mu_1\neq\mu_2$	Deep Ambient		Shallow Ambient	
			F-test Result	*t-Test Result*	*F-test Result*	*t-Test Result*
	Variable 2	Deep Cycled	$\sigma_1^2=\sigma_2^2$	$\mu_1=\mu_2$		
		Shallow Cycled			$\sigma_1^2=\sigma_2^2$	$\mu_1=\mu_2$

Note: F-test hypothesis were H_O: $\sigma_1^2=\sigma_2^2$ and H_A: $\sigma_1^2\neq\sigma_2^2$

Table 11-21. t-Test Results for Brand Y Material

Material: Brand Y			Variable 1			
Depth Comparison	*t-Test:*	H_O: $\mu_1=\mu_2$ H_A: $\mu_1<\mu_2$	Shallow Cycled		Shallow Ambient	
			F-test Result	*t-Test Result*	*F-test Result*	*t-Test Result*
	Variable 2	Deep Cycled	$\sigma_1^2=\sigma_2^2$	$\mu_1<\mu_2$		
		Deep Ambient			$\sigma_1^2=\sigma_2^2$	$\mu_1=\mu_2$
Post-Curing Comparison	*t-Test:*	H_O: $\mu_1=\mu_2$ H_A: $\mu_1\neq\mu_2$	Deep Ambient		Shallow Ambient	
			F-test Result	*t-Test Result*	*F-test Result*	*t-Test Result*
	Variable 2	Deep Cycled	$\sigma_1^2=\sigma_2^2$	$\mu_1=\mu_2$		
		Shallow Cycled			$\sigma_1^2=\sigma_2^2$	$\mu_1=\mu_2$

Note: F-test hypothesis were H_O: $\sigma_1^2=\sigma_2^2$ and H_A: $\sigma_1^2\neq\sigma_2^2$

Table 11-22. t-Test Results for Brand Z Material

Material: Brand Z			Variable 1			
Depth Comparison	*t-Test:*	H_O: $\mu_1=\mu_2$ H_A: $\mu_1<\mu_2$	Shallow Cycled		Shallow Ambient	
			F-test Result	*t-Test Result*	*F-test Result*	*t-Test Result*
	Variable 2	Deep Cycled	$\sigma_1^2=\sigma_2^2$	$\mu_1<\mu_2$		
		Deep Ambient			$\sigma_1^2=\sigma_2^2$	$\mu_1=\mu_2$
Post-Curing Comparison	*t-Test:*	H_O: $\mu_1=\mu_2$ H_A: $\mu_1\neq\mu_2$	Deep Ambient		Shallow Ambient	
			F-test Result	*t-Test Result*	*F-test Result*	*t-Test Result*
	Variable 2	Deep Cycled	$\sigma_1^2=\sigma_2^2$	$\mu_1=\mu_2$		
		Shallow Cycled			$\sigma_1^2\neq\sigma_2^2$	$\mu_1=\mu_2$

Note: F-test hypothesis were H_O: $\sigma_1^2=\sigma_2^2$ and H_A: $\sigma_1^2\neq\sigma_2^2$

As shown in Table 11-20 through Table 11-22, the null hypothesis was rejected when comparing the population means of the shallow cycled specimens to the deep cycled specimens for each of the three repair materials. In other words, given a 5-percent level of significance, the population mean of the shallow cycled specimens is less than the population mean of the deep cycled specimens. For all other bond tensile strength mean comparisons, the null hypothesis was accepted, meaning that there was no statistical reason to believe that the population means are not equal.

Prior to performing bond tensile strength testing, it was expected that there might be a difference between the specimens of different post curing conditions. It was thought that thermally cycling two different materials, with presumably different thermal expansion coefficients, would result in shearing stresses across the repair-substrate interface. These stresses could negatively impact bond tensile strength. However, results did not indicate this to be the case, as evidenced by the t-tests.

In addition, no statistical difference was expected between different depth repairs subjected to the same post curing conditions. However, thermal cycling does appear to have had an impact on the mean bond tensile strength with repairs of different thickness. A reason has not been established as to why the lower mean bond tensile strength was observed in the shallow repair specimens.

11.3.3.3.4 Comparison of Bond Tensile Strengths Based on Failure Mode

Overall, a majority of the bond tensile strength failures occurred at the repair-substrate interface (see Table 11-15). To determine whether the mean failure stress at the repair-substrate interface was lower than the mean failure stress of failures entirely within the repair mortar or substrate, t-tests were performed. The alternate hypothesis was structured such that H_A: $\mu_1<\mu_2$ with variable 1 being the mode C-D-E failures and variable 2 being either the mode B or mode F failures. See Figure 11-6 for an illustration of the failure modes.

T-tests were performed for failures within the same repair material and for all repair materials. Due to a large number of interface failures, mean bond tensile strength results for Brand X material could not be compared between failure mode C-D-E and modes B or F. Similarly, a mean comparison between the mode C-D-E and mode F failures for Brand Y material could not be performed.

As before, F-tests were performed prior to conducting the t-tests because the population variances for each of the failure modes were unknown. For each F-test, the result indicated that the null hypothesis should be accepted; therefore the population variances were assumed to be equal, but unknown.

The results of the t-tests are shown in Table 11-23.

Table 11-23. t-Test of Bond Tensile Strength Per Failure Mode

Material: Brand Y			Variable 1	
Failure Mode Comparison	*t-Test:*	H_O: $\mu_1=\mu_2$ H_A: $\mu_1<\mu_2$	Failure Mode C-D-E	
			F-test Result	*t-Test Result*
	Variable 2	Failure Mode B	$\sigma_1^2=\sigma_2^2$	$\mu_1=\mu_2$
		Failure Mode F	Insufficient Data	
Material: Brand Z			Variable 1	
Failure Mode Comparison	*t-Test:*	H_O: $\mu_1=\mu_2$ H_A: $\mu_1<\mu_2$	Failure Mode C-D-E	
			F-test Result	*t-Test Result*
	Variable 2	Failure Mode B	$\sigma_1^2=\sigma_2^2$	$\mu_1=\mu_2$
		Failure Mode F	$\sigma_1^2=\sigma_2^2$	$\mu_1<\mu_2$
Material: All Repair Materials			Variable 1	
Failure Mode Comparison	*t-Test:*	H_O: $\mu_1=\mu_2$ H_A: $\mu_1<\mu_2$	Failure Mode C-D-E	
			F-test Result	*t-Test Result*
	Variable 2	Failure Mode B	$\sigma_1^2=\sigma_2^2$	$\mu_1=\mu_2$
		Failure Mode F	$\sigma_1^2=\sigma_2^2$	$\mu_1<\mu_2$

The results of the t-tests indicated that there was no reason to believe that, given a 5-percent level of significance, there is any difference between the population means of the failures at the repair-substrate interface (mode C-D-E) and failures within the repair mortar (mode B). However, the alternate hypothesis was accepted when comparing interface and substrate failure modes. In other words, the population means of the mode F failures is greater than the population mean of the mode C-D-E failures. As indicated in Table 11-23, these statements are true when comparing the mean failure stresses of all repair materials as well as the mean failure stresses of the Brand Y and Z repairs.

11.3.3.4 *Bond Tensile Strength of Substrate*

In order to assess the effects of selective demolition on a substrate and determine the bond tensile strength of the substrate, four specimens were cast for the specific purpose of performing bond tensile strength tests. These control specimens were cast at the same time, followed the same initial curing procedures, and were subjected to each type of post-curing conditions as the repair substrate specimens. For this study, half of the control specimens were placed in a laboratory ambient post-curing environment and the others were subjected to thermally cycled post-curing conditions.

Additional surface preparation above that used for performing bond tensile strength testing on repair specimens was required in order to perform testing on the control specimens. Due to the very rough surface on the control specimens, the outer 1/8 to 1/4–inch of the finished surface was removed by passing the specimen through the masonry saw. The resulting surface was, in most cases, level enough to permit sufficient adhesive bond between the substrate and the steel disk. However, one test location, CA2-3, was noted to have an uneven surface after sawing. Not surprisingly, this test location produced a mode "A" failure during bond tensile strength testing.

After the outer surface of the control specimens had been sawn, the test locations were drilled following a procedure similar to that used for the repair specimens. Unlike the repair specimens, three test locations were created on the control specimens centered at 4, 10-1/2, and 17-in from the top of the specimen. These test locations were designated as no. 1, 2, and 3, from the top of the specimen, down. A depth of drilling into the substrate of 1-in was used for the control specimens, which matches the desired substrate drilling depth in all repair specimens in this study.

Procedures for test location cleaning, steel disk application, adhesive curing, and loading were similar to those followed for testing of the repair specimens. Refer to the earlier section in this chapter, *Bond Tensile Strength of Repairs*, for additional information on these procedures. Testing procedures also match those previously described. Test results for each specimen, including information at various testing stages, failure loads, equivalent stresses, failure modes, and observations are included in Appendix K of Kasper's report (Kasper, 2002).

Bond tensile strength failure modes for the control specimens were, by design of the test, limited to a mode A or mode F failure, because no repair material was present. Please refer to the earlier section in this chapter, *11.3.3.3.1 Failure Modes*, for illustrations of these failure modes. Mode A failures constitute a bond failure at the disk-repair interface while mode F failures are a cohesive failure of the substrate.

A summary of test statistics for bond tensile strength tests performed on the control specimens is provided in Table 11-24.

Table 11-24. Summary of Bond Tensile Strength Test Statistics – Substrate Control Specimens

Failure Mode	Statistic	Post-Curing		Total
		Cycled	Ambient	
A	No. Failures		1	1
	Mean (psi)		361	361
	COV			
F	No. Failures	6	5	11
	Mean (psi)	461	387	426
	COV	4%	22%	16%
All Modes	No. Failures	6	6	
	Mean (psi)	461	382	
	COV	4%	20%	

The mean of all bond tensile strength tests performed on thermally cycled control specimens was 461-psi, with a coefficient of variation of 16 percent. This corresponds to a value of roughly $6.5\sqrt{f_c}$, where f_c is the 28-day compressive strength. Expressed in different terms, the bond tensile strength was roughly 9 percent of f_c. This generally corresponds to the expected range of concrete tensile strength being within 8 to 15 percent of f_c (MacGregeor, 1992).

It is apparent from Table 11-24 that cycled control specimens had fairly uniform bond tensile strength test results. Greater dispersion about the mean ambient bond tensile strength was also observed. With only one low outlying mode F test result disregarded from the ambient bond tensile strength data, the mean increases to 411-psi with a coefficient of variation of 8 percent.

11.3.3.5 *Comparison of Bond Tensile Strength to Mean Mortar Compressive Strength*

Results from the bond tensile strength testing were compared to the mortar compressive strength data for each repair material to see if any trends exist between the two variables. Scatter plots were used to make a comparison between the end of post-curing mean compressive strength (thermally cycled and laboratory ambient strengths for each repair material) versus the mean bond tensile strength for each repair material with a given repair depth and post-curing conditioning. These plots are presented in Figure 11-7 through Figure 11-10.

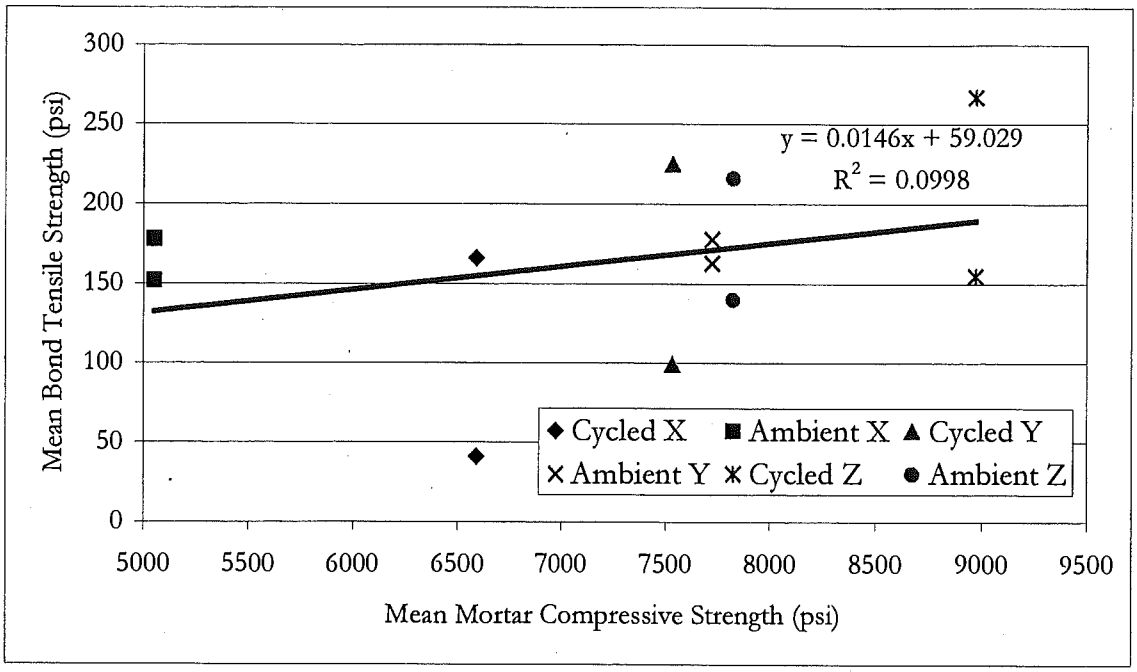

Figure 11-7. Mean Bond Tensile Strength vs. Mean Mortar Compressive Strength - All Specimens

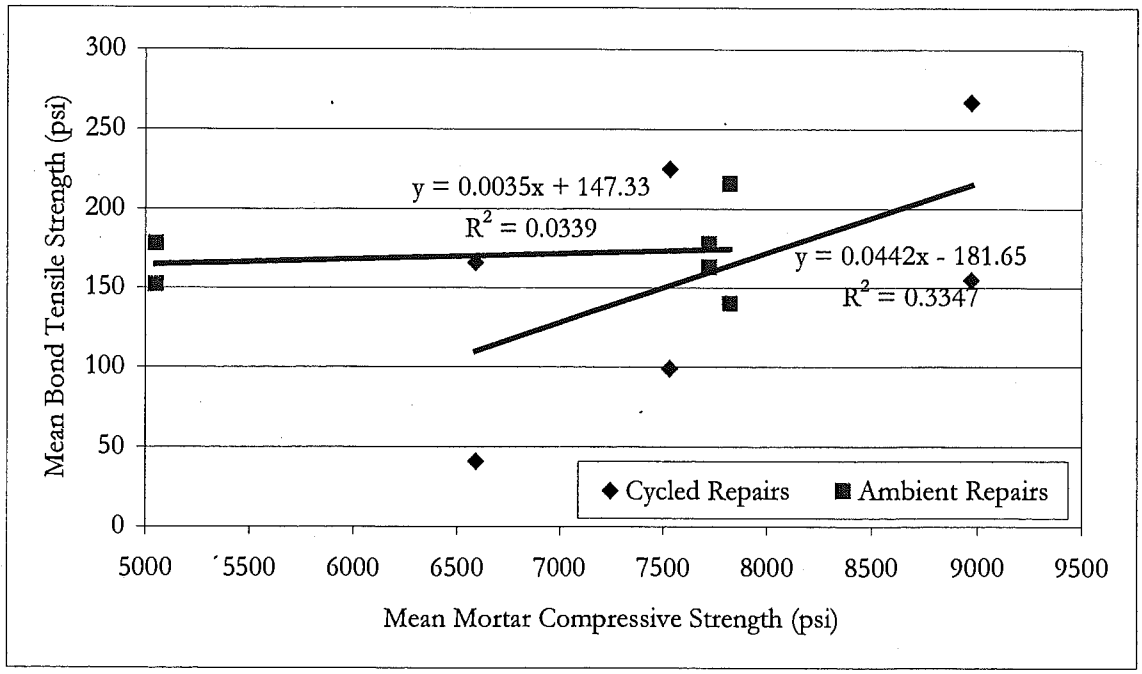

Figure 11-8. Mean Bond Tensile Strength vs. Mean Mortar Compressive Strength – Cycled vs. Ambient Post-Cured Specimens

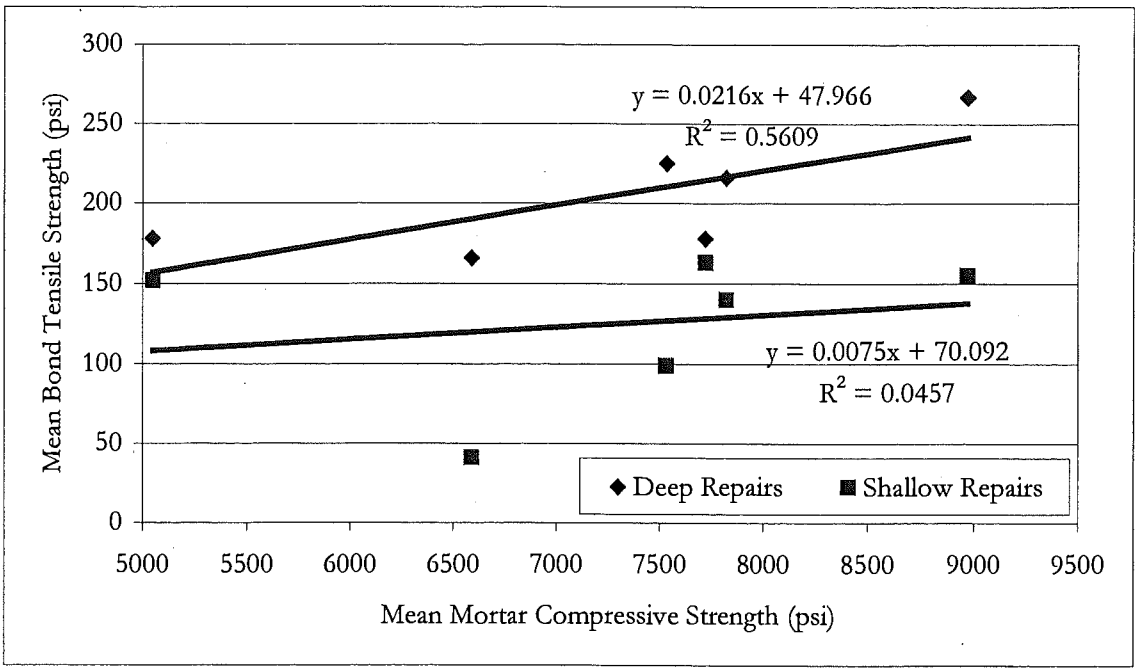

Figure 11-9. Mean Bond Tensile Strength vs. Mean Mortar Compressive Strength – Shallow vs. Deep Repair Specimens

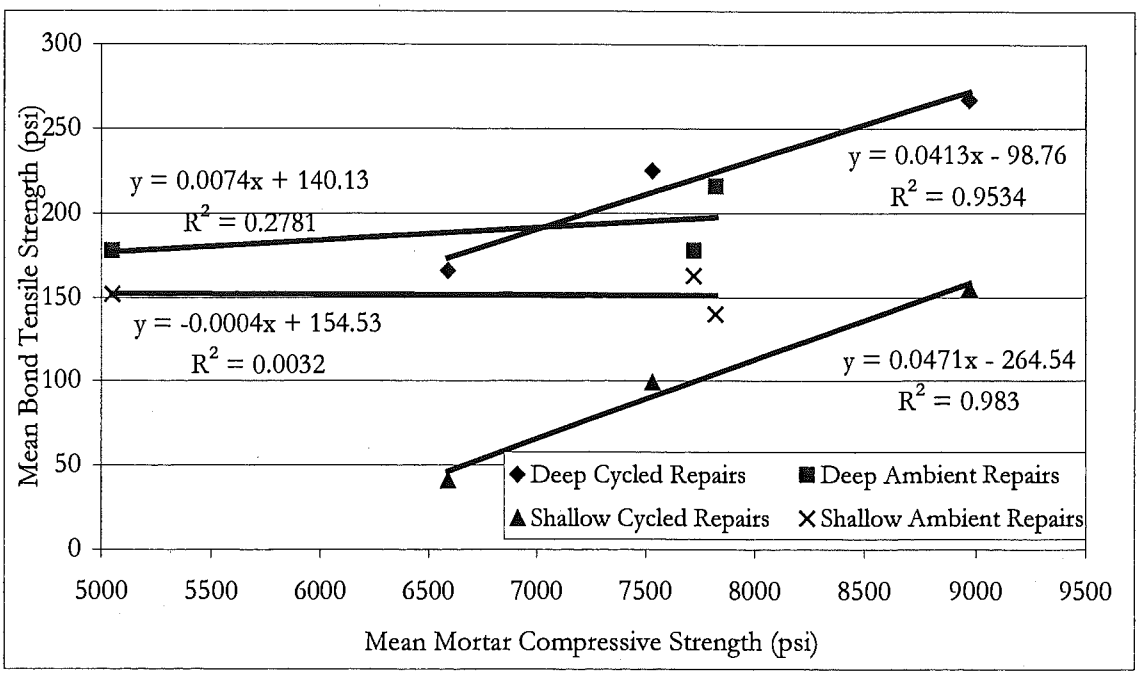

Figure 11-10. Mean Bond Tensile Strength vs. Mean Mortar Compressive Strength – Individual Depth and Post-Curing Conditions

Figure 11-7 shows a scatter plot generated from the mean compressive strength and mean bond tensile strength data. The compressive strength of the Brand Z specimens that were

post-cured in laboratory ambient conditions has been estimated to equal the 28-day compressive strength, because a mean strength could not be obtained from the actual test data. This strength (7820 psi) was used in all bond tensile vs. compressive strength plots for this study. A linear regression analysis was performed on the data in Figure 11-7 and indicates slowly increasing mean bond tensile strengths with increasing mean compressive strength. However, the data was spread widely about the regression function, as evidenced by the coefficient of determination, R^2, which was approximately 0.1. The coefficient of determination can range from 0 to 1. An R^2 value of 1 indicates that there is no variation of the data about the regression line. In contrast, a R^2 value of 0 indicates that the best estimate of the data is the mean.

Linear regression analyses generate the rate of change in one variable compared to another. This rate of change is the slope of the regression line (b_1) where the regression line can be described by the general relationship: $y = b_1 x + b_0$. For Figure 11-7, b_1 was calculated to be 0.0146. A t-test was performed to evaluate whether b_1 is equal to zero or not. If the slope of the regression line was found to be statistically equal to zero, then one could say that the best estimate of any mean bond tensile strength for a given mean mortar compressive strength would be the mean bond tensile strength. For this test, the null hypothesis was stated such that H_O: $\beta_1 = 0$, where β_1 was the slope of the population of mean bond tensile strength. The alternate hypothesis was structured such that H_A: $\beta_1 \neq 0$. Assuming a 5-percent level of confidence, the t-test indicated that the null hypothesis be accepted and that, considering all test data, the best estimate of any mean bond tensile strength for a given mean mortar compressive strength would be the mean bond tensile strength. That is, with a line slope equal to zero, the bond tensile strength is constant over the compressive strength range tested, and the best estimate is the mean of the bond tensile strength.

Another comparison was made with the data, this time looking at the specimens that were thermally cycled after curing compared to those that were in laboratory ambient conditions after curing. This plot is shown in Figure 11-8. A linear regression analysis was again performed on this data and showed, for repairs that were conditioned in laboratory ambient conditions after curing, there was little gain in mean bond tensile strength, with increasing mean compressive strength, regardless of repair depth. A t-test was also performed on each set of data in Figure 11-8 to determine if the slope of the regression line for the data was representative of a slope with a population mean equal to zero. Testing was performed similar to the analysis used for the regression of all compressive strength – bond tensile strength data points (Figure 11-7). The t-test indicated that the null hypothesis should be accepted for each regression analysis in Figure 11-8; the best estimate of any mean bond tensile strength for a given mean mortar compressive strength would be the mean bond tensile strength of the cycled or ambient post-cured repairs. However, the coefficient of determination of each regression analysis (0.33 and 0.03) indicated that the linear regression did not explain the mean bond tensile strength well.

As shown in Figure 11-9, the strength data was re-evaluated, this time considering the different depths of the repair and not considering the post-curing conditions. Linear regression analyses performed on this data indicate a general trend of increasing bond tensile strength with increasing compressive strength. t-testing of the regressions shown in Figure 11-9 was performed, similar to the analysis used for the regression of all mean compressive strength – mean bond tensile strength data points (Figure 11-7). The t-test indicated that the

null hypothesis should be accepted for each regression analysis in Figure 11-9; the best estimate of any mean bond tensile strength for a given mortar compressive strength would be the mean bond tensile strength. However, the coefficient of determination of each regression analysis (0.56 and 0.05) indicated that the linear regression did not explain the mean bond tensile strength well.

Lastly, a means comparison was performed for each repair depth and post-curing scenario. This scatter plot is shown in Figure 11-10. Linear regression analyses was performed on these four data sets and indicated an overall poor relationship between the mean bond tensile strength for the deep and shallow ambient repairs compared to the mortar compressive strength. This is indicated by the low coefficients of determination, 0.28 and 0.00 for the deep and shallow ambient repairs, respectively. A strong relationship between the mean bond tensile strength and mean mortar compressive strength can be observed in Figure 11-10 for the deep and shallow cycled repairs; R^2 for these data were 0.95 and 0.98, respectively. t-testing of the regressions shown in Figure 11-10 was performed, similar to the analysis used for the regression of all mean compressive strength – mean bond tensile strength data points (Figure 11-7). The t-test indicated that the null hypothesis should be accepted for each regression analysis in Figure 11-10; the best estimate of any mean bond tensile strength for a given mortar compressive strength would be the mean bond tensile strength.

An alternate presentation of the data in Figure 11-7 through Figure 11-10 is to compare individual bond tensile strength data, rather than the mean strengths. As the data in Figure 11-10 appeared to show the most promise for providing the most conclusive results, the regression analyses in this Figure were re-calculated, based on the actual test data, rather than the mean strengths. These plots are presented in Figure 11-11 through Figure 11-14.

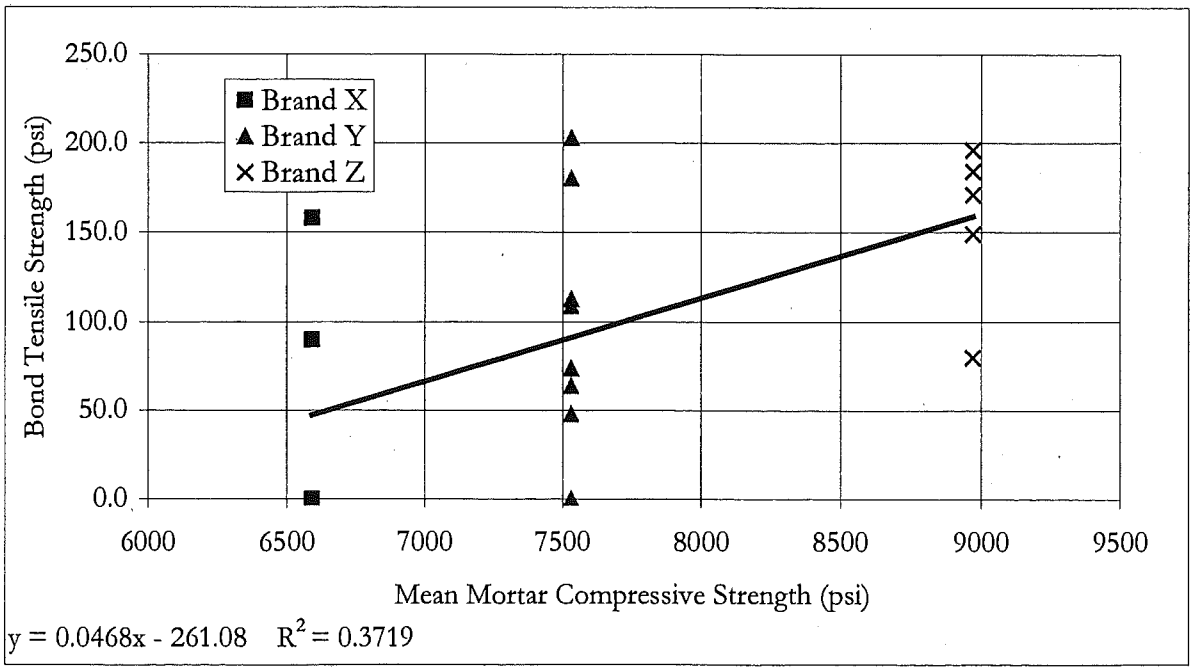

Figure 11-11. Bond Tensile Strength Data vs. Mean Mortar Compressive Strength - Shallow Cycled Specimens

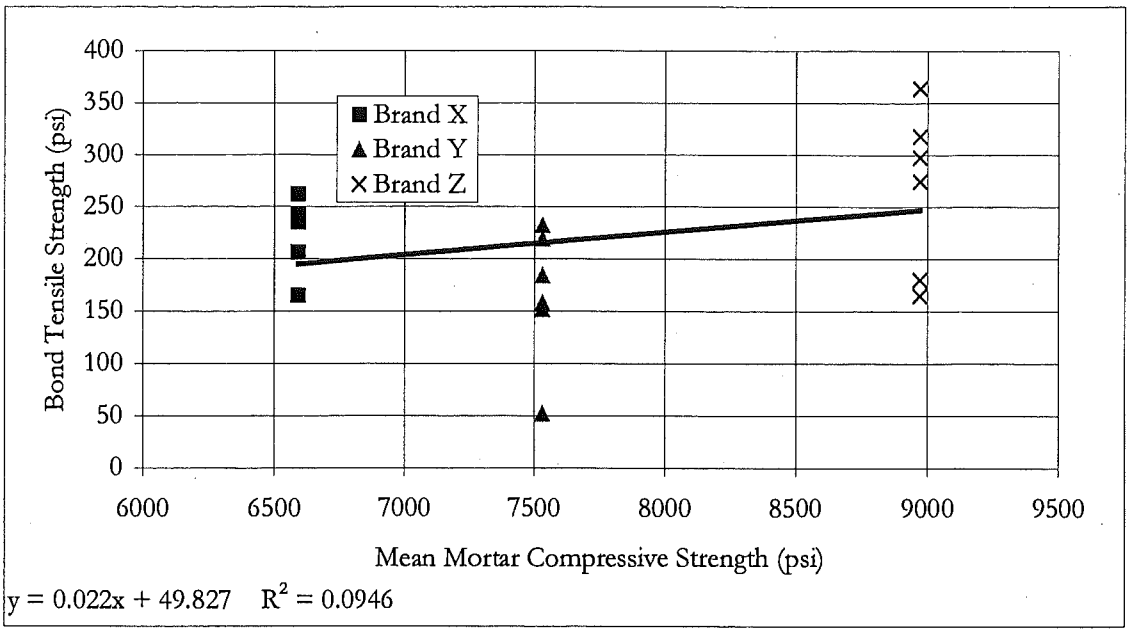

Figure 11-12. Bond Tensile Strength Data vs. Mean Mortar Compressive Strength - Deep Cycled Specimens

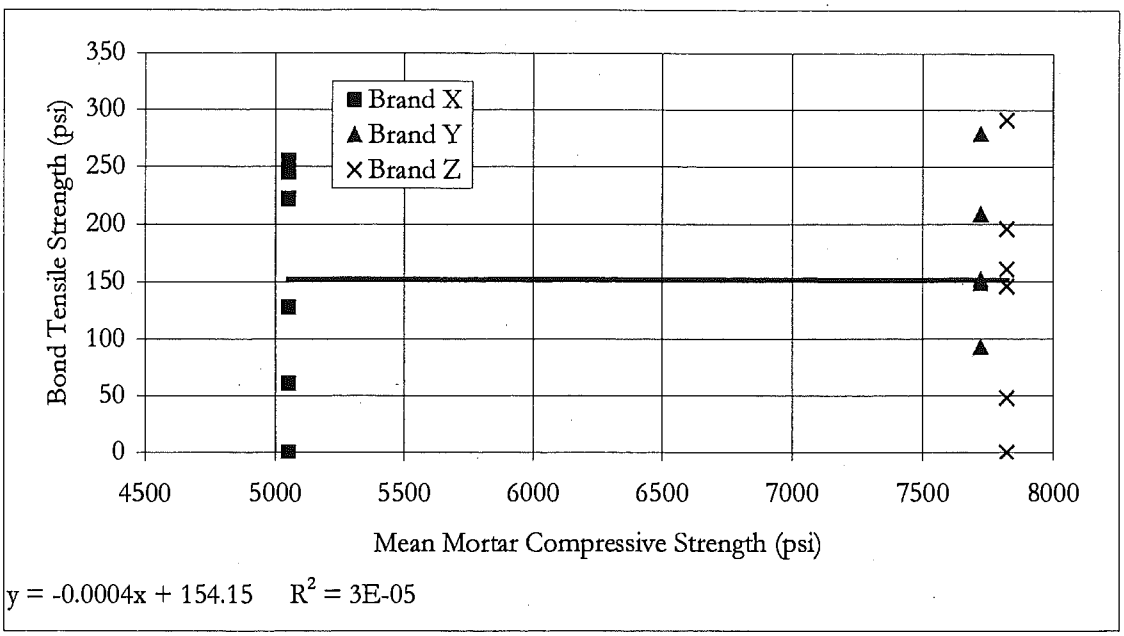

Figure 11-13. Bond Tensile Strength Data vs. Mean Mortar Compressive Strength – Shallow Ambient Specimens

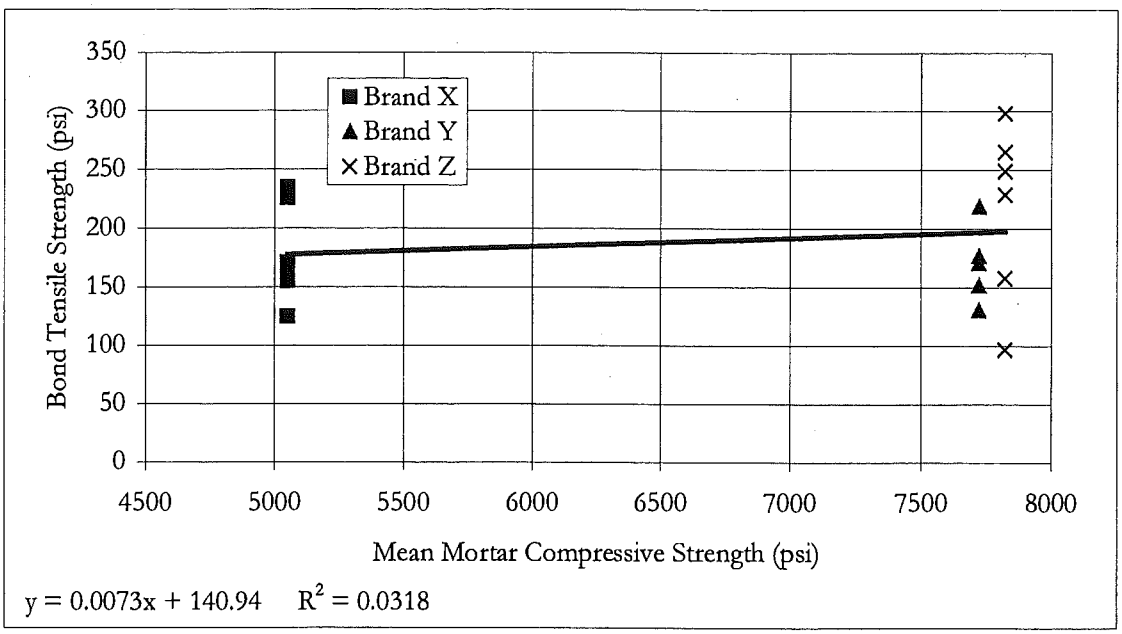

Figure 11-14. Bond Tensile Strength Data vs. Mean Mortar Compressive Strength – Deep Ambient Specimens

A trend that is present in the bond tensile strength data scatter plots compared to the mean bond tensile strength plots is that the slope of the regression lines generally remained the same. However, the goodness of fit of the regression functions decreased significantly for linear regression analyses performed on individual bond tensile strength data. Table 11-25 summarizes a comparison between the t-test results, the regression slope, and the coefficient of determination for both the mean and individual bond tensile strength data.

Table 11-25. Comparison of Test Statistics and Regression Analyses - Mean vs. Individual Bond Tensile Strength Data

Specimen Group	Mean Bond Tensile Strength Data			Individual Bond Tensile Strength Data		
	t-test of b_1	Regression Slope	R^2	t-test of b_1	Regression Slope	R^2
Deep Cycled	$\beta_1=0$	0.0413	0.9534	$\beta_1=0$	0.0220	0.0946
Deep Ambient	$\beta_1=0$	0.0074	0.2781	$\beta_1=0$	0.0073	0.0318
Shallow Cycled	$\beta_1=0$	0.0471	0.9830	$\beta_1\neq0$	0.0468	0.3719
Shallow Ambient	$\beta_1=0$	-0.0004	0.0032	$\beta_1=0$	-0.0004	0.00003

In summary, it was found that based on the mean bond tensile failure stress for each repair depth and post curing conditioning, there appears to be a trend for increasing mean bond tensile strength with increasing mean compressive strength for specimens that had been in a

thermally cycled post-curing environment. Trends for all other comparisons showed no significant increase in mean bond tensile strength with increasing mean mortar compressive strength. T-tests performed on the slope of the linear regression function for each mean-mean comparison indicated that the null hypothesis should be accepted; the best estimate of any mean bond tensile strength for a given mean mortar compressive strength would be the mean bond tensile strength. Statistically, mean mortar compressive strength has no impact on the mean bond tensile strength. Coefficient of determination statistics calculated for the regression analyses shown in Figure 11-7 through Figure 11-10 generally indicated a poor fit of the regression line to the data. Exceptions to this observation are evident in specimens that were thermally cycled after curing, especially when considering different repair depths individually. R^2 statistics for these regression analyses approached 1, indicating little variation about the regression line.

Additional poorly fit regressions were observed when plotting actual bond tensile strength data to the mean mortar compressive strength. Table 11-25 shows how the quality of the regression model decreased with the second comparison. The results of the t-tests on the individual bond tensile strength data indicated that there was no statistical difference between the regression line slope and a slope of zero, except for the shallow repair that were thermally cycled after curing. In other words, for each case, the best estimate of the bond tensile strength for each case corresponds to the mean of all failure modes as listed in Table 11-16 through Table 11-19 (e.g., deep repair specimens undergoing thermal cycles can be expected to have a bond tensile strength of 219 psi from Table 11-16).

11.3.3.5.1 Performance Evaluation Based on Bond-Tensile Strength of Repairs

In the introduction to this chapter, it was stated that one of the requirements of a repair material was to develop sufficient bond to assist the parent member in carrying load and at a minimum not de-bond from the substrate. The long-term success of a repair material cannot be based on one test alone; however, past research has also shown that, in general, improved performance of repair materials can be expected with increasing tensile strength (McDonald et al, 2002). Analysis to determine a required bond tensile strength value for a particular condition is beyond the scope of this study. However, a minimum bond tensile strength of 400-psi has been suggested for non-structural or protective repairs (McDonald et al, 2002). While the BSI 1881: Part 207 test was used for bond tensile strength in this study, the procedure does not list a minimum performance criterion for strength. As such, the limit suggested by McDonald was employed.

None of the repair materials tested met the 400 psi performance criteria for bond tensile strength. In fact, less than 3 percent of the repair specimens (2 out of 78 tests) yielded bond tensile strengths greater than 300 psi. If repair material and repair-substrate interface strengths are improved, bond tensile strengths greater than 400 psi can be attained. This is evident from review of the control specimen strength data. Unless preparation, placement, and curing procedures are modified from those followed for this study, it appears that suggested minimum bond tensile strength cannot be reached.

An earlier section in this chapter, *Brand Y Repaired Specimens*, discussed how delamination of the repair material had occurred on two specimens. Delaminated regions can be considered to have zero bond tensile strength to the substrate. Spalling of these repairs is likely in a field situation, such as a beam-end beneath a defective transverse deck joint.

11.3.4 Shrinkage Evaluation

As stated in the *Visual Review of Repair Surfaces* section of this chapter, an important property in the performance of concrete repairs is the ability of resist cracking (McDonald et al, 2002). This requires dimensional compatibility between the repair material and concrete substrate, because the repair material and concrete substrate are physically connected to the same structure, but yet may have significantly different material properties.

As mentioned in the section *Performance Evaluation Based on Visual Observations*, cracking of a restrained material will occur if the tensile stresses generated exceed the tensile strength of the material. In the case of a restrained repair, such as the one used in this study, the amount of tensile stress that develops will depend on many properties. These include the amount of shrinkage, quality of bond on all bonded edges, creep or relaxation properties of the repair, and thermal expansion properties of mortar and substrate (ACI, 1990). It is not well understood how material properties affect dimensional compatibility, how material properties interrelate, and what values should be specified to achieve durable repairs (McDonald et al, 2002).

This component of the study attempted to evaluate the restrained shrinkage properties of various repair materials in different repair geometries and post-curing temperature conditions. Various tests exist for measuring the restrained shrinkage of a portland cement concrete material (McDonald et al, 2002). These tests include casting concrete rings, prisms, or bars (Emmons and Vaysburd, 1995). These tests commonly either use cracking or deflection as the performance measure of the material. However, none of these tests were used in this study, primarily because they are performed on separately cast test specimens that are not part of an actual repair itself. In other words, this study aimed to observe the in-situ restrained shrinkage performance rather than on an isolated test specimen.

The intended performance measure for this component of the study was to record dimensional changes at the repair-substrate joint, such as cracking, by performing periodic measurements between surface mounted monuments (DEMEC points). The locations of the monuments were shown in Figure 11-1. They were positioned to document lengths, and therefore length changes over time on the substrate, repair material, and at the substrate-repair joint. Monuments were placed at these locations in an effort to later subtract contributions to the crack width from substrate activity at the conclusion of the experiment (i.e. after final distance measurements were obtained).

However, in developing the model for analyzing the data after the experiment was completed, two large sources of experimental error were found. The first of these error sources was that relative humidity measurements were not obtained during the course of the study. Relative humidity has a significant impact on drying shrinkage and swelling of portland cement concrete (Nawy, 2000). The second error was the position of the monuments on the specimen. As shown in Figure 11-1, the monuments were located at various distances from the free edges of the substrate or repair material. The distance of a monument to a free edge can impact localized moisture in the specimen (e.g. moisture content closer to a free edge can be different than moisture content at a distance into the specimen) and therefore impact distance measurements. This error, when combined with the impacts of relative humidity, makes the data impractical to analyze at this time.

11.4 Summary

11.4.1 Overview

Although the integrity and durability of a repair can generally never be as good as the original member, repairs are recognized for their ability to extend service life in the short-term at an attractive cost. A significant portion of this study involved laboratory experiments that focused on the performance of concrete repairs for corrosion-induced beam-end deterioration. Research has been conducted recently that looked at the performance of various concrete repair materials for repair depths similar to those used in this study (McDonald et al, 2002). However, this study was unique in that the specimen fabrication, selective demolition, repair, curing, conditioning, and testing were done using methods similar to those that would actually be used in the field on distressed beam ends. An example of one of the more unique aspects of this research is that the repairs were performed in vertical and overhead positions, something that was not discussed in any literature reviewed for this study. Major variables in the fabrication of the repair specimens included shallow (1-in nominal) and deep (3-in nominal) repairs as well as laboratory ambient and cycled post-curing temperatures. Some important findings during fabrication of the repairs were:

- Concrete selective demolition can be performed with conventional hand-held tools, however concrete breakers should be less than a 15-lb. class of hammer to reduce damage to the substrate.
- A surface microscopic evaluation of substrates prepared by mechanical wire brushing and sandblasting did not reveal a significant difference in surface characteristics between the two surface preparation methods.
- Concrete repair in the vertical and overhead position with prepackaged repair mortars is feasible. Each of the materials evaluated in this study were equally easy to work with in small batches.
- Shallow repairs should be completed from the top down to reduce sagging. Deep repairs must be completed in successive lifts to reduce sagging.
- Consolidation of repair mortars with tools having a large surface area (e.g. flat side of a putty knife compared to a round-nosed rod) tended to produce the densest repairs. Over-consolidation can result in repair mortar sagging.
- Improper finishing can lead to sagging and tearing of the finished repair surface.
- Sufficient release agent must be applied to formwork. Removal of forms or initiation of wet curing prior to sufficient set can damage the repairs.

Although a concrete repair must have many properties in order to be durable in-service, perhaps two of the most important properties are crack resistance and substrate adhesion (bond). Crack resistance is needed to prohibit ingress of contaminants that can adversely affect the performance of the repair. Adhesion is required to assist the parent member in carrying loads as well as protecting the parent member (or repair) steel reinforcement from corrosion. A performance evaluation of the repairs was also conducted for this study and

focused on evaluating crack development and repair bond tensile strength at the conclusion of the post-curing period. Repair mortar compressive strength testing was also performed in this study to verify conformance to manufacturer specifications. In addition, compressive strength testing is relatively easy to perform. It was therefore desirable to see if any relationships exist between mortar compressive strength and other performance tests (i.e. bond tensile strength).

The performance measure for repair cracking width for this study was 6-mils, based on industry recommendations (ACI, 1990). Based on the relatively short time in which the repairs needed to perform (approximately 60 days), it could be argued that this criteria is un-conservative and that any cracking or finer crack widths would be cause for finding a repair unsatisfactory.

Visual observations of repair condition at the conclusion of the post-curing period revealed cracking within the repair material itself and at the repair-substrate joints (i.e. top and bottom repair joints). Not considering the cracking at these joints, some observations made were:

- All brands of repair material showed cracking greater than 6-mils in width.
- Those specimens with fine-width (2-mil) pattern cracking generally did not exhibit cracks within the repair greater than 6-mils in width.
- Those specimens repaired with materials produced with a liquid polymer exhibited more cracking than the material mixed with potable water (Figure 11-2).
- Repair depth did not have an impact on frequency of cracked specimens relative to the total number of specimens tested (Figure 11-3). About one-third of each repair depth group exhibited cracking greater that 6 mils.
- Post-curing environment showed 43% of specimens exceeded the 6-mil performance measure, whereas 28% of ambient cured specimens exceeded the measure (Figure 11-4).

For bond tensile strength, two sets of performance measures were observed. First, repairs cannot delaminate from the substrate and second, a bond tensile strength of 400 psi was required. As discussed in this chapter, over 1/3 of the repair specimens did not meet the cracking performance criteria and none of the specimens were able to develop a bond tensile strength of greater than 400 psi.

From statistical analysis of the mean bond tensile strength data, the following conclusions can be made for the different materials, repair depths, and post-curing conditions used in this study:

- For each repair material, the population mean bond tensile strengths were equal between the:
  - Shallow ambient and deep ambient repairs
  - Deep ambient and deep cycled repairs
  - Shallow ambient and shallow cycled repairs
- For each repair material, the population mean bond tensile strength of the shallow cycled specimens was less than the population mean of the deep cycled specimens.

One of six failure modes is possible for the bond tensile strengths performed in this study (see Figure 11-6). The majority of failures (77-percent) were at the repair-substrate interface. Statistically evaluating the bond tensile strength results on the basis of failure mode, the following conclusions can be drawn:

- The population mean bond tensile strengths were equal between mode B (repair material) and mode C-D-E (repair-substrate interface) failures for the:
    - Brand Y repair material
    - Brand Z repair material
    - All materials together (independent of brand)

- The population mean bond tensile strength for mode F failures (substrate) were greater than the mode C-D-E (repair-substrate interface) failures for the:
    - Brand Z repair material
    - All All materials together (independent of brand)

Compressive strength testing performed on the concrete substrate and repair mortar was also evaluated statistically. From these analyses, the following observations can be drawn:

- The 28-day compressive strength of the substrate used for this study is from a population having a compressive strength of 5000-psi.

- The end of post-curing compressive strength test results for the substrate concrete cycled and ambient are from the same population.

- The end of post-curing compressive strength test results for the Brand Y material cycled and ambient are from the same population.

- The end of post-curing compressive strength test results for the Brand X material cycled and ambient are not from the same population (Brand Z was inconclusive.)

Some trends can be drawn when relating mean bond tensile strength to mean mortar compressive strength. These trends are evident by evaluating the data in a scatter plot and performing linear regression analyses. Additional statistical testing of the rate of change in mean compressive strength to mean bond tensile strength (slope of regression, b_1) revealed that, considering all repair materials, and each unique repair depth / post-curing combination:

- The best estimate of any bond tensile strength data for a given mean mortar compressive strength would be the mean bond tensile strength for:
    - Deep cycled specimens (219-psi, Table 11-16)
    - Deep ambient specimens (191-psi, Table 11-17)
    - Shallow ambient specimens (152-psi, Table 11-19)
    - Shallow cycled specimens did not meet the criteria, see next comment.

- There is reason to believe that the slope of the regression is not equal to zero for the shallow cycled specimens.

- The coefficient of determination for each linear regression performed on a bond tensile strength data vs. mean mortar compressive strength was less than 0.4. In other words, the regression functions do not explain the individual data very well, but do indicate overall trends.

- Trends in the regression analyses performed indicate relatively little change in bond tensile strength (mean or individual data) with increasing mortar compressive strength for laboratory ambient post-cured specimens.

- Trends in the regression analyses performed indicate increasing bond tensile strength (mean or individual data) with increasing mortar compressive strength for thermally cycled post-cured specimens.

11.4.2 Significance and Limitations of Results

Findings and techniques from this experimental study will likely be used in aiding other engineers to make better-educated decisions on which techniques to use and why. For example, this study synthesized many available preventive maintenance and repair alternatives both currently and not currently being used by state departments of transportation. Appendix J contains a summary of the techniques identified in the literature review and state surveys separated into the four different approaches for addressing corrosion-induced deterioration of prestressed concrete I-beam ends. It should be stressed that if the mechanism of deterioration is not from corrosion-induced deterioration by deicer penetration significantly different approaches for preventive maintenance and repair will be needed. Appendix J can be used as a quick reference to see what alternatives are available.

Overall, the performance of the repairs was not favorable. Cracking, sagging, delaminations, and lower-than-expected bond tensile strengths suggest that at best, repairs can provide only short-term increased service life. It must be noted that the poor overall performance cannot be attributed to any one material, each had conditions or properties that were less than desirable for durable repairs. In addition, there were a multitude of different approaches that could have been taken while performing the repairs: different demolition, surface preparation, material placement, and curing.

Based on the findings and procedures used in this experimental study, those persons specifying one of the three repair materials evaluated in this study can expect the repairs to crack. The severity, frequency, and location of cracking will likely vary based on the repair material used. However, the repairs should develop a bond tensile strength of approximately 200-psi (± 100-psi) and not delaminate from the substrate shortly after placement. Because repairs to beam-ends are in a thermally cycled environment, specifiers should expect to see increased bond tensile strength with increasing repair material compressive strength, especially for deeper repairs. In addition, the mean bond tensile strength of deep repairs should be expected to be greater than mean bond tensile strength of shallow repairs in a thermally cycled environment.

12.0 Bridge Management for I-Girder End Condition

12.1 Introduction

One specific goal of this research is to develop an inspection or health monitoring procedure for prestressed concrete I-beam bridges and to develop/recommend protection and repair techniques corresponding to each state of health. The primary expectation from the health monitoring procedure is to identify the prestressed concrete I-beams that are vulnerable to end deterioration, including tendon corrosion. The health monitoring procedure is based on an extensive analysis of the Michigan bridge inventory and condition data, a multi-state survey in the US to learn about the experience of other State Departments of Transportation, and the detailed field inspection of twenty highway bridges in Michigan.

It is also important to relate the protection and repair techniques to funding categories specified as "Capital Scheduled Maintenance (CSM)", "Capital Preventive Maintenance (CPM)", "Rehabilitation (R1)" and "Replacement (R2)". CSM activities are for sustaining the current condition of the bridges, CPM is to address the needs of bridges in fair condition, and R1 and R2 are for improving the condition of the bridges.

The long-term brigde health-monitoring goal in Michigan is to utilize fleet management tools and procedures in planning and scheduling maintenance and repair activities. In fleet-management tools, analytical models are incorporated for predicting service life of bridge components, specifically with respect to corrosion-initiated distress (Enright and Frangopol 2000). Practical issues such as traffic control and re-routing necessitate that the repair and maintenance activities be performed on highway corridors. In this approach, repair and maintenance are performed only on the bridges along and on the corridors planned for that budget year. The objective of the bridge repair and maintenance activities is to improve the condition of all the components to above "satisfactory." Keeping this reality in mind, the health monitoring procedure includes a table with maintenance and repair techniques for each common distress state found in the ends of prestressed concrete I-beams. The distress states are described in Chapter 6 and tabulated in Table 6-2. The maintenance repair procedures, when implemented, will improve the girder condition from its current state to a "good" condition.

12.2 I-Beam End Management

As described, the maintenance and repairs on the bridges are currently scheduled along selected corridors. The bridges with distresses that cannot be deferred and which are not on the repair schedules are often dealt with temporary shoring and strengthening procedures until the corridor bridges are scheduled. When bridges on a corridor are scoped, the beam-end conditions described in Table 6-2 are often observed. In order to help with the maintenance/repair replacement decision for the beam-ends from the scoping reports, a process is developed.

In this process the twelve condition states identified for the beam-end described in Chapter 6 are lumped into the following five General Condition Categories:

1. No Obvious Distress
2. Corrosion
3. Corrosion with Delamination and/or Spall
4. Loss of Deformability (Non-Functional Bearing)
5. Reduction in Beam Capacity

In order to assist with the necessary corrective action and the available means, Table 12-1 and Table 12-2 are presented. Table 12-1 shows the relation between the condition states (presented in Table 6-3) and the General Condition Categories. The goals presented in Table 12-1 would be achieved if the preventative maintenance and/or repair techniques given in Table 12-2 were enacted.

Table 12-2 was generated to provide a link between beam-end distress and common repair and maintenance procedures specific to that distress. Utilizing the twelve condition states that were established in Chapter 6.0, techniques are applied to the prestressed concrete I-beam bridge fleet. The maintenance and repair activity required for each condition state is identified as shown in the Table 12-2. Also shown is the relationship between the condition states developed and those specified by FHWA for safety assessment of the bridge. It should be noted that the FHWA requirement is to assure bridges are at least in fair condition.

Table 12-1. General Condition Categories

General Condition Categories	Condition States	Goals		
No Obvious Distress	1	Prevent Corrosion Initiation	-	-
Corrosion	2,3,4,5,7,8,9	Stop Corrosion	Prevent Corrosion Reinitiation	-
Corrosion with Delamination and/or Spall	10,11	Stop Corrosion	Prevent Corrosion Reinitiation	Esthetic Restoration of Beam-end
Loss of Deformability (Non-Functional Bearing)	6	Stop Corrosion	Restore Functionality	-
Reduction in Beam Capacity	12	Replace Beam-end	Prevent Corrosion Initiation	-

For beam-ends in the most severe condition state, Michigan has already developed and utilized an overcasting repair procedure. Prior to encasing the beam end, the Michigan procedure specifies removal of deteriorated web and flange concrete. The overcast section on the beam-end is also integrated with a new diaphragm. Repair concrete for this design is MDOT Grade D polymer (latex) modified concrete. MDOT plans were prepared detailing an end repair method for prestressed concrete I-beams with and without end blocks. This repair technique was executed in 1999 in Lower Michigan. The cost of repairing prestressed concrete I-beam ends using this procedure was reported to be 35 to 69 percent of full-replacement cost (Needham, 2000). These tables provide categories for the condition of I-beam end and the appropriate preventative maintenance or repair technique.

Table 12-2. Condition States of Prestressed Concrete I-Beam Ends with Suggested Preventative Maintenance & Repair Techniques

Condition State		Photos Describing the Condition State	FHWA Condition Rating and Description	Preventative Maintenance / Repair Technique
1	No cracks observed, No staining	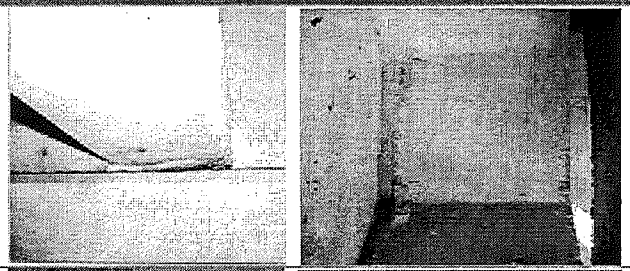	**N** - NOT APPLICABLE & **9 & 8** - EXCELLENT CONDITION	----
2	Efflorescence, water-stains, and/or corrosion	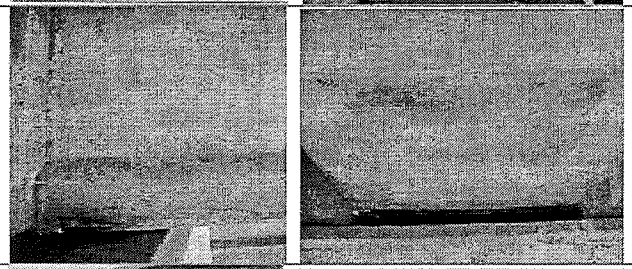	**7** - GOOD CONDITION	▪ Surface Insulating Methods *(Penetrating, Surface, Sealers, Coatings, and Crack Sealants)*
3	Hairline cracks: horizontal, vertical, and/or diagonal	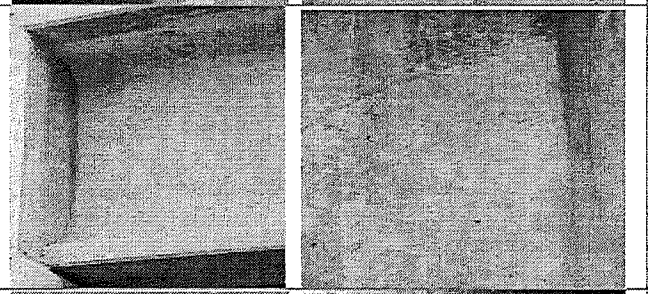		▪ Surface Insulating Methods *(Penetrating, Surface, Sealers, Coatings, and Crack Sealants)*
4	Map Cracks	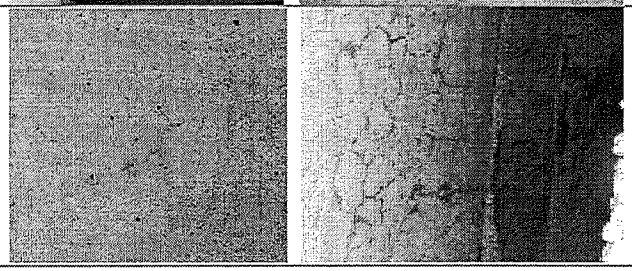		▪ Surface Insulating Methods *(Penetrating, Surface, Sealers, Coatings, and Crack Sealants)*, ▪ Electron Control Methods *(Surface Applied Corrosion Inhibitors, Sacrificial Anodes, Impressed Cathodic Protection)*,

5	Hairline Cracks with efflorescence, water-stains, and/or corrosion with a horizontal crack propagating from the sole plate	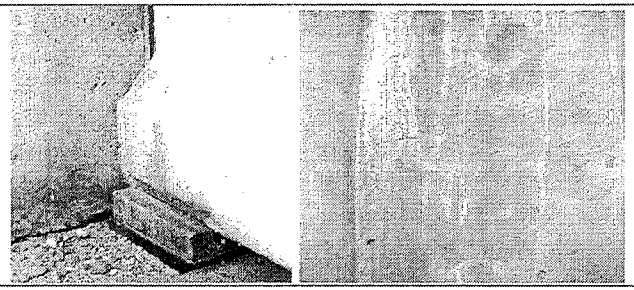		▪ Surface Insulating Methods *(Penetrating, Surface, Sealers, Coatings, and Crack Sealants)*, ▪ Electron Control Methods *(Surface Applied Corrosion Inhibitors, Sacrificial Anodes, Impressed Cathodic Protection)*, ▪ Environment Modifying Methods
6	Cracked and deformed neoprene pad, probably non-functional		**6 -** SATISFACTORY CONDITION	▪ Remove Rust from Bearing ▪ Replace Neoprene Pad
7	Moderate Cracks	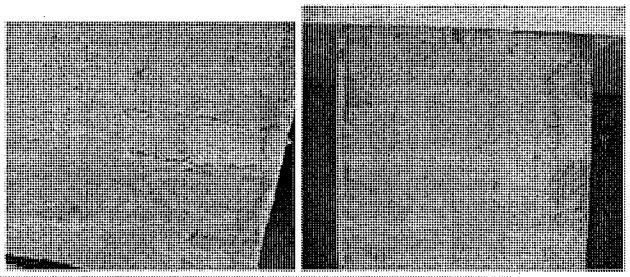		▪ Electron Control Methods *(Surface Applied Corrosion Inhibitors, Sacrificial Anodes, Impressed Cathodic Protection)* ▪ Surface Insulating Methods *(Penetrating, Surface, Sealers, Coatings, and Crack Sealants)*, Reinforcement Surface Preparation *(Epoxies, Liquid Corrosion Inhibitors, Zinc-rich Paint)*
8	Moderate cracks with efflorescence, water-stains, and/or corrosion	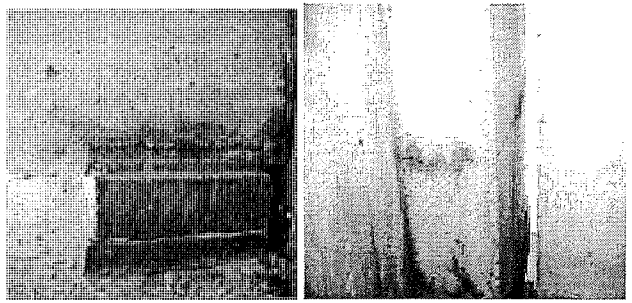		▪ Secondary Framing Modification *(Replace Diaphragms)*, ▪ Surface Sealers, ▪ Re-alkalization, Chloride Ion Extraction, ▪ Concrete Surface Preparation *(Compressed Air, High Pressure Water, Grit and Sand Blasting, Scrabbling, Wire Brushing)*, ▪ Electron Control Methods *(Surface Applied Corrosion Inhibitors, Sacrificial Anodes, Impressed Cathodic Protection)*

9	Major Cracks with efflorescence, water-stains, and/or corrosion	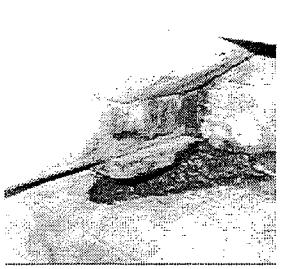 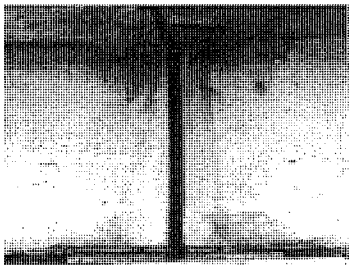		▪ Support Member Modification *(New Haunch and New Bearing)*, ▪ Primary Framing Modification *(Supplemental Beam, Full Beam Replacement)*, ▪ Environment Modification Methods *(Re-Alkalization, Chloride Ion Extraction, DC Current Impressed, and Surface Applied Barriers)* ▪ Partial Depth Beam Repair *(Concrete Removal, Concrete Surface Preparation, Reinforcement Cleaning, Reinforcement Surface Preparation,*
10	Delamination with moderate and/or major cracks	 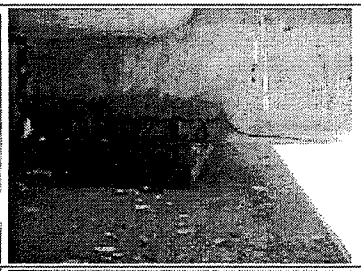	**5** -FAIR CONDITION	▪ Support Member Modification ▪ Deck Modifications *(Joint Repair, New Joint, Overlay, New CLL Deck)*, ▪ Primary Framing Modification *(Supplemental Beam, Full Beam Replacement)*, ▪ Electron Control Methods *(Surface Applied Corrosion Inhibitors, Sacrificial Anodes, Impressed Cathodic Protection)*, ▪ Environment Modification Methods ▪ Partial Depth Beam Repair *(Concrete Removal, Concrete Surface Preparation, Reinforcement Cleaning, Reinforcement Surface Preparation, Partial Depth Patching)*
11	Spall, delamination, corrosion, and cracks	 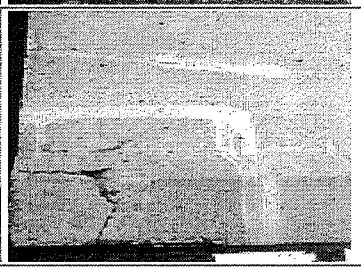		
12	Spall, exposed reinforcement and corrosion	 	**4** -POOR CONDITION	▪ Environment Modification Methods ▪ Partial Depth Beam Repair *(Concrete Removal, Concrete Surface Preparation, Reinforcement Cleaning, Reinforcement Surface Preparation, Partial Depth Patching)* ▪ Chip and Overcast procedure used by MDOT R-1373 and RR-1380. ▪ Replacement of the superstructure and substructure elements

13.0 Conclusions

The study had three components: field inspection, experimental study, and analytical modeling. The purpose of the field inspection was to document the beam-end distress states and collect data in order to understand the causes of girder-end distress. The experimental study dealt with evaluating shallow and deep patches for beam-end repair. The analytical study looked into the influence of prestressing actions and additional live and intrinsic loads on girder-end distress. The research procedure had five steps: first—document the level and extent of beam-end distress; second—develop a hypothesis for determining the cause(s) of beam-end distress; third—develop a test for the hypothesis; fourth—analyze the impact of beam-end distress on bridge safety; and fifth—perform experiments for developing viable repair methods for moderate levels of beam-end distress.

The major conclusions are described below:

1. The prestressed concrete I-beam ends are often cracked. The cracking with the presence of moisture accelerates the girder-end deterioration primarily by accelerating the chloride ingress process and corrosion initiation of shear reinforcement and prestressing tendons.
2. The recent deck design using the continuous for live-load system eliminates the expansion joint and consequently provides a roof over the beam-end. Moisture access to the beam-end and the ingress of chlorides is subsequently reduced. However, spray from traffic below and new diaphragm details, which encase the beam-end and traps moisture, still make beam-ends a vulnerable portion of the I-beam bridges. The diaphragm in this configuration also conceals the beam-end, which makes visual inspection impossible. The primary approach for improving beam durability should be the elimination or reduction of beam-end cracking. In all existing bridges, beam ends with any width cracks should be sealed.
3. Analytical models showed that the cracking potential is very high on straight and draped prestressed strand girders. The cracking potential is lower but still exists in sheathed or debonded girders, which affect the more recent manufacturing process. Prestressed concrete beam-end cracking is due to the transverse and shear stresses generated by axial load change along transfer length. These loads cannot be eliminated, but cracking can be minimized with the use of confinement steel near beam-ends. Further study is needed to determine the exact arrangement and size of confinement steel.
4. Conclusions related to full bridge analysis include the effect of diaphragms and bearings on the stresses at the beam-ends. The purpose of diaphragms is for girder stability during erection and transfer of shear between girders under live loads. It is seen in the analyses that

the diaphragm geometry and material properties do not generate significant influence on the beam-end stresses. The recent diaphragm design and material properties may require changes. Steel X bracings may be a proper alternative, which provide ventilation for the beam-ends. An efficient detail with steel X-braced girders and beam-ends free of diaphragm should be further investigated.

5. The beam-end stresses are amplified due to neoprene bearing, which is sometimes nonfunctional. Analytical studies show that beam-end vulnerability is a concern for bridge safety for two reasons. First, the deteriorated portion of the girder-end is often within the path of live load transfer to the bearings. Second, the loss of bond near the ends reduces the prestressing force affecting the moment capacity. Load path is established under dead and service loads to assess when the deteriorated portions of beam-end intrude into the load-path.
6. Shallow and deep patch repairs on delaminated girder ends can be a way of restoring the cross-section and preventing further progression of tendon corrosion. All patching materials, however, are not equal and may show significant differences in expected performance. The three repair materials evaluated herein showed non-acceptable cracking, and none met the minimum adhesion criteria through bond tensile strength testing.
7. The bridge scoping, assessment, maintenance, and rehabilitation are often currently performed on roadway corridors. The scoping inspections are performed within a designated corridor. Beam-ends at various condition states can be encountered. Utilizing the inspection data and further studies using the Pontis database, common beam-end distress are categorized into twelve condition states. The first six of these conditions can be dealt with using Capital Preventive Maintenance.

14.0 Recommendations for Future Work

14.1 Introduction

This research provides a solid foundation for understanding issues related to the deterioration of prestressed concrete I-beam ends used in Michigan bridges. The focus of this work has been the maintenance and repair of prestressed concrete I-beam bridges. We established girder condition states and recommended repair and maintenance procedures for each condition state. We also tested patch techniques for the repair of spalled/delaminated beam-ends. We attempted to understand the reasons for the beam-end vulnerability by developing analytical models and conducting response analysis for discrete girders as well as full bridges.

However, as with most research projects, several questions remain unanswered and deserve future attention. The following discussion constitutes a list of research items that should be considered.

The focus of the next phase of work should be safety assessment. In order to understand the relation between girder-end condition states and their load performance, the approach should be the development of an analytical model for various bridge types calibrated by the full-scale testing of decommissioned girders. In order to successfully implement this approach, future research will have an analytical and experimental component. The experimental component should be further divided into laboratory experiments for condition characterization of in-service girders and field-testing of full-scale girders.

14.2 Future Analytical Modeling

Analytical studies focused on two finite element models: a discrete beam and the full model bridge. These models have helped to identify cracking potential and the significance of some elements on the overall behavior. With the models developed, many additional topics are worthy of further study. The models should be used to improve on current design details so that detrimental mechanisms can be avoided. Details to be considered include the effectiveness of various reinforcement approaches for eliminating end cracking.

Additional cracking at the ends of the I-beam was noted in the field investigation. The analytical model should be used to introduce cracks into the end of members at actual field-noted locations.

While the problem of unknown crack depth extension exists, a conservative approach may be to "insert" a crack the full width of the member. Modeling the influence of all cracks at the same time can provide insight into expected behavior under a cracked state. Unsound, spalled, and delaminated concrete can all be modeled by using a member of reduced cross section. Cross-sectional area reduction should be investigated to determine when a structural capacity reduction occurs. From field investigation notes, 6 to 12-in from the end of the beam in conjunction with an exposed reinforcing cage may be a good starting point. Additional cross-sectional reduction could be used to simulate more aggressive concrete loss, say to behind the reinforcing cage.

Similarly, loss of prestressing strand and mild steel reinforcement in both bond and cross-sectional area can also influence the strength of the member and should be investigated. Corroded bars and strands may or may not be effective in contributing to the flexural, shear, and bearing capacity. Corroded and debonded strands some distance away from the bearing area may accelerate strength loss to an even greater degree.

The I-beams are designed to operate in a simple-supported structural system. Analytical models developed for the full bridge showed that the diaphragms and end beams over abutments result in a structural system that is not really simply supported. The utilization of link-slab as well as the continuous for live load decks also generates end restraints. Design details such as bearing pads and diaphragms can be improved upon by the utilization a of three-dimensional realistic analytical model of a full bridge.

14.3 Future Laboratory Studies

The limited laboratory study included in this research has provided valuable information into the effectiveness of partial depth patching for vertical and overhead repairs in a moderate state of distress. While the three latex-modified polymer repair mortars were specified with corrosion inhibitors, the excessive cracking noted in all three materials (two materials showed wide cracks greater than 6 mils and one material showed significant fine map cracking) warrants them as potentially ineffective in protecting the reinforcing and prestressing strands from further deterioration. Additional materials need to be reviewed for effectiveness in protecting the steel once a repair has been made.

Enhancing the bond of the repair material needs to be addressed. While only a few specimens showed delaminations of the repair material from the concrete substrate, the bond tensile strength results did not meet the performance metric of 400-psi strength. All repairs must adhere to be effective. Additional repair materials as well as bonding agents need to be reviewed for effectiveness in providing adhesion once a repair has been made.

Further investigation into the damage caused to sound concrete by various methods of concrete removal needs to be addressed. While concrete removal using a small rotary hammer is an accepted practice, laboratory results indicate that some damage is done to the sound concrete. Direct bond test results on non-repaired concrete showed higher bond strengths than on repaired specimens that broke in the concrete substrate. Petrographic analysis can be a direct method to determine the concrete removal damage done to the concrete microstucture.

Laboratory and environmental conditions used in this study were relatively mild when compared to actual field conditions. Thermal cycling varied between 32 and 95 degrees Fahrenheit, and no moisture cycles were integrated into this experimental study. Once more suitable repair materials are found to successfully undergo the minimum performance metrics of crack width and adhesion using the above testing methods, the repairs should be subjected to more representative field conditions, including free-thaw cycles and de-icing compound applications.

NOTE: all repaired specimens used in this study will be stored for up to one year (until August 2003) in the event that further study is desired using those specimens.

14.4 Field Testing and Other Studies

Valuable information can be gained from actual field studies. Materials testing and petrographic analysis are ways to evaluate field conditions in a laboratory environment. The use of decommissioned bridges for research can provide information relative to the soundness of the materials used. Testing can include chloride content determination, level of strand and reinforcement deterioration, and linking alkali-silica reactivity (ASR) to end deterioration. While some work has been done by MDOT to correlate elevated chloride levels to deterioration of beams and reduction in strand tensile strength, limiting testing was performed and additional attention to the issue is warranted.

Bridges that are taken out of service can be evaluated for performance in many more ways than just material testing. Evaluation of actual beam structural capacity is needed to truly understand the damage due to deterioration. Full-scale testing results of individual beams in flexure and shear can give insight into the actual strength reduction and can be compared with analytical models. Corresponding models can then be used for future bridge analysis of deteriorated structures to more accurately determine the capacity of the structure. In addition, repaired beams can also be tested for effectiveness in restoring strength.

Additionally, inspection based assessment studies should investigate the performance of Michigan prestressed concrete bridges built with and without corrosion inhibitors. Bridges built during the period of 1989 to 1997 used a corrosion inhibitor that was added to the concrete mixture at the precast plant prior to casting. The corrosion inhibitor additive assists the concrete in providing added protection for the steel by reducing the rate of corrosion. Performance of bridge beams made with the corrosion inhibitors needs to be compared to beams without corrosion inhibitors that experience similar traffic and environmental conditions. This valuable information may show that the use of corrosion inhibitors is the single most important protector to assist beams in achieving long-term performance. Documentation of the condition of these beams will also assist in future decisions regarding the use of corrosion inhibitors in precast concrete bridge beams.

To assist field inspectors and MDOT in selecting appropriate tests to identify the beam-end distress severity, such as noted in Table 7-1, further work is warranted. An optimization technique can be applied to define which test or observation to perform, and based on a test's importance rating, the test results can be used to determine the distress level.

14.5 Future Life-Cycle-Cost-Benefit Optimization Studies

A performance analysis matrix was initialized to aid in selecting appropriate preventative maintenance techniques. I-beam end deterioration appears to be mainly a product of corrosion induced deterioration caused by ineffective transverse deck joints. With over 400 sealers and coatings on the market, as well as hundreds of patching materials and now the use of cathodic protection, the initial cost of such a preventative maintenance technique or repair can be confusing. In addition, the long-term cost associated with preventative maintenance and repair or replacement influences the cost. The process of deciding if one repair is less costly than another is straightforward. Similarly, the process of deciding if a repair performs better than another is somewhat straightforward. However, when these requirements are combined and optimization of both cost and multi-criteria performance is sought, it is not as simple. A decision-making technique similar to Bayesian decision theory needs to be employed to combine the different parameters on which the decision is to be based. Further work is warranted if one is to decide the cost-benefit of the many solutions.

References

3M (1998). "3M Zinc-Hydrogel Anode 4727 Technical Data," http://www.3m.com/intl/kr/img/pdf/4727_Zinc-Hydrogel_Anode.pdf (August 21, 2001).

3M (2001). "3M (TM) Specialty tapes & products: 3M(TM) Zinc-Hydrogel Anode 4727." http://products.mmm.com/usenglish/mfg_industrial/mfg_industrial_specialty.jhtml?powurl=GSTSMRQS8JbeGSNYTMLW46geGST1T4S9TCgvGSNTN0VJCLgl (August 21, 2001)

AASHTO (1996). with interims. "Standard Specifications for Highway Bridges, 16th edition". American Association of State Highway and Transportation Officials, Washington, D.C.

AASHTO (1999). Maintenance Manual: *The Maintenance and Management of Roadways and Bridges*, American Association of State Highway and Transportation Officials, Washington, D.C.

AASHTO (2000). "Manual for Condition Evaluation of Bridges, 2nd Edition". American Association of State Highway and Transportation Officials, Washington, D.C.

AASHTO (2001). "2001 Interim Revisions to Manual for Condition Evaluation of Bridges, 2nd Edition." American Association of State Highway and Transportation Officials, Washington, D.C.

AASHTO (2001). *Pontis (Version 3.4.3). Computer Software.* American Association of State Highway and Transportation Officials, Washington, D.C.

ABAQUS/Standard Version 5.5 Manual (1998), Hibbitt, Karlson & Sorensen, Inc., Pawtucket, RI.

http://www.abaqus.com

ACI (1956). "ACI 318-56 – Building Code Requirements for Reinforced Concrete", American Concrete Institute, Farmington Hills, Michigan.

ACI (1963). "ACI 318-63 – Building Code Requirements for Reinforced Concrete", American Concrete Institute, Farmington Hills, Michigan.

ACI (1971). "ACI 318-71 – Building Code Requirements for Reinforced Concrete", American Concrete Institute, Farmington Hills, Michigan.

ACI (1980) "ACI 224R-8: – Control of Cracking in Concrete Structures," American Concrete Institute, Farmington Hills, Michigan.

ACI (1989). "ACI 318-89 – Building Code Requirements for Reinforced Concrete," American Concrete Institute, Farmington Hills, Michigan.

ACI (1990). "ACI 116R-90 - Cement and Concrete Terminology", American Concrete Institute, Farmington Hills, Michigan.

ACI (1990b). "ACI 224R-90 – Control of Cracking in Concrete Structures", American Concrete Institute, Farmington Hills, Michigan.

ACI (1992). "ACI 201.2R-92 - Guide to Durable Concrete", American Concrete Institute, Farmington Hills, Michigan.

ACI (1994). "ACI 364.1R-94 - Guide for Evaluation of Concrete Structures Prior to Rehabilitation", American Concrete Institute, Farmington Hills, Michigan.

ACI (1995). "ACI 318-95 - Building Code Requirements for Structural Concrete", American Concrete Institute, Farmington Hills, Michigan.

ACI (1996). "ACI 222R-96 - Corrosion of Metals in Concrete", American Concrete Institute, Farmington Hills, Michigan.

ACI (1999). "ACI 318-99 - Building Code Requirements for Structural Concrete and Commentary", American Concrete Institute, Farmington Hills, Michigan.

ACI, "Building Code Requirements for Structural Concrete", ACI 318-02, MI, 2002

Ahlborn, T.M, Aktan, H., Kasper, J.M., and Ovanesova, A.V. (2001). "Interim Report: Causes and Cures for Prestressed Concrete I-beam End Deterioration". Michigan Technological University, Houghton, Michigan.

Al-Qadi, I.L., Prowell, B.D., Weyers, R.E., Dutta, T., Gouru, H., and Berke, N. (1993) "Concrete Bridge Protection and Rehabilitation: Chemical and Physical Techniques, Corrosion Inhibitors and Polymers.", SHRP-S-666, National Research Council, Washington, D.C.

Andrews-Phaedonos, F., Collins, F. G., Green, W. K., and Peek, A. M. (1997). "Assessment of Protective Coatings for Concrete Bridges in Marine or Saline Environments", *Materials Technology Department Proceedings,* Corrosion Prevention. Paper 010, pp.1-10.

Arner, R. C., and Panganiban, R. R. (1986). *Cathodic Deck Protection and Latex Modified Concrete Overlay on Steel I-Beam and on Prestressed Concrete Box Beam Bridges*, Research Projects No. 83-09A and B, Pennsylvania Department of Transportation, Harrisburg, Pennsylvania.

ASCE (2002). "New Polls Show Voters Worried About Aging Infrastructure; Will Affect Candidate Choice." http://www.asce.org/publicpolicy/vgrelease.cfm (February 4, 2002).

ASTM International (2001). *C31/C31M-00e1 Standard Practice for Making and Curing Concrete Test Specimens in the Field.* ASTM International, West Conshohocken, Pennsylvania.

ASTM International (2001). *C39/C39M-01 Standard Test Method for Compressive Strength of Cylindrical Concrete Specimens.* ASTM International, West Conshohocken, Pennsylvania.

ASTM International (2000). *C143/C143M-00 Standard Test Method for Slump of Hydraulic Cement Concrete.* ASTM International, West Conshohocken, Pennsylvania.

ASTM International (1999). *C876-91(1999) Standard Test Method for Half-Cell Potentials of Uncoated Reinforcing Steel in Concrete.* ASTM International, West Conshohocken, Pennsylvania.

ASTM International (1999). *C109/C109M-99 (1999) Standard Test Method for Compressive Strength of Hydraulic Cement Mortars*. ASTM International, West Conshohocken, Pennsylvania.

ASTM International (1998). *C511-98 Standard Specification for Moist Cabinets, Moist Rooms, and Water Storage Tanks Used in the Testing of Hydraulic Cements and Concretes*. ASTM International, West Conshohocken, Pennsylvania.

ASTM International (1997). *C231-97e1 Standard Test Method for Air Content of Freshly Mixed Concrete by the Pressure Method*. ASTM International, West Conshohocken, Pennsylvania.

Ayyub, B.M. and McCuen, R.H. (1997). *Probability, Statistics, and Reliability for Engineers*. CRC Press, New York, 514 pages.

Beaudette, M. R. (2001a). "Norcure Chloride Removal Systems", http://www.norcure.com/index.htm (August 23, 2001).

Beaudette, M. R. (2001b). "Galvashield®XP", http://www.norcure.com/GSdatasheet.htm (August 23, 2001).

Beaudette, M. R. (2001c). "Galvashield®CC", http://www.norcure.com/CCdatasheet.htm (August 23, 2001).

Beaudette, M. R. (2001d). "Galvashield®XP Project Reference Lists", http://www.norcure.com/refer2.htm (August 23, 2001).

Beaudette, M.R. (2002a). "Chloride Removal – Technical Papers", http://www.norcure.com/criteria.htm (March 6, 2002).

Beaudette, M.R. (2002b). "Re-Alkalization-Technical Papers", http://www.norcure.com/criter2.htm (March 6, 2002).

Billington, D. P. (1976). "Historical Perspectives on Prestressed Concrete", *PCI Journal*, pp. 48-71.

Breen, J. E. (1990). "Prestressed Concrete: The State of the Art in North America", *PCI Journal*, pp. 62-67.

British Standards Institution (1992). *"BS 1881:Part 207 - Recommendations for the Assessment of Concrete Strength by Near-to-Surface Tests"*, British Standards Institution, London, United Kingdom

Broomfield, J. P., Davies, K., and Hladky, K. (1999). "Permanent Corrosion Monitoring For New & Existing Reinforced Concrete Structures" Structural Faults + Repair-99, 8th International Conference, London, UK, 13-15 July.

Bullard, S. J., Covino Jr., B. S., Cramer, S. D., Holcomb, G. R., and McGill, G. E. (1996). "Thermal-Sprayed Zinc Anodes for Cathodic Protection of Steel-Reinforced Concrete Bridges" CORROSION/96, Denver, Colorado, March 24-29.

Burns, D. (2001). *Telephone Conversation.* Assistant Manager, Vector Corrosion Technologies. June 25.

Cady, P. D. (1994). "Sealers For Portland Cement Concrete Highway Facilities". NCHRP Synthesis 209 – *A synthesis of Highway Practice*. Transportation Research Board, National Research Council, Washington, DC.

Cairns, J., and Millard, S. (1999). " Reinforcement Corrosion and Its Effect on Residual Strength of Concrete Structures", "STRUCTURAL FAULTS + REPAIR-99", 8th International Conference London, UK, 13-15 July 1999.

CFR Title 23—Highways, Chapter I--Federal Highway Administration, Department of Transportation, Part 650--Bridges, Structures, and Hydraulics (1999). http://www.access.gpo.gov/nara/cfr/waisidx_99/23cfr650_99.html (August 21, 2001).

Clear, K.C. (1989). "Measruing Rate of Corrosion of Steel in Field Concrete Structures", *Transportation Research Record No. 1211*, pp. 28-37.

Collins, M.P, and Mitchell, D. (1991) "Prestressed Concrete Structures", Prentice-Hall, Englewood Cliffs, New Jersey. (crack discussion on pages 114 and 115).

Chemrex (2002a). "ThoRoc Product Specifier" http://www.chemrex.com/thoroc/product_thc.asp (March 19, 2002).

Chemrex (2002b). "MBT Product Specifier." http://www.chemrex.com/mbt/product_mbt.asp (March 19, 2002).

Cox, R. (2001). *Telephone Conversation.* Field Operations Section Director, Texas Department of Transportation. August 10.

Dillard, J.D., Glanville, J.O., Collins, W.D., Weyers, R.E., and Al Qadi, I.L (1993) "Concrete Bridge Protection and Rehabilitation: Chemical and Physical Techniques, Feasibility Studies of New Rehabilitation Techniques.", SHRP-S-665, National Research Council, Washington, D.C.

Draft Interim Standard Specifications for Construction, (2001). Michigan Department of Transportation, Lansing, Michigan.

Emmons, P. H. (1994). *Concrete Repair and Maintenance Illustrated*, R.S. Means Company, Inc., Kingston, Massachusetts.

Emmons, P.H., (1994). *Concrete Repair and Maintenance Illustrated*, R.S. Means Company, Inc., Kingston, Massachusetts.

Enright, M. P., and Frangopol, D. M. (2000). "Survey and Evaluation of Damaged Concrete Bridges", Journal of Bridge Engineering, February, pp. 31-38.

Ersoy, U., "Reinforced Concrete", METU, Ankara, 1997

Federal Highway Administration (FHWA) (1997). "Evaluation of Digital Camera Technology For Bridge Inspection", Publication No: FHWA-SA-97-100.

Funahashi, M., and Daily, S. F. (1996). "New Sacrificial Anode for Cathodic Protection of Reinforced Concrete Structures", *Proceedings of the Materials Engineering Conference (Conference Title: Proceedings of the 1996 4th Materials Engineering Conference. Part 2 (of 2))*, Vol. 2, pp. 1256-1262.

Ganji, V., Tabrizi, K., and Vittilo, N. (2000). "Project Level Application of Portable Seismic Pavement Analyzer." *Structural Material Technology IV - an NDT Conference, 2000*, S. Alampalli, ed., Technomic, 205-210.

Gawedzinski, M. (2001). *Telephone Conversation.* Illinois Department of Transportation. August 9.

Gee, C. K., and Hover, K. C. (1987). "Cathodic Protection for Prestressed Structures", *Concrete International: Design and Construction,* Vol. 9, pp. 26-30.

Geidl, V. A., and Khafagi, B. K. (1988). "Reliability of Cracked, Prestressed Girders", *Probabilistic Methods in Civil Engineering, Proceedings of the 5th ASCE Specialty Conference,* New York, pp. 309-312.

Gergely, P., and M.A. Sozen. Design of Anchorage-Zone Reinforcement in Prestressed Concrete Beams. PCI Journal, April 1967, pp. 63-75.

Ghosh, S. K., and Fintel, M. "Development Length of Prestressing Strands, Including Debonded Strands, and Allowable Concrete Stresses in Prestensioned Members", *"PCI Journal"*, September-October 1986.

Graybeal, B. A., Rolander, D. D., Phares, B. M., Moore, M. E., and Washer, G. A. (2001). "Highway Bridge Inspection: State-Of-The-Practice Survey", Transportation Research Board, 80th Annual Meeting, Conference Paper, Washington D.C., January 7-11.

Gucunski, N., Vitillo, N., and Maher, A. (2000). "Bridge Deck Delamination Using Integrated Seismic Devices." *Structural Material Technology IV - an NDT Conference, 2000*, S. Alampalli, ed., Technomic, 329-334.

Hag-Elsafi, O., and Alampalli, S. (2000). "Strengthening Prestressed Concrete Beams Using Bonded FRP Laminates." *Structural Material Technology IV - an NDT Conference, 2000*, S. Alampalli, ed., Technomic, 287-292.

Halstead, J. P., O'Connor, J. S., Alampalli, S., and Minser, A. (2000). "Evaluating FRP Wrap with NDT Methods." *Structural Material Technology IV - an NDT Conference, 2000*, S. Alampalli, ed., Technomic, 275-280.

Hartle, R. A., Amrhein, W. J., Wilson, K. E., Baughman, D. R., and Tkacs, J. J. (1995). *Bridge Inspectors Training Manual 90*, Federal Highway Administration, Washington, D.C.

Heldt, L. D. (2001). Corrosion workshop at Michigan Technological University. July 11.

Henderson, M. E., Costley, R. D., and Dion, G. N. (2000). "Acoustic Inspection of Concrete Bridges with the HollowDeck." *Structural Material Technology IV - an NDT Conference, 2000*, S. Alampalli, ed., Technomic, 184-189.

HyperMesh 2.0 Documentation (1995). Altair Computing, Inc., Troy, Michigan.

http://www.altairmodel.com

HyperMesh 4.0 Documentation (2000). Altair Computing, Inc., Troy, Michigan.

http://www.altairmodel.com

Illinois Department of Transportation (IDOT) (2001). "Final Report, 3M Corporation, Corrosion Abatement System 4727 Zinc-Hydrogel Anode" ftp://ftp.dot.state.il.us/pub/ (August 15, 2001).

Iowa State University, " Steel Diaphragms in Prestressed Concrete Girder Bridges TR-424", http:// http://www.ctre.iastate.edu, May 2002

Ishii, K., Seki, H., Fukute, T., and Ikawa, K. (1998). "Cathodic Protection for Prestressed Concrete Structures", *Construction and Building Materials,* Vol. 12, No. 2-3, pp. 125-132.

Jadun, S. (1990). "Michigan Experience with Prestressed Concrete Bridges," *MATES*, Michigan Department of Transportation, Materials and Technology Division, Issue No. 49, December 1990.

Jones, D. A. (1992). *Principles and Prevention of Corrosion*, Macmillan Publishing Company, New York, New York.

Juntunen, D. A. (2000). *Cracks and Deterioration of Prestressed Beams*, Michigan Department of Transportation, Lansing, Michigan.

Kasper, J. M., (2002). "A Performance Evaluation of Repair Materials for Corrosion Induced Deterioration of Prestressed Concrete Bridges," Master of Science Thesis, Michigan Technological University.

Keating, P. B., and Fisher, J. W. (1987). "Repair, Rehabilitation, and Strengthening of Highway Bridges in the United States." *Bridge Evaluation Repair and Rehabilitation*, E. Absi, and A. S. Nowak, ed., The University of Michigan, Ann Arbor, Michigan, 185-196.

Kennedy, R. C. (1991). *Cathodic Deck Protection and Latex Modified Concrete Overlay on Steel I-Beam Bridge*, Pennsylvania Department of Transportation, Montoursville, Pennsylvania.

Kosaka, Yasuo, Miura, Takashi, Tsukada, and Yukihiro. (1999). "Salt- Damage And Retrofitting Of Prestressed Concrete Bridges At The Japanese Sea Coast In North – Japan", Structural Faults + Repair-99, 8th International Conference, London, UK, 13-15 July 1999

Kosmatka, S. H., and Panarese, W. C. (1988). *Design and Control of Concrete Mixtures, Thirteenth Edition*, Portland Cement Association, Skokie, Illinois

Kosmatka, S.H., Kerkhoff, B., and Panarese, W.C., (2002), *Design and Control of Concrete Mixtures, EB001, 14th edition*, Portland Cement Association, Skokie, Illinois, 372 pages.

Krauss, P. D., and Nmai, C. K. (1996). "Preliminary Corrosion Investigation of Prestressed Concrete Piles in a Marine Environment: Deerfield Beach Fishing Pier", *ASTM Special Technical Publication (Conference Title: Proceedings of the 1994 Symposium on Techniques to Assess the Corrosion Activity of Steel Reinforced Concrete),* Vol. 1276, pp.161-172.

Lanyi, R. S. (1994). "Field prestressing repairs to precast concrete bridge girders" SP-151 American Concrete Institute, Farmington Hills, Michigan

Legat, A., Kuhar, V., Bevc, L., and Vehovar, L. (1996). "Some Considerations of Potential-Mapping as a Method for the Detection of Corrosion in Reinforced and Prestressed Concrete Structures", *13th International Corrosion Congress Proceedings,* Paper 186, pp.1-6.

Lenschow, R.J., and M.A. Sozen. Practical Analysis of the Anchorage Zone Problem in Prestressed Beams. Journal of the American Concrete Institute, November 1965, pp. 1421-1439.

Leonhardt, F. (1964). Prestressed Concrete Design and Construction, Wilhelm Ernst & Sohn, Berlin.

Lin, T. Y., and Burns, N. H. (1981). "Design of Prestressed Concrete Structures", Third Edition, John Wiley & Sons

Liu, W., Hunsperger, R., and Kunz, E. (2001). "Nondestructive Corrosion Monitoring of Prestressed HPC Bridge Beams Using Time Domain Reflectometry", Transportation Research Board, Conference Paper, Washington D. C, January 7- 11.

MacGregor, J.G. (1992). "Reinforced Concrete Mechanics and Design, Second Edition." Prentice-Hall, Englewood Cliffs, New Jersey. p. 46.

Mari, R. A., and Valdes, M. (2000). "Long-Term Behavior of Continuous Precast Concrete Girder Bridge Model", Journal of Bridge Engineering, pp. 22-30.

McDonald, J.E., Vaysburd, A.S., Emmons, P.H., Poston, R.W., and Kesner, K. (2002). "Selecting Durable Repair Materials: Performance Criteria – Summary". Concrete International, American Concrete Institute, January, pp 37-44.

MDOT (1984a). *MDOT Design Division Informational Memorandum 320-B*, Michigan Department of Transportation, Lansing, Michigan.

MDOT (1984b). *MDOT Design Division Informational Memorandum 332-B*, Michigan Department of Transportation, Lansing, Michigan.

MDOT (1989). *MDOT Design Division Informational Memorandum 411-B*, Michigan Department of Transportation, Lansing, Michigan.

MDOT (1991). *MDOT Design Division Informational Memorandum 402-B*, Michigan Department of Transportation, Lansing, Michigan.

MDOT (1992). *MDOT Design Division Informational Memorandum 447-B*, Michigan Department of Transportation, Lansing, Michigan.

MDOT (1996). *Standard Specifications for Construction*, Michigan Department of Transportation, Lansing, Michigan.

MDOT (1997a). *MDOT Design Division Informational Memorandum 484-B*, Michigan Department of Transportation, Lansing, Michigan.

MDOT (1997b). *Michigan Structure Inventory and Appraisal Coding Guide.* Michigan Department of Transportation, Lansing, Michigan.

MDOT (1999). *Michigan Pontis Bridge Inspection Manual.* Michigan Department of Transportation, Lansing, Michigan.

MDOT (2000). *Special Provision for Vertical and Overhead Structure Repairs.* Michigan Department of Transportation, Lansing, Michigan.

MDOT (2001a). *Bridge Design Manual.* Michigan Department of Transportation, Lansing, Michigan.

MDOT (2001b). *Bridge Design Guides.* Michigan Department of Transportation, Lansing, Michigan.

MDOT (2001c). *MDOT - 2001 Materials Source Guide –Index.* http://www.mdot.state.mi.us/mappub/materialsguide/ (March 9, 2002).

Mindess, S. and Young, J.F. (1981). *Concrete.* Prentice-Hall, Englwood Cliffs, New Jersey.

Monterio, P. J. M., Frank, M., and Frangos, W. (1998). "Nondestructive Measurement of Corrosion State of Reinforcing Steel in Concrete", *ACI Material,* Vol. 95, No. 6, pp.704-709.

Moore, D. G., Klodt, D. T., and Hensen, R. J. (1970). "Protection of Steel in Prestressed Concrete Bridges" *NCHRP Report No. 90.* National Research Council, Washington, D.C.

Narasimhan, E. S., and Wallbank, E. J. (1999). "Bridge Inspections - Current Thinking And Regimes" Structural Faults + Repair-99, 8th International Conference, London, UK, 13-15 July.

National Association of Corrosion Engineers (1970). "*NACE Basic Corrosion Course*", NACE, Houston, Texas.

Nawy, E.G. (2000) *Prestressed Concrete – A Fundamental Approach*, Third Edition, Prentice Hall, Upper Saddle River, New Jersey, p. 49.

Needham, D. (1999). *Prestressed Concrete Beam End Repair (Interim Report)*, Research Report R-1373, Michigan Department of Transportation, Lansing, Michigan.

Needham, D. (2000). *Prestressed Concrete Beam End Repair*, Research Report RR-1380, Michigan Department of Transportation, Lansing, Michigan.

Needham, D. (2001). "Development and Evaluation of Passive Cathodic Protection Systems Used on PCI-Beam Ends", Transportation Research Record No. 00795442, Transportation Research Board, Washington, D.C.

Needham, D., and Juntunen, D. A. (1997). *Investigation of Condition of Prestressed Concrete Bridges in Michigan*, Research Report R-1348, Michigan Department of Transportation, Lansing, Michigan.

Nogueira, C. L. (1999). "Bridge Evaluation Using Nondestructive Testing In Bridge Inspections As A Tool For Bridge Management Systems", Structural Faults + Repair-99, 8th International Conference, London, UK, 13-15 July.

Ohio Department of Transportation (OhDOT) (2001). http://www-ltap.eng.ohio-state.edu/bms/beams/pcibeams.htm (September 25, 2001).

Ohyama, H., Fujiwara, T., Kawakami, M., Shoyn, M., and Kosaka, Y. (1999). "Investigation & Retrofitting of Prestressed Concrete Bridges In Northeastern District of Japan", Structural Faults + Repair-99, 8th International Conference, London, UK, 13-15 July.

Ota, M., Numata, A., and Kondo, S. (1985). "Life Time Test of Prestressed Concrete", *Ocean Space Utilization '85, Proceedings of the International Symposium,* Tokyo, pp. 463.

Park,R.,Paulay,T., "Reinforced Concrete Structures", 1975

Pascale, G., Bonfiglioli, B., Carli, R., and Arduini, M. (1999). "Bridge RC Beams: Repair & Monitoring", Structural Faults + Repair-99, 8th International Conference, London, UK, 13-15 July.

PCI Design Handbook, Fifth Edition, (1999). Raths, Raths, & Johnson, Inc., editor, Prestressed Concrete Institute, Chicago, Illinois

Pedeferri, P. (1996). "Cathodic Protection and Cathodic Prevention", *Construction and Building Materials,* Vol. 10, No. 5, pp. 391-402.

Perenchio, W. F., Fraczek, J., and Preiffer, D. W. (1989). "Corrosion Protection of Prestressing Systems in Concrete Bridges" *NCHRP Report No. 313*, National Research Council, Washington D.C.

Petrangeli, M. P., and Sarno, R. (1999). "NDT Of Prestressing Cables By Impact-Echo Method" Structural Faults + Repair-99, 8th International Conference, London, UK, 13-15 July.

Portland Cement Association (PCA) (2001). "Concrete Information: Effects of Substances on Concrete and Guide to Protective Treatments." IS001, Portland Cement Association, Skokie, Illinois.

Preston, H. K., Osborn, A. E. N., and Roach, C. E. (1987). *Restoration of Strength in Adjacent Prestressed Concrete Box Beams*, Wiss, Janey, Elstner Associates, Inc., Princeton Junction, New Jersey.

Puzey, C. (2001). *Telephone Conversation.* Bridge Investigations and Repair Plans Unit Chief, Illinois Department of Transportation. August 9.

Rabbat, B.G. and Aswad, A. (2002) "Design of Precast Prestressed Girders Made Continuous" www.portcement.org/br/design_for_continuity.pdf (May 6, 2002).

Rabbat, B. G., and Russell, H. G. (1982). "Optimized Sections for Precast Prestressed Bridge Girders", PCI Journal, pp. 88-104.

Rengaswamy, N. S., and Rajagopalan, K. S. (1977). "Corrosion of High-Strength Steel in Prestressed Concrete: 1- Electrochemical Studies," *Indian Concrete Journal*, Vol. 51, No. 10, October, pp. 301-304.

Russell, B. W. "Measurements of Transfer Lengths on Pretensioned Concrete Elements", *Journal of Structural Engineering*, May 1997

S-B Power Tool Company (2002). "Product List" http://www.boschtools.com/Tools+and+Accessories/Tools/product_list.htm?link=product&hierarchy_id=59141 (March 19, 2002).

Sealants and Coatings.com (2001). http://www.sealantsandcoatings.com/frameset.cfm?sheetLink=http%3A%2F%2Fwww%2Edelamtools%2Ecom%2Fpages%2Fdel2000%2Ehtml (August 22, 2001).

Settipani, A. (1987). "Inspection of Reinforced and Prestressed Concrete by means of Gammagraphy." *Bridge Evaluation Repair and Rehabilitation*, E. Absi, and A. S. Nowak, ed., The University of Michigan, Ann Arbor, Michigan, 498-505.

Shanafelt, G. O., and Horn, W. B. (1985). "Guidelines for Evaluation and Repair of Prestressed Concrete Bridge Members." *NCHRP Report No. 280*, Transportation Research Board, Washington D.C.

Shanafelt, G. O., and Horn, W. B. (1980). "Damage Evaluation and Repair of Prestressed Concrete Bridge Members." *NCHRP Report No. 226*, Transportation Research Board, Washington D.C.

Sika USA (2002). "Welcome to Sika USA." http://www.sikausa.com/ (March 19, 2002).

Smith, J. L., and Virmani, Y. P. (2000). "Materials and Methods for Corrosion Control of Reinforced and Prestressed Concrete Structures in New Construction", Report Submitted to Federal Highway Agency, Report No. FHWA-RD-00-081.

Staton, J. (2001). *Re: Approval process for vertical and overhead concrete repair materials.* E-mail to James Kasper. November 27, 2001.

Sterritt, G., and Chryssanthopoulos, M. K. (1999). "Deterioration Prediction & Updating As A Means Of Structure Specific Bridge Management", Structural Faults + Repair-99, 8th International Conference, London, UK, 13-15 July.

Texas Transportation Institute (TTI) (1998). "Innovative Highway Technologies," http://leadstates.tamu.edu/All/information.stm (August 30, 2001).

Till, R. D. (2001a). *PC I-Beam End Project.* E-mail to Project Team with Attachments. March 16, 2001.

Till, R. D. (2001b). *Re: Q1 report comments.* E-mail to Project Team with Attachment. July 18, 2001.

Till, R.D. (2001c). *Re: mix design for lab tests.* Facsimile to Project Team. December 18.

Tilly, G. P. (1987). "Performance and serviceability of concrete bridges." *Bridge Evaluation Repair and Rehabilitation*, E. Absi, and A. S. Nowak, ed., The University of Michigan, Ann Arbor, Michigan, 119-134.

Titman, D. J. (1999). "Applications Of Thermography In NDT Of Structures", Structural Faults + Repair-99, 8th International Conference, London, UK, 13-15 July.

Tortorete, J (2001) "Bridge Deck Resurfacing" Presentation at the 2001 Michigan Bridge Conference, Mount Plesant, Michigan, May 30.

TxDOT (1993). ftp://ftp.dot.state.tx.us/pub/txdot-info/cmd/cserve/specs/1993/spec/es4302.pdf (September 25, 2001).

USACE (1992). "CRD-C 164-92 Standard Test Method for Direct Tensile Strength of Cylindrical Concrete or Mortar Specimens," *Handbook for Concrete and Cement*, U.S. Army Corps of Eingineers Waterways Experiment Station, Vicksburg, Mississippi.

Vaysburd, A.M. and McDonald, J.E. (1999). "An Evaluation of Equipment and Procedures for Tensile Bond Testing of Concrete". Technical Report REMR-CS-61, U.S. Army Corps of Engineers, Washington D.C.

Vector Corrosion Technologies (2001). "Galvashield® CC Project History – City of Winnipeg, Prestressed Girder Rehabilitation", Vector Corrosion Technologies, Winnipeg, Manitoba, Canada.

Virmani, Y.P and Clemena, G.G (1998). "Corrosion Protection – Concrete Bridges", *FHWA-RD-98-088*, Federal Highway Administration, McLean, Virginia.

Weyers, R. E., Prowell, B. D., Sprinkel, M. M., and Vorster, M. (1993). "Concrete Bridge Protection, Repair, and Rehabilitation relative to Reinforcement Corrosion: A Methods Application Manual," *SHRP-S-360*, National Research Council, Washington, D.C.

Whiting, D. A., Stejskal, B. G., and Nagi, M. A. (1993). "Conditions of prestressed concrete bridge components: Technology review and field surveys." FHWA-RD-93-037, Federal Highway Administration, Washington, D.C.

Whiting, D. A., Stejskal, B. G., and Nagi, M. A. (1998). "Rehabilitation of Prestressed Concrete Bridge Components By Non-Electrical (Conventional) Methods." FHWA-RD-98-189, Federal Highway Administration, Washington, D.C.

Whiting, D. A., Ost, B., Nagi, M., and Cady, P. D. (1992). "Condition Evaluation of Concrete Bridges Relative to Reinforcement Corrosion, Volume 5: Methods for Evaluating the Effectiveness of Penetrating Sealers." SHRP-S /FR-92-107, Strategic Highway Research Program, Washington, D.C.

Xanthakos, P. P. (1996). *Bridge Strengthening and Rehabilitation*, Prentice-Hall PTR, New Jersey

Yazdani N., Eddy S., Cai C.S., "Effect of Bearing Pads on Precast Concrete Bridges". Journal of Bridge Engineering. Vol. 5, August 2000, pp. 224-232

Zemajtis, J., and Weyers, R. E. (1998). "Corrosion Protection Service Life of Low Permeable Concretes and Low Permeable Concrete with a Corrosion Inhibitor", Transportation Research Board 77th Annual Meeting, Conference Paper, Washington, D.C., January 11-15.

Zhang, J., Monterio, P. J. M., and Morrison, F. H. (2001). "Non Invasive Surface Measurement of the Corrosion Impedance of Rebar in Concrete Part I", *ACI Material Journal*, pp.116-126.

Additional Documents

The interested reader may also refer to the following documents for information on the inspection, assessment, preventive maintenance, and repair of prestressed concrete I-beams.

"ACI 201.1R-92 - Guide for Making a Condition Survey of Concrete in Service." (1992). American Concrete Institute, Farmington Hills, Michigan.

"ACI 222.2R-01: Corrosion of Prestressing Steels." (2001). American Concrete Institute, Farmington Hills, Michigan.

"ACI 224.1R-93 - Causes, Evaluation, and Repair of Cracks in Concrete Structures." (1993). American Concrete Institute, Farmington Hills, Michigan.

"ACI 228.2R-98 - Nondestructive Test Methods for Evaluation of Concrete in Structures." (1998). American Concrete Institute, Farmington Hills, Michigan.

"ACI 364.1R-94 - Guide for Evaluation of Concrete Structures Prior to Rehabilitation." (1994). American Concrete Institute, Farmington Hills, Michigan.

"ACI 546.1R-80: Guide for Repair of Concrete Bridge Superstructures" (1980). American Concrete Institute, Farmington Hills, Michigan.

"ACI 546R-96 - Concrete Repair Guide." (1996). American Concrete Institute, Farmington Hills, Michigan.

"Condition Evaluation of Prestressed Strands in Bridges." NCHRP Project 10-53

"FHWA-SHRP Showcase - Assessment of Physical Condition of Concrete Bridge Components." (1996) CONCORR Inc., Ashburn, Virginia

"ICRI Guideline No. 03730 - Guide for Surface Preparation for the Repair of Deteriorated Concrete Resulting from Reinforcing Steel Corrosion." International Concrete Repair Institute

"ICRI Guideline No. 03733 - Guide for Selecting and Specifying Materials for Repair of Concrete Surfaces." International Concrete Repair Institute

"ICRI Guideline No. 03734 - Guide for Verifying Field Performance of Epoxy Injection of Concrete Cracks." International Concrete Repair Institute

"Management of Highway Structures" ed. P.C. Das, Thomas Telford Publishing, London, 1999.

"Safety of Bridges", ed. P.C. Das, Thomas Telford Publishing, London, 1997.

Chase, S. B. and Washer, G., "Nondestructive Evaluation for Bridge Management in the Next Century", Turner-Fairbank Highway Research Center, July 1997

Ciolko, A. T. and Tabatabai, H., "Nondestructive Methods for Condition Evaluation of Prestressing Steel Strands in Concrete Bridges", National Cooperative Highway Research Program, Transportation Research Board, and National Research Council, NCHRP Project 10-53, March 1999

Das., P. C., Frangopol, D. M. and Nowak, A. S., ed., "Bridge Design, Construction and Maintenance", International Conference in Singapore, Thomas Telford, London, October 1999.

Das., P. C., Frangopol, D. M. and Nowak, A. S., ed., "Bridge Design, Construction and Maintenance", International Conference in Singapore, Thomas Telford, London, October 1999.

Fam, A.Z., Rizkala, S.H., and Tadros, G. (1997). "Behavior of CFRP for Prestressing and Shear Reinforcements of Concrete Highway Bridges." ACI Structural Journal (1/97), American Concrete Institute, Farmington Hills, Michigan.

Federal Highway Administration, (1981). "Detection of Flaws in Reinforcing Steel in Prestressed Concrete Bridge Members", Contract No: DOT-FH-11-8999

Federal Highway Administration, (1989). "Salt Penetration and Corrosion in Prestressed Concrete Members", Publication No: FHWA-SA-97-100.

Federal Highway Administration, (1997). "Evaluation of Digital Camera Technology For Bridge Inspection", Publication No: FHWA-PD-91-015

Federal Highway Administration, (2000). "Materials and Methods for Corrosion Control of Reinforced and Prestressed Concrete Structures in New Construction", Publication No: FHWA-RD-00-081. On microfiche in JRVP: TD 2.30:00-081

Feldman, L.R., Jirsa, J.O., and Kowal, E.S. (1998). "Repair of Bridge Impact Damage." Concrete International (2/98), American Concrete Institute, Farmington Hills, Michigan.

Fiorato, A. E., "Inspection Guide for Reinforced Concrete Vessels", USDOT, US Coast Guard, Contract No: DOT-CG-832171-A, October, 1981

Freitag, S. A., Bruce, S. M., and Hickman, W, E., "Reinforcement Corrosion in New Zealand Concrete", Advances in Concrete Technology, ACI SP-171, 1997

Hachem, Y., Zografos, K., and Soltani, M., "Bridge Inspection Strategies", Journal of Performance of Constructed Facilities, Vol. 5, No.1, February, 1991

Kim, S., Nowak, A.S., and Saraf, V., "Field Evaluation of Existing Bridges", US-Canada-Europe Workshop on Bridge Engineering, Zurich, Switzerland, July 1997.

Konig, G. and Nowak, A.S., ed., "Bridge Rehabilitation", Ernst & Sohn, Berlin, Germany, 1992.

Lamberson, E.A. (1983). "Post-tensioning Concepts for Strengthening and Rehabilitation of Bridges." ASCE Structures Congress, Preprint SC-10, Houston.

Management of Highway Structures, ed. P.C. Das, Thomas Telford Publishing, London, 1999.

Medlock, R. D., and Laffrey, D. C., ed., "Structural Materials Technology III: An NDT Conference." Texas Dept. of Transportation, Austin, Texas, 1998.

Naaman, A.E. (1985). "Partially Prestressed Concrete Review and Recommendations." PCI Journal, Vol. 30, No. 6.

Nawy, E.G. (1996). Prestressed Concrete. A Fundemental Approach.

Novokshxhenov, V., "Prestressed Bridges and Marine Environment", Journal of Structural Engineering, Vol. 116, No. 11, November, 1990

Nowak, A.S. and Kim, S. , "Development of a Guide for Evaluation of Existing Bridges, Part I", UMCEE 98-12, Final Report submitted to MDOT, June 1998.

Nowak, A.S., ed., "Bridge Evaluation, Repair and Rehabilitation," NATO ASI Series E, Vol. 187, Kluwer Academic Publishers, Dordrecht, Netherlands, 1990.

Nowak, A.S., Sanli, A., Kim, S. Eom, J., and Eamon C., "Development of a Guide for Evaluation of Existing Bridges, Part II", UMCEE 98-13, Final Report submitted to MDOT, June 1998.

Nowak, A.S., Saraf, V. and Kim, S., "Evaluation of Bridges using Field Testing", International Conference on Rehabilitation and Development of Civil Eng. Infrastructure Systems, Beirut, Lebanon, June 1997, Vol. I, pp. 391-402.

Safety of Bridges, ed. P.C. Das, Thomas Telford Publishing, London, 1997.

Saraf, V., Nowak, A.S. and Kim, S., "Nondestructive Testing of Bridges", Fourth National Workshop on Bridge Research in Progress, Buffalo, NY, June 1996, pp. 45-50.

Shubinsky, G., "Visual & Infrared Imaging for Bridge Inspection", Northwestern University BIRL Basic Industrial Research Laboratory, June 1994

Tabsh, S. W., "Sensitivity Analysis of Damaged Concrete Bridge Girders", Designing Concrete Structures for Serviceability and Safety, ACI SP-133, 1992

Van Begin, C., "Durability of Concrete Bridges in Belgium—Balance of the Systematic Inspection", Concrete Durability, ACI SP-100, Vol. 1, 1987

Veshosky, D., Beidleman, C. R., Buetow, G. W., and Demir, M., "Comparative Analysis of Bridge Superstructure Deterioration", Journal of Structural Engineering, Vol. 120, No. 7, July, 1994

Workshop on Optimal Maintenance of Structures, Delft, The Netherlands, October 2000